AN INVESTIGATION OF THE MECHANICS OF WIRE DRAWING WITH THE SUPERPOSITION OF AN OSCILLATORY DRAWING STRESS

by

C.E.Winsper B.Sc. G.I.Mech.E.

Submitted in fulfilment of the requirements for the degree of Doctor of Philosophy.

University of Aston in Birmingham.

September 1966.

Faculty of Engineering.

Dept. of Mech. Eng.

Supervisor,

Dr.D.H.Sanso

Synopsis

A number of investigators have studied the application of oscillatory energy to a metal undergoing plastic deformation. Their results have shown that oscillatory stresses reduce both the stress required to initiate plastic deformation and the friction forces between the tool and workpiece. The first two sections in this thesis discuss historically and technically the development of the use of oscillatory energy techniques to aid metal forming with particular reference to wire drawing. The remainder of the thesis discusses the research undertaken to study the effect of applying longitudinal oscillations to wire drawing.

Oscillations were supplied from an electric hydraulic vibrator at frequencies in the range 25 to 500 c/s., and drawing tests were performed at drawing speeds up to 50 ft/m. on a 2000 lbf. bull-block. Equipment was designed to measure the drawing force, drawing torque, amplitude of die and drum oscillation and drawing speed. Reasons are given for selecting mild steel, pure and hard aluminium, stainless steel and hard copper as the materials to be drawn, and the experimental procedure and calibration of measuring equipment are described.

Results show that when oscillatory stresses are applied at frequencies within the range investigated :

(a) There is no reduction in the maximum drawing load.

(b) Using sodium stearate lubricant there is a negligible reduction in the coefficient of

friction between the die and wire.

(c) Pure aluminium does not absorb sufficient oscillatory energy to ease the movement of dislocations.

(d) Hard aluminium is not softened by oscillatory energy accelerating the diffusion process.

(e) Hard copper is not cyclically softened.

A vibration analysis of the bull-block and wire showed that oscillatory drawing in this frequency range, is a mechanical process of straining and unstraining the drawn wire, and is dependent upon the stiffness of the material being drawn and the drawing machine.

Directions which further work should take are suggested.

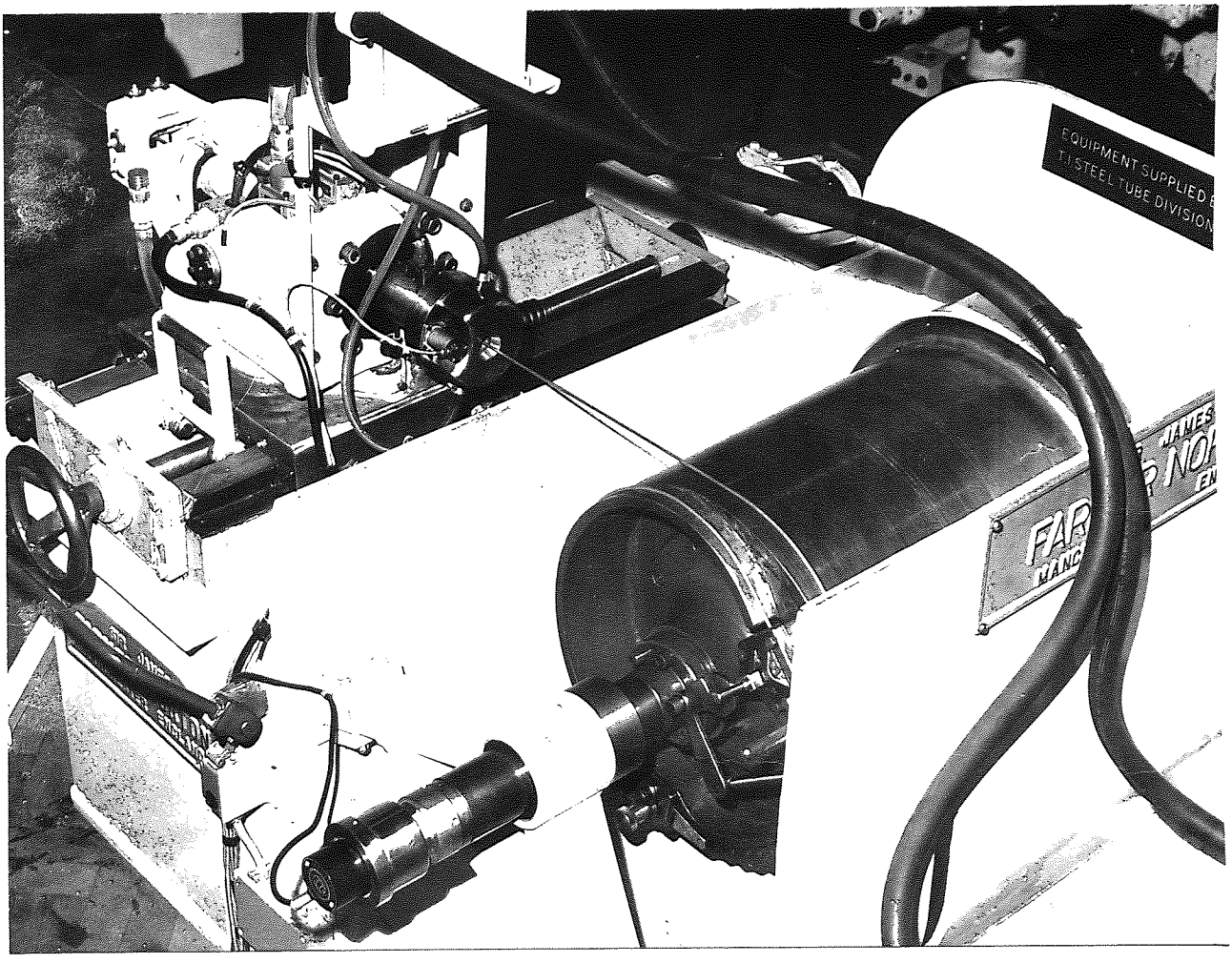

FRONTISPIECE

List of Contents

Nomenclature

a	Velocity of propogation of stress waves in material, and radius of disc in Trifilar suspension
A	Cross-sectional area of wire
c	Length of wire
C	Damping coefficient
d	Diameter of shafts (bull-block drive)
E	Young's Modulus
F	Drawing force
G	Modulus of rigidity
I	Moment of inertia of drum
J	Polar moment of inertia of shafts
k	Radius of gyration
K	Linear stiffness of wire and loadmeter
ℓ	Length of shafts (bull-block drive)
L	Length of wire between die and drum, and length of wire used in Trifilar suspension
m	Mass of die and die holder assembly
N	Speed of revolution
r	Radius of drum, radius of wire and radius of disc used in Trifilar suspension
R	Gear ratio
S	Torsional stiffness of bull-block drive
t	Time
T	Applied torque
u	Displacement of cross-section of wire
V	Drawing speed
W	Weight of aluminium disc used in Trifilar suspension

x	Amplitude of die oscillation and rectilinear displacement
x'	Displacement of end of wire
X	Amplitude of oscillation and normal function
Y	Yield stress of material (tension)
α	Semi-die angle
γ	Angle, (Trifilar suspension)
ε	Natural strain
$\bar{\varepsilon}$	Generalised strain
θ	Angle of twist of drum and drive shafts
μ	Coefficient of friction
ρ	Density of material
σ	True stress
ω	Frequency of oscillation

suffix 1, refers to wire entry conditions

suffix 2, refers to wire exit conditions

radial natural strain $= \varepsilon_1 = \ln \frac{r_1}{r_2}$

longitudinal natural strain $= \varepsilon_2 = \ln \frac{A_1}{A_2}$

circumferential natural strain $= \varepsilon_3 = \ln \frac{r_1}{r_2}$

and $$\bar{\varepsilon} = \frac{2}{3} \sqrt{\varepsilon_1^2 + \varepsilon_2^2 + \varepsilon_3^2}$$

reduction in area $= \frac{A_1 - A_2}{A_1}$

1. Introduction

1. Introduction.

In 1955, Blaha and Langenecker (1)*, performed an experiment in which they superimposed oscillatory energy on the applied stress during a tensile test on a single crystal of zinc. Surprisingly, these vibrations substantially reduced the stress necessary to cause plastic deformation. This increase in plasticity was also observed by Tarpley et. al. (2), when joining two pieces of metal with a single spot weld. Tarpley showed that the pieces being joined could be readily swivelled about the axis of the weld as the weld was being subjected to oscillatory energy. On removal of the energy source, the weldment abruptly resumed normal rigidity.

In 1957, workers at Aeroprojects Incorporated (USA) (3), observed that oscillatory energy also substantially reduced frictional forces. Metal components with interference fits were readily assembled when subjected to vibration. They further observed, that the application of vibrational energy resulted in a minimum scoring of the mating surfaces and a reduction in force necessary to perform the assembly.

The possible potential of applying these observed phenomena to metal working processes was soon realised and consequently, interest in the effect of oscillatory stresses on the deformation of metals began to increase rapidly. Extensive studies have been made in the USSR and the USA and

---

* Numbers in parentheses designate references listed at end of thesis.

in most cases quite remarkable results have been reported. As a result of these findings, some oscillatory stress techniques have now been patented and applied in the metal working industries in these countries.

Results of investigations can be summarised briefly as follows :-

Comparing a metal deforming operation in which oscillatory stresses are applied with a similar non-oscillatory operation, it appeared that :-

(1) The loads required to achieve the deformation are reduced on account of

(a) A reduction in stress necessary to initiate plastic deformation of the metal.

(b) A reduction of friction between the deforming metal and the tools.

(2) The strain to fracture is increased.

(3) The deformation is more uniform, ie. the redundant deformation is reduced.

(4) With some reservation, the reduction of yield stress is directly proportional to the amplitude of oscillation.

(5) The rate of work hardening is decreased.

(6) Within wide limits the frequency of oscillation has little or no effect.

In view of these encouraging results, it was decided to

initiate a thorough investigation into the application of longitudinal oscillatory stresses during wire drawing, studying such variables as :-

(a) Frequency of oscillation

(b) Amplitude of oscillation

(c) Drawing speed

(d) Reduction of area and

(e) Diameter of drawn wire.

with a view to obtaining optimum drawing conditions.

This thesis, (i) describes the historical and technical development of the application of oscillatory energy to metal working processes and (ii) discusses the research undertaken to study the mechanics of wire drawing with a superimposed oscillatory drawing stress.

2. Historical and Technical Review

2. Historical and Technical Review.

2.1. Introduction.

The application of oscillatory energy to a metal undergoing plastic deformation has been studied by a number of investigators (3). Their results have shown that, with the superimposed oscillatory stress, the deformation may be achieved with significantly reduced forces. This force reduction has been observed under conditions of pure tension and during actual metal working operations. The magnitudes of the reductions ranging from barely detectable to as high as 80 per cent.

The effects of oscillatory energy can be considered to be twofold, namely a surface effect and a volume effect. The surface effect relates to a reduction in external friction between the die and the deforming metal, while the volume effect applies to internal changes taking place within the deforming metal under the action of the oscillator stress waves. The mechanism underlying the phenomenon of reduced stress necessary to initiate plastic deformation of a metal, has not yet been adequately explained. It is thought that some, or all of the vibrational energy is absorbed preferentially at dislocation sites, but the mode by which the energy is absorbed is not known.

The following sections of this chapter, outline the historical and technical development of the application of oscillatory energy to metal working processes. Section

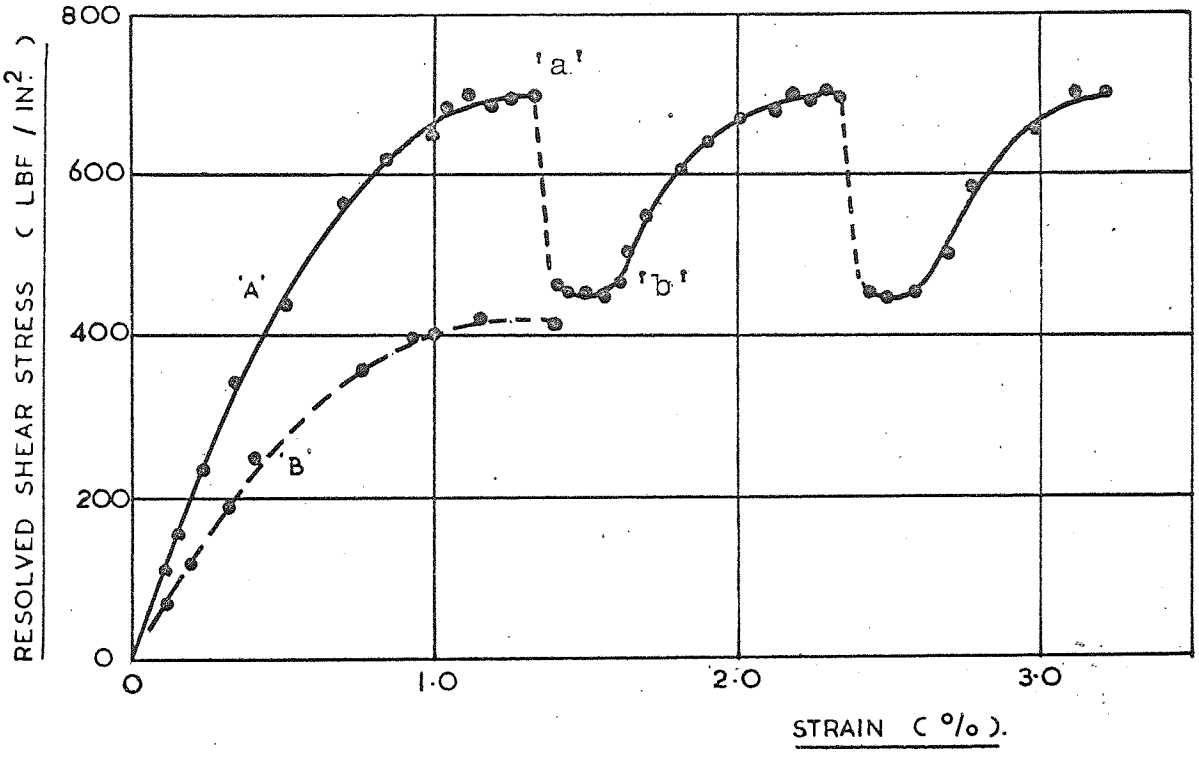

FIG. NO. 1 SHEAR STRESS STRAIN CURVE FOR A SINGLE CRYSTAL OF ZINC.

(BLAHA AND LANGENECKER . 1955)

2.2. describes early work on the effect of vibrational stresses on the mechanical properties of materials, and section 2.3. discusses the mechanism underlying the observed reduction in stress necessary to cause yielding. Section 2.4. considers the reduction in external friction and discusses the mechanisms by which the coefficient of friction could be reduced. Section 2.5. describes the application of oscillatory energy to various metal working processes e.g. forging, rolling, coining, extruding etc., culminating in a seperate section 2.6, on wire and tube drawing. Section 2.7 discusses the implication of oscillatory energy to the metal working industries.

2.2. The Effect of Oscillatory Stresses on the Mechanical Properties of Metals.

As outlined on page 1, Blaha and Langenecker first observed the phenomenon of a reduction in stress necessary to initiate plastic deformation of a metal when an oscillatory stress is superimposed on the steadily applied stress. Their experiments consisted of superimposing a vibrating load, in the direction of the specimen axis, on the steadily applied load, while tensile testing single crystals of zinc. The frequency of oscillation they chose was 800×10^3 c/s. A shear stress-strain curve obtained from these experiments is shown in Fig. No.1.

The dotted curve, curve 'A', shows the effect of applying oscillatory energy intermittently. 'a' is the point at which oscillatory energy was applied and is marked by a sudden reduction of shear stress of approximately 30 per cent. This level of stress was then maintained until the oscillatory energy was removed at point 'b', when the shear stress rapidly increased to its original non-oscillatory level. Curve 'B' was obtained by continually straining the zinc crystal with a superimposed oscillatory stress. Langenecker et al (4,5,6,7), obtained similar results when tensile testing single crystals of aluminium and cadmium and also with polycrystalline specimens of zinc, aluminium, cadmium, beryllium, tungsten and 18-8 stainless steel at frequencies in the range 15 to 25 x 10^3 c/s. Langenecker further observed that the magnitude of stress reduction was independent of the frequency for the above range, but dependent upon the amplitude of vibration.

Additional investigations by Langenecker, Colberg and Fransden 1962 (8), and Langenecker 1963 (9), using frequencies of vibration up to 10^6 c/s., further confirmed the observed reduction in the steady stress required to initiate yielding. During these investigations Langenecker also noted that stress-strain curves obtained at room temperature under various conditions of oscillatory stressing, resembled curves obtained under non-oscillatory conditions

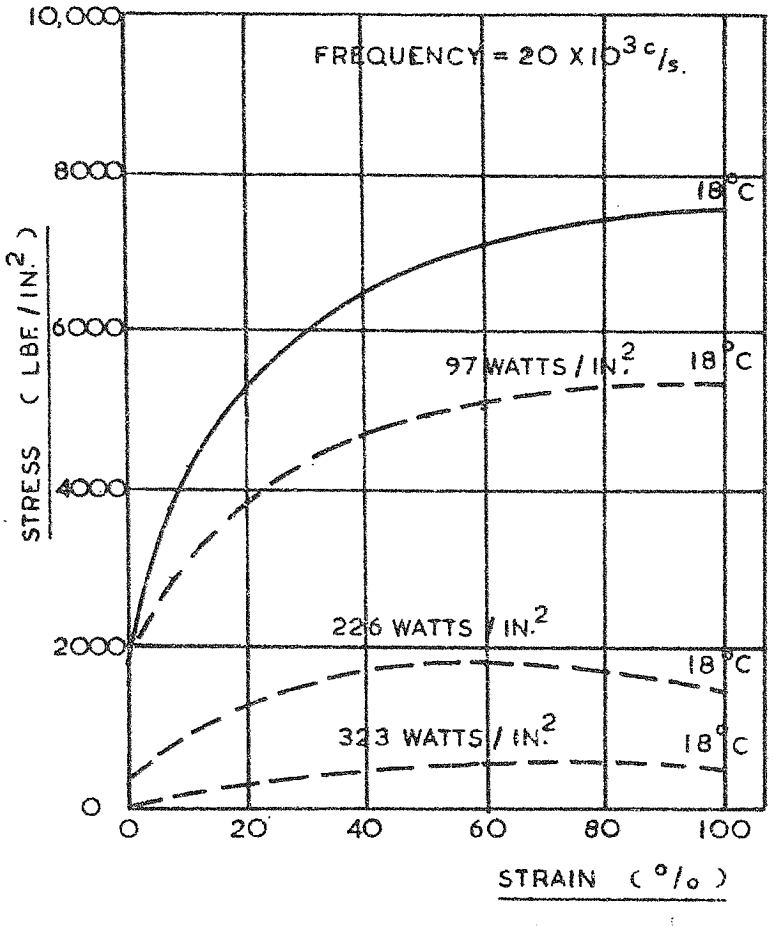

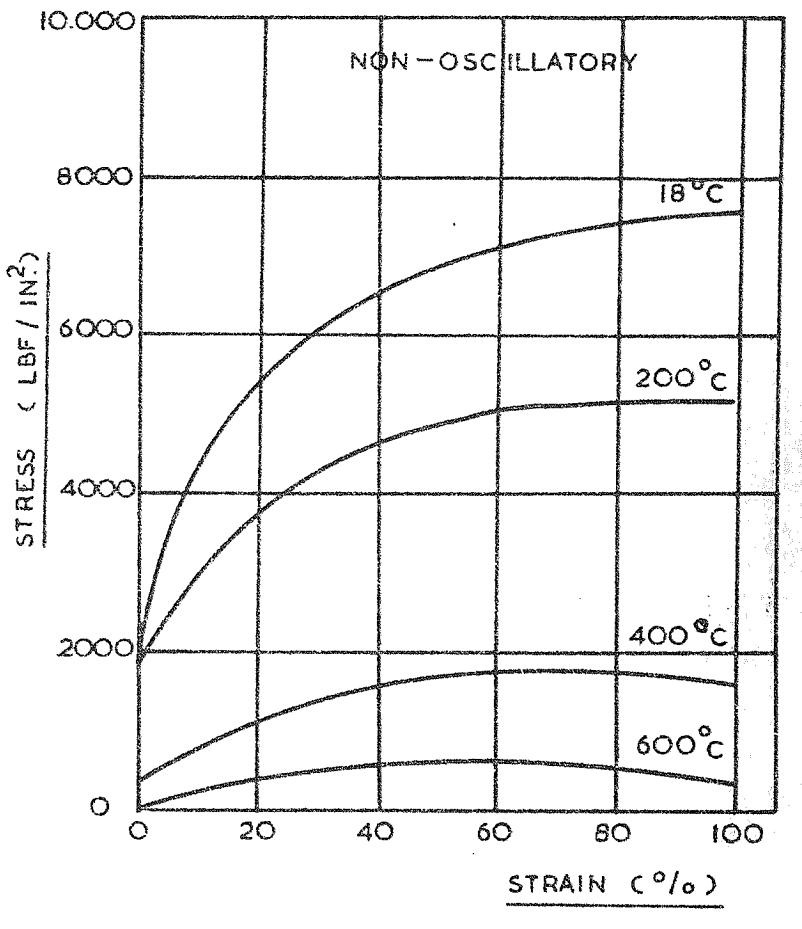

FIG. NO. 2 STRESS STRAIN CURVES FOR ALUMINIUM SINGLE CRYSTALS.

(LANGENECKER, 1959)

at elevated temperatures.

Fig. No.2 compares stress-strain curves obtained by Langenecker for single crystals of aluminium obtained at room temperature under conditions of superimposed oscillatory energy, with stress strain curves obtained at various temperatures under non-oscillatory conditions. The curves also show that the yield stress for aluminium is almost reduced to zero, when oscillatory energy at 323 watts/in.^{2} is applied to the crystal.

During these later investigations, Langenecker observed that no changes appeared in the physical properties of the metals after the application of oscillatory energy, provided low amplitude oscillatory stress waves were applied. If, however, oscillatory stress waves were applied having amplitudes exceeding a critical value, this value being dependent on the metal, permanent changes in the physical properties, particularly in strength, ocurred. For example Langenecker noted that the shear stress of single crystals of zinc and aluminium was increased by up to five and three times respectively, while the ductility remained unaffected, when the crystals were subjected to oscillatory energy exceeding the critical value.

During the period 1957 to 1961, Fitzgerald (10,11,12), developed a device in which specimens were clamped in compression and subjected to a sinusoidally varying shear

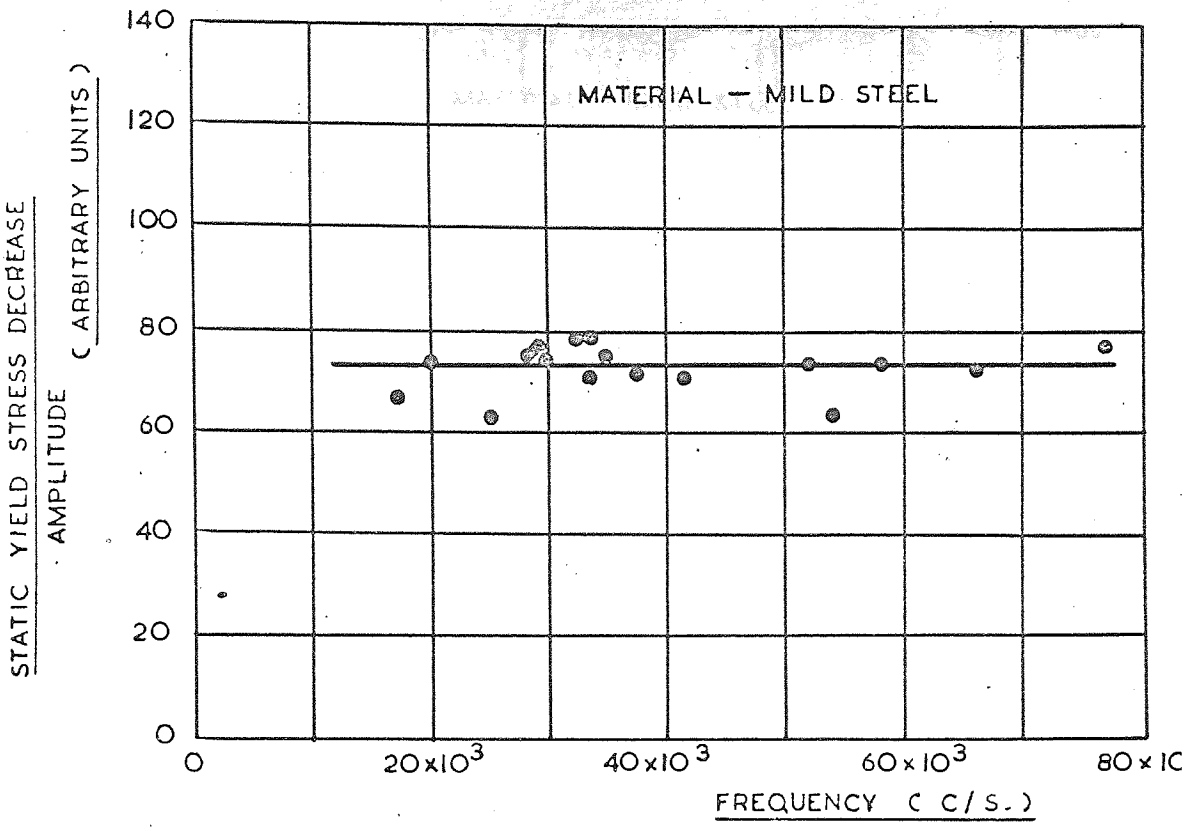

FIG. NO. 3 FREQUENCY OF VIBRATION PLOTTED AGAINST THE STATIC YIELD STRESS DECREASE AT ROOM TEMPERATURE

(NEVILL AND BROTZEN. 1957)

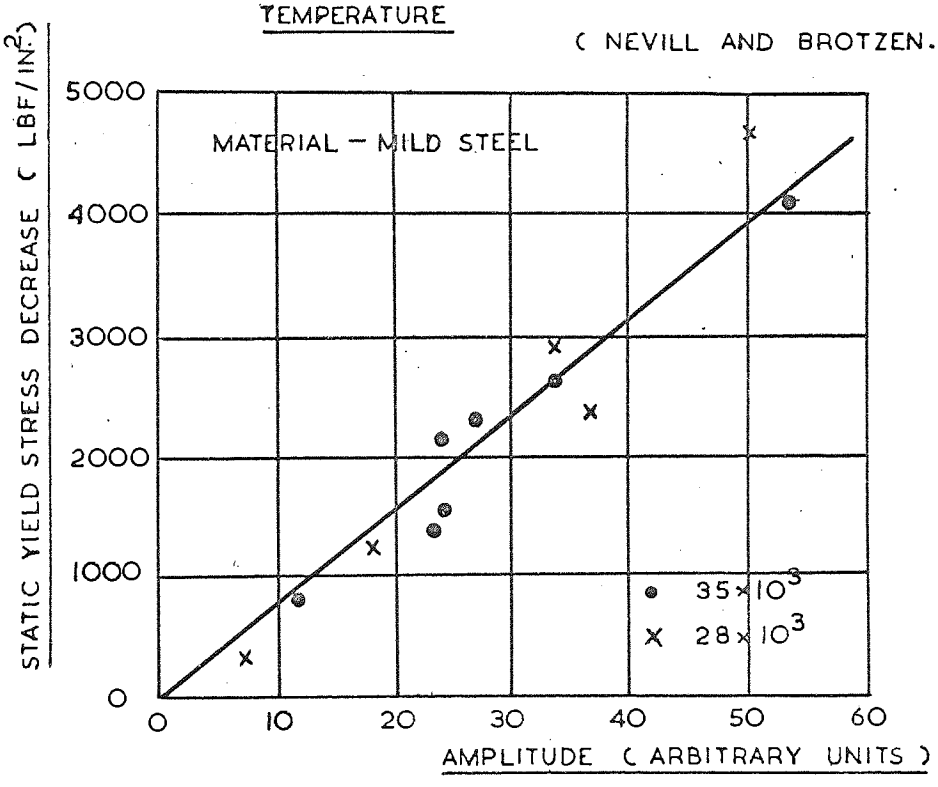

FIG. NO. 4 AMPLITUDE OF VIBRATION PLOTTED AGAINST THE STATIC YIELD STRESS DECREASE AT ROOM TEMPERATURE

(NEVILL AND BROTZEN. 1957)

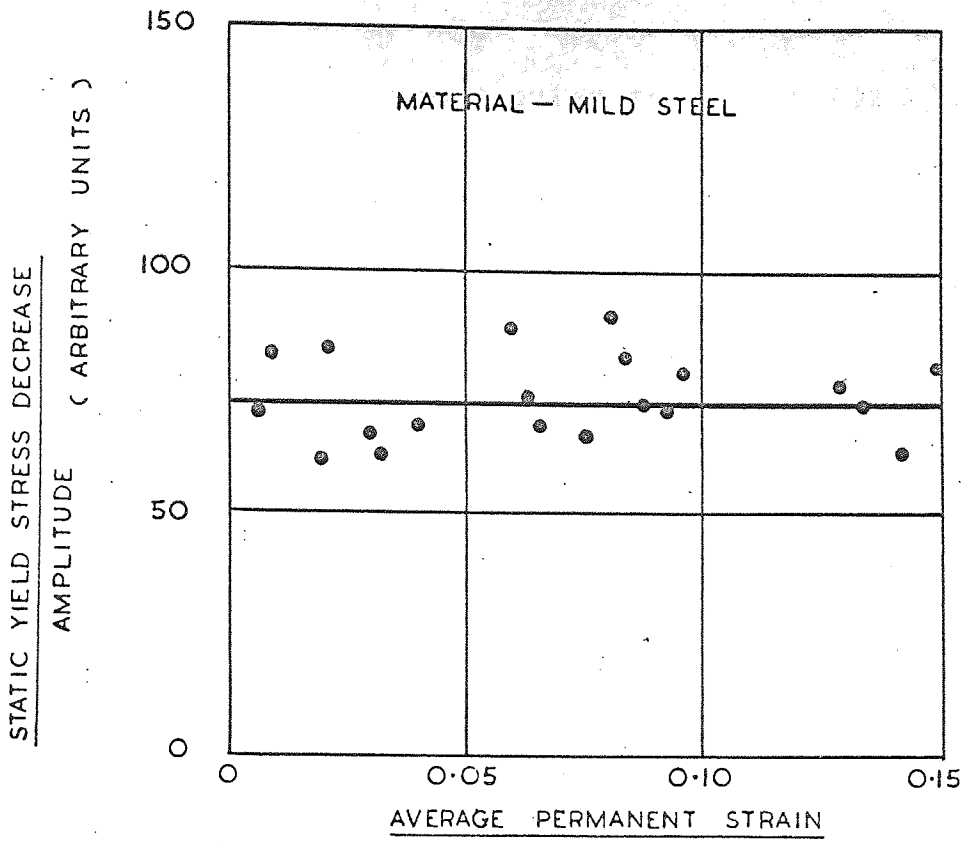

FIG. NO. 5 AVERAGE PERMANENT STRAIN PLOTTED AGAINST THE STATIC YIELD DECREASE DUE TO VIBRATION AT ROOM TEMPERATURE AND FREQUENCY 20×10^3 C/S.

(NEVILL AND BROTZEN. 1957)

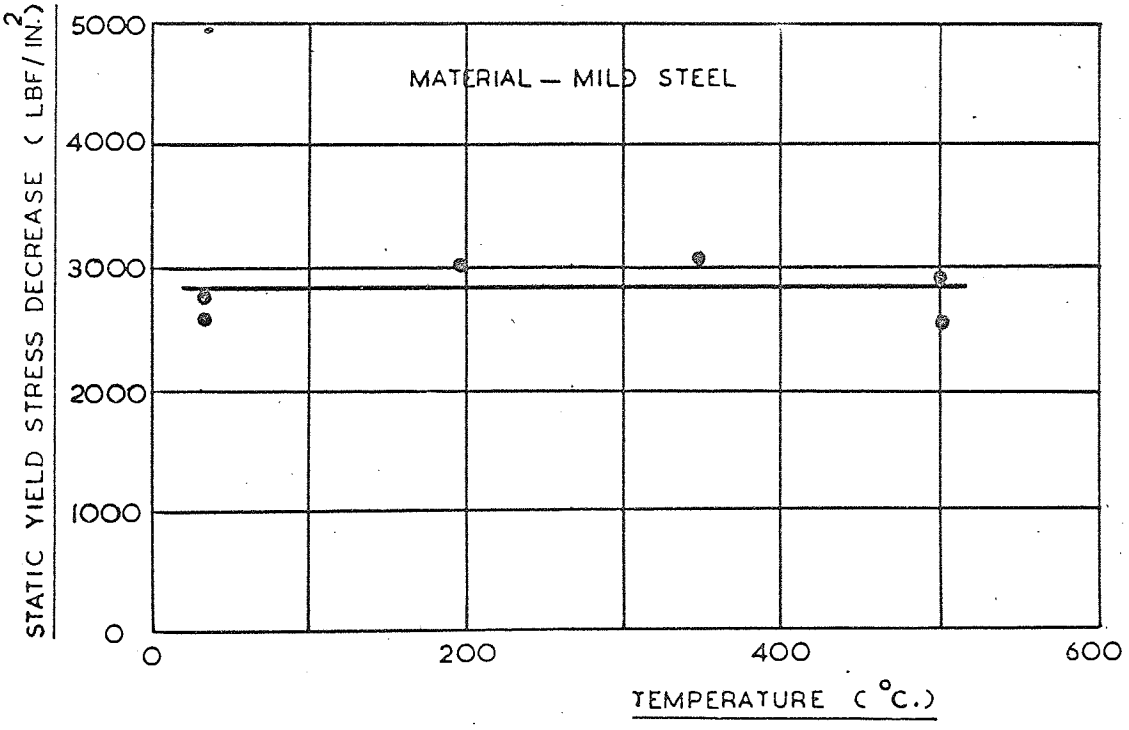

FIG. NO. 6 TEMPERATURE PLOTTED AGAINST THE STATIC YIELD STRESS DECREASE DUE TO VIBRATION AT CONSTANT AMPLITUDE AND FREQUENCY 20×10^3 C/S.

(NEVILL AND BROTZEN. 1957)

stress in a direction perpendicular to the static clamping stress. Specimens of aluminium, zinc, and platinum were tested at frequencies of vibration in the range 100 to 500 c/s. Under oscillatory stress conditions, Fitzgerald observed shear strains much higher than those which had been recorded under static conditions. He concluded that this was due to a reduction in shear stress required to cause plastic deformation. Thus Fitzgerald's experiments provided independent confirmation of Langenecker's findings.

In 1957, Nevill and Brotzen (13), further confirmed the work of Langenecker and Fitzgerald by tensile testing low carbon steel wire with a superimposed oscillatory stress. They summarised their work by stating that :-

(1) In the frequency range 15×10^3 to 80×10^3 c/s., the decrease in stress necessary to initiate yielding was independent of the frequency of vibrations (Fig. No.3)

(2) The observed reduction in stress was directly proportional to the amplitude of vibration (Fig. No.4)

(3) The decrease in stress was independent of the prior strain for values of average permanent elongation up to 15 per cent (Fig. No.5) and

(4) In the temperature range 30 to 500 degrees Celsius the yield stress reduction was independent of temperature (Fig. No.6)

Other investigators, Siegel 1959 (14), Oelschlagel 1962 (15), and Severdenko and Klubovich 1964 (16), have noted the phenomenon of reduction in the steady stress required to initiate yielding from tests on coil springs of copper wire and single crystals of zinc at frequencies of 0.8×10^6 c/s. and copper wire at a frequency of 23×10^3 c/s.

Meleka and Harris in 1962 (17), described tensile tests on pure zinc with superimposed oscillatory stresses at a frequency of 20 c/s. They observed that under the influence of the added cyclic stress, the specimen could withstand strains more than 100 per cent greater than those possible with non-cyclic straining. They further observed that this increase in strain to fracture was independent of the initial strain and proportional to the stress amplitude. Meleka summarised his work by stating that the application of an oscillatory stress has the same effect as a rise in temperature, thus confirming the findings of Langenecker, Nevill and Brotzen, and Fitzgerald.

2.3. The Mechanism Underlying the Observed Reduction in Yield Stress.

The mechanism underlying the observed reduction in yield stress was first considered by Blaha and Langenecker (4). They believed that the reduction was due to an interaction between oscillatory stress waves and dislocations such that the stress required for deformation was reduced. Nevill and

Brotzen (13), expounded these comments by stating that the strength of a given metal depended primarily on obstacles to the movement of dislocations and hence any reduction in yield stress would have to involve some mechanism by which these obstacles could be overcome. Meleka and Harris (17), endorsed these comments and concluded further that the application of a cyclic stress supplied the energy to impart dynamic mobility to the dislocations, thus enabling them to overcome obstacles not readily surmounted by a static stress alone. Langenecker et al. (4,5,6,7) and Oelschlagel (15), provided experimental and theoretical data to substantiate these concepts of energy absorption, but they were unable to reach any conclusion on the mode in which the dislocations absorbed the energy.

Nevill and Brotzen considered three mechanisms by which dislocations might absorb oscillatory energy and overcome obstacles namely, resonance, relaxtion and hysteresis. However, they were unable to obtain correlation between their experimental findings and these theories. They concluded their work by attributing the phenomenon of reduced yield stress to a mechanism of a superposition of steady and alternating stresses. This mechanism for reduced yield stress was generally accepted, but Langenecker, showed that this interpretation failed in some cases. For example Langenecker stated that the theory did not account for the 100 per cent reduction in yield stress in zinc,

aluminium, stainless steel, beryllium and tungsten, which he had observed at room temperature when these metals were exposed to oscillatory energy at a frequency of vibration of 20×10^3 c/s. Langenecker explained large stress reductions by stating that defects in a metal, such as dislocations and grain boundaries, absorb sufficient energy through inelastic scattering of the oscillatory stress waves that the scattered atoms approach melting temperature. Within milliseconds, the temperature of these atoms is raised and the stress required to cause their mobility suddenly decreases. Thus the metals can yield under the influence of oscillatory stresses having magnitudes much lower than the yield stress at room temperature but comparable to the yield stress at elevated temperatures. He summarised his remarks by likening the absorption of energy to that of a temperature rise and concluded that since oscillatory energy was absorbed preferentially at dislocation sites and thermal energy was absorbed by all atoms, the application of oscillatory energy was a more effective method of reducing the stress necessary to cause plastic elongation of a metal. Langenecker demonstrated this concept when he showed that the yield stress of aluminium could be reduced to zero either by a given thermal energy or by 32 per cent less oscillatory energy.

2.4. The Effect of Oscillatory Energy on Friction Forces.

It was outlined on page 1 that workers at Aeroprojects Incorporated (USA)(2), noted that oscillatory energy could substantially reduce frictional forces. They observed that oscillatory activation could reduce the sliding friction between a plastic sheet and a steel surface to about one-seventh of its non-oscillatory value. They also noted that vibration effectively reduced friction forces between two contact surfaces when they inserted a stepped mandrel in a tube and where the clearance between the mandrel and the inside of the tube was progressively decreased to zero. They further observed that the scoring of the mating surfaces was minimised.

In 1959, Boborykin (19), investigated frictional conditions between the workpiece and tool when forming sheet steel specimens round a former using a vibrating tool at a frequency in the range 16 to 22 c/s. He noted that the coefficient of friction between tool and workpiece was reduced significantly, approaching the value for a highly polished, lubricated surface. Also in 1959, Fridman and Levesque (20), carried out a series of experiments designed to study the effect of vibration on the coefficient of friction between metallic surfaces. Their experiments consisted of measuring the force required to slide a steel block down an inclined plane which was being subjected to a vibration perpendicular to the block movement. They showed

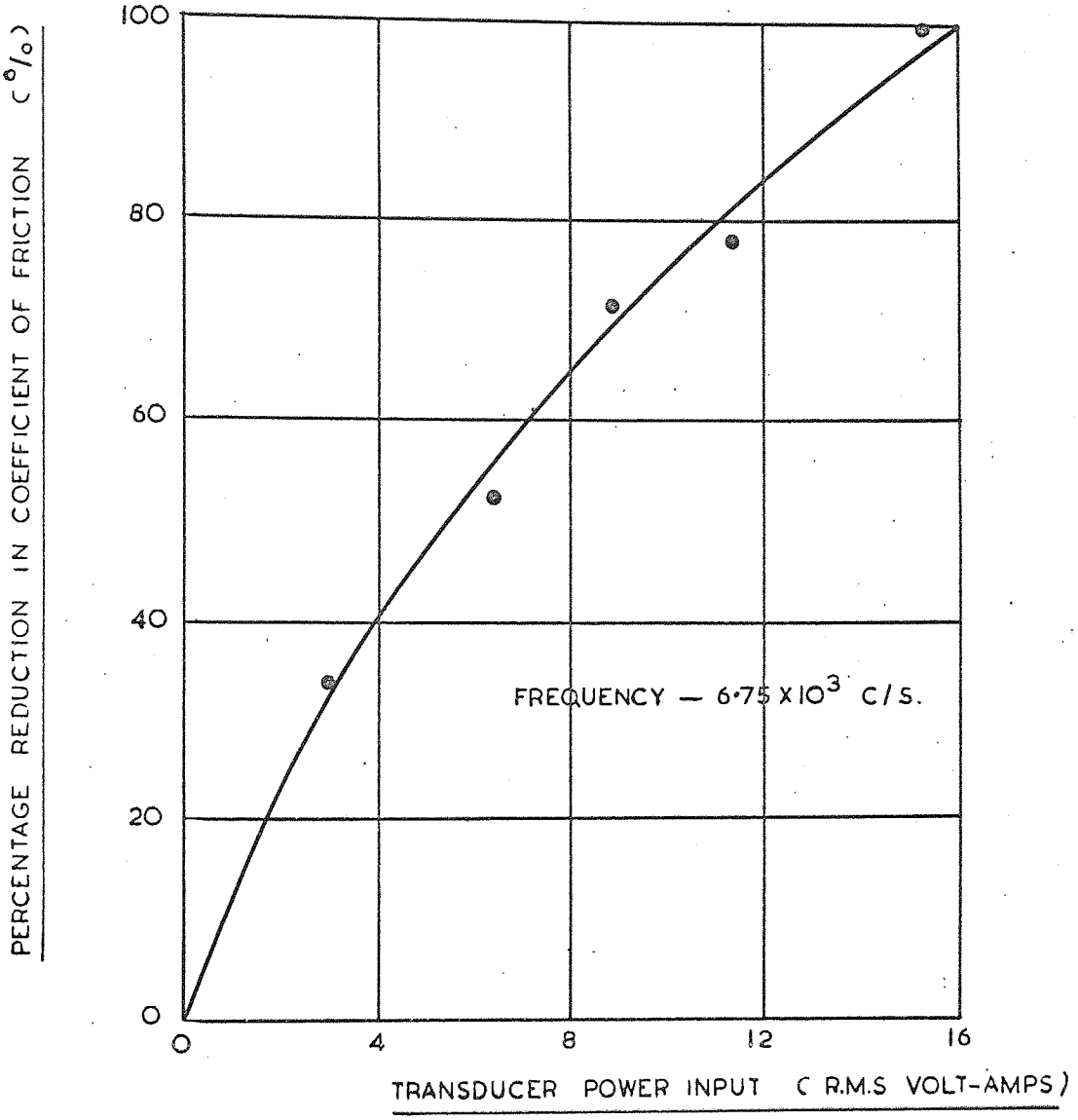

FIG. NO. 7

PERCENTAGE REDUCTION IN COEFFICIENT OF FRICTION PLOTTED AGAINST TRANSDUCER POWER INPUT.

(FRIDMAN AND LEVESQUE. 1959)

that the coefficient of friction could be reduced almost to zero as a result of vibrations at frequencies in the range 6×10^3 to 42×10^3 c/s.

Fig. No.7 plots the results obtained by Fridman and Levesque. The percentage reduction in the coefficient of friction was drawn against the power input to the vibratory transducer for a highly polished steel surface subjected to vibration at a frequency of 41×10^3 c/s. The curve shows: (a) that the higher the transducer power input, the greater the reduction in coefficient of friction and (b) for a transducer input of 16 volt-amperes the coefficient of friction can be reduced by 100 per cent.

Fridman and Levesque attempted to explain the mechanism of frictional forces as follows : They described the contact area between two metallic surfaces as being made of a number of very small welds formed as a result of the load between the surfaces and the 'plasticity' of the surface asperities. When one surface moves relative to the other then these minute welds must be sheared, therefore a force dependent on the strength of such welded junctions must be exerted to start the motion of the surfaces relative to each other. They concluded that when a vibration was set up between two such surfaces, the welded junctions break because of the force exerted on them by the acceleration

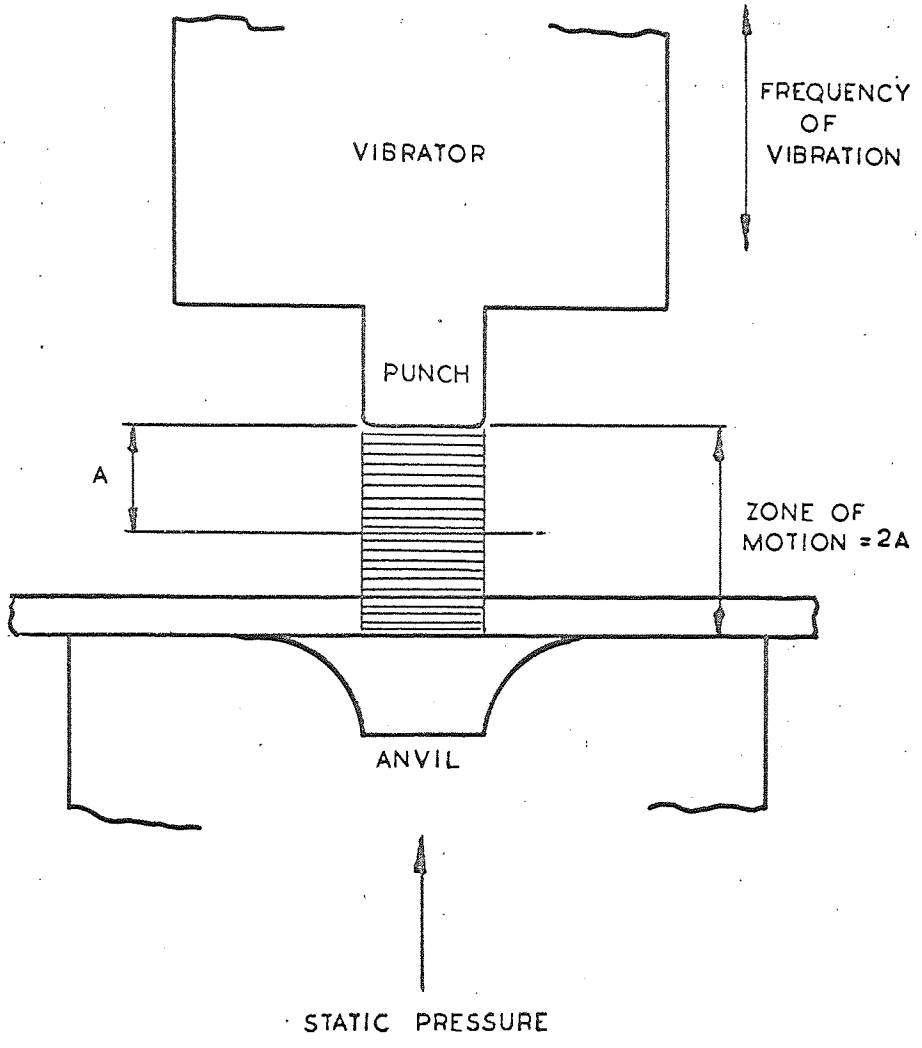

FIG. NO. 8 DIAGRAM ILLUSTRATING THE 'ZONE OF MOTION'

(BALMOUTH . 1961)

of the wave form amplitude. The horizontal force required to make the block slide therefore, depends on the normal force exerted on each welded junction which will be determined by the amplitude and acceleration of the wave form.

Balamuth, 1961(21), also considered the mechanism of reduced friction forces when describing the design of an oscillatory press. He stated that while a workpiece is in the zone of motion (Fig. No.8), the working surfaces are in contact for only a fraction of each cycle of vibration. He concluded that this contact time was often less than one-twentieth of the period time and so friction forces were very small.

Balamuth demonstrated this effect by placing a sheet metal specimen between two metal platens, one of which was the output face of an oscillator, and pressed the two surfaces tightly together so that it was impossible to move the specimen horizontally between them. He then showed that when the vibration was switched on, only a very small pressure was required to slide the metal strip horizontally between the platens, even though a large static force was still pressing the platens against the specimen.

2.5. The Application of Oscillatory Energy to Metal Working Processes.

It will be clear from the four previous sections, that the benefits to be gained by applying oscillatory energy to a metal undergoing plastic deformation are numerous. As a result of these investigations, the phenomena of reduction in friction between the workpiece and tool and the reduction in stress required to initiate yielding have been harnessed in a number of metal deformation processes. The remainder of this chapter outlines the historical and technical development of oscillatory stress techniques to forging, rolling, coining, extruding, dimpling and stretch forming, and drawing, culminating in a section discussing the implications of these findings to the metal working industries.

2.5.1. Forging.

In 1958, Shestakov and Kornov (22), published a paper on the results of work on aluminium and steel, forged, with and without the application of oscillatory loads. Tests were performed on a specially constructed 'vibro-press'. This press, similar to a conventional hydraulic press, incorporated a mechanical vibrator which enabled an oscillatory stress to be superimposed on the steady stress during the forging operation. A frequency of vibration of 21 c/s., was used with amplitudes up to 1.0 in. Shestakov concluded that the variation of hardness, the distortion

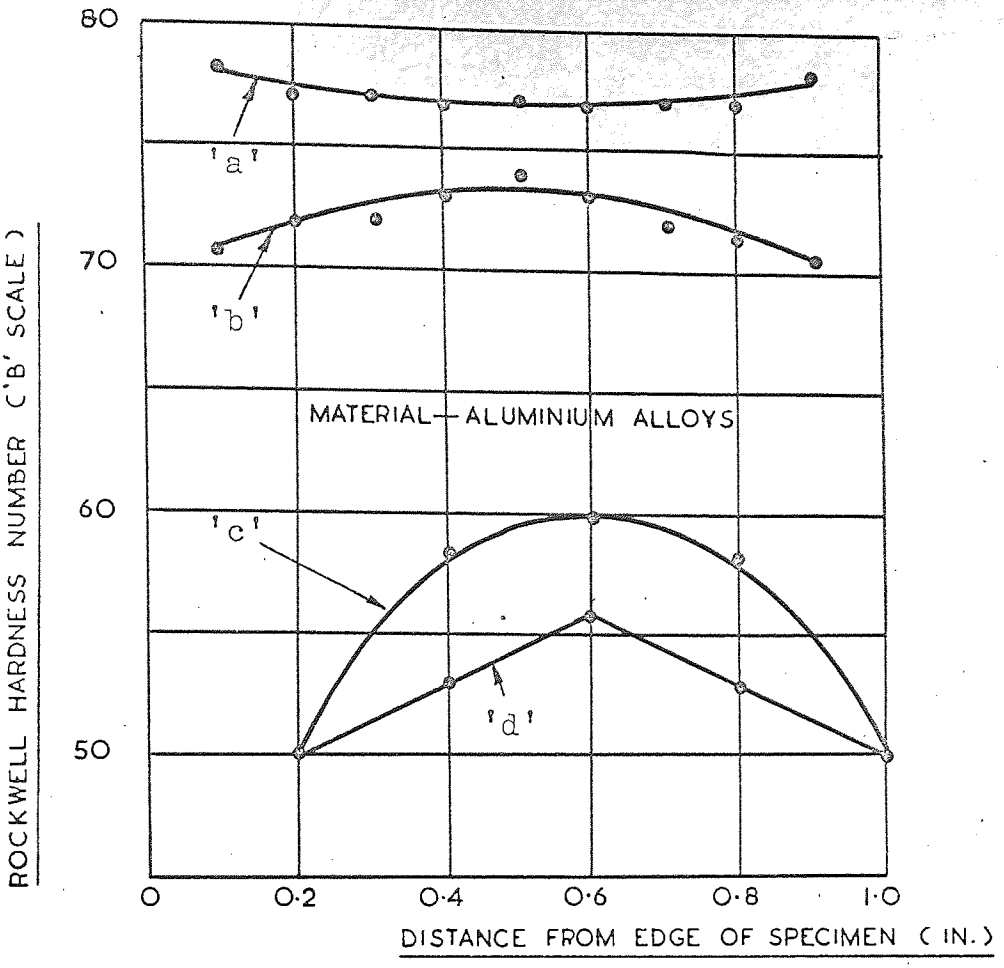

FIG. NO. 9 VARIATION OF HARDNESS ACROSS END FACE OF FORGED SPECIMENS

(SOGRISHIN. 1959.)

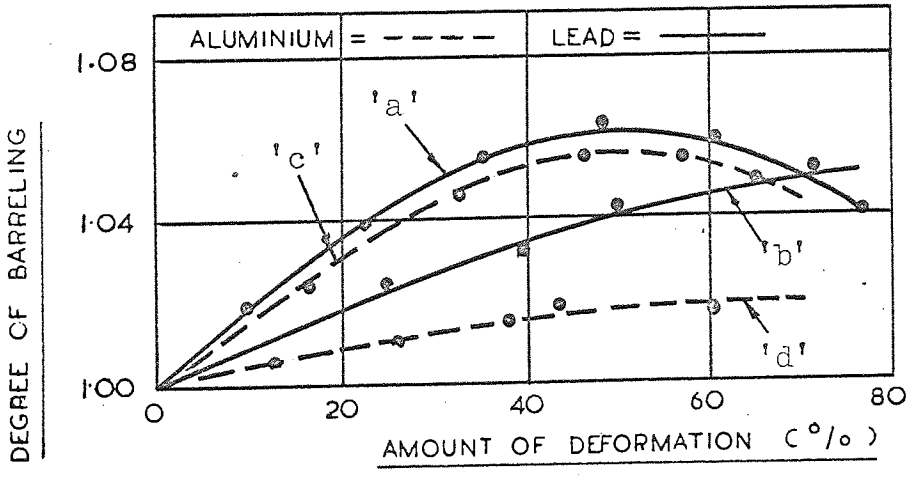

FIG. NO. 10 DEGREE OF BARRELING PLOTTED AGAINST AMOUNT OF DEFORMATION

(SOGRISHIN. 1959.)

of the structure, and the deformation loads were least when vibration was applied. All these effects were attributed to a reduction in friction. Sogrishin, 1959 (23), and Kornov and Shestakov, 1959 (24), obtained similar results when 'vibro-forging' specimens of aluminium and lead using frequencies in the range 16 to 37 c/s, and amplitudes of vibration up to 0.4 in.

Results obtained by Sogrishin are shown graphically in Fig. No.9 and 10. Fig. No.9, plots the variation of hardness across the end faces of two different aluminium alloy specimens, and Fig. No.10 shows the degree of barrelling plotted against the amount of deformation for specimens of aluminium and lead. In both figures curves 'a' and 'c' were obtained under non-oscillatory conditions and curves 'b' and 'd' under oscillatory conditions.

In 1959, Lysak and Sogrishin (25), performed similar forging tests on cylindrical specimens of aluminium to investigate the effects of vibrational loading on residual stresses. They concluded that for a frequency of vibration in the range 24 to 37 c/s., the magnitude of residual stress was smaller than that for non-oscillatory forging; also that the magnitude of the residual stress was dependent upon the amplitude and duration of the vibration.

Kornov and Voronin (26), published a paper in

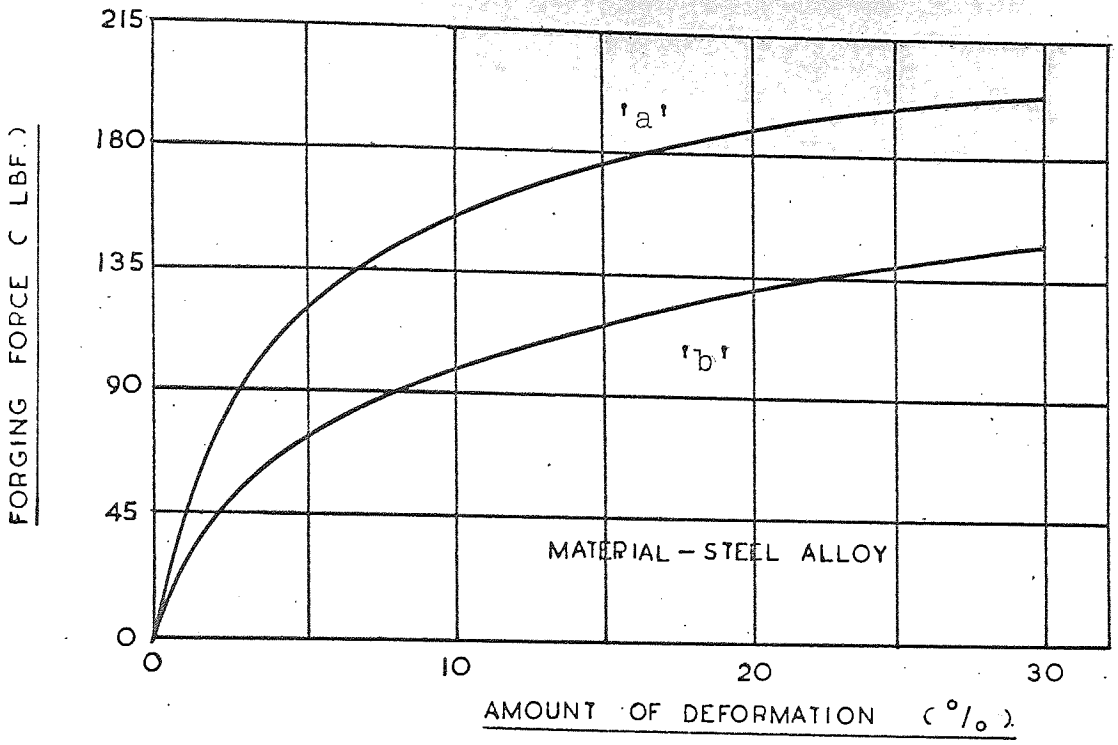

FIG. NO. 11 FORGING FORCE PLOTTED AGAINST AMOUNT OF DEFORMATION

(KARNOV 1961.)

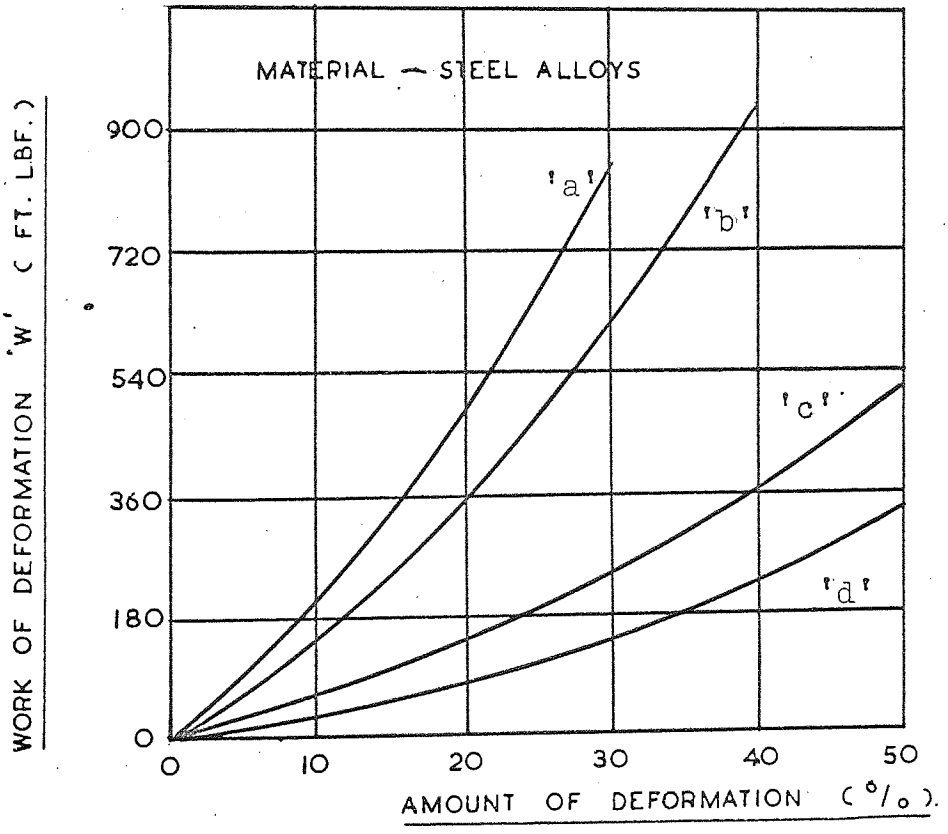

FIG. NO. 12 WORK OF DEFORMATION PLOTTED AGAINST AMOUNT OF DEFORMATION

(KARNOV 1961.)

1960 on upsetting tests on steel and aluminium alloys, both cold and hot, with and without vibration, in which they studied 'plasticity', hardness and other mechanical properties. They observed that oscillatory loads applied at 21 c/s., resulted in, (i) a more uniform deformation of the metal, (ii) a reduction in friction of up to 60 per cent, (iii) an increased elongation of up to 40 per cent and (iv) a reduction in the force required to perform the deformation of as much as 50 per cent. The precision and surface finish of the forged parts was also improved. Kornov, 1961 (27), obtained similar results when upsetting aluminium and steel specimens using frequencies of vibration up to 17 c/s. In 1961, Kornov (28), also attempted to determine the work of deformation under conditions of vibrational loading during forging. He concluded that the force of deformation 'P' could be represented as a power function,

$$\text{ie.} \quad P = A.(dh.)^n$$

hence giving the work of deformation 'W' equal to,

$$W = \frac{(dh.)^{n+1}}{n+1} .A.$$

Where 'A' and 'n' are constants and dh. represents the reduction in height.

Figs. No.11 and 12, plot the results obtained by Kornov. Fig. No.11, shows the relationship between the forging force and the amount of deformation

under non-oscillatory, curve 'a', and oscillatory, curve 'b', conditions. Fig. No. 12 shows the work of deformation 'W', plotted against the amount of deformation during the forging of two different steel alloy specimens. Curves 'a' and 'c' represent non-oscillatory forging, and curves 'b' and 'd' oscillatory forging.

Fleischhacker, 1961 (29), reported on forging tests carried out on aluminium at frequencies of vibration of 120 and 180 c/s. He observed that the application of an oscillatory stress promoted the flow of the test piece at 120 c/s, but that at 180 c/s., no benefit to plastic flow was to be gained. No explanation was given for the 180 c/s. results and hence these tests must be regarded with some doubt in view of the findings of all other investigators.

Severdenko and Klubovich, 1961 (30), and 1965 (31), published results on upsetting tests carried out on aluminium and copper cylinders with superimposed oscillatory loads at frequencies of vibration of 23.5×10^3, and 23.0×10^3 c/s. respectively. They noted that, under the action of an oscillatory stress, the load to cause deformation could be reduced by 50 to 60 per cent. In addition, their experiments showed that these high frequency vibrations also reduced the 'barrelling' effect by 30 to 40 per cent.

2.5.2. Rolling.

A paper by Rosenfield 1963, (3), in a symposium held in the same year on the effect of the application of oscillatory energy to metal working processes, reported on rolling tests performed on narrow strip aluminium, steel and commercially pure copper. A transducer was developed which, when incorporated inside the rolls applied a radial mode of vibration at an unspecified frequency in the ultrasonic range. It was observed that, under the action of the oscillatory loading, the roll separating force was reduced significantly and larger reductions in thickness per pass were possible.e.g. 230 to 530 per cent more. Similar results were obtained when rolling zinc wire.

2.5.3. Coining.

In 1961, Kobayashi, Bocharov and Thomson (32), published results on coining tests performed on pure lead and aluminium, with and without the application of oscillatory energy. Experiments were performed on a 40 tonf. hydraulic press which had provision for superimposing an oscillatory load, at 130 c/s. on the static press load. In the absence of a lubricant it was observed that, with applied vibrational energy, the deformation pressure was reduced by 35 per cent when coining lead specimens, and 7 per cent when coining aluminium. The smaller effect on aluminium was attributed to the fact that the amplitude of the superimposed vibratory stress was small compared with the higher

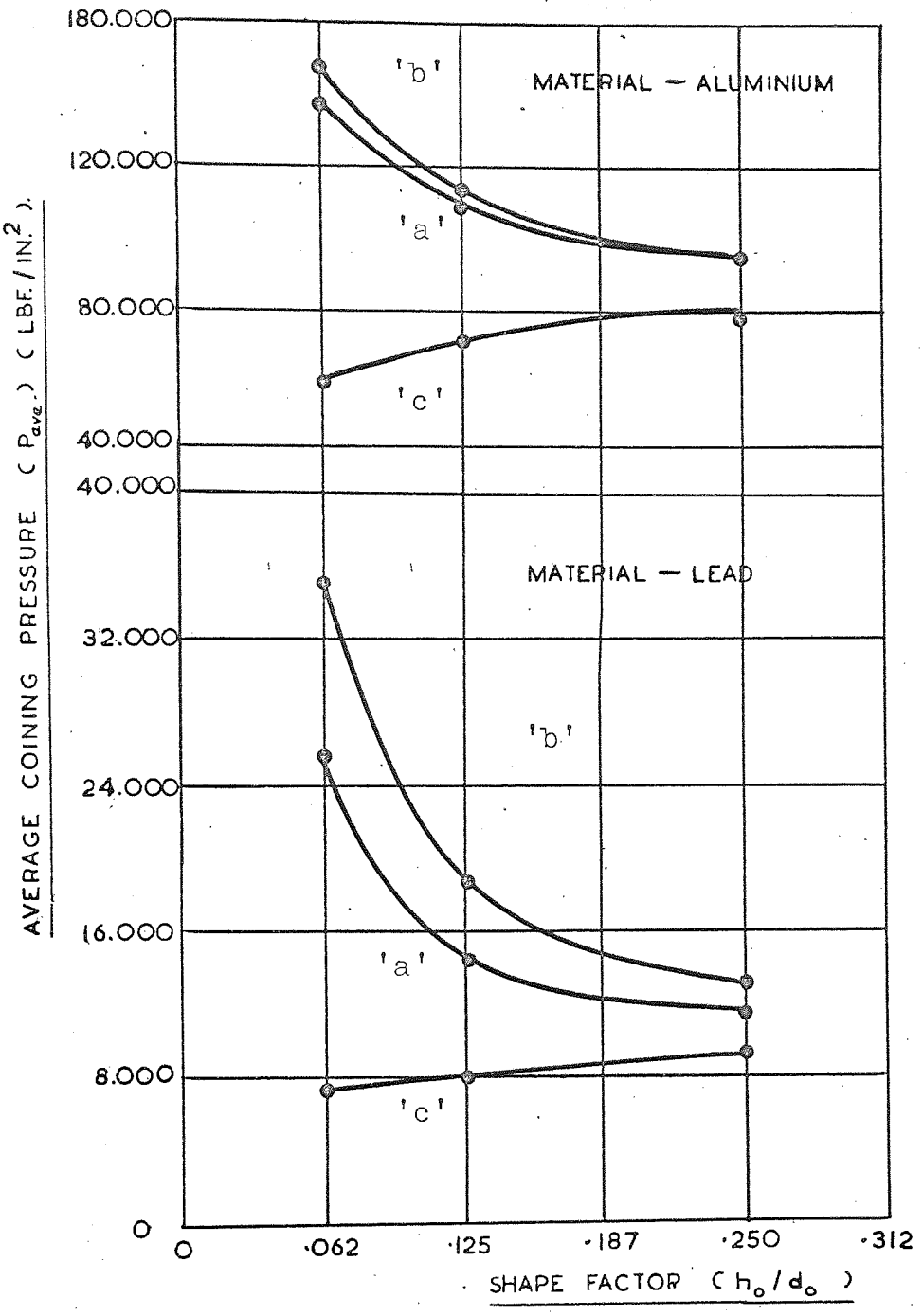

FIG. NO. 13 AVERAGE COINING PRESSURE PLOTTED AGAINST SHAPE FACTOR (KOBAYASHI ET. AL. 1962).

coining stress. When a lubricant was employed, it was observed that the non-oscillatory coining pressure was lower than that required for unlubricated specimens coined with a superimposed oscillatory stress. Furthermore, it was noted that for lubricated specimens the application of oscillatory loading had no effect on the coining pressure. From these findings Kobayashi et al. concluded that the effect of applying an oscillatory stress was to reduce the contact friction.

Fig. No. 13 shows graphically the relationship between the average coining pressure, P_{ave} and the shape factor (h_o/d_o) as obtained by Kobayashi et.al. (h_o/d_o = ratio of initial height to initial diameter of specimen). Curves marked 'a', refer to unlubricated coining with a superimposed oscillatory load. Curves marked 'b', refer to non-oscillatory unlubricated coining and curves marked 'c' refer to both oscillatory and non-oscillatory, lubricated coining.

2.5.4. Extruding.

Jones and Maropis (33), 1959, described extrusion tests performed on lead and aluminium tubes, hot and cold, with and without the application of oscillatory stresses. A 15 tonf. laboratory press which had provision for vibrating the die, ram and container in the direction of extrusion at 20×10^3 c/s. was used in the experiment. It was observed

that, for the same rate of extrusion, the press force was reduced by 15 to 30 per cent under oscillatory conditions; and similarly for a constant extrusion force the rate was increased by 150 to 300 per cent. The maximum effect from oscillatory loading ocurred when the container was vibrated. Similar results and improved surface finish have been observed by Tarpley, Yocom and Pheasant (34), 1961, when cold extruding and pressing ceramic pellets.

2.4.5 Dimpling, Deep Drawing and Stretch Forming.

Peacock 1961 (35), described dimpling tests performed on aluminium and titanium alloys, with and without superimposed oscillatory stresses. Vibrations were applied to the die in the direction of dimpling at 14×10^{3} c/s. with an amplitude of 0.8×10^{-3} in. It was observed that dimples formed at room temperature, under oscillatory conditions, were comparable with those formed with heated dies under non-oscillatory conditions.

Langenecker, Fountain and Jones 1964 (36), reported on cup forming tests performed on copper, with and without the application of oscillatory energy. Cups were formed by oscillating the punch in the direction of forming at an unspecified frequency in the megacycle range. It was observed that the 200 lbf. forming force required under non-oscillatory conditions could be reduced to 70 lbf. when an oscillatory stress was applied. It was also observed that a greater depth of cup was obtained under

vibrational conditions and that this depth was dependent on the magnitude of the vibrational energy employed. Similar results were reported by Rosenfield 1963 (3), when performing deep drawing tests on aluminium alloys.

2.6. The Application of Oscillatory Stresses to Wire and Tube Drawing.

In 1961, Tarpley and Kartluke (37), reported on a preliminary investigation into the application of oscillatory stresses to the drawing of niobium, Zircaloy-2 and copper tubes. They observed that, when drawing with a longitudinal oscillation of the die of 20 x 10^3 c/s. the speed of drawing was increased 13 times for copper and 100 times for Zircaloy -2. They observed further that the load on the die was reduced by 40 to 80 per cent when drawing copper and 15 per cent when drawing niobium. Metallographic and metallurgical examination of the finished tubes drawn, with and without superimposed vibration, showed no quantitative difference in surface finish and no difference in mechanical properties.

Following the work of Tarpley, Boyd and Maropis (3), reported on multi-pass drawing tests carried out on very thin tin wire. They observed that the drawing tension could be reduced by one half to two thirds when the die was oscillated parallel to the axis of drawing. They further noted that, for a given power input to the oscillatory transducer, the reduction in drawing tension became

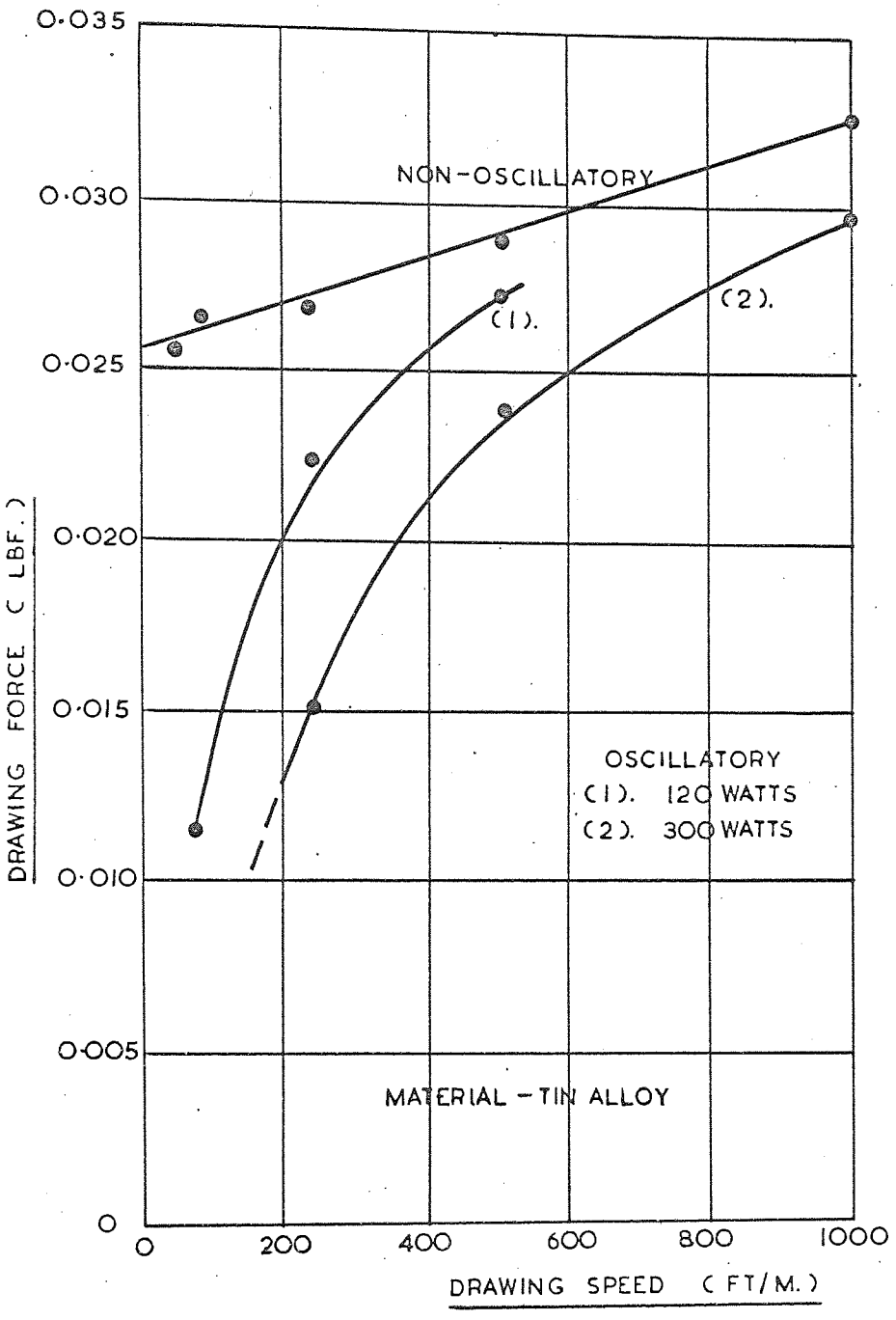

FIG. NO. 14 DRAWING FORCE PLOTTED AGAINST DRAWING SPEED

(BOYD AND MAROPIS. 1963.)

progressively smaller as the drawing speed was increased. Graphical representation of this observation is shown in Fig. No. 14.

In 1963, Mainwaring (3), reported on plug drawing tests performed on aluminium tubes, with and without applied oscillatory energy. He showed that, with a superimposed longitudinal oscillatory stress of 20 x 10^3 c/s., the tubes could be reduced by 50 per cent in two successive draws. The reductions were achieved at a drawing speed of 125 ft/m., and the tubes decreased in size from 0.61 in. outside diameter and 0.0378 in. wall thickness, down to 0.336 in. outside diameter and 0.018 in. wall thickness. Under non-oscillatory conditions it required three draws to obtain this overall reduction in area. During these tests Mainwaring also showed that oscillatory energy improved the surface finish of the material, particularly on the inside of the tube.

In 1963, Severdenko and Klubovich (38), described drawing tests on copper wire, with and without the application of oscillatory stresses. Experiments were performed at a drawing speed of 1.67 ft/m. and a reduction in area of 35 per cent. They observed that with a longitudinal oscillation of the die of 20 x 10^3 c/s., the drawing load was reduced by 50 per cent.

In 1963, Robinson (39), at the U.S. Naval Ordnance Test Station commenced a programme of work designed to

investigate the drawing of wire with ultrasonically activated dies. His initial tests, with a longitudinal die oscillation of 20 x 10^3 c/s., showed that when drawing iron wire with a reduction of area of 13 per cent and a drawing speed of 2.0 in./s., the drawing force could be reduced by up to 35 per cent. His results up to the summer 1966, have shown that the observed reduction in drawing load is dependent on the amplitude of die vibration and independent of the drawing speed in the range 0 to 500 ft./m., provided that the energy density (ie. the power input to the vibrating transducer per unit volume of material drawn), remains constant. In 1965, the Steel Company of Canada (40), confirmed the observed reduction in die load when drawing steel wire at a speed of 1.0 ft./m. through a longitudinally oscillated die at 22.4 x 10^3 c/s. However, unlike Robinson and Boyd, they were unable to detect any reduction in drawing load for drawing speeds greater than 1.28 ft./m.

In 1966, Nosal and Rymsha(41), published results on sinking tests made on steel tubes. They showed that the drawing force was reduced by 20-40 per cent when an oscillatory stress, of frequency 20 x 10^3 c/s. was superimposed on the normal drawing stress. They attributed these load reductions to a mechanism of reduced friction.

2.7. Implications to the Metal Working Industries.

It will have been noted from the previous sections that by applying oscillatory energy to the workpiece during a metal working process, (i) the forces on the tools are reduced, (ii) the metal flows more readily and (iii) the product quality is improved. The implications of these findings to the metal working industries can be summarised briefly as follows.

(1) Since the power required to perform the operation is reduced, then the capacity or the ability to deform difficult materials, of existing machinery will be extended.

(2) Where new plant is envisaged, smaller more compact machines may be purchased, eg. smaller rolling mills with fewer, lighter stands, smaller and lighter presses etc.

(3) The reduced loads may mean that greater reduction of area per pass will be achieved and therefore a component may be formed in, for example, two operations instead of three.

(4) The reduction in load may also indicate that the number of interstage anneals can be reduced.

(5) The reduction in frictional forces and smoother finished surfaces may mean that the life of tools and dies will be increased, and adverse effects such as galling, chatter and scoring may be minimised.

(6) Lubrication requirements may be less stringent and in some cases the need for a lubricant eliminated.

A list of patents involving the application of oscillatory energy techniques is given in Appendix No. 16.11.

3. Discussion of Published Work on Oscillatory Wire and Tube Drawing

3. Discussion of Published Work on Oscillatory Wire and Tube Drawing.

As a result of Tarpley's preliminary investigations, a number of research workers have reported on the application of oscillatory stresses to wire and tube drawing. All these investigators have oscillated the die in a longitudinal mode at frequencies of the order of 20×10^3 c/s. This chapter discusses these publications with particular reference to

(i) the difficulties experienced when applying oscillatory stress techniques.

(ii) theoretical considerations.

The first extensive study of oscillatory wire drawing was undertaken by Robinson et.al. in 1963. Their programme, sponsored by the U.S. Naval Ordnance Department, was designed to study the feasibility of applying oscillatory energy to the drawing of metals, and to study the effects of high frequency oscillatory stresses on the mechanism of plastic flow.

During their early tests, Robinson et.al. (39 and 42), frequently found that when drawing with superimposed oscillatory stresses, practically no oscillatory power was being delivered to the wire. Investigations showed that this was due to poor mounting of the die-transducer assembly and it was found that in order to gain

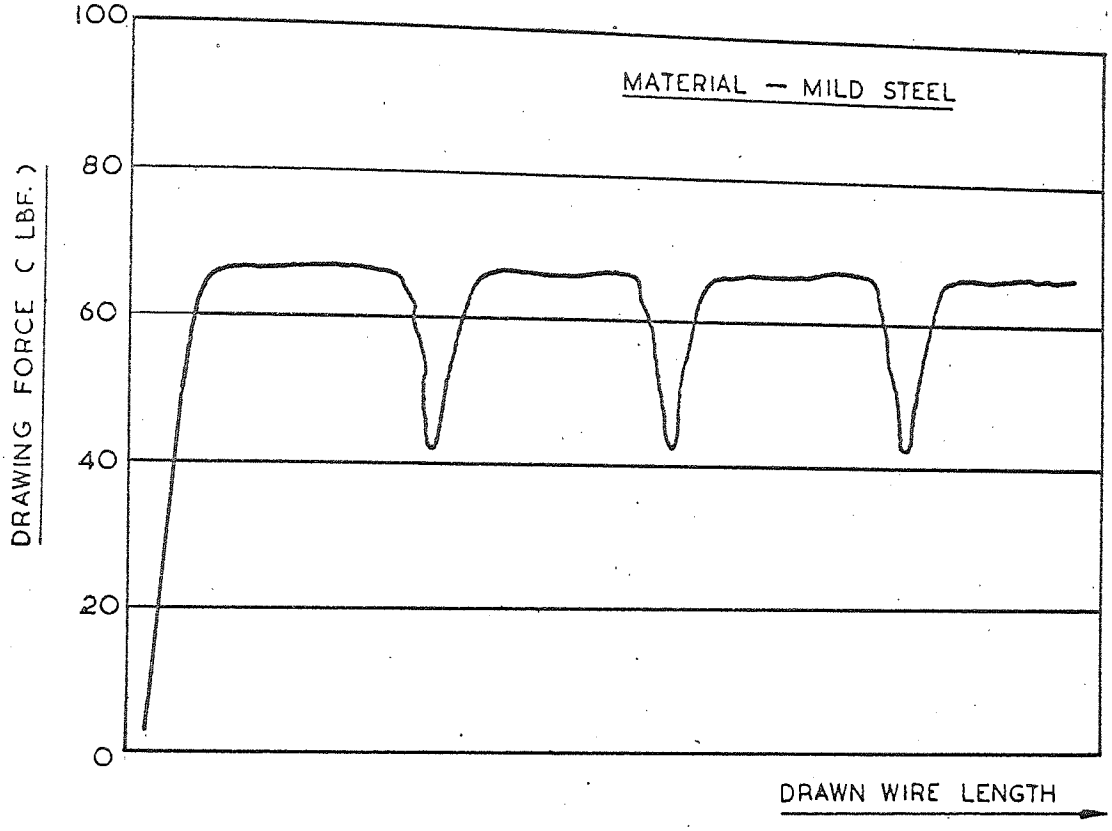

FIG. NO. 15 DRAWING FORCE VARIATION WITH DRAWN WIRE LENGTH

(ROBINSON ET. AL. 1963)

the maximum transference of energy from transducer to die, the assembly must be made very rigid. Also during these early tests, Robinson observed that the load-time curves showed periodic load fluctuations varying in amplitude from 30 to 50 per cent, when short lengths of wire were being drawn with superimposed oscillatory energy. Fig.No.15 shows this phenomenon with a load fluctuation of approximately 40 per cent. Further analysis of this problem revealed that only at the troughs of the force-time curve was the system operating at its intended resonant condition. At points in between these observed troughs the system resonance was lost and it was noted that there was very little oscillatory power going into the deformation zone. Robinson showed that the fluctuation of load had a constant period and could be related to the drawing speed. He found that the resonance of the system could be maintained only when the wire length between the die and the gripping jaws was equal to multiples of a certain distance. In order to eliminate the characteristic of varying length, an isolator system was designed which could be placed between the die and the gripping jaws. The isolator consisted of a drum round which the wire made a 360 degree loop. The effect of this isolator was to damp out the motion of the longitudinal waves transmitted from the die along the length of the wire. Robinson placed the isolator at different positions from the die and obtained an optimum

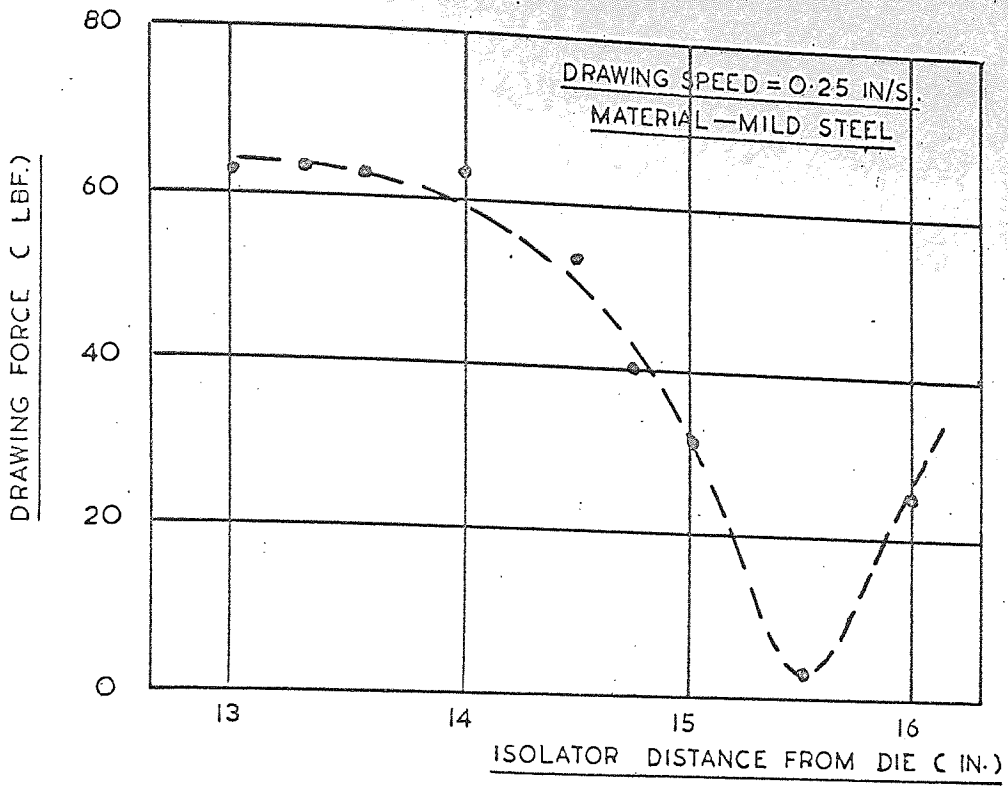

FIG.NO. 16 EFFECT OF POSITION OF ISOLATOR ON DRAWING FORCE

(ROBINSON ET. AL. 1963)

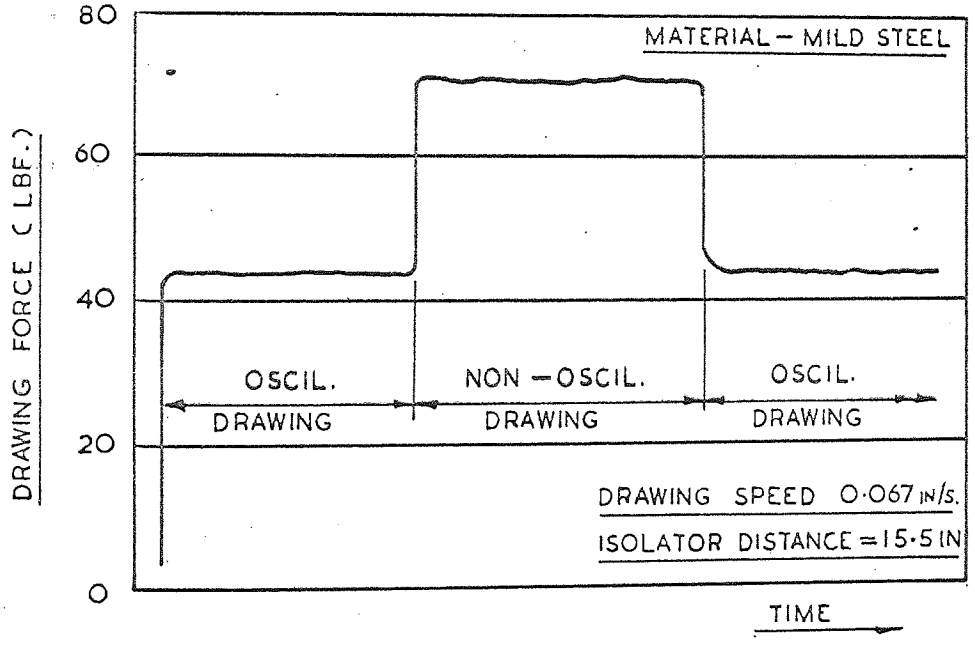

FIG.NO. 17 DRAWING FORCE WITH AND WITHOUT OSCILLATORY ENERGY

(ROBINSON ET. AL. 1963)

distance for drawing. The effect of isolator position relative to the die is shown in Fig. No.16. With the isolator located at an optimum position it was found that resonance could be maintained during continuous drawing, resulting in a force-time curve of constant amplitude similar to that shown in Fig. No. 17.

The phenomenon of critical length has also been observed by investigators at the Steel Company of Canada. During their tests they found that the distance between the die and the gripping jaws was a very important parameter, and that significant results could be obtained only when this distance had a certain value. They showed that the calculated half wave length of the magnetostrictive transducer was 4.625 in. and the measured critical die-to-gripping jaws distance was 4.25 in. They concluded that this critical point was in reality an antinodal point and that when the length of drawn wire was equal to this distance, or an integral number of half wave lengths, then resonant conditions prevailed.

Further experiments performed by Robinson et.al. again stressed the importance of optimum coupling between the workpiece and the transducer, and the need for precise location of the die with respect to the longitudinal stress waves. These later tests also showed that with the isolator in position a stationary wave was set up in the wire between the die and the gripping jaws. The

consequence of this was that in addition to the high oscillatory energy input to the die there was also localised energy absorption, resulting in heating at specified points along the length of the wire. These points of maximum heating corresponded to antinodal points of the stationary acoustic wave. Robinson showed that provided the wire was drawn sufficiently fast then this additional heat could be absorbed in the volume of the drawn wire. However, if the speed was reduced and the power input to the transducer high, then the temperature at localised points approached the melting temperatures of the metal being drawn, and the wire broke.

This local melting of the wire during oscillatory activation of the die, has also been experienced by Severdenko and Klubovich while drawing copper wire at a frequency of vibration of 23×10^3 c/s. They observed that oscillatory stress waves were propagated along the wire resulting in the wire becoming heated at the exit from the die. This heating ultimately caused breakage of the wire at a distance from the die equal to one-fourth of the wavelength. In order to attenuate these induced oscillations a movable isolator, similar to that developed by Robinson, was incorporated in their experimental apparatus. However, unlike Robinson, Severdenko and Klubovich calculated the position for the isolator on the basis of the following deliberations.

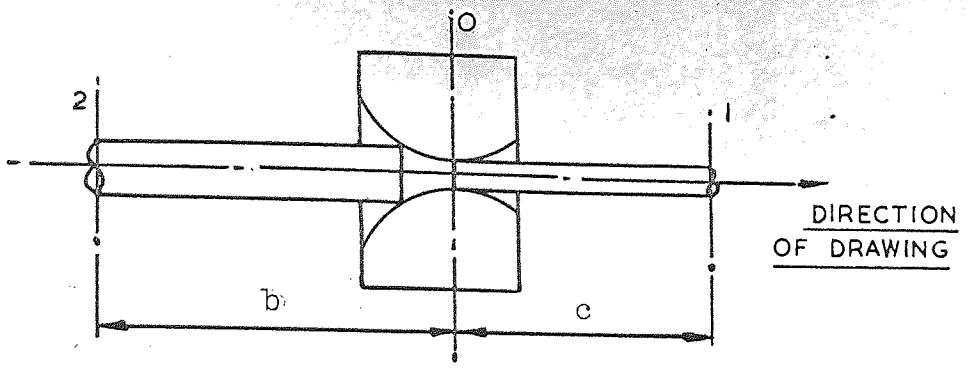

FIG. NO. 18 DIAGRAM OF DRAWING
(SEVERDENKO AND KLUBOVICH)

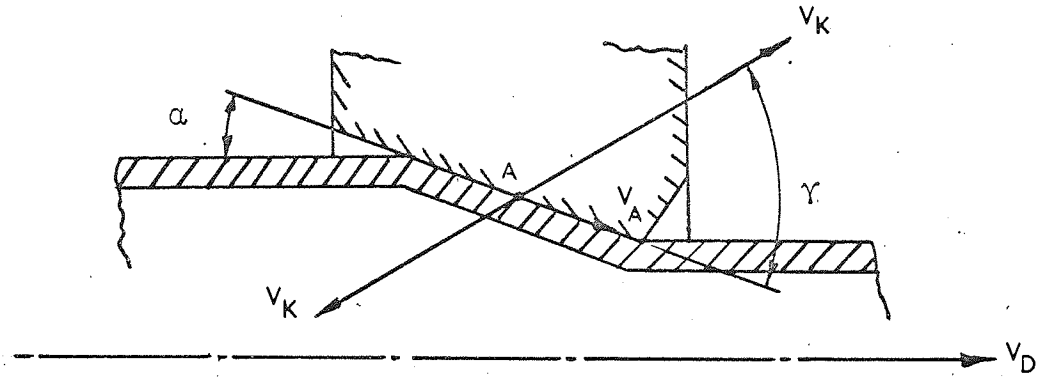

FIG. NO. 19 SECTION OF ZONE OF DEFORMATION
(NOSAL AND RYMSHA 1966)

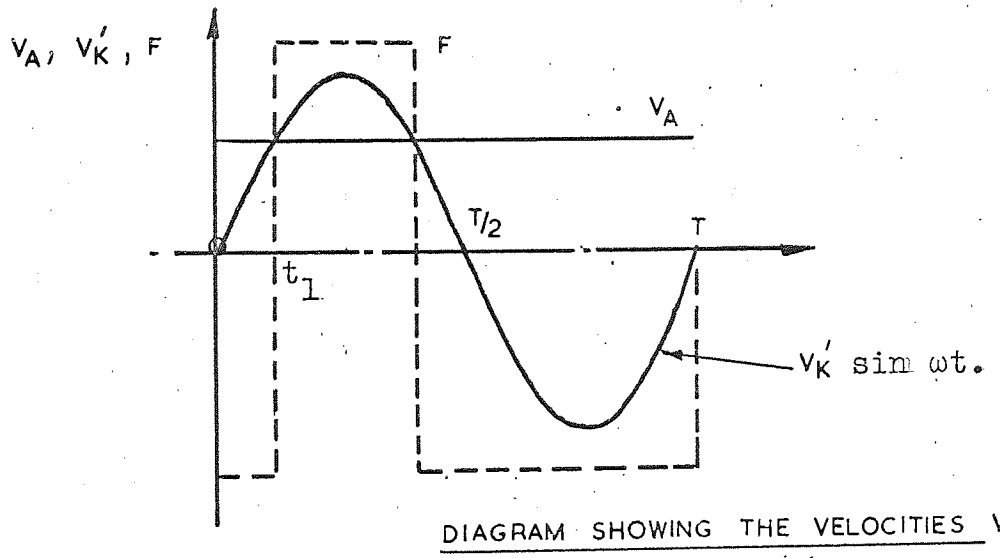

FIG. NO. 20 DIAGRAM SHOWING THE VELOCITIES V_A, V_K' AND FRICTION FORCE F, PLOTTED AGAINST THE TIME 't'
(NOSAL AND RYMSHA 1966.)

They considered that point 'o', (see Fig. No.18), was the position at which the drawing force acted and under oscillatory conditions changed as-

$$F=F_o \sin \omega t. \qquad \text{(1)}$$

where F_o = amplitude of the oscillatory force.
They concluded further that the displacements of particles in the wire at sections 'c' and 'b' could then be written as follows -

$$\left.\begin{aligned} U_1 &= B_1 \sin \frac{\omega}{a}(x + c)\sin \omega t. \\ U_2 &= B_2 \sin \frac{\omega}{a}(x - b)\sin \omega t. \end{aligned}\right\} \qquad \text{(2)}$$

where 'B_1' and 'B_2' were the respective displacements, 'c' and 'b' were respective distances from the die, and 'a' = the velocity of sound in the material.
Since the points 'c' and 'b' on the wire were secured, then the following conditions prevailed.

$$U_1 (c,t) = 0 = U_2 (b,t)$$

For continuity at point 'o', $U_1 (0) = U_2 (0)$ from which can be written

$$B_1 \sin \frac{\omega}{a} c + B_2 \sin \frac{\omega}{a} b = 0 \qquad \text{(3)}$$

The forces at 'o' were in equilibrium and therefore

$$E.A. \left[\frac{\partial U_1}{\partial x} (0) - \frac{\partial U_2}{\partial x} (0) \right] = F \qquad \text{(4)}$$

Substituting the derivatives of U_1 and U_2 into equation (4)

$$\frac{\omega}{a} E.A.B_1 \cos \frac{\omega}{a} c - \frac{\omega}{a} E.A.B_2 \cos \frac{\omega}{a} b = F_o \qquad (5)$$

therefore

$$B_1 \cos \frac{\omega}{a} c - B_2 \cos \frac{\omega}{a} b = \frac{F_o}{E.A} \cdot \frac{a}{\omega} = B_o \frac{a}{\omega} \qquad (6)$$

By solving equations (3) and (6), Severdenko and Klubovich obtained the following expressions for the amplitudes B_1 and B_2.

$$\left.\begin{aligned} B_1 &= B_o \frac{a}{\omega} \frac{\sin \frac{\omega}{a} b}{\sin \frac{\omega}{a} (c + b)} \\ B_2 &= B_o \frac{a}{\omega} \frac{\sin \frac{\omega}{a} c}{\sin \frac{\omega}{a} (c + b)} \end{aligned}\right\} \qquad (7)$$

and consequently the respective strains were

$$\left.\begin{aligned} e_1 &= \frac{\partial U_1}{\partial x} = B_o \frac{\sin \frac{\omega}{a} b}{\sin \frac{\omega}{a} (c + b)} \cos \frac{\omega}{a} (x + c) \\ e_2 &= \frac{\partial U_2}{\partial x} = B_o \frac{\sin \frac{\omega}{a} c}{\sin \frac{\omega}{a} (c + b)} \cos \frac{\omega}{a} (x - b) \end{aligned}\right\} \qquad (8)$$

Severdenko and Klubovich then selected the values of 'c' and 'b' such that :- $\sin \frac{\omega}{a} c = 0$ and $\sin \frac{\omega}{a} b = 1$ resulting in the strain at the exit from the die as follows

$$c_1 = B_o \cos \frac{\omega}{a} (x + c) \qquad (9)$$

From this equation they observed that the strain in the wire and consequently the liberation of heat at points 'c' and 'o' would be a maximum. They concluded that under these conditions the wire leaving the die would not be heated. Tests performed with the isolator positioned at these calculated antinodal points have shown that wire can be drawn without fracture when subjected to oscillatory energy. However, when the drawing process was stopped, or the wire was drawn very slowly, they observed that the wire could still rupture due to considerable localised heating.

No reference has been made in the published papers on oscillatory wire and tube drawing, of a force variation being present in the drawn material between the die and the gripping jaws. It is thought that some of the oscillatory energy would be transmitted from the die to the wire resulting in a force variation being induced in the wire as it leaves the die. Investigators studying oscillatory drawing have used low frequency response instruments for recording the loadmeter output signals. As a result of this, the signals have been severely attenuated and hence any force variation present in the wire has been concealed. It will be shown in this thesis

that, for low frequencies of die oscillation (ie. 25 to 500 c/s.), a force variation is induced in the drawn material. For all drawing conditions the maximum value of this variation was observed to be greater than the non-oscillatory drawing force, but the mean value was observed to be less than the non-oscillatory force and it is this mean value of drawing force which low frequency response instruments record.

Severdenko adn Klubovich's analysis predicted a force variation in the wire as follows :-

The strain at the isolator was shown to be equal to

$$e_1 = B_o \cos \frac{\omega}{a} c\,(x + c)$$

and therefore the force in the wire was given by

$$F = F_o \cos \frac{\omega}{a} c\,(x + c)$$

However, since the value of F_o was not included in their paper it was not possible to calculate the magnitude of the variation.

Although there was thought (by the author of this thesis) to be a force variation induced in the wire, because of the small amplitudes of oscillation employed, it was considered to be small when compared with the non-oscillatory force. The following analysis illustrates the presence of a force variation and shows its dependency on

the amplitude of oscillation.

If the oscillatory drawing process can be considered as a wire fixed rigidly at both the gripping jaws and the die, while the die was being subjected to a sinusoidal displacement, then the force variation can be expressed as

$$F = \frac{X.A.E.\omega}{a} \operatorname{cosec} \frac{\omega L}{a} \cos \frac{\omega x}{a} \sin \omega t.$$

(page 135, Mechanical Vibrations : Seto).

This analysis over simplifies the problem of oscillatory drawing and gives high values of force. By substituting experimental results obtained by Severdenko and Klubovich when drawing copper wire, it is seen that the force variation is small, ie. less than 4.5 per cent by comparison with the non-oscillatory force.

For example:- $X = 0.0016$ in. peak to peak.

$A = 0.0019$ in.^{2}

$E = 17 \times 10^6$ lbf./in.^{2}

$\omega = 23 \times 10^3$ c/s.

$a = 1.44 \times 10^5$ in/s.

$x = L$ = position of isolator.

Therefore the force variation $F \pm 4$ lbf. The recorded non-oscillatory drawing force = 90 lbf., but their instrumentation precluded their being able to record force variation.

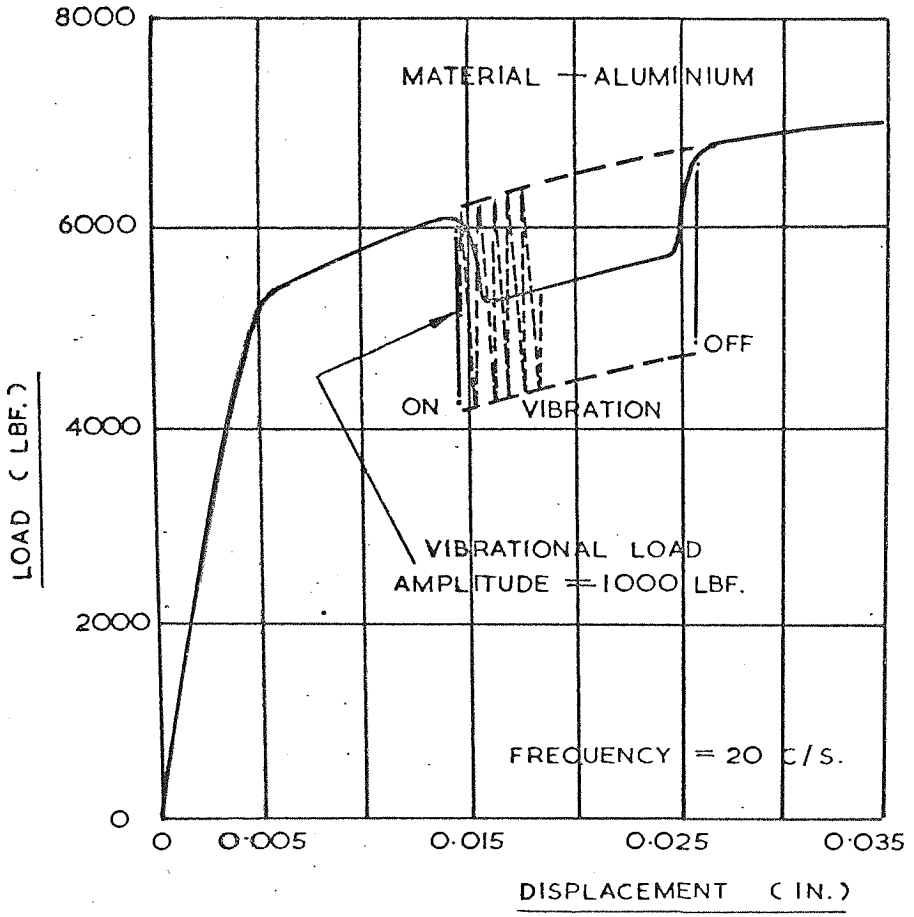

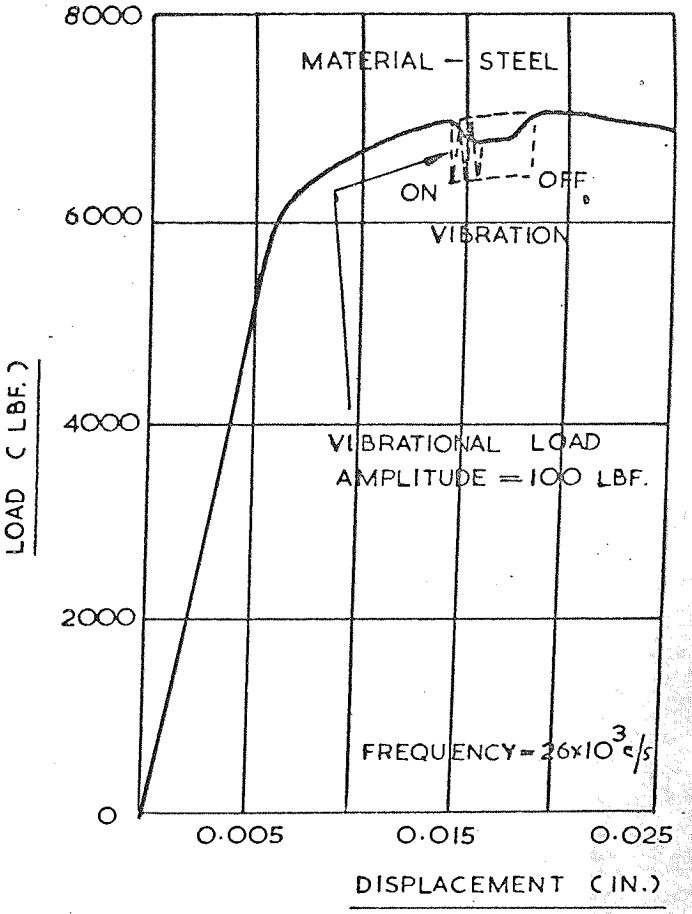

FIG.NO. 21 LOAD DISPLACEMENT CURVES OBTAINED FROM TENSILE TESTS ON STEEL AND ALUMINIUM SPECIMENS

(HAVERBECK AND WEBER 1963)

The possibility that there is a force variation induced in a metal specimen undergoing plastic deformation seems to have been ignored by the majority of investigators. It is still not clear from the literature whether there is a reduction in yield stress, or whether a stress variation is induced in the specimen, whose maximum value is coincident with or even above the non-oscillatory stress. This later phenomenon has been observed by Haverbeck and Weber (18), when tensile testing aluminium and steel and suggests a mechanical process of stressing and unstressing the specimen under test. (Fig. No.21). However, it must be concluded from most of the published results that a purely mechanical process of loading and unloading can not account for the 100 per cent reductions in yield stress observed by Langenecker et al.

The remainder of this chapter discusses the theoretical aspects of oscillatory wire and tube drawing as presented by: (i) Boyd, Maropis and Kartluke 1963, and (ii) Nosal and Rymsha 1966.

(i). Boyd, Maropis and Kartluke.

Boyd and Maropis considered the process of drawing wire in its simplest form and neglected (a) friction at the die surface, (b) work hardening and (c) redundant deformation.

Therefore the work expended per unit volume when reducing a wire in cross section from area A_1 to A_2 is

$$W = Y \ln. \frac{A_1}{A_2}$$

Also, the work done in producing unit length of wire is $\sigma . A_2$, and therefore the work done per unit volume is equal to the drawing stress, σ, and therefore:-

$$\sigma = Y \ln. \frac{A_1}{A_2}$$

$$\text{or} \quad \frac{F}{A_2} = Y \ln. \frac{A_1}{A_2} \qquad \text{(1)}$$

where F = the drawing force.

Since this expression neglected frictional effects, work hardening and redundant deformation, Boyd and Maropis introduced an empirical efficiency, and therefore

$$\frac{F}{A_2} = \frac{1}{\beta} Y \ln. \frac{A_1}{A_2} \qquad \text{(2)}$$

$$\text{where } \beta = \frac{F_1}{F}$$

F_1 = the theoretical drawing force obtained from equation (1), and F = the actual measured drawing force. Boyd and Maropis concluded that, for a range of oscillatory powers and drawing velocities, the effect of applying oscillatory energy to the drawing process could be expressed

in terms of its influence upon the drawing efficiency.

$$\text{ie. } \beta = \beta_o + KP \qquad \text{——————————(3)}$$

(The derivation of this equation is considered on page 40)

β_o = The drawing efficiency for non-oscillatory drawing. P = The oscillatory power, expressed in terms of the electrical input to the transducer, and K = a constant.

In order to take account of the drawing speed V, they assumed that the reduction in drawing force was dependent upon the energy density and therefore equation (3) was modified to

$$\beta = \beta_o + \frac{K_2 P}{V}$$

Note - since the power input to the transducer was expressed in terms of energy per unit time, and the drawing velocity was proportional to the volume rate of flow through the die, then the ratio of these two quantities was proportional to the energy density.

K_2 was the proportionality constant.

The drawing force without oscillatory activation of the die was given by -

$$\frac{F_o}{A_2} = \frac{1}{\beta_o} Y \ln.\frac{A_1}{A_2} \qquad \text{——————————(4)}$$

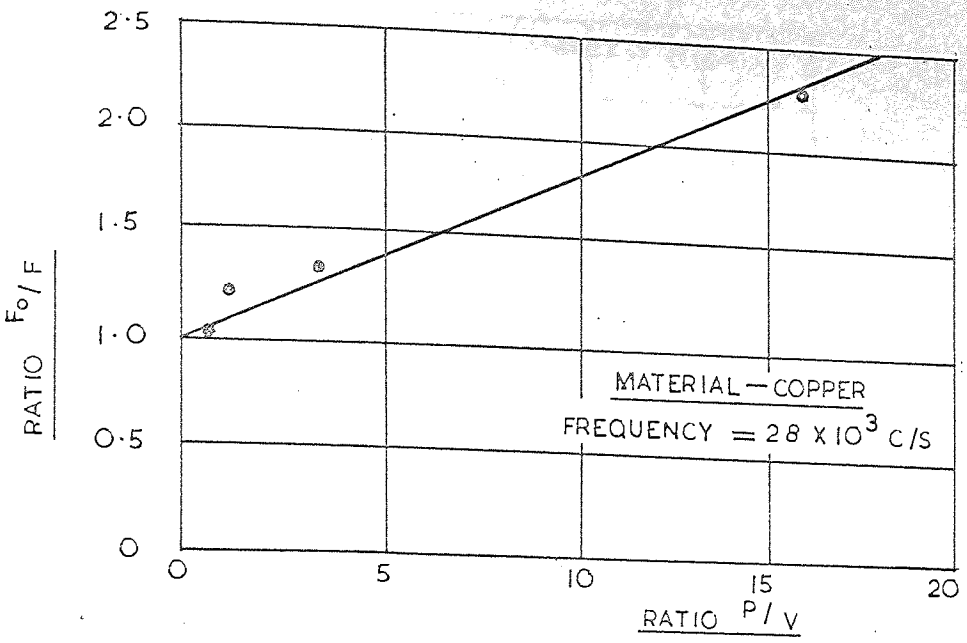

FIG. NO. 22

VARIATION OF F_o/F WITH P/V FOR COPPER WIRE

(BOYD ET AL 1963)

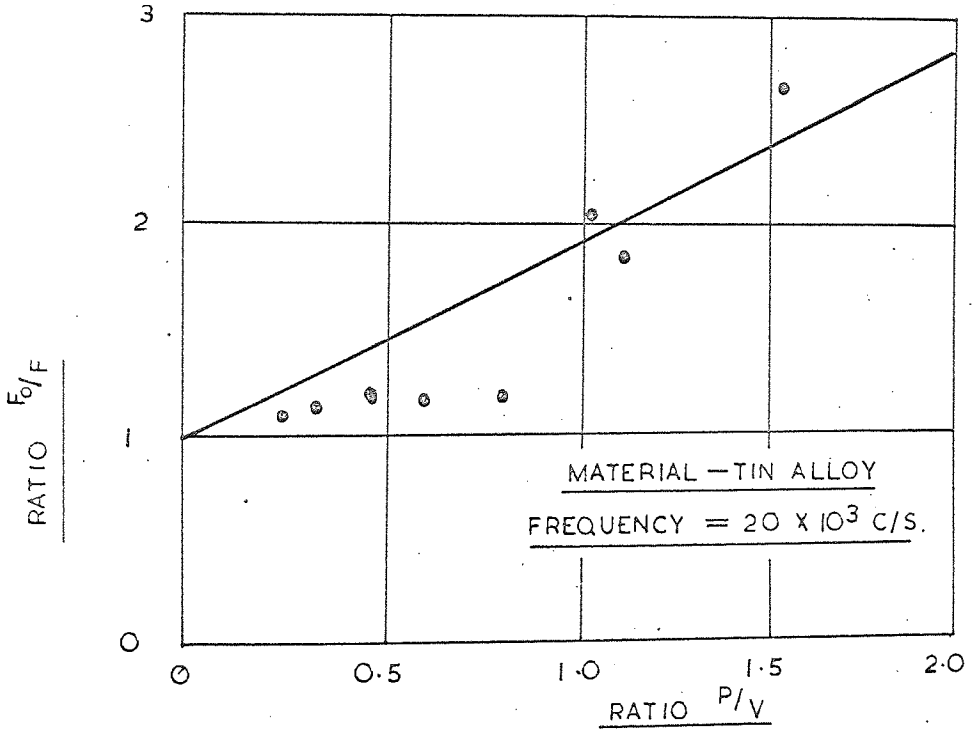

FIG. NO. 23

VARIATION OF F_o/F WITH P/V FOR TIN ALLOY

(BOYD ET. AL. 1963)

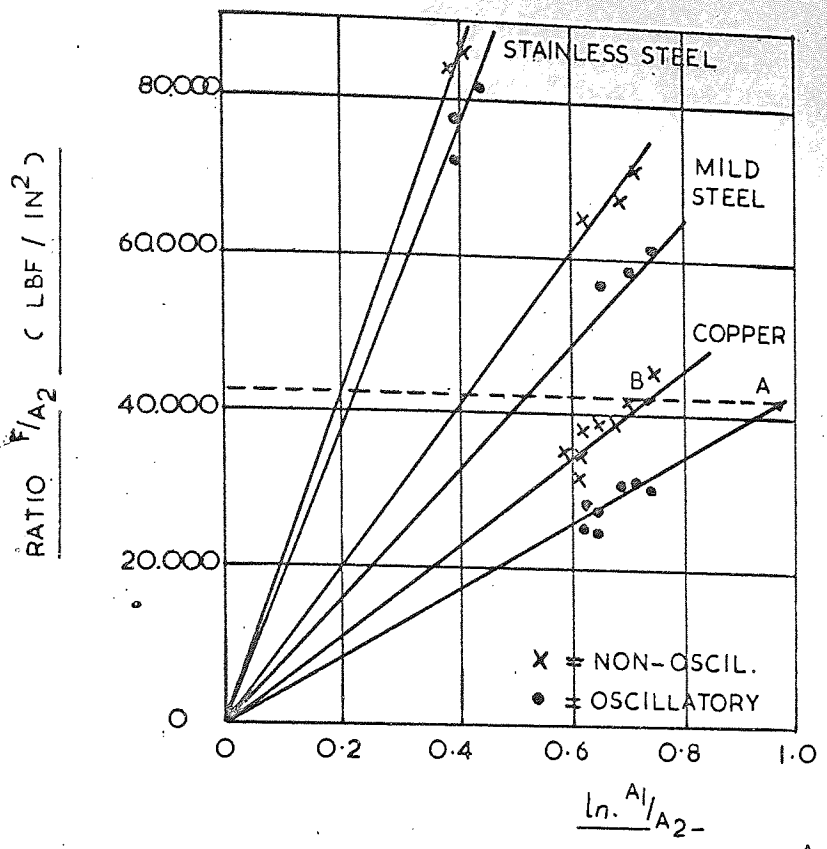

FIG.NO. 24 VARIATION OF F/A_2 WITH $\ln. A_1/A_2$ FOR STAINLESS STEEL, MILD STEEL AND COPPER

(BOYD ET. AL. 1963)

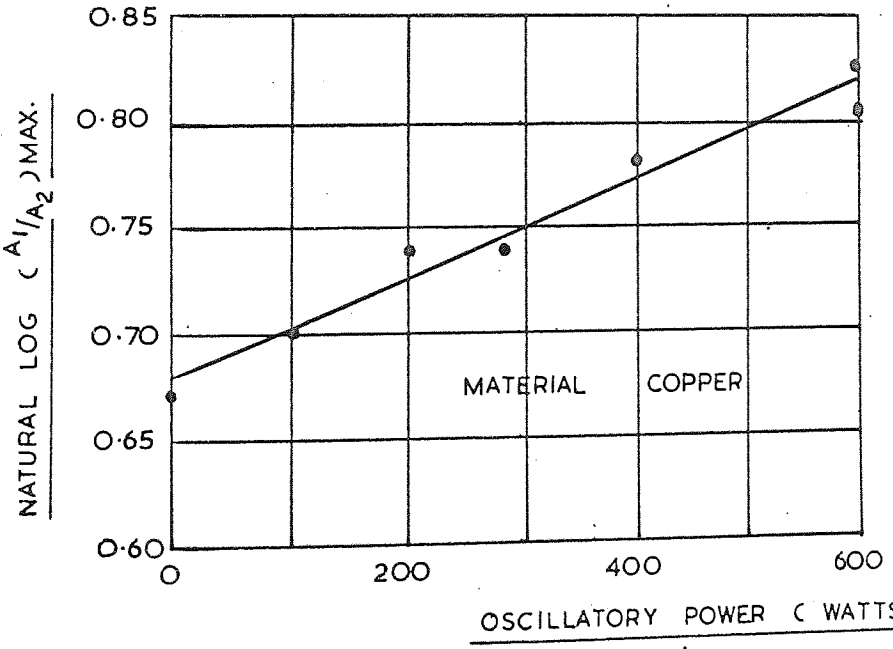

FIG.NO. 25. VARIATION OF $\ln. A_1/A_2$ WITH OSCILLATORY POWER 'P'

(BOYD ET. AL. 1963)

and for a given oscillatory power level and drawing velocity -

$$\frac{F}{A_2} = \frac{1}{\left(\rho_o + \frac{K_2 P}{V}\right)} Y \ln.\frac{A_1}{A_2} \qquad \text{(5)}$$

since A_1, A_2 and Y were assumed to remain constant then the ratio of the drawing forces was expressed as -

$$\frac{F_o}{F} = 1 + \frac{K_2}{\rho_o}.\frac{P}{V}$$

$$\frac{F_o}{F} = 1 + K_3.\frac{P}{V} \qquad \text{(6)}$$

where $K_3 = K_2/\rho_o$.

Boyd and Naropis plotted the ratios of F_o/F, and P/V, for experiments performed on a tin alloy wire and obtained a linear relationship as predicted by equation (6). This graph, and a similar plot from data obtained when drawing copper wire are shown in Fig. No. 22 and Fig. No. 23.

Boyd and Kartluke extended the above semi-empirical analysis to tube drawing and plotted results obtained when drawing copper, mild steel and stainless steel tubes, according to the functional form of equation (2). see Fig. No. 24.

Note - Boyd and Kartluke used ultimate stress values in place of Y. They assumed that the ultimate stress was proportional to the average yield stress of the material and hence they concluded that the slopes of the curves in Fig. No. 24 gave a measure of $1/\beta$.

Determination of the equation $\beta = \beta_o + K_2 P$.

Boyd and Kartluke determined the maximum drawing ratio, ($\ln. A_1/A_2$), that could be obtained without breakage, as a function of the oscillatory power input. This data was plotted (see Fig. No.25) and indicated a function of the form -

$$\ln.\frac{A_1}{A_2}_{\substack{\text{max.}\\ \text{oscil.}}} = \ln.\frac{A_1}{A_2}_{\substack{\text{max.}\\ \text{non-oscil.}}} + K_3 P \qquad \text{------(7)}$$

Also, from Fig. No. 24 they observed that for a constant drawing stress, at points A and B -

$$\frac{F}{A_2} = \frac{Y}{\beta} \ln.\frac{A_1}{A_2}_{\substack{\text{max.}\\ \text{oscil.}}} = \frac{Y}{\beta_o} \ln.\frac{A_1}{A_2}_{\substack{\text{max.}\\ \text{non-oscil.}}}$$

and therefore

$$\ln.\frac{A_1}{A_2}_{\text{oscil.}} = \frac{\beta}{\beta_o} \ln.\frac{A_1}{A_2}_{\text{non-oscil.}}$$

also from equation (7)

$$\frac{\beta}{\beta_o} \ln.\frac{A_1}{A_2}_{\text{non-oscil.}} = \ln.\frac{A_1}{A_2}_{\text{non-oscil.}} + K_3 P$$

and therefore

$$\beta = \beta_o + \frac{\beta_o K_3 P}{\ln.\frac{A_1}{A_2}_{\text{non-oscil.}}}$$

$$\beta = \beta_o + KP \qquad \text{(3)}$$

where $$K = \frac{\beta_o K_3}{\ln.\frac{A_1}{A_2}_{\text{non-oscil.}}}$$

The simple analysis of wire and tube drawing developed by Boyd et al. shows correlation with experimental results and is therefore considered a satisfactory method for comparing the effects of oscillatory energy when drawing different types of metals. However, this comparison is limited to materials which have been drawn with the same apparatus. (ie. The experimental oscillatory power levels were recorded in terms of electrical power input to the transducer. Because of mechanical and electrical losses, inherent in magnetostrictive transducers, the actual power at the deformation zone in the die will be dependent upon the efficiency of coupling and hence the particular apparatus in use).

Boyd's analysis is inadequate in that it does not incorporate the two fundamentals of oscillatory metal working. No attempt was made in the theory to include the phenomena of reduction in stress necessary to cause plastic deformation and the reduction in the coefficient of friction. The high reduction in drawing load of 80 per cent recorded by Boyd and Haropis when drawing tin alloy wire with a superimposed oscillatory stress, suggests that both phenomena of load reduction were present. Using a value of 0.025 for the coefficient of friction as suggested by Wistreich (43), for drawing mild steel with a dry soap lubricant, then a reduction in the coefficient to zero could only account for a decrease in drawing force of about 13 per cent.

---

(2) Nosal and Rymsha.

In 1966, Nosal and Rymsha published a paper on their analysis of oscillatory tube drawing. Their theory was based on a reduction in contact time, and therefore a reduction in the friction forces, between the die and the deforming metal. The analysis was presented as follows -

They stated that when a die was oscillated, the vibratory waves distributed themselves along the contact surface between the die and the deforming metal. For the most general case they considered that the longitudinal waves formed an angle 'γ' with the direction in which the metal advanced along the die surface. (see Fig. No.19).

Point 'A' on the contact surface moved along the die profile with a velocity of V_A and also oscillated at a velocity V_K at an angle 'γ' to the die surface.

Nosal and Rymsha postulated that -

(i) When $V_A < V_K \cos \gamma < V_K'$.

The vector of the relative velocity at point 'A' changed in direction simultaneously with the change in the direction of the oscillatory velocity. At certain time intervals within the period 'T', the relative velocity coincided with the displacement of the metal along the contact surface, and at other times it was directed in the opposite direction.

(ii) When $V_A > V_K \cos \gamma > V_K'$.

Then the direction of the relative velocity always coincided with the direction of drawing.

Fig. No. 20 shows that for the time interval $(T/2 + 2t_1)$ the force of friction was negative (ie. it opposed the advancement of metal in the die), and for the time interval $(T/2 - 2t_1)$ the force of friction was positive (ie. it assisted the motion of the metal by decreasing the drawing force).

Nosal and Rymsha concluded that the ratio of the sum of these two time intervals to the difference, ie. $T/4t$, was the coefficient of reduction of mean friction force. They gave the ratio the symbol 'n'.

$$\text{Period } T = \frac{1}{F} = \frac{2\pi}{\omega} \qquad \text{(1)}$$

$$\text{also } V_A = X\,\omega \sin \omega t_1 = V_K' \sin \omega t. \qquad \text{(2)}$$

where X = the amplitude of die oscillation.

therefore

$$\omega t_1 = \sin^{-1} \frac{V_A}{V_K'}$$

$$\text{also } V_K' = V_K \cos \gamma \quad \text{and therefore}$$

$$\omega t_1 = \sin^{-1} \frac{V_A}{V_K \cos \gamma} \qquad \text{(3)}$$

Substituting into the equation $n = T/4t_1$

$$n = \frac{\pi}{2} \cdot \frac{1}{\sin^{-1} \dfrac{V_A}{V_K \cos \gamma}} \qquad \text{(4)}$$

Nosal and Rymsha concluded that for small values of ωt_1, equation (4) simplified to -

$$n = \frac{\pi}{2} \cdot \frac{V_K \cos \gamma}{V_A} \qquad \text{(5)}$$

They then replaced the velocity V_A with a mean velocity -

$$V = V_D \cdot \frac{\delta \cos \alpha + 1}{2\delta \cos \alpha}$$

where δ = a drawing coefficient = the ratio of areas (A_1/A_2).

By substituting in equation (4), they obtained

$$n = \frac{\pi}{2} \frac{V_K \cos \gamma}{\sin^{-1} \frac{V_D(\delta \cos \alpha + 1)}{2\delta \cos \alpha}}$$

or approximately

$$n = \frac{\pi . \omega . X . \delta \cos \alpha}{V_D(\delta \cos \alpha + 1)} \cos \gamma \qquad \text{(6)}$$

Nosal and Rymsha concluded from equation (6), that the important factor affecting the efficiency of the oscillatory drawing process was the correct selection of the oscillatory speed and drawing speed relationship. A high oscillatory speed could be obtained under great technical difficulties but, it would not be economically acceptable. It was therefore considered necessary to select a range of V_D/V_K ratios that would produce an economic reduction of the drawing force with a corresponding increase in the reduction of area per pass.

Nosal and Rymsha then considered the following equation -

$$P_Z = P_Y + P_X = P_Y(1 + \mu \cot \alpha)$$

where P_Z = the drawing force

P_Y = the force required to overcome the resistance to deformation

P_{ZY} = the total drawing force with superimposed oscillatory energy.

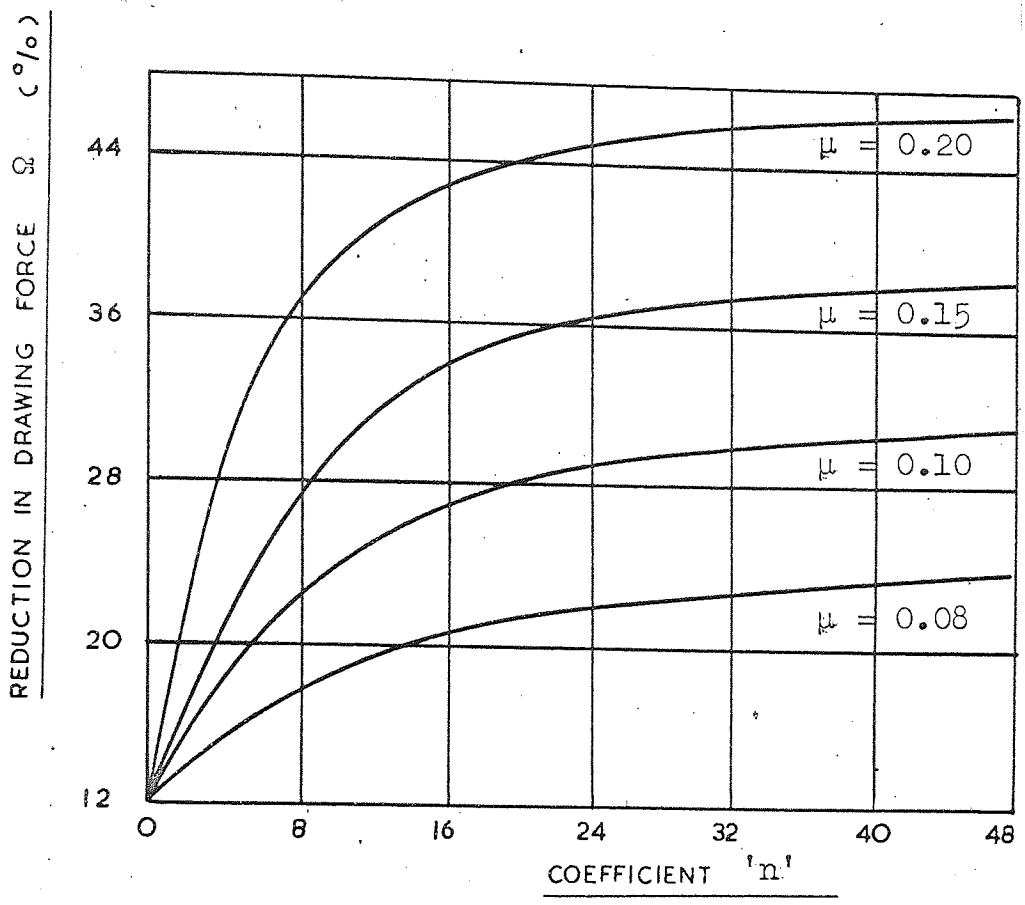

FIG. NO. 26 REDUCTION IN DRAWING FORCE PLOTTED AGAINST COEFFICIENT 'n'

(NOSAL AND RYMSHA)

P_X = the force required to overcome friction.

μ = the coefficient of friction.

When oscillatory energy was applied during the drawing process, then the equation became -

$$P_{ZY} = P_Y \left(1 + \frac{\mu \cot \alpha}{n} \right) \qquad \text{(9)}$$

or rewriting as a percentage reduction in force, Ω

$$\Omega = \frac{(P_Z - P_{ZY})}{P_Z} \cdot 100 = \frac{\mu \cot \alpha}{1+\mu \cot \alpha} \left[1 - \frac{1}{n} \right] 100 \qquad \text{(10)}$$

This relationship was shown graphically in Fig. No. 26. In order to check their theory, Nosal and Rymsha proceeded to draw steel tubes without a mandrel with a longitudinal die oscillation of 20×10^3 c/s., (ie. $\gamma = 0$). They observed that, when drawing at a speed of 0.94 in./s., and an amplitude of oscillation of 4.0×10^{-5} in., the drawing force was reduced by approximately 35 per cent. When substituting the appropriate values into equations(6) and (10), they obtained a reduction in force of 40 per cent.

Although Nosal and Rymsha's analysis shows good correlation with experimental findings, it was considered to be based on a doubtful postulate. Their concept of reduced friction forces was similar to that described by Balmouth (21), and postulates that frictional forces are reduced because of a

reduction in contact time between the die surface and the deforming metal. They assumed that, because the die travelled with a greater velocity than the metal being drawn, there would be relative movement between the die and the deforming metal, when the die was moving in the direction of drawing. This postulate is considered to be incorrect because of observations made during the research programme described in this thesis. It will be shown that, when testing with die oscillation speeds greater than the drawing speed, the die did not move relative to the deformation zone. It was found that this was because the elastic recovery of the machine and the wire was sufficiently large, that contact between the deforming metal and the die was always maintained. This observation showed that the contact time was not reduced and therefore rendered Nosal and Rymsha's postulate meaningless. It was thought that there could only be relative movement between the die and the metal being drawn when the velocity of the die was greater than the velocity of stress propagation in the material, or when the amplitude of the die oscillation was greater than the extension present in the drawn wire due to the non-oscillatory drawing force.

The magnitude of the friction forces between two surfaces depends on the load between them and the 'plasticity' of the surface asperities. When one surface moves relative to

the other a force sufficient to overcome the shear strength of welded junctions must be exerted. If the application of oscillatory energy results in a lowering of yield stress of a material than the shear stress of these weldments must also be reduced and hence the force required for shearing reduced. It was concluded therefore, that the phenomenon of a reduction in friction forces is closely associated with the phenomenon of reduction in yield stress.

4. A Discussion on the Course to be Followed by this Investigation

4. A Discussion of the Course to be followed by this Investigation.

At the start of this research programme, very little work had been published on the application of oscillatory energy to metal working processes, and therefore this investigation was undertaken to see whether the observed phenomena of reduction in yield stress and reduction in friction forces, could be harnessed to aid metal forming. An extensive study into wire drawing with superimposed longitudinal oscillatory stresses was initiated, the programme being designed to study the effects of such variables as -

(1) Frequency of oscillation.

(2) Amplitude of oscillation.

(3) Drawing speed.

(4) Reduction in area and

(5) Diameter of drawn wire on the drawing process and to obtain so far as may be possible both experimentally and theoretically, the optimum parameters for oscillatory drawing. Wire drawing was selected as the metal working process to be studied because it was considered that

(1) A steady state process was desirable.

(2) The die could be readily oscillated.

(3) It was desirable to maintain a constant radial stress when drawing, (ie. if tube

was selected, in order to prevent a variation in radial stress, it would be necessary to draw the tube with a plug. This would present additional engineering difficulties when trying to support, or oscillate, the plug during oscillatory drawing.).

(4) Because there was good understanding of the mechanics of the non-oscillatory process.

(5) Raw material and machinery was not expensive.

(6) Materials are easily cold worked in a University.

(7) Process likely to indicate what would happen in other cold working processes.

It was thought that, if oscillatory energy techniques proved advantageous to drawing, then existing technological theories of wire drawing could be used and modified to incorporate the effects of oscillatory energy by the selection of appropriate values for the yield stress 'Y', and the coefficient of friction 'μ'.

The drawing tests were performed on a 2000 lbf. bull-block and the superimposed vibrational energy was supplied in a longitudinal mode from an electro-hydraulic oscillator. To take advantage of modern strain gauge

techniques and dynamic strain recording equipment, it was decided to measure the drawing force by situating a loadmeter in series with the die and the actuator, and to measure the torque by locating a torquemeter on the drum shaft between the drum and the drive pinion. Instrumentation was also installed to measure the drawing speed and the amplitude of die oscillation.

During the course of the investigation, it became apparent that the magnitude of the force variation in the wire leaving the die as measured by the loadmeter, differed from that predicted by the torquemeter. In order to understand this, a vibration analysis of the bull-block and drive was undertaken and it became apparent that the inertia force of the drum was an important parameter. The moment of inertia for the drum was measured and additional instrumentation incorporated to record the torsional displacement of the drum and shaft. Furthermore, in order to obtain a direct measurement of the force variation in the wire and therefore to confirm the analysis, a strain gauge bridge was mounted directly on to the wire.

The initial slow speed drawing tests were performed with a mild steel wire (EN.2B). Five reductions of area were drawn the values being selected to give equal increments of generalised strain. Further slow speed tests, at fixed reductions in area, were performed with a pure aluminium, a precipitation hardening aluminium alloy (HG.9), a

stainless steel and a high conductivity copper. In order to check the effect of drawing speed, the copper was drawn at increasing speeds, up to a maximum of 50 ft/m.

Lastly, a number of stress strain curves were obtained for the materials in the following conditions -

(1) 'as received'

(2) non-oscillatory drawn

(3) drawn with superimposed oscillatory energy,

to determine the effect of oscillatory energy on the mechanical properties of the drawn wire.

4.1. Selection of Mode of Oscillation.

Oscillatory stresses could be applied to the deformation zone during drawing by oscillating the die in either, (i) a radial mode or,(ii)a longitudinal mode. However, to provide radial oscillation to the die was a difficult engineering problem. Furthermore,it was thought that radial vibrations may result in the drawn wire having an undulating surface. Therefore,because of these two factors, it was decided to perform the drawing tests with the die oscillating in a longitudinal mode.

4.2. Selection of Frequency and Amplitude Range.

Work on the effect of oscillatory stresses on the deformation of metals has been carried out with frequencies of vibration ranging from 15 c/s up to 1000×10^3 c/s. In order to investigate the application of oscillatory stresses during wire drawing over this entire range of frequencies,

FREQUENCY RANGE	0 — 500 C/S.	500 — 10×10^3 C/S.	10×10^3 — 1000×10^3 C/S.
TYPE OF OSCILLATOR	ELECTRO — HYDRAULIC	ELECTRO — MAGNETIC	MAGNETOSTRICTIVE
AMPLITUDE OF OSCILLATION	LARGE ± 0·100 IN.	SMALL ± 0·001 IN.	VERY SMALL ± 0·0001 IN.
TYPE OF UNIT FOR COMPARABLE POWER	SMALL AND COMPACT. READILY ADAPTABLE	VERY LARGE. NOT READILY ADAPTABLE	LARGE NOT READILY ADAPTABLE

FIG. NO. 27 TABLE SHOWING TYPES OF OSCILLATORY SYSTEMS REQUIRED TO PROCESS WIRE 0·25 IN. DIAMETER

three separate types of vibration system would have been required as shown in Fig. No.27. However, previous investigators have concluded that the results obtained with superimposed oscillatory energy were independent of the frequency of vibration but dependent upon the amplitude of vibration. Therefore, it was considered that for the present series of experiments an oscillator which enabled a wide range of amplitudes to be tested, rather than a wide range of frequencies should be used. Thus it was proposed to carry out the programme of work using an electro-hydraulic vibrator. This type of oscillator had additional advantages in that it was readily adaptable to the problem of wire drawing, and also the additional power available enabled heavy gauge wire (ie. 0.25 in. diameter) to be drawn. A brief description of the oscillator is given in Appendix No. 16.2.

4.3. Selection of Wire Drawing Machine.

To maintain a constant length of drawn wire between the die and the gripping jaws, a horizontal bull-block was used for the test. The machine was conventional in design, but special care was taken during its design and manufacture to ensure that the machine was very rigid, ie. plain bearings were used wherever possible and clearances were cut to a minimum. A 'stiff' machine was considered desirable to ensure that the oscillatory energy was transferred from the vibrator to the deformation zone and not absorbed

DIAMETER OF DIE THROAT = 0·158 IN. (φ4mm)			
INCREMENT OF GENERALIZED STRAIN '$\bar{\varepsilon}$'	REDUCTION IN AREA (%)	EFFECTIVE SEMI — DIE ANGLE 'α' (DEGREES)	DIAMETER OF WIRE (IN.)
0·105	10	2° 59′	0·173
0·308	26	5° 15′	0·192
0·511	41	6° 56′	0·212
0·714	51	8° 25′	0·235
0·916	60	9° 49′	0·260

FIG.NO. 28 TABLE SHOWING DETAILS OF SEMI-DIE ANGLES AND WIRE DIAMETERS

in the system because of poor mechanical coupling. A complete specification of the machine was included in Appendix No. 16.1.

4.4. Selection of Drawing Dies.

In order to maintain a constant diameter of drawn wire and therefore a constant stiffness of wire between the die and the gripping jaws, it was decided to keep the die size constant and to obtain different reductions in area by varying the material size. Five reduction in area were chosen between 10 and 60 per cent, their magnitudes selected to give equal increments of generalised strain (see Fig.No.28). It was considered unlikely that a 60 per cent reduction in area would be achieved under non-oscillatory conditions, but it was hoped that it would be possible with superimposed oscillatory energy. It was decided that the maximum diameter of material to be drawn would be 0.25 (ϕ6.25) in. and therefore, for a 60 per cent reduction in area the die throat diameter was calculated to be 0.158 in. Radius profile dies were selected in preference to conical dies to eliminate the effects of length of parallel and blend radius and hence to maintain geometrically similar zones of deformation for all stock sizes. An optimum equivalent semi-die angle was chosen for the die, ie. for a 60 per cent reduction in area a semi-angle of approximately 10 degrees was used, in accordance with Wistreich's (43), conclusions.

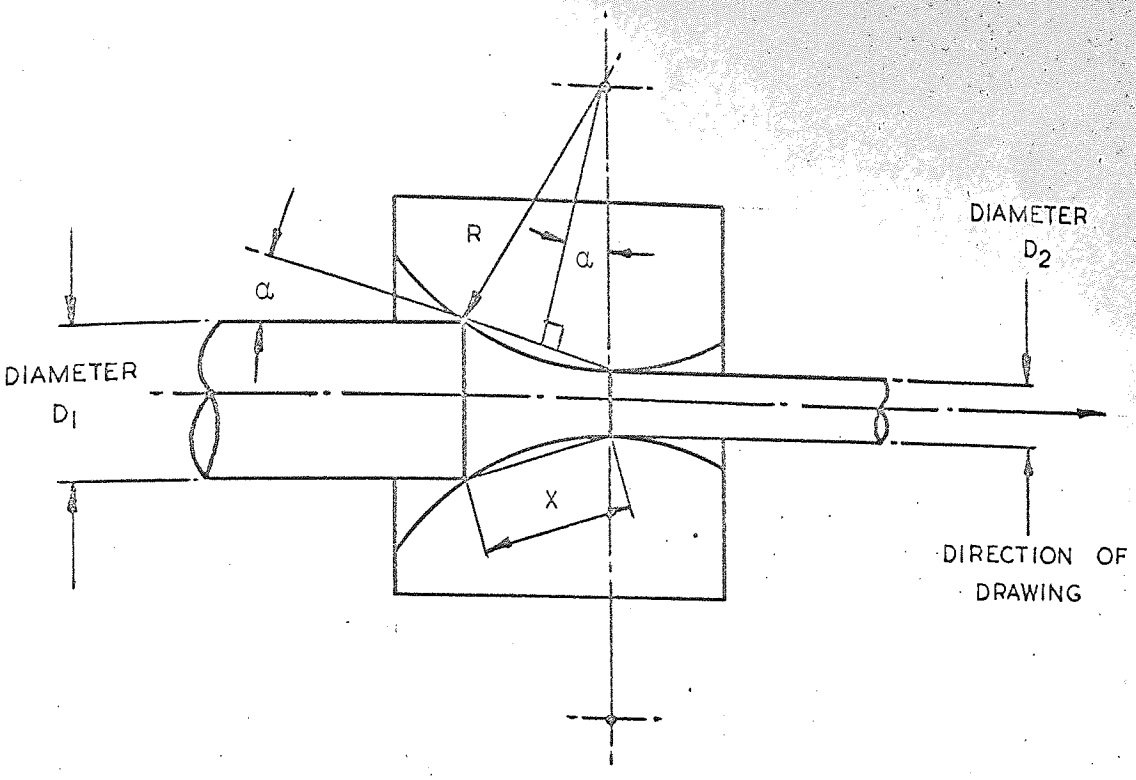

$$\frac{\frac{D_1 - D_2}{2}}{X} = \sin \alpha.$$

$$\therefore D_1 - D_2 = 2.X \sin \alpha. \text{ ——— (1).}$$

IF 'α' IS SMALL THEN

$$\frac{X}{2} = R. \sin \alpha.$$

$$\therefore X = 2.R \sin \alpha. \text{ ——— (2).}$$

SUBSTITUTING EQUATION (2). IN (1).

$$D_1 - D_2 = 4R \sin^2 \alpha \text{ ——— (3).}$$

FIG. NO. 29 EQUIVALENT SEMI-DIE ANGLE

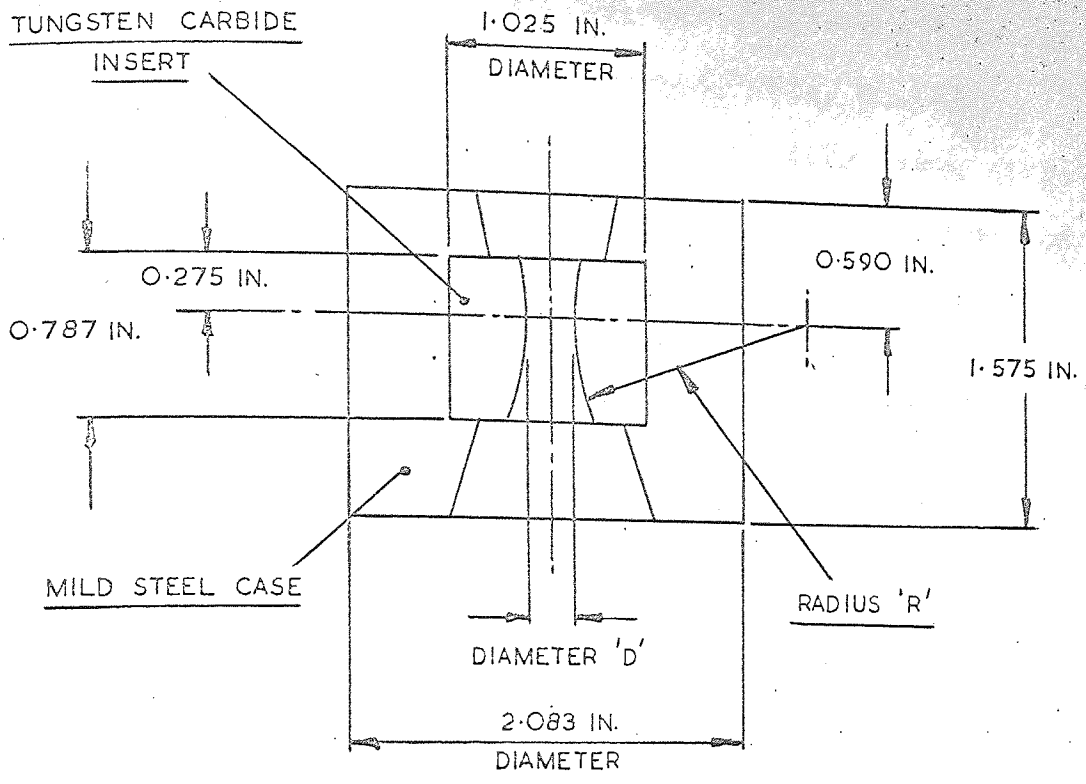

R (IN.)	D (IN.)
0·833	0·167
0·923	0·184
1·021	0·205
1·129	0·226
1·250	0·250

FIG. NO. 30. DETAILS OF DRAWING DIES

Note :- The equivalent semi-die angle was taken as the mean angle over the arc of contact. (Fig. No.29).

To suppress the yield point of the mild steel wire, the coils were given a sizing pass of 7 per cent reduction in area prior to the main series of tests. Four further dies were required for this operation and in order to maintain geometrical similarity between them and the existing die, the semi-die angle was used as a criterion. (ie. all the die dimensions were selected so that for a reduction of area of 60 per cent, the equivalent die angles would be approximately 10 degrees).

The dies were manufactured from tungsten carbide pellets which were brazed into mild steel cases. The accuracy of the profile radius and the throat diameter was checked by the manufacturer at a magnification of 50 times, giving an accuracy of $\pm$ .0001 in. Details of the dies are given in Fig. No. 30.

4.5. Selection of Materials.

4.5.1. Mild Steel (EN.2B)

The initial tests were carried out using a 0.15 per cent carbon steel EN.2B. This material was chosen because of its characteristic elastic-plastic stress-strain curve, its availability and its commercial implications. In order to try and maintain uniform mechanical properties and surface finish, all wire was supplied from the same cast. The material was received in the following diameters

0.173 in., 0.192 in., 0.212 in., 0.240 in. and 0.260 in., fully annealed and lubricated with a phosphate coating. A specification of the material is included in Appendix No. 16.8.

The remaining tests were performed with four other metals - stainless steel, two types of aluminium and copper. The reasons for selecting these materials will be explained in the following sections -

4.5.2. Stainless Steel.

Meleka and Harris have observed that oscillatory energy can reduce the rate of work hardening in a material. In an attempt to establish whether this phenomenon occurred in oscillatory wire drawing, a material which exhibited a very high rate of work hardening was selected ie. stainless steel. It was anticipated that, during oscillatory drawing, the stainless steel would react as predicted by Meleka and Harris and hence the drawing force would be reduced.

The stainless steel used was, 0.212 in. diameter, niobium stabilised, SAE 305 and had received an approximate reduction in area of 7 per cent. It was supplied copper coated to a depth of 3×10^{-4} to 5×10^{-4} in., and was further lubricated with a phosphate coating. A complete specification is included in Appendix No.16.8.

4.5.3. Aluminium Alloy (HG.9)

When a precipitation hardening aluminium alloy

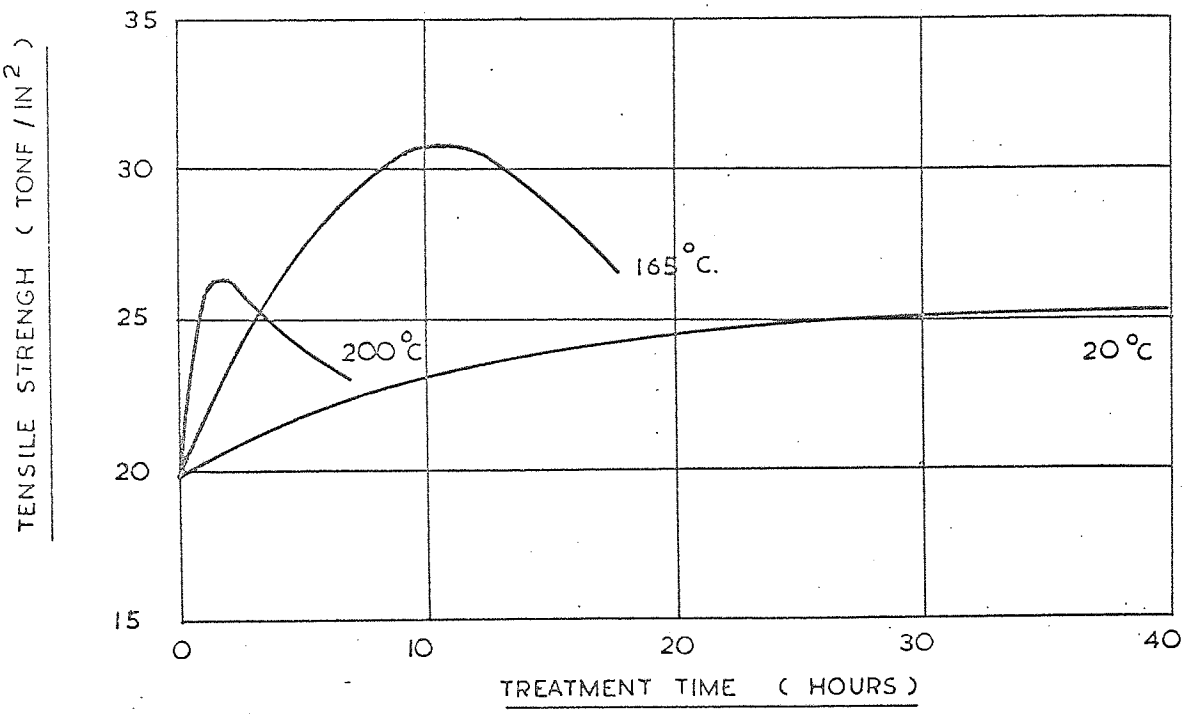

FIG.NO. 31 TENSILE STRENGH PLOTTED AGAINST TREATMENT TIME FOR AGE HARDENING AN ALUMINIUM ALLOY (HIGGINS 1957.).

is quenched and then allowed to remain at room temperature, it will be found that its tensile strength will gradually increase and reach a maximum in about six days. After this time has elapsed no further appreciable changes in strength take place. An improvement in properties over those obtained by ordinary age hardening can be obtained by heating the quenched alloy at temperatures up to 200 degrees Celsius for short periods. This treatment causes diffusion of the copper atoms to take place and this proceeds up to a point where further heating results in a rapid decrease in the tensile strength. This phenomenon is shown in Fig. No.31. When heating takes place at temperatures above 200 degrees Celsius, the diffusion process is rapidly accelerated and softening takes place almost instantaneously.

Many investigators have reported that oscillatory energy affects a material in much the same way as a temperature rise. It was therefore anticipated that, if a precipitation hardening alloy was drawn under oscillatory conditions, the vibrational energy, acting in a way similar to thermal energy, would accelerate the diffusion process and cause rapid softening of the wire. As a result, it was anticipated that the drawing force would be reduced and the finished material would be in a softer condition.

In order to investigate this, a precipitation hardening aluminium alloy HG.9 was used in the tests. The material was received 0.212 in. diameter and was supplied

in its hardest condition. A complete specification of the aluminium is included in Appendix No.16.8.

4.5.4. Pure Aluminium.

Langenecker has observed that defects in metals such as grain boundaries and dislocation sites, absorb oscillatory energy so that the stress required to cause the mobility of the atoms is reduced. He likened the absorption of energy to a temperature rise and concluded that, since oscillatory energy was absorbed preferentially at dislocation sites and thermal energy was absorbed by all atoms, then the application of oscillatory energy was a more effective method of lowering the yield stress of a material. In an attempt to incorporate this phenomenon of dislocation movement during drawing, a pure aluminium was selected. It was anticipated that during oscillatory drawing, the energy would impart dynamic mobility to the dislocations and hence lower the yield stress of the material and consequently lower the drawing force.

Note - The mechanism for absorbing oscillatory energy and assisting dislocation movement, differs from that for accelerating the diffussion process, although both are dependent upon a rise in temperature.

The aluminium used was 99.8 per cent pure, and was supplied at 0.212 in. diameter, fully annealed. A complete specification is included in Appendix No.16.8.

4.5.5. Oxygen Free High Conductivity Copper.

In 1966, Oldroyd, Burns and Benham (50), reported on strain cycling tests which had been performed on a number of different metals. Their tests consisted of subjecting metal specimens to tension-compression cycles of plastic deformation. During these investigations they showed that some materials ie. nickel chrome steel EN.25 and cold worked copper, were rapidly work softened as a result of stress reversals.

During the preliminary investigations into oscillatory wire drawing, it was observed that a large stress variation was induced into the wire as it left the die. Although this variation was always tensile, it was thought that it may be possible to observe the phenomenon of cyclic softening during the oscillatory drawing of certain metals. If this was the case, the drawing force and also the tensile strength of the finished wire would be reduced.

In order to investigate this effect, a coil of 0.212 in. diameter, oxygen free, high conductivity copper wire was purchased. The wire was supplied in a cold-worked condition, having received a 40 per cent reduction in area. A complete specification of the copper is included in Appendix No. 16.8.

Note :- This type of load reduction was not envisaged when the research programme was initiated but, because of the importance to metal working of Oldroyd,

Burns and Benham's results, it was considered desirable to include an investigation to establish whether the effect occurred.

4.6. Selection of Drawing Lubricants.

The initial drawing tests on mild steel were performed using a dry soap, Swift's Teliximet MCF. This lubricant is a form of sodium stearate and was chosen for its low coefficient of friction when used as a drawing lubricant (ie. $\mu = 0.025$), and its commercial implications.

In order to avoid the use of a wet lubricant and to maintain constant lubrication conditions, this soap was also used for drawing the aluminium, stainless steel and copper wires.

5. Design of Measuring and Recording Apparatus

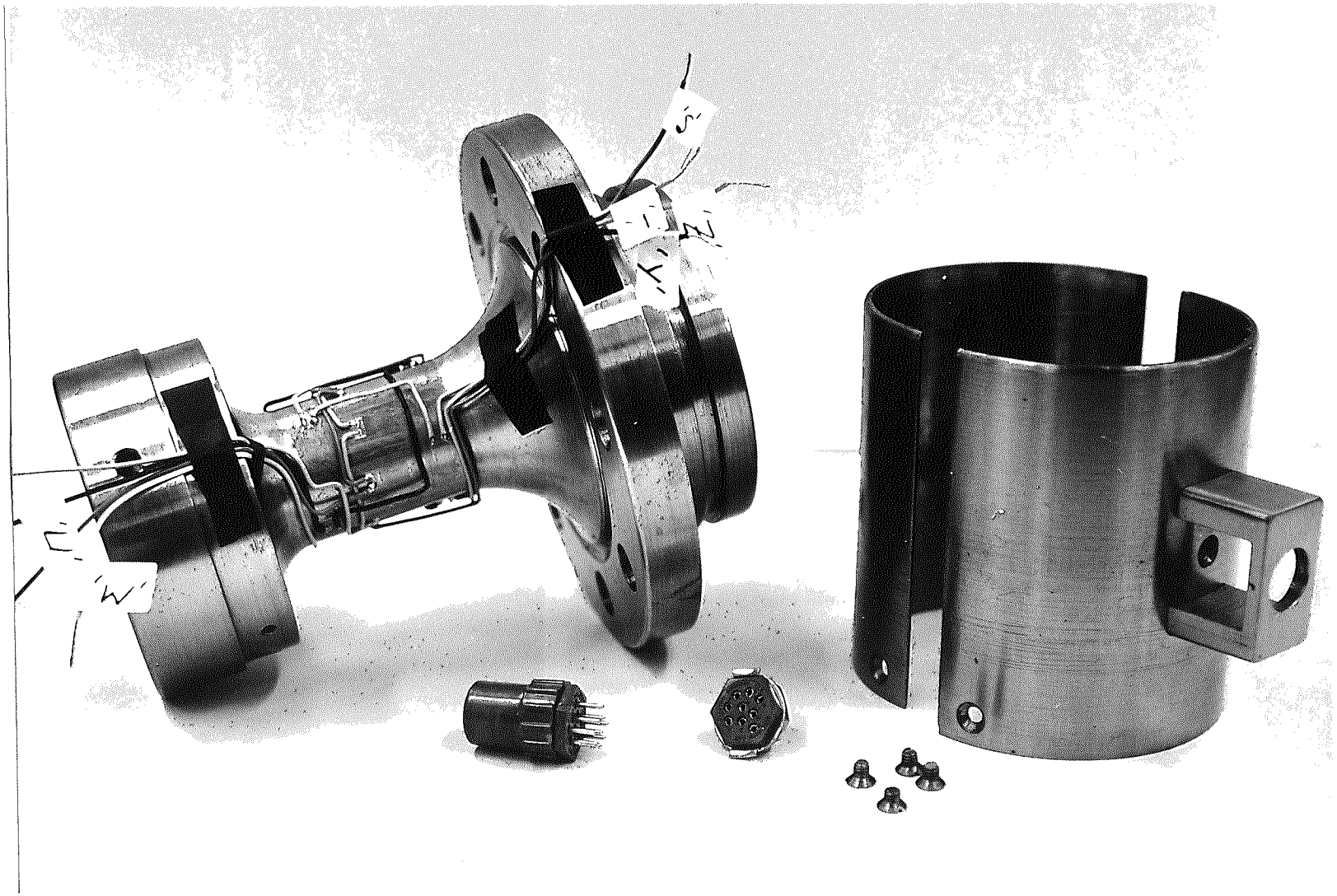

FIG.NO. 32. LOADMETER DESIGN DETAILS

TERMINAL BRIDGE
MATL: M.S. EN.6A

3/4"

3/4"

1 13/32" RAD.

SECTION YY.

3 HOLES 4 B.A. C'SK. TO SUIT SCREW HD.

10°

10°

2 HOLES 6.B.A. C'SK ON INSIDE TO SUIT SCREW HD.

1/2" DIA. HOLE

1/8" RAD.

1/4"

1/4"

1/16"

1 1/8"

1 1/8"

1/4"

Y

Y

LOADMETER COVER
MATL: M.S. EN.6A.

1/32" RAD.

2 HOLES 6.B.A. TAPPED 5/16" DEEP.

1/16"

2·814" DIA. (OUTSIDE)

2·748" DIA. (INSIDE)

2 7/8" DIA.

X

10°

10°

8 HOLES 7/16" DIA. EQUALLY SPACED ON 3 7/8" P.C. DIA.

X

10°

10°

SECTION ZZ.

3 HOLES 4.B.A. C'SK TO SUIT SCREW HD.

2 HOLES TAPPED 1/4" B.S.F. RIGHT THROUGH.

3/4"

1/2"

2 3/4"

1/16" RAD.

3/8" RAD.

2·750" DIA.

1·00" DIA.

1·200" DIA.

2·812" DIA.

2·750" DIA.

1/32" RAD.

7/32" RAD.

3/4"

7/32"

6 HOLES TAPPED 4.B.A. 1/4" DEEP.

1/2"

7/8"

5/32"

0·188"

5/16"

1/16" RAD.

1/2" RAD.

5/16"

2·125" DIA.

2·500" DIA.

2·875" DIA.

3·121" DIA.

1" RAD.

0·115"

SECTION XX.

LOADMETER MATL H.T.S EN.24. CONDITION Z.

3 3/8"

Z

Z

1·500" DIA.

1·125" DIA.

4 3/4" DIA.

1/16"

2·814" DIA. (OUTSIDE)

2·748" DIA. (INSIDE)

FRACTIONAL DIMENSIONS ±·010"

LOADMETER DESIGN DETAILS

FIGURE NO. 33

The centre cylinder of the loadmeter was ground to size, the outer and inner diameters being calculated to give a 0.02 per cent strain for a load of 2000 lbf., which was the maximum rated capacity of the bull-block. The end flanges of the loadmeter were machined intergrally with the main body and large fillet radii were ground at the junctions between them and the cylinder. This was considered necessary in order to reduce the tendency for cracking during heat treatment and subsequent vibrational working. One end of the meter was designed so that it could be screwed and locked on to the oscillator piston, while the other end was designed for mounting a die and the die holder assembly.

The mild steel cover was made in two halves and was fixed on to the loadmeter body by six screws. A small hole was provided in the cover to allow the leads to be connected to a plug which was mounted on a terminal bridge.

Sixteen 75 ohm. foil gauges were bonded on the ground surface of the loadmeter with Araldite (an epoxey resin adhesive). This type of gauge was chosen because of its known characteristics and sensitivity. Prior to mounting the gauges, the surface of the loadmeter cylinder was roughened and cleaned with a degreasing agent, trichlorethylene. Eight gauges were aligned longitudinally with the axis of the loadmeter, while the remaining eight were lined transversely. The relative positions of the

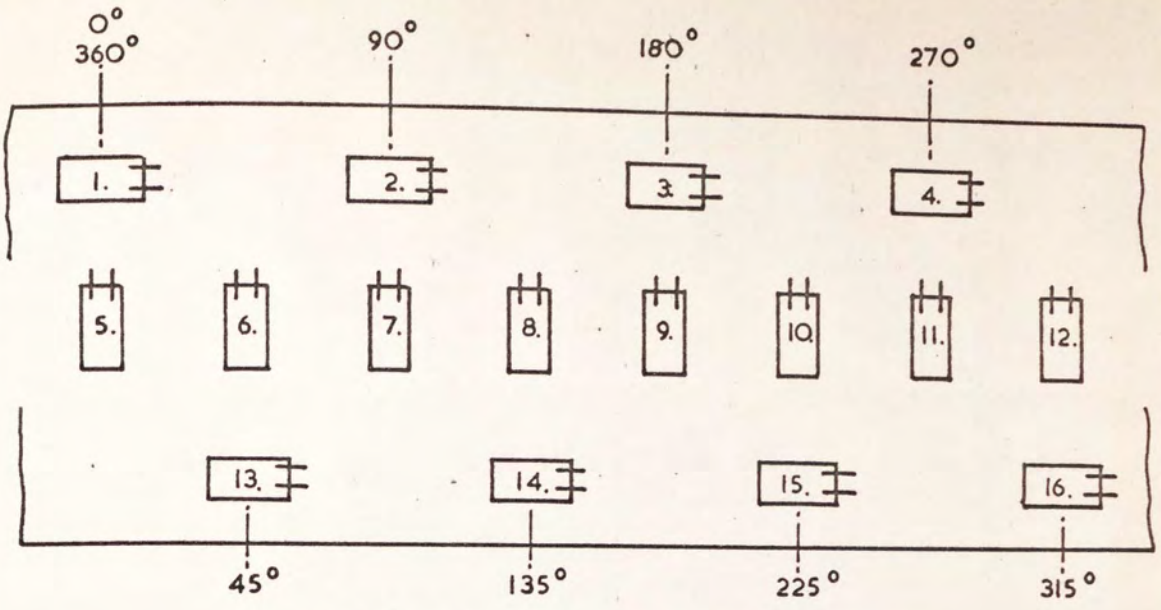

DEVELOPMENT OF LOADMETER COLUMN

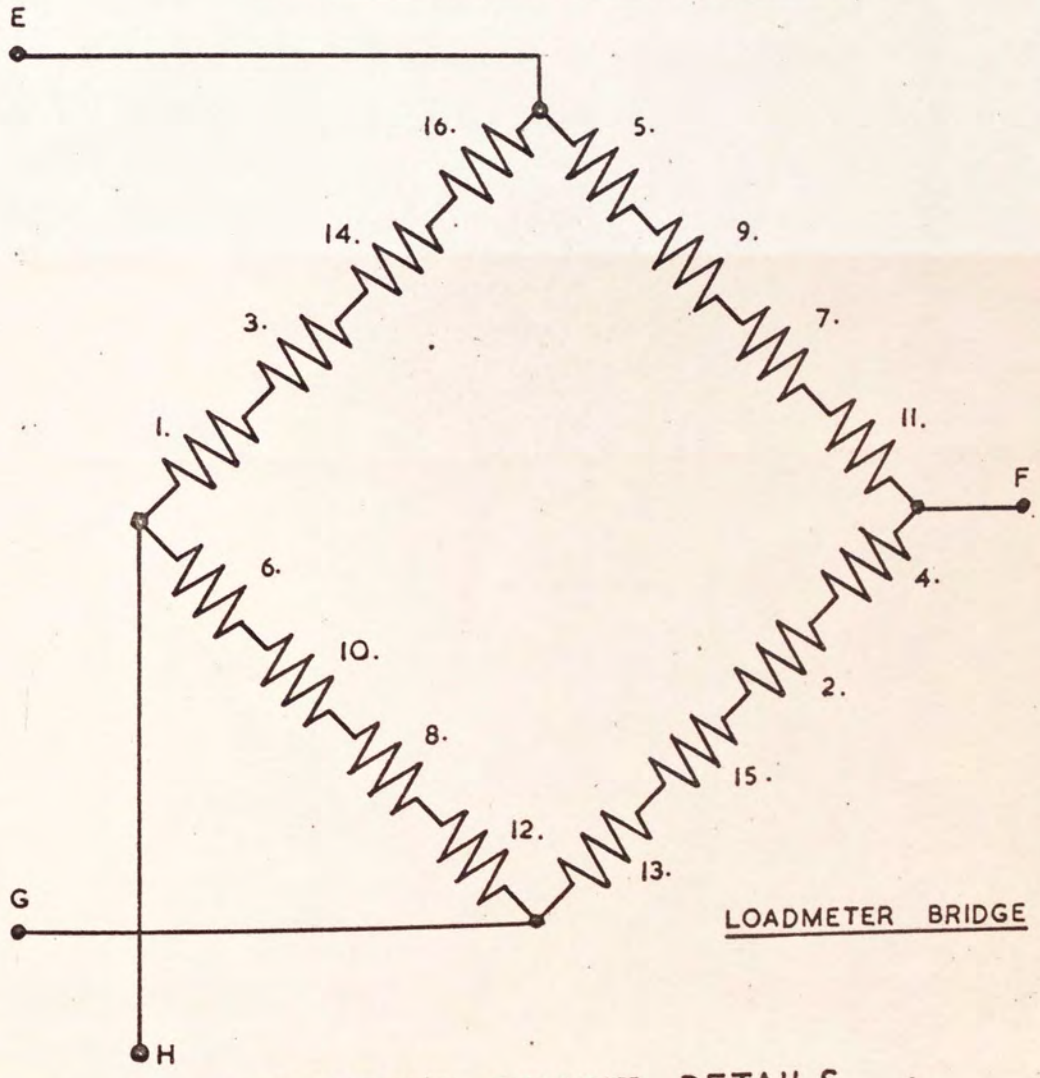

LOADMETER BRIDGE

LOADMETER CIRCUIT DETAILS

FIGURE NO. 34

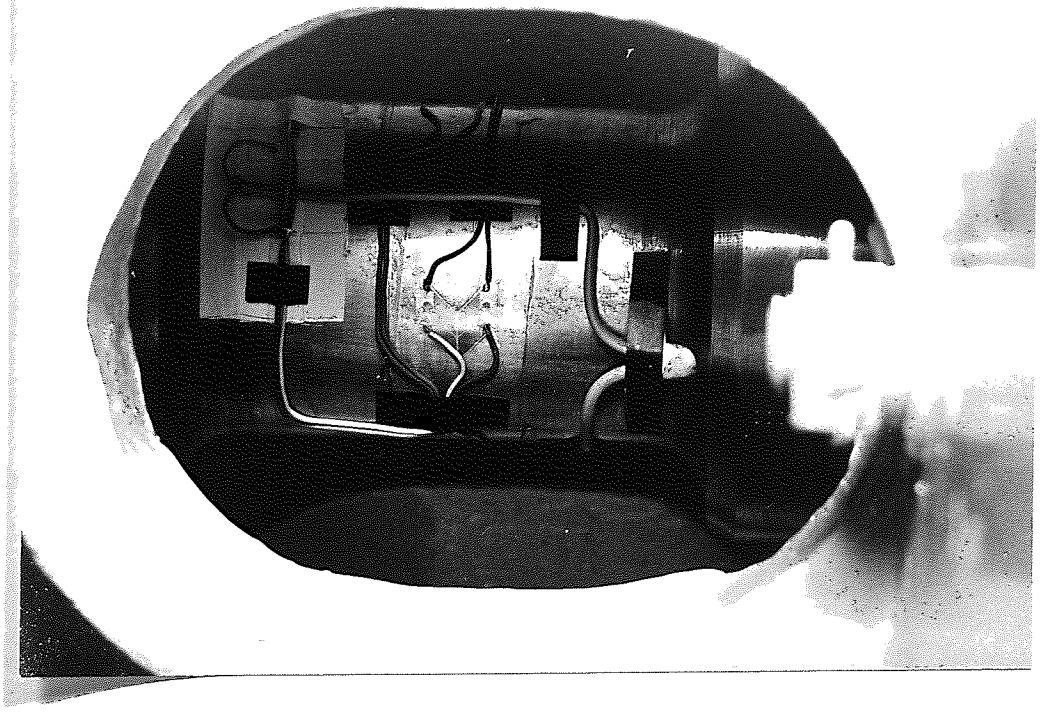

FIG.NO. 35. TORQUEMETER STRAIN GAUGE BRIDGE

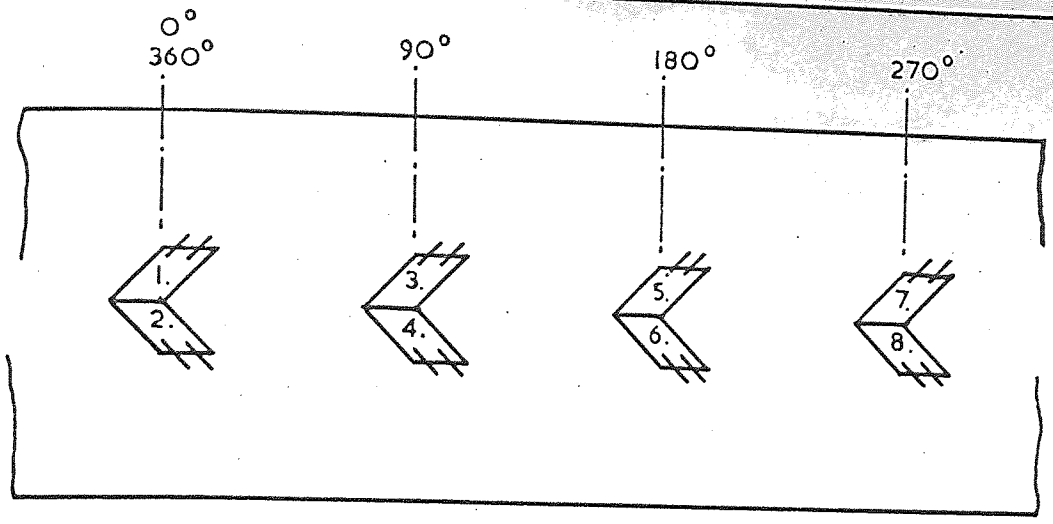

DEVELOPMENT OF TORQUEMETER COLUMN

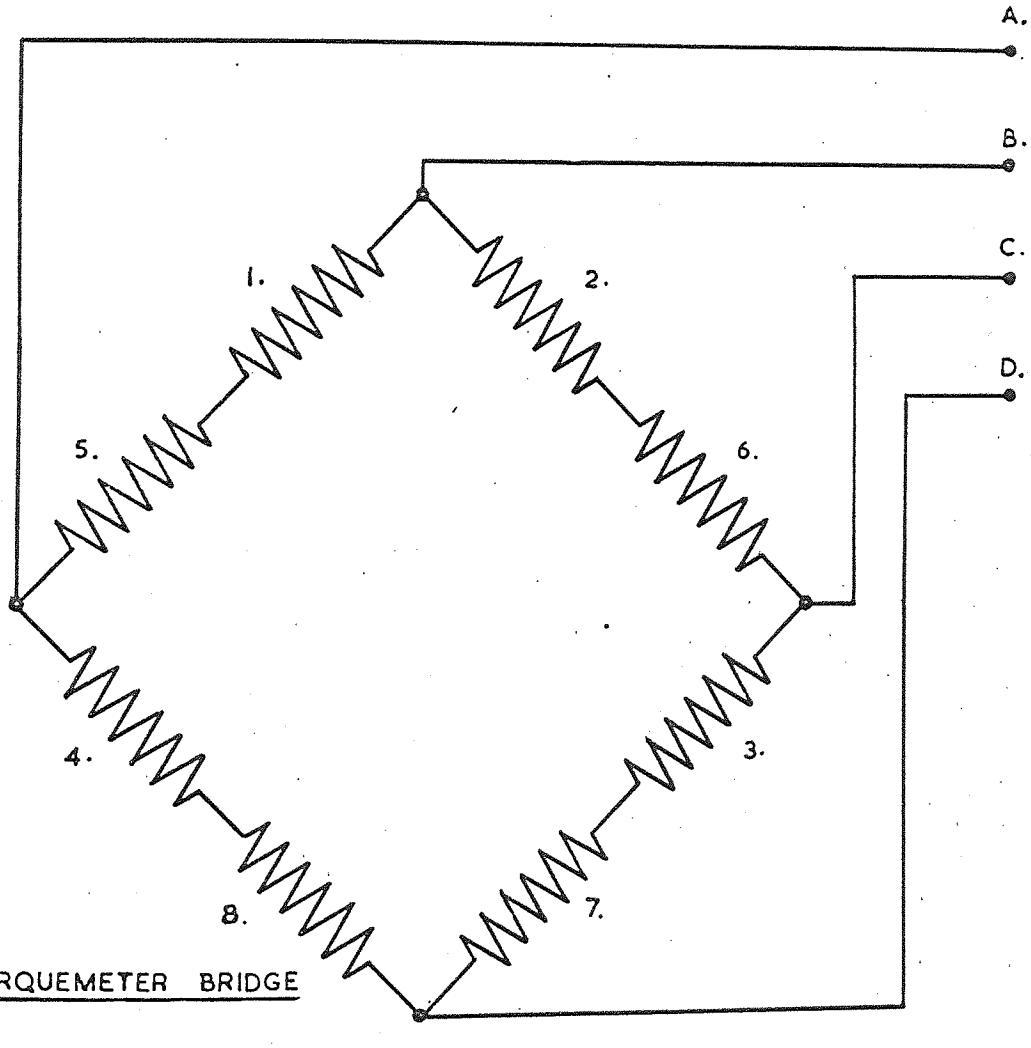

TORQUEMETER BRIDGE

TORQUEMETER CIRCUIT DETAILS

FIGURE NO. 36

gauges are shown diagrammatically in Fig. No. 34 .

After bonding, each gauge was checked for continuity and resistance to earth. The gauges were connected into a Wheatstone bridge as shown in Fig. No. 34. The bridge was connected this way to ensure that the loadmeter was fully temperature compensated and that any bending effects caused by the application of eccentric loads were eliminated. When the gauges had been connected, the loadmeter was allowed to dry in an oven at a temperature of 60 degrees Celsius for a period of 24 hours. The bridge continuity and resistance to earth were again checked, and at this point in the preparation of the loadmeter, the resistance to earth was found to in excess of 100 megohms.

Lastly, in order to make the strain gauge bridge moisture proof, di-jell was heated until molten and then poured into the space between the gauges and the cover. The gauges were protected against too rapid a rise in temperature by a thin layer of di-jell. When the loadmeter had cooled it was again tested for continuity and insulation resistance. The latter was found to be greater than 100 megohms.

5.2. Torquemeter.

The torquemeter details are shown in Figs. No.35 and 36. Four torque foil gauges, 300 ohms each, were bonded to the drum shaft which had been roughened, degreased and cleaned. After bonding, the gauges were tested, 'wired-up',

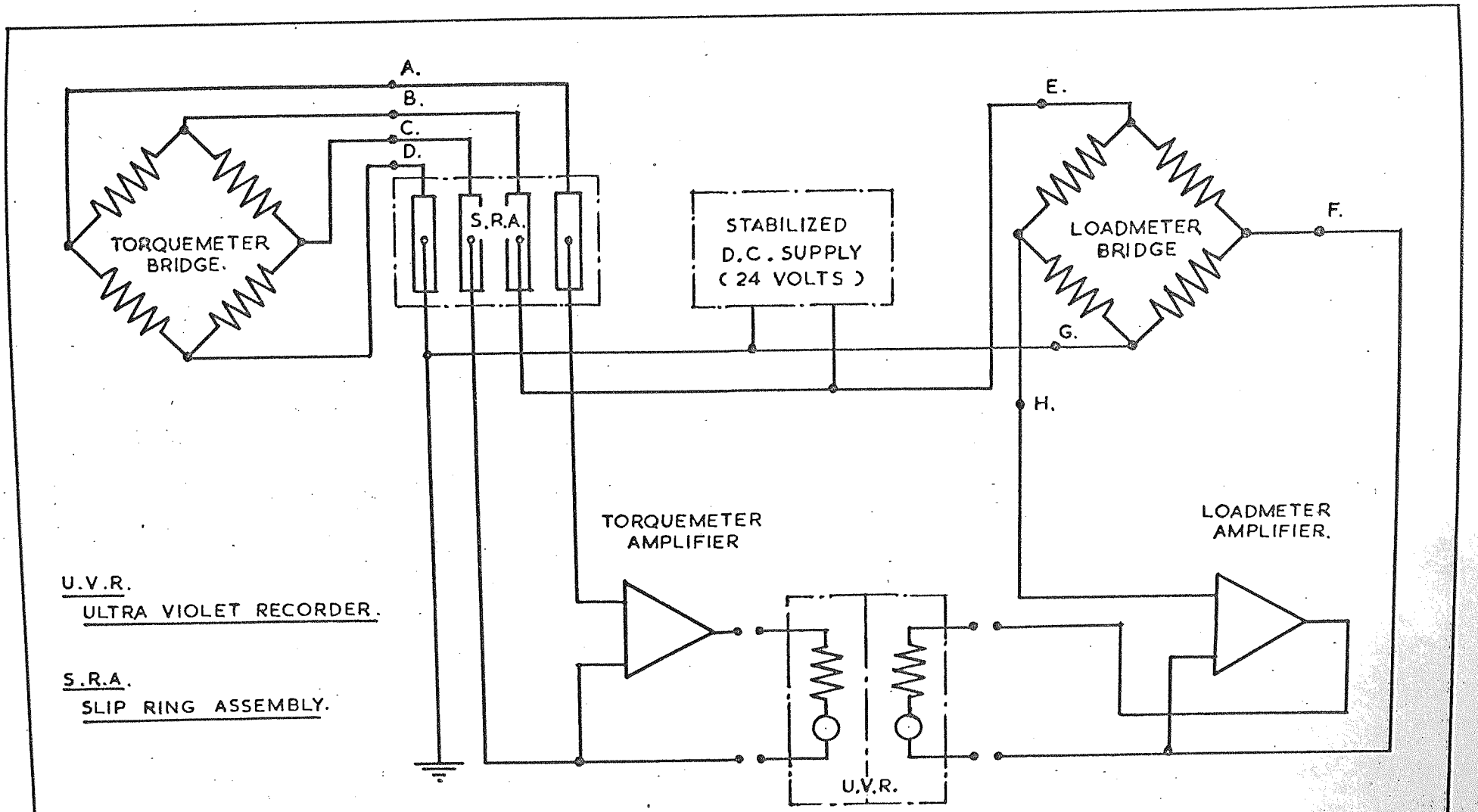

LOADMETER AND TORQUEMETER CIRCUIT DIAGRAM

FIGURE NO. 37

sealed against moisture and finally tested again by the same procedure that was adopted during the construction of the loadmeter.

The leads from the torquemeter bridge were connected to a slip ring assembly which was mounted at the drive end of the shaft. This assembly had silver graphite brushes and gave an electrical noise level of less than 8 micro-volts per milliampere. A complete specification of the slip ring assembly is included in Appendix No.16.9.

The torquemeter was connected in parallel with the loadmeter as shown in Fig. No.37. The bridge input currents were supplied from a 24 volt stabilised d.c. supply, while the bridge outputs were recorded on two channels of an ultra violet galvanometer recorder. A specification of the recorder is included in Appendix No.16.9. Because of the high frequency response galvanometer required (ie. 500 c/s.), it was necessary to incorporate two d.c. amplifiers in the circuit between the bridge outputs and the galvanometer inputs. Details of the amplifiers are given in section 5.3.

Throughout the circuitry special attention was given to insulation and screening. It was found essential to screen each pair of input and output leads and to earth and screen the amplifiers. The loadmeter-torquemeter circuit with all other electrical equipment was earthed to the bull-block. Special care was paid to the types of cable and plugs used. Heavily insulated, twin core, screened

cable was employed to reduce capacitive effects, and gold plated multi-pin plugs were used to provide good electrical contact.

5.3. D.C. Amplifiers.

In order to provide sufficient current to drive the galvanometers, it was necessary to amplify the loadmeter and torquemeter outputs, ie. a current of the order of 1.5 milli-amperes was required to drive the galvanometer and is equivalent to a drawing force of 1500 lbf. A number of commercially available amplifiers were tested but at the relatively low gain required, approximately 100, the pick up and noise levels were found to be excessive. To overcome this problem it was decided to design and build two fixed gain amplifiers.

The amplifiers were two stage, transistorised and gave a gain of 100 times. Although the amplifiers were built for a fixed gain, it was possible to change this by increasing or decreasing the first stage output resistors R_1 and R_2. If these two resistors were increased twofold, then the gain would be approximately doubled. However, by increasing the gain in this way the noise level and drift would also be increased. The amplifiers were designed to operate with a 300 ohm bridge and a 24 volt stabilised d.c. supply. The latter being used to drive the amplifier and to supply the strain gauge bridge input current. The amplifiers were also manufactured to incorporate the following -

(1) A Bridge Balance - In order to balance the strain gauge bridge outputs to zero for a zero strain, a 1000 ohm variable resistance was provided in each amplifier.

(2) Drift Compensation - This was achieved in two ways as follows -

(a) To overcome drifting due to small variations in the supply voltage, the components in each stage were matched as closely as possible.

and (b) To overcome drifting due to temperature variations in this amplifier, each pair of stage transistors was incorporated in a heat sink and connected so that the algebraic sum of the drifts caused by each transistor would be zero.

(3) Damping Resistance - In an attempt to provide the galvanometers with the correct damping resistance and hence obtain a 'flat' frequency response, a capacitance-resistance network was incorporated into each amplifier.

Before finally connecting the amplifiers in the loadmeter-torquemeter circuits, a series of commissioning tests were performed. The results of these tests were as follows -

(1) When the bridge out-of-balance was large, it was found that there was insufficient resistance to balance the bridge, and hence it was necessary to increase the variable resistance to 2000 ohms.

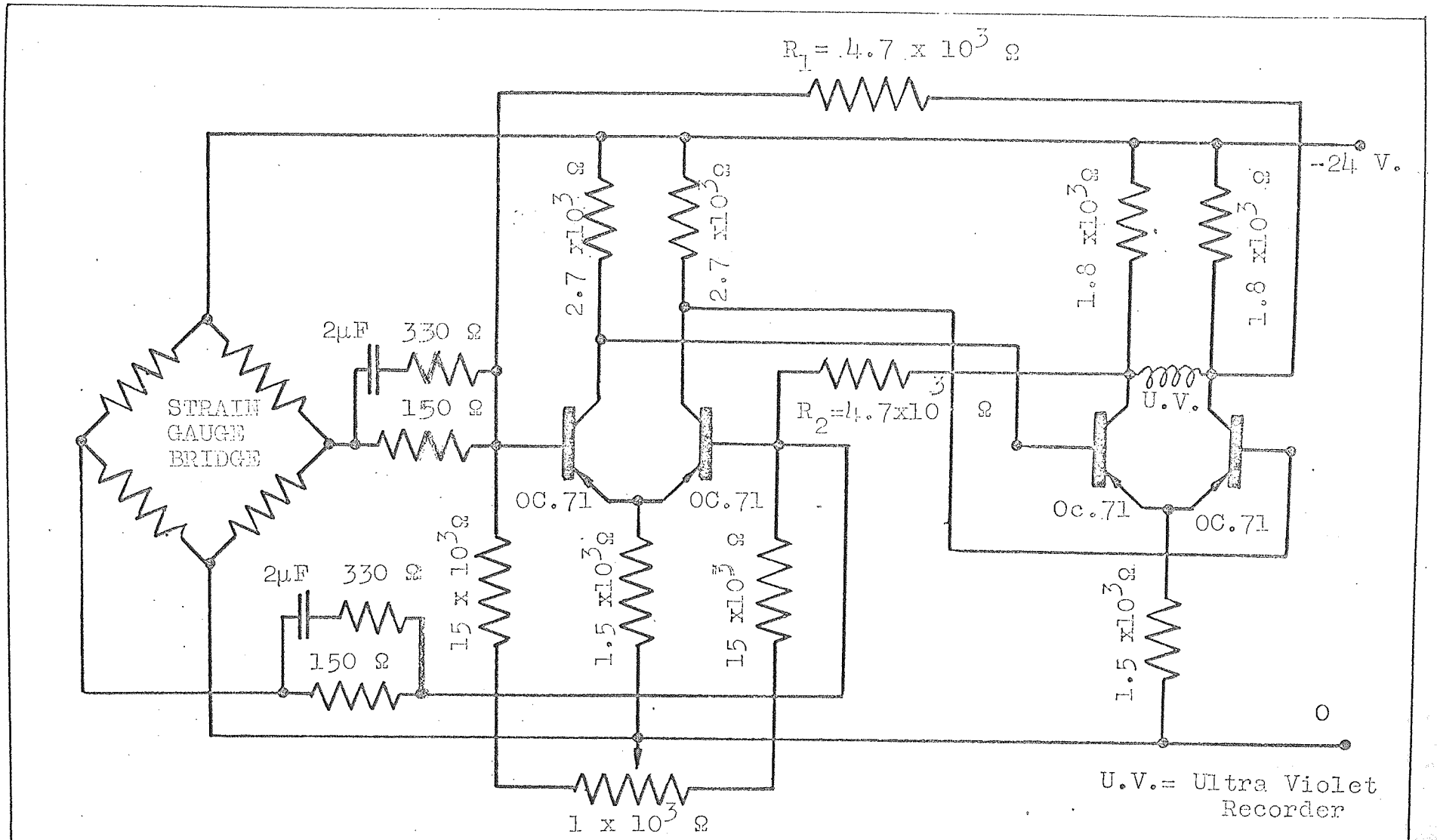

FIG. NO. 38. CIRCUIT DIAGRAM OF D.C. AMPLIFIER

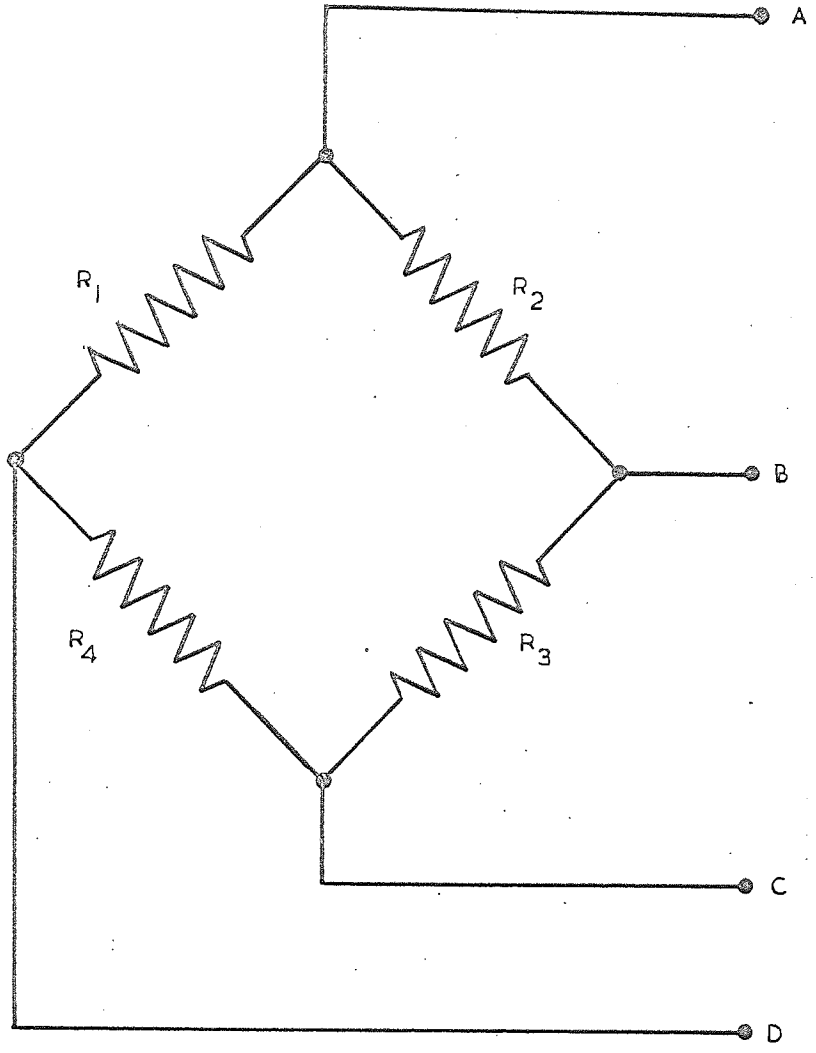

R1 = ACTIVE GAUGE

R2 = R3 = R4 = INACTIVE GAUGES

FIG. NO. 39 STRAIN GAUGE BRIDGE ON WIRE CIRCUIT DETAILS

(2) The drift was found to be negligible, amounting to approximately 25 micro-volts per degree Celsius.

(3) The damping characteristics of the galvanometer were found to vary considerably and hence it was only possible to match each amplifier to a particular galvanometer. Because of the difficulty of modifying the amplifier to suit each galvanometer used, it was decided to accept the variation and to obtain a number of frequency response curves for each galvanometer used.

These curves are included in Appendix No.16.13.

(4) No electrical noise level was detected.

A circuit diagram of the amplifier is shown in Fig. No.38.

5.4. Strain Gauge Bridge on Wire.

To check the magnitude of the force variation induced in the wire as it left the die, a series of tests was carried out with a strain gauge bridge on the wire. The bridge consisted of two active gauges mounted directly on the wire and six dummy gauges mounted on a dummy length of wire made from the material being drawn. The dummy gauges were bonded on the block by the same procedure as that adopted when preparing the load and torquemeters, and then connected to form three arms of a Wheatstone bridge as shown in Fig. No.39. The two active gauges were aligned

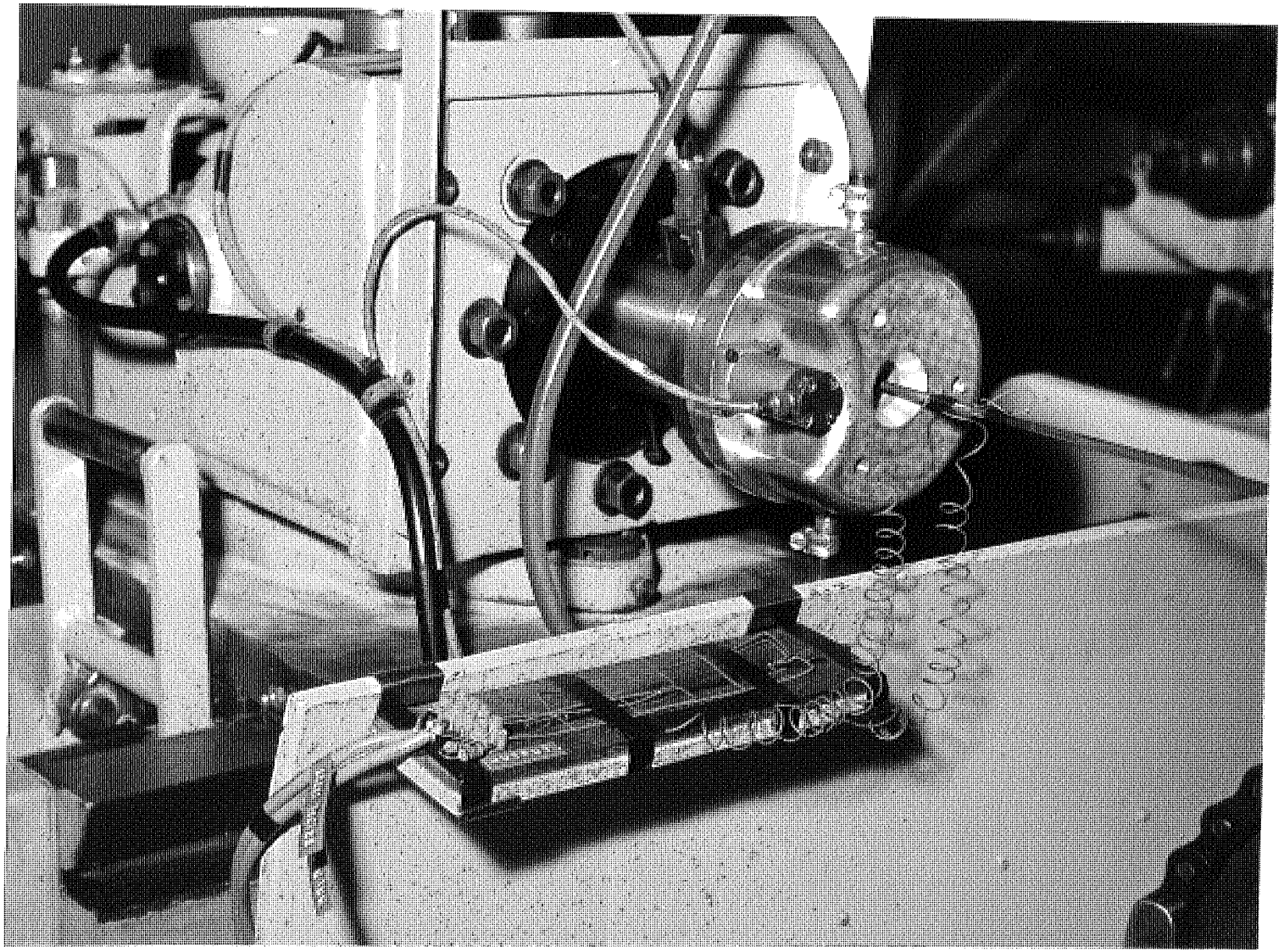

FIG. NO. 40

STRAIN GAUGE BRIDGE ON WIRE PRIOR TO THE START OF A TEST

longitudinally with the axis of the wire at points round the circumference 180 degrees apart. The procedure for mounting each set of active gauges was as follows -

(1) Before bonding the gauges, the wire was roughened, degreased and cleaned.

(2) The gauges were checked for continuity and bonded to the wire with Araldite.

(3) The gauges were held in place on the wire by a simple wooden clamp and the adhesive was allowed to cure under an infra red light source at a temperature of approximately 80 degrees Celsius for a period of two hours.

(4) The gauges were tested for continuity and resistance to earth and finally 'wired-up' to form the remaining arm of the Wheatstone bridge as shown in Fig. No.39.

Fig. No. 40, shows the strain gauge bridge circuit on the wire prior to the start of a test.

5.5. Modification of D.C. Amplifier for Strain Gauge Bridge on Wire.

For a given drawing force, the strain produced in the wire was greater then that produced in the loadmeter, Hence, the strain gauge bridge on the wire required an amplifier which had a smaller gain than the amplifiers used with the loadmeter and torquemeter circuits. To achieve this, a third amplifier was built, but its design was

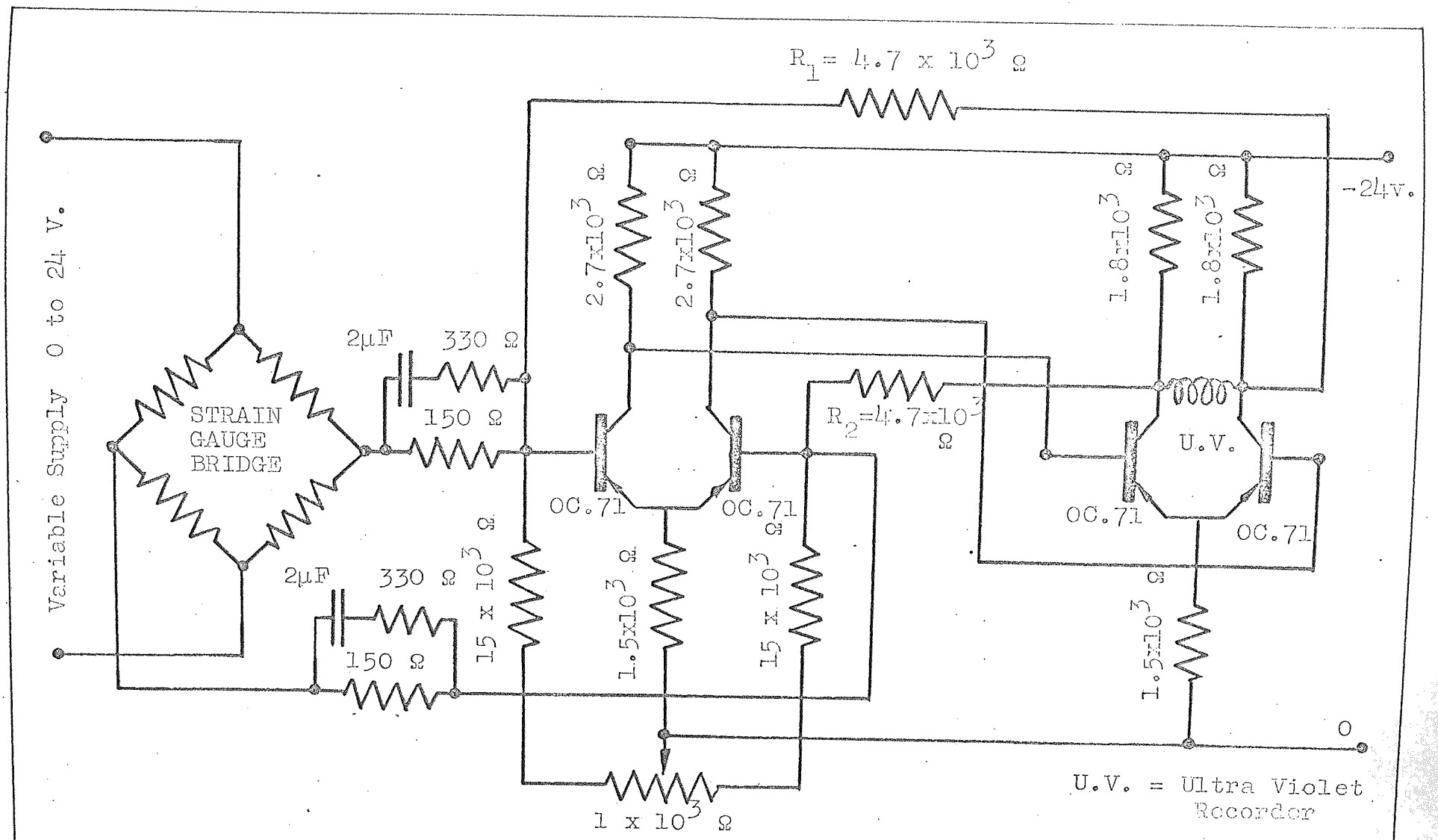

FIG. NO. 41. MODIFIED CIRCUIT DIAGRAM OF D.C. AMPLIFIER

modified to include a variable gain. This modification is shown in Fig. No. 41, and was as follows -

Instead of driving the amplifier and supplying the bridge current from the same voltage source, the bridge was supplied with a separate variable source (ie. variable from 0 to 24 volt). For the majority of tests, a bridge voltage of between 5 and 10 volt was used.

In order to use the basic design of the amplifier, it was necessary to arrange for the strain gauge bridge to have a resistance of 300 ohm. However, this proved to be difficult and could only be obtained by using two 130 ohm gauges and a 40 ohm fixed resistance in each arm of the bridge. The effect of adding a resistance was to reduce the sensitivity of the bridge, but since an amplifier was to be used, this was not considered to be a disadvantage. Furthermore, since care was taken in selecting four resistors of equal magnitude, and the bridge was calibrated before and after each test, the effect on the stability of the circuit was negligible.

5.6. Transducers for Measuring Amplitudes of Die and Drum Oscillation.

To measure the linear amplitude of die oscillation and the torsional amplitude of drum oscillation, two seismic-mass transducers were used. The outputs from these transducers were connected to two channels of a vibration meter. The meter had provision for monitoring directly

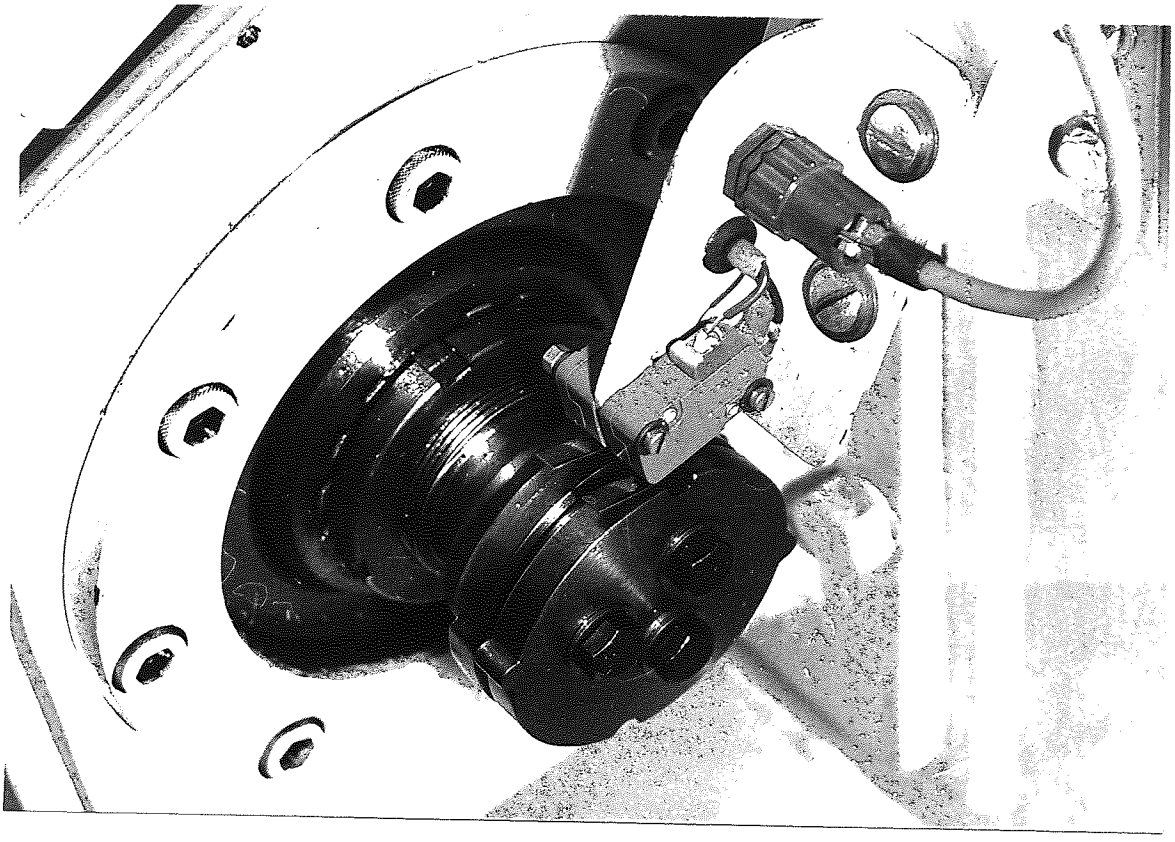

FIG. NO. 42 DETAILS OF DRAWING SPEED MEASUREMENT

the linear displacement and velocity, in (in.) and (in/s.), and the torsional displacement and velocity, in (degrees) and (degrees/s.).

A specification of the transducers and the vibration meter is included in Appendix No. 16.9.

5.7. Measurement of Drawing Speed.

The drawing speed was obtained by measuring the time taken for the worm shaft to rotate through a quarter of a revolution. The conversion of time to drawing speed was made from geometrical considerations of the drive pinion-worm shaft assembly. The computation of the drawing speed is given in Appendix No.16.3. The time interval was recorded on a digital counter, the details of which are included in Appendix No.16.9. The mechanism developed for triggering the counter was as follows -

Two circular cams were mounted on the worm shaft, each having been machined with two projections on its circumference at points 180 degrees apart. The cams were assembled so that these projections were arranged at 90 degree intervals round the shaft. The projections were provided to operate two micro-switches which were secured above the cams as shown in Fig. No.42. The micro-switches were connected in circuit with the digital counter, which also acted as a voltage source. The system operated as follows -

When the cam closed the micro-switch in circuit 'B'

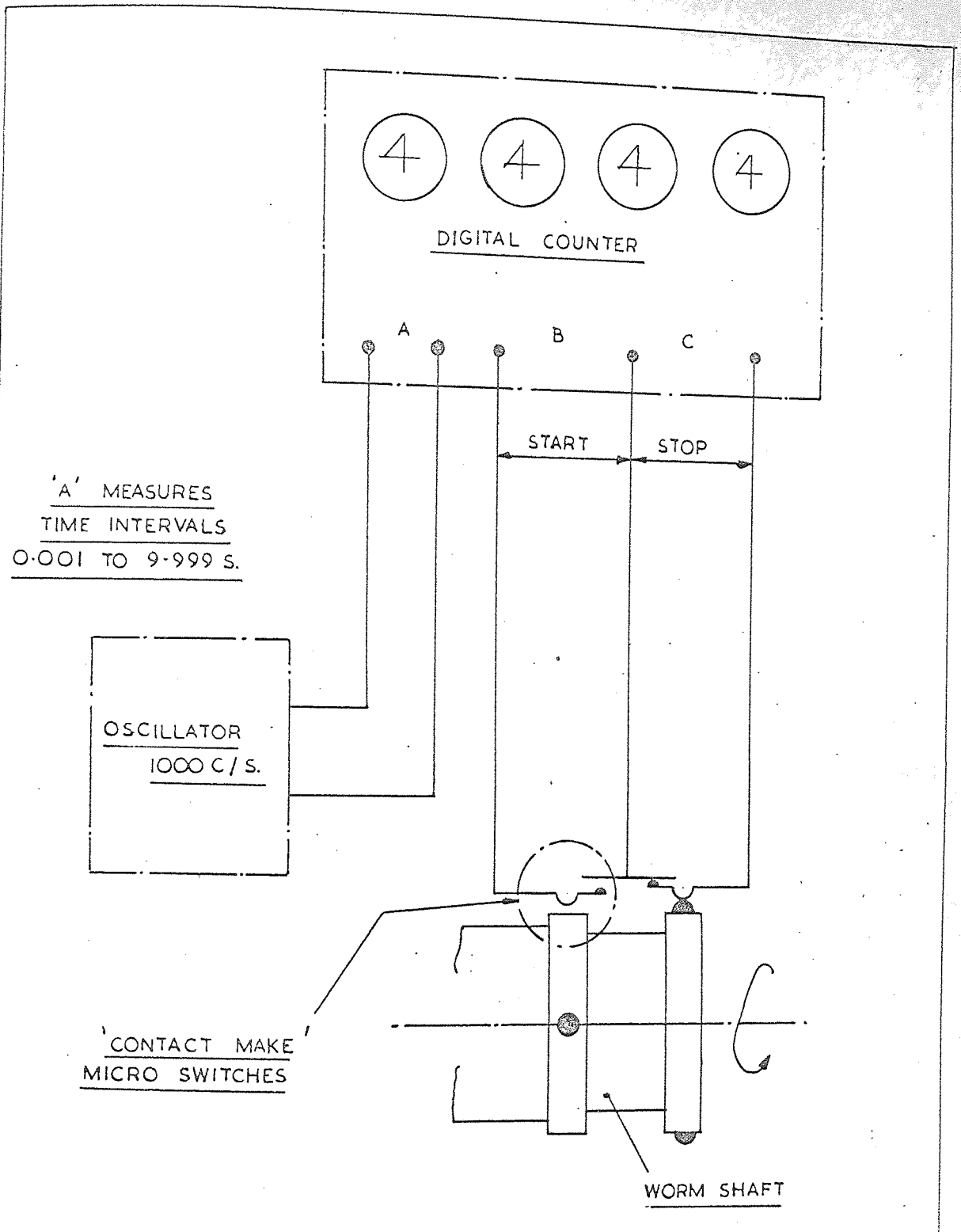

FIG. NO. 43 SCHEMATIC DIAGRAM OF DRAWING SPEED MEASUREMENT

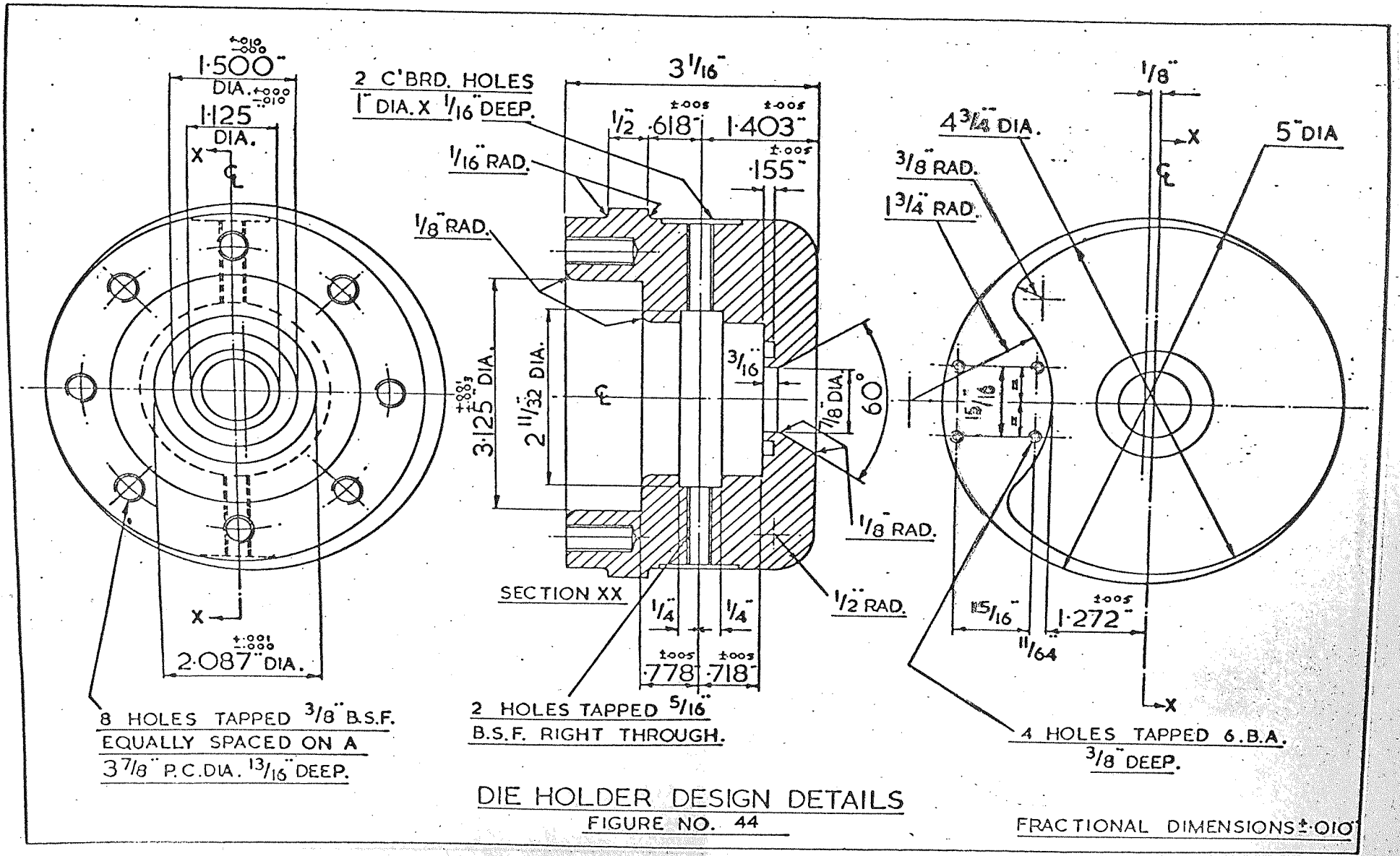

DIE HOLDER DESIGN DETAILS

FIGURE NO. 44

FRACTIONAL DIMENSIONS ±·010"

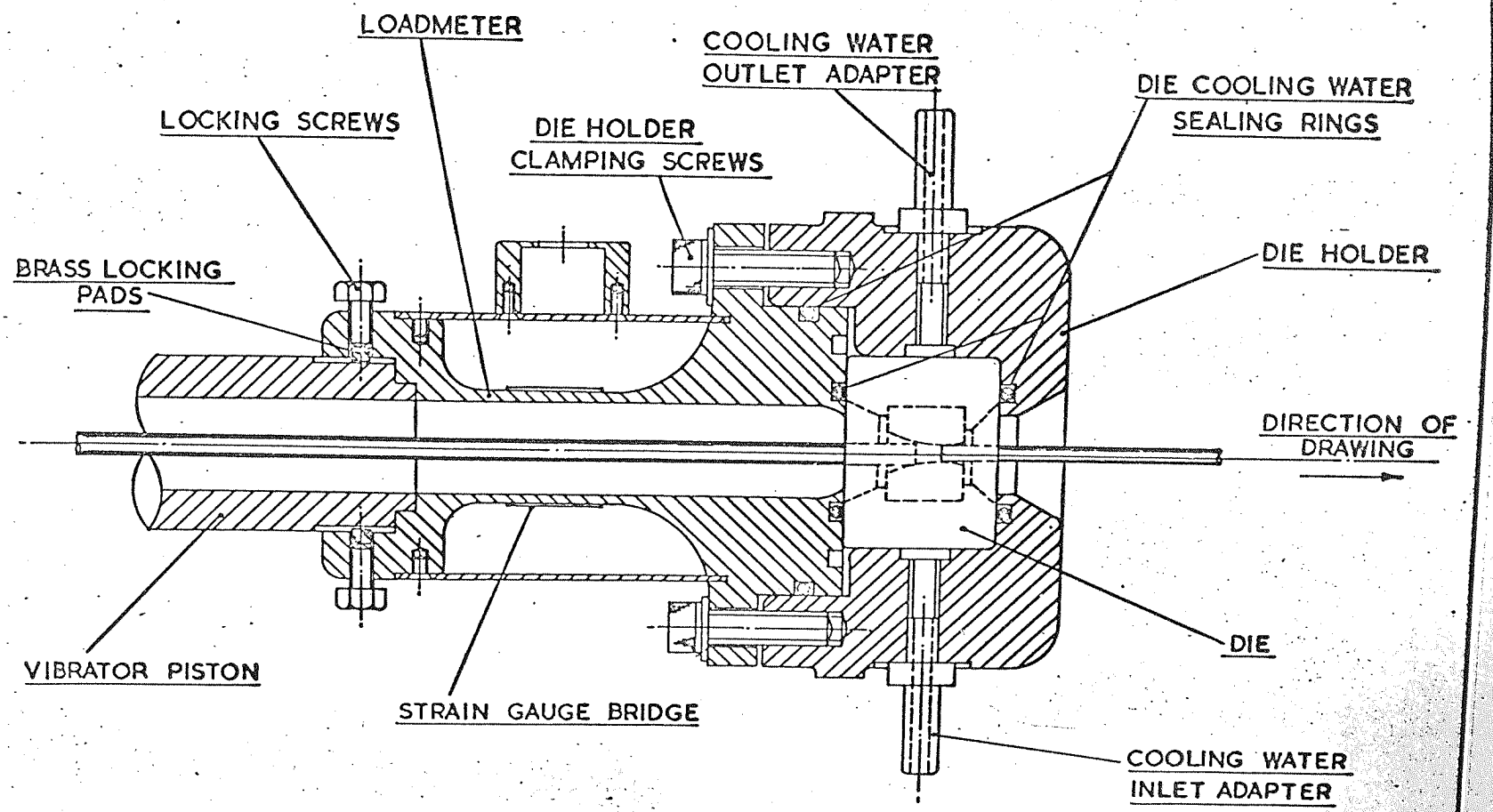

ASSEMBLY OF DIE AND LOADMETER

FIGURE NO. 45

(see Fig. No. 43), an electrical pulse instructed the counter to commence recording. The timing operation proceeded until the shaft rotated through 90 degrees and the second cam operated the micro-switch in circuit 'C'. An electrical pulse was again generated and the counter was instructed to finish recording. The system was arranged so that during the first quarter of a revolution of the shaft the counter recorded the time interval and during the second quarter of a revolution it monitored the recorded time. This cycle of recording and monitoring was repeated every one-half of a revolution of the worm shaft.

An accuracy of $\pm$ 0.001s. was obtained by supplying the counter with a reference signal of 1000 c/s.

5.8. Design of Die Holder Assembly.

To support the die on the loadmeter a die holder was manufactured as shown in Fig. No. 44. It was made from a solid bar and was designed to provide location for the linear seismic transducer. The holder was machined internally so that sealing rings could be incorporated to prevent the cooling water from escaping or from contaminating the soap lubricant.

The holder was clamped to the loadmeter by eight 3/8 B.S.F. cap screws as shown in Fig. No.45.

The analysis undertaken to correlate the loadmeter and torquemeter readings, revealed that the inertia of the die holder assembly was an important parameter. Therefore,

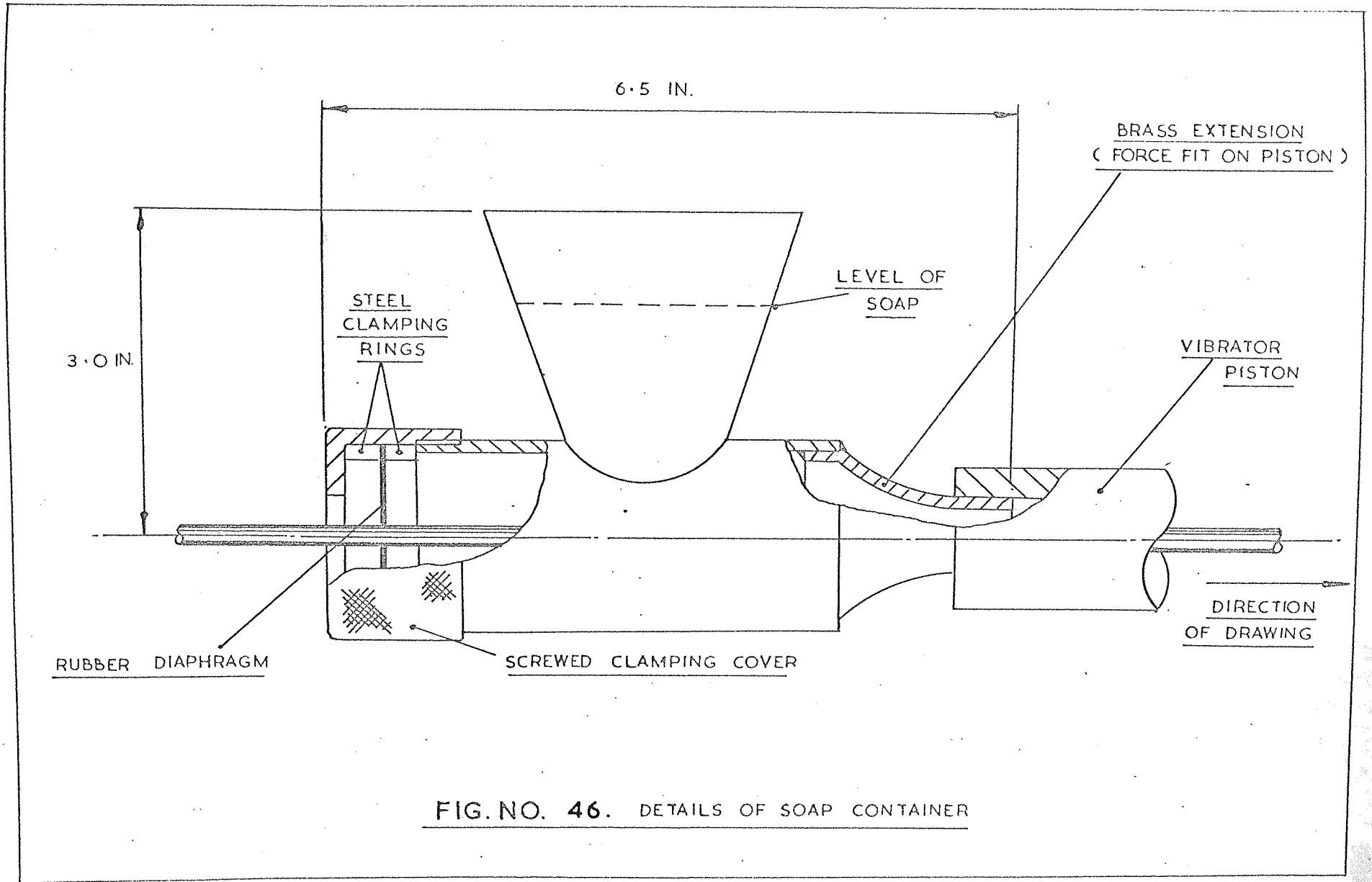

FIG. NO. 46. DETAILS OF SOAP CONTAINER

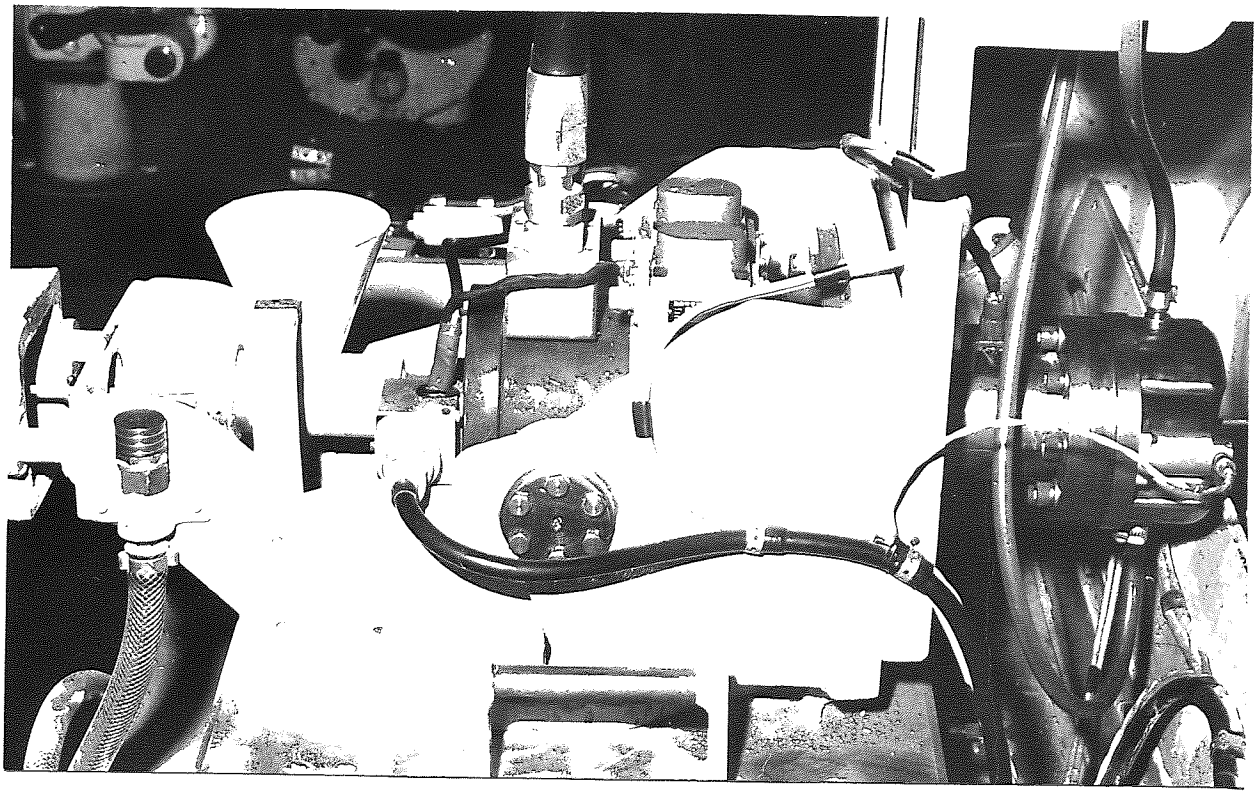

FIG. NO. 47 GENERAL VIEW OF DIE-LOADMETER - OSCILLATOR ASSEMBLY

to investigate this variable, two holders were manufactured, one from an alloy steel, Vibrac 45,and the other from an aluminium alloy, Duralumin. This resulted in equivalent die holder assembly weights of 21.2 and 13.8 lbf. respectively.

The die cooling water was supplied from a reservoir situated directly above the die assembly. The inlet and outlet pipes were provided by two 3/8 in. diameter plastic tubes.

Prior to entering the die, the wire passed through a soap container, details of which are given in Fig. No.46. A rubber diaphragm was used to prevent the soap from escaping from the container at the wire entry. The diaphragm was designed with a hole in it,approximately 0.050 in. smaller in diameter than the material being drawn, and hence the tightness of the rubber on the wire formed a seal.

A general view of the oscillator-loadmeter-die assembly is shown in Fig. No. 47.

6. Calibration of Apparatus

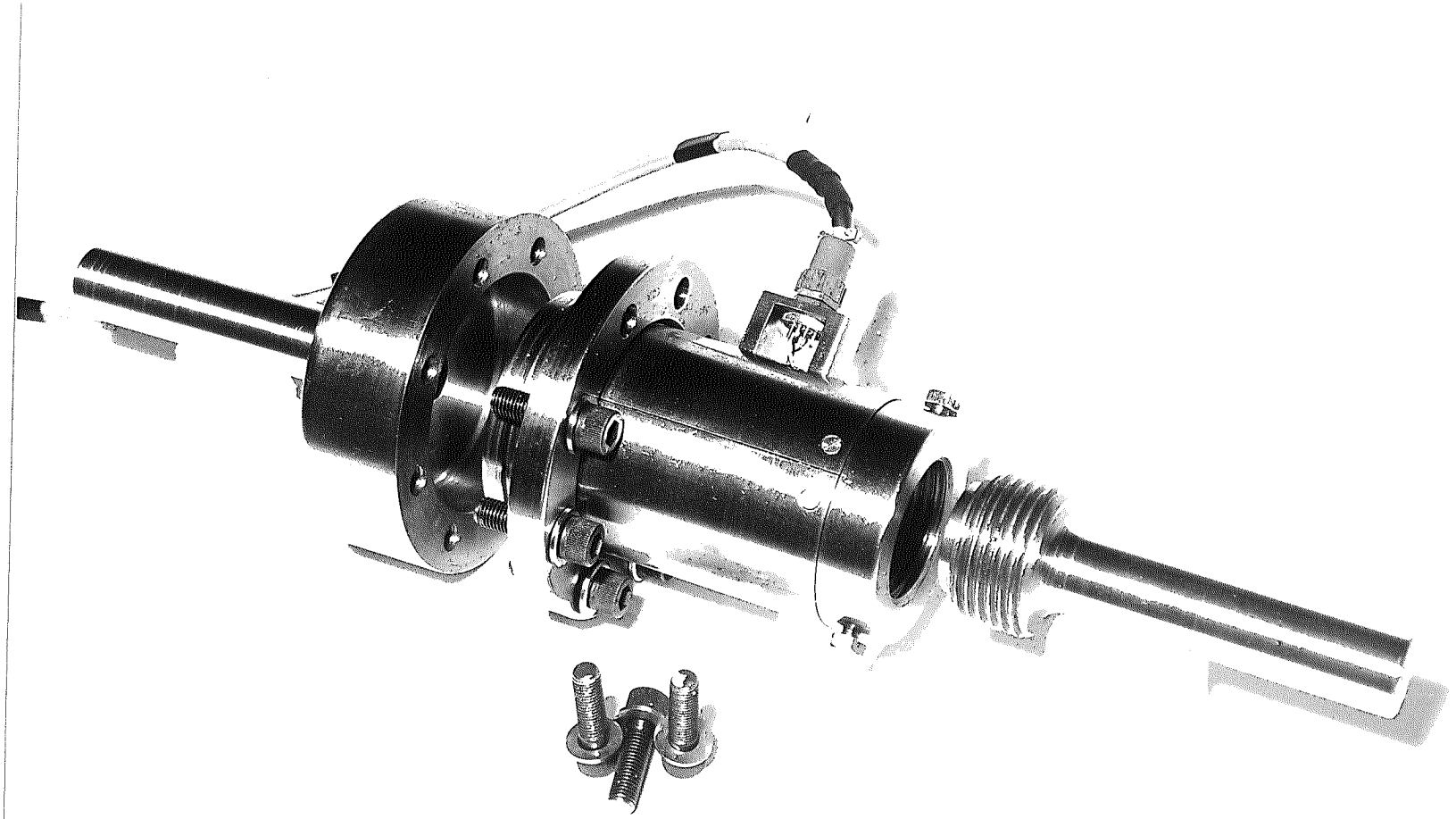

FIG.NO. 48. LOADMETER WITH ADAPTORS FOR CALIBRATION

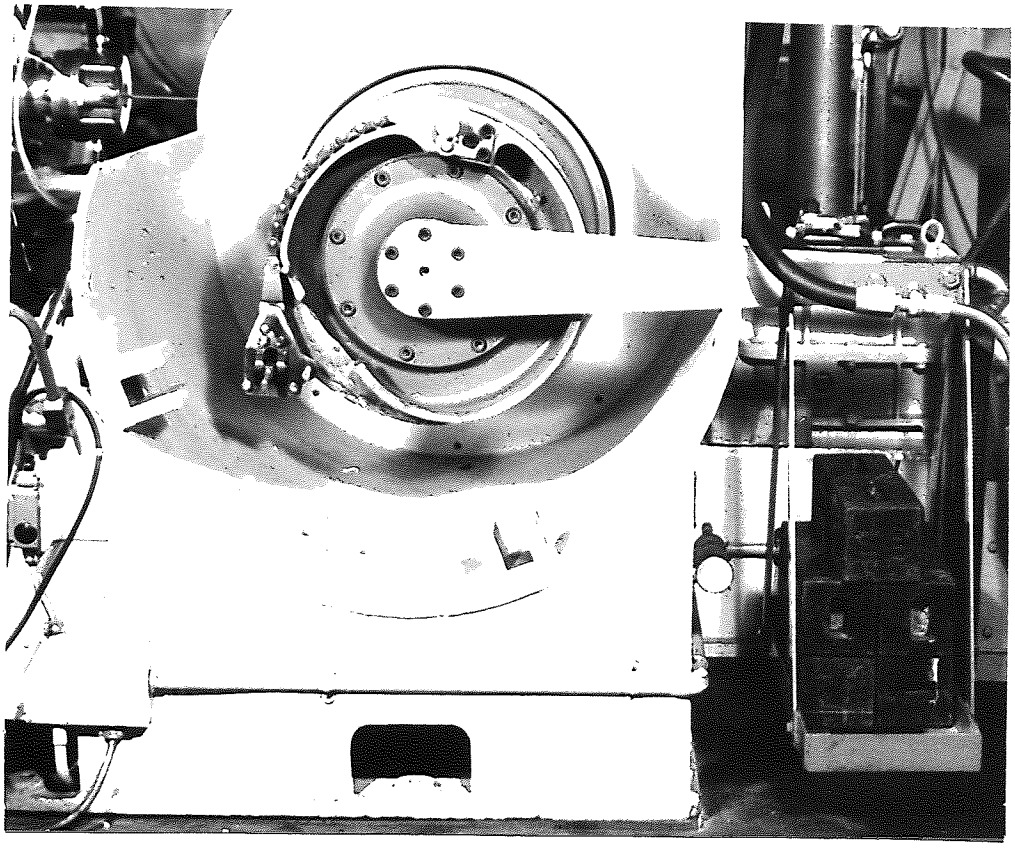

FIG. NO. 49. TORQUEMETER CALIBRATION

6. Calibration of Apparatus.

6.1. Loadmeter.

The loadmeter was calibrated in tension using a Denison dead weight testing machine. To enable the loadmeter to be held in the machine jaws, it was necessary to design two adapters. These were machined from mild steel, EN.6A, and were manufactured as shown in Fig. No.48.

Prior to each calibration, the electronic equipment was allowed to 'warm-up' for a period of approximately 30 minutes to allow the d.c. amplifier to obtain stable conditions.

Loads were applied to the loadmeter in steps of 200 lbf. rising to a maximum of 2000 lbf. and returning to zero. The deflection of the galvanometer trace was related to each load step. This procedure was repeated several times to enable an accurate mean curve to be obtained.

Two galvanometers of different sensitivities were used in the recorder and typical calibration curves for these are included in Appendix No.16.12.

6.2. Torquemeter.

The torquemeter was calibrated by loading weights on a torque arm which was fixed to the drum shaft. The torque arm had a radius of 24 inches, and was mounted at the free end of the shaft as shown in Fig. No.49. To prevent rotation of the drum during loading, the shaft

drive pinion was locked in position with the torque arm horizontal.

The procedure for allowing the circuit to attain stable temperature conditions, was the same as that adopted for calibrating the loadmeter.

Weights were applied to (or removed from) the torque arm in increments of 100 lbf. up to a maximum of 800 lbf. This maximum load was equal to a torque of 1600 lbf. ft. and a drawing force of 2120 lbf. A representative calibration curve is included in Appendix No. 16.12.

Note :- for reasons of simplicity of calibration, the torquemeter was calibrated by subjecting it to a torque in the opposite direction to that which it experienced during wire drawing. This was considered justifiable because

(1) Only small elastic strains were present.

and (2) The non-oscillatory drawing force predicted by the torquemeter agreed, to with $\pm$ 2.5. per cent, with that predicted by the loadmeter.

The loadmeter and torquemeter were calibrated at regular intervals during the experimental work, but no detectable variation was found.

6.3. Strain Gauge Bridge on Wire.

The strain gauge bridge on the wire was calibrated against the loadmeter and torquemeter. The calibration was carried out before and after each test and was achieved

as follows -

While a length of wire was being drawn under non-oscillatory conditions, the d.c. bridge voltage was arranged so that a galvanometer deflection of the order of 5 cm. was obtained. The magnitude of the drawing force corresponding to this deflection was determined from the loadmeter and torquemeter records. The deflection of the galvanometer was assumed to be directly proportional to the force in the wire and hence a calibration factor 'a' was determined.

$$\text{i.e. Calibration factor 'a'} = \frac{\text{force in wire (lbf.)}}{\text{galvanometer deflection (cm)}}$$

When drawing with superimposed oscillatory energy, the force variation in the wire was obtained by multiplying the recorded galvanometer deflection by the calculated calibration factor 'a'.

The assumption that the galvanometer deflection was directly proportional to the drawing force was considered to be justifiable since, both the load and torque meters, produced linear calibrations using very similar amplifier circuits.

6.4. Amplifier Frequency Response.

To calibrate the d.c. amplifiers for frequency response, the amplifier circuits were modified as shown

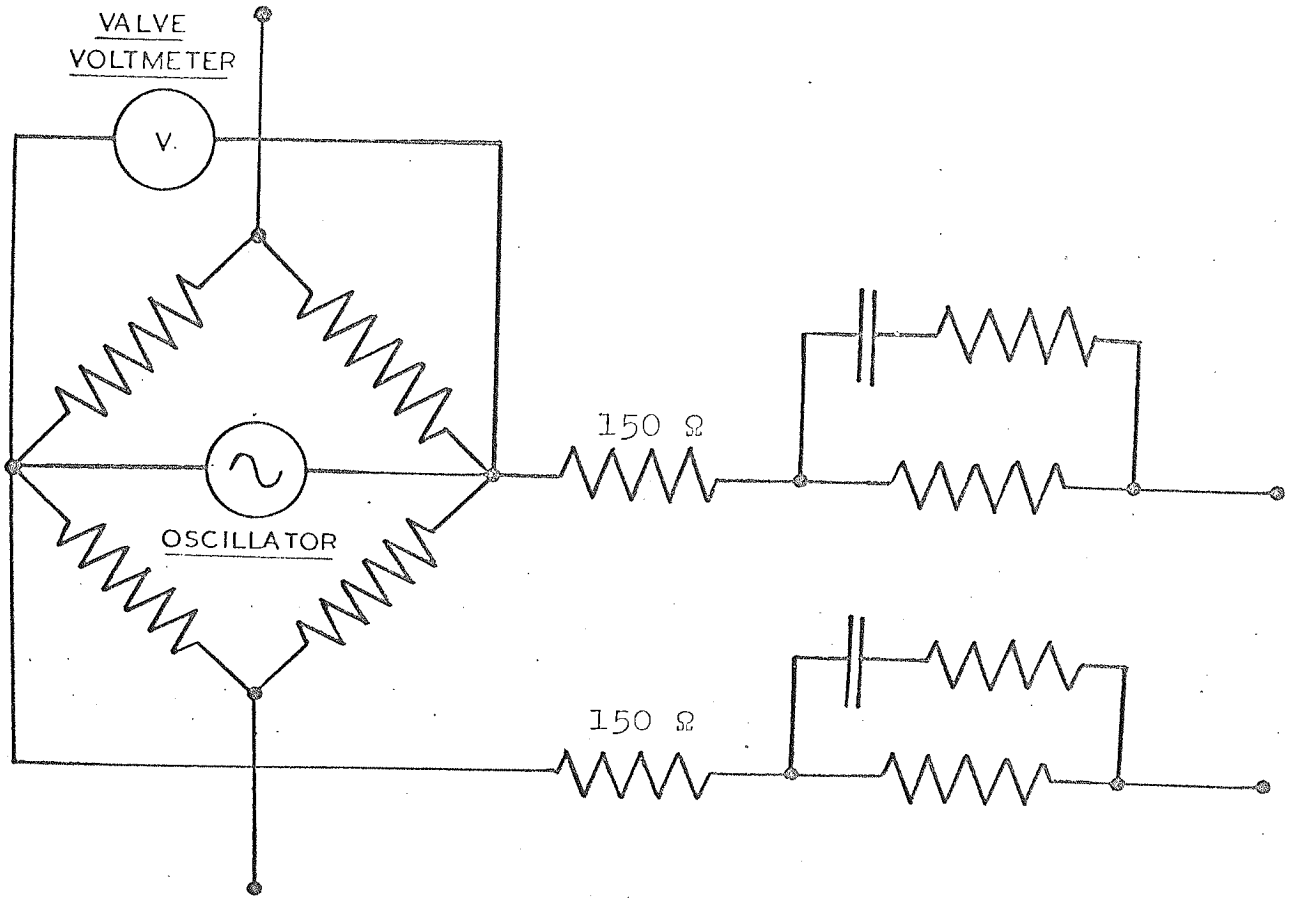

FIG. NO. 50. MODIFICATION TO D.C. AMPLIFIERS FOR FREQUENCY RESPONSE TESTS

in Fig. No.50. The two 150 ohm resistors were added to the circuits so that the oscillator, connected across the bridge output, was fed into an equivalent 300 ohm bridge. The transistorised oscillator superimposed a sinusoidal voltage on the equivalent bridge circuit. The signal was maintained constant by connecting a valve voltmeter in parallel with the oscillator. The frequency response curves were obtained as follows -

(1) The oscillator was arranged to supply a 0.001 volt signal and the corresponding galvanometer deflection was recorded.

(2) The signal was kept constant and the frequency was varied from d.c. up to 500 c/s. in 100 c/s. intervals.

(3) A frequency response curve of the ratio of recorded to 'true' galvanometer deflection against frequency, was plotted.

Note - the 'true' galvanometer deflection was the deflection corresponding to the d.c. signal.

The above procedure was repeated for voltage signals of 0.003, 0.006 and 0.009 volt, but the degree of attenuation or amplification of the input signals was found to be independent of the magnitude of the input voltage. The response curves are included in Appendix No. 16.13.

6.5. Torsiograph.

The Bell and Howell torsiograph had been designed so that its output was matched directly to the impedance of the vibration meter. The calibration of the torsiograph was carried out by the instrument manufacturer. During the early oscillatory drawing tests, it was believed that the torsiograph was producing an error of two, ie. it was thought that the instrument was recording the zero to peak amplitude of drum oscillation and not the peak to peak amplitude as indicated in the instrument specification. To check this phenomenon, the Bell and Howell torsiograph was calibrated against a Southern Instruments transdueer. This instrument had the advantage of a direct mechanical calibration but the disadvantage that it required complicated associated electronic control equipment. The calibration revealed that, as anticipated, the Bell and Howell instrument was reading the zero to peak amplitude, but otherwise, it was found to give accurate values of torsional amplitude.

6.6. Linear Transducer.

The linear transducer operated on the same principle as the torsiograph and therefore it was considered necessary to calibrate it prior to testing. The calibration was performed with a cathetometer as follows -

(1) The die was set to oscillate at a peak to peak amplitude indicated by the vibration meter.

(2) A cathetometer viewed a point on the die holder and checked the vibration reading.

A number of amplitude and frequency settings were checked. The calibrations showed that the transducer was reading peak to peak amplitudes of vibration as indicated by the instrument specification, and also that the amplitudes monitored were accurate ($\pm$ 2 per cent) within the range of amplitudes used in this research project.

7. Experimental Procedure and Technique

7. Experimental Procedure and Technique.

7.1. Slow Speed Drawing Tests - 1.3 ft/m.

Before carrying out a drawing test, the oscillator power unit was set in operation and oil was delivered under pressure to both sides of the actuator piston. The piston was thus supported so that when a drawing force was applied, the piston was prevented from colliding with, and possibly damaging, the oil seals.

At the start of each test, the loadmeter and torquemeter bridge circuits were balanced and the galvanometer position corresponding to zero force observed. The wire to be tested was 'tagged' in a swaging machine and a length was drawn under non-oscillatory conditions. The resulting galvanometer deflection was recorded. The oscillator was adjusted to operate at the required frequency and amplitude and a length of wire was drawn with superimposed oscillatory energy. The corresponding galvanometer deflection was again noted. During oscillatory drawing, the torsional amplitude of drum oscillation was also measured and from this, and the galvanometer deflection, the non-oscillatory and oscillatory drawing forces were computated. The above procedure was repeated for all frequency and amplitude settings.

Drawing tests were performed at frequencies of 25, 50, 75, 100 and 125 c/s., with amplitudes of die oscillation increasing to a value where either, the maximum

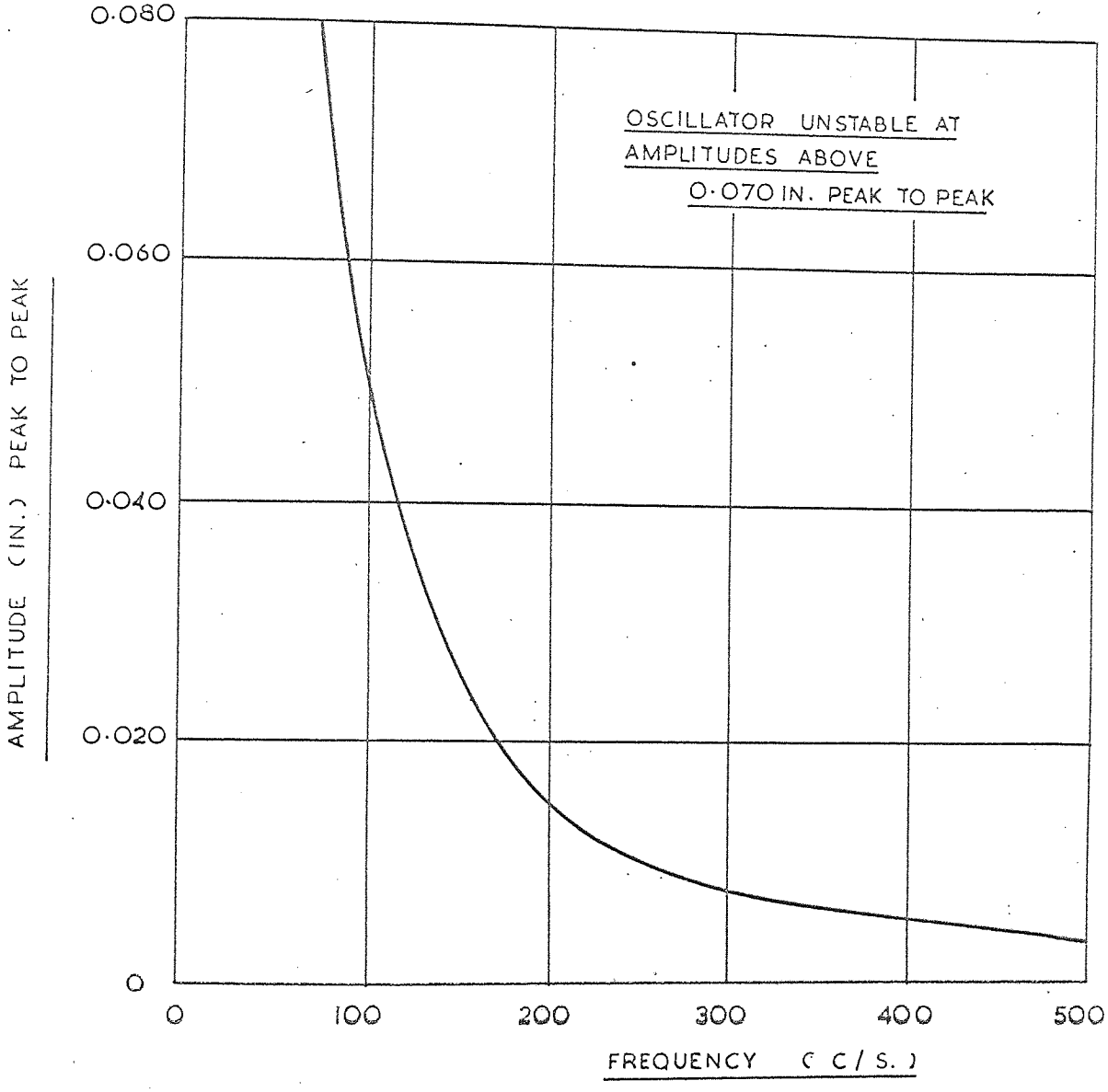

FIG. NO. 51 OSCILLATOR AMPLITUDE AND FREQUENCY CHARACTERISTICS

oscillator output was reached, or the minimum value of the force variation in the wire was equal to zero drawing force. For certain drawing settings, the amplitudes corresponding to this latter condition were found to be considerably lower than the maximum oscillator output.

The characteristic of the hydraulic oscillator was such that as the frequency of vibration was increased, the maximum amplitudes obtainable were greatly reduced, ie. for frequencies above 300 c/s., the amplitudes obtainable were less than 0.007 in. peak to peak (see Fig. No. 51). Furthermore, at frequencies equal to, and above 200 c/s., the torsional amplitudes of the drum oscillation were very small and were undetectable by the torsiograph. Therefore, for drawing tests at frequencies of 200, 300, 400 and 500 c/s. the force variation in the wire was obtained from a strain gauge bridge mounted on the wire between the die and the drum.

To check the analysis developed to determine the magnitude of force variation in the wire, 20 per cent of the slow speed results were obtained by direct strain gauge measurements on the wire.

7.2. High Speed Drawing Tests.

To investigate the effect of drawing speed during oscillatory drawing, a number of high speed tests were performed on copper wire. The procedure was the same as that adopted for the slow speed tests except that

frequencies of die oscillation above 125 c/s.were not tested. This was because the amplitudes available at these higher frequencies were so small that the effect on the drawing force was negligible.

Speeds of 10, 20, 35 and 50 ft/m. were tested. At speeds greater than 50 ft/m. no detectable reduction in mean drawing force was observed.

7.3. Determination of Stress-Strain Curves.

A number of stress-strain curves were obtained for the wires in the following conditions - (1) 'as received', (2) drawn under non-oscillatory conditions and (3) drawn with superimposed oscillatory energy. The specimens were tensile tested in a 50 tonf. Denison testing machine, and load-extension curves were obtained from a Weidmann-Baldwin autographic recorder. Three specimens were tested at each of the above conditions and the average of the three results was recorded. True stress, 'σ' - natural strain, 's', curves were plotted (Graph No's.93 to 100 incl)

To obtain Young's Modulus for the materials being drawn, a series of tensile tests was carried out. The tests were performed in a Hounsfield testing machine, and the extensions of the specimens were recorded with a Hounsfield extensometer. Load-extension curves were plotted as shown in Appendix No. 16.14.

8. A Discussion on the Analysis of the Torquemeter and Loadmeter Records

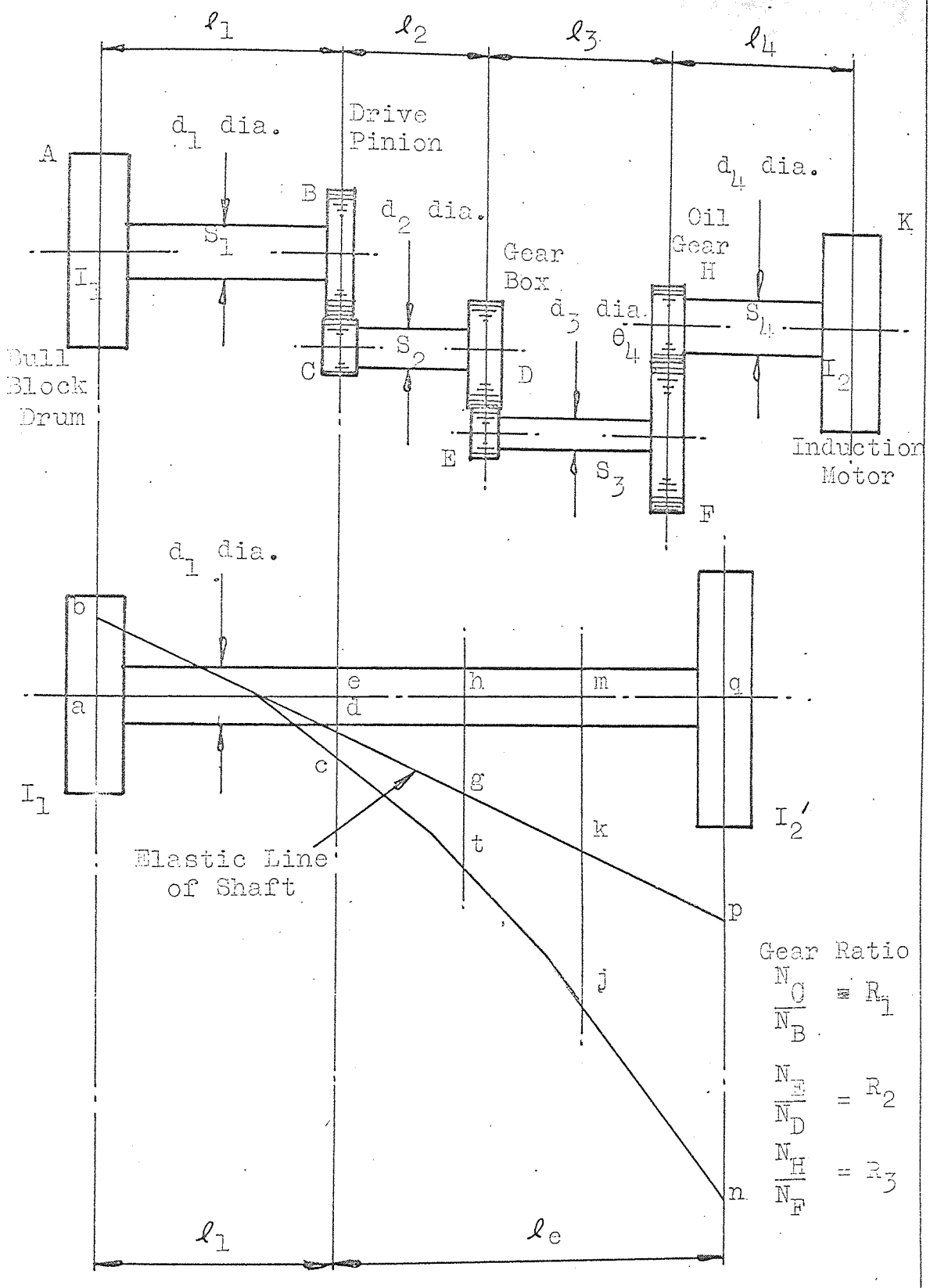

Gear Ratio

$$\frac{N_C}{N_B} = R_1$$

$$\frac{N_E}{N_D} = R_2$$

$$\frac{N_H}{N_F} = R_3$$

FIG. NO. 52. DETAILS OF BULL BLOCK DRIVE

8. A Discussion on the Analysis of the Torquemeter and Loadmeter Records.

During the early investigations, it became apparent that the magnitude of the force variation in the wire leaving the die as predicted by the torquemeter, differed from the value predicted by the loadmeter. Furthermore, a complete understanding of the process of oscillatory drawing was required, and therefore a vibration analysis of the bull-block and its drive was undertaken and is shown in the following section.

8.1. Theoretical Analysis of the Bull-block.

To obtain a speed variation from 1.3 up to 500 ft/m. the bull-block drive was designed as follows -

A 15 hp. induction motor was connected to a Carter oil gear through a belt drive. The oil gear was coupled directly to a four speed gear box which was in turn coupled to the drum shaft by a worm and pinion gear.

To enable an equivalent stiffness and inertia of the system to be determined, the drive was simplified as shown in Fig. No.52, ie. reduced to a system having two rotors mounted on an equivalent shaft, one at each end.

For purposes of analysis the rotor 'K' was assumed to be fixed and the gear 'H' was subjected to a torque, causing it to twist through an angle of θ_4 degrees. The corresponding angle of twist of the gear 'F' was therefore equal to θ_4/R_3 degrees, where R_3 = the gear ratio.

Similarly, the angle of twist at gear 'E' equals $(\theta_3 + \theta_4/R_3)$ and hence the angle at gear 'D' equals $(\theta_3 + \theta_4/R_3)\ 1/R_2$.

Therefore, the total angle of twist of the drum 'A' relative to the induction motor 'K' equals -

$$\theta_T = \theta_1 + \left[\theta_2 + \left(\theta_3 + \frac{\theta_4}{R_3} \right) \frac{1}{R_2} \right] \frac{1}{R_1}$$

therefore

$$\theta_T = \theta_1 + \frac{\theta_2}{R_1} + \frac{\theta_3}{R_1 R_2} + \frac{\theta_4}{R_1 R_2 R_3} \qquad \text{——(1)}$$

If a torque 'T', is applied to the rotor 'A', then the torques at 'C', 'E' and 'H' are -

$$\left.\begin{aligned} &\text{at 'C' the torque} = \frac{T}{R_1} \\ &\text{at 'E' " } = \frac{T}{R_1 R_2} \\ &\text{and at 'H' " } = \frac{T}{R_1 R_2 R_3} \end{aligned}\right\} \qquad \text{——(2)}$$

If G = the modulus of rigidity, and J = the polar moment of inertia of the shafts then -

$$\frac{T}{J} = \frac{G\,\theta}{\ell} \quad \text{and therefore} \quad \theta = \frac{T\ell}{J\,G} \qquad \text{——(3)}$$

By substituting equations (2) and (3) in equation (1),

$$\theta_T = \frac{T\ell_1}{J_1 G} + \frac{T\ell_2}{R_1^2 J_2 G} + \frac{T\ell_3}{R_1^2 R_2^2 J_3 G} + \frac{T\ell_4}{R_1^2 R_2^2 R_3^2 J_4 G} = \frac{T\ell_e}{J_1 G}$$

where ℓ_e = the equivalent length of shaft of diameter = d_1.

Also the stiffness $S = JG/\ell$, and therefore

$$\frac{1}{S_e} = \frac{1}{S_1} + \frac{1}{R_1^2 S_2} + \frac{1}{R_1^2 R_2^2 S_3} + \frac{1}{R_1^2 R_2^2 R_3^2 S_4} \qquad (4)$$

where S_e = the equivalent stiffness.

$$\text{Also } \theta_T = \frac{T}{G}\left[\frac{\ell_1}{J_1} + \frac{\ell_2}{R_1^2 J_2} + \frac{\ell_3}{R_1^2 R_2^2 J_3} + \frac{\ell_4}{R_1^2 R_2^2 R_3^2 J_4}\right]$$

therefore

$$\theta_T = \frac{T}{GJ_1}\left[\ell_1 + \frac{\ell_2}{R_1^2}\cdot\frac{J_1}{J_2} + \frac{\ell_3}{R_1^2 R_2^2}\cdot\frac{J_1}{J_3} + \frac{\ell_4}{R_1^2 R_2^2 R_3^2}\cdot\frac{J_1}{J_4}\right]$$

$$\theta_T = \frac{T}{GJ_1}\left[\ell_1 + \frac{\ell_2}{R_1}\left[\frac{d_1}{d_2}\right]^4 + \frac{\ell_3}{R_1^2 R_2^2}\left[\frac{d_1}{d_3}\right]^4 + \frac{\ell_4}{R_1^2 R_2^2 R_3^2}\left[\frac{d_1}{d_4}\right]^4\right]$$

$$\theta_T = \frac{T}{GJ_1}\left[\ell_1 + \ell_e\right] \qquad (5)$$

$$\text{where } \ell_e = \frac{\ell_2}{R_1^2}\left[\frac{d_1}{d_2}\right]^4 + \frac{\ell_3}{R_1^2 R_2^2}\left[\frac{d_1}{d_3}\right]^4 + \frac{\ell_4}{R_1^2 R_2^2 R_3^2}\left[\frac{d_1}{d_4}\right]^4 \qquad (6)$$

Since the maximum angular velocity of a rotor is directly proportional to the amplitude of oscillation, it will be seen from Fig. No. 52 also, that for a geared system the maximum kinetic energy is proportional to -

$$I_1 (ab)^2 + I_2 (qn)^2$$

(neglecting the inertia of the gears)

For the equivalent two rotor system, the maximum kinetic energy is proportional to -

$$I_1 (ab)^2 + I_2' (qp)^2$$

Therefore equating the kinetic energy of the actual system to the equivalent system -

$$I_1 (ab)^2 + I_2 (qn)^2 = I_1 (ab)^2 + I_2' (qp)^2$$

and therefore $$I_2' = \left[\frac{qn}{qp}\right]^2 I_2 \qquad \text{(7)}$$

now $\frac{ec}{ed} = R_1$; $\frac{ht}{hg} = R_1R_2$ and $\frac{mj}{mk} = \frac{qn}{qp} = R_1R_2R_3$

and therefore from equation (7)

$$I_2' = (R_1R_2R_3)^2 I_2 \qquad \text{(8)}$$

For the bull-block drive (ie. at a drawing speed of 1.3 ft/m)

$$S_c = 4.48 \times 10^6 \text{ in. lbf/ rad.}$$

and $$I_2' = (14.66)^2(3.7)^2(50.0)^2 I_2$$

The calculations for the above are given in Appendix No.16.4

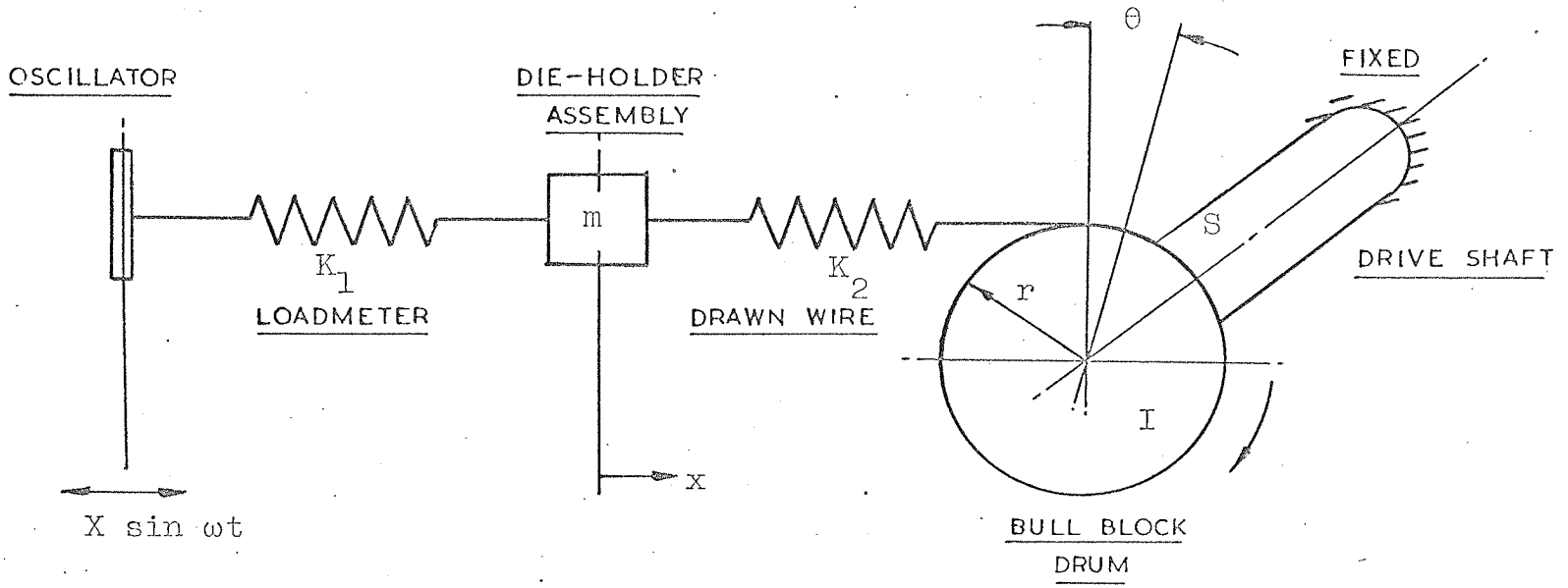

FIG. NO. 53. SIMPLIFICATION OF BULL BLOCK AND WIRE

I_2' is likely to be large compared with I_1, therefore the two rotor system can be reduced further to a shaft fixed rigidly at one end carrying a rotor of inertia I_1 at its free end. (see Fig. No. 53.)

Determination of Natural Frequencies of Bull-block.

If the length of drawn wire can be considered as a spring fixed rigidly at both the die and the drum, then the bull-block assembly can be treated as a system of springs and masses as shown in Fig. No. 53.

The forces acting on the die holder are -

$$K_1 (X \sin \omega t - x') = K_2 (x' - r\theta) + m\frac{d^2x'}{dt^2} + C_1\frac{dx'}{dt} \quad \text{---(1)}$$

and neglecting $C_1 dx'/dt$ because friction at the die is small

$$m \frac{d^2x'}{dt^2} + K_2x' - K_2r\theta = K_1X \sin \omega t - K_1x'$$

$$m \frac{d^2x'}{dt^2} + (K_1 + K_2)x' - K_2r\theta = K_1X \sin \omega t \quad \text{---(1a)}$$

From a consideration of the torques acting on the drum -

$$K_2(x' - r\theta)r = S\theta + I \frac{d^2\theta}{dt^2} + C_2 \frac{d\theta}{dt} \quad \text{---(2)}$$

is obtained and if, for purposes of calculating the natural frequencies, friction and therefore damping is neglected then

$$I \frac{d^2\theta}{dt^2} + S\theta + K_2r^2\theta - K_2rx' = 0$$

$$I\frac{d^2\theta}{dt^2} + (S + K_2r^2)\theta - K_2rx' = 0 \qquad \text{(2a)}$$

To solve equations (1a) and (2a),

let $x' = A \sin \omega t$.

therefore $\frac{d^2x'}{dt^2} = -A\omega^2 \sin \omega t$

and $\theta = B \sin \omega t$

therefore $\frac{d^2\theta}{dt^2} = -B\omega^2 \sin \omega t$

substituting in equations (1a) and (2a),

$$m(-A\omega^2 \sin \omega t) + (K_1 + K_2)A \sin \omega t - K_2rB \sin \omega t = K_1X \sin \omega t$$

and $I(-B\omega^2 \sin \omega t) + (S + K_2r^2)B \sin \omega t - K_2rA \sin \omega t = 0$

therefore

$$-A\omega^2m + A(K_1 + K_2) - BK_2r = K_1X$$

and $$-B\omega^2I + B(S + K_2r^2) - AK_2r = 0$$

therefore

$$A(K_1 + K_2 - \omega^2m) - BK_2r = K_1X \qquad \text{(3)}$$

and $$-AK_2r + B(S + K_2r^2 - \omega^2I) = 0 \qquad \text{(4)}$$

multiply equation (3), by $(S + K_2r^2 - \omega^2I)$

$$A(K_2 + K_1 - \omega^2m)(S + K_2r^2 - \omega^2I) - BK_2r(S + K_2r^2 - \omega^2I) = K_1X(S + K_2r^2 - \omega^2I) \qquad \text{(5)}$$

and multiply equation (4) by rK_2

$$-AK_2^2r^2 + B(\ rK_2\ )(S + K_2r^2 - \omega^2 I) = 0 \qquad \text{(6)}$$

adding equations (5) and (6)

$$A(K_1 + K_2 - \omega^2 m)(S + K_2r^2 - \omega^2 I) - AK_2^2r^2 = K_1X(S + K_2r^2 - \omega^2 I)$$

$$A(K_1S + K_1K_2r^2 - K_1\omega^2 I + K_2S + K_2^2r^2 - K_2\omega^2 I - \omega^2 mS - \omega^2 mK_2r^2 + \omega^4 Im) - AK_2^2r^2 = K_1XS + K_1K_2Xr^2 - K_1X\omega^2 I$$

$$A\left[\omega^4 Im - \omega^2(K_1 I + K_2 I + mS + mK_2r^2) + K_1S + K_2S + K_1K_2r^2\right] = K_1X(S + K_2r^2 - \omega^2 I)$$

$$A = \frac{K_1X(S + K_2r^2 - \omega^2 I)}{\omega^4 Im - \omega^2\left[I(K_1 + K_2) + m(S + K_2r^2)\right] + S(K_1 + K_2) + K_1K_2r^2}$$

and also from equation (4)

$$B = \frac{K_1K_2Xr}{\omega^4 Im - \omega^2\left[I(K_1 + K_2) + m(S + K_2r^2)\right] + S(K_1 + K_2) + K_1K_2r^2}$$

therefore

$$x' = \frac{K_1X(S + K_2r^2 - \omega^2 I)\sin \omega t}{\omega^4 Im - \omega^2\left[I(K_1 + K_2) + m(S + K_2r^2)\right] + S(K_1 + K_2) + K_1K_2r^2} \qquad \text{(7)}$$

and

$$\theta = \frac{K_1 K_2 Xr \sin \omega t}{\omega^4 Im - \omega^2\left[I(K_1 + K_2) + m(S + K_2 r^2)\right] + S(K_1 + K_2) + K_1 K_2 r^2} \qquad (8)$$

re-writing equations (3) and (4) as a determinant

$$\begin{vmatrix} (K_2 + K_1 - \omega^2 m) & -K_2 r \\ -K_2 r & (S + K_2 r^2 - \omega^2 I) \end{vmatrix} = 0$$

solving the determinant

$$(K_1 + K_2 - \omega^2 m)(S + K_2 r^2 - \omega^2 I) - (-K_2 r)(-K_2 r) = 0$$

$$K_1 S + K_1 K_2 r^2 - K_1 \omega^2 I + K_2 S + K_2^2 r^2 - K_2 \omega^2 I - \omega^2 mS - \omega^2 m K_2 r^2 + \omega^4 Im - K_2^2 r^2 = 0$$

$$\omega^4 Im - \omega^2(K_1 I + K_2 I + mS + mK_2 r^2) + K_1 S + K_1 K_2 r^2 + K_2 S = 0$$

$$\omega^4 Im - \omega^2\left[I(K_1 + K_2) + m(S + K_2 r^2)\right] + S(K_1 + K_2) + K_1 K_2 r^2 = 0$$

$$\omega^4 - \omega^2\left[\frac{K_1 + K_2}{m} + \frac{S + K_2 r^2}{I}\right] + \frac{S(K_1 + K_2)}{Im} + \frac{K_1 K_2 r^2}{Im} = 0$$

solving the quadratic equation for ω^2

$$\omega^2 = \frac{1}{2}\left[\frac{K_1 + K_2}{m} + \frac{S + K_2 r^2}{I}\right] \pm \frac{1}{2}\sqrt{\left[\frac{K_1 + K_2}{m} + \frac{S + K_2 r^2}{I}\right]^2 - 4\left[\frac{S(K_1 + K_2) + K_1 K_2 r^2}{Im}\right]}$$

$$\omega^2 = \frac{I(K_1+K_2)+m(S+K_2r^2) \pm \sqrt{\left[I(K_1+K_2)+m(S+K_2r^2)\right]^2 - 4Im\left[S(K_1+K_2)+K_1K_2r^2\right]}}{2Im} \quad (10)$$

8.2. Discussion on the Analysis.

The foregoing analysis simplifies the problem of oscillatory drawing in that it assumes that the die and wire are rigidly connected. This is not so, as wire is being drawn through the die, however, since some oscillatory energy is transmitted to the wire as it leaves the die, then the wire and bull-block vibrates as a spring system and so this simplification is justifiable. In the analysis, the value of 'x'' refers to the amplitude of displacement of the wire and not the amplitude of die oscillation, which was recorded by the linear transducer.

Equations (1) and (2) show that the variation of force in the wire between the die and the drum is dependent upon the stiffness of the wire being drawn, the inertia of the die-loadmeter assembly, the inertia of the drum and the damping forces present in the system. Furthermore, the equations show that the loadmeter and torquemeter recordings are not equal to the force variation in the wire, but are equivalent to the algebraic sum of various forces in the system. For example, to obtain the magnitude of force variation in the wire from the loadmeter records, the inertia force of the die-loadmeter assembly must be subtracted algebraically from the loadmeter signal. Moreover,

to obtain the magnitude of the force variation from the torquemeter records, it is necessary to add both the drum inertia torque and the damping torque algebraically to the torquemeter signal.

By substituting the appropriate parameters in equation (10), for drawing mild steel wire EN2B, 0.158 in. diameter, the natural frequencies of the bull-block were calculated to be 57 c/s. and 2271 c/s. This suggests that for frequencies of die oscillation below the fundamental frequency (ie. < 57 c/s.), the die and drum will vibrate in phase and for frequencies of oscillation between 57 c/s. and 2271 c/s. the die and drum will vibrate 180 degrees out of phase. This phase relationship will not be exactly 0 and 180 degrees because of the effect of damping in the system. All frequency calculations are included in Appendix No.16.5.

The following section discusses the experiments designed to check the validity of the analysis and to see whether correlation could be obtained between the loadmeter and torquemeter signals.

8.3. Tests Designed to Check the Analysis.

Before starting the experiments to check the bull-block analysis, the inertia of the drum was determined as described in Appendix No. 16.7. The following tests were then undertaken.

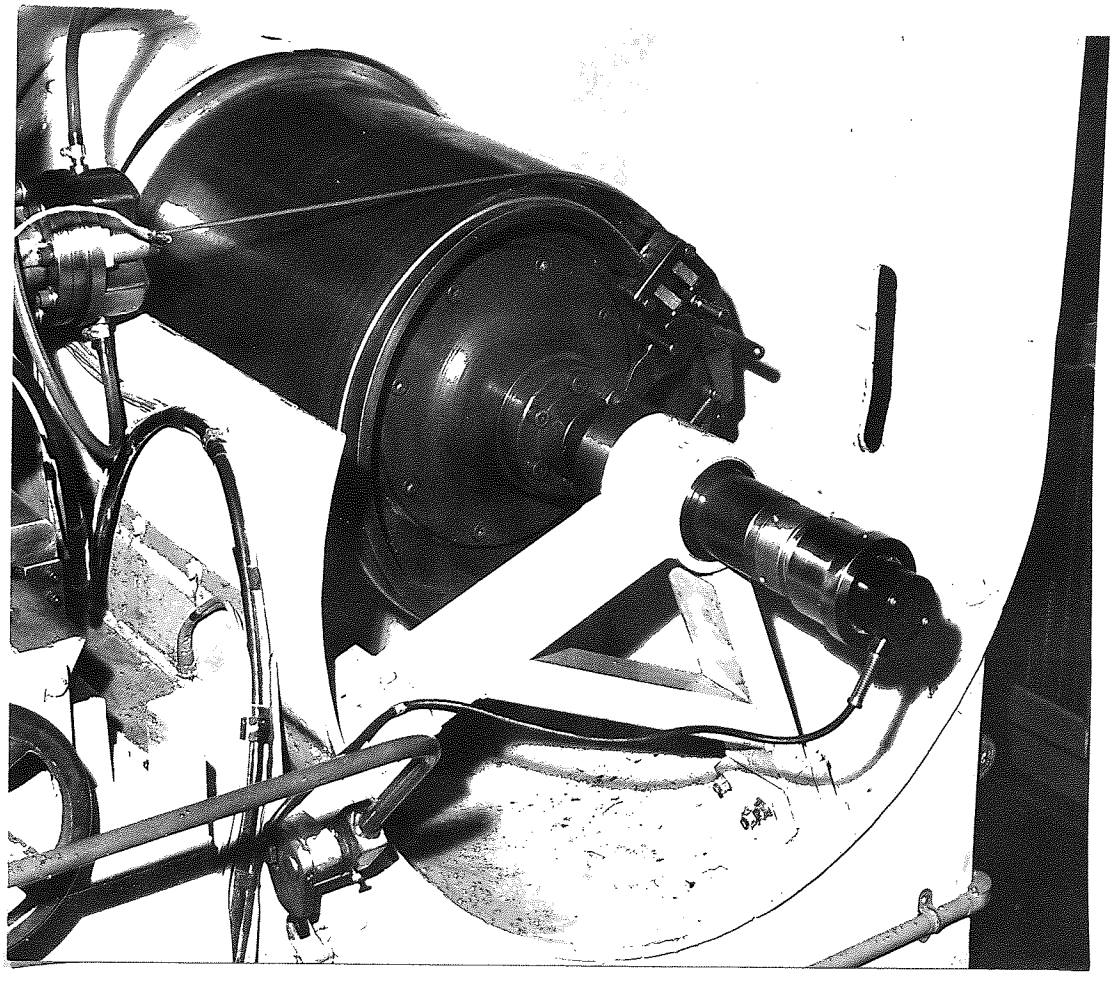

FIG.NO. 54. SHOWING PEDESTAL IN PLACE

8.3.1. Determination of Natural Frequency.

The bull-block and oscillator unit were arranged to draw mild steel wire at 1.3 ft/m. with superimposed oscillatory energy. The oscillator amplitude was set at 0.015 in. peak to peak with frequencies of vibration between 25 and 125 c/s. At each frequency setting the amplitude of drum oscillation was recorded and a curve of frequency against amplitude of drum oscillation was plotted. (see Graph No.1) From this graph, the natural frequency of the complete bull-block and wire system was determined.

8.3.2. Determination of Damping Coefficient.

From the graph of drum amplitude against frequency of oscillation the damping coefficient 'C' was calculated as described by Den Hartog (51).

8.3.3. Determination of the Effect of Drum Oscillation.

The bull-block analysis was confined to torsional oscillations of the drum, however, since the drum was mounted as a cantilever it was thought that it may be experiencing other modes of vibration. To investigate this possibility a pedestal was designed which was mounted at the free end of the drum shaft. The object of the pedestal was to eliminate all secondary modes of vibration by ensuring that the shaft could only oscillate torsionally. The pedestal was secured to the bull-block frame and supported the shaft in a phosphur bronze bearing as shown in Fig. No. 54. To study the effect of supporting the

drum, two oscillatory drawing tests were performed, one with the pedestal in place and the other with it removed. The tests were carried out with frequency and amplitude settings of 50 c/s. and 0.025 in. peak to peak respectively. The material drawn was mild steel and the speed of drawing was 1.3 ft/m.

8.3.4. Determination of the Effect of Die-Loadmeter Inertia.

To investigate the effect of the inertia of the die-loadmeter assembly on the loadmeter record, two tests were carried out using die holders of different weights. Both tests were performed at a drawing speed of 1.3 ft/m., with mild steel wire and frequency and amplitude settings of 50 c/s. and 0.025 in. peak to peak respectively. One test was performed with an aluminium die holder and the other with a steel holder.

8.3.5. Check on Loadmeter-Torquemeter Correlation.

With the aluminium die holder in position and the pedestal removed, five tests were carried out drawing mild steel wire at a drawing speed of 1.3 ft/m. The tests were performed at frequencies of 25, 50, 75, 100 and 125 c/s. with an amplitude of die oscillation of 0.015 in. peak to peak.

During the tests described in sub-sections 8.3.3., 8.3.4. and 8.3.5, strain gauge bridges were mounted on the wires and the variation of force in the wire was

measured directly.

The results from the above five series of experiments are included in the following section.

8.4. Results of Tests.

Fig. No's. 56 to 63 plot drawing forces measured by the load and torque meters, and the amplitudes of die and drum oscillation.

The drawing forces, computed from the torquemeter records, are plotted with the drum inertia and drum damping forces. The force variation in the wire is then plotted by adding these three curves algebraically. Similarly, the drawing forces as seen by the loadmeter are plotted with the die-assembly inertia forces. The force variation in the wires as predicted by the loadmeter is then plotted by subtracting these two curves algebraically. Finally to compare the force variation in the wires, the records obtained from the strain gauge bridges on the wire are plotted. All of the above curves are plotted against time on the abscissa.

In these figures the following notation is employed-

X_D = Torsional amplitude of drum oscillation.

X_A = Amplitude of die oscillation.

F_D = Drawing force (lbf.)

F_M = Mean drawing force (lbf.)

F_I = Inertia force (lbf.)

F_F = Drum damping force.

The next four symbols apply when the bull-block is viewed from the operators position.

C.C.W. : Counter clockwise rotation of drum.

C.W. : Clockwise rotation of drum.

(+ ve) : Movement of die towards drum.

(- ve) : Movement of die away from drum.

AMPLITUDE OF DIE OSCILLATION = 0·015 IN. PEAK TO PEAK			
FREQUENCY (C/S.)	AMPLITUDE OF DRUM 'θ' (RADS.)	FREQUENCY (C/S.)	AMPLITUDE OF DRUM 'θ' (RADS.)
25	$3·31 \times 10^{-4}$	52·5	$6·28 \times 10^{-4}$
30	4·18 "	55	5·05 "
35	4·79 "	60	3·66 "
40	5·92 "	70	2·79 "
45	8·02 "	80	2·09 "
47·5	10·12 "	100	1·13 "
50	8·54 "	125	0·61 "

FIG. NO. 55. TABLE SHOWING AMPLITUDES AND FREQUENCIES OF DRUM OSCILLATION

DETERMINATION OF THE FUNDAMENTAL NATURAL FREQUENCY AND THE DAMPING COEFF.

GRAPH NO. 1

DAMPING RATIO $= K = \dfrac{\omega_2 - \omega_1}{\omega_n}$

$K = \dfrac{51.5 - 43.5}{48} = 0.0834$

DAMPING COEFFICIENT $'C' = 2 K I \omega_n$

$= 2.0.0834.53.77.48.2.\pi.$

$\therefore C = 225$ FT. LBF S./RAD

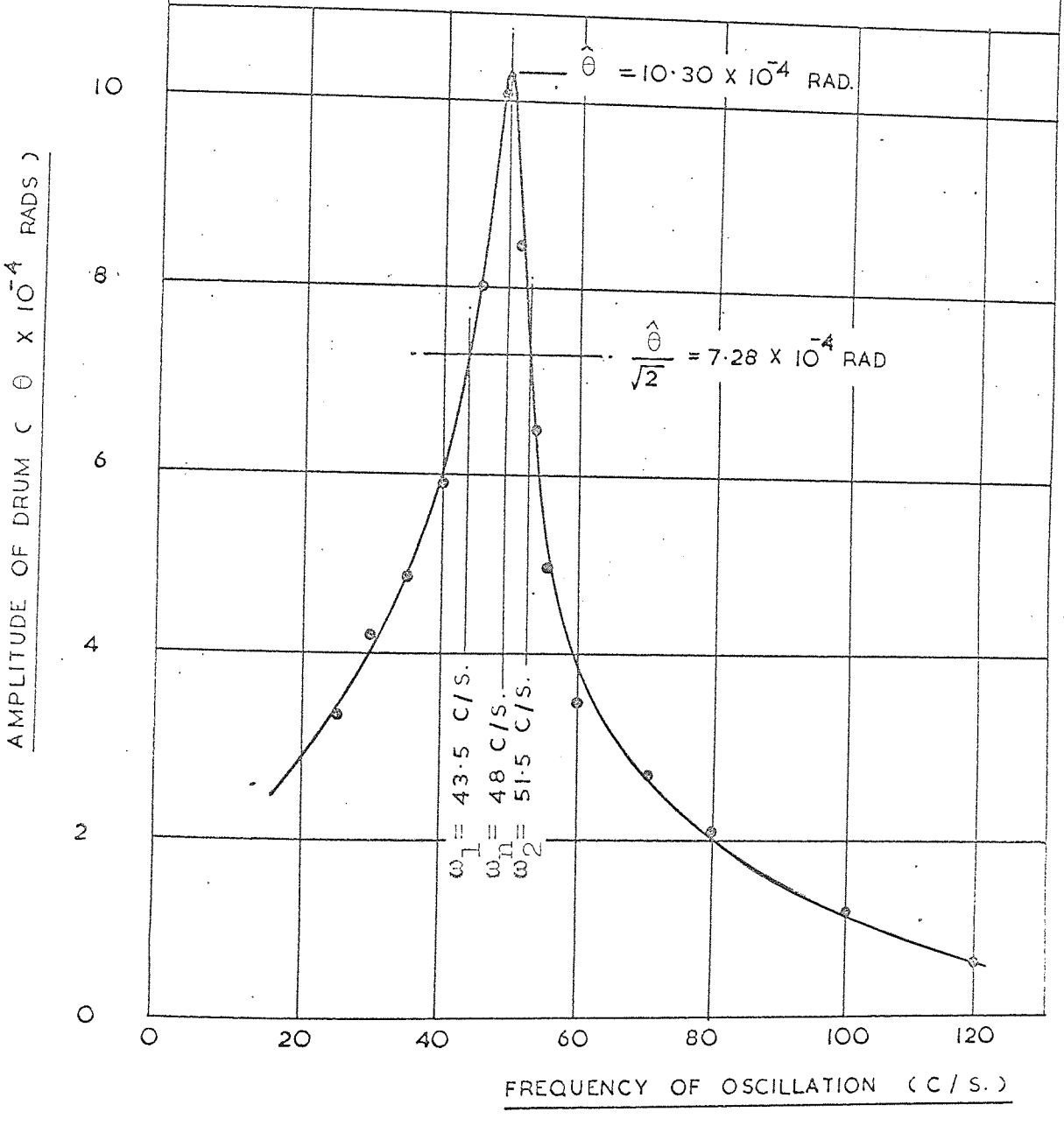

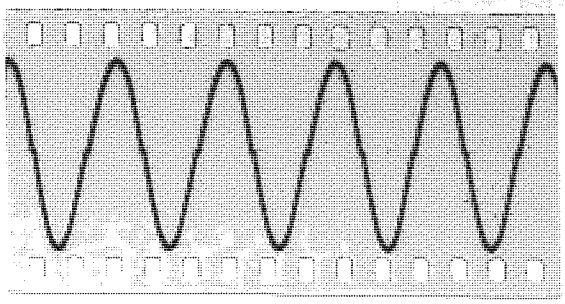

50 C/S.

(1) AMPLITUDE (PEAK TO PEAK) OF DIE OSCILLATION = 0·035 IN.
(FREE OSCILLATION)

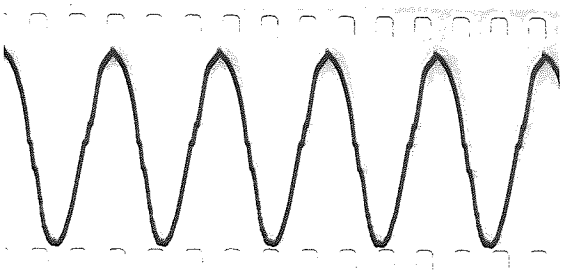

50 C/S.

(2). VELOCITY OF DIE OSCILLATION = 11·0 IN / S. (FREE OSCILLATION)

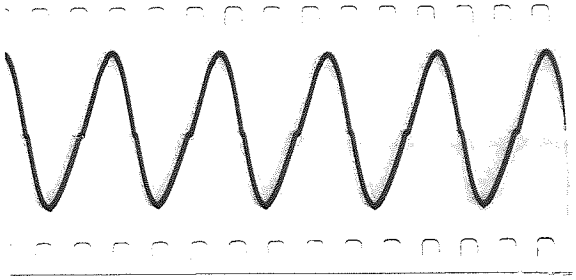

50 C/S.

(3). AMPLITUDE (PEAK TO PEAK) OF DIE OSCILLATION = 0·035 IN.
(DRAWING WIRE)

(4). VELOCITY OF DIE OSCILLATION = 11·0 IN / S. (DRAWING WIRE)

FIG. NO. 64

OSCILLOGRAMS SHOWING AMPLITUDE AND VELOCITY OF DIE OSCILLATION

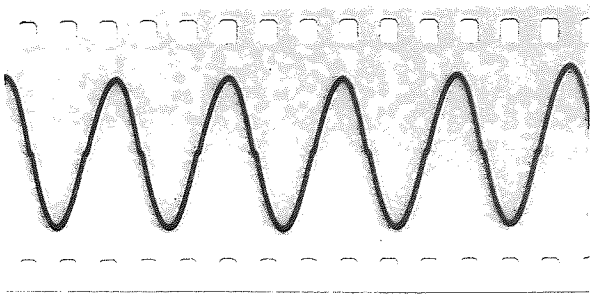

50 C/S.

(1). AMPLITUDE (PEAK TO PEAK) OF DRUM OSCILLATION 36×10^{-4} RADIAN

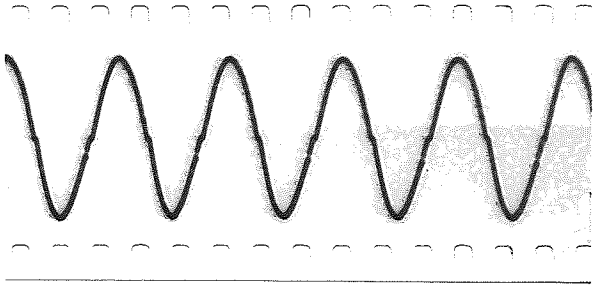

50 C/S.

(2) VELOCITY OF DRUM OSCILLATION $= 113 \times 10^{-4}$ RADIAN / S.

FIG. NO. 65. OSCILLOGRAMS SHOWING AMPLITUDE AND VELOCITY OF DRUM OSCILLATION

6.5. Discussion of Results.

The fundamental natural frequency of the bull-block when drawing mild steel wire, 0.158 in. diameter, was measured to be 48 c/s., while the value calculated from the theoretical analysis was found to be 57 c/s. The difference between these two values was attributed to the assumptions made in the analysis. It was assumed that the damping present in the system was negligible and the wire and die were rigidly fixed. However, because of the good agreement between the two frequencies and because of the reasons discussed in section 6.2., these assumptions were considered to be justifiable.

The test designed to determine the first natural frequency also revealed that the damping coefficient, and hence the damping force, in the system was small when compared with the non-oscillatory drawing force. The damping force was dependent upon the amplitude of oscillation of the drum and was therefore a maximum at frequencies close to the natural frequency, ie. at a frequency of 50 c/s., the peak to peak damping force was equal to 156 lbf., while at a frequency of 125 c/s., it was equal to 34 lbf. (see Fig No's 60 and 63). Since the damping force was 90 degrees out of phase with both, the torquemeter and the drum inertia traces, then the effect on the force variation in the wire was small, amounting to approximately 5 per cent of the peak to peak value at 50 c/s.

The main effect of damping was to introduce a phase lag between the torquemeter and loadmeter signals, but again this effect was small, resulting in a maximum phase difference of 20 degrees when drawing with the pedestal in place. (Fig. No.56). From the above observations, it was concluded that the omission of the damping term in the analysis was justifiable, and as a result of this, it was decided to neglect damping when computing the variation of force in the wires being drawn.

The phenomenon of a phase change between the torsional oscillation of the drum and linear oscillation of the die is shown in Fig. No's. 56 to 63. It was noted that for oscillatory drawing tests at a peak to peak die amplitude of 0.015 in. and a frequency of 25 c/s., the drum and die oscillated in phase and the mean drawing force was reduced by approximately 6 per cent. For the same amplitude of die oscillation and for all frequencies tested above the natural frequency, the die and drum vibrated nearly 180 degrees out of phase and the mean drawing force was reduced by approximately 16 per cent. The phenomenon of a phase change is predicted by the bull-block analysis and further confirms that the process of oscillatory drawing can be considered as a system of springs and masses.

The results of including a pedestal are shown in Fig. No's 56 and 57. The desired effect of minimising any

secondary modes of oscillation was realised and consequently the bull-block stiffness was increased. As a result of this the torsional amplitude of drum oscillation was increased and the mean drawing force was reduced a further 2.5 per cent, while the force variation in the wire was increased by 10 per cent. During these tests, the force variation in the wire, computed from the load and torque meters, agreed to within $\pm$ 1.2 per cent with the values recorded by the strain gauge bridges bonded to the wires. Since the effects of secondary modes of vibration of the drum were small and since good loadmeter-torquemeter correlation was obtained with the pedestal removed, it was decided to perform the main series of tests without a pedestal.

It is pertinent at this stage in the discussion to mention briefly a difficulty incurred when trying to obtain correlation between the loadmeter and torquemeter records because of an error of 2 introduced by an incorrectly calibrated torsiograph. It was only after several weeks of extensive study of the problem, that it was found that the torsiograph was reading the amplitude of drum oscillation and not the peak to peak value as indicated by the instrument specification. This point has since been taken up with the instrument makers.

The effects of varying the inertia forces of the die-loadmeter assembly are shown in Fig. No's. 57 and 58.

During this series of tests it was observed that the signal from the loadmeter was distorted (ie. not a pure sine wave), and for a given amplitude and frequency of die oscillation the effect of increasing the die assembly weight was to increase the degree of distortion. Therefore in order to obtain the minimum distortion possible, it was decided to incorporate the aluminium die holder for all of the remaining tests.

Fig. No's. 59 to 63 show the effect of varying the frequency of die oscillation. During these tests, it was again observed that the die inertia force, and the loadmeter wave forms were distorted. Furthermore, it was noted that as the acceleration of the die was increased, then the amount of distortion was increased also. The distortion of the sine waves was so marked at high accelerations, that at frequencies above 75 c/s., it was necessary to adopt the following procedure to obtain the peak to peak values of force -

It was assumed that, provided the amplitude and frequency of the die oscillation were constant, then the inertia force would remain constant. Furthermore, it was assumed that the inertia force remained constant during both, oscillatory drawing and free oscillation of the die, although the force was distributed differently. The inertia energy of the die, for half a cycle, was determined

by measuring the area under the die inertia force-time curve. The area under the loadmeter record was measured also, and the two areas were then subtracted . The area remaining equalled the variation of energy in the wire and this was converted to a sinusoidal force- time curve. Correlation between loadmeter and torquemeter records was obtained for all frequency settings, and the magnitudes of force agreed to within $\pm$ 3.0 per cent with the values obtained from the strain gauge readings on the wires.

To investigate the distortion of the die inertia and loadmeter wave-forms, the amplitude of die oscillation was viewed on an oscilloscope. Note - the signal was obtained from the linear seismic transducer. It was found that the amplitude wave-form was a good sine wave although slight distortion was noted at the mid-point of the piston stroke. The manufacturer of the oscillator has stated that this type of wave-form is characteristic of hydraulic oscillators and the distortion can only be eliminated by carrying out expensive modifications. By differentiating the amplitude signal, it was possible to inspect the die velocity wave-form and this showed a considerable degree of distortion. When viewing the same parameter during oscillatory drawing it was observed that the velocity wave-form was again severely distorted, but in a different manner from that when the die

was oscillating freely. The amplitude and velocity wave-forms corresponding to a die frequency of 50 c/s. are shown in Fig. No. 64. Conversely the torsional amplitude and torsional velocity of the drum showed very little distortion (see Fig. No.65). It was therefore concluded that, in order to simplify the analysis for the main series of experiments, the force variation in the wire should be computed from the torquemeter traces, and the loadmeter records used only to confirm the mean and non-oscillatory drawing forces.

8.6. Conclusions.

(1) The fundamental natural frequency of the bull-block when drawing mild steel was found to be 48 c/s.; the calculated value was 57 c/s.

(2) The damping coefficient 'C', was found to be 225 ft.lbf.s/rad.

(3) The effect of damping on the variation of force in the wire was small ie. amounting to 5 per cent of the peak to peak value at a frequency of 50 c/s.,and therefore for the main series of tests it was decided to neglect damping.

(4) The pedestal minimised all secondary modes of oscillation of the drum and increased the bull-block stiffness other than the torsional stiffness. However, since correlation of the loadmeter-torquemeter records was good with the pedestal removed, it was decided to perform the main series of tests without the additional support of the drum by the pedestal.

(5) The force variation in the wire as computated from the loadmeter and torquemeter records agreed to within $\pm$ 3 per cent with the values measured directly with strain gauges on the wires.

(6) The loadmeter traces were badly distorted and hence analysis of them was difficult. Therefore it was decided to obtain the force variation in the wire from the torquemeter records and to use the loadmeter to check the non-oscillatory and mean drawing forces.

(7) The effect of increasing the die holder weight was to increase the degree of distortion of the loadmeter records and therefore it was decided to use the light aluminium holder for all remaining experiments.

9. Theoretical Considerations

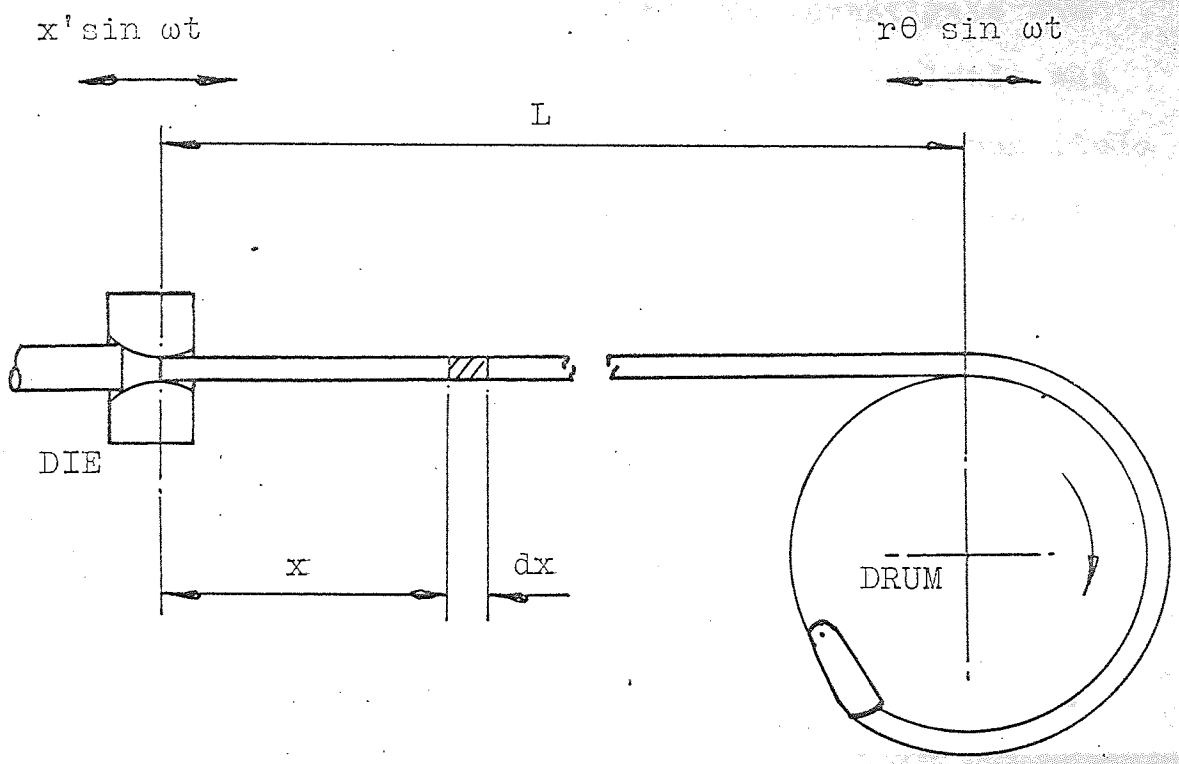

FIG.NO. 66 LONGITUDINAL VIBRATIONS IN THE DRAWN WIRE

9. Theoretical Considerations.

The results obtained in the preceding section suggested that the process of oscillatory drawing was a purely mechanical process and could therefore be considered as a system of springs and weights. To investigate the process further, the following theoretical analysis was undertaken to obtain an equation to predict the magnitude of the force variation induced in the drawn wire as it leaves the die.

For the purpose of analysis, the drawn wire was considered to be a bar subjected to a sinusoidal displacement at both ends, ie. corresponding to the die and drum amplitudes of oscillation.

From Fig. No. 66

let the displacement at the die = $x' \sin \omega t$

and the displacement at the drum = $r\theta \sin \omega t$

Note :- x' = the displacement of the wire and not the displacement of the die recorded by the linear transducer.

If the wire is uniform in cross-section, made of homogeneous and isotropic material, and obeys Hooke's law, then the equation of motion for longitudinal oscillations in the wire is given by -

$$\frac{\partial^2 u}{\partial t^2} = a^2 \frac{\partial^2 u}{\partial x^2} \qquad \text{(1)}$$

where u = the displacement of any cross-section

a = the velocity of sound in the material = $\sqrt{\frac{E\,g}{\rho}}$

ρ = the density of the wire and

x = the co-ordinate along the longitudinal axis

$$\text{let} \quad u\,(x,t) = X(x) \sin \omega t \qquad \text{——————(2)}$$

which is the general solution for steady state forced vibrations in the wire.

Therefore from the equation of motion (1),

$$\frac{d^2X}{dx^2} + \frac{\omega^2 X}{a^2} = 0$$

the solution is then

$$X(x) = A_1 \cos \frac{\omega x}{a} + A_2 \sin \frac{\omega x}{a}$$

where A_1 and A_2 are constants.

Substituting in equation (2),

$$u\,(x,t) = \left[A_1 \cos \frac{\omega x}{a} + A_2 \sin \frac{\omega x}{a} \right] \sin \omega t \qquad \text{——(3)}$$

when $x = 0$, $u(0,t) = x' \sin \omega t$, and therefore from equation (3),

$$A_1 \sin \omega t = x' \sin \omega t$$

therefore, $A_1 = x'$

Substituting in equation (3),

$$u(x,t) = \left[x' \cos \frac{\omega x}{a} + A_2 \sin \frac{\omega x}{a} \right] \sin \omega t \quad \text{_____(4)}$$

when $x = L$, $u(L,t) = r\theta \sin \omega t$, and therefore from equation (4),

$$\left[x' \cos \frac{\omega L}{a} + A_2 \sin \frac{\omega L}{a} \right] \sin \omega t = r\theta \sin \omega t$$

$$A_2 \sin \frac{\omega L}{a} = r\theta - x' \cos \frac{\omega L}{a}$$

$$A_2 = r\theta \operatorname{cosec} \frac{\omega L}{a} - x' \cot \frac{\omega L}{a}$$

Substituting in equation (4),

$$u(x,t) = \left[x' \cos \frac{\omega x}{a} + \left(r\theta \operatorname{cosec} \frac{\omega L}{a} - x' \cot \frac{\omega L}{a} \right) \sin \frac{\omega x}{a} \right] \sin \omega t \quad \text{_____(5)}$$

The force variation in the wire = $F = AE\, \partial u/\partial x$ and therefore from equation (5),

$$F = AE \left[- \frac{x'\omega}{a} \sin \frac{\omega x}{a} + \frac{\omega}{a} \cos \frac{\omega x}{a} \left(r\theta \operatorname{cosec} \frac{\omega L}{a} - x' \cot \frac{\omega L}{a} \right) \right] \sin \omega t$$

$$F = \frac{AE\omega}{a} \left[r\theta \operatorname{cosec} \frac{\omega L}{a} \cos \frac{\omega x}{a} - x' \left(\cos \frac{\omega x}{a} \cot \frac{\omega L}{a} + \sin \frac{\omega x}{a} \right) \right] \sin \omega t \quad \text{_____(6)}$$

Equation (6), is true for all frequencies below the fundamental natural frequency where the die and drum oscillate in phase, but for frequencies above the natural frequency the die and drum oscillate nearly 180 degrees out of phase and therefore the equation must be modified as follows -

Let the displacement of the wire at the die $= -x' \sin \omega t$ and the displacement at the drum $= r\theta \sin \omega t$, therefore equation (6) becomes,

$$F = \frac{AE\omega}{a}\left[r\theta \operatorname{cosec} \frac{\omega L}{a} \cos \frac{\omega x}{a} + x' \left(\cos \frac{\omega x}{a} \cot \frac{\omega L}{a} + \sin \frac{\omega x}{a}\right)\right] \sin \omega t \qquad (7)$$

Equations (6) and (7), show that the magnitude of force variation in the drawn wire varies with the distance x, from the die. However, within the frequency range tested during this investigation the variation is small, ie. at 100 c/s. when x = 0, (at the die), $\cos \frac{\omega x}{a} = 1.000$ and $\sin \frac{\omega x}{a} = 0$, and when x = 17.8 in., (at the drum), $\cos \frac{\omega x}{a} = \cos \frac{\omega L}{a} = 0.998$, and $\sin \frac{\omega x}{a} = \sin \frac{\omega L}{a} = 0.056$, and therefore equations (6) and (7) can be simplified as follows -

$$F = \frac{AE\omega}{a}\left[r\theta \operatorname{cosec} \frac{\omega L}{a} - x' \left(\cot \frac{\omega L}{a} + \sin \frac{\omega L}{a}\right)\right] \sin \omega t \qquad (8)$$

and

$$F = \frac{AE\omega}{a}\left[r\theta \operatorname{cosec} \frac{\omega L}{a} + x'\left(\cot \frac{\omega L}{a} + \sin \frac{\omega L}{a}\right)\right] \sin \omega t \quad \text{---(9)}$$

The values of θ, were recorded with a torsiograph, while the values of x', were calculated from equations (7) and (8), on pages 88 and 89.

10. Graphical Results

10. Graphical Results.

(1) For a given material, reduction in area and drawing speed the mean drawing force was plotted against the amplitude of die oscillation for all frequencies tested above the natural frequency of the bull-block and wire. (ie. 50, 75, 100, 125, 200, 300, 400 and 500 c/s.)
Graph No's. 2, 9, 16, 23, 32, 39, 46, 53, 61, 68, 75 and 76.

(2) Also, the mean drawing force was plotted against the amplitude of die oscillation at frequency settings of 50, 75, 100 and 125 c/s., and the maximum and minimum drawing forces were computed graphically from the torquemeter records as described in section 8.
Graph No's. (4 to 7), (11 to 14), (18 to 21), (25 to 28), (34 to 37), (41 to 44), (48 to 51), (55 to 58), (63 to 66) and (70 to 73).

(3) The maximum and minimum values of drawing force were then re-plotted on the graphs described in (1) above.

(4) For a given material, reduction in area and drawing speed, the maximum, mean and minimum drawing forces were plotted against the amplitude of die oscillation for a frequency of oscillation of 25 c/s.
Graph No's. 3, 10, 17, 24, 33, 40, 47, 54, 62 and 69.

(5) For all reductions in area tested when drawing mild steel wire two graphs were plotted of mean and maximum drawing force against amplitude of die oscillation.

At frequencies of 50 to 500 c/s. - Graph No. 30. at a frequency of 25 c/s.-Graph No.31.

(6) For all materials tested, the maximum and mean drawing forces were plotted against the amplitudes of die oscillation at frequencies within the range 50 to 500 c/s.
Graph No.60.

(7) For a given material, reduction in area and drawing speed, the magnitudes of force variation as determined from the theoretical analysis were plotted on graphs reproduced from (1), at frequencies of 75, 100 and 125 c/s.
Graph No's. 8, 15, 22, 29, 38, 45, 52, 59, 67 and 74.

(8) The magnitudes of force variation at a frequency of 25 c/s. were plotted on the graphs described in (4) along with the experimental results.

(9) For hard drawn copper, the mean and maximum drawing forces were plotted against the drawing speed for constant amplitudes of die oscillation at frequencies of 50, 75, 100 and 125 c/s.
Graph No's. 77 to 84 inclusive.

(10) The above (9), was repeated for a frequency of oscillation of 25 c/s.
Graph No's. 85 to 92 inclusive.

(11) Finally, a series of stress-strain curves were plotted for all materials drawn
Graph No's 93 to 100 inclusive.

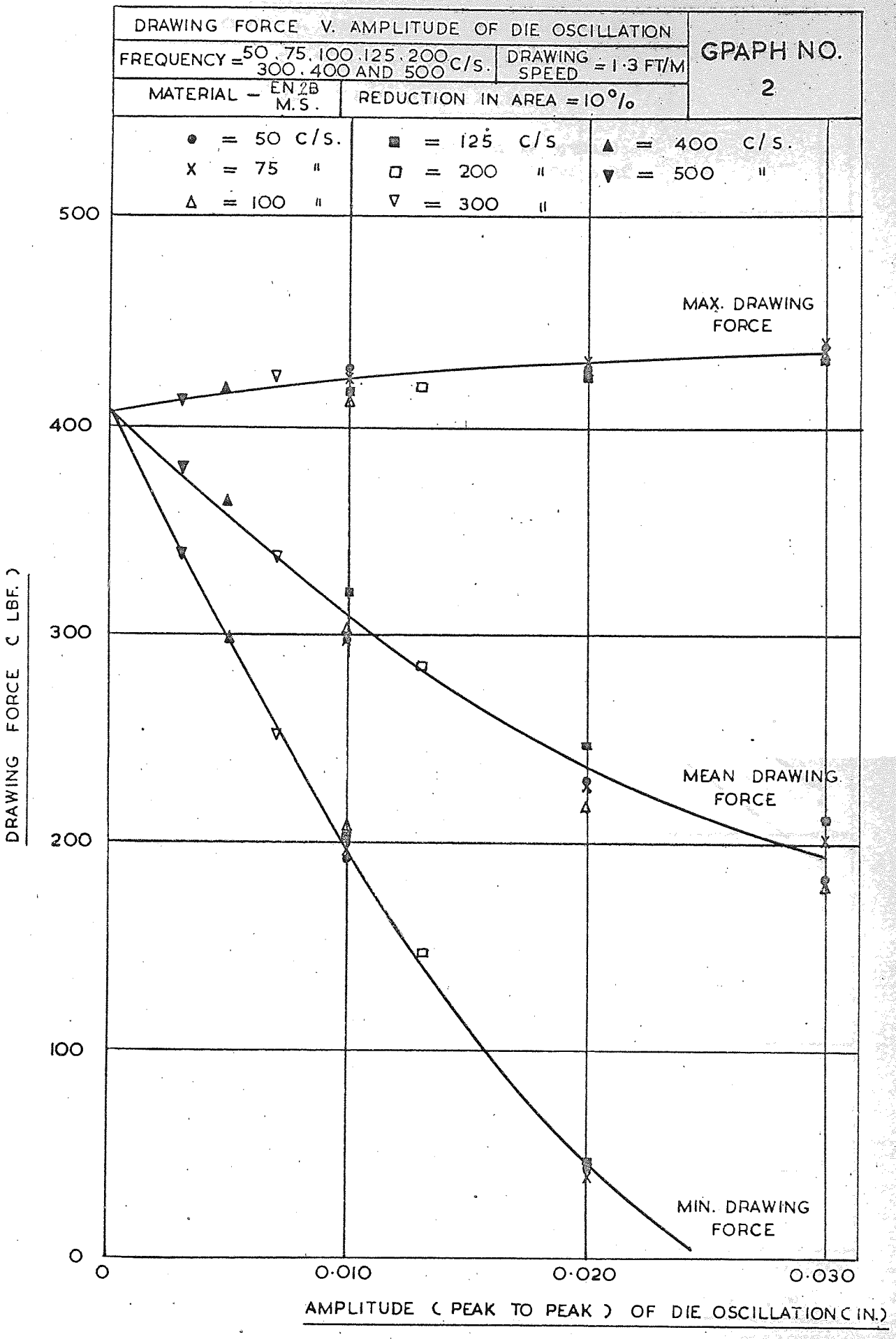
DRAWING FORCE V. AMPLITUDE OF DIE OSCILLATION
FREQUENCY = 50, 75, 100, 125, 200, 300, 400 AND 500 C/S.
DRAWING SPEED = 1·3 FT/M
MATERIAL – EN 2B M.S.
REDUCTION IN AREA = 10%
GPAPH NO. 2
● = 50 C/S.
X = 75 "
Δ = 100 "
■ = 125 C/S
□ = 200 "
▽ = 300 "
▲ = 400 C/S.
▼ = 500 "
MAX. DRAWING FORCE
MEAN DRAWING FORCE
MIN. DRAWING FORCE
DRAWING FORCE (LBF.)
500
400
300
200
100
0
0
0·010
0·020
0·030
AMPLITUDE (PEAK TO PEAK) OF DIE OSCILLATION (IN.)

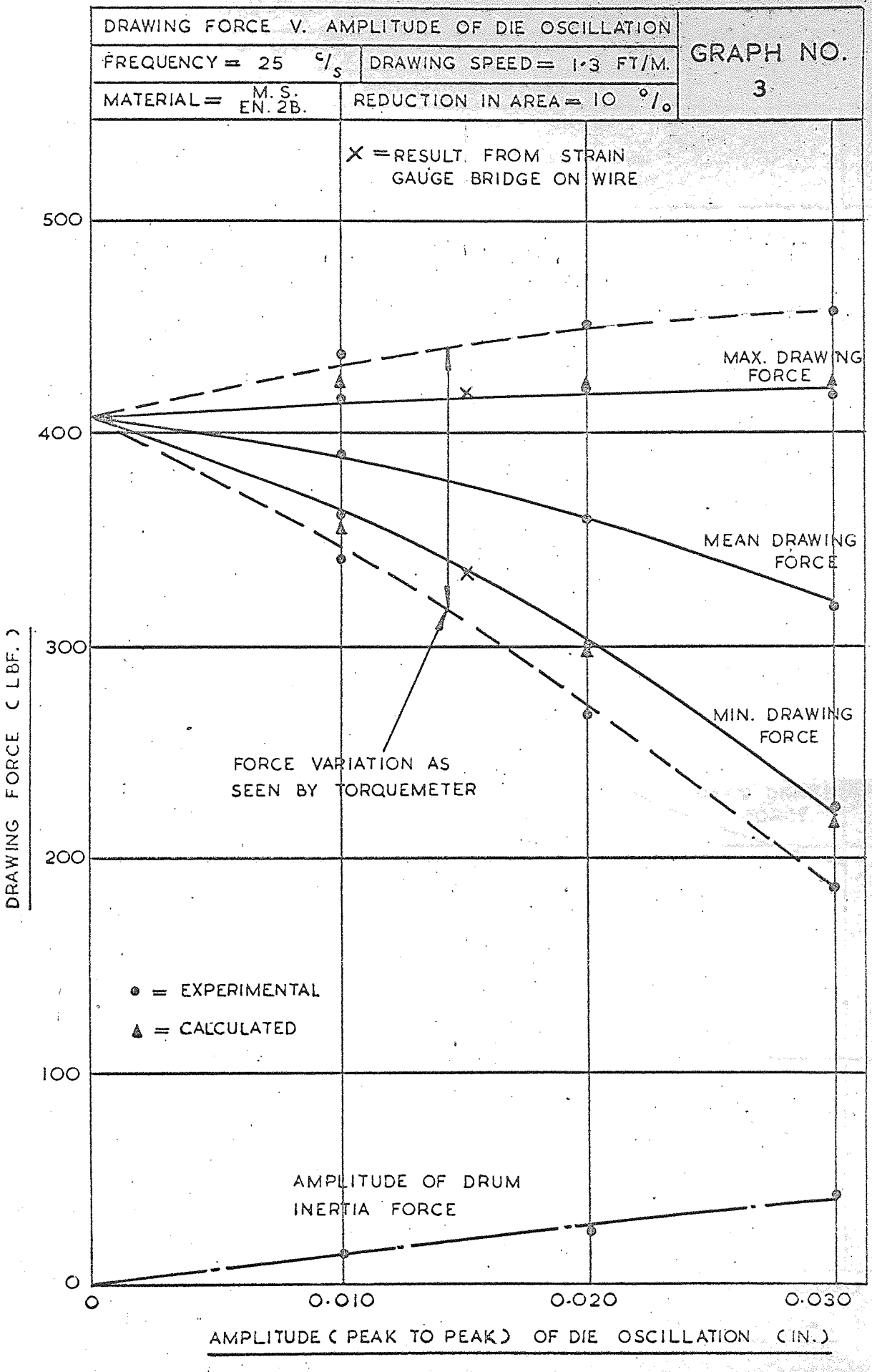
DRAWING FORCE V. AMPLITUDE OF DIE OSCILLATION
FREQUENCY = 25 c/s
DRAWING SPEED = 1·3 FT/M.
MATERIAL = M.S. EN. 2B.
REDUCTION IN AREA = 10 %
GRAPH NO. 3
X = RESULT FROM STRAIN GAUGE BRIDGE ON WIRE
MAX. DRAWING FORCE
MEAN DRAWING FORCE
MIN. DRAWING FORCE
FORCE VARIATION AS SEEN BY TORQUEMETER
AMPLITUDE OF DRUM INERTIA FORCE
● = EXPERIMENTAL
▲ = CALCULATED
DRAWING FORCE (LBF.)
500
400
300
200
100
0
0
0·010
0·020
0·030
AMPLITUDE (PEAK TO PEAK) OF DIE OSCILLATION (IN.)

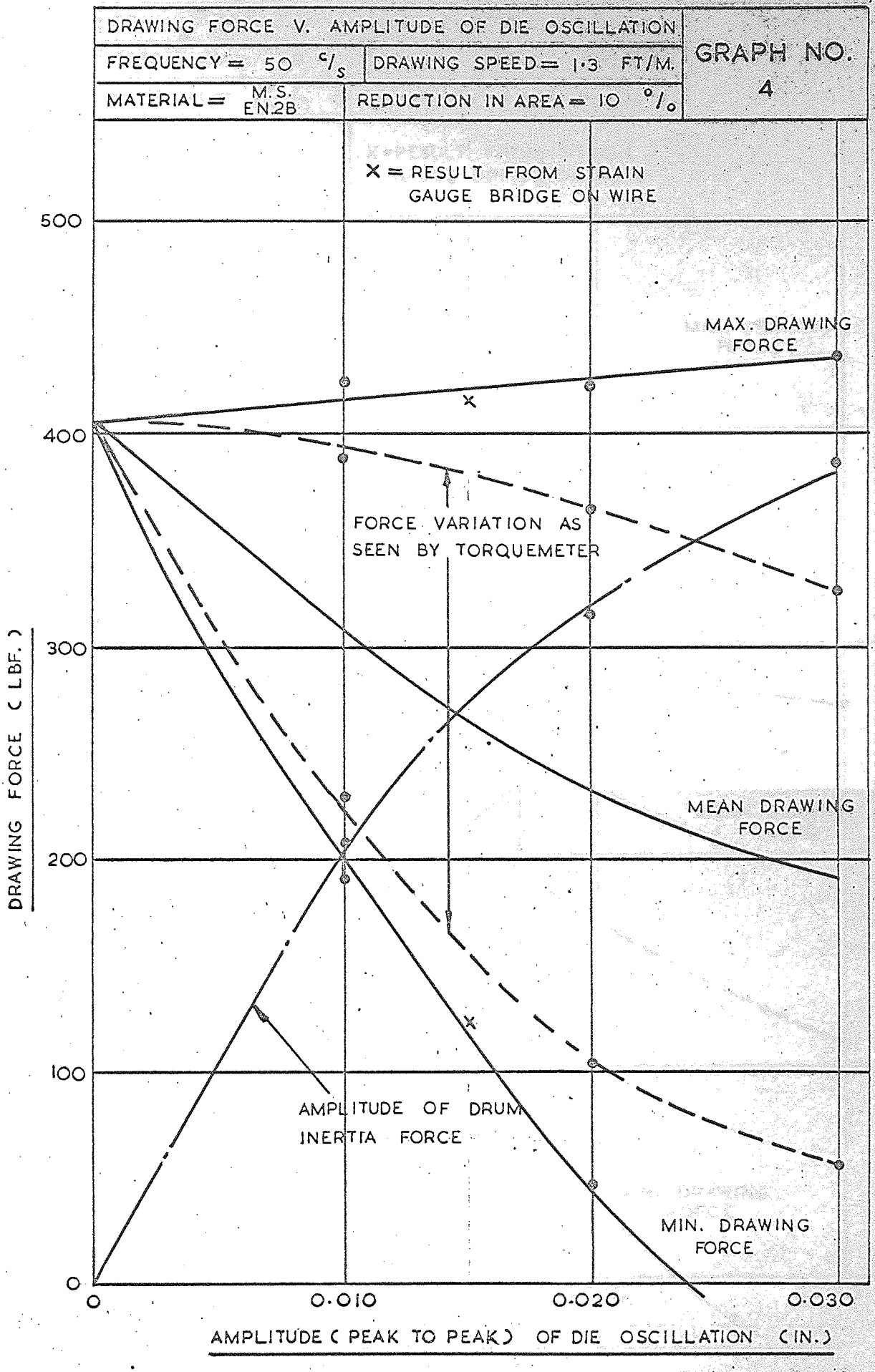
DRAWING FORCE V. AMPLITUDE OF DIE OSCILLATION
FREQUENCY = 50 c/s
DRAWING SPEED = 1·3 FT/M.
MATERIAL = M.S. EN.2B
REDUCTION IN AREA = 10 %
GRAPH NO. 4
X = RESULT FROM STRAIN GAUGE BRIDGE ON WIRE
MAX. DRAWING FORCE
FORCE VARIATION AS SEEN BY TORQUEMETER
MEAN DRAWING FORCE
AMPLITUDE OF DRUM INERTIA FORCE
MIN. DRAWING FORCE
DRAWING FORCE (LBF.)
500
400
300
200
100
0
0
0·010
0·020
0·030
AMPLITUDE (PEAK TO PEAK) OF DIE OSCILLATION (IN.)

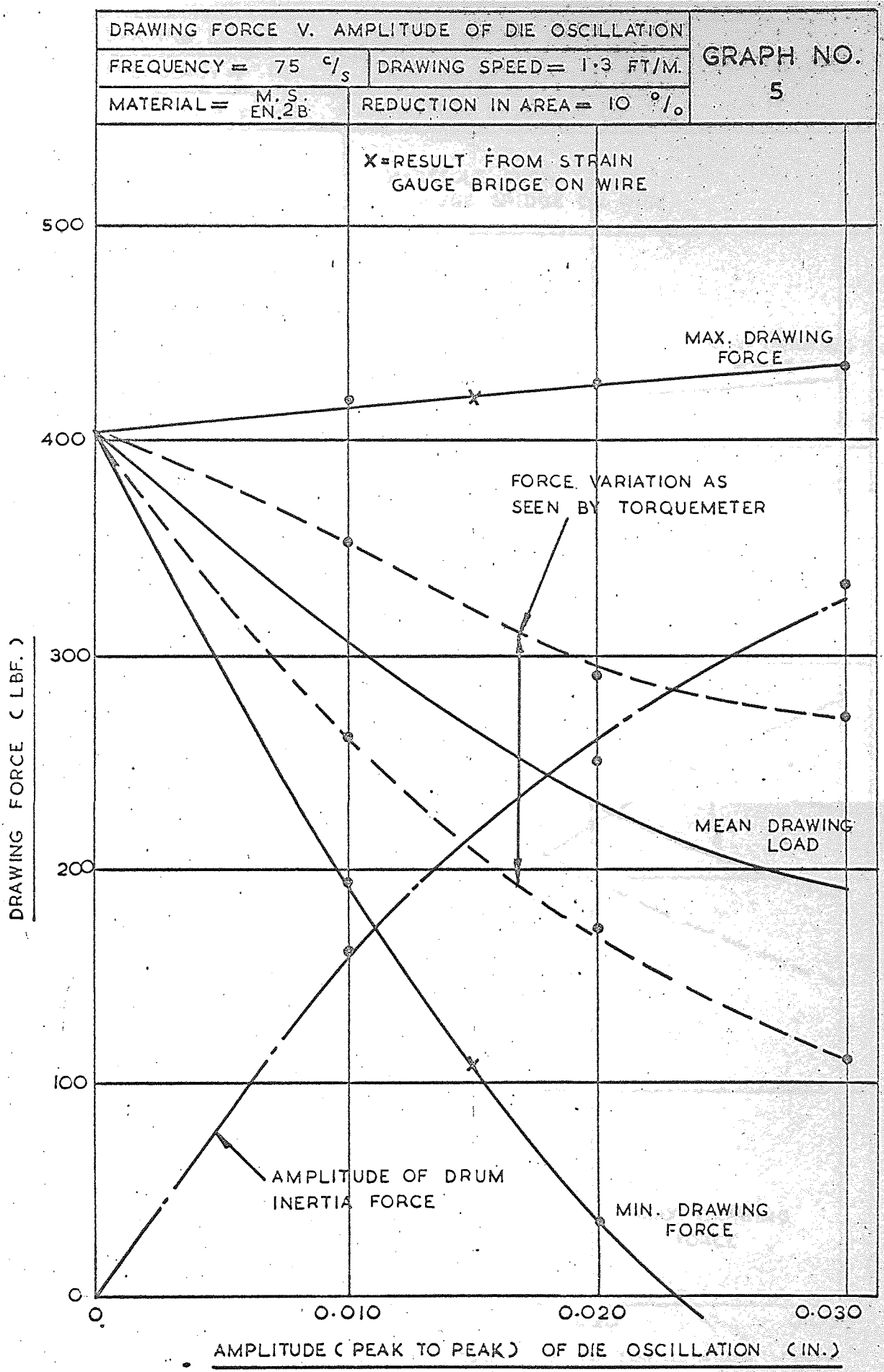
DRAWING FORCE V. AMPLITUDE OF DIE OSCILLATION
FREQUENCY = 75 c/s
DRAWING SPEED = 1·3 FT/M.
MATERIAL = M.S. EN.2B
REDUCTION IN AREA = 10 %
GRAPH NO. 5
X = RESULT FROM STRAIN GAUGE BRIDGE ON WIRE
MAX. DRAWING FORCE
FORCE VARIATION AS SEEN BY TORQUEMETER
MEAN DRAWING LOAD
AMPLITUDE OF DRUM INERTIA FORCE
MIN. DRAWING FORCE
DRAWING FORCE (LBF.)
500
400
300
200
100
0
0
0·010
0·020
0·030
AMPLITUDE (PEAK TO PEAK) OF DIE OSCILLATION (IN.)

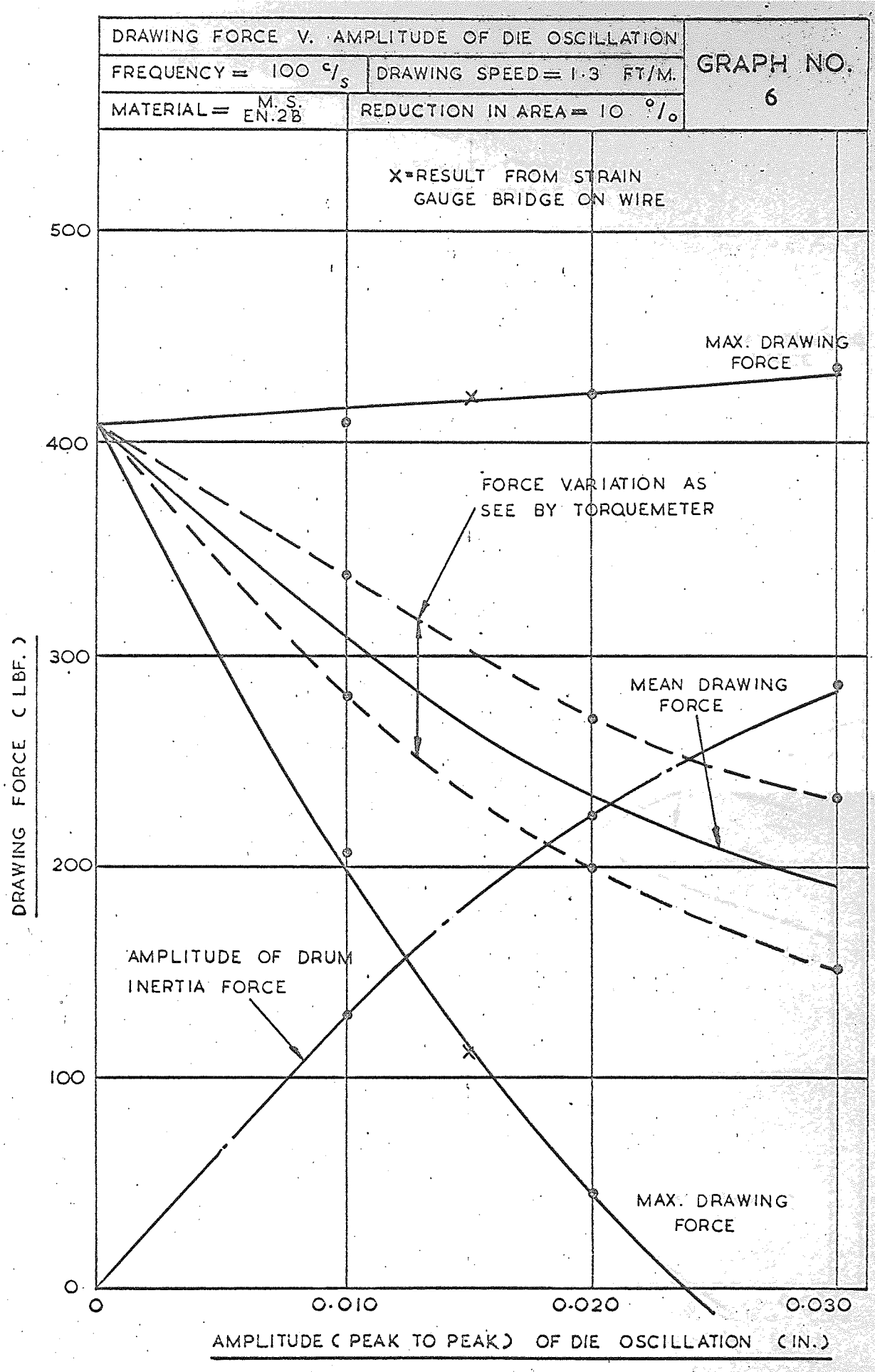
DRAWING FORCE V. AMPLITUDE OF DIE OSCILLATION
FREQUENCY = 100 c/s
DRAWING SPEED = 1·3 FT/M.
MATERIAL = M.S. EN.2B
REDUCTION IN AREA = 10 %
GRAPH NO. 6
X = RESULT FROM STRAIN GAUGE BRIDGE ON WIRE
MAX. DRAWING FORCE
FORCE VARIATION AS SEE BY TORQUEMETER
MEAN DRAWING FORCE
AMPLITUDE OF DRUM INERTIA FORCE
MAX. DRAWING FORCE
DRAWING FORCE (LBF.)
500
400
300
200
100
0
0
0·010
0·020
0·030
AMPLITUDE (PEAK TO PEAK) OF DIE OSCILLATION (IN.)

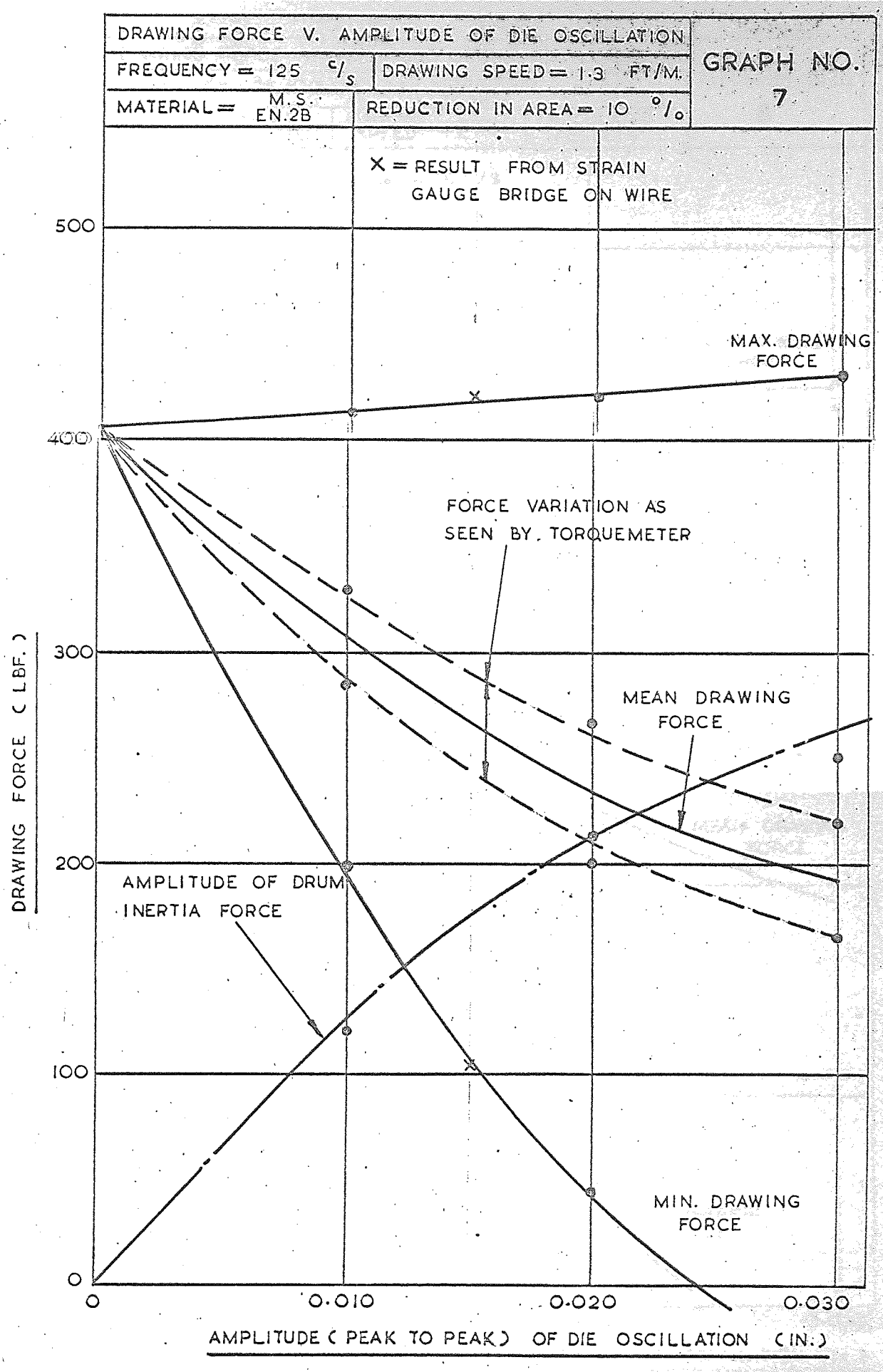
DRAWING FORCE V. AMPLITUDE OF DIE OSCILLATION
FREQUENCY = 125 c/s
DRAWING SPEED = 1.3 FT/M.
MATERIAL = M.S. EN.2B
REDUCTION IN AREA = 10 %
GRAPH NO. 7
X = RESULT FROM STRAIN GAUGE BRIDGE ON WIRE
MAX. DRAWING FORCE
FORCE VARIATION AS SEEN BY TORQUEMETER
MEAN DRAWING FORCE
AMPLITUDE OF DRUM INERTIA FORCE
MIN. DRAWING FORCE
DRAWING FORCE (LBF.)
500
400
300
200
100
0
0
0·010
0·020
0·030
AMPLITUDE (PEAK TO PEAK) OF DIE OSCILLATION (IN.)

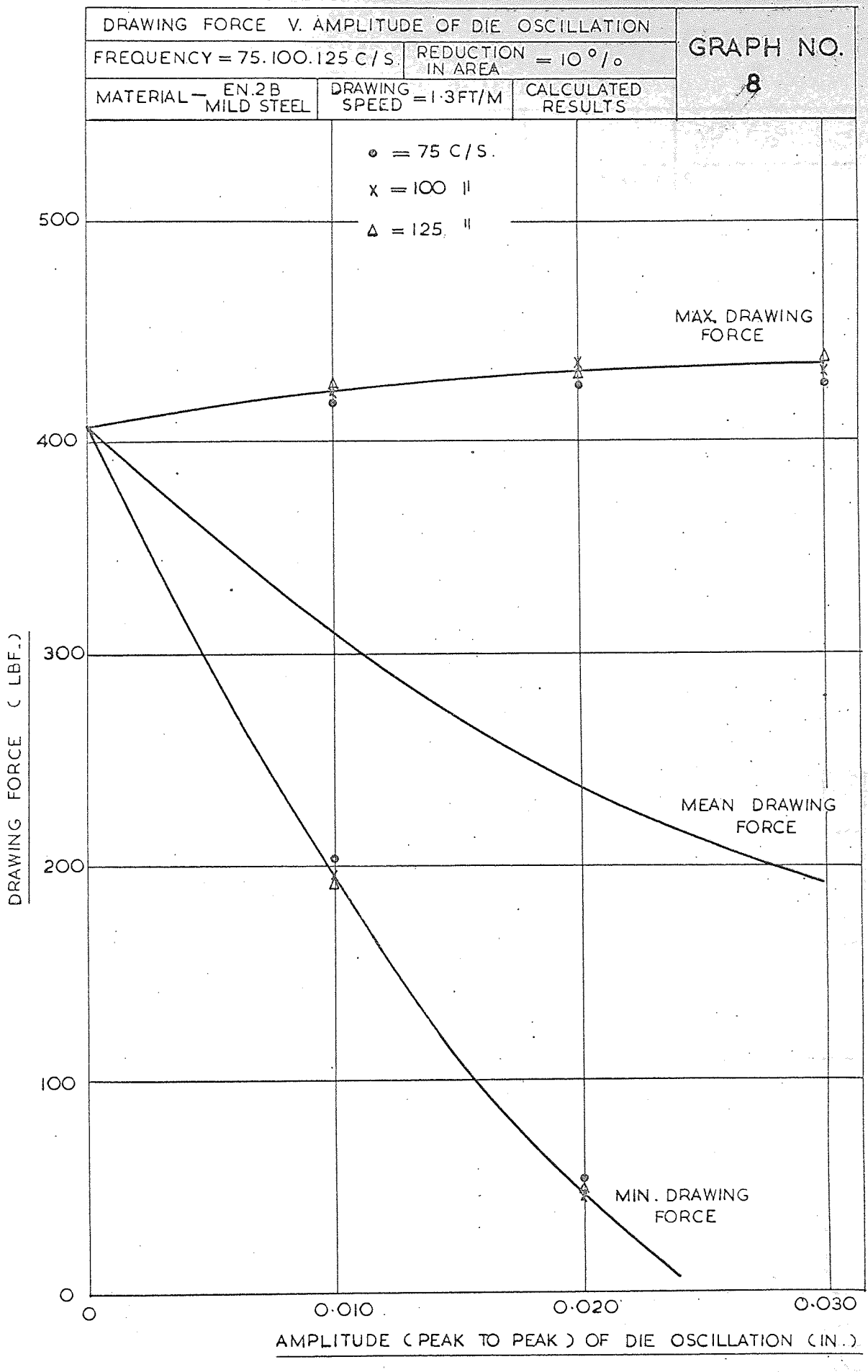
DRAWING FORCE V. AMPLITUDE OF DIE OSCILLATION
FREQUENCY = 75. 100. 125 C/S.
REDUCTION IN AREA = 10 %
MATERIAL — EN.2B MILD STEEL
DRAWING SPEED = 1·3FT/M
CALCULATED RESULTS
GRAPH NO. 8
● = 75 C/S.
X = 100 "
Δ = 125 "
MAX. DRAWING FORCE
MEAN DRAWING FORCE
MIN. DRAWING FORCE
DRAWING FORCE (LBF.)
500
400
300
200
100
0
0
0·010
0·020
0·030
AMPLITUDE (PEAK TO PEAK) OF DIE OSCILLATION (IN.)

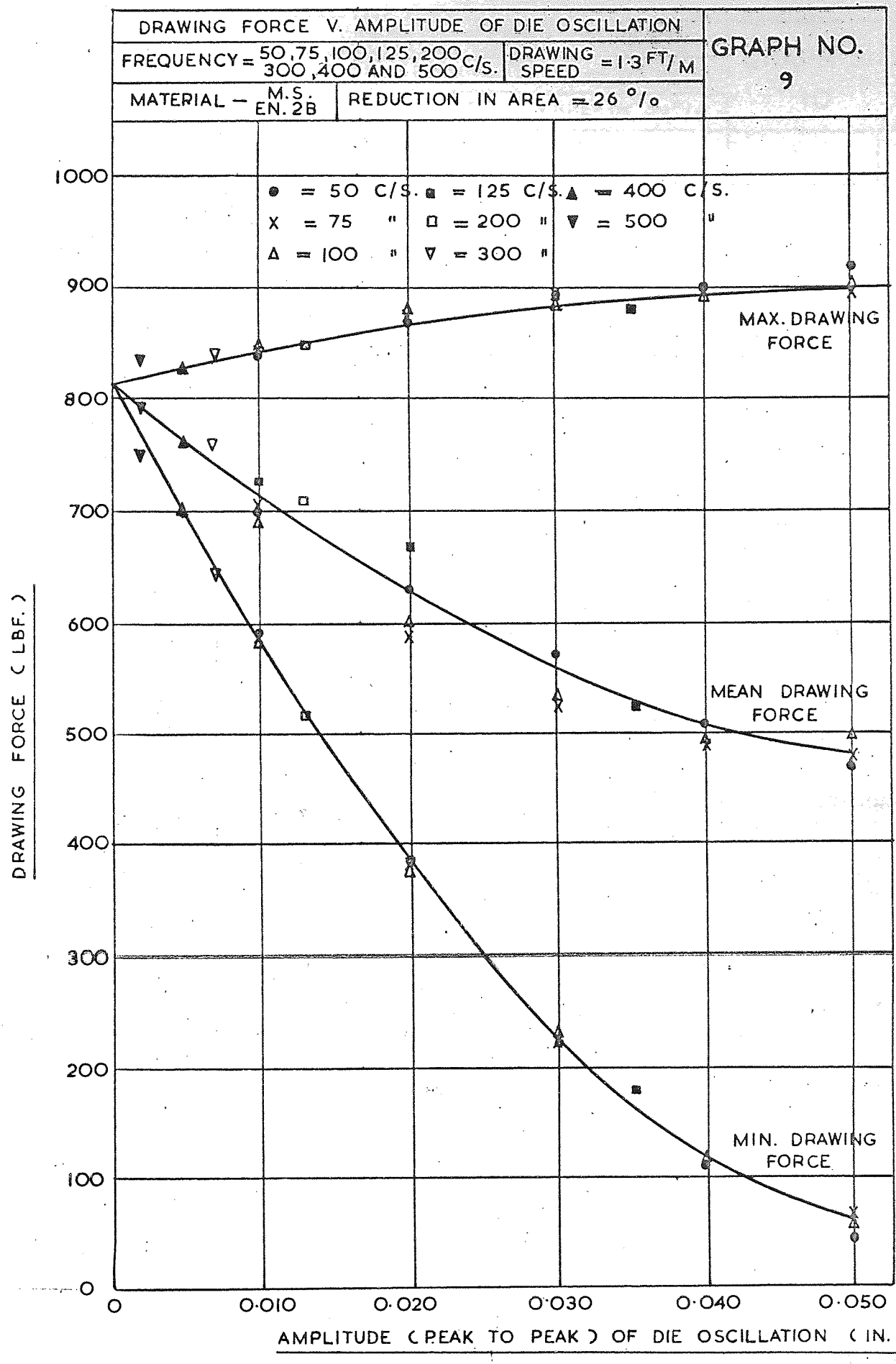
DRAWING FORCE V. AMPLITUDE OF DIE OSCILLATION
FREQUENCY = 50, 75, 100, 125, 200, 300, 400 AND 500 C/S.
DRAWING SPEED = 1·3 FT/M
MATERIAL — M.S. EN. 2B
REDUCTION IN AREA = 26 %
GRAPH NO. 9
● = 50 C/S. ■ = 125 C/S. ▲ = 400 C/S.
X = 75 " □ = 200 " ▼ = 500 "
Δ = 100 " ▽ = 300 "
MAX. DRAWING FORCE
MEAN DRAWING FORCE
MIN. DRAWING FORCE
DRAWING FORCE (LBF.)
1000
900
800
700
600
500
400
300
200
100
0
0
0·010
0·020
0·030
0·040
0·050
AMPLITUDE (PEAK TO PEAK) OF DIE OSCILLATION (IN.)

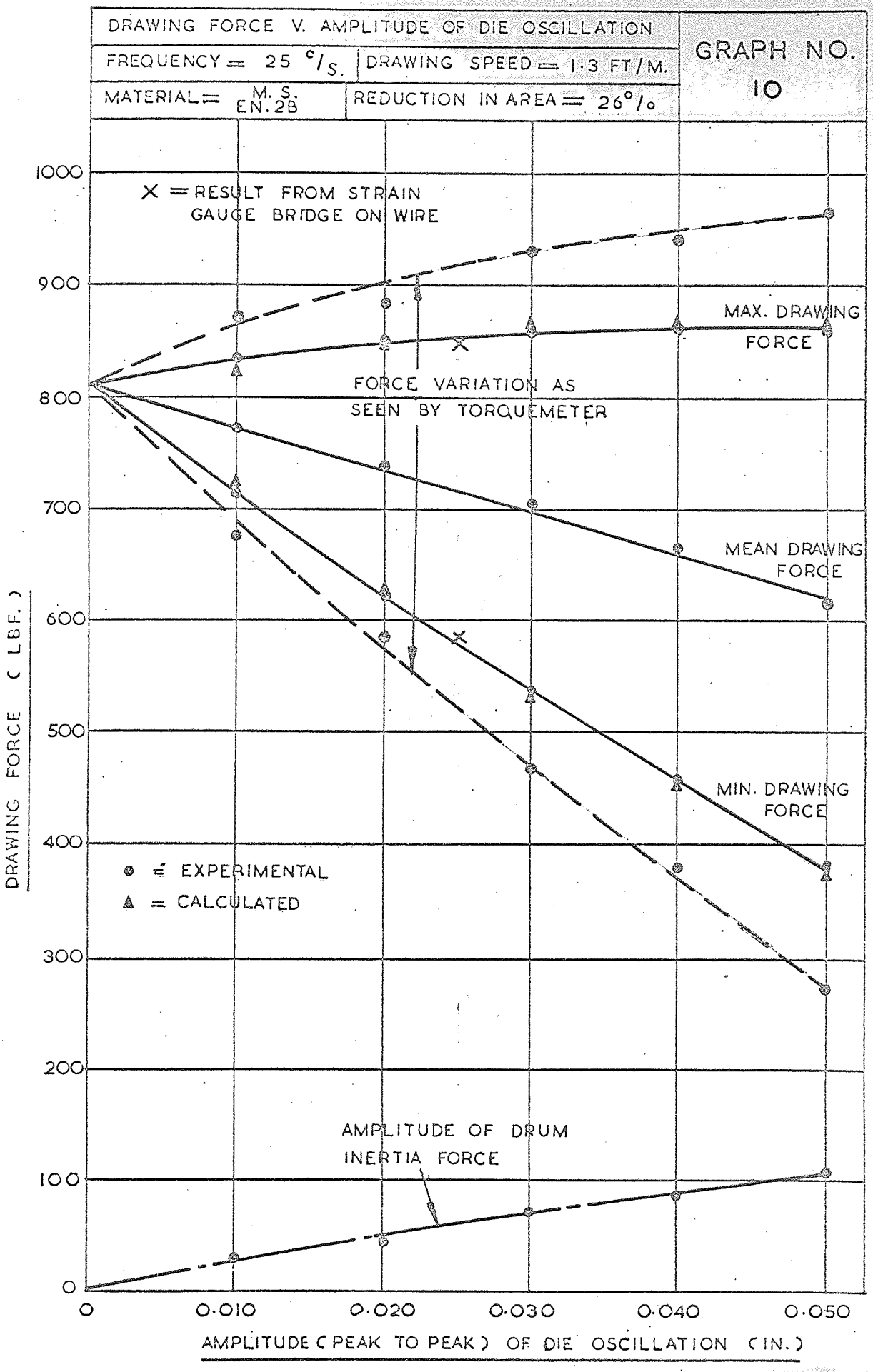
DRAWING FORCE V. AMPLITUDE OF DIE OSCILLATION
FREQUENCY = 25 c/s.
DRAWING SPEED = 1·3 FT/M.
MATERIAL = M.S. EN.2B
REDUCTION IN AREA = 26%
GRAPH NO. 10
X = RESULT FROM STRAIN GAUGE BRIDGE ON WIRE
MAX. DRAWING FORCE
FORCE VARIATION AS SEEN BY TORQUEMETER
MEAN DRAWING FORCE
MIN. DRAWING FORCE
● = EXPERIMENTAL
▲ = CALCULATED
AMPLITUDE OF DRUM INERTIA FORCE
DRAWING FORCE (LBF.)
1000
900
800
700
600
500
400
300
200
100
0
0
0·010
0·020
0·030
0·040
0·050
AMPLITUDE (PEAK TO PEAK) OF DIE OSCILLATION (IN.)

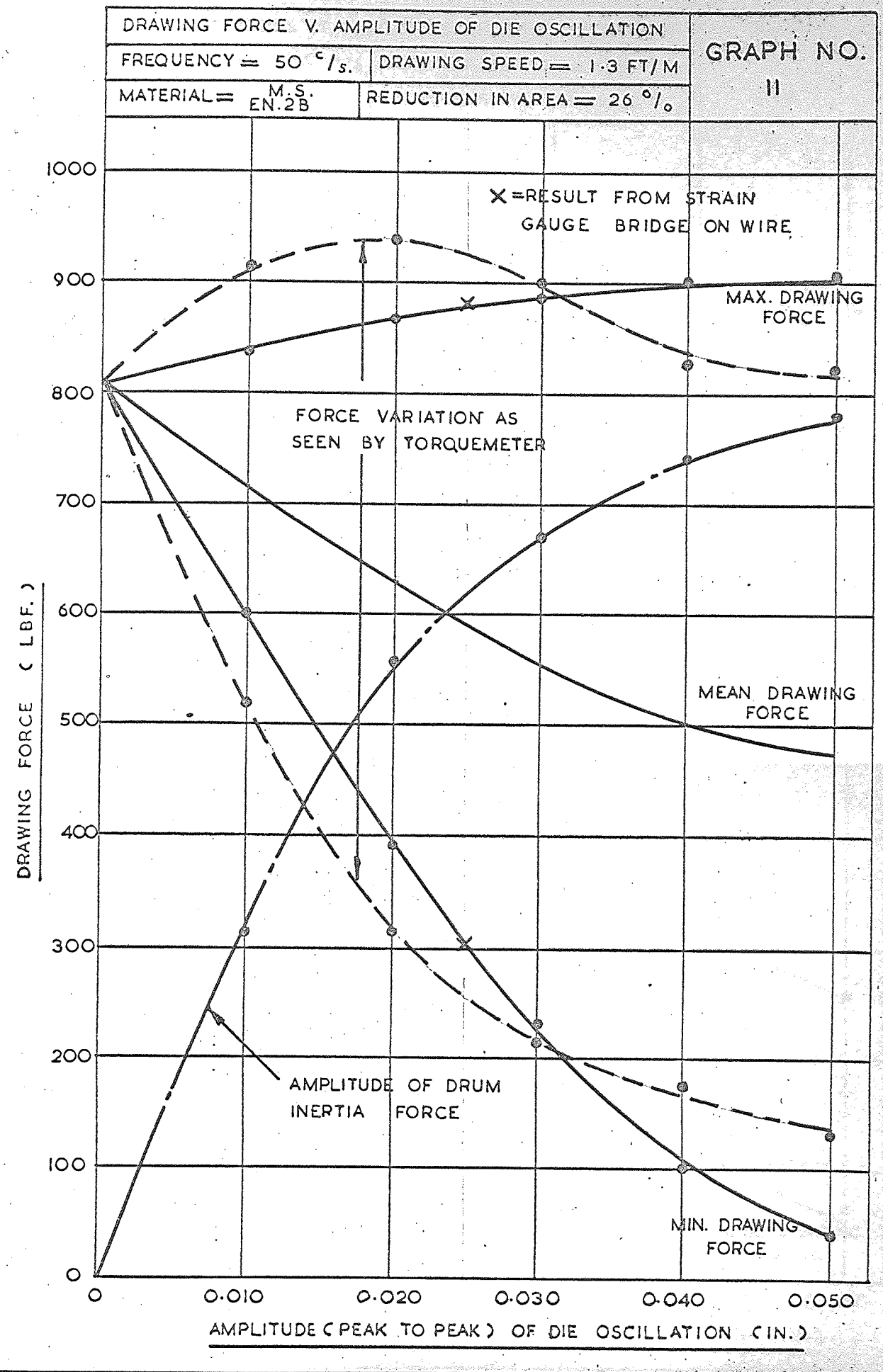
DRAWING FORCE V. AMPLITUDE OF DIE OSCILLATION
FREQUENCY = 50 c/s.
DRAWING SPEED = 1·3 FT/M
MATERIAL = M.S. EN.2B
REDUCTION IN AREA = 26 %
GRAPH NO. 11
X = RESULT FROM STRAIN GAUGE BRIDGE ON WIRE
MAX. DRAWING FORCE
FORCE VARIATION AS SEEN BY TORQUEMETER
MEAN DRAWING FORCE
AMPLITUDE OF DRUM INERTIA FORCE
MIN. DRAWING FORCE
DRAWING FORCE (LBF.)
1000
900
800
700
600
500
400
300
200
100
0
0
0·010
0·020
0·030
0·040
0·050
AMPLITUDE (PEAK TO PEAK) OF DIE OSCILLATION (IN.)

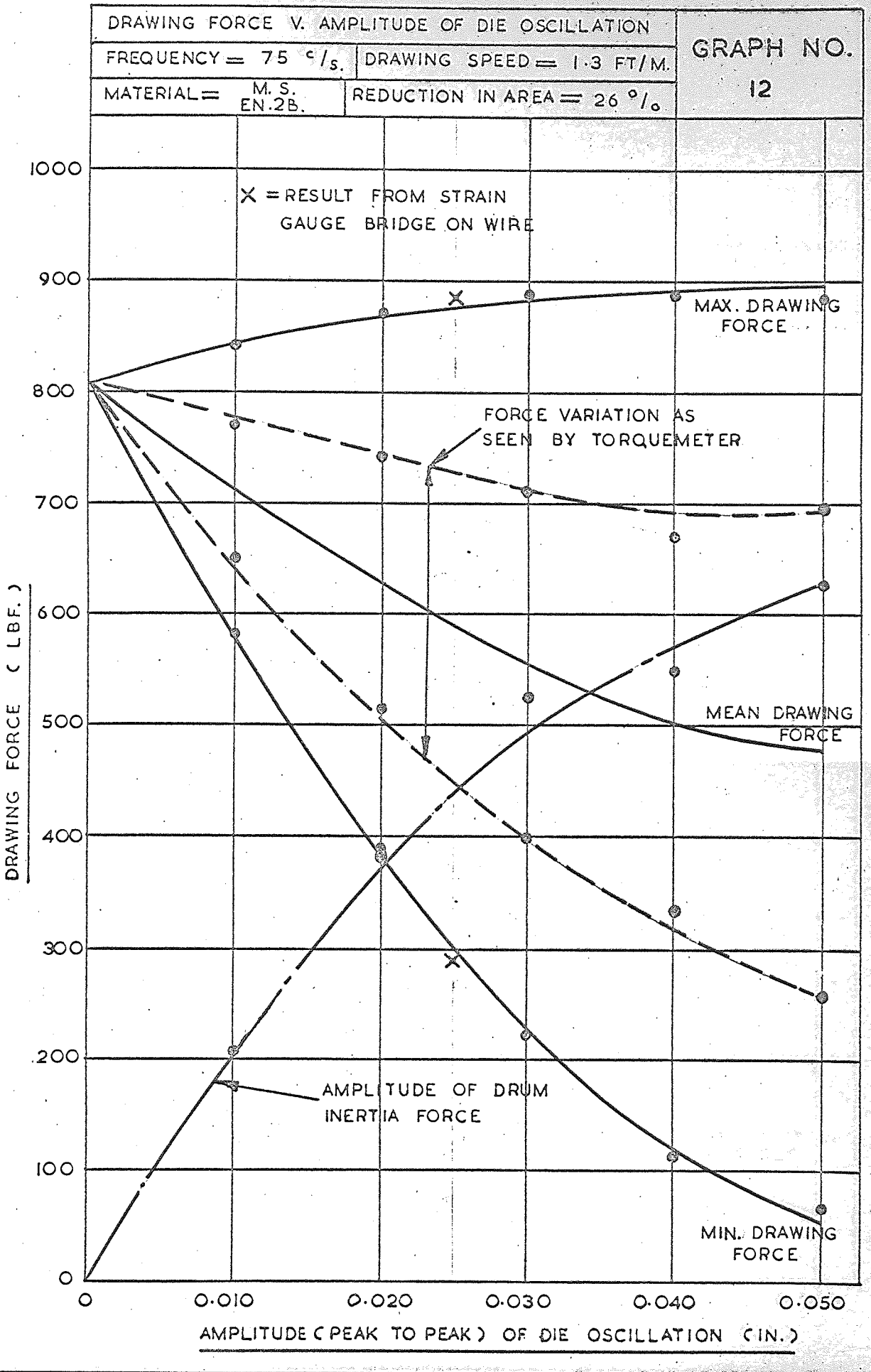
DRAWING FORCE V. AMPLITUDE OF DIE OSCILLATION
FREQUENCY = 75 c/s.
DRAWING SPEED = 1·3 FT/M.
MATERIAL = M.S. EN.2B.
REDUCTION IN AREA = 26 %
GRAPH NO. 12
X = RESULT FROM STRAIN GAUGE BRIDGE ON WIRE
MAX. DRAWING FORCE
FORCE VARIATION AS SEEN BY TORQUEMETER
MEAN DRAWING FORCE
AMPLITUDE OF DRUM INERTIA FORCE
MIN. DRAWING FORCE
DRAWING FORCE (LBF.)
1000
900
800
700
600
500
400
300
200
100
0
0
0·010
0·020
0·030
0·040
0·050
AMPLITUDE (PEAK TO PEAK) OF DIE OSCILLATION (IN.)

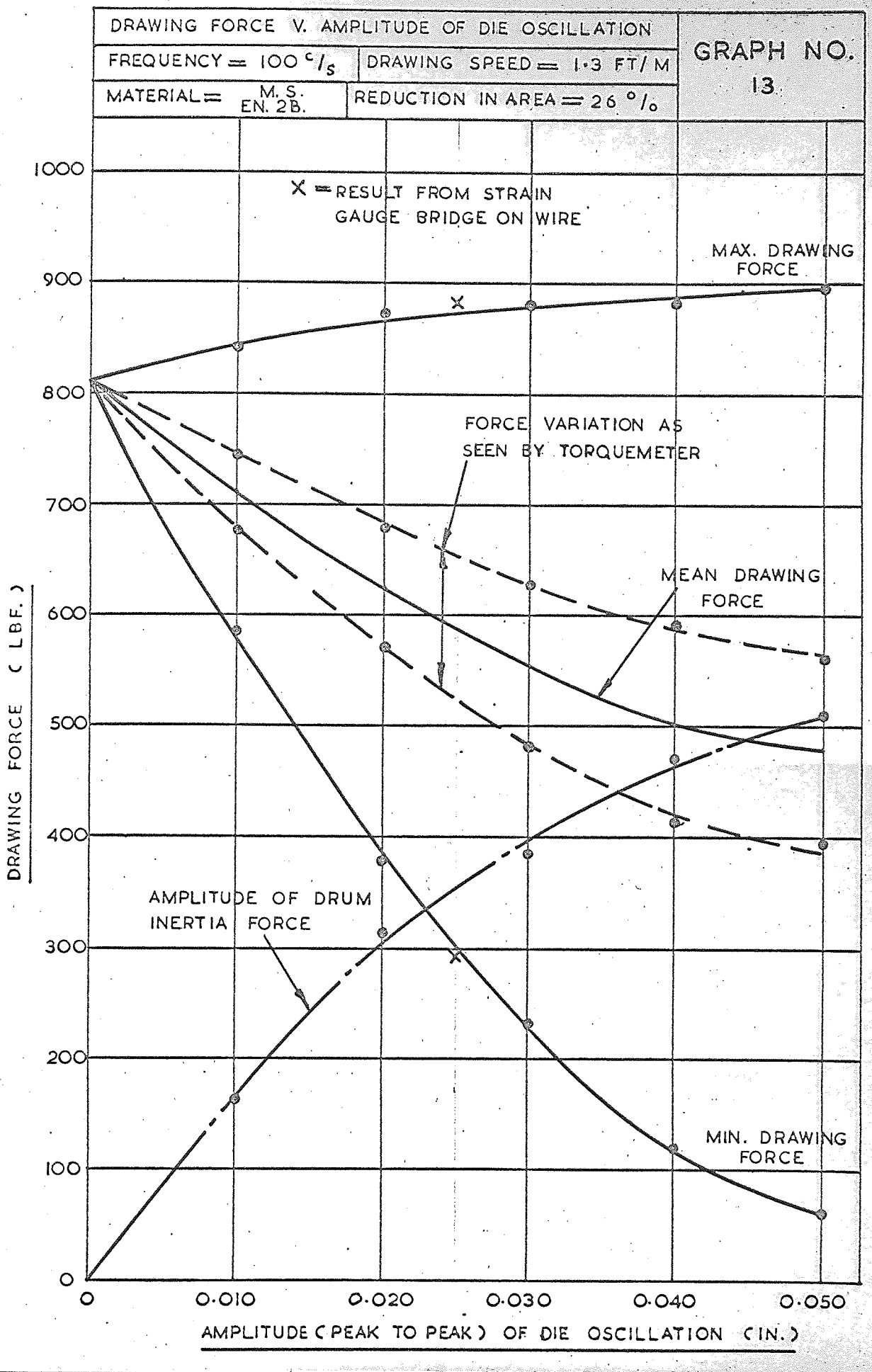
DRAWING FORCE V. AMPLITUDE OF DIE OSCILLATION
FREQUENCY = 100 c/s
DRAWING SPEED = 1·3 FT/M
MATERIAL = M.S. EN. 2B.
REDUCTION IN AREA = 26 %
GRAPH NO. 13
X = RESULT FROM STRAIN GAUGE BRIDGE ON WIRE
MAX. DRAWING FORCE
FORCE VARIATION AS SEEN BY TORQUEMETER
MEAN DRAWING FORCE
AMPLITUDE OF DRUM INERTIA FORCE
MIN. DRAWING FORCE
DRAWING FORCE (LBF.)
1000
900
800
700
600
500
400
300
200
100
0
0
0·010
0·020
0·030
0·040
0·050
AMPLITUDE (PEAK TO PEAK) OF DIE OSCILLATION (IN.)

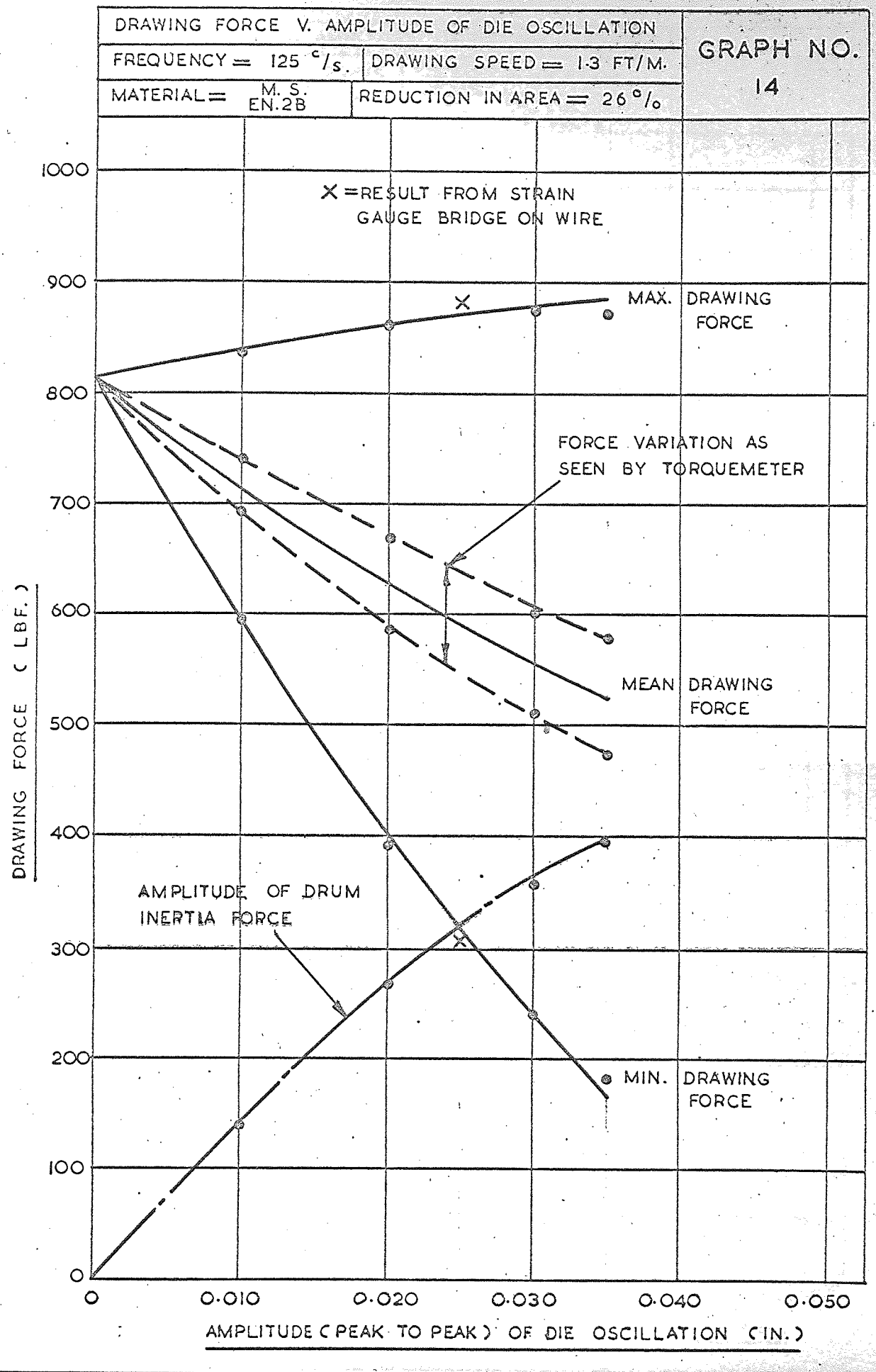
DRAWING FORCE V. AMPLITUDE OF DIE OSCILLATION
FREQUENCY = 125 c/s.
DRAWING SPEED = 1·3 FT/M.
MATERIAL = M.S. EN.2B
REDUCTION IN AREA = 26 %
GRAPH NO. 14
X = RESULT FROM STRAIN GAUGE BRIDGE ON WIRE
MAX. DRAWING FORCE
FORCE VARIATION AS SEEN BY TORQUEMETER
MEAN DRAWING FORCE
AMPLITUDE OF DRUM INERTIA FORCE
MIN. DRAWING FORCE
DRAWING FORCE (LBF.)
1000
900
800
700
600
500
400
300
200
100
0
0
0·010
0·020
0·030
0·040
0·050
AMPLITUDE (PEAK TO PEAK) OF DIE OSCILLATION (IN.)

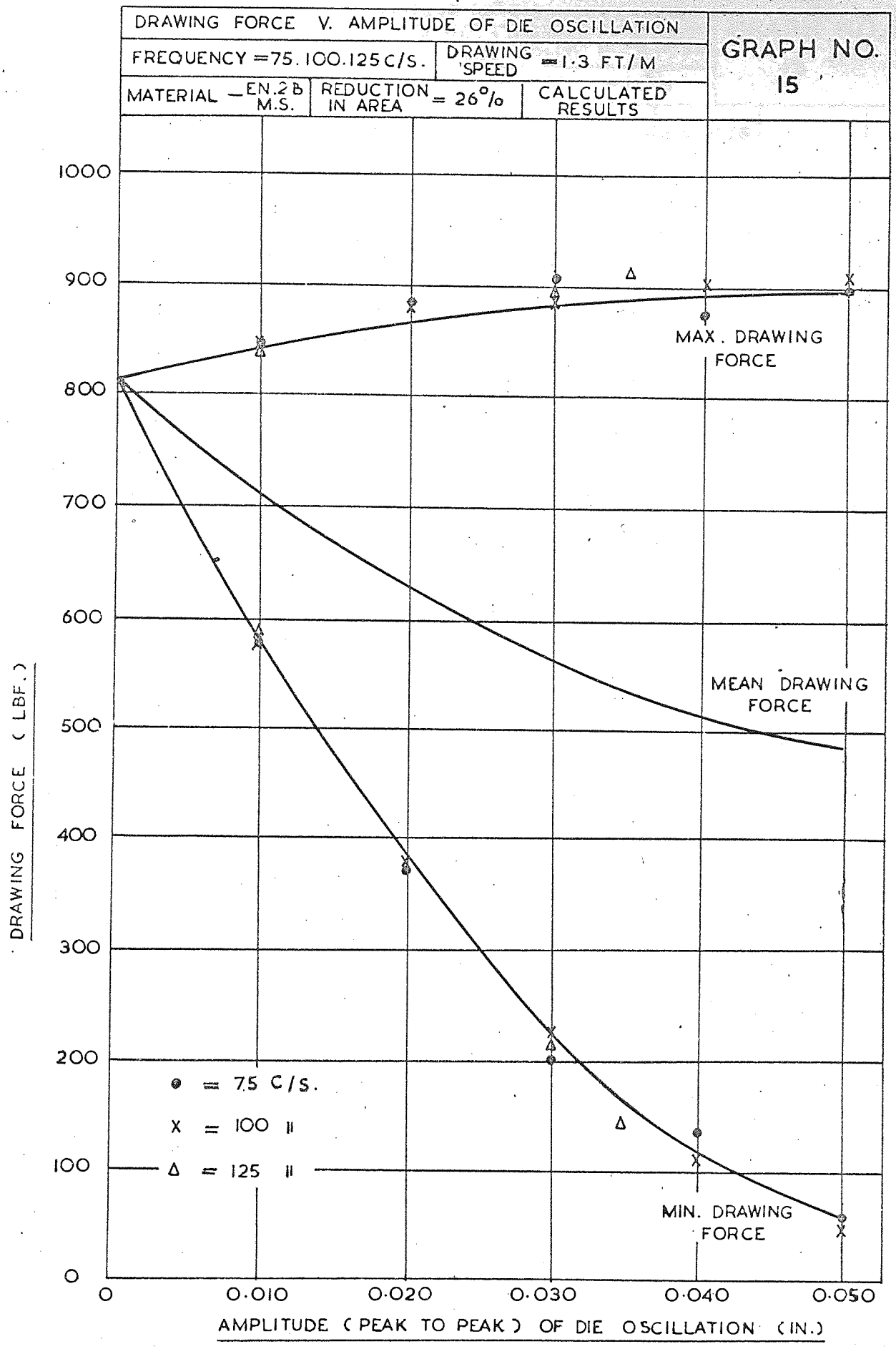
DRAWING FORCE V. AMPLITUDE OF DIE OSCILLATION
FREQUENCY = 75. 100. 125 C/S.
DRAWING SPEED = 1·3 FT/M
MATERIAL — EN.2B M.S.
REDUCTION IN AREA = 26%
CALCULATED RESULTS
GRAPH NO. 15
MAX. DRAWING FORCE
MEAN DRAWING FORCE
MIN. DRAWING FORCE
● = 7.5 C/S.
X = 100 "
Δ = 125 "
DRAWING FORCE (LBF.)
AMPLITUDE (PEAK TO PEAK) OF DIE OSCILLATION (IN.)
0
100
200
300
400
500
600
700
800
900
1000
0·010
0·020
0·030
0·040
0·050

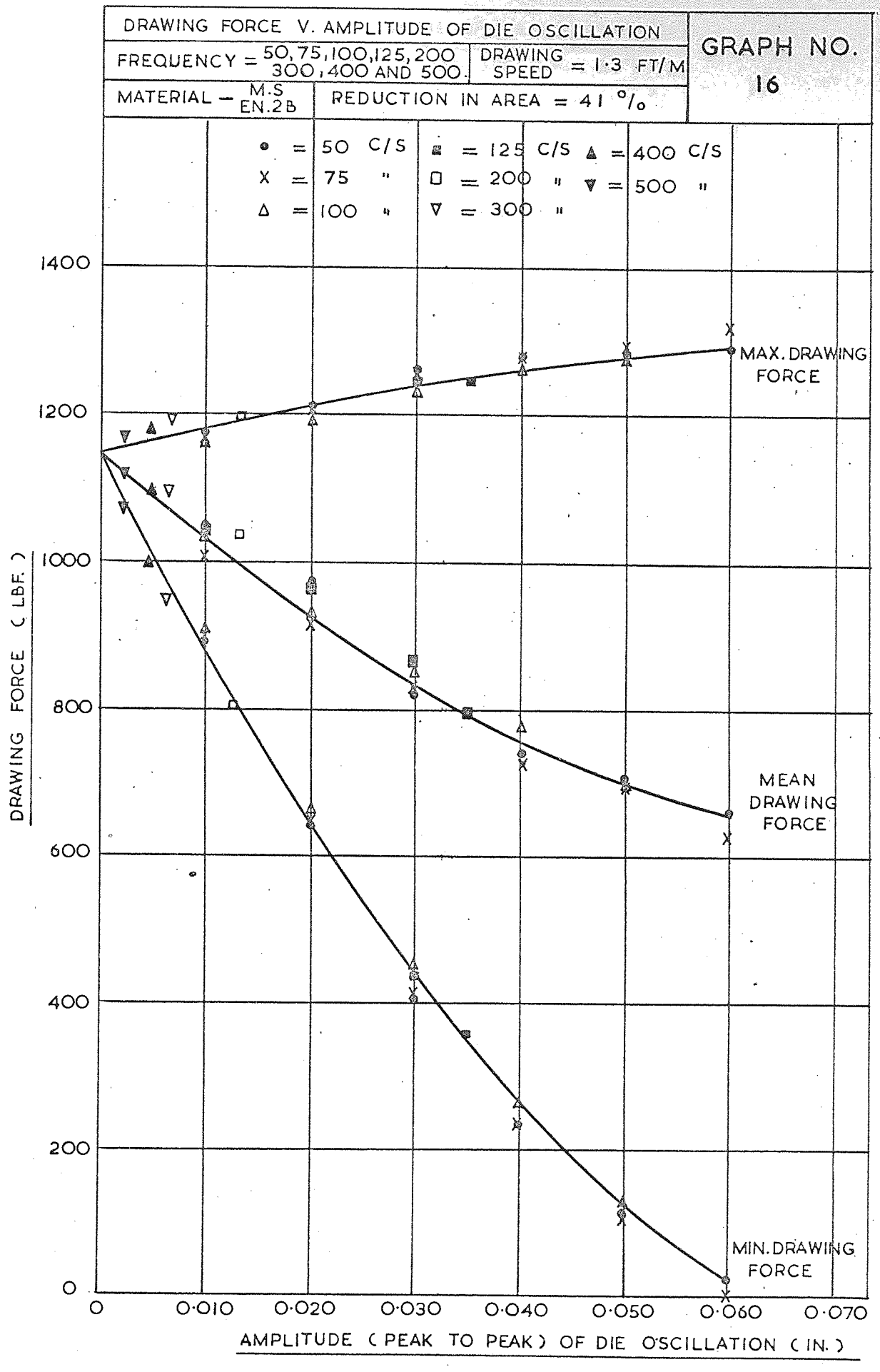
DRAWING FORCE V. AMPLITUDE OF DIE OSCILLATION
FREQUENCY = 50, 75, 100, 125, 200 300, 400 AND 500.
DRAWING SPEED = 1·3 FT/M
MATERIAL — M.S EN.2B
REDUCTION IN AREA = 41 %
GRAPH NO. 16
● = 50 C/S
X = 75 "
Δ = 100 "
■ = 125 C/S
□ = 200 "
▽ = 300 "
▲ = 400 C/S
▼ = 500 "
MAX. DRAWING FORCE
MEAN DRAWING FORCE
MIN. DRAWING FORCE
DRAWING FORCE (LBF.)
1400
1200
1000
800
600
400
200
0
0
0·010
0·020
0·030
0·040
0·050
0·060
0·070
AMPLITUDE (PEAK TO PEAK) OF DIE OSCILLATION (IN.)

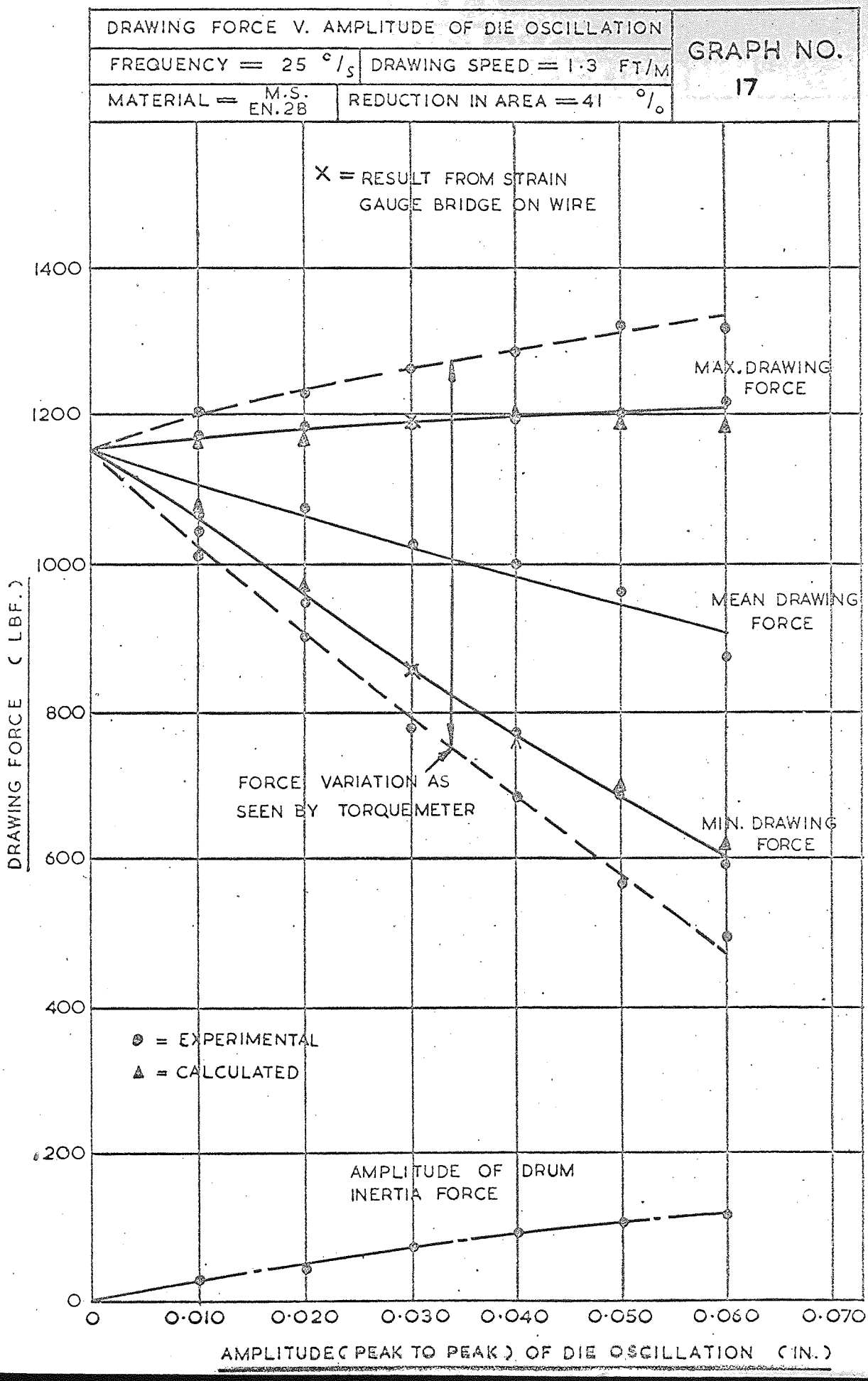
DRAWING FORCE V. AMPLITUDE OF DIE OSCILLATION
FREQUENCY = 25 °/S
DRAWING SPEED = 1·3 FT/M
MATERIAL = M.S. EN.2B
REDUCTION IN AREA = 41 %
GRAPH NO. 17
X = RESULT FROM STRAIN GAUGE BRIDGE ON WIRE
MAX. DRAWING FORCE
MEAN DRAWING FORCE
MIN. DRAWING FORCE
FORCE VARIATION AS SEEN BY TORQUEMETER
AMPLITUDE OF DRUM INERTIA FORCE
● = EXPERIMENTAL
▲ = CALCULATED
DRAWING FORCE (LBF.)
1400
1200
1000
800
600
400
200
0
0
0·010
0·020
0·030
0·040
0·050
0·060
0·070
AMPLITUDE (PEAK TO PEAK) OF DIE OSCILLATION (IN.)

DRAWING FORCE V. AMPLITUDE OF DIE OSCILLATION

FREQUENCY = 50 $^{c}/_{s}$ | DRAWING SPEED = 1·3 FT/M

MATERIAL = M·S. EN.2B. | REDUCTION IN AREA = 41 $^{o}/_{o}$

GRAPH NO. 18

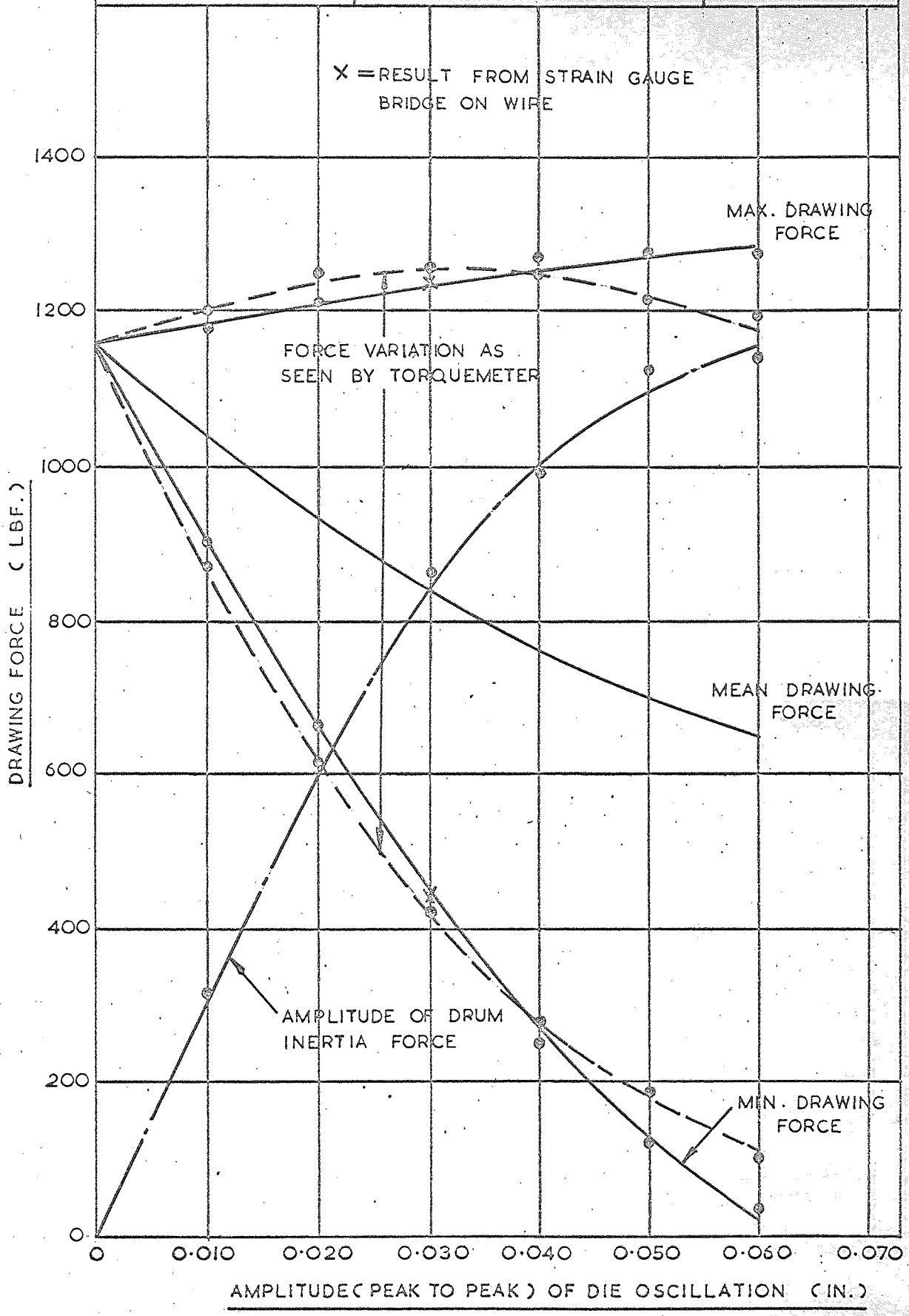

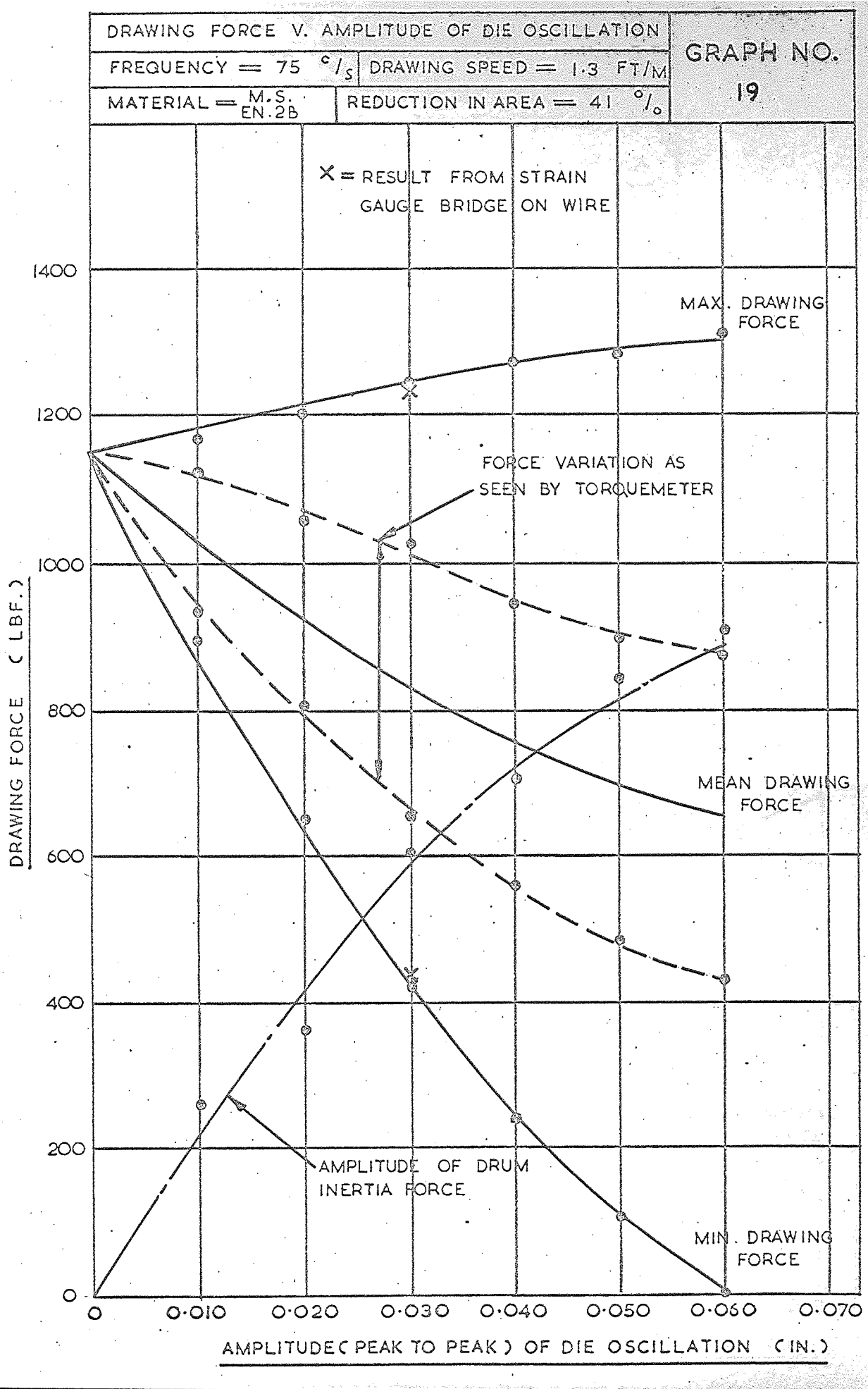
DRAWING FORCE V. AMPLITUDE OF DIE OSCILLATION
FREQUENCY = 75 c/s
DRAWING SPEED = 1.3 FT/M
MATERIAL = M.S. EN.2B
REDUCTION IN AREA = 41 %
GRAPH NO. 19
× = RESULT FROM STRAIN GAUGE BRIDGE ON WIRE
MAX. DRAWING FORCE
FORCE VARIATION AS SEEN BY TORQUEMETER
MEAN DRAWING FORCE
AMPLITUDE OF DRUM INERTIA FORCE
MIN. DRAWING FORCE
DRAWING FORCE (LBF.)
1400
1200
1000
800
600
400
200
0
0
0·010
0·020
0·030
0·040
0·050
0·060
0·070
AMPLITUDE (PEAK TO PEAK) OF DIE OSCILLATION (IN.)

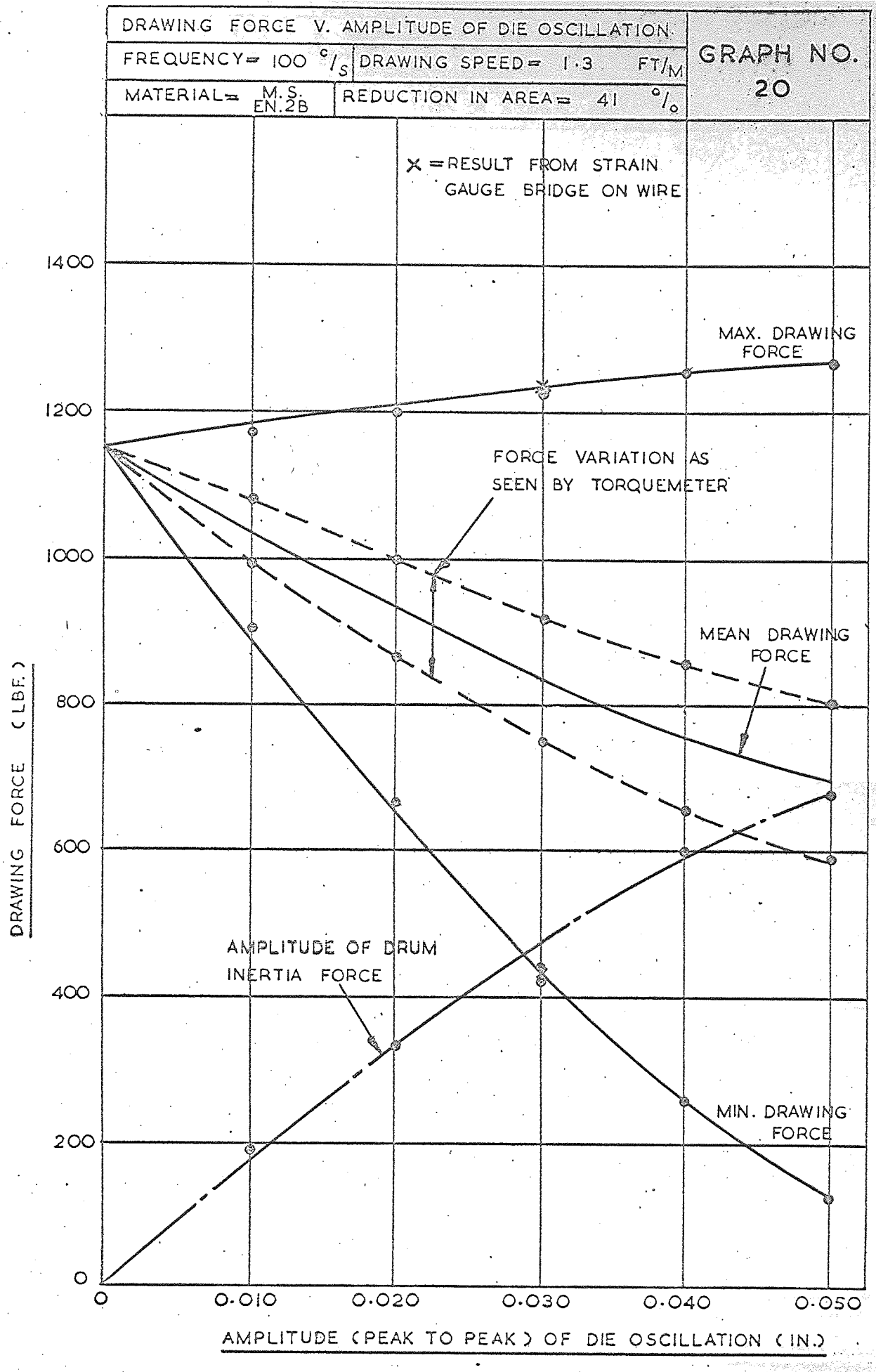
DRAWING FORCE V. AMPLITUDE OF DIE OSCILLATION
FREQUENCY = 100 °/S
DRAWING SPEED = 1·3 FT/M
MATERIAL = M.S. EN.2B
REDUCTION IN AREA = 41 %
GRAPH NO. 20
× = RESULT FROM STRAIN GAUGE BRIDGE ON WIRE
MAX. DRAWING FORCE
FORCE VARIATION AS SEEN BY TORQUEMETER
MEAN DRAWING FORCE
AMPLITUDE OF DRUM INERTIA FORCE
MIN. DRAWING FORCE
DRAWING FORCE (LBF.)
1400
1200
1000
800
600
400
200
0
0
0·010
0·020
0·030
0·040
0·050
AMPLITUDE (PEAK TO PEAK) OF DIE OSCILLATION (IN.)

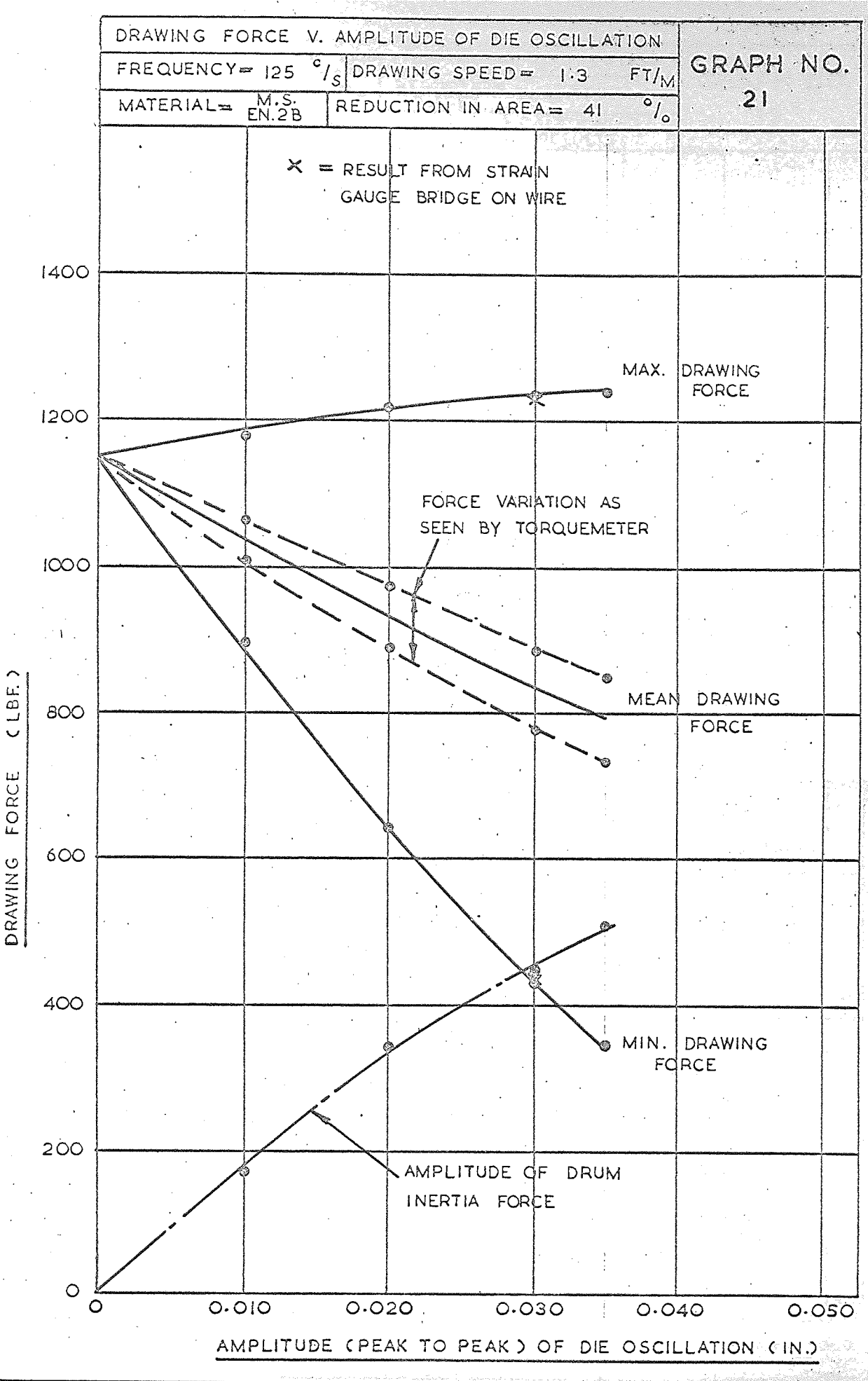
DRAWING FORCE V. AMPLITUDE OF DIE OSCILLATION
FREQUENCY = 125 °/S
DRAWING SPEED = 1·3 FT/M
MATERIAL = M.S. EN.2B
REDUCTION IN AREA = 41 %
GRAPH NO. 21
× = RESULT FROM STRAIN GAUGE BRIDGE ON WIRE
MAX. DRAWING FORCE
FORCE VARIATION AS SEEN BY TORQUEMETER
MEAN DRAWING FORCE
MIN. DRAWING FORCE
AMPLITUDE OF DRUM INERTIA FORCE
DRAWING FORCE (LBF.)
1400
1200
1000
800
600
400
200
0
0
0·010
0·020
0·030
0·040
0·050
AMPLITUDE (PEAK TO PEAK) OF DIE OSCILLATION (IN.)

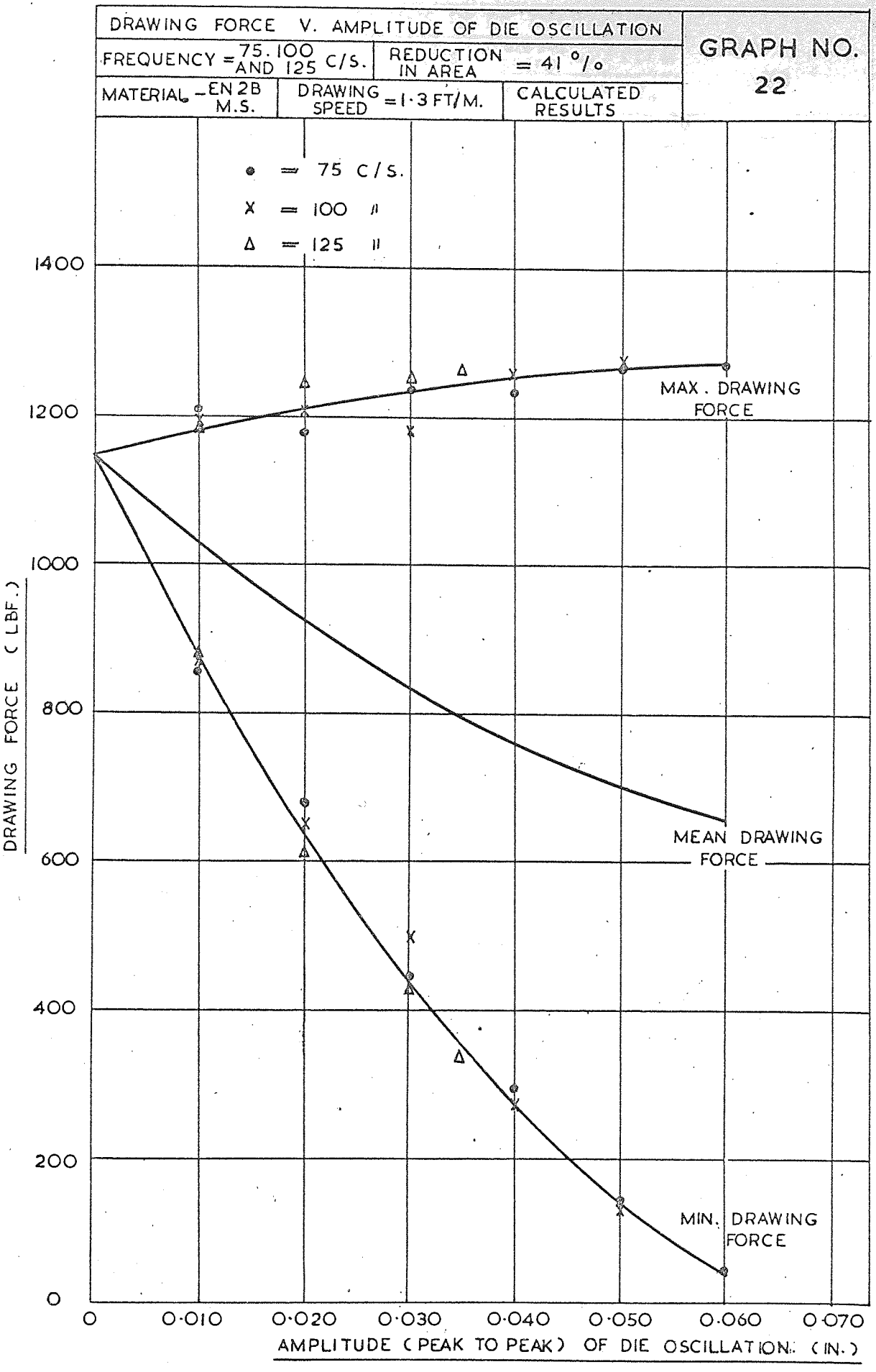
DRAWING FORCE V. AMPLITUDE OF DIE OSCILLATION
FREQUENCY = 75. 100 AND 125 C/S.
REDUCTION IN AREA = 41 %
MATERIAL – EN 2B M.S.
DRAWING SPEED = 1·3 FT/M.
CALCULATED RESULTS
GRAPH NO. 22
● = 75 C/S.
X = 100 "
Δ = 125 "
MAX. DRAWING FORCE
MEAN DRAWING FORCE
MIN. DRAWING FORCE
DRAWING FORCE (LBF.)
1400
1200
1000
800
600
400
200
0
0
0·010
0·020
0·030
0·040
0·050
0·060
0·070
AMPLITUDE (PEAK TO PEAK) OF DIE OSCILLATION. (IN.)

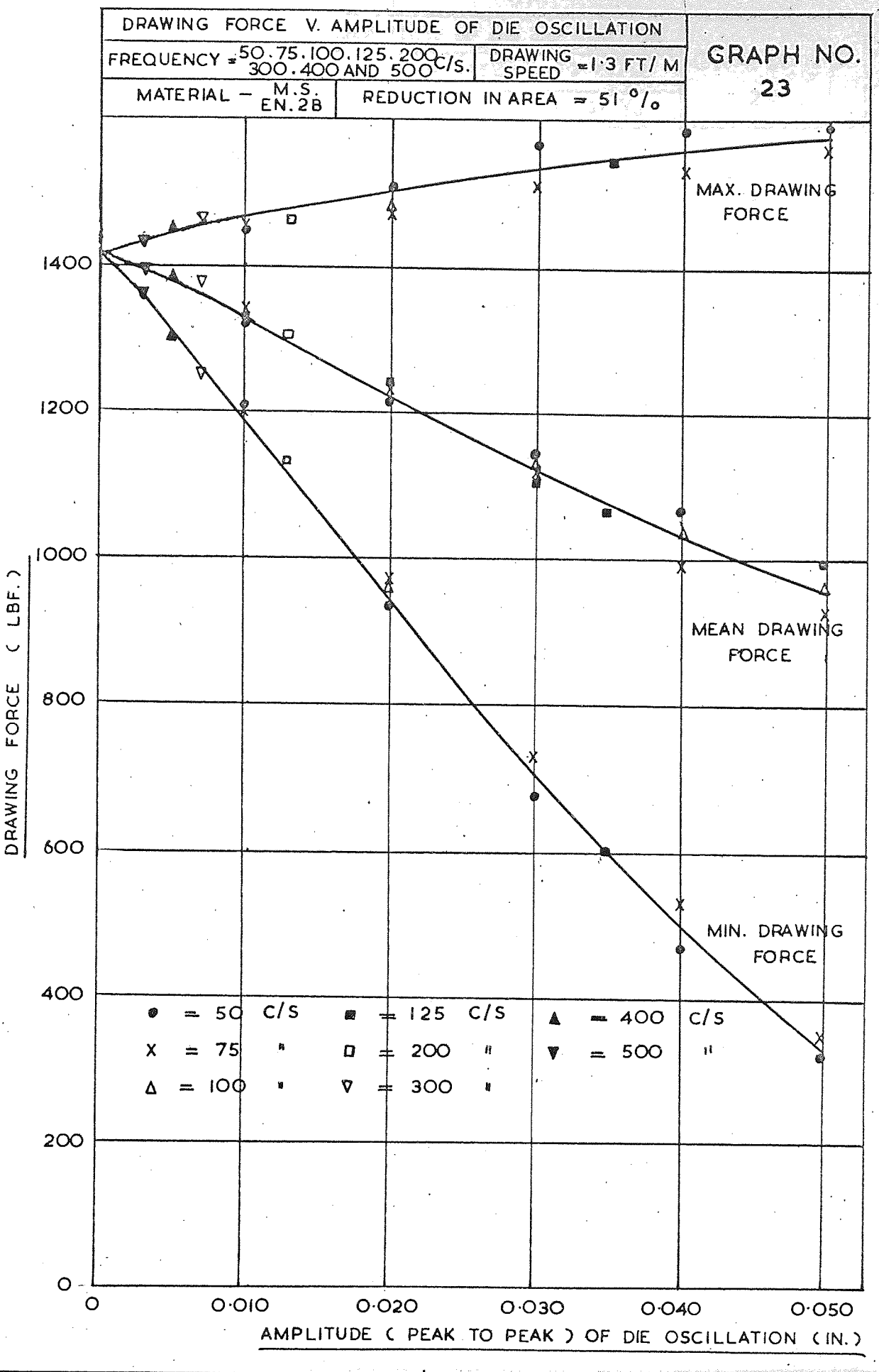
DRAWING FORCE V. AMPLITUDE OF DIE OSCILLATION
FREQUENCY = 50. 75. 100. 125. 200. 300. 400 AND 500 C/S.
DRAWING SPEED = 1·3 FT/ M
MATERIAL – M.S. EN. 2B
REDUCTION IN AREA = 51 %
GRAPH NO. 23
MAX. DRAWING FORCE
MEAN DRAWING FORCE
MIN. DRAWING FORCE
DRAWING FORCE (LBF.)
AMPLITUDE (PEAK TO PEAK) OF DIE OSCILLATION (IN.)
0
200
400
600
800
1000
1200
1400
0·010
0·020
0·030
0·040
0·050
● = 50 C/S
X = 75 "
Δ = 100 "
■ = 125 C/S
□ = 200 "
▽ = 300 "
▲ = 400 C/S
▼ = 500 "

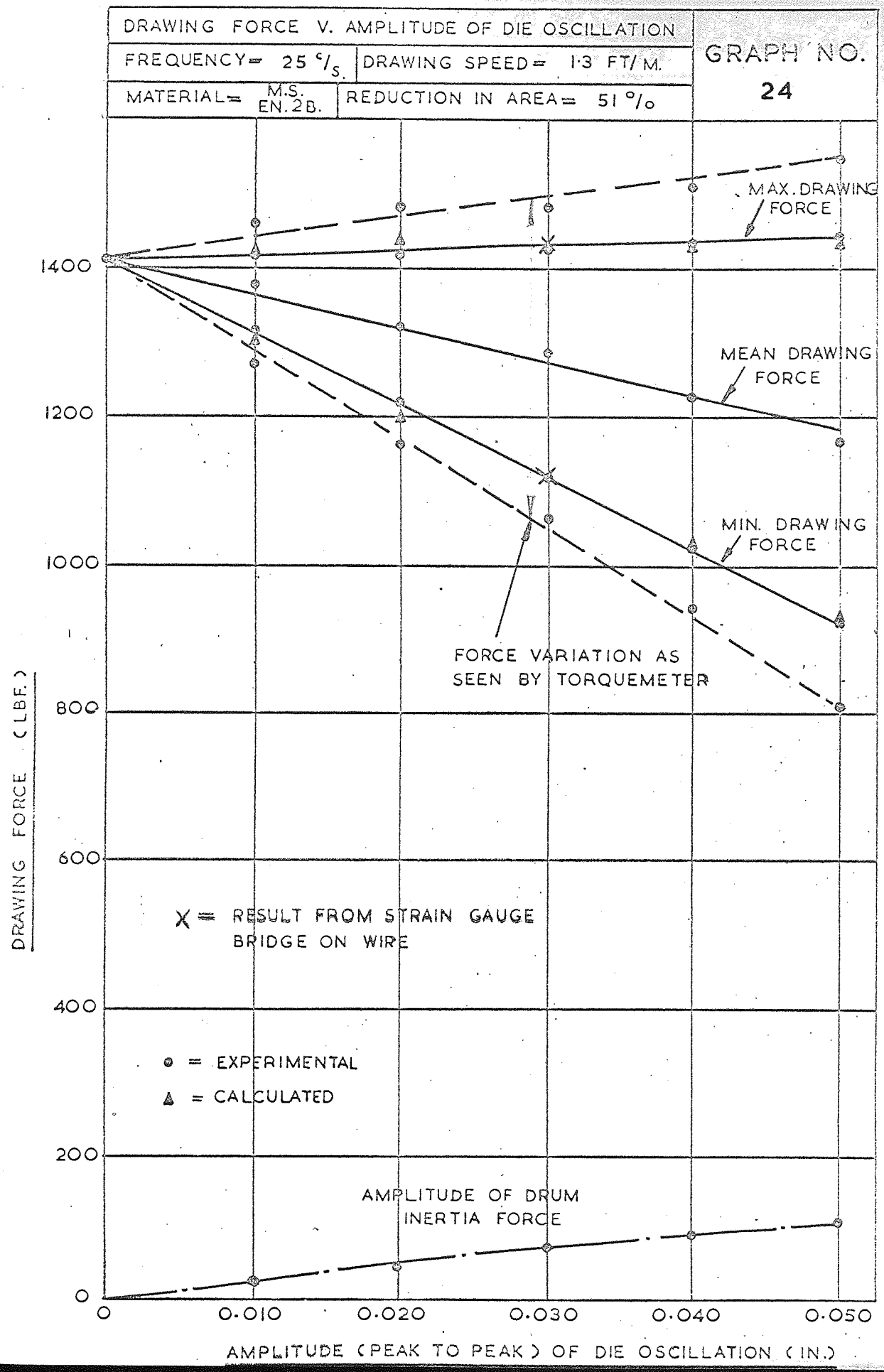
DRAWING FORCE V. AMPLITUDE OF DIE OSCILLATION
FREQUENCY = 25 c/s
DRAWING SPEED = 1·3 FT/M.
MATERIAL = M.S. EN. 2B.
REDUCTION IN AREA = 51 %
GRAPH NO. 24
MAX. DRAWING FORCE
MEAN DRAWING FORCE
MIN. DRAWING FORCE
FORCE VARIATION AS SEEN BY TORQUEMETER
X = RESULT FROM STRAIN GAUGE BRIDGE ON WIRE
= EXPERIMENTAL
= CALCULATED
AMPLITUDE OF DRUM INERTIA FORCE
DRAWING FORCE (LBF.)
1400
1200
1000
800
600
400
200
0
0
0·010
0·020
0·030
0·040
0·050
AMPLITUDE (PEAK TO PEAK) OF DIE OSCILLATION (IN.)

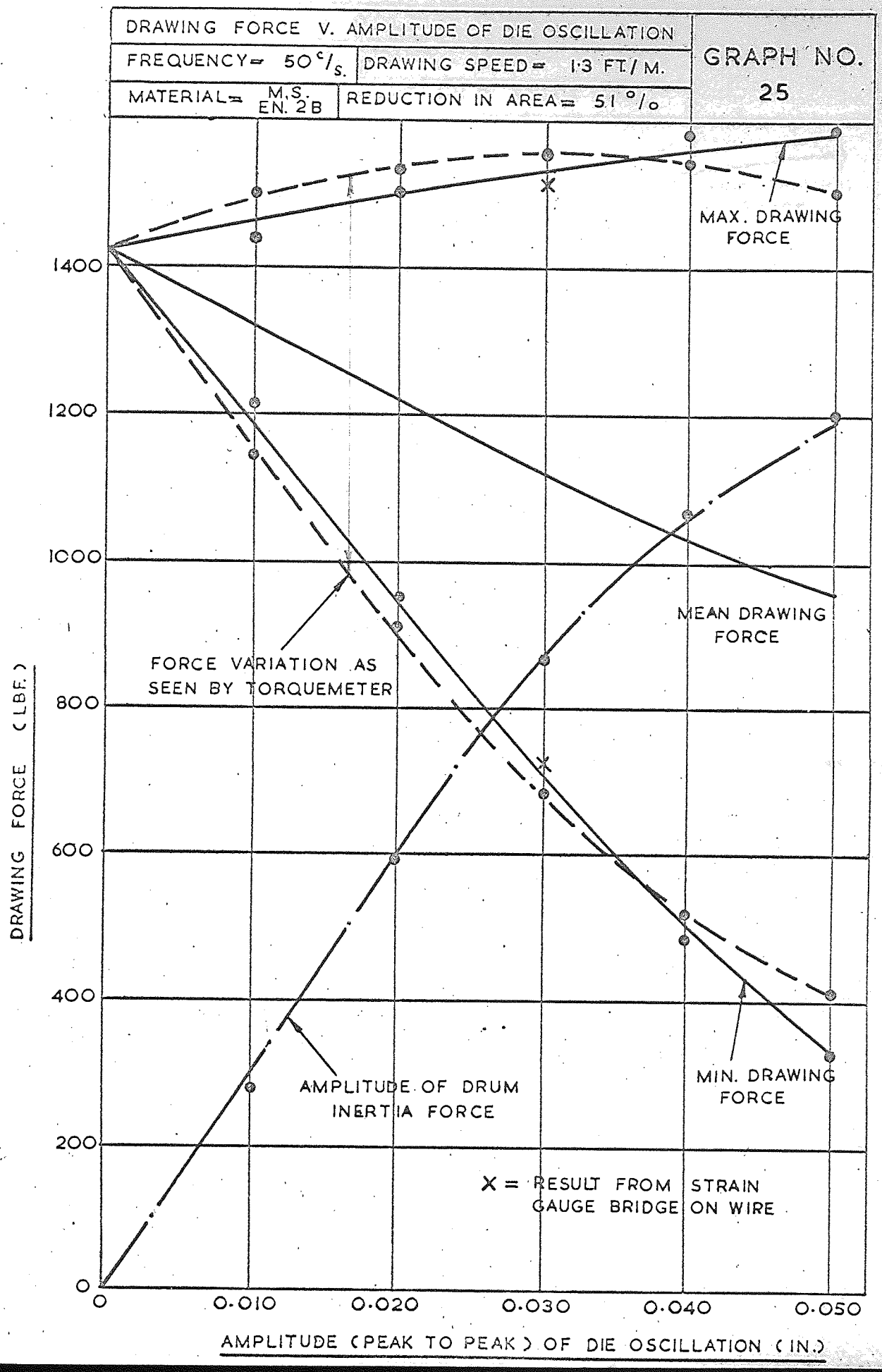
DRAWING FORCE V. AMPLITUDE OF DIE OSCILLATION
FREQUENCY = 50 c/s.
DRAWING SPEED = 1·3 FT./M.
MATERIAL = M.S. EN. 2B
REDUCTION IN AREA = 51 %
GRAPH NO. 25
MAX. DRAWING FORCE
MEAN DRAWING FORCE
FORCE VARIATION AS SEEN BY TORQUEMETER
MIN. DRAWING FORCE
AMPLITUDE OF DRUM INERTIA FORCE
X = RESULT FROM STRAIN GAUGE BRIDGE ON WIRE
DRAWING FORCE (LBF.)
1400
1200
1000
800
600
400
200
0
0
0·010
0·020
0·030
0·040
0·050
AMPLITUDE (PEAK TO PEAK) OF DIE OSCILLATION (IN.)

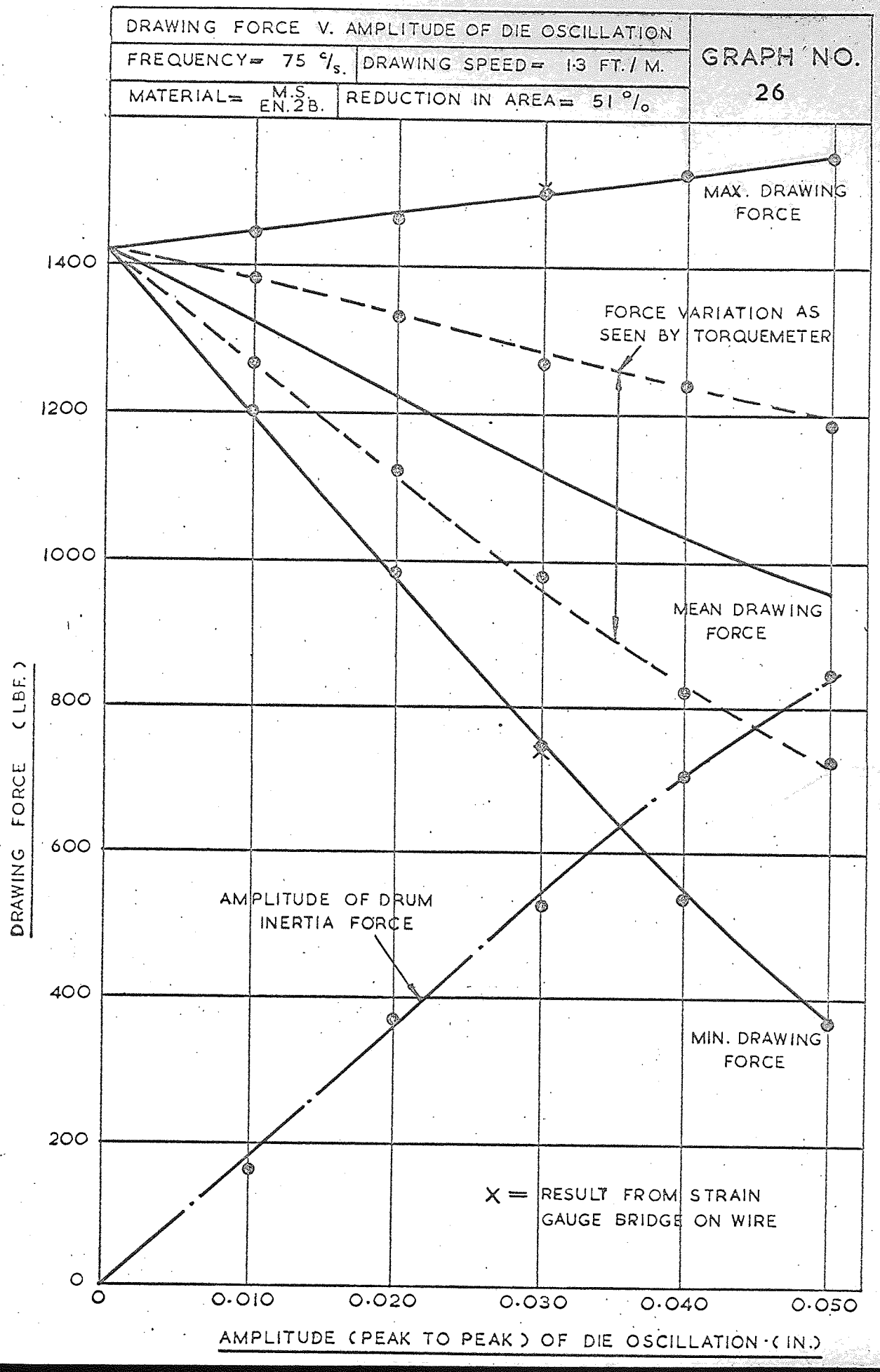
DRAWING FORCE V. AMPLITUDE OF DIE OSCILLATION
FREQUENCY = 75 c/s.
DRAWING SPEED = 1·3 FT./M.
MATERIAL = M.S. EN.2B.
REDUCTION IN AREA = 51 %
GRAPH NO. 26
MAX. DRAWING FORCE
FORCE VARIATION AS SEEN BY TORQUEMETER
MEAN DRAWING FORCE
AMPLITUDE OF DRUM INERTIA FORCE
MIN. DRAWING FORCE
X = RESULT FROM STRAIN GAUGE BRIDGE ON WIRE
DRAWING FORCE (LBF.)
0
200
400
600
800
1000
1200
1400
0
0·010
0·020
0·030
0·040
0·050
AMPLITUDE (PEAK TO PEAK) OF DIE OSCILLATION (IN.)

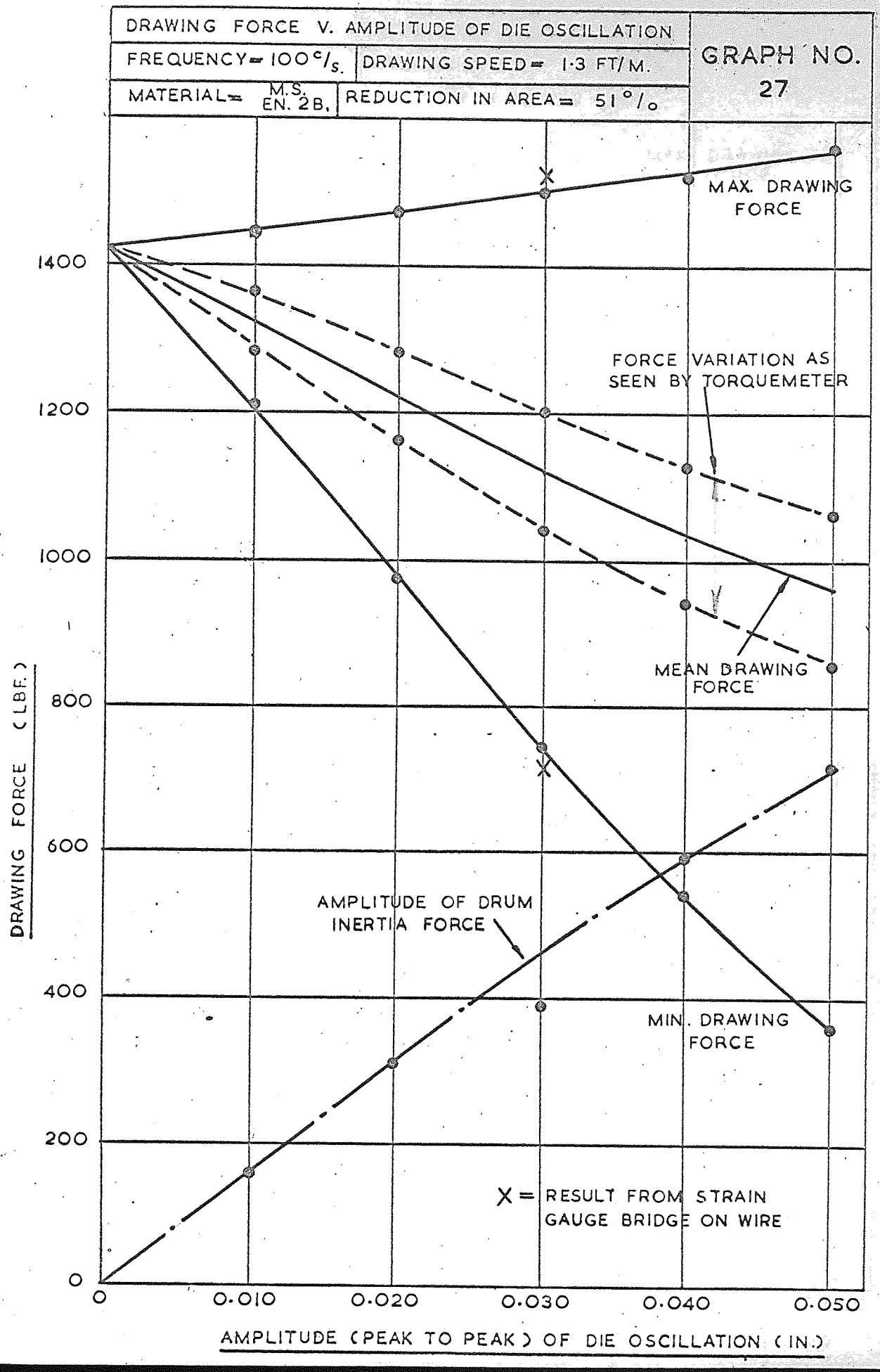
DRAWING FORCE V. AMPLITUDE OF DIE OSCILLATION
FREQUENCY = 100 c/s.
DRAWING SPEED = 1·3 FT/M.
MATERIAL = M.S. EN. 2B.
REDUCTION IN AREA = 51 %
GRAPH NO. 27
MAX. DRAWING FORCE
FORCE VARIATION AS SEEN BY TORQUEMETER
MEAN DRAWING FORCE
AMPLITUDE OF DRUM INERTIA FORCE
MIN. DRAWING FORCE
X = RESULT FROM STRAIN GAUGE BRIDGE ON WIRE
DRAWING FORCE (LBF.)
0
200
400
600
800
1000
1200
1400
0
0·010
0·020
0·030
0·040
0·050
AMPLITUDE (PEAK TO PEAK) OF DIE OSCILLATION (IN.)

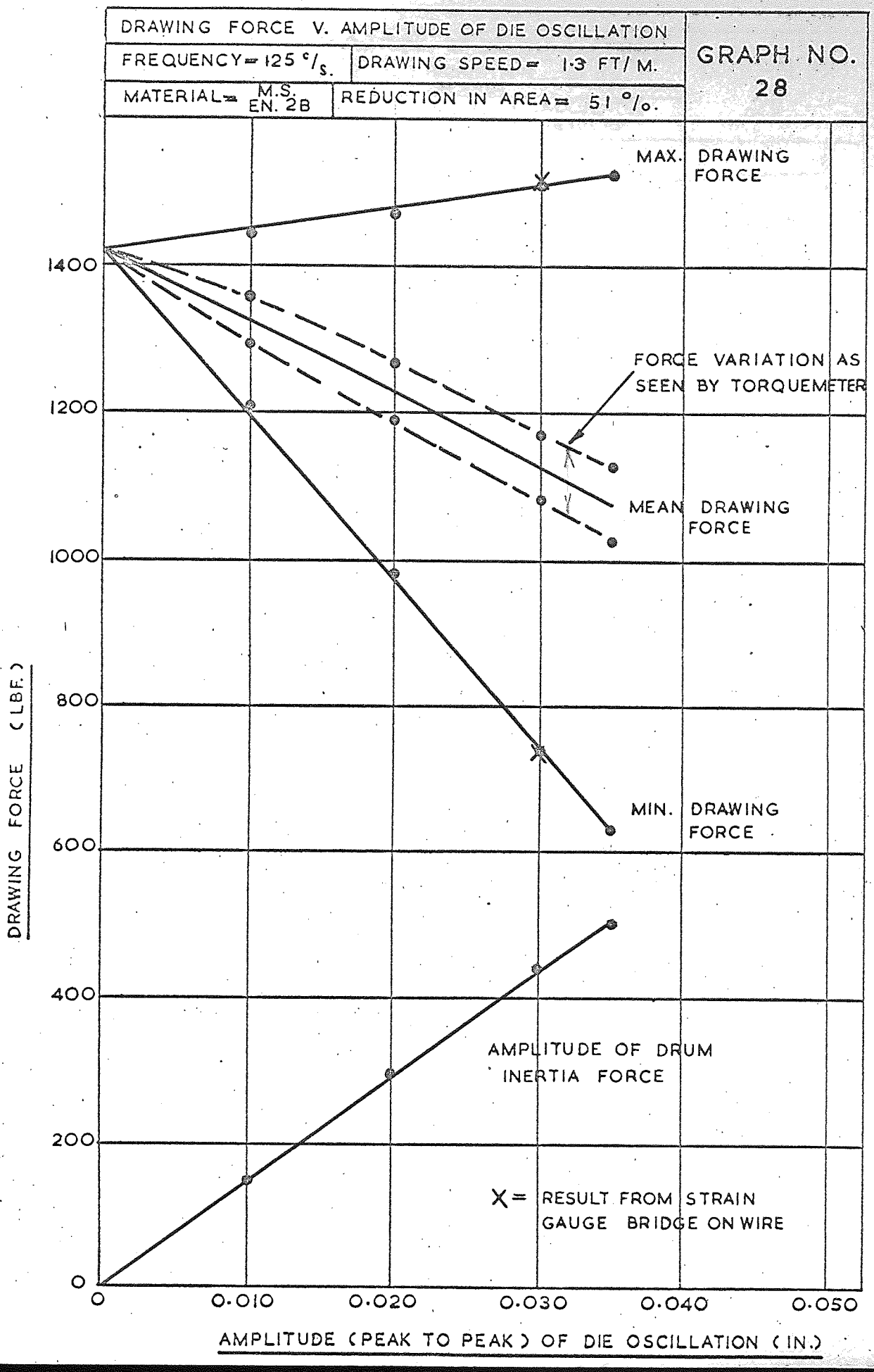
DRAWING FORCE V. AMPLITUDE OF DIE OSCILLATION
FREQUENCY = 125 °/s.
DRAWING SPEED = 1·3 FT/M.
MATERIAL = M.S. EN. 2B
REDUCTION IN AREA = 51 %.
GRAPH NO. 28
MAX. DRAWING FORCE
FORCE VARIATION AS SEEN BY TORQUEMETER
MEAN DRAWING FORCE
MIN. DRAWING FORCE
AMPLITUDE OF DRUM INERTIA FORCE
X = RESULT FROM STRAIN GAUGE BRIDGE ON WIRE
DRAWING FORCE (LBF.)
1400
1200
1000
800
600
400
200
0
0
0·010
0·020
0·030
0·040
0·050
AMPLITUDE (PEAK TO PEAK) OF DIE OSCILLATION (IN.)

DRAWING FORCE V. AMPLITUDE OF DIE OSCILLATION

FREQUENCY = 75 . 100 . 125 C/S | REDUCTION IN AREA = 51 °/o

MATERIAL – M.S. EN.2B | DRAWING SPEED = 1·3 FT/M | CALCULATED RESULTS.

GRAPH NO. 29

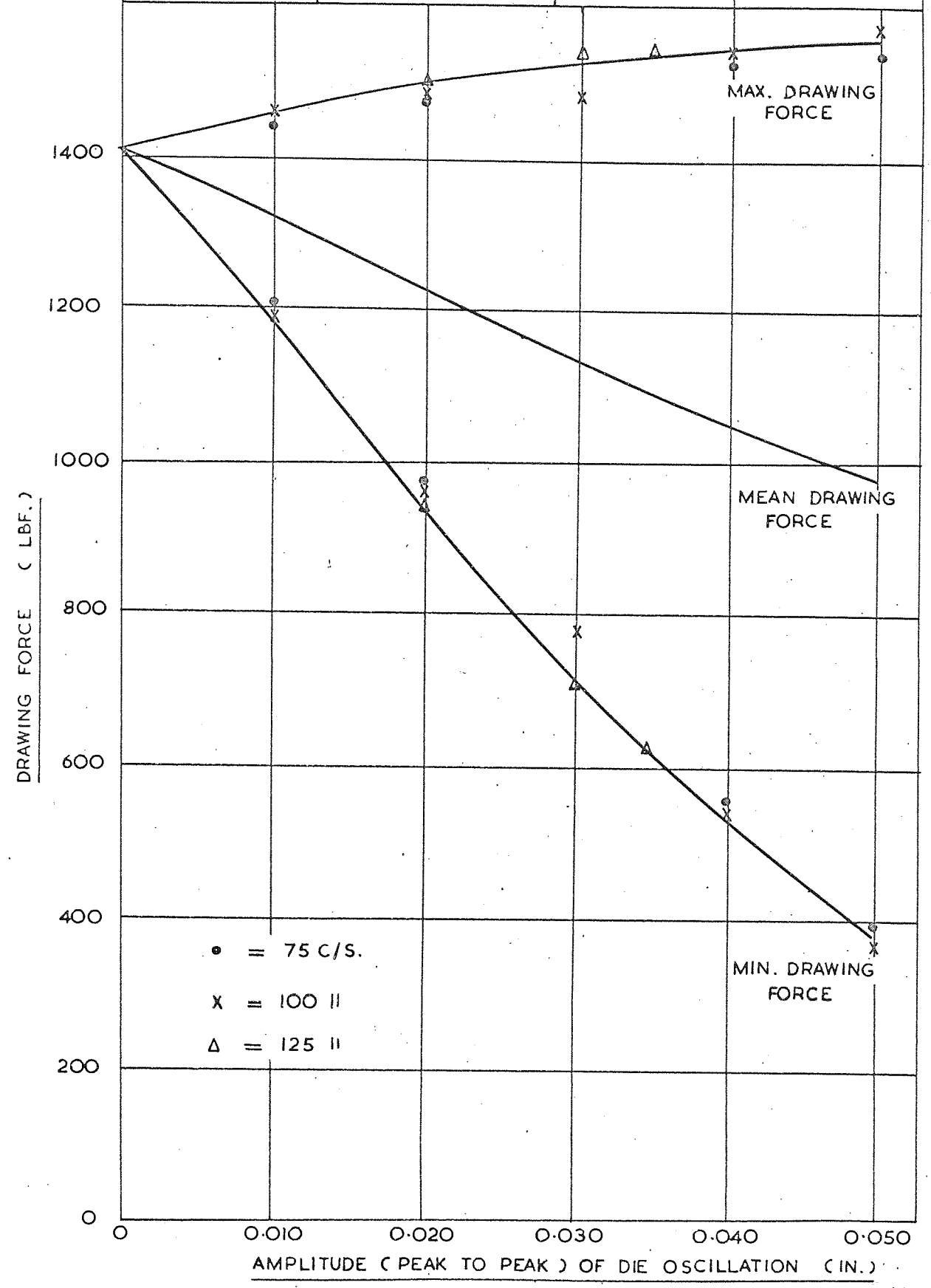

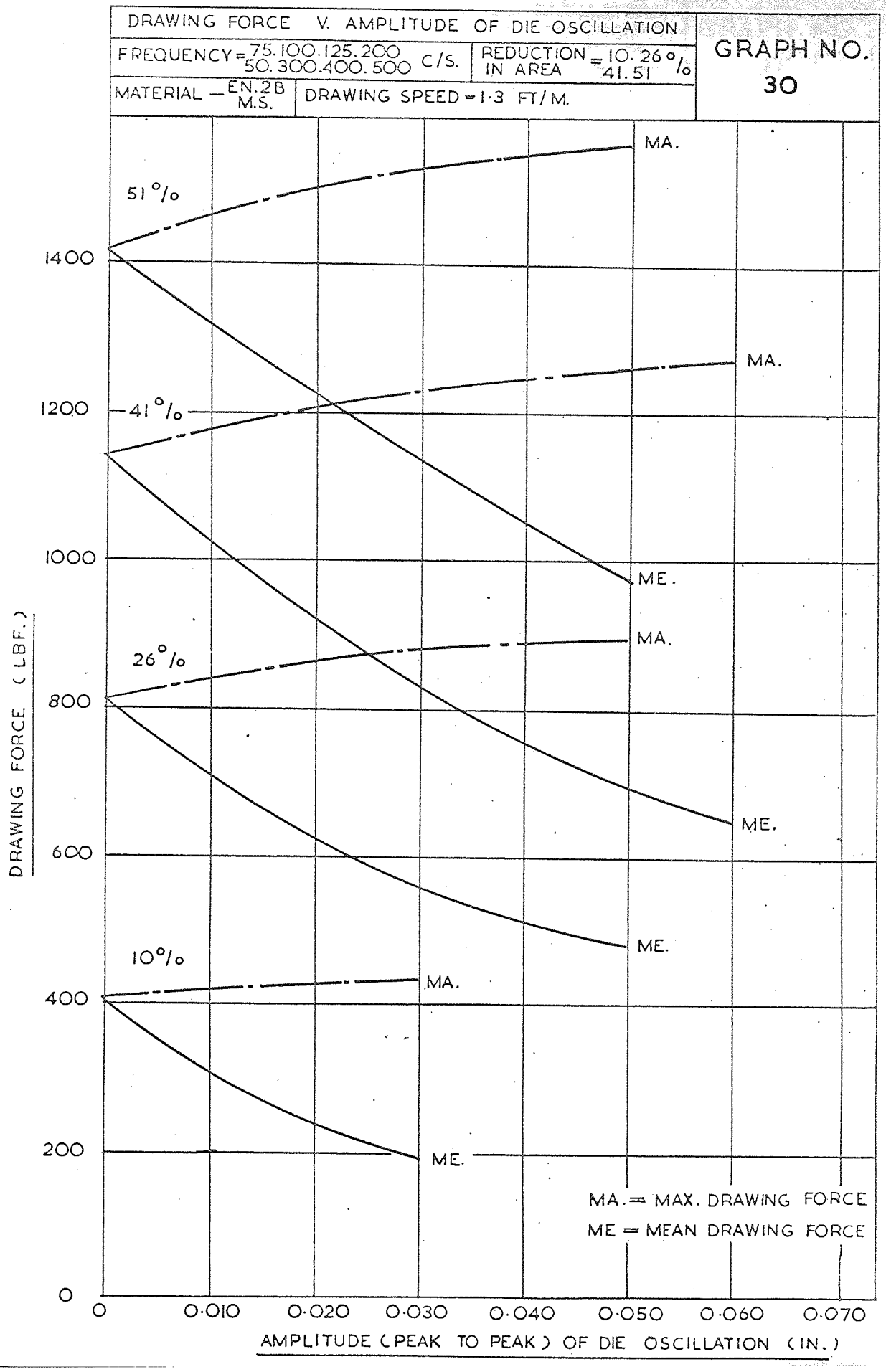
DRAWING FORCE V. AMPLITUDE OF DIE OSCILLATION
FREQUENCY = 75.100.125.200 / 50.300.400.500 C/S.
REDUCTION IN AREA = 10.26 % / 41.51
MATERIAL — EN.2B M.S.
DRAWING SPEED = 1·3 FT/M.
GRAPH NO. 30
51 %
41 %
26 %
10 %
MA.
ME.
1400
1200
1000
800
600
400
200
0
DRAWING FORCE (LBF.)
0
0·010
0·020
0·030
0·040
0·050
0·060
0·070
AMPLITUDE (PEAK TO PEAK) OF DIE OSCILLATION (IN.)
MA. = MAX. DRAWING FORCE
ME = MEAN DRAWING FORCE

DRAWING FORCE V. AMPLITUDE OF DIE OSCILLATION

FREQUENCY = 25 C/S. | REDUCTION IN AREA = 10. 26. 41. 51 %

MATERIAL — M. S. EN.2B | DRAWING SPEED = 1·3 FT/M.

GRAPH NO. 31

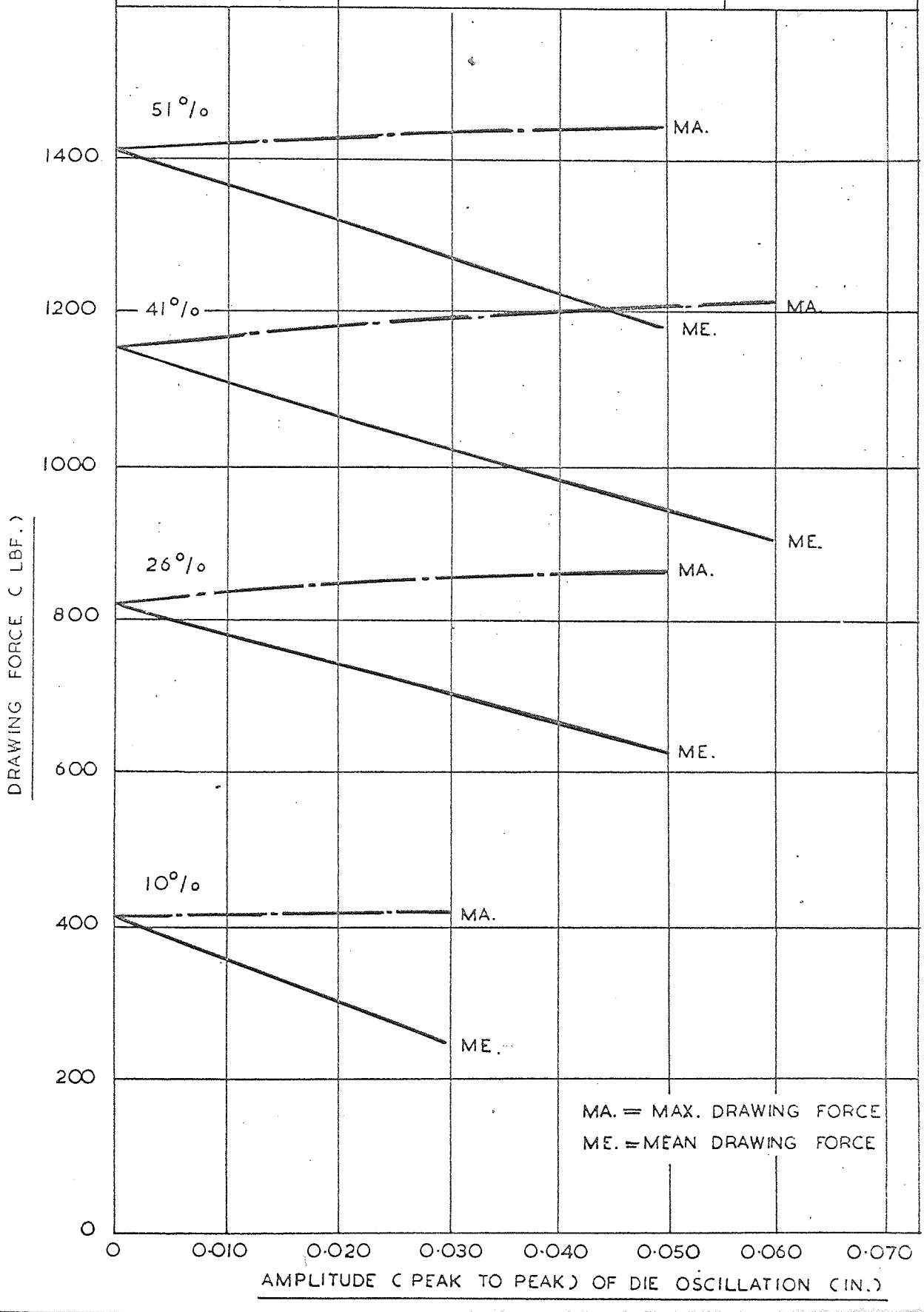

DRAWING FORCE V. AMPLITUDE OF DIE OSCILLATION

FREQUENCY = 50·100·125·200·300·400 AND 500 C/S. | DRAWING SPEED = 1·3 FT/M.

MATERIAL — STAINLESS STEEL | REDUCTION IN AREA = 44·5 %

GRAPH NO. 32

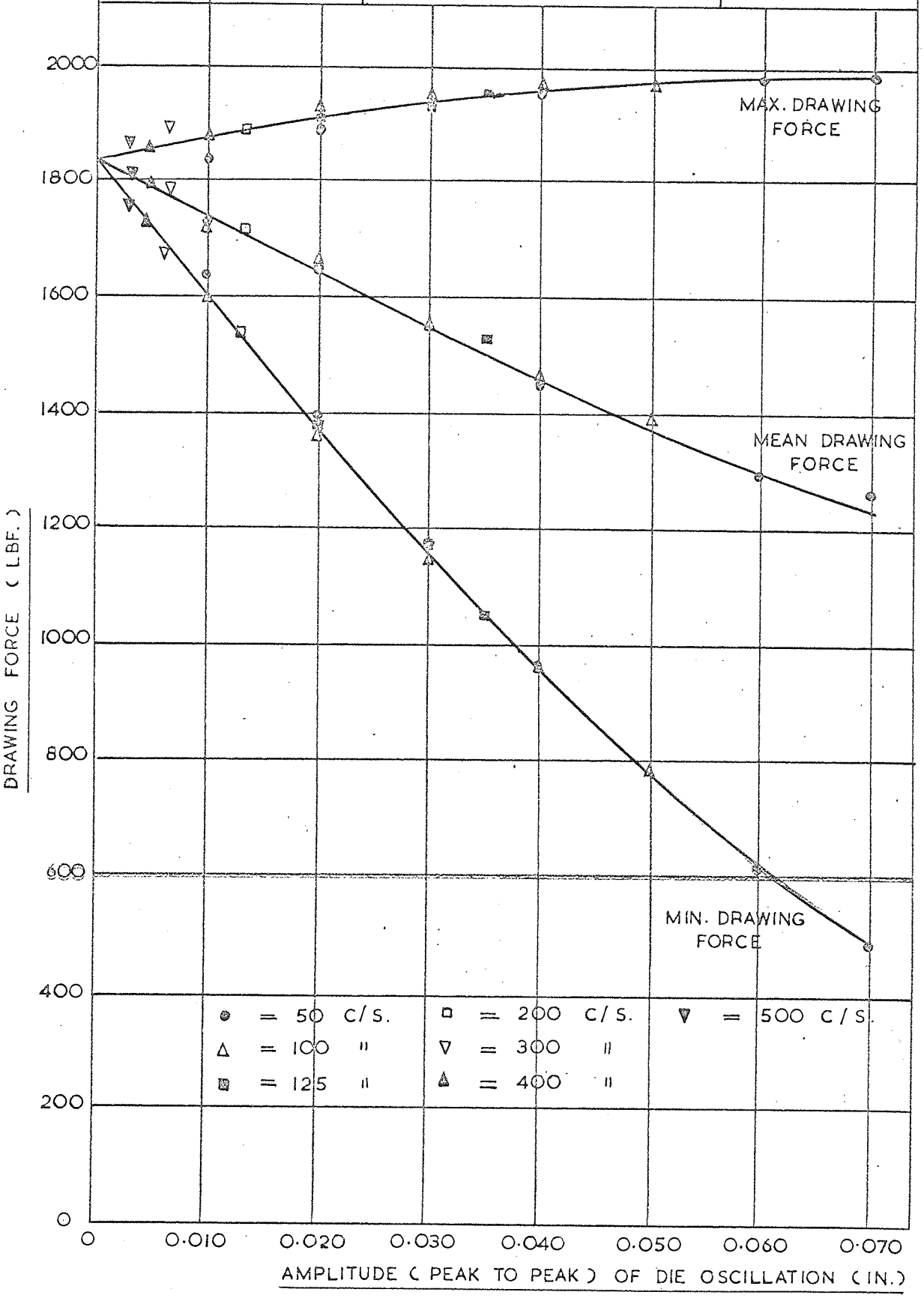

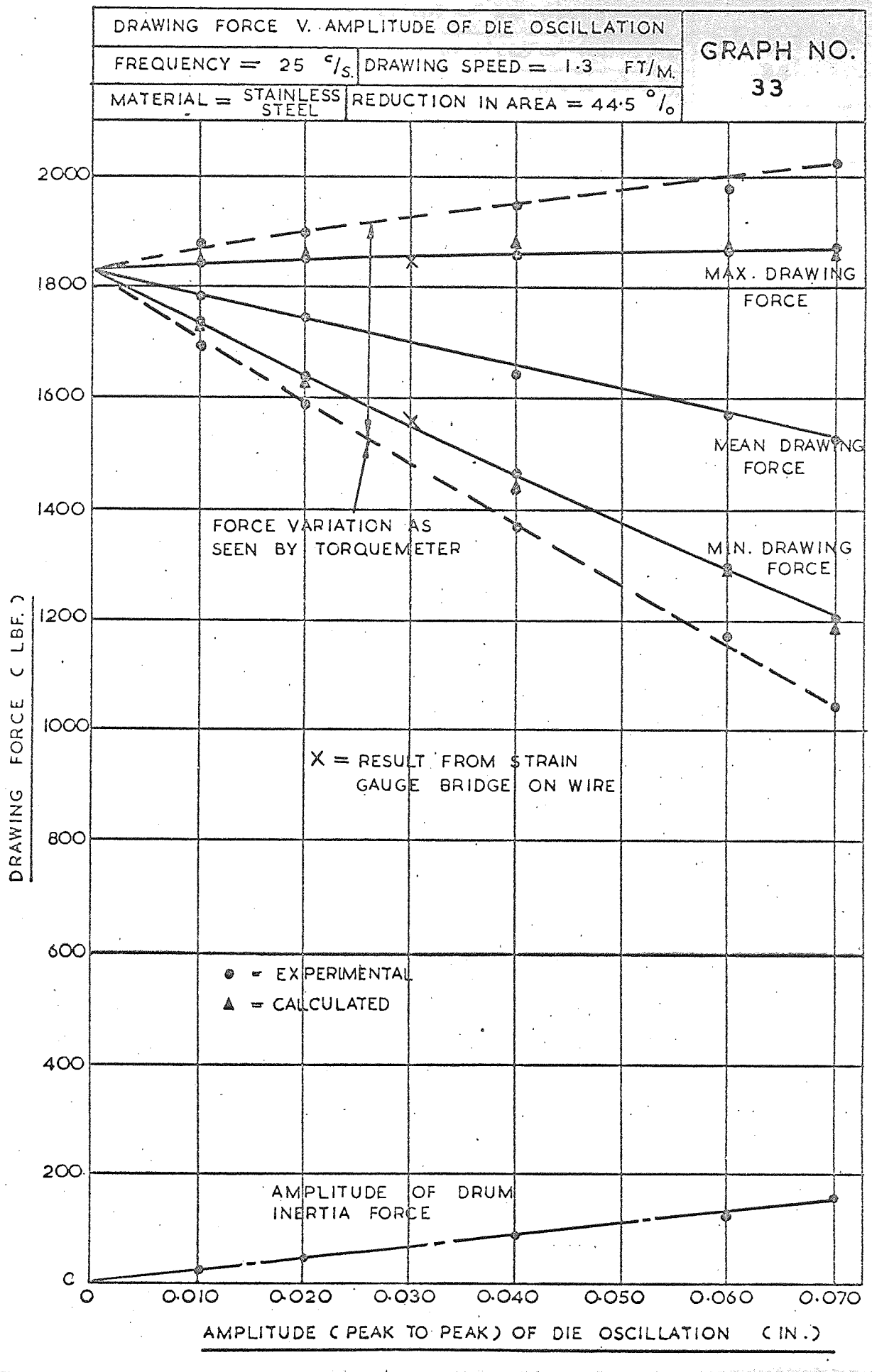
DRAWING FORCE V. AMPLITUDE OF DIE OSCILLATION
FREQUENCY = 25 c/s.
DRAWING SPEED = 1·3 FT/M.
MATERIAL = STAINLESS STEEL
REDUCTION IN AREA = 44·5 %
GRAPH NO. 33
MAX. DRAWING FORCE
MEAN DRAWING FORCE
MIN. DRAWING FORCE
FORCE VARIATION AS SEEN BY TORQUEMETER
X = RESULT FROM STRAIN GAUGE BRIDGE ON WIRE
● = EXPERIMENTAL
▲ = CALCULATED
AMPLITUDE OF DRUM INERTIA FORCE
DRAWING FORCE (LBF.)
2000
1800
1600
1400
1200
1000
800
600
400
200
0
0·010
0·020
0·030
0·040
0·050
0·060
0·070
AMPLITUDE (PEAK TO PEAK) OF DIE OSCILLATION (IN.)

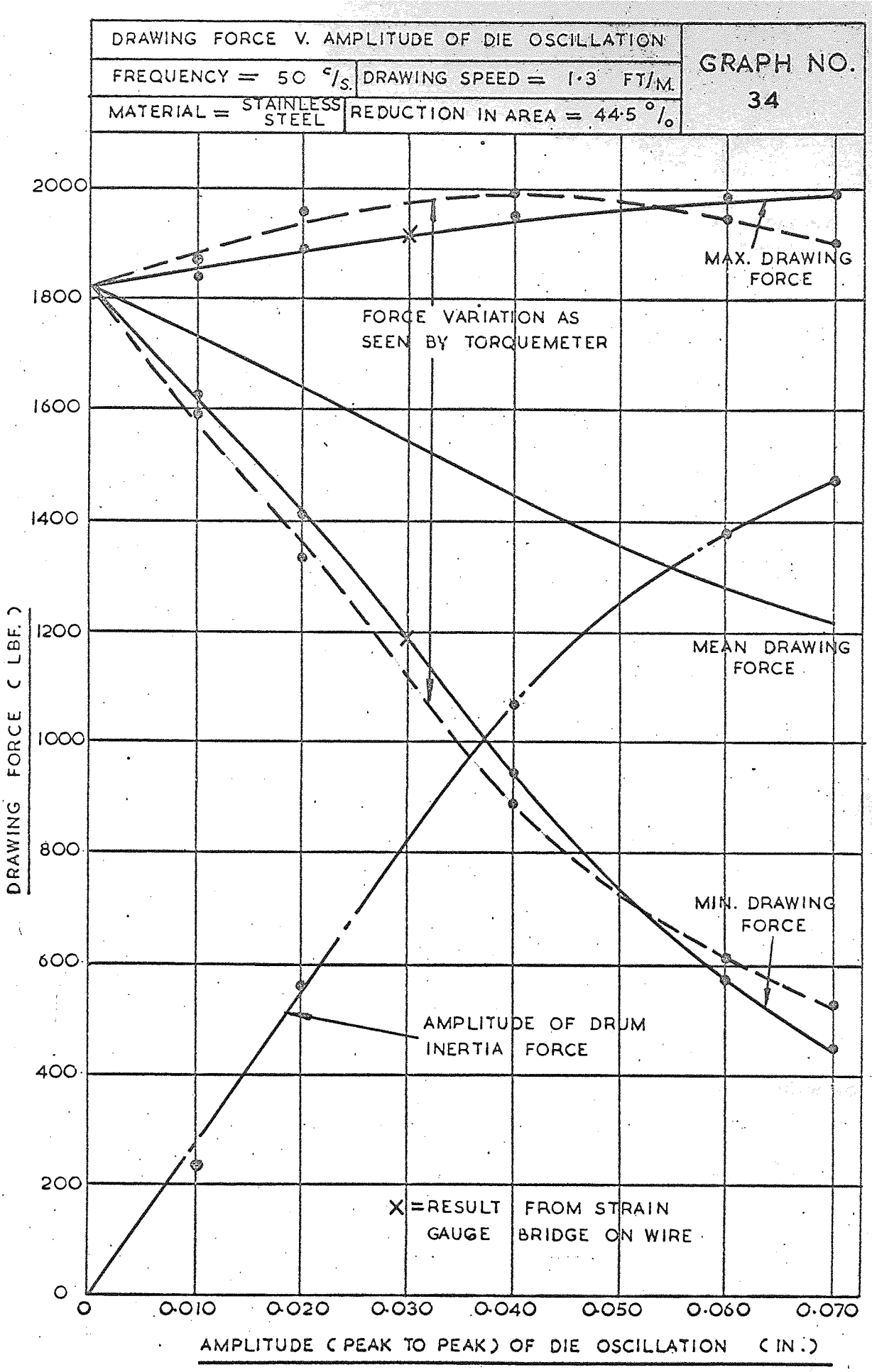
DRAWING FORCE V. AMPLITUDE OF DIE OSCILLATION
FREQUENCY = 50 c/s.
DRAWING SPEED = 1·3 FT/M.
MATERIAL = STAINLESS STEEL
REDUCTION IN AREA = 44·5 %
GRAPH NO. 34
2000
1800
1600
1400
1200
1000
800
600
400
200
0
DRAWING FORCE (LBF.)
MAX. DRAWING FORCE
FORCE VARIATION AS SEEN BY TORQUEMETER
MEAN DRAWING FORCE
MIN. DRAWING FORCE
AMPLITUDE OF DRUM INERTIA FORCE
X = RESULT FROM STRAIN GAUGE BRIDGE ON WIRE
0
0·010
0·020
0·030
0·040
0·050
0·060
0·070
AMPLITUDE (PEAK TO PEAK) OF DIE OSCILLATION (IN.)

DRAWING FORCE V. AMPLITUDE OF DIE OSCILLATION

FREQUENCY = 75 $^{c}/_{s}$ | DRAWING SPEED = 1·3 FT/M.

MATERIAL = STAINLESS STEEL | REDUCTION IN AREA = 44·5 %

GRAPH NO. 35

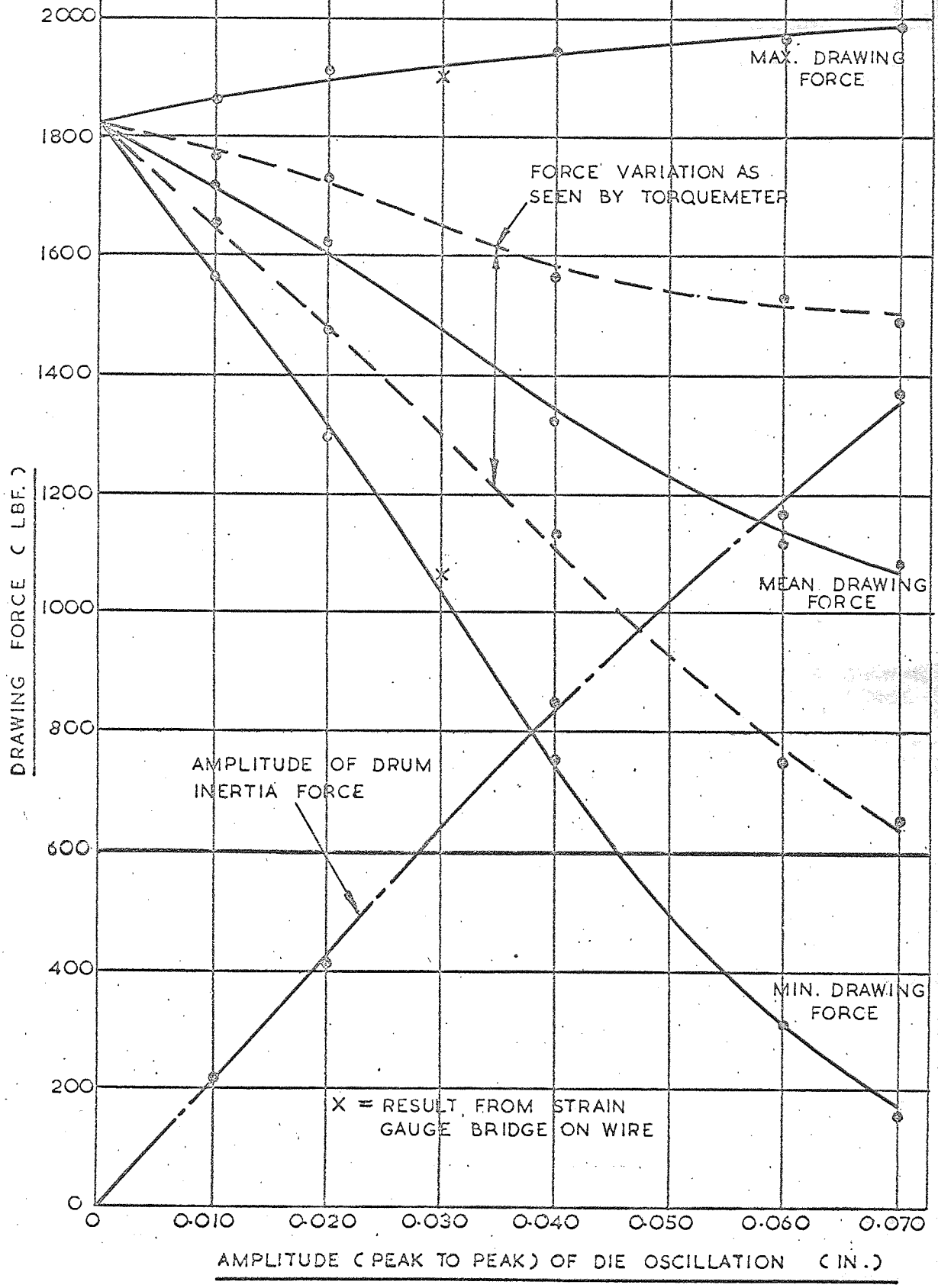

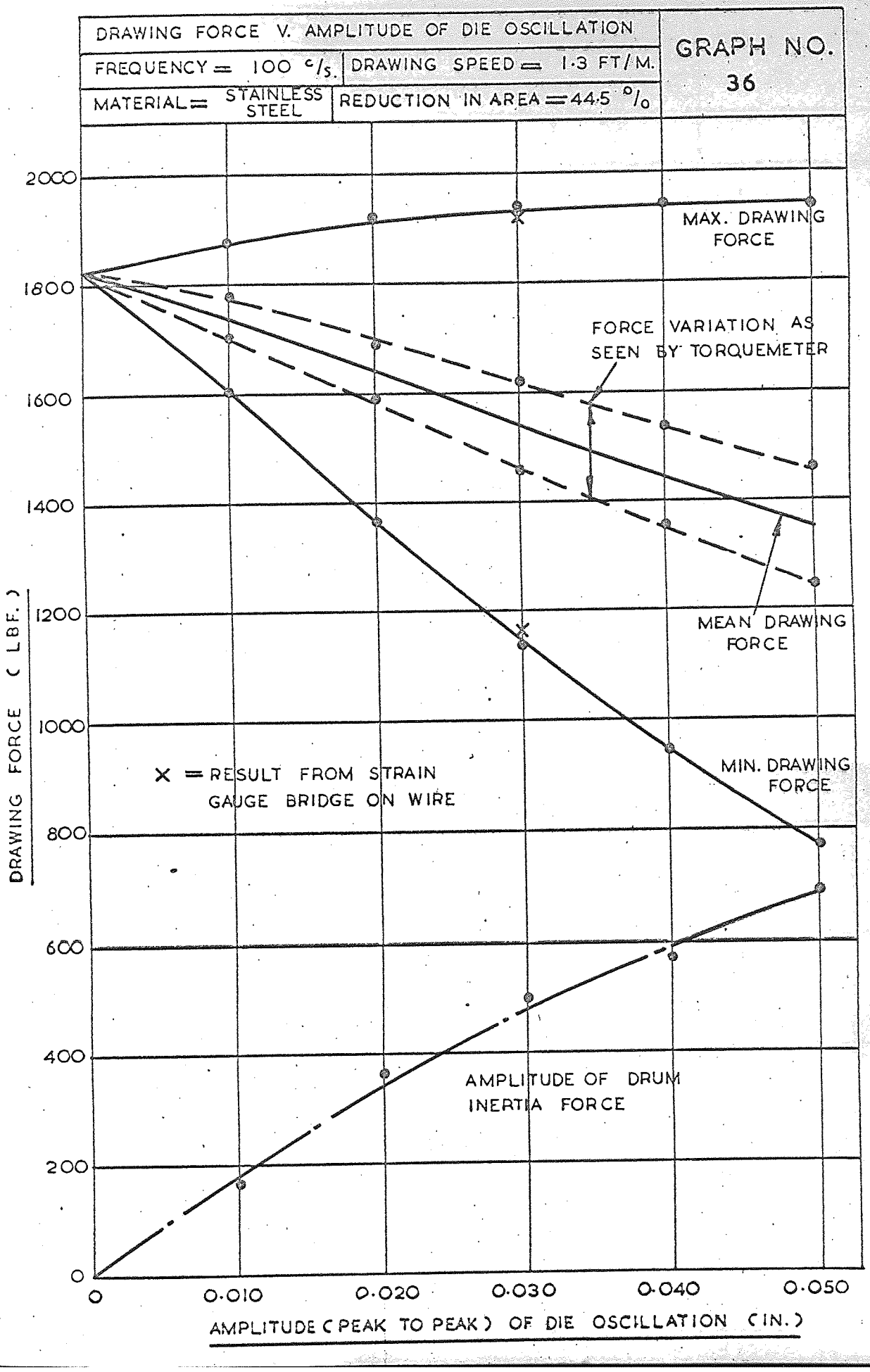
DRAWING FORCE V. AMPLITUDE OF DIE OSCILLATION
FREQUENCY = 100 c/s.
DRAWING SPEED = 1·3 FT/M.
MATERIAL = STAINLESS STEEL
REDUCTION IN AREA = 44·5 %
GRAPH NO. 36
MAX. DRAWING FORCE
FORCE VARIATION AS SEEN BY TORQUEMETER
MEAN DRAWING FORCE
MIN. DRAWING FORCE
× = RESULT FROM STRAIN GAUGE BRIDGE ON WIRE
AMPLITUDE OF DRUM INERTIA FORCE
DRAWING FORCE (LBF.)
2000
1800
1600
1400
1200
1000
800
600
400
200
0
0
0·010
0·020
0·030
0·040
0·050
AMPLITUDE (PEAK TO PEAK) OF DIE OSCILLATION (IN.)

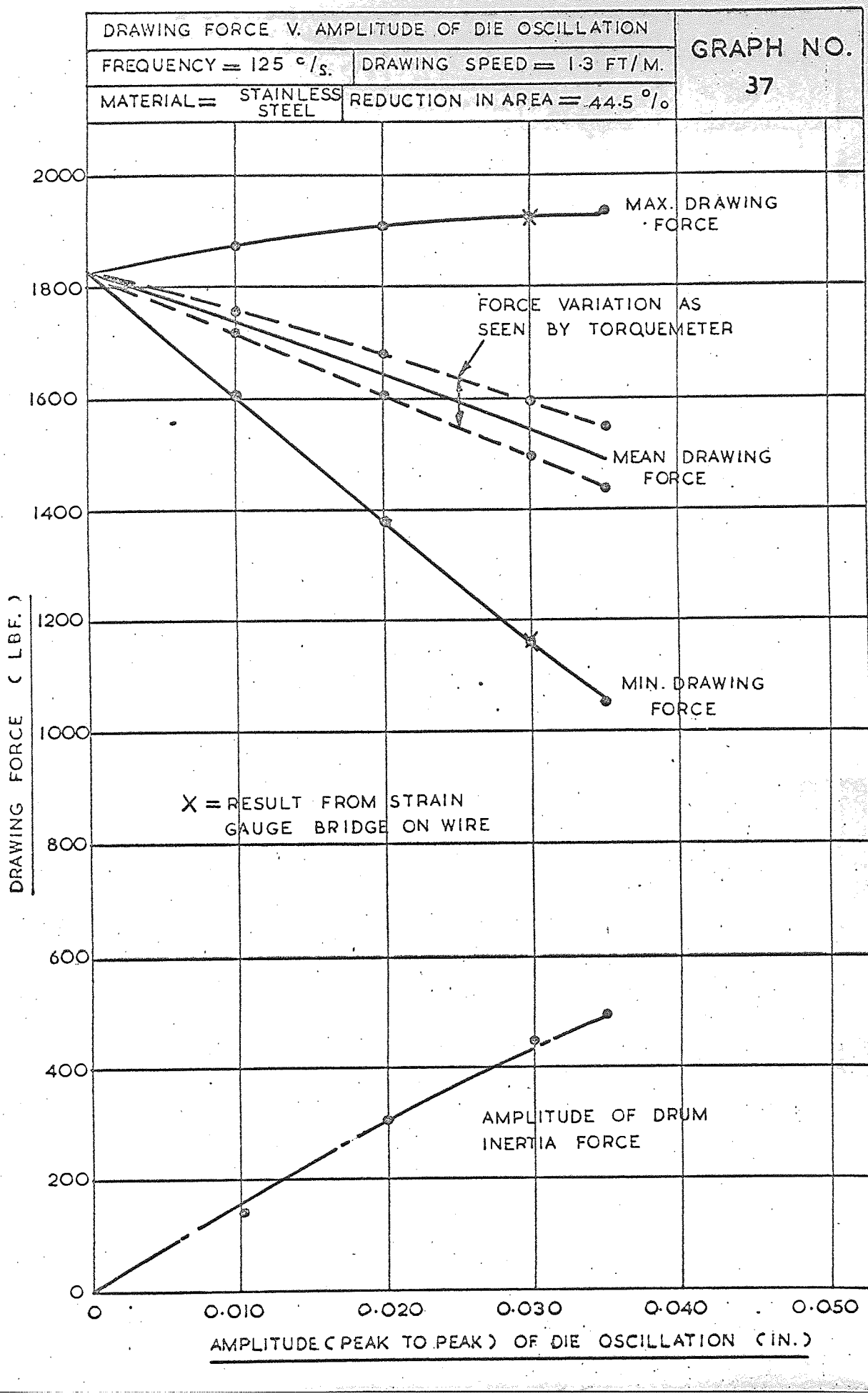
DRAWING FORCE V. AMPLITUDE OF DIE OSCILLATION
FREQUENCY = 125 c/s.
DRAWING SPEED = 1·3 FT/M.
MATERIAL = STAINLESS STEEL
REDUCTION IN AREA = 44·5 %
GRAPH NO. 37
2000
1800
1600
1400
1200
1000
800
600
400
200
0
DRAWING FORCE (LBF.)
MAX. DRAWING FORCE
FORCE VARIATION AS SEEN BY TORQUEMETER
MEAN DRAWING FORCE
MIN. DRAWING FORCE
X = RESULT FROM STRAIN GAUGE BRIDGE ON WIRE
AMPLITUDE OF DRUM INERTIA FORCE
0
0·010
0·020
0·030
0·040
0·050
AMPLITUDE (PEAK TO PEAK) OF DIE OSCILLATION (IN.)

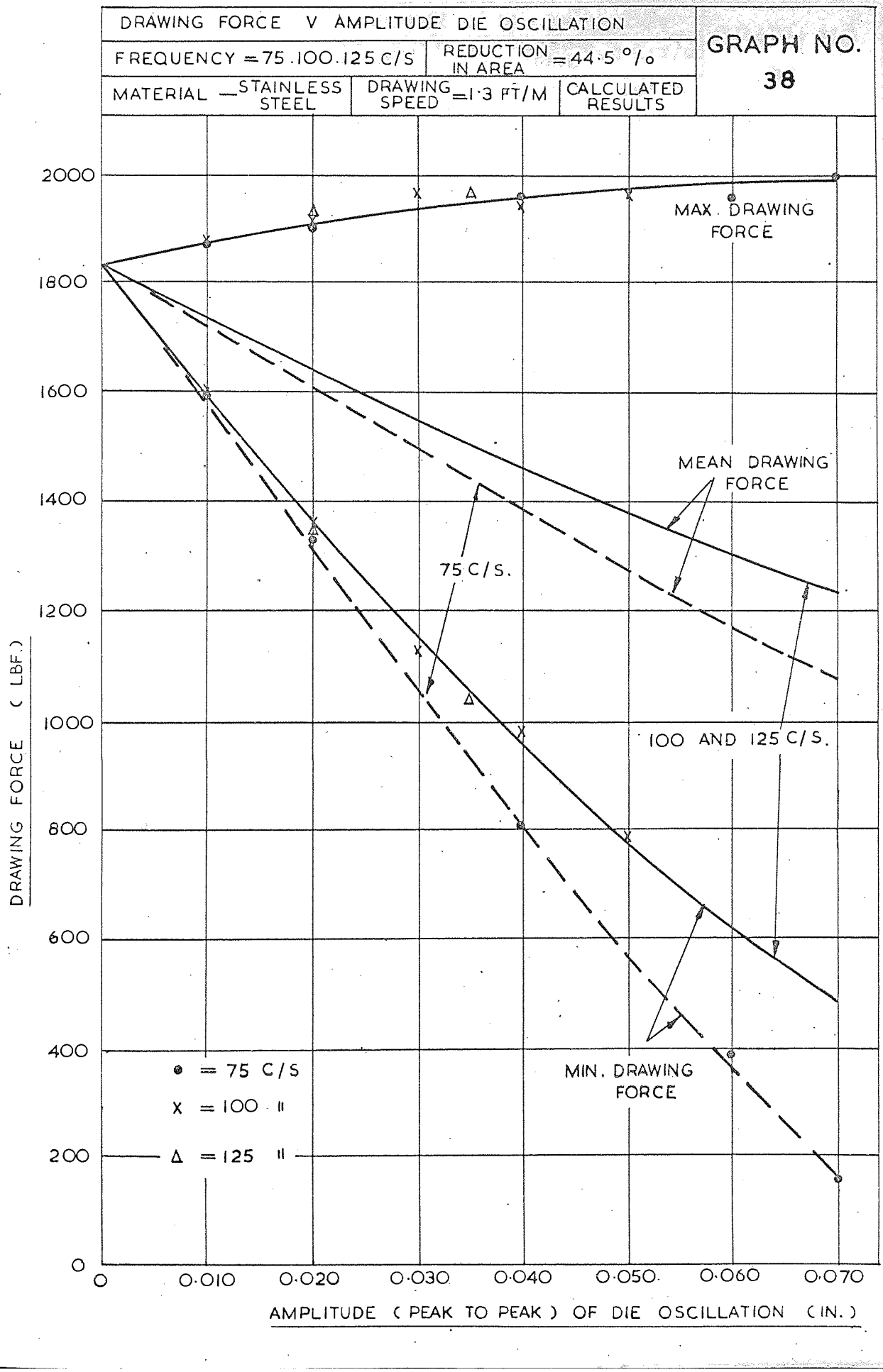
DRAWING FORCE V AMPLITUDE DIE OSCILLATION
FREQUENCY = 75 . 100 . 125 C/S
REDUCTION IN AREA = 44·5 %
MATERIAL — STAINLESS STEEL
DRAWING SPEED = 1·3 FT/M
CALCULATED RESULTS
GRAPH NO. 38
MAX. DRAWING FORCE
MEAN DRAWING FORCE
75 C/S.
100 AND 125 C/S.
MIN. DRAWING FORCE
● = 75 C/S
X = 100 "
Δ = 125 "
DRAWING FORCE (LBF.)
2000
1800
1600
1400
1200
1000
800
600
400
200
0
0
0·010
0·020
0·030
0·040
0·050
0·060
0·070
AMPLITUDE (PEAK TO PEAK) OF DIE OSCILLATION (IN.)

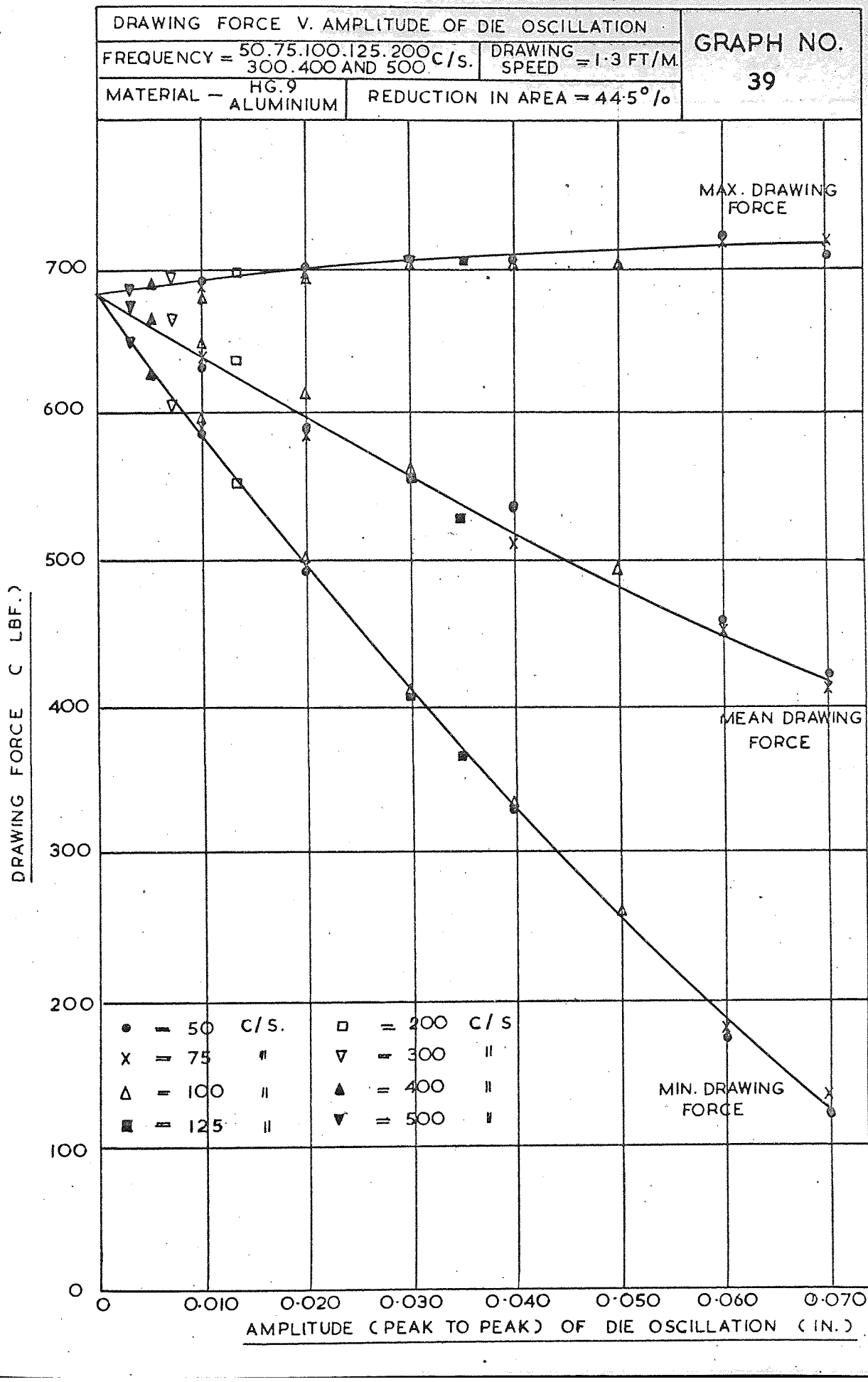
DRAWING FORCE V. AMPLITUDE OF DIE OSCILLATION
FREQUENCY = 50.75.100.125.200 300.400 AND 500 C/S.
DRAWING SPEED = 1·3 FT/M.
MATERIAL — HG.9 ALUMINIUM
REDUCTION IN AREA = 44·5°/o
GRAPH NO. 39
MAX. DRAWING FORCE
MEAN DRAWING FORCE
MIN. DRAWING FORCE
DRAWING FORCE C LBF.)
AMPLITUDE (PEAK TO PEAK) OF DIE OSCILLATION (IN.)
0
100
200
300
400
500
600
700
0·010
0·020
0·030
0·040
0·050
0·060
0·070
● = 50 C/S.
X = 75 "
Δ = 100 "
■ = 125 "
□ = 200 C/S
▽ = 300 "
▲ = 400 "
▼ = 500 "

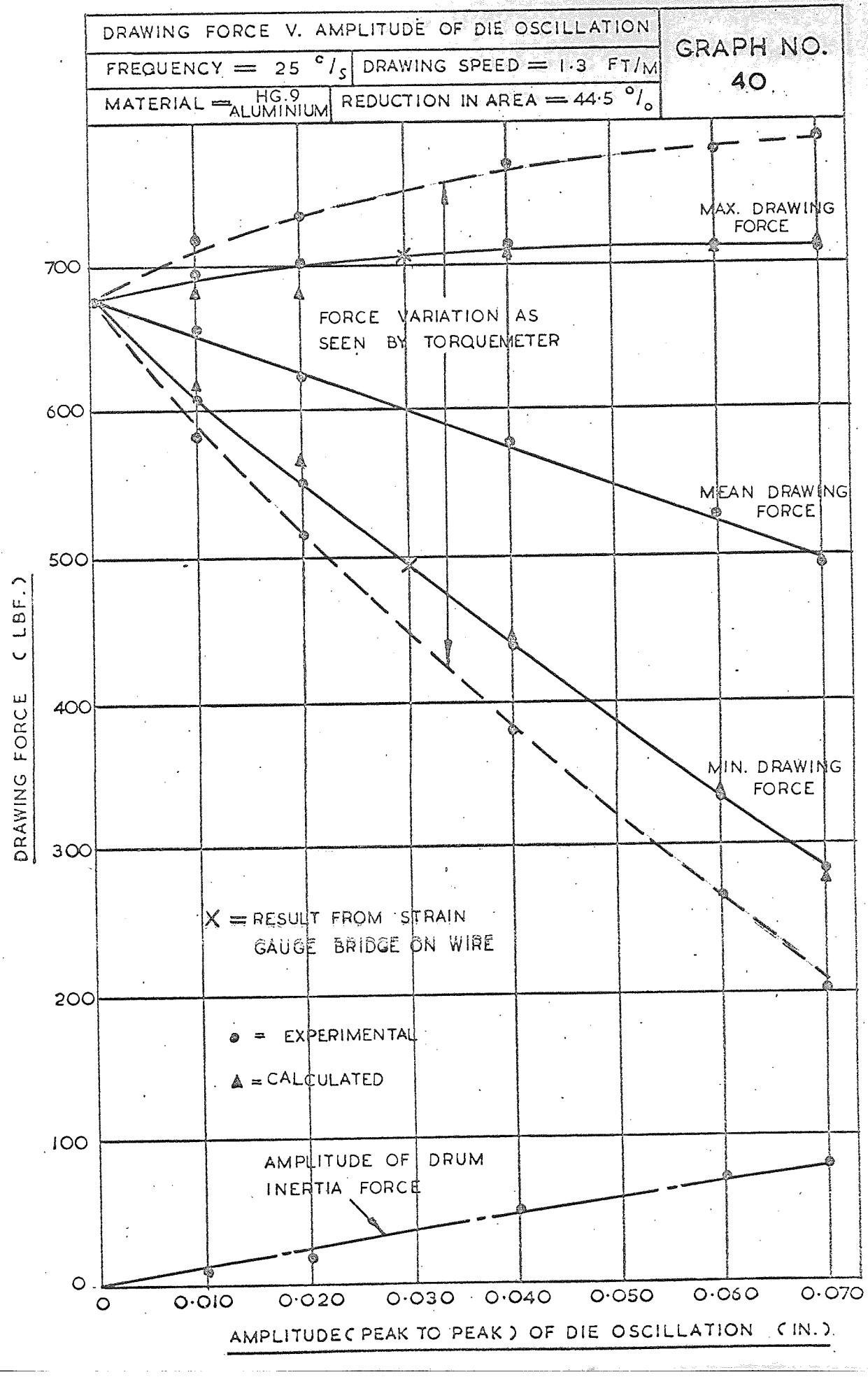
DRAWING FORCE V. AMPLITUDE OF DIE OSCILLATION
FREQUENCY = 25 c/s
DRAWING SPEED = 1·3 FT/M
MATERIAL = HG.9 ALUMINIUM
REDUCTION IN AREA = 44·5 %
GRAPH NO. 40
MAX. DRAWING FORCE
FORCE VARIATION AS SEEN BY TORQUEMETER
MEAN DRAWING FORCE
MIN. DRAWING FORCE
X = RESULT FROM STRAIN GAUGE BRIDGE ON WIRE
● = EXPERIMENTAL
▲ = CALCULATED
AMPLITUDE OF DRUM INERTIA FORCE
DRAWING FORCE (LBF.)
0
100
200
300
400
500
600
700
0
0·010
0·020
0·030
0·040
0·050
0·060
0·070
AMPLITUDE (PEAK TO PEAK) OF DIE OSCILLATION (IN.)

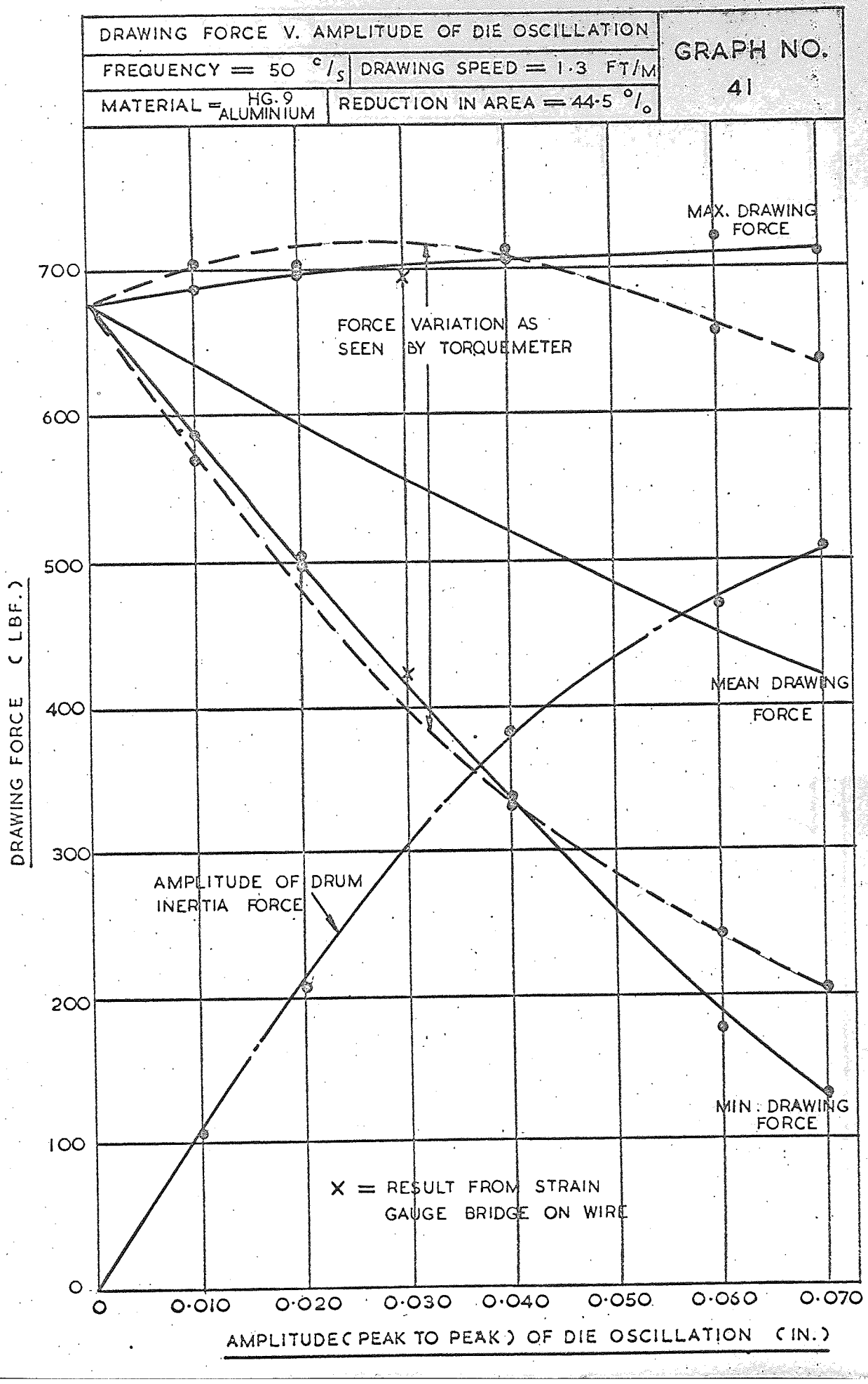
DRAWING FORCE V. AMPLITUDE OF DIE OSCILLATION
FREQUENCY = 50 c/s
DRAWING SPEED = 1·3 FT/M
MATERIAL = HG. 9 ALUMINIUM
REDUCTION IN AREA = 44·5 %
GRAPH NO. 41
MAX. DRAWING FORCE
FORCE VARIATION AS SEEN BY TORQUEMETER
MEAN DRAWING FORCE
AMPLITUDE OF DRUM INERTIA FORCE
MIN. DRAWING FORCE
X = RESULT FROM STRAIN GAUGE BRIDGE ON WIRE
DRAWING FORCE (LBF.)
0
100
200
300
400
500
600
700
0
0·010
0·020
0·030
0·040
0·050
0·060
0·070
AMPLITUDE (PEAK TO PEAK) OF DIE OSCILLATION (IN.)

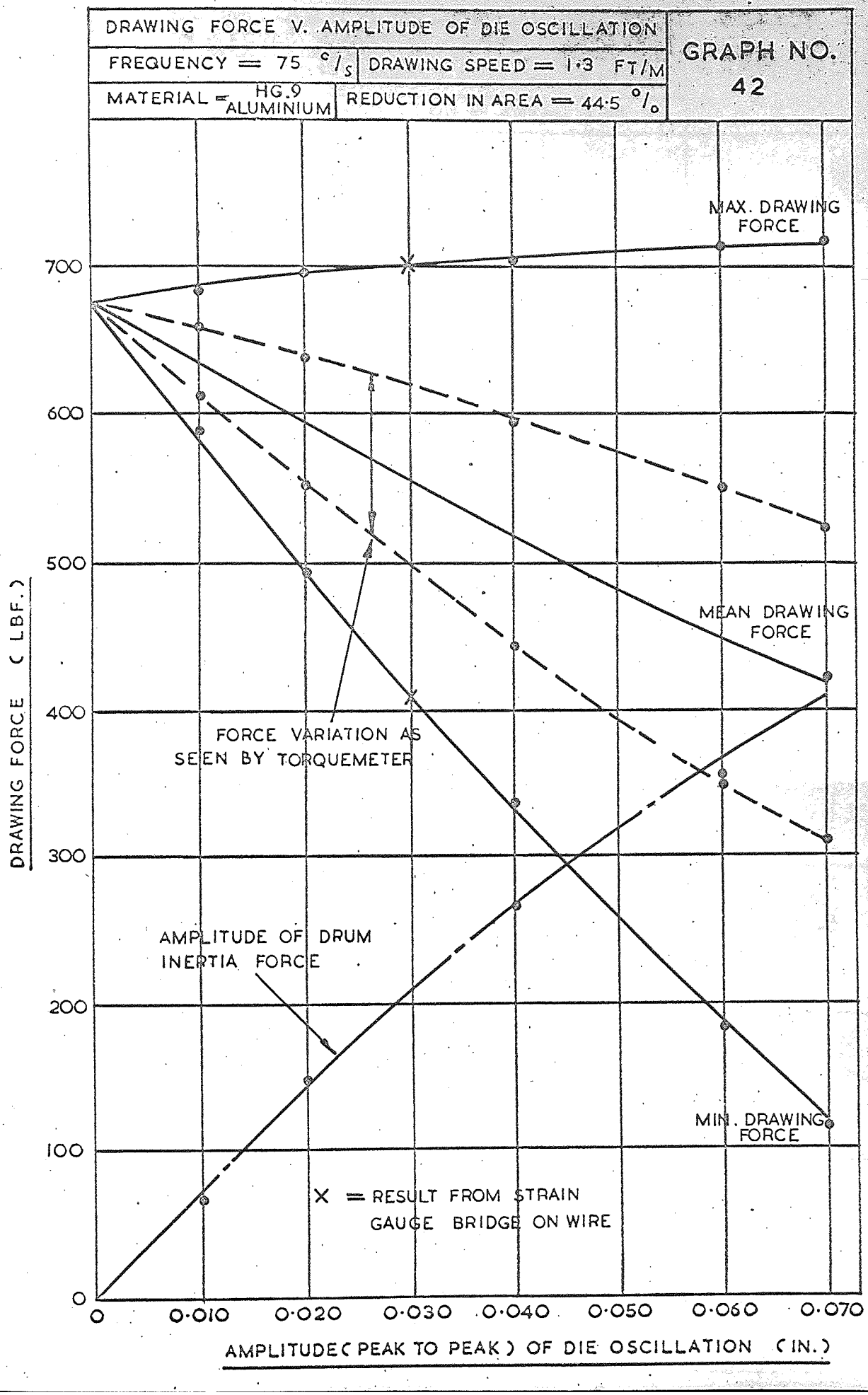
DRAWING FORCE V. AMPLITUDE OF DIE OSCILLATION
FREQUENCY = 75 °/S
DRAWING SPEED = 1·3 FT/M
MATERIAL = HG.9 ALUMINIUM
REDUCTION IN AREA = 44·5 %
GRAPH NO. 42
MAX. DRAWING FORCE
MEAN DRAWING FORCE
FORCE VARIATION AS SEEN BY TORQUEMETER
AMPLITUDE OF DRUM INERTIA FORCE
MIN. DRAWING FORCE
X = RESULT FROM STRAIN GAUGE BRIDGE ON WIRE
DRAWING FORCE (LBF.)
0
100
200
300
400
500
600
700
0
0·010
0·020
0·030
0·040
0·050
0·060
0·070
AMPLITUDE (PEAK TO PEAK) OF DIE OSCILLATION (IN.)

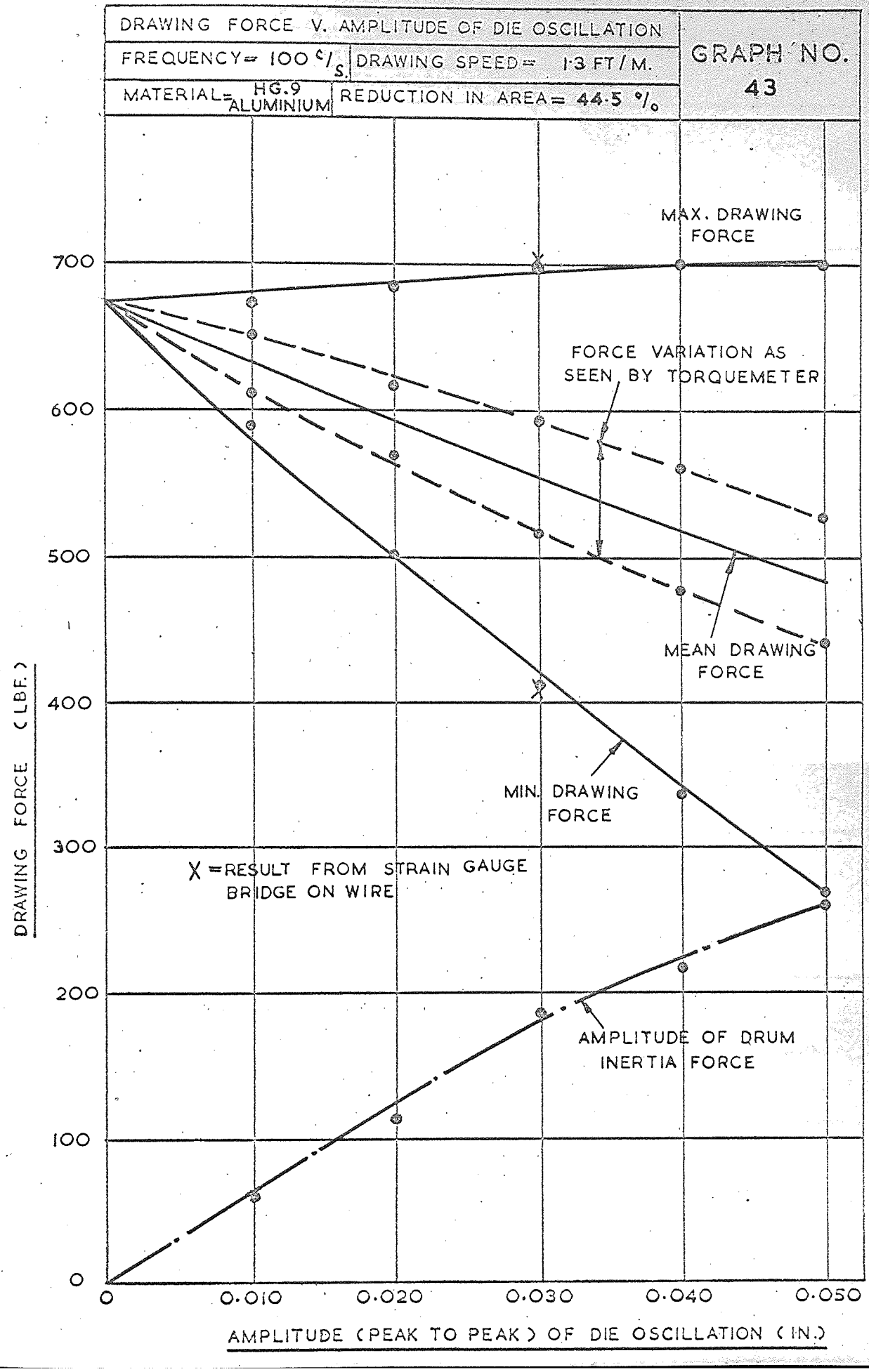
DRAWING FORCE V. AMPLITUDE OF DIE OSCILLATION
FREQUENCY = 100 c/s.
DRAWING SPEED = 1·3 FT/M.
MATERIAL = HG.9 ALUMINIUM
REDUCTION IN AREA = 44·5 %
GRAPH NO. 43
MAX. DRAWING FORCE
FORCE VARIATION AS SEEN BY TORQUEMETER
MEAN DRAWING FORCE
MIN. DRAWING FORCE
X = RESULT FROM STRAIN GAUGE BRIDGE ON WIRE
AMPLITUDE OF DRUM INERTIA FORCE
DRAWING FORCE (LBF.)
700
600
500
400
300
200
100
0
0
0·010
0·020
0·030
0·040
0·050
AMPLITUDE (PEAK TO PEAK) OF DIE OSCILLATION (IN.)

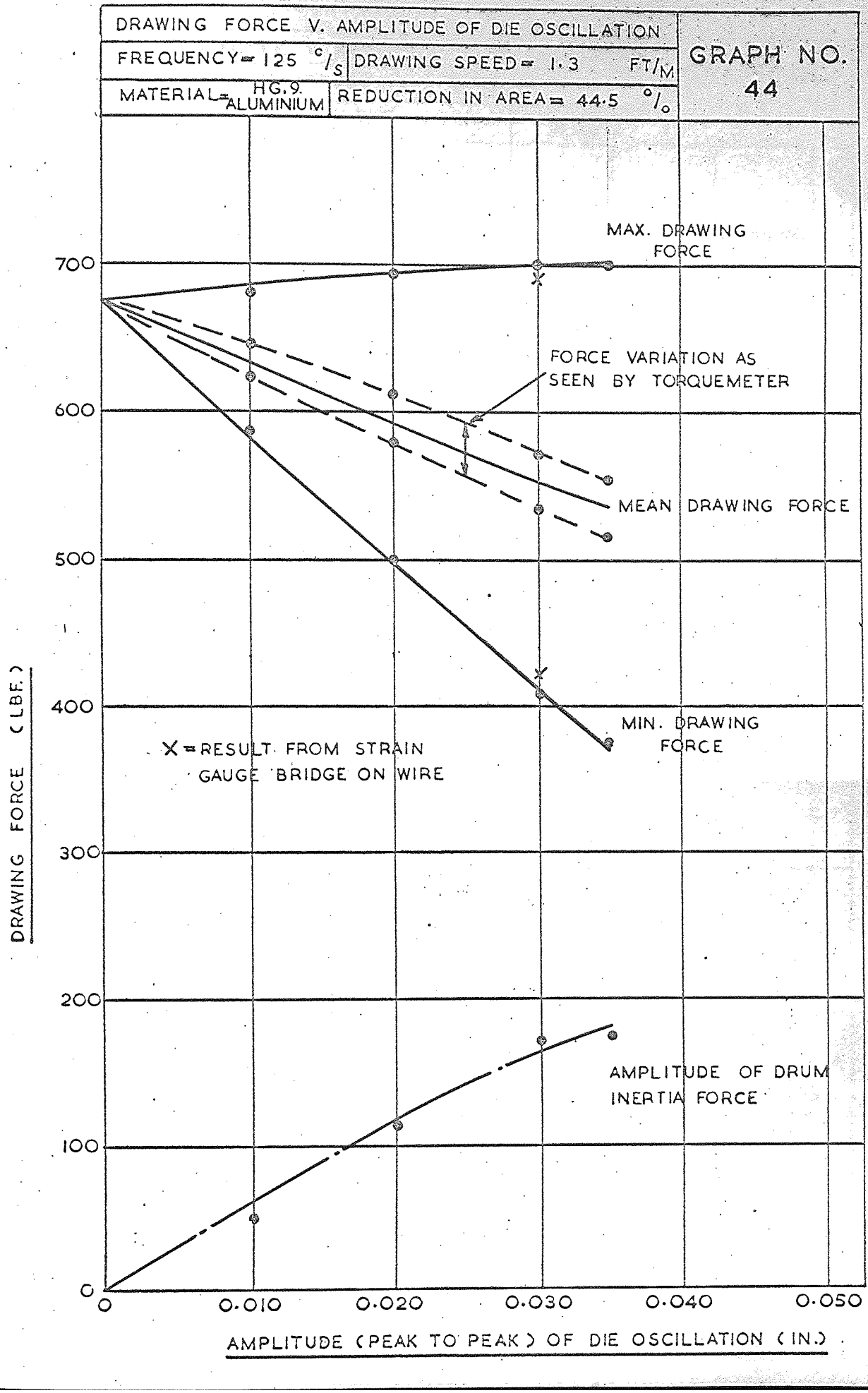
DRAWING FORCE V. AMPLITUDE OF DIE OSCILLATION
FREQUENCY = 125 c/s
DRAWING SPEED = 1·3 FT/M
MATERIAL = HG.9. ALUMINIUM
REDUCTION IN AREA = 44·5 %
GRAPH NO. 44
MAX. DRAWING FORCE
FORCE VARIATION AS SEEN BY TORQUEMETER
MEAN DRAWING FORCE
MIN. DRAWING FORCE
X = RESULT FROM STRAIN GAUGE BRIDGE ON WIRE
AMPLITUDE OF DRUM INERTIA FORCE
DRAWING FORCE (LBF.)
700
600
500
400
300
200
100
0
0
0·010
0·020
0·030
0·040
0·050
AMPLITUDE (PEAK TO PEAK) OF DIE OSCILLATION (IN.)

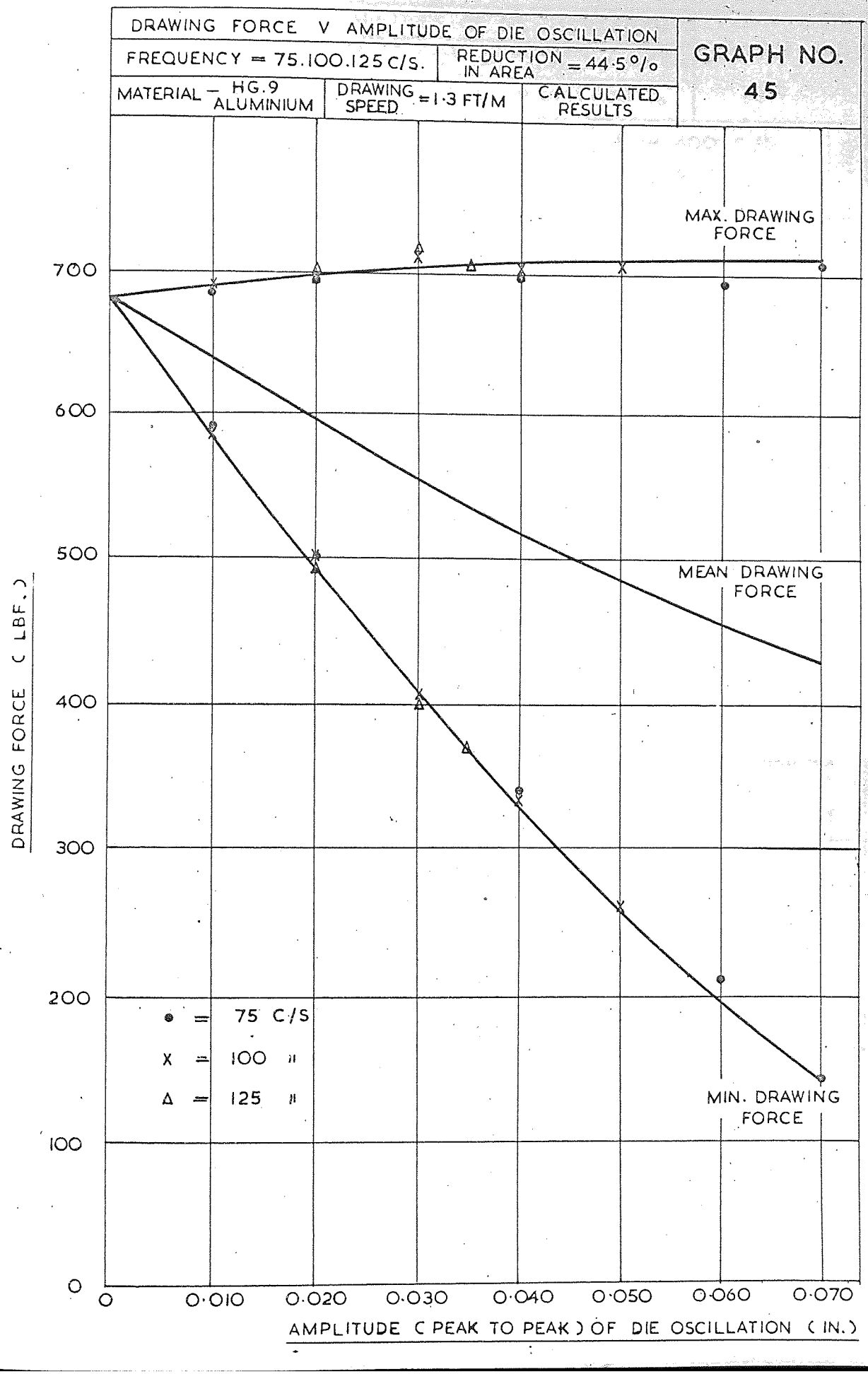
DRAWING FORCE V AMPLITUDE OF DIE OSCILLATION
FREQUENCY = 75.100.125 C/S.
REDUCTION IN AREA = 44·5%
MATERIAL – HG.9 ALUMINIUM
DRAWING SPEED = 1·3 FT/M
CALCULATED RESULTS
GRAPH NO. 45
MAX. DRAWING FORCE
MEAN DRAWING FORCE
MIN. DRAWING FORCE
● = 75 C/S
X = 100 "
Δ = 125 "
DRAWING FORCE (LBF.)
0
100
200
300
400
500
600
700
0
0·010
0·020
0·030
0·040
0·050
0·060
0·070
AMPLITUDE (PEAK TO PEAK) OF DIE OSCILLATION (IN.)

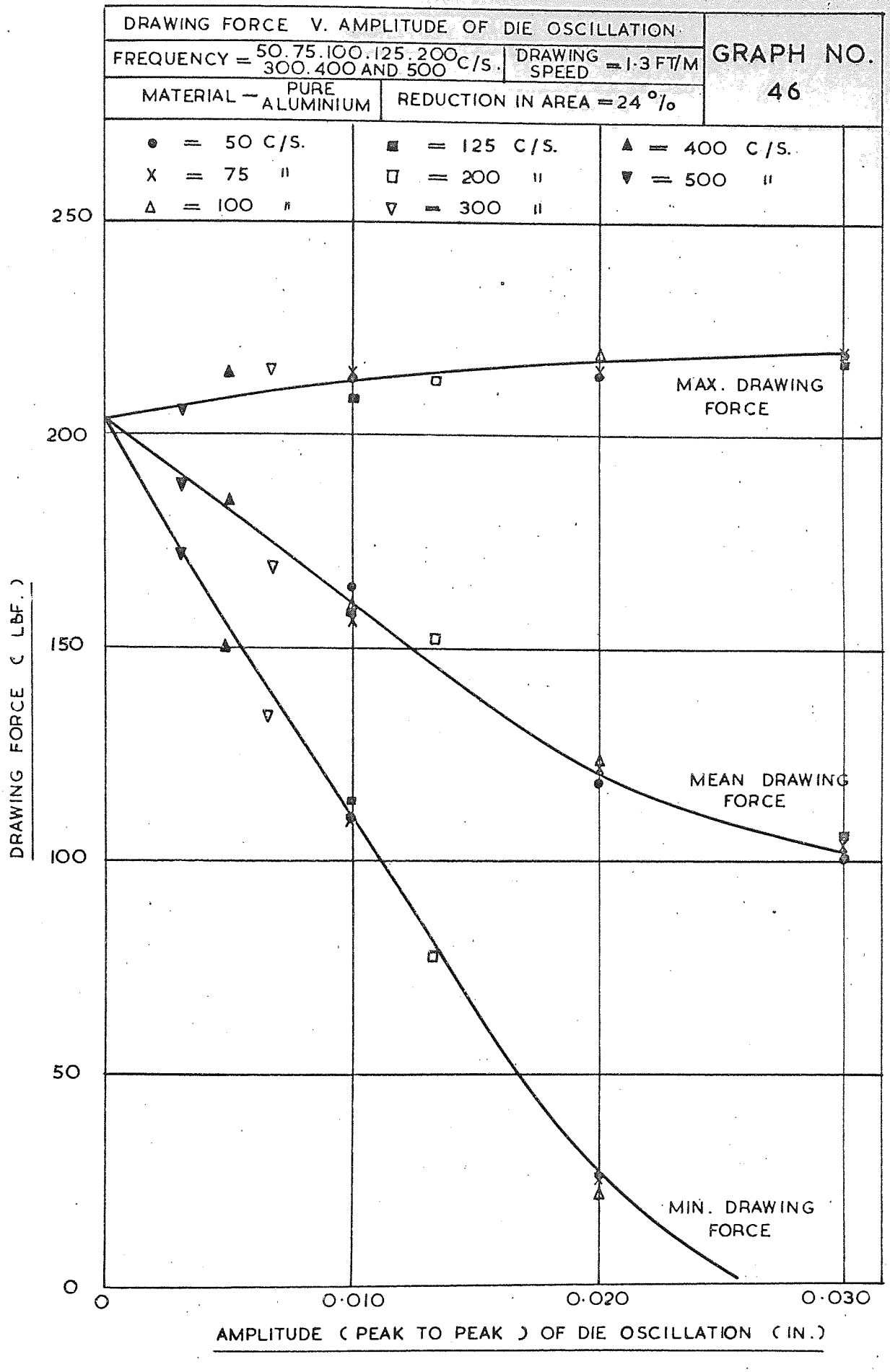
DRAWING FORCE V. AMPLITUDE OF DIE OSCILLATION
FREQUENCY = 50. 75. 100. 125. 200 300. 400 AND 500 C/S.
DRAWING SPEED = 1·3 FT/M
MATERIAL — PURE ALUMINIUM
REDUCTION IN AREA = 24 %
GRAPH NO. 46
● = 50 C/S.
X = 75 "
Δ = 100 "
■ = 125 C/S.
□ = 200 "
▽ = 300 "
▲ = 400 C/S.
▼ = 500 "
MAX. DRAWING FORCE
MEAN DRAWING FORCE
MIN. DRAWING FORCE
DRAWING FORCE (LBF.)
250
200
150
100
50
0
0
0·010
0·020
0·030
AMPLITUDE (PEAK TO PEAK) OF DIE OSCILLATION (IN.)

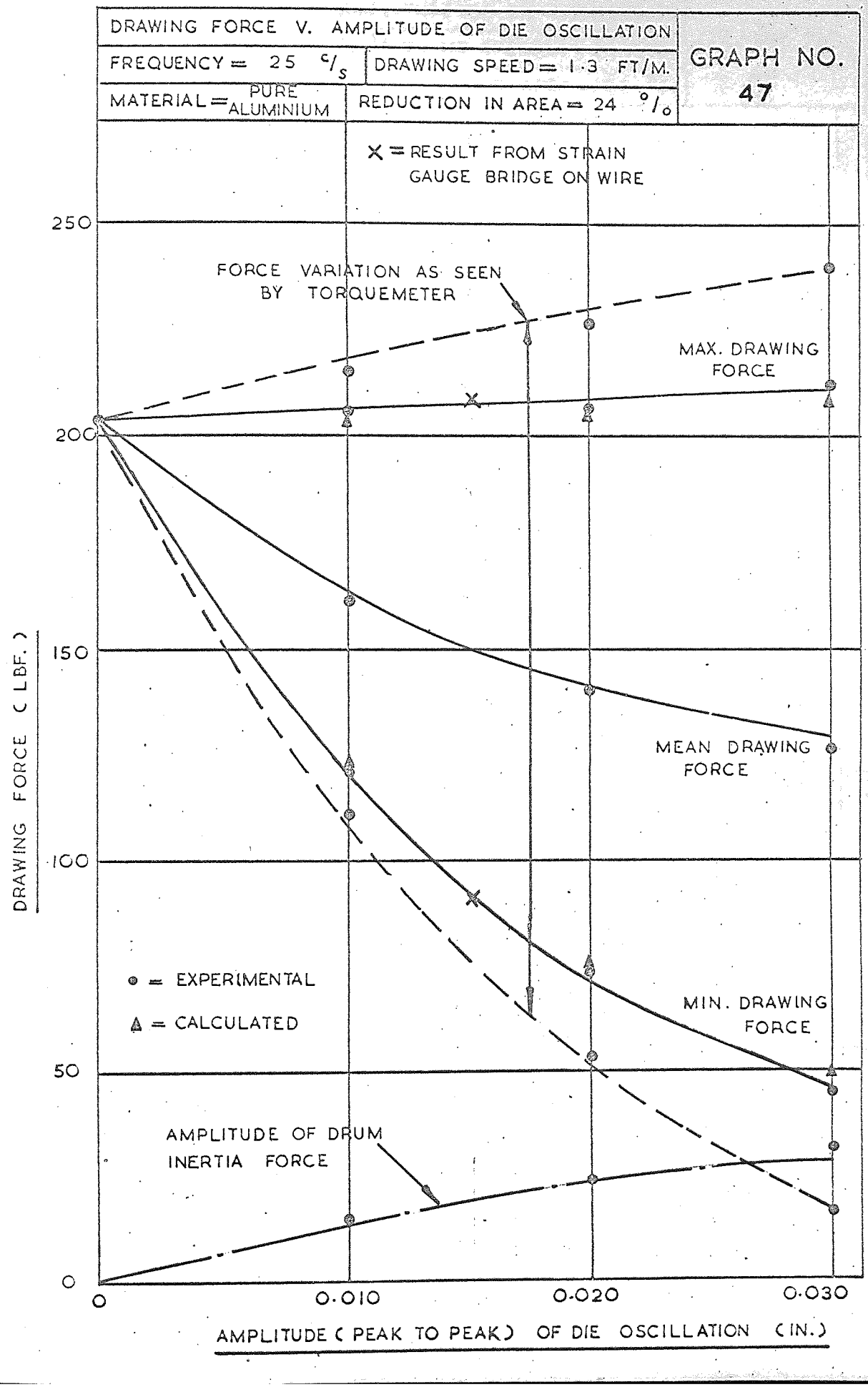
DRAWING FORCE V. AMPLITUDE OF DIE OSCILLATION
FREQUENCY = 25 c/s
DRAWING SPEED = 1·3 FT/M.
MATERIAL = PURE ALUMINIUM
REDUCTION IN AREA = 24 %
GRAPH NO. 47
X = RESULT FROM STRAIN GAUGE BRIDGE ON WIRE
FORCE VARIATION AS SEEN BY TORQUEMETER
MAX. DRAWING FORCE
MEAN DRAWING FORCE
MIN. DRAWING FORCE
AMPLITUDE OF DRUM INERTIA FORCE
● = EXPERIMENTAL
▲ = CALCULATED
DRAWING FORCE (LBF.)
250
200
150
100
50
0
0
0·010
0·020
0·030
AMPLITUDE (PEAK TO PEAK) OF DIE OSCILLATION (IN.)

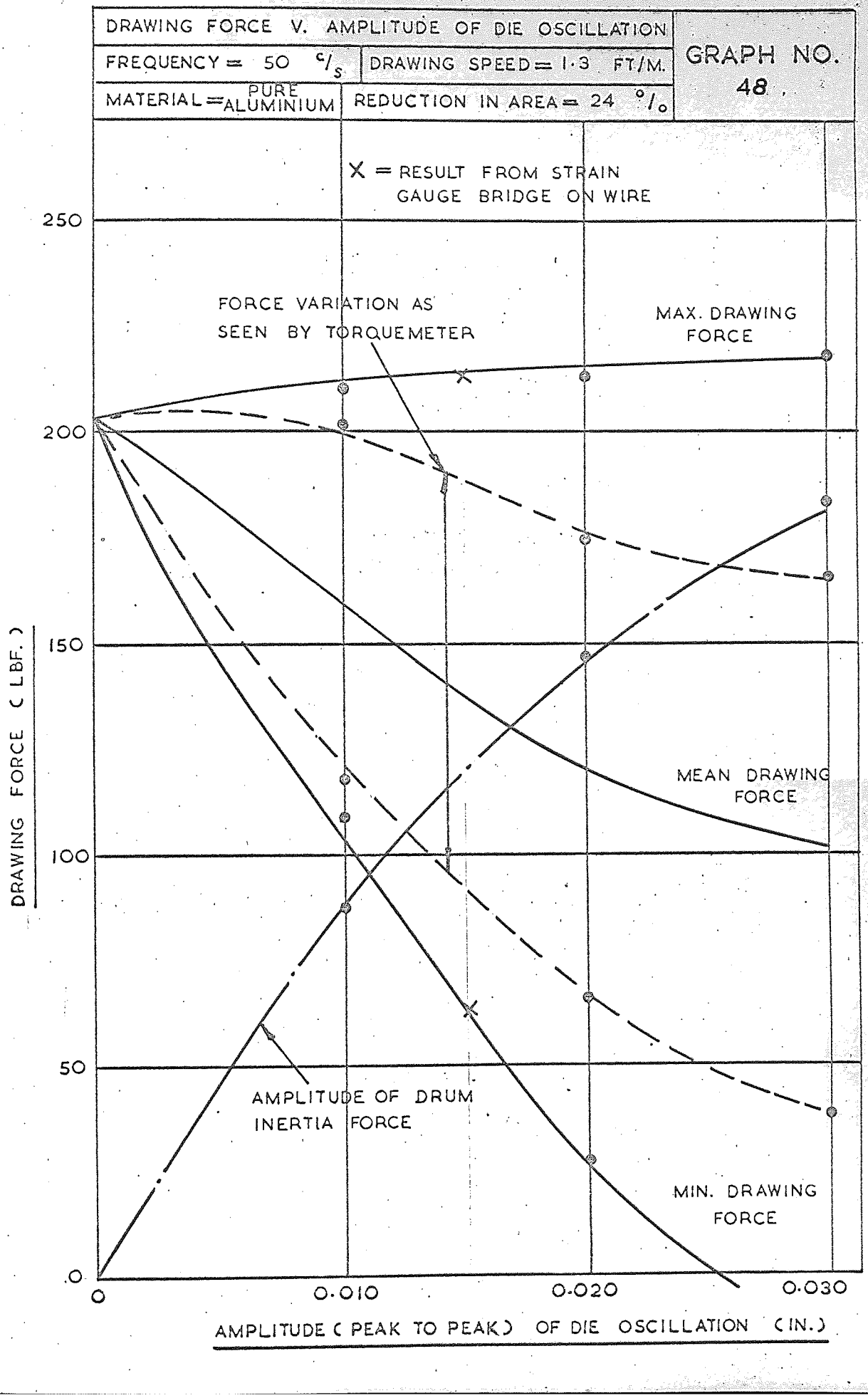
DRAWING FORCE V. AMPLITUDE OF DIE OSCILLATION
FREQUENCY = 50 c/s
DRAWING SPEED = 1·3 FT/M.
MATERIAL = PURE ALUMINIUM
REDUCTION IN AREA = 24 %
GRAPH NO. 48.
X = RESULT FROM STRAIN GAUGE BRIDGE ON WIRE
FORCE VARIATION AS SEEN BY TORQUEMETER
MAX. DRAWING FORCE
MEAN DRAWING FORCE
MIN. DRAWING FORCE
AMPLITUDE OF DRUM INERTIA FORCE
DRAWING FORCE (LBF.)
250
200
150
100
50
0
0
0·010
0·020
0·030
AMPLITUDE (PEAK TO PEAK) OF DIE OSCILLATION (IN.)

DRAWING FORCE V. AMPLITUDE OF DIE OSCILLATION

FREQUENCY = 75 c/s | DRAWING SPEED = 1·3 FT/M.

MATERIAL = PURE ALUMINIUM | REDUCTION IN AREA = 24 %

GRAPH NO. 49

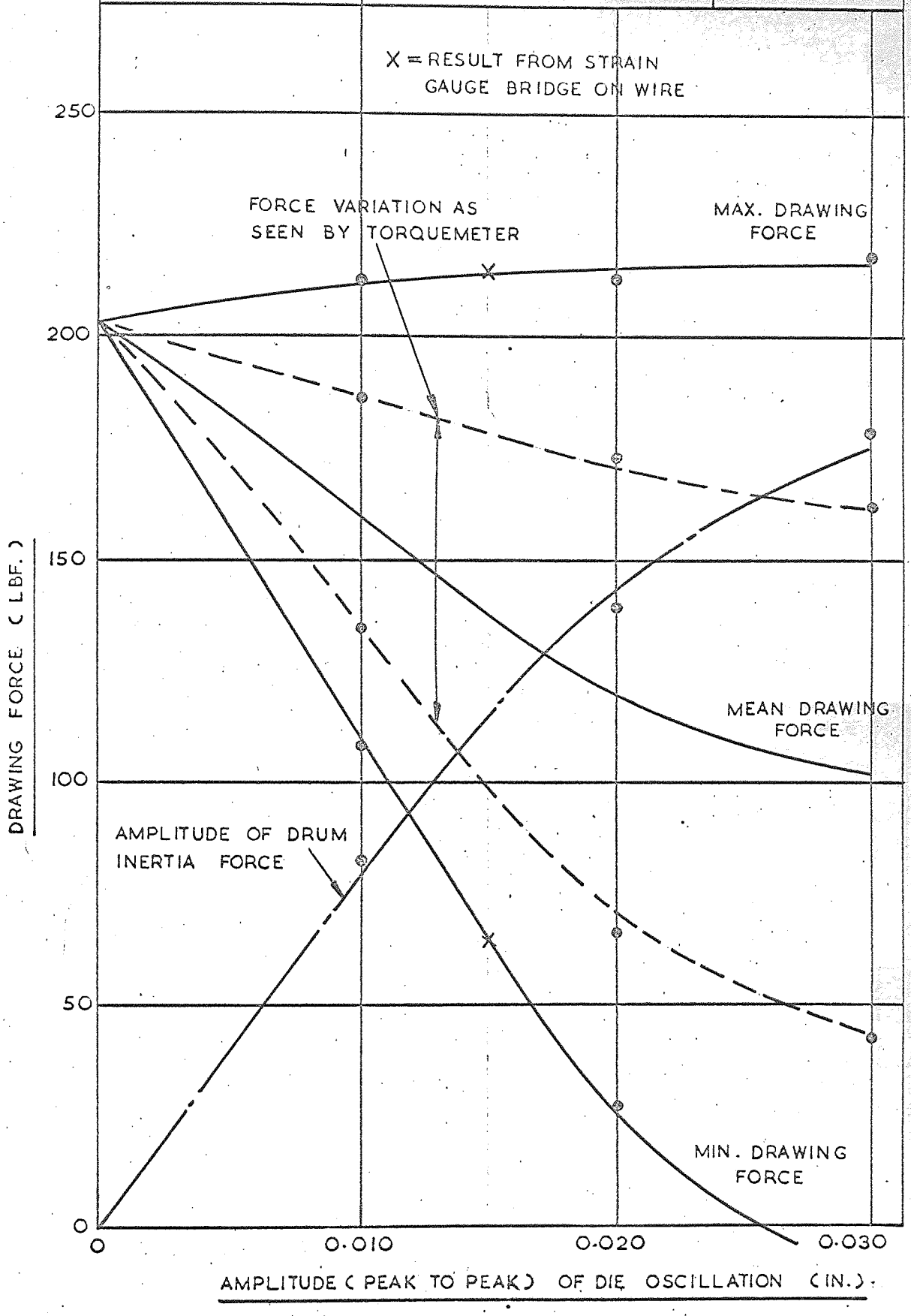

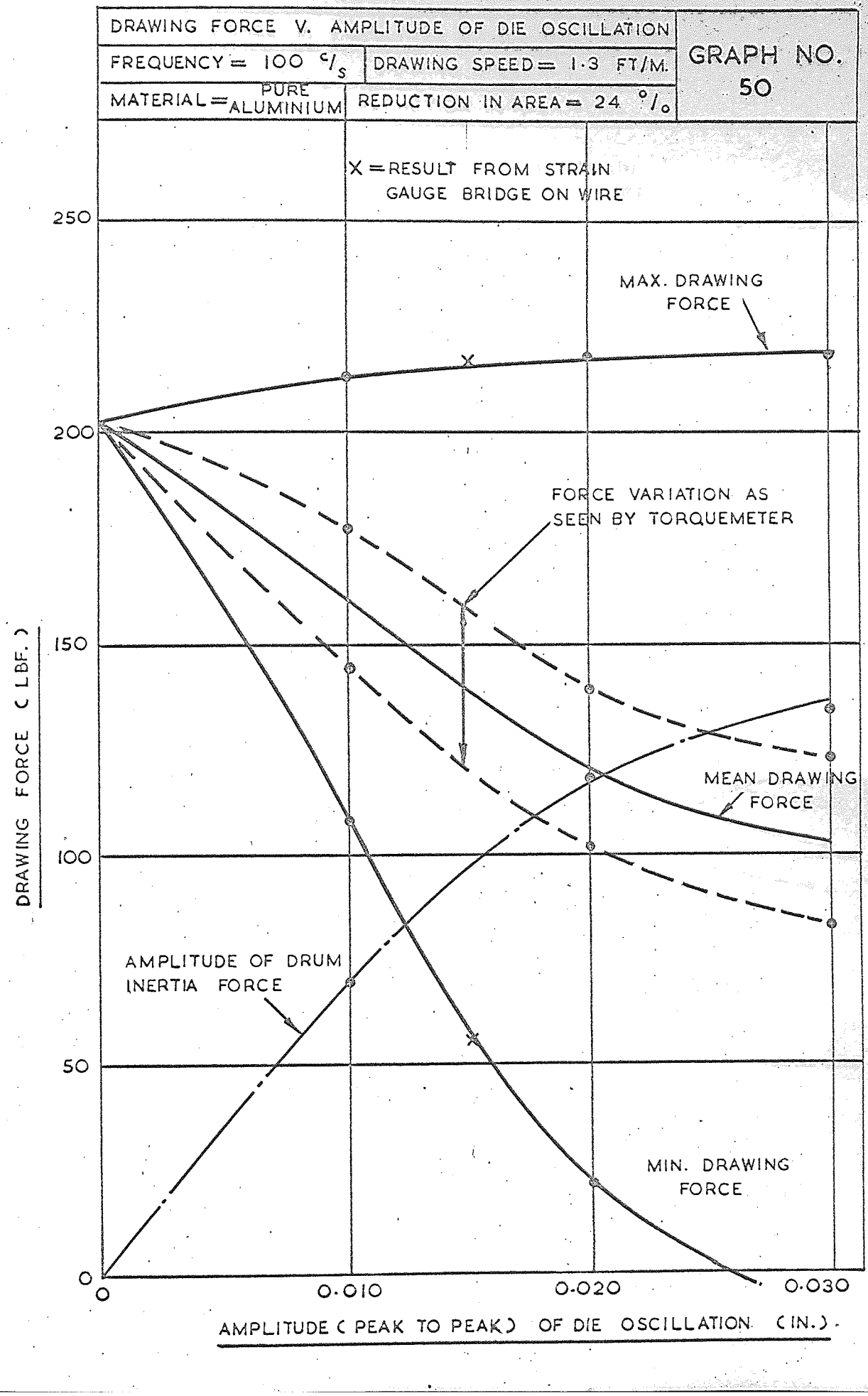
DRAWING FORCE V. AMPLITUDE OF DIE OSCILLATION
FREQUENCY = 100 c/s
DRAWING SPEED = 1·3 FT/M.
MATERIAL = PURE ALUMINIUM
REDUCTION IN AREA = 24 %
GRAPH NO. 50
X = RESULT FROM STRAIN GAUGE BRIDGE ON WIRE
MAX. DRAWING FORCE
FORCE VARIATION AS SEEN BY TORQUEMETER
MEAN DRAWING FORCE
AMPLITUDE OF DRUM INERTIA FORCE
MIN. DRAWING FORCE
DRAWING FORCE (LBF.)
250
200
150
100
50
0
0
0·010
0·020
0·030
AMPLITUDE (PEAK TO PEAK) OF DIE OSCILLATION (IN.).

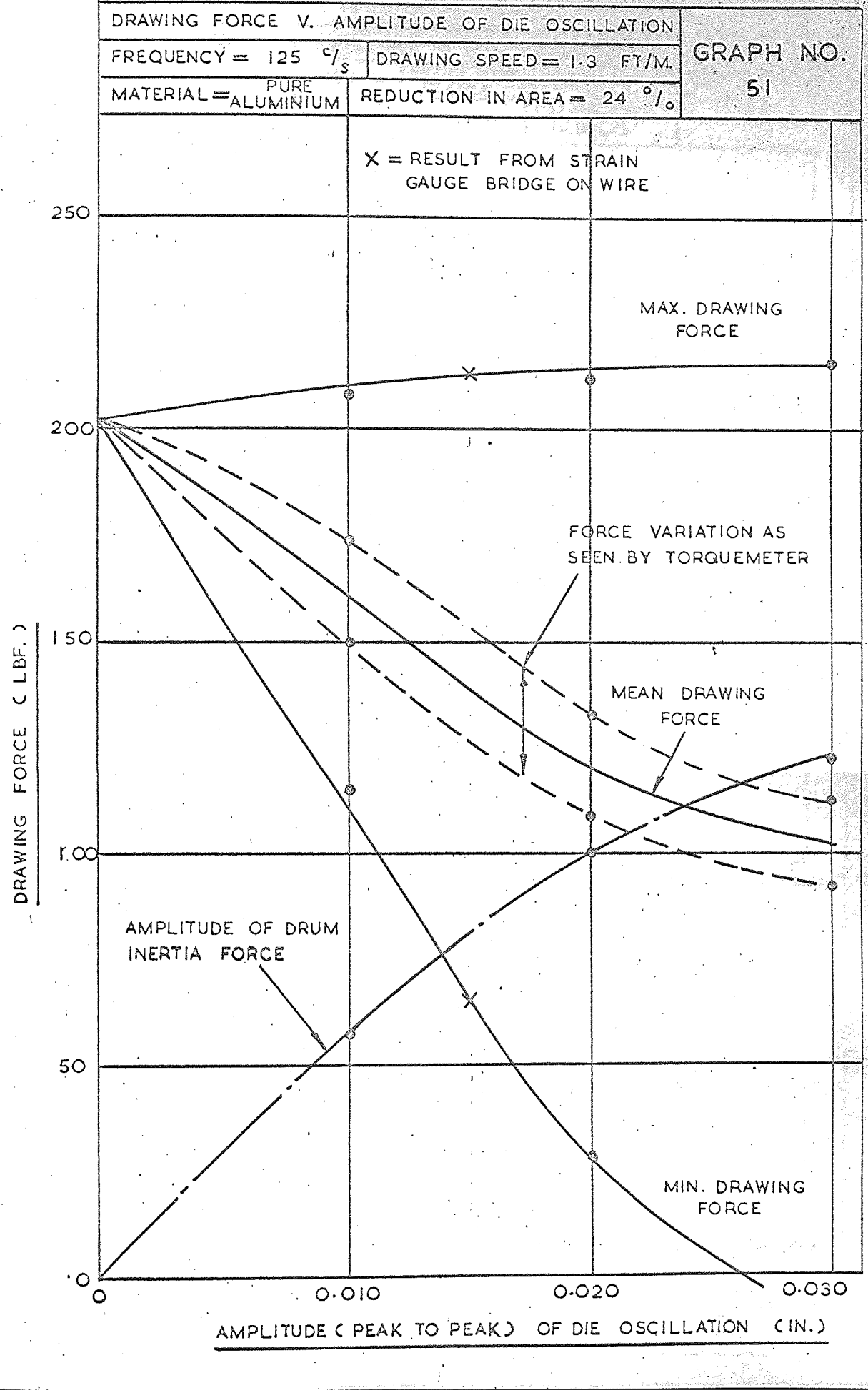
DRAWING FORCE V. AMPLITUDE OF DIE OSCILLATION
FREQUENCY = 125 c/s
DRAWING SPEED = 1·3 FT/M.
MATERIAL = PURE ALUMINIUM
REDUCTION IN AREA = 24 %
GRAPH NO. 51
X = RESULT FROM STRAIN GAUGE BRIDGE ON WIRE
MAX. DRAWING FORCE
FORCE VARIATION AS SEEN BY TORQUEMETER
MEAN DRAWING FORCE
AMPLITUDE OF DRUM INERTIA FORCE
MIN. DRAWING FORCE
DRAWING FORCE (LBF.)
250
200
150
100
50
0
0
0·010
0·020
0·030
AMPLITUDE (PEAK TO PEAK) OF DIE OSCILLATION (IN.)

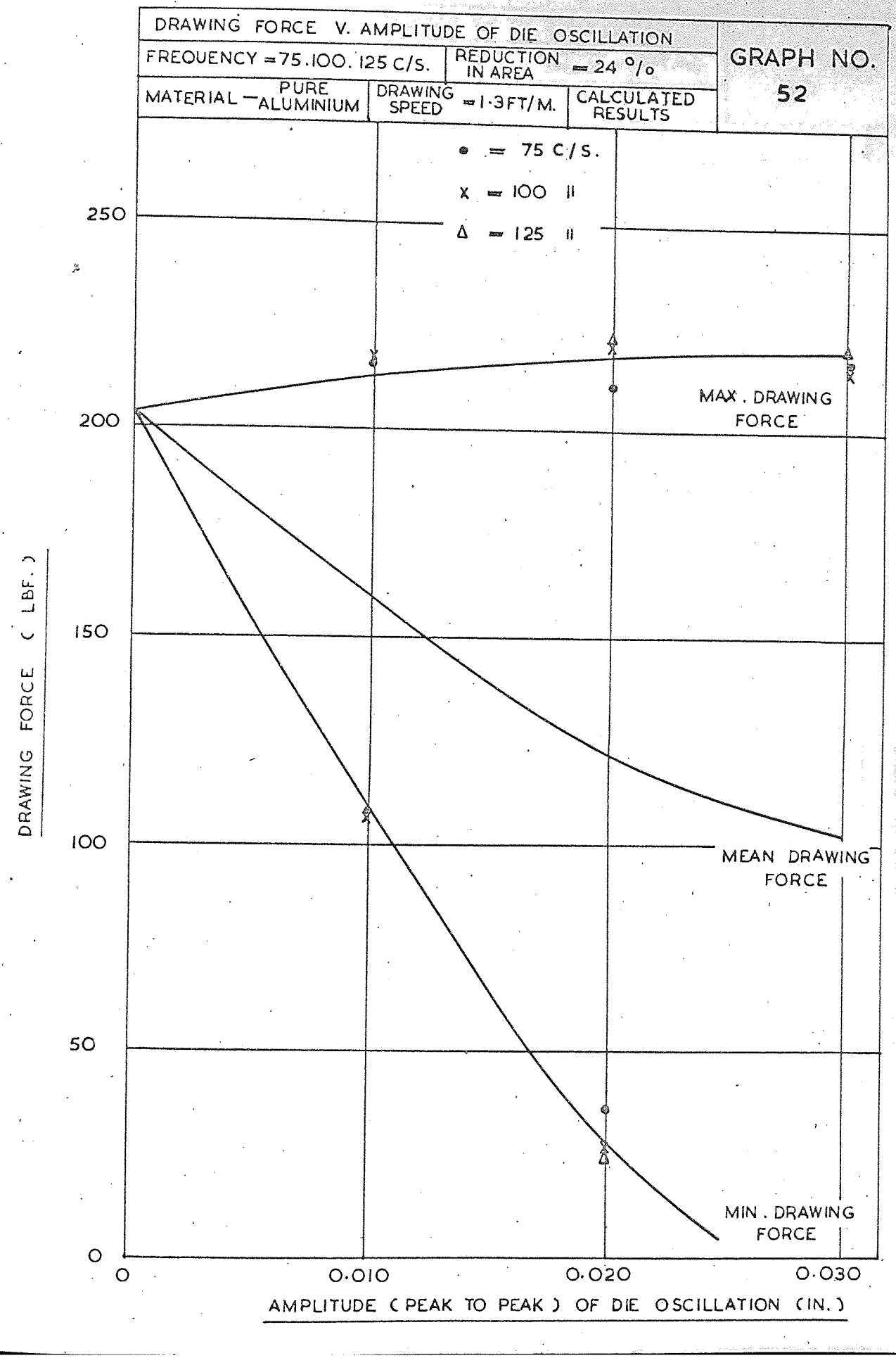
DRAWING FORCE V. AMPLITUDE OF DIE OSCILLATION
FREQUENCY = 75. 100. 125 C/S.
REDUCTION IN AREA = 24 %
MATERIAL — PURE ALUMINIUM
DRAWING SPEED = 1·3 FT/M.
CALCULATED RESULTS
GRAPH NO. 52
● = 75 C/S.
X = 100 "
Δ = 125 "
MAX. DRAWING FORCE
MEAN DRAWING FORCE
MIN. DRAWING FORCE
DRAWING FORCE (LBF.)
250
200
150
100
50
0
0
0·010
0·020
0·030
AMPLITUDE (PEAK TO PEAK) OF DIE OSCILLATION (IN.)

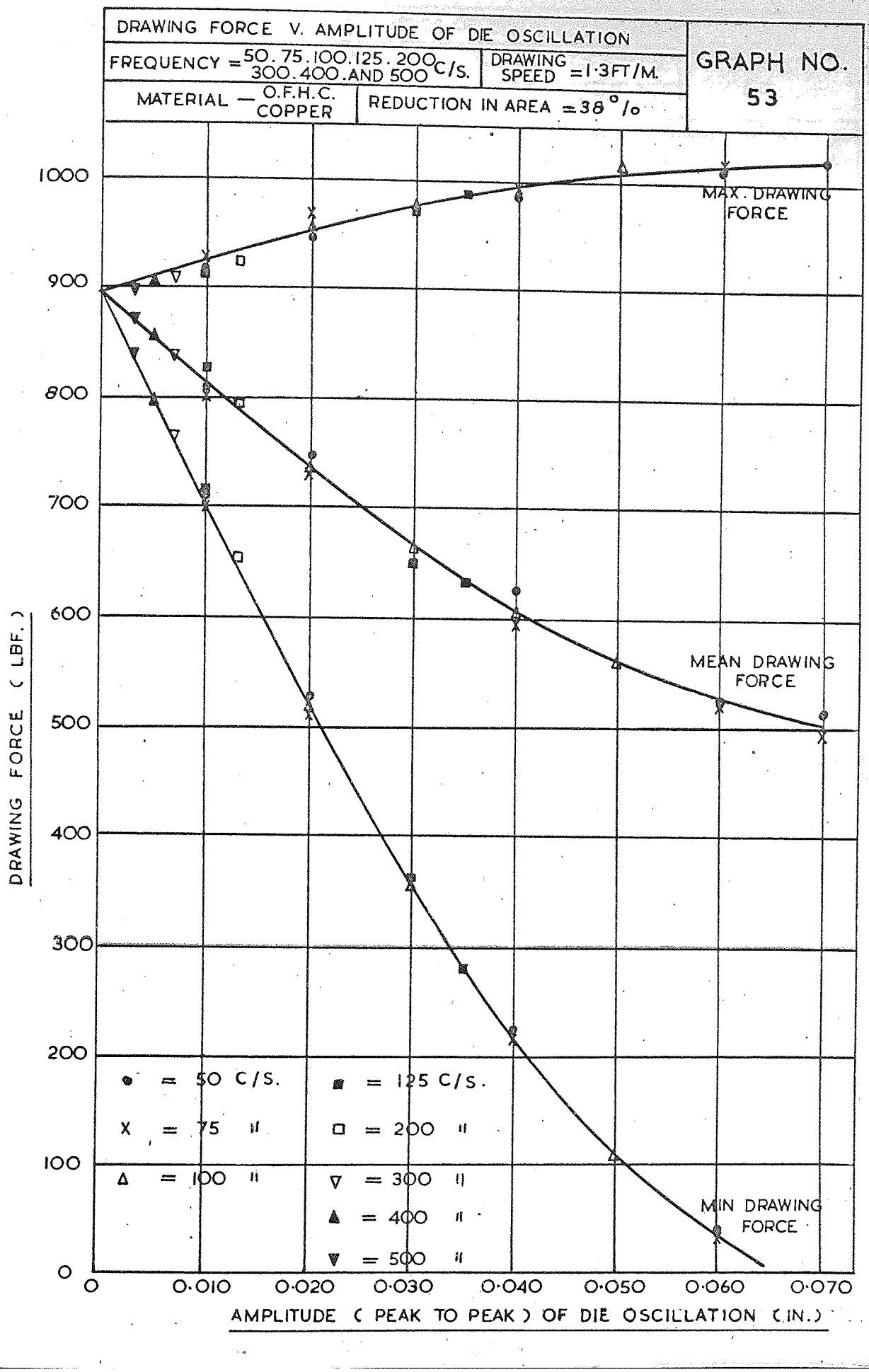
DRAWING FORCE V. AMPLITUDE OF DIE OSCILLATION
FREQUENCY = 50. 75. 100. 125. 200 300. 400. AND 500 C/S.
DRAWING SPEED = 1·3 FT/M.
MATERIAL — O.F.H.C. COPPER
REDUCTION IN AREA = 38 %
GRAPH NO. 53
MAX. DRAWING FORCE
MEAN DRAWING FORCE
MIN DRAWING FORCE
DRAWING FORCE (LBF.)
AMPLITUDE (PEAK TO PEAK) OF DIE OSCILLATION (IN.)
1000
900
800
700
600
500
400
300
200
100
0
0·010
0·020
0·030
0·040
0·050
0·060
0·070
● = 50 C/S.
X = 75 "
Δ = 100 "
■ = 125 C/S.
□ = 200 "
▽ = 300 "
▲ = 400 "
▼ = 500 "

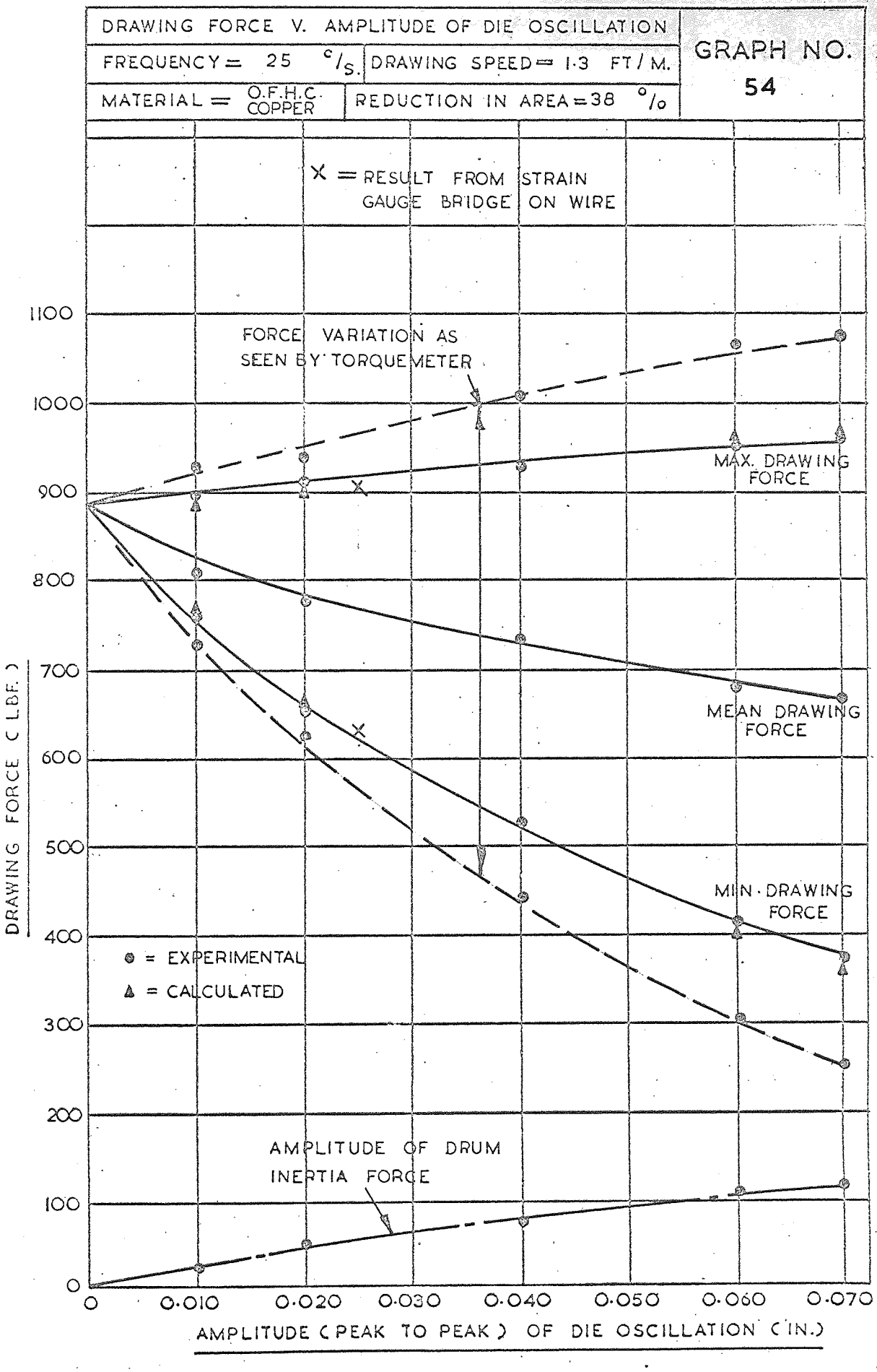
DRAWING FORCE V. AMPLITUDE OF DIE OSCILLATION
FREQUENCY = 25 c/s.
DRAWING SPEED = 1·3 FT/M.
MATERIAL = O.F.H.C. COPPER
REDUCTION IN AREA = 38 %
GRAPH NO. 54
X = RESULT FROM STRAIN GAUGE BRIDGE ON WIRE
FORCE VARIATION AS SEEN BY TORQUE METER
MAX. DRAWING FORCE
MEAN DRAWING FORCE
MIN. DRAWING FORCE
● = EXPERIMENTAL
▲ = CALCULATED
AMPLITUDE OF DRUM INERTIA FORCE
DRAWING FORCE (LBF.)
1100
1000
900
800
700
600
500
400
300
200
100
0
0
0·010
0·020
0·030
0·040
0·050
0·060
0·070
AMPLITUDE (PEAK TO PEAK) OF DIE OSCILLATION (IN.)

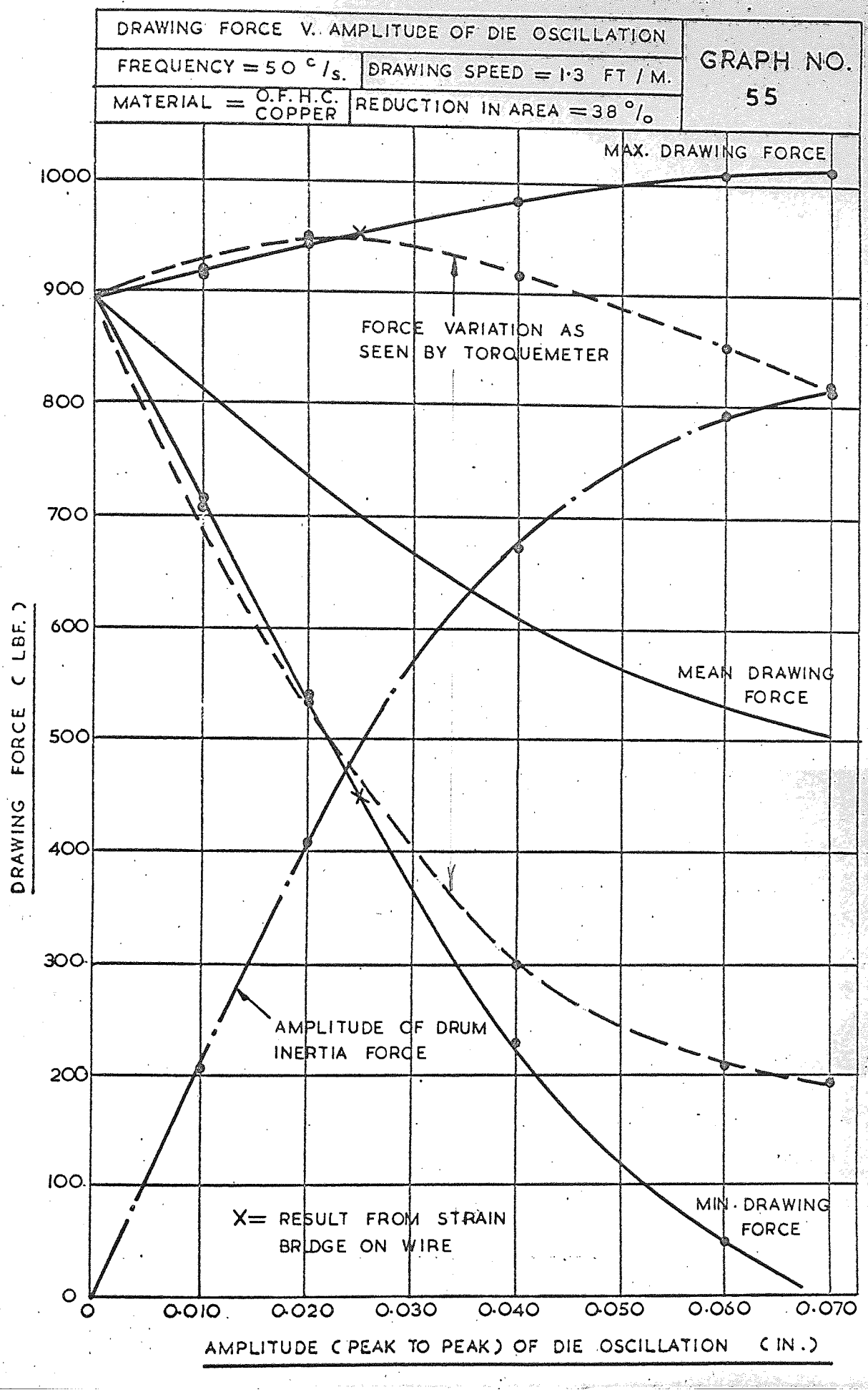
DRAWING FORCE V. AMPLITUDE OF DIE OSCILLATION
FREQUENCY = 50 c/s.
DRAWING SPEED = 1·3 FT / M.
MATERIAL = O.F. H.C. COPPER
REDUCTION IN AREA = 38 %
GRAPH NO. 55
MAX. DRAWING FORCE
FORCE VARIATION AS SEEN BY TORQUEMETER
MEAN DRAWING FORCE
AMPLITUDE OF DRUM INERTIA FORCE
X= RESULT FROM STRAIN BRIDGE ON WIRE
MIN. DRAWING FORCE
DRAWING FORCE (LBF.)
1000
900
800
700
600
500
400
300
200
100
0
0
0·010
0·020
0·030
0·040
0·050
0·060
0·070
AMPLITUDE (PEAK TO PEAK) OF DIE OSCILLATION (IN.)

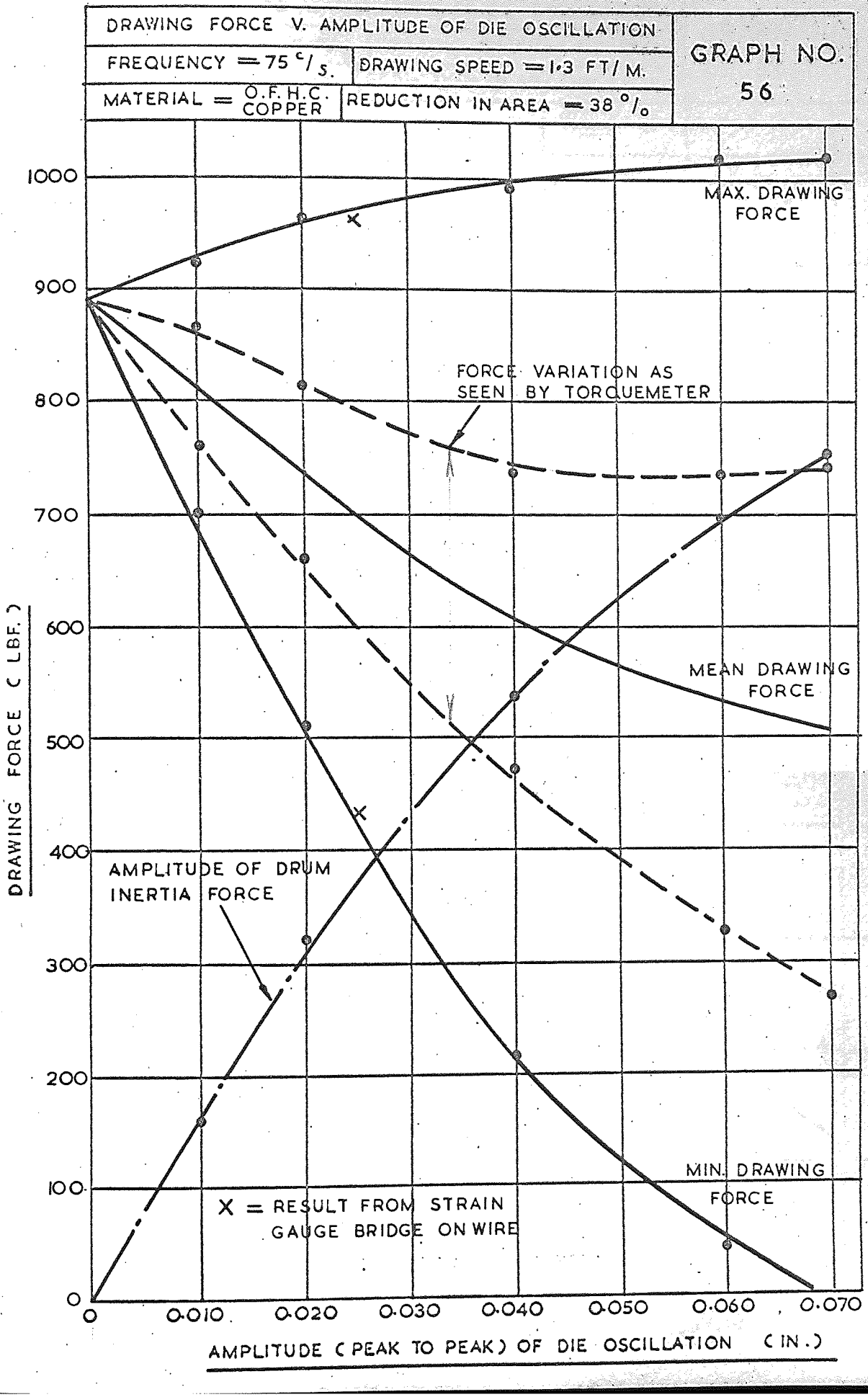
DRAWING FORCE V. AMPLITUDE OF DIE OSCILLATION
FREQUENCY = 75 c/s.
DRAWING SPEED = 1·3 FT/M.
MATERIAL = O.F.H.C. COPPER
REDUCTION IN AREA = 38 %
GRAPH NO. 56
MAX. DRAWING FORCE
FORCE VARIATION AS SEEN BY TORQUEMETER
MEAN DRAWING FORCE
AMPLITUDE OF DRUM INERTIA FORCE
MIN. DRAWING FORCE
X = RESULT FROM STRAIN GAUGE BRIDGE ON WIRE
DRAWING FORCE (LBF.)
1000
900
800
700
600
500
400
300
200
100
0
0
0·010
0·020
0·030
0·040
0·050
0·060
0·070
AMPLITUDE (PEAK TO PEAK) OF DIE OSCILLATION (IN.)

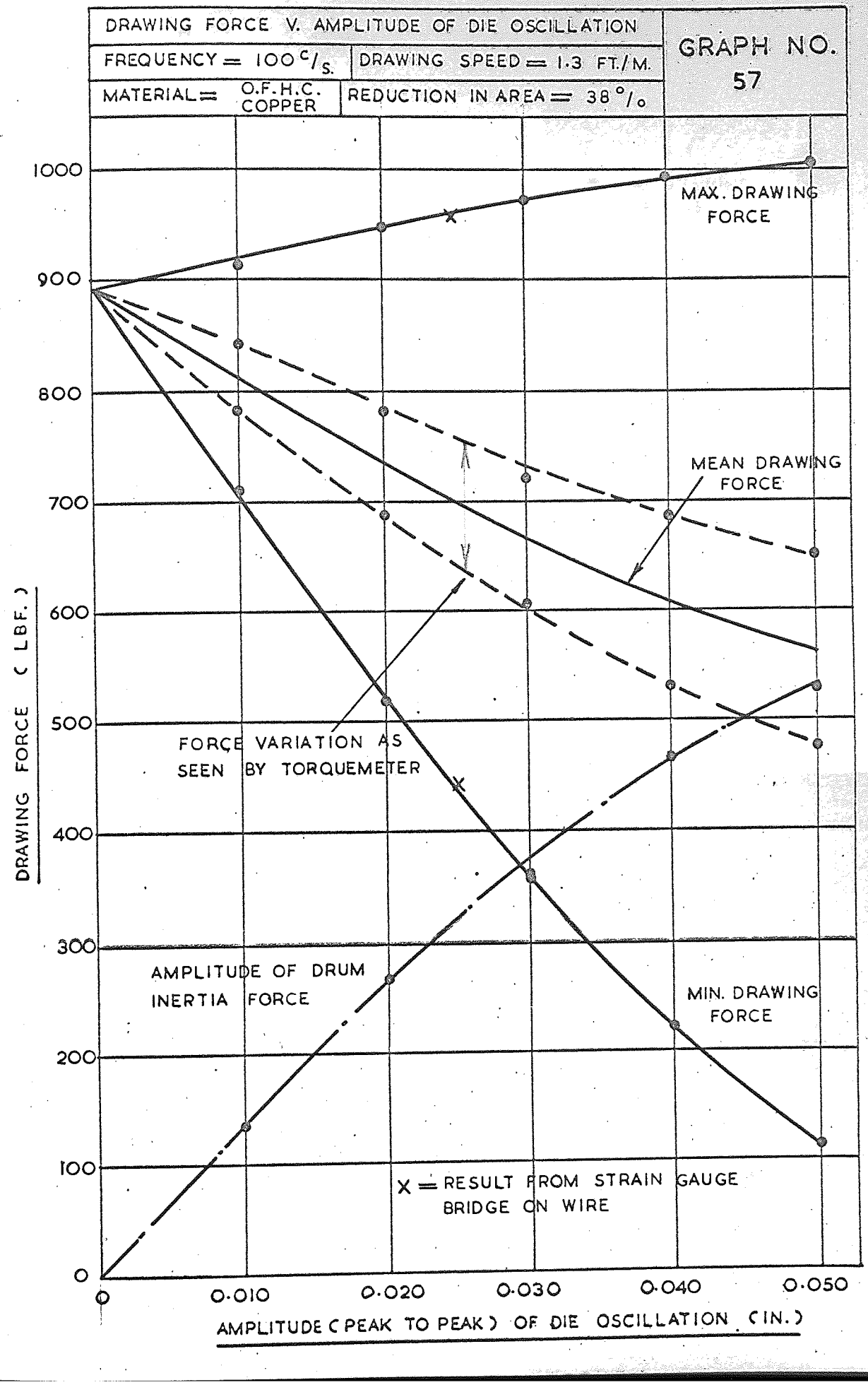
DRAWING FORCE V. AMPLITUDE OF DIE OSCILLATION
FREQUENCY = 100 C/S.
DRAWING SPEED = 1.3 FT./M.
MATERIAL = O.F.H.C. COPPER
REDUCTION IN AREA = 38 %
GRAPH NO. 57
MAX. DRAWING FORCE
MEAN DRAWING FORCE
FORCE VARIATION AS SEEN BY TORQUEMETER
AMPLITUDE OF DRUM INERTIA FORCE
MIN. DRAWING FORCE
X = RESULT FROM STRAIN GAUGE BRIDGE ON WIRE
DRAWING FORCE (LBF.)
1000
900
800
700
600
500
400
300
200
100
0
0
0.010
0.020
0.030
0.040
0.050
AMPLITUDE (PEAK TO PEAK) OF DIE OSCILLATION (IN.)

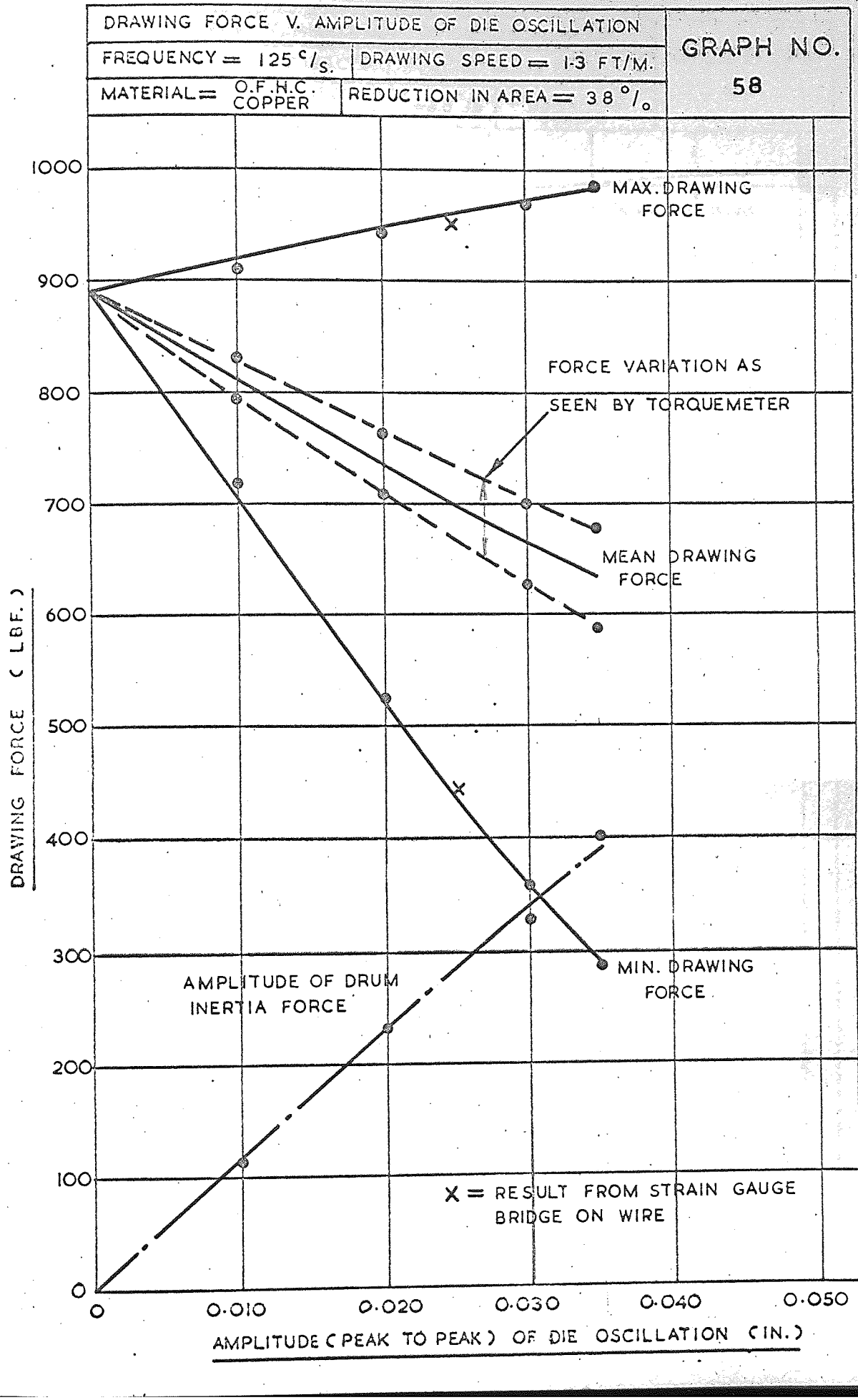
DRAWING FORCE V. AMPLITUDE OF DIE OSCILLATION
FREQUENCY = 125 c/s.
DRAWING SPEED = 1·3 FT/M.
MATERIAL = O.F.H.C. COPPER
REDUCTION IN AREA = 38 %
GRAPH NO. 58
MAX. DRAWING FORCE
FORCE VARIATION AS SEEN BY TORQUEMETER
MEAN DRAWING FORCE
MIN. DRAWING FORCE
AMPLITUDE OF DRUM INERTIA FORCE
X = RESULT FROM STRAIN GAUGE BRIDGE ON WIRE
DRAWING FORCE (LBF.)
1000
900
800
700
600
500
400
300
200
100
0
0
0·010
0·020
0·030
0·040
0·050
AMPLITUDE (PEAK TO PEAK) OF DIE OSCILLATION (IN.)

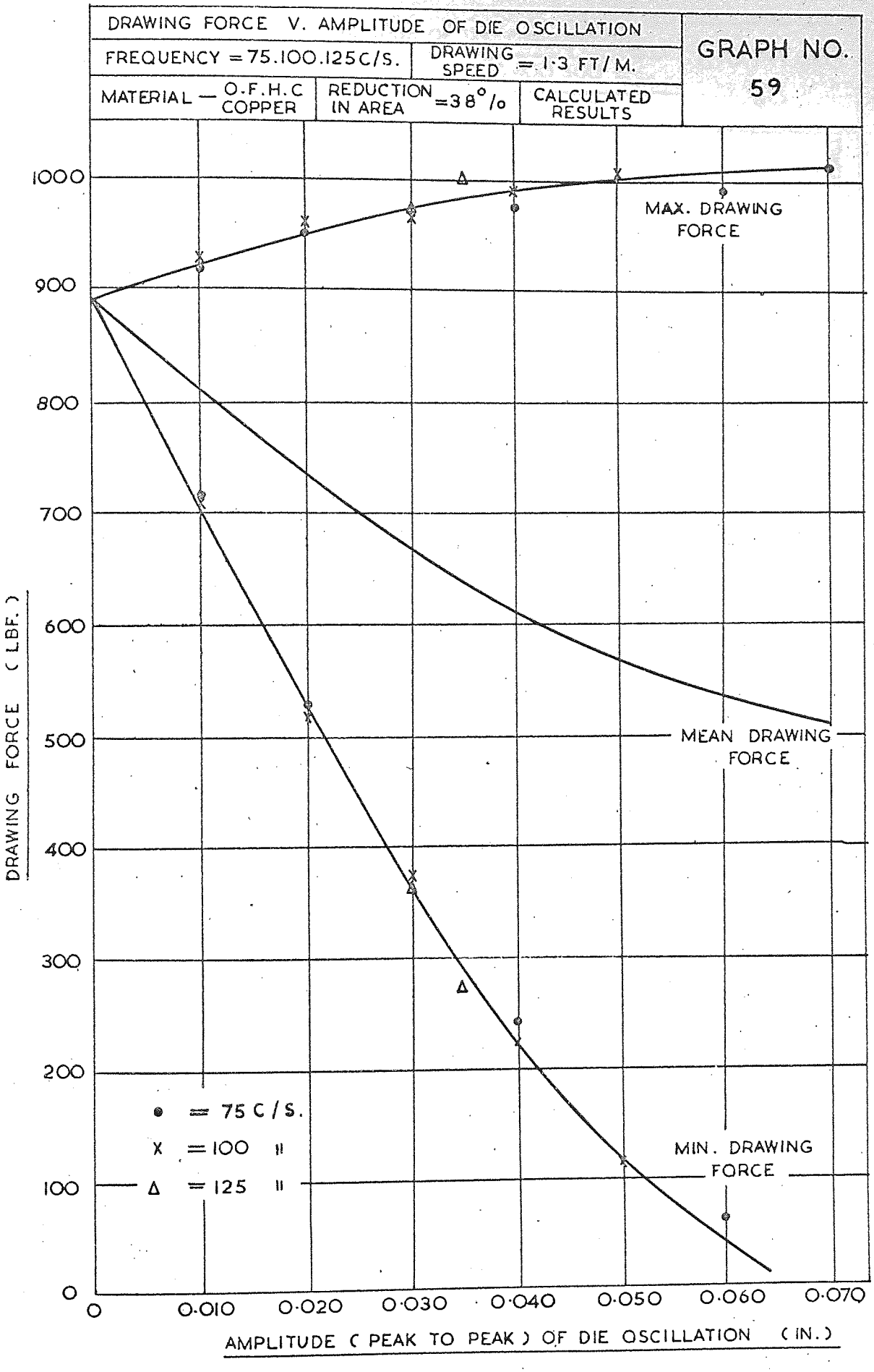
DRAWING FORCE V. AMPLITUDE OF DIE OSCILLATION
FREQUENCY = 75.100.125 C/S.
DRAWING SPEED = 1·3 FT/M.
MATERIAL — O.F.H.C COPPER
REDUCTION IN AREA = 38 %
CALCULATED RESULTS
GRAPH NO. 59
MAX. DRAWING FORCE
MEAN DRAWING FORCE
MIN. DRAWING FORCE
● = 75 C/S.
X = 100 "
Δ = 125 "
DRAWING FORCE (LBF.)
AMPLITUDE (PEAK TO PEAK) OF DIE OSCILLATION (IN.)
0
100
200
300
400
500
600
700
800
900
1000
0·010
0·020
0·030
0·040
0·050
0·060
0·070

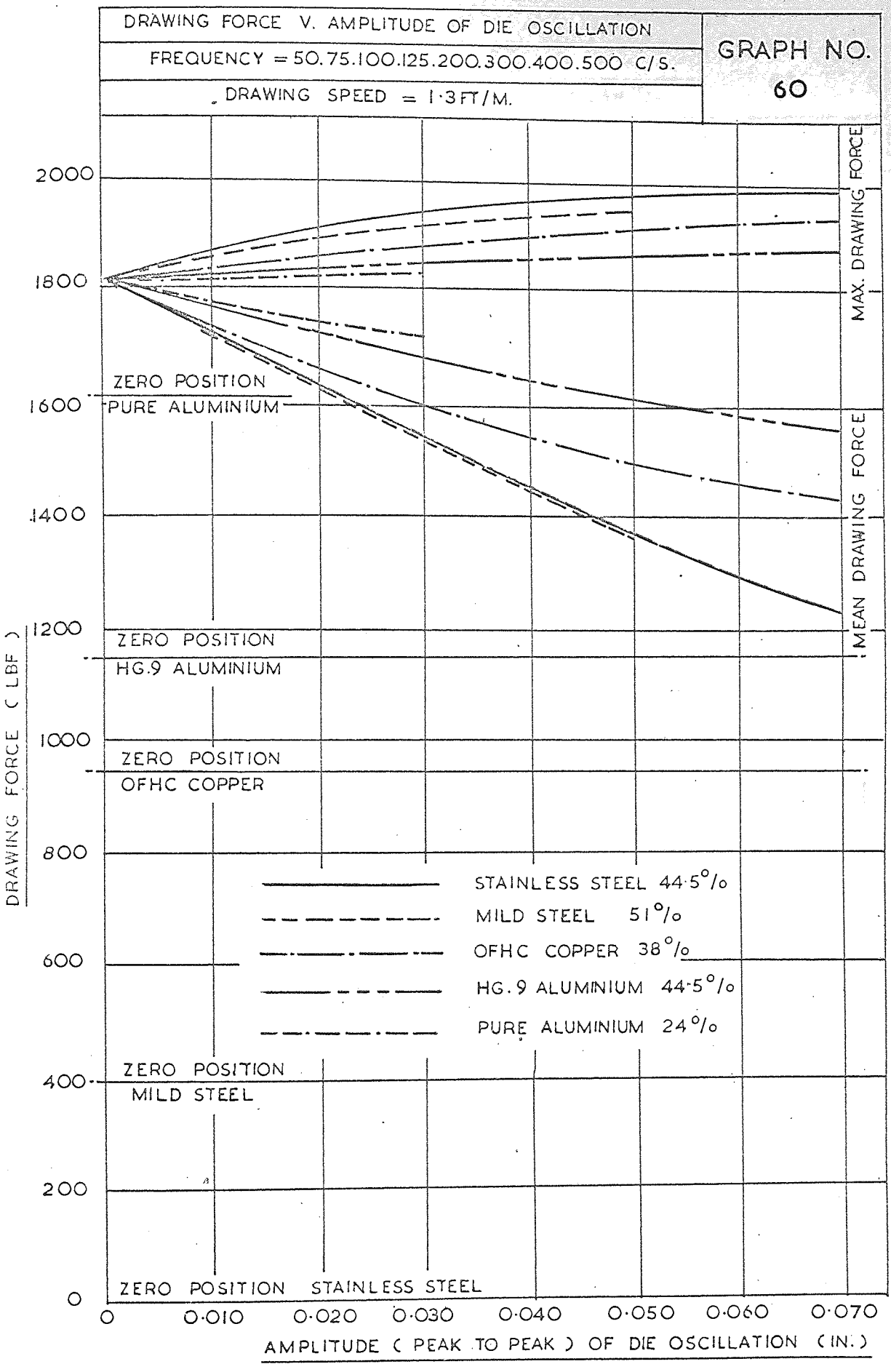
DRAWING FORCE V. AMPLITUDE OF DIE OSCILLATION
FREQUENCY = 50.75.100.125.200.300.400.500 C/S.
DRAWING SPEED = 1·3 FT/M.
GRAPH NO. 60
MAX. DRAWING FORCE
MEAN DRAWING FORCE
DRAWING FORCE (LBF)
2000
1800
1600
1400
1200
1000
800
600
400
200
0
ZERO POSITION PURE ALUMINIUM
ZERO POSITION HG.9 ALUMINIUM
ZERO POSITION OFHC COPPER
ZERO POSITION MILD STEEL
ZERO POSITION STAINLESS STEEL
STAINLESS STEEL 44·5°/o
MILD STEEL 51°/o
OFHC COPPER 38°/o
HG.9 ALUMINIUM 44·5°/o
PURE ALUMINIUM 24°/o
0
0·010
0·020
0·030
0·040
0·050
0·060
0·070
AMPLITUDE (PEAK TO PEAK) OF DIE OSCILLATION (IN.)

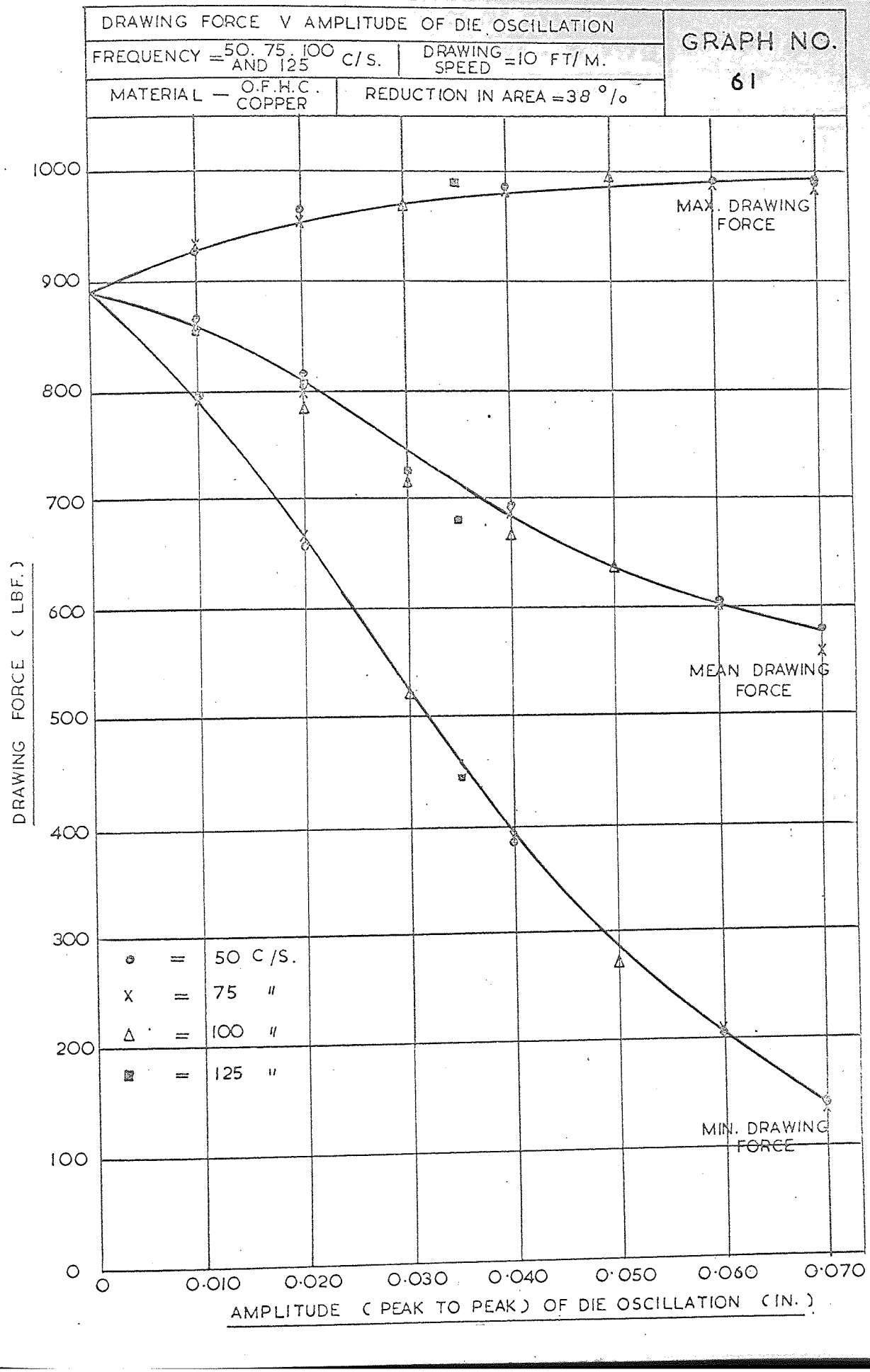
DRAWING FORCE V AMPLITUDE OF DIE OSCILLATION
FREQUENCY = 50, 75, 100 AND 125 C/S.
DRAWING SPEED = 10 FT/M.
MATERIAL — O.F.H.C. COPPER
REDUCTION IN AREA = 38 %
GRAPH NO. 61
MAX. DRAWING FORCE
MEAN DRAWING FORCE
MIN. DRAWING FORCE
⊙ = 50 C/S.
X = 75 "
Δ = 100 "
▨ = 125 "
DRAWING FORCE (LBF.)
1000
900
800
700
600
500
400
300
200
100
0
0
0·010
0·020
0·030
0·040
0·050
0·060
0·070
AMPLITUDE (PEAK TO PEAK) OF DIE OSCILLATION (IN.)

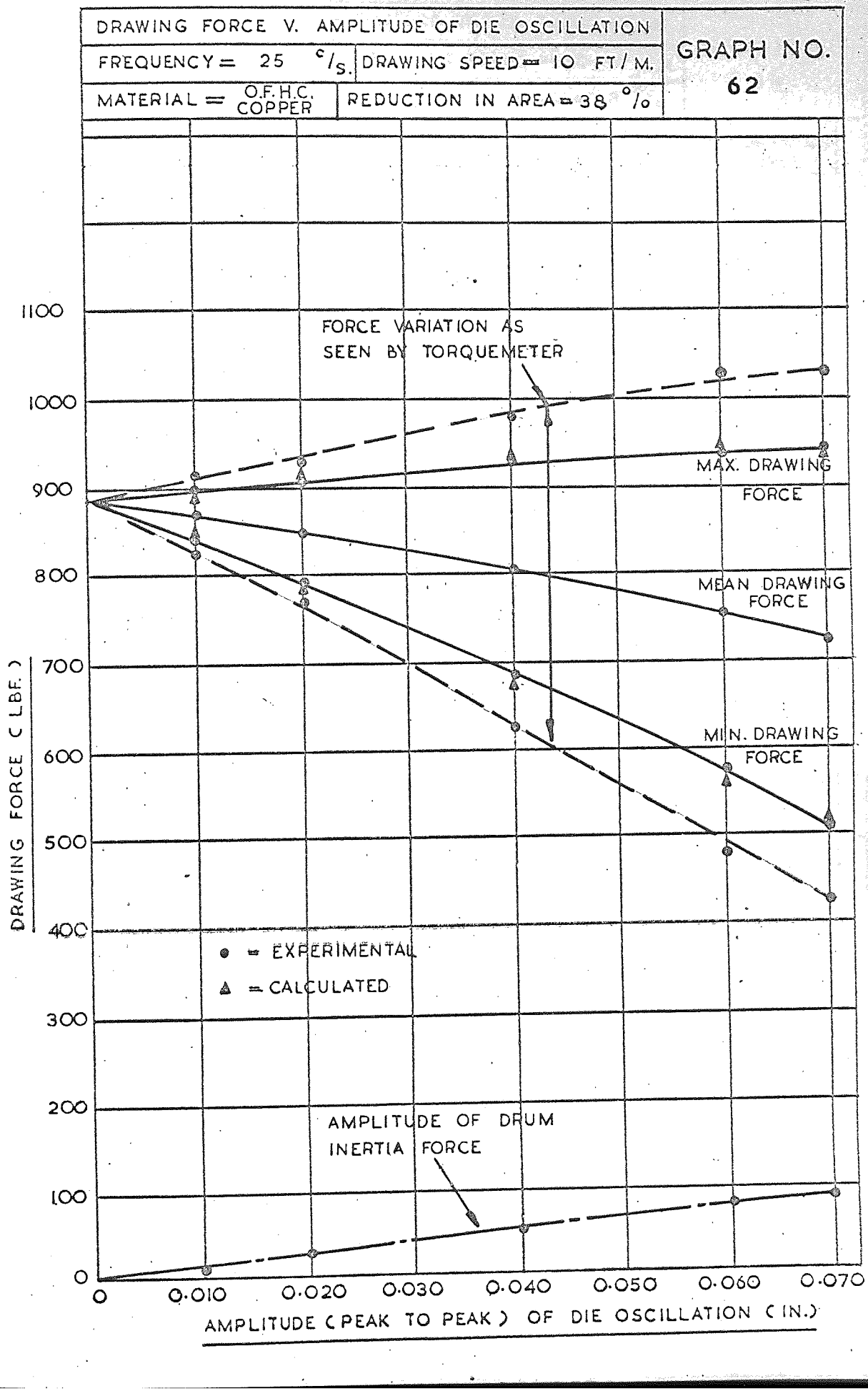
DRAWING FORCE V. AMPLITUDE OF DIE OSCILLATION
FREQUENCY = 25 c/s.
DRAWING SPEED = 10 FT/M.
MATERIAL = O.F.H.C. COPPER
REDUCTION IN AREA = 38 %
GRAPH NO. 62
FORCE VARIATION AS SEEN BY TORQUEMETER
MAX. DRAWING FORCE
MEAN DRAWING FORCE
MIN. DRAWING FORCE
● = EXPERIMENTAL
▲ = CALCULATED
AMPLITUDE OF DRUM INERTIA FORCE
DRAWING FORCE (LBF.)
1100
1000
900
800
700
600
500
400
300
200
100
0
0
0.010
0.020
0.030
0.040
0.050
0.060
0.070
AMPLITUDE (PEAK TO PEAK) OF DIE OSCILLATION (IN.)

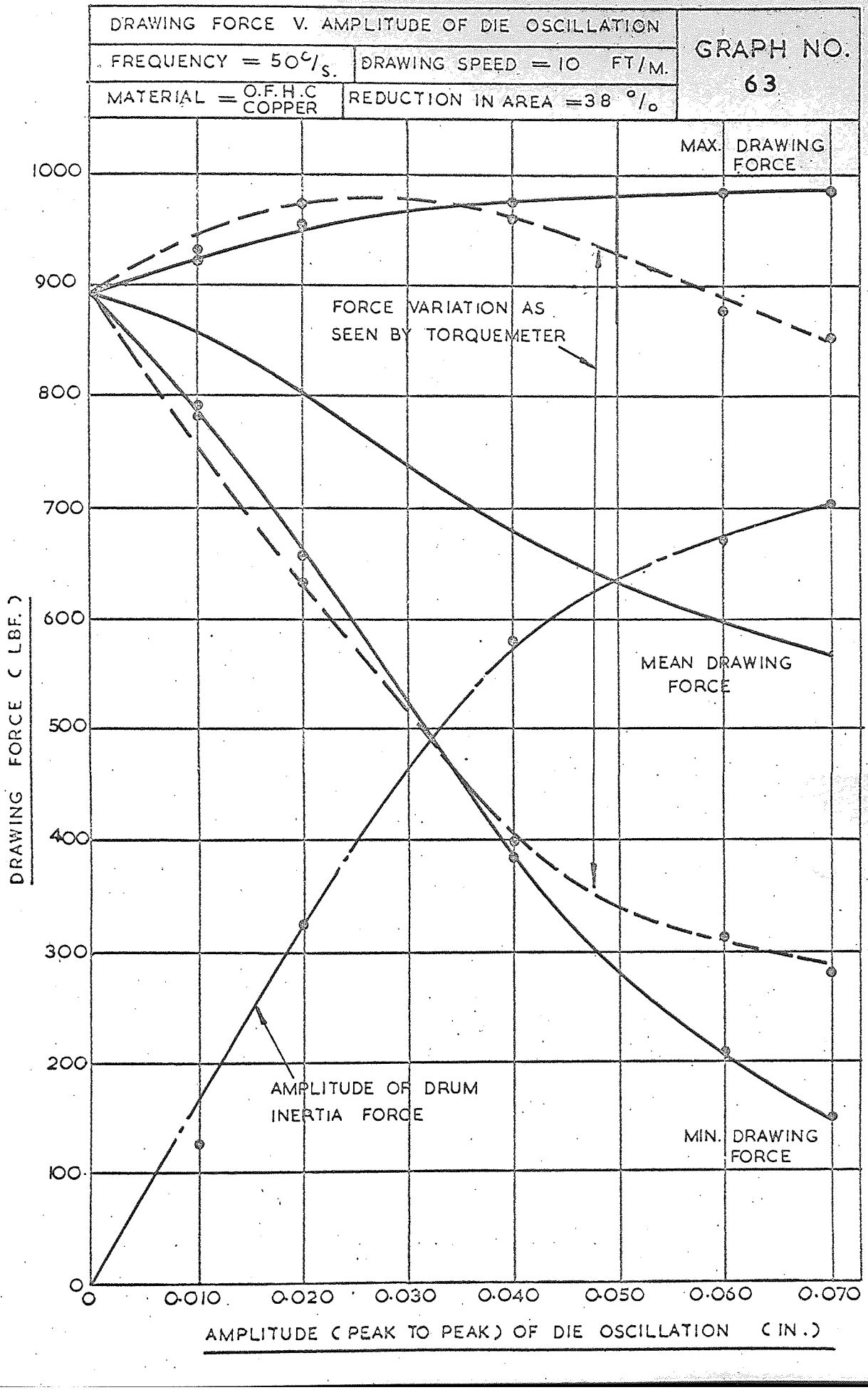
DRAWING FORCE V. AMPLITUDE OF DIE OSCILLATION
FREQUENCY = 50 ~/S.
DRAWING SPEED = 10 FT/M.
MATERIAL = O.F.H.C COPPER
REDUCTION IN AREA = 38 %
GRAPH NO. 63
MAX. DRAWING FORCE
FORCE VARIATION AS SEEN BY TORQUEMETER
MEAN DRAWING FORCE
AMPLITUDE OF DRUM INERTIA FORCE
MIN. DRAWING FORCE
DRAWING FORCE (LBF.)
1000
900
800
700
600
500
400
300
200
100
0
0
0·010
0·020
0·030
0·040
0·050
0·060
0·070
AMPLITUDE (PEAK TO PEAK) OF DIE OSCILLATION (IN.)

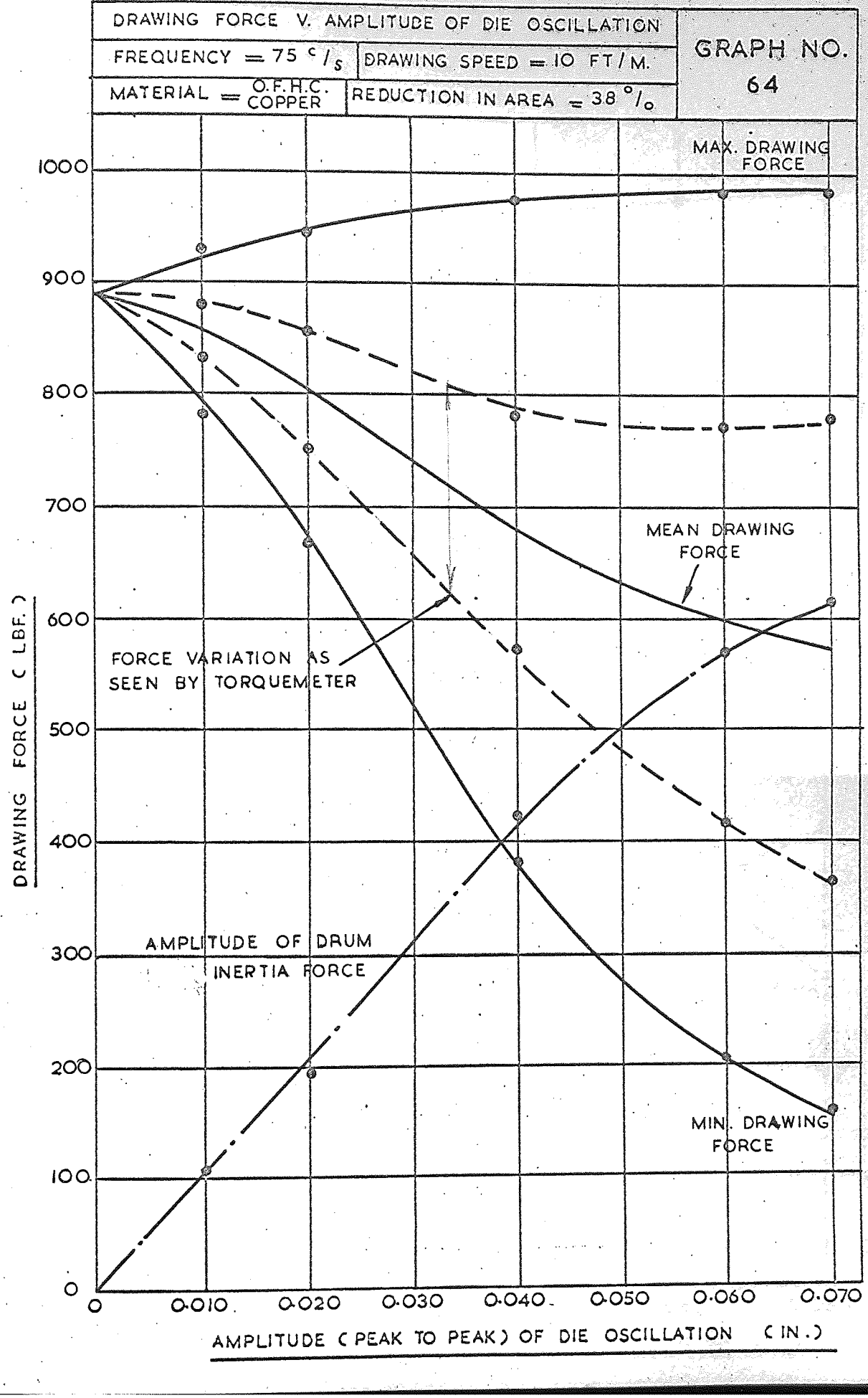
DRAWING FORCE V. AMPLITUDE OF DIE OSCILLATION
FREQUENCY = 75 c/s
DRAWING SPEED = 10 FT/M.
MATERIAL = O.F.H.C. COPPER
REDUCTION IN AREA = 38 %
GRAPH NO. 64
MAX. DRAWING FORCE
MEAN DRAWING FORCE
FORCE VARIATION AS SEEN BY TORQUEMETER
AMPLITUDE OF DRUM INERTIA FORCE
MIN. DRAWING FORCE
DRAWING FORCE (LBF.)
1000
900
800
700
600
500
400
300
200
100
0
0
0.010
0.020
0.030
0.040
0.050
0.060
0.070
AMPLITUDE (PEAK TO PEAK) OF DIE OSCILLATION (IN.)

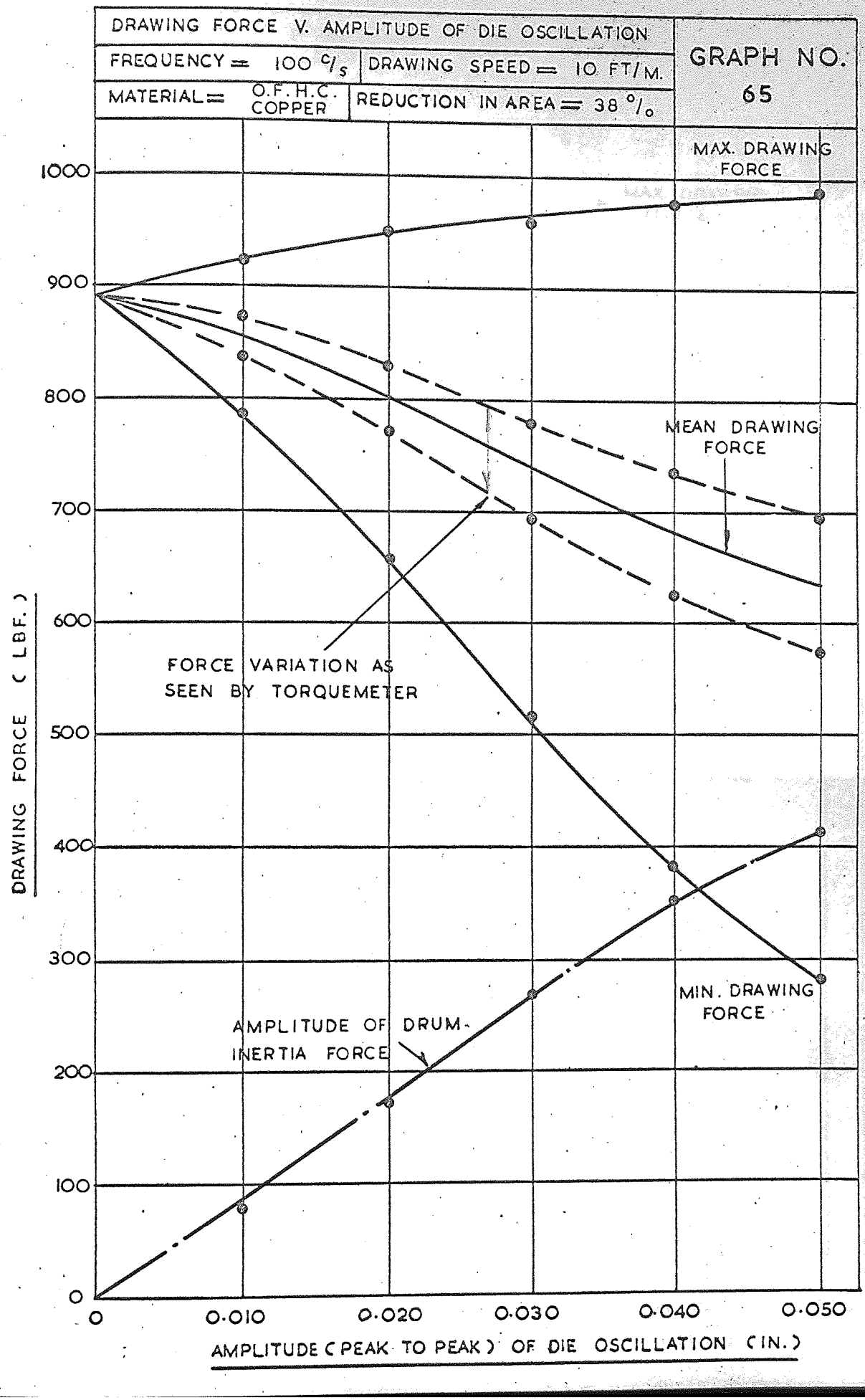
DRAWING FORCE V. AMPLITUDE OF DIE OSCILLATION
FREQUENCY = 100 c/s
DRAWING SPEED = 10 FT/M.
MATERIAL = O.F.H.C. COPPER
REDUCTION IN AREA = 38 %
GRAPH NO. 65
MAX. DRAWING FORCE
MEAN DRAWING FORCE
FORCE VARIATION AS SEEN BY TORQUEMETER
MIN. DRAWING FORCE
AMPLITUDE OF DRUM-INERTIA FORCE
DRAWING FORCE (LBF.)
1000
900
800
700
600
500
400
300
200
100
0
0
0.010
0.020
0.030
0.040
0.050
AMPLITUDE (PEAK TO PEAK) OF DIE OSCILLATION (IN.)

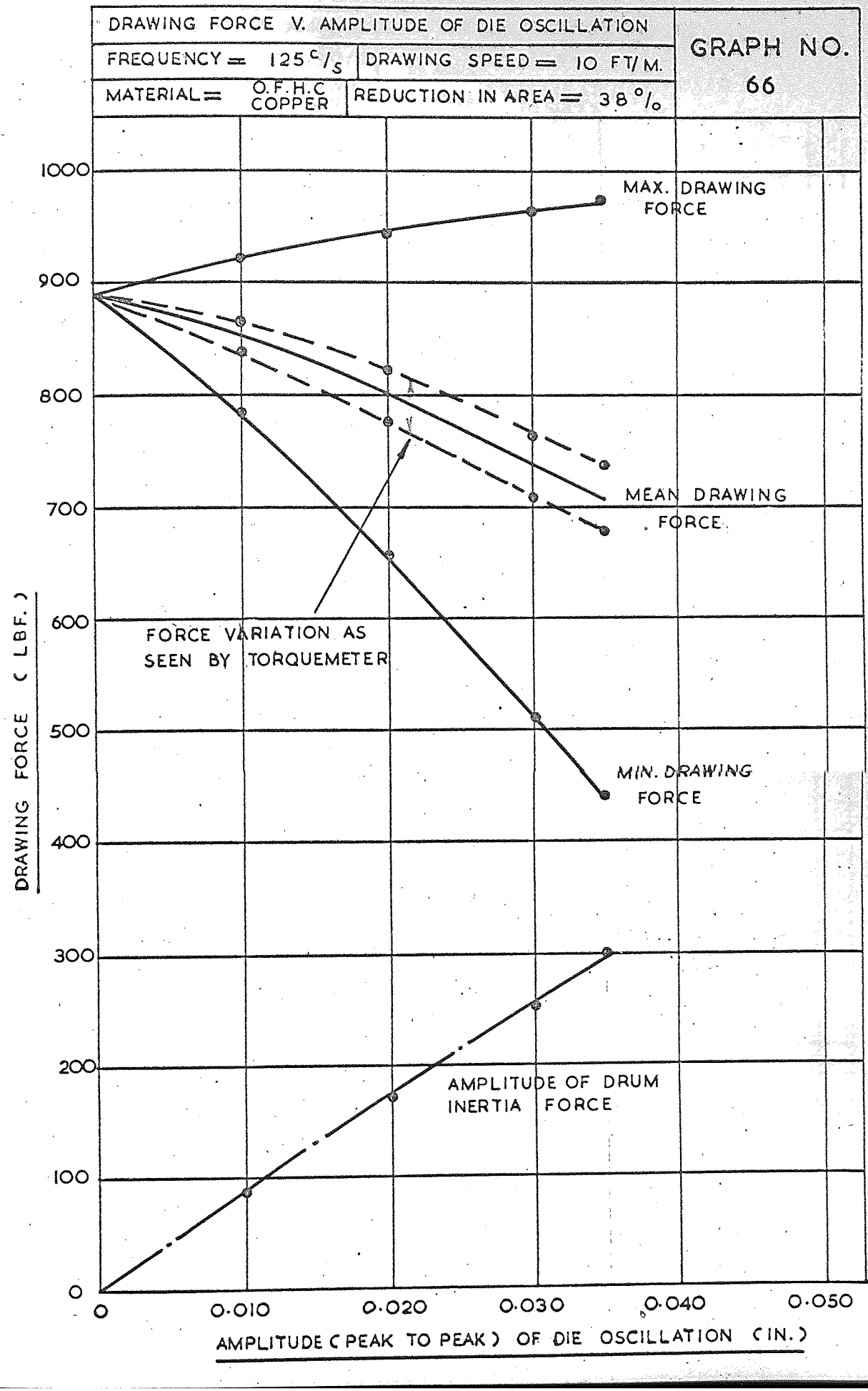
DRAWING FORCE V. AMPLITUDE OF DIE OSCILLATION
FREQUENCY = 125 c/s
DRAWING SPEED = 10 FT/M.
MATERIAL = O.F.H.C COPPER
REDUCTION IN AREA = 38 %
GRAPH NO. 66
MAX. DRAWING FORCE
MEAN DRAWING FORCE
FORCE VARIATION AS SEEN BY TORQUEMETER
MIN. DRAWING FORCE
AMPLITUDE OF DRUM INERTIA FORCE
DRAWING FORCE (LBF.)
1000
900
800
700
600
500
400
300
200
100
0
0
0·010
0·020
0·030
0·040
0·050
AMPLITUDE (PEAK TO PEAK) OF DIE OSCILLATION (IN.)

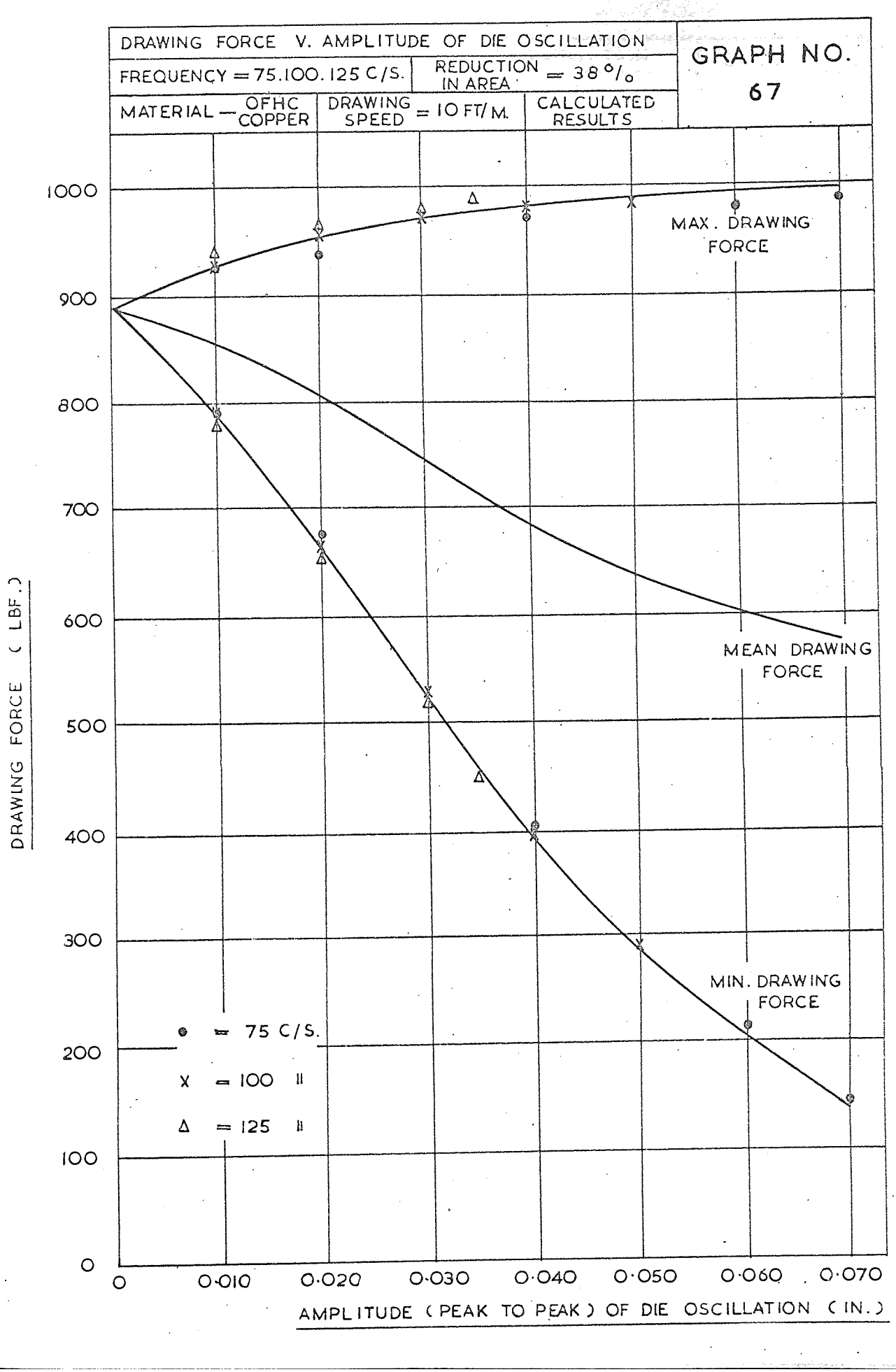
DRAWING FORCE V. AMPLITUDE OF DIE OSCILLATION
FREQUENCY = 75.100.125 C/S.
REDUCTION IN AREA = 38 %
MATERIAL — OFHC COPPER
DRAWING SPEED = 10 FT/M.
CALCULATED RESULTS
GRAPH NO. 67
MAX. DRAWING FORCE
MEAN DRAWING FORCE
MIN. DRAWING FORCE
● = 75 C/S.
X = 100 "
Δ = 125 "
DRAWING FORCE (LBF.)
AMPLITUDE (PEAK TO PEAK) OF DIE OSCILLATION (IN.)
0
100
200
300
400
500
600
700
800
900
1000
0·010
0·020
0·030
0·040
0·050
0·060
0·070

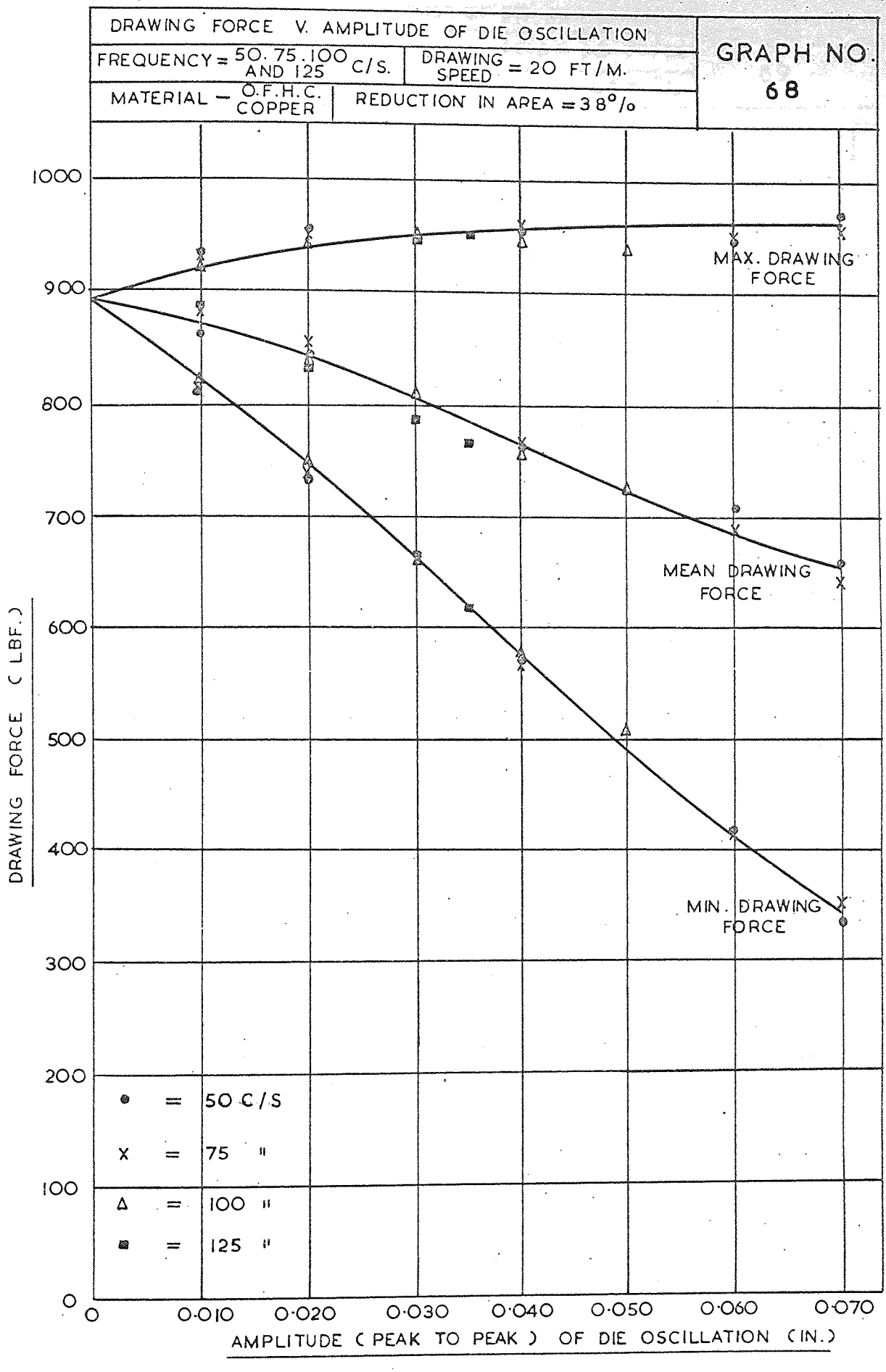
DRAWING FORCE V. AMPLITUDE OF DIE OSCILLATION
FREQUENCY = 50. 75. 100 AND 125 C/S.
DRAWING SPEED = 20 FT/M.
MATERIAL — O.F.H.C. COPPER
REDUCTION IN AREA = 38%
GRAPH NO. 68
MAX. DRAWING FORCE
MEAN DRAWING FORCE
MIN. DRAWING FORCE
DRAWING FORCE (LBF.)
1000
900
800
700
600
500
400
300
200
100
0
0
0·010
0·020
0·030
0·040
0·050
0·060
0·070
AMPLITUDE (PEAK TO PEAK) OF DIE OSCILLATION (IN.)
● = 50 C/S
X = 75 "
Δ = 100 "
■ = 125 "

DRAWING FORCE V. AMPLITUDE OF DIE OSCILLATION

FREQUENCY = 25 $^{c}/_{s.}$ | DRAWING SPEED = 20 FT/M.

MATERIAL = O.F.H.C COPPER | REDUCTION IN AREA = 38 %

GRAPH NO. 69

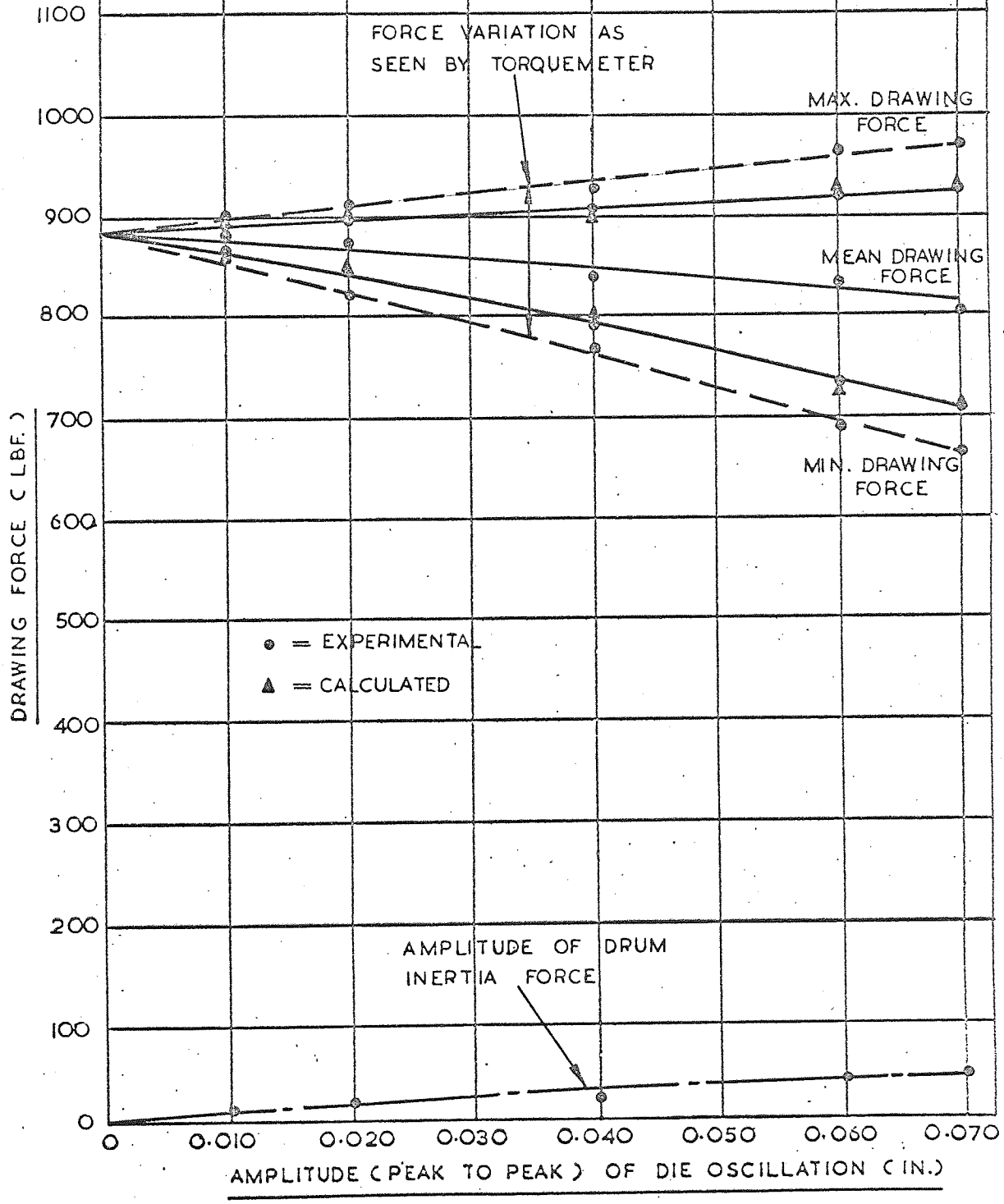

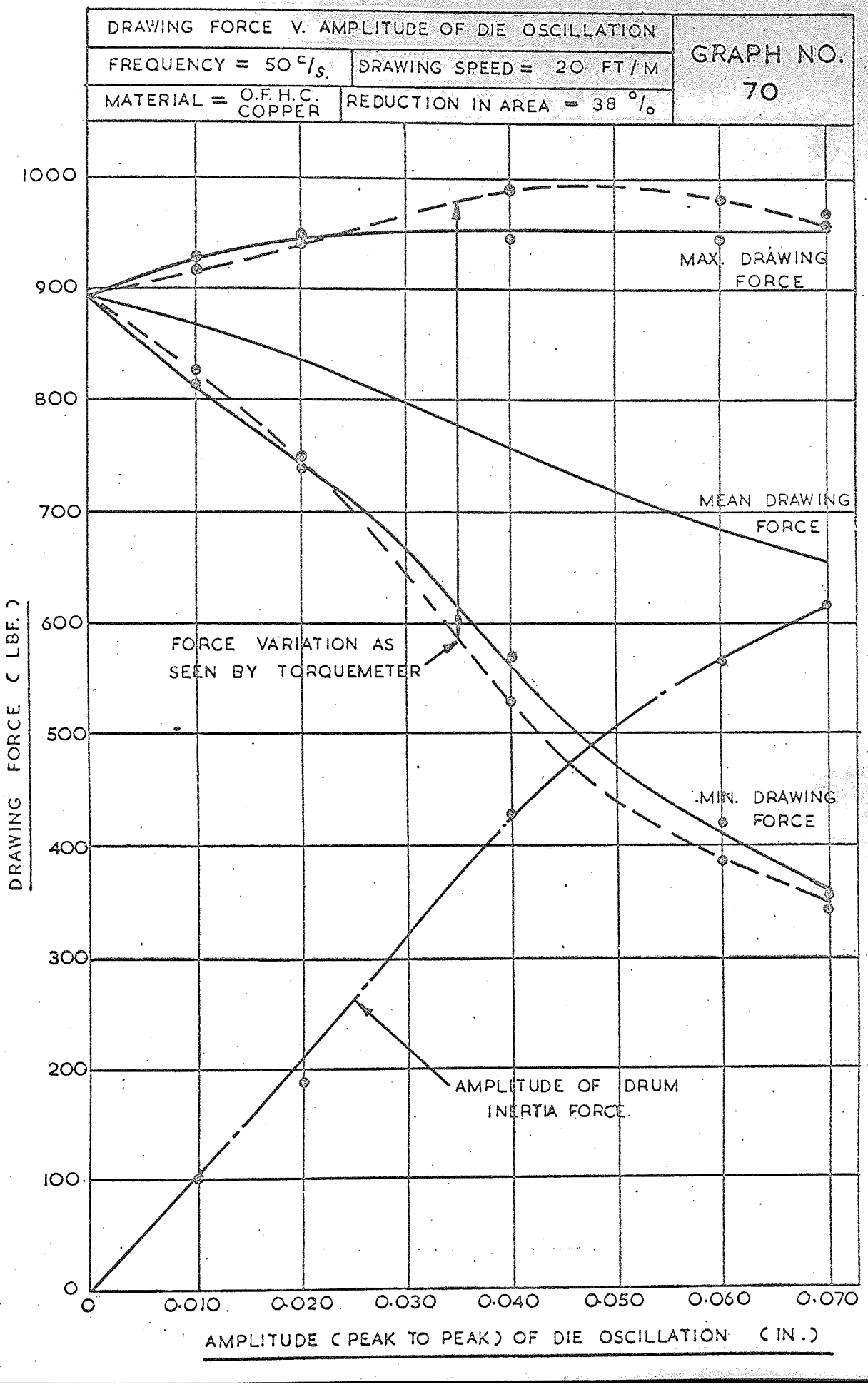
DRAWING FORCE V. AMPLITUDE OF DIE OSCILLATION
FREQUENCY = 50 c/s.
DRAWING SPEED = 20 FT/M
MATERIAL = O.F.H.C. COPPER
REDUCTION IN AREA = 38 %
GRAPH NO. 70
MAX. DRAWING FORCE
MEAN DRAWING FORCE
FORCE VARIATION AS SEEN BY TORQUEMETER
MIN. DRAWING FORCE
AMPLITUDE OF DRUM INERTIA FORCE.
DRAWING FORCE (LBF.)
1000
900
800
700
600
500
400
300
200
100
0
0"
0.010
0.020
0.030
0.040
0.050
0.060
0.070
AMPLITUDE (PEAK TO PEAK) OF DIE OSCILLATION (IN.)

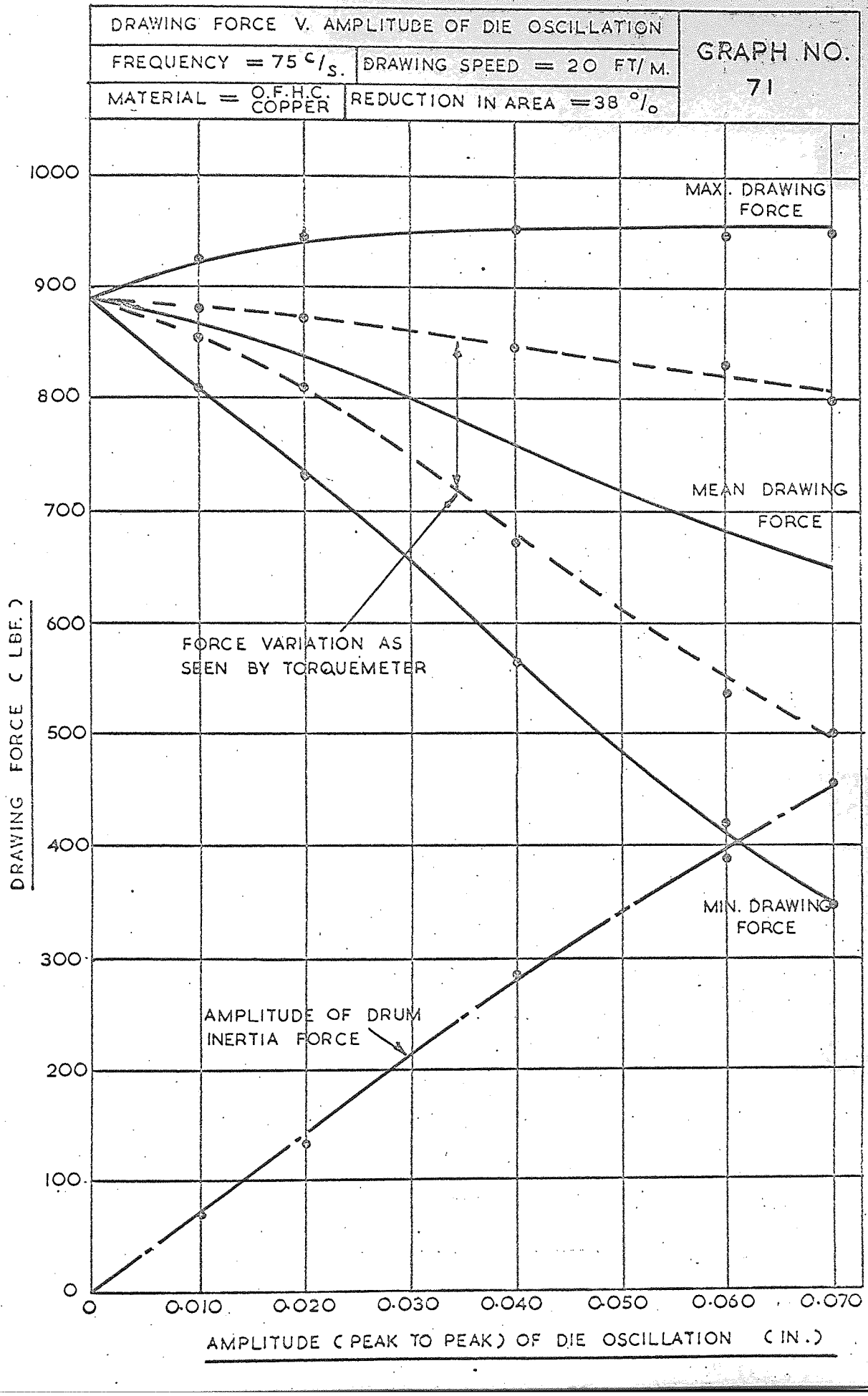
DRAWING FORCE V. AMPLITUDE OF DIE OSCILLATION
FREQUENCY = 75 C/S.
DRAWING SPEED = 20 FT/M.
MATERIAL = O.F.H.C. COPPER
REDUCTION IN AREA = 38 %
GRAPH NO. 71
MAX. DRAWING FORCE
MEAN DRAWING FORCE
FORCE VARIATION AS SEEN BY TORQUEMETER
MIN. DRAWING FORCE
AMPLITUDE OF DRUM INERTIA FORCE
DRAWING FORCE (LBF.)
1000
900
800
700
600
500
400
300
200
100
0
0
0·010
0·020
0·030
0·040
0·050
0·060
0·070
AMPLITUDE (PEAK TO PEAK) OF DIE OSCILLATION (IN.)

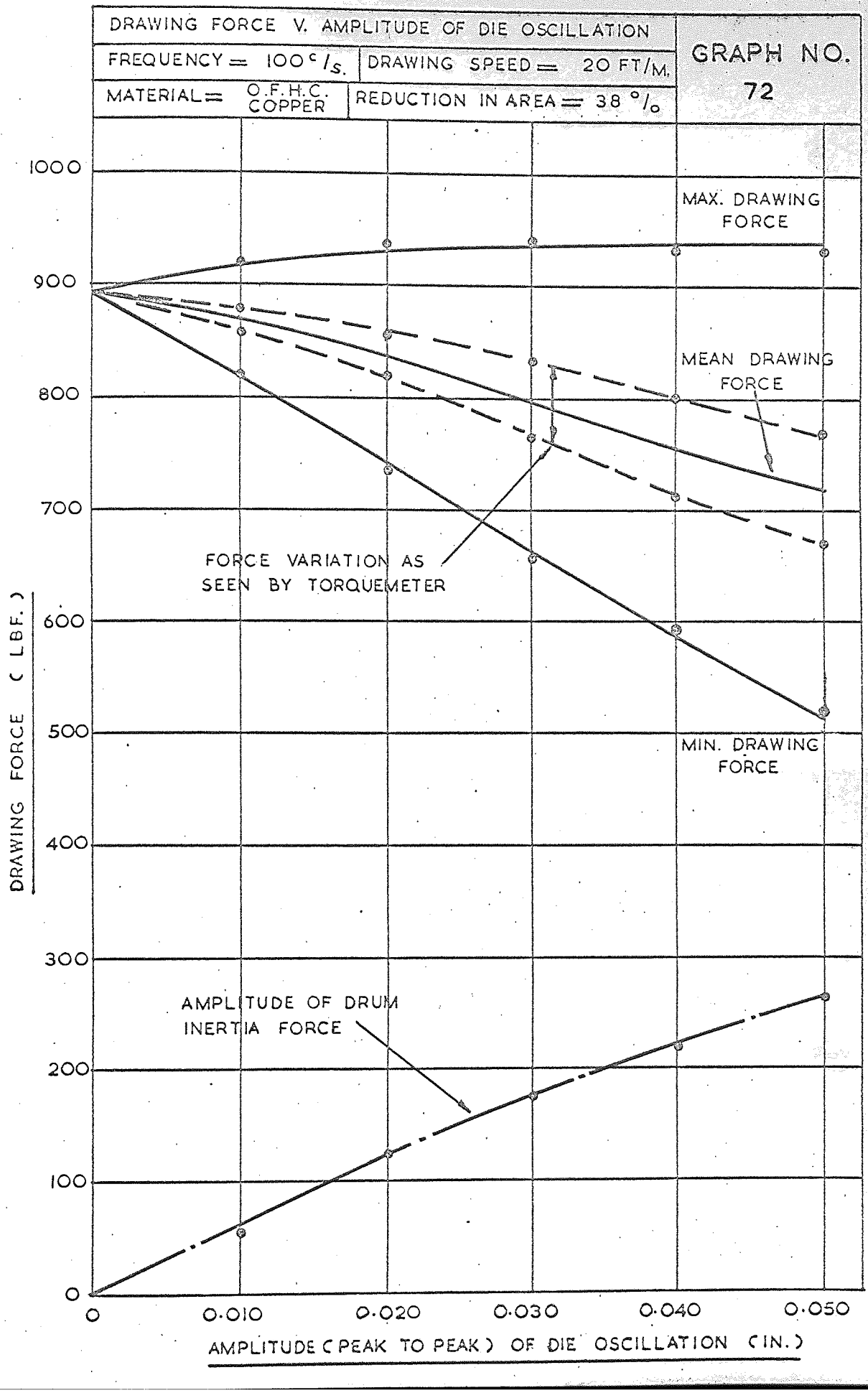
DRAWING FORCE V. AMPLITUDE OF DIE OSCILLATION
FREQUENCY = 100 c/s.
DRAWING SPEED = 20 FT/M.
MATERIAL = O.F.H.C. COPPER
REDUCTION IN AREA = 38 %
GRAPH NO. 72
MAX. DRAWING FORCE
MEAN DRAWING FORCE
FORCE VARIATION AS SEEN BY TORQUEMETER
MIN. DRAWING FORCE
AMPLITUDE OF DRUM INERTIA FORCE
DRAWING FORCE (LBF.)
1000
900
800
700
600
500
400
300
200
100
0
0
0.010
0.020
0.030
0.040
0.050
AMPLITUDE (PEAK TO PEAK) OF DIE OSCILLATION (IN.)

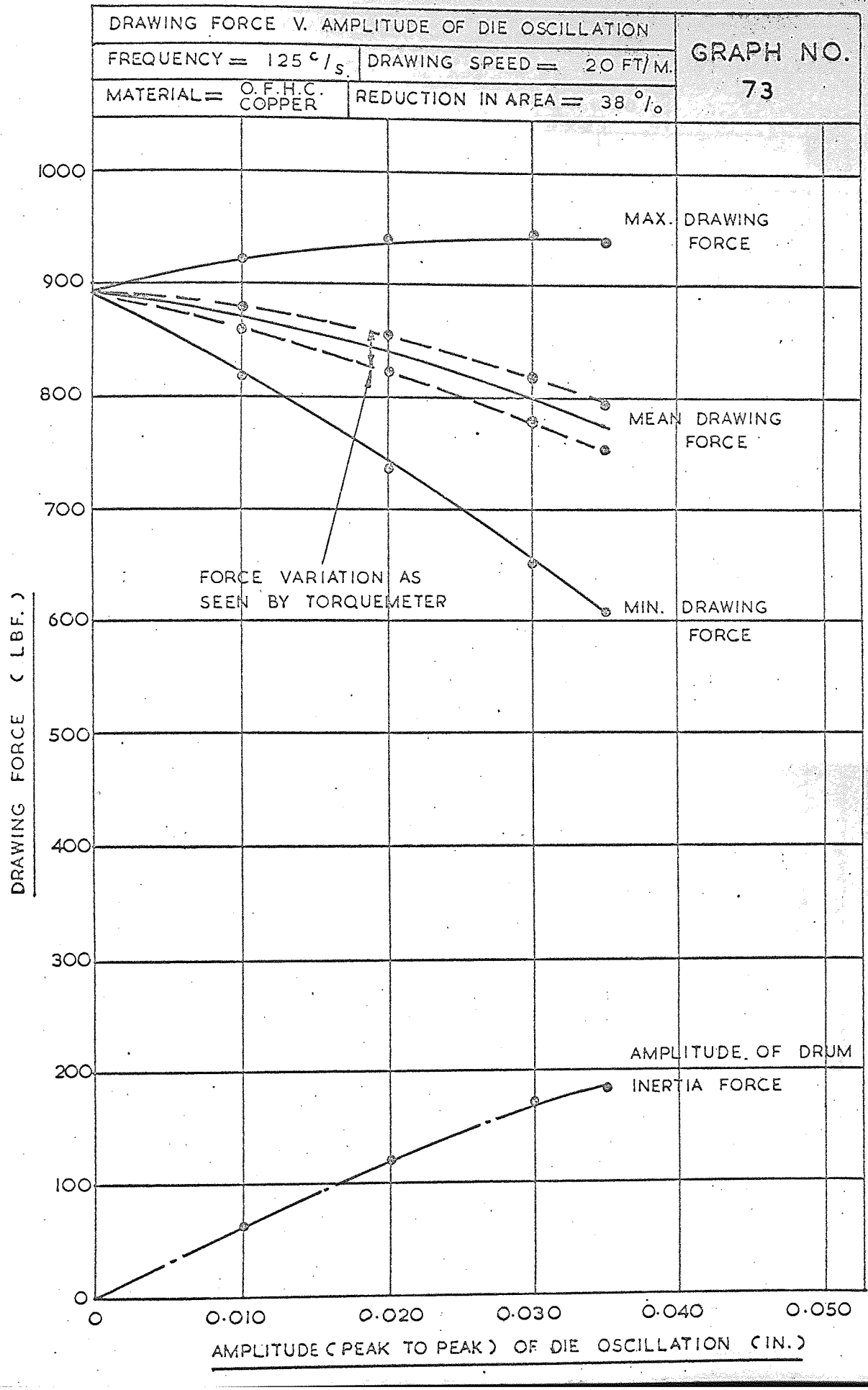
DRAWING FORCE V. AMPLITUDE OF DIE OSCILLATION
FREQUENCY = 125 c/s
DRAWING SPEED = 20 FT/M.
MATERIAL = O.F.H.C. COPPER
REDUCTION IN AREA = 38 %
GRAPH NO. 73
MAX. DRAWING FORCE
MEAN DRAWING FORCE
MIN. DRAWING FORCE
FORCE VARIATION AS SEEN BY TORQUEMETER
AMPLITUDE OF DRUM INERTIA FORCE
DRAWING FORCE (LBF.)
1000
900
800
700
600
500
400
300
200
100
0
0
0.010
0.020
0.030
0.040
0.050
AMPLITUDE (PEAK TO PEAK) OF DIE OSCILLATION (IN.)

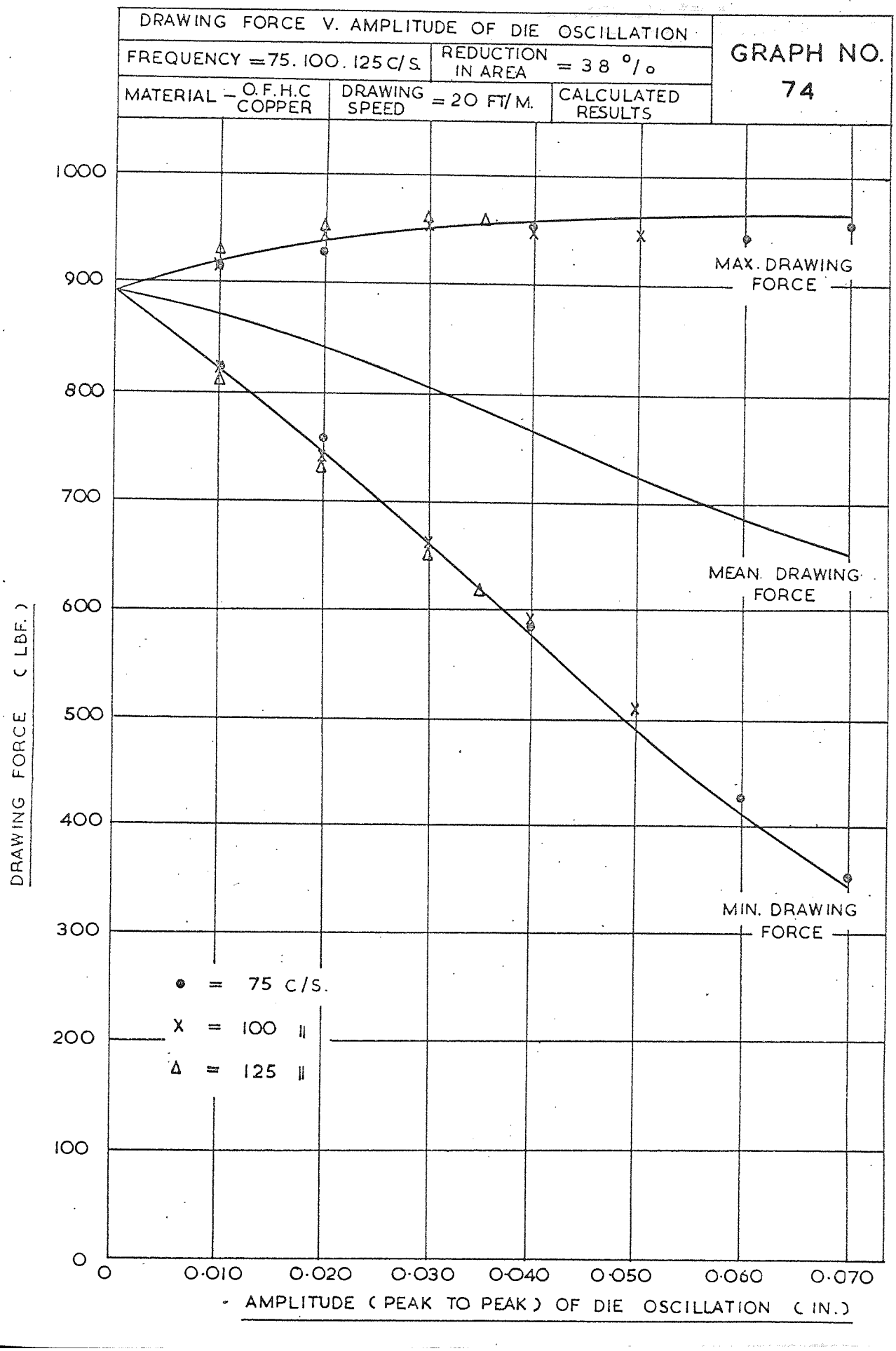
DRAWING FORCE V. AMPLITUDE OF DIE OSCILLATION
FREQUENCY = 75. 100. 125 C/S.
REDUCTION IN AREA = 38 %
MATERIAL – O.F.H.C COPPER
DRAWING SPEED = 20 FT/M.
CALCULATED RESULTS
GRAPH NO. 74
MAX. DRAWING FORCE
MEAN. DRAWING FORCE
MIN. DRAWING FORCE
● = 75 C/S.
X = 100 "
Δ = 125 "
DRAWING FORCE (LBF.)
1000
900
800
700
600
500
400
300
200
100
0
0
0·010
0·020
0·030
0·040
0·050
0·060
0·070
AMPLITUDE (PEAK TO PEAK) OF DIE OSCILLATION (IN.)

DRAWING FORCE V. AMPLITUDE OF DIE OSCILLATION

FREQUENCY = 50 c/s. | DRAWING SPEED = 35 FT/M.

MATERIAL = O.F.H.C. COPPER | REDUCTION IN AREA = 38 %

GRAPH NO. 75

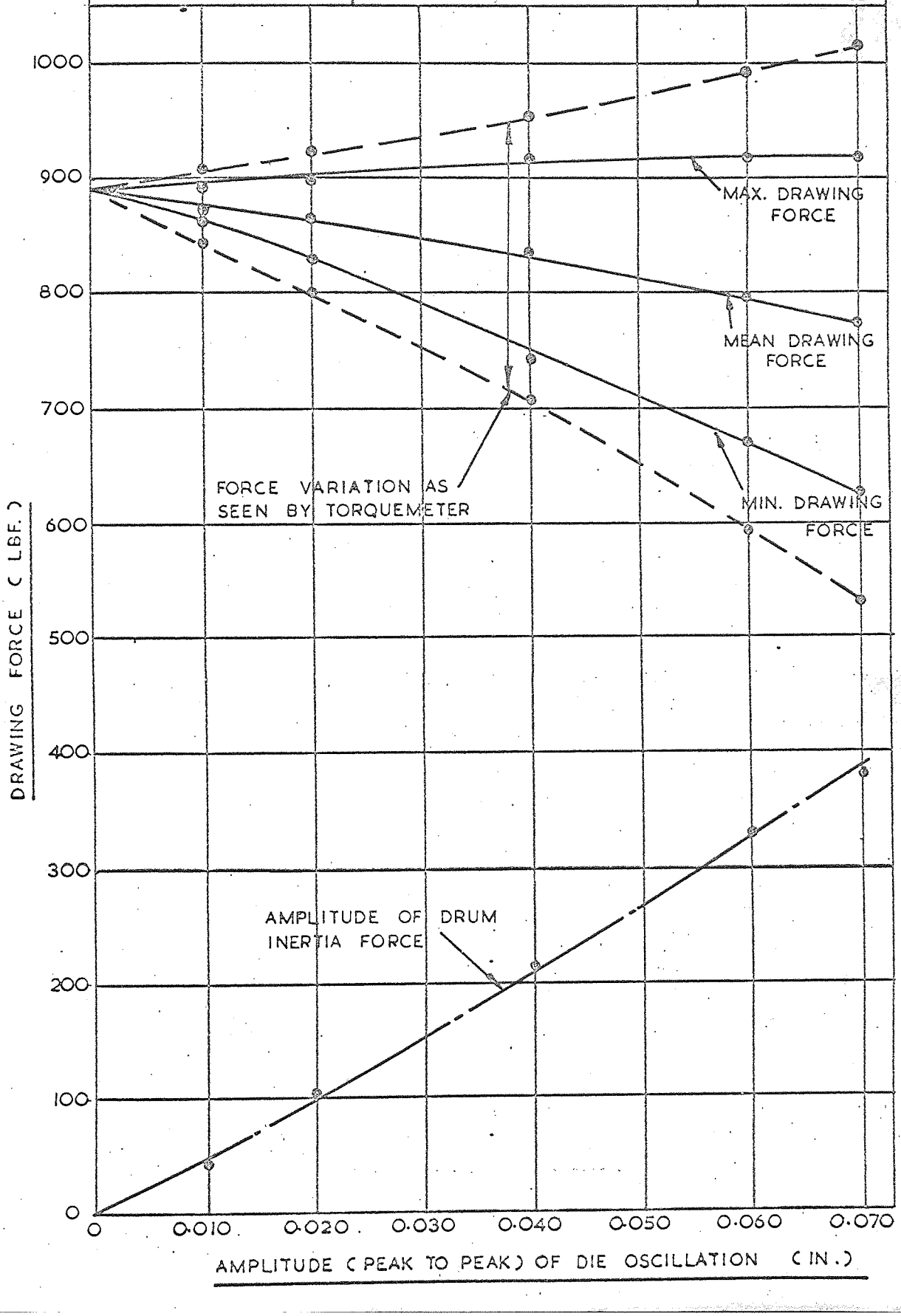

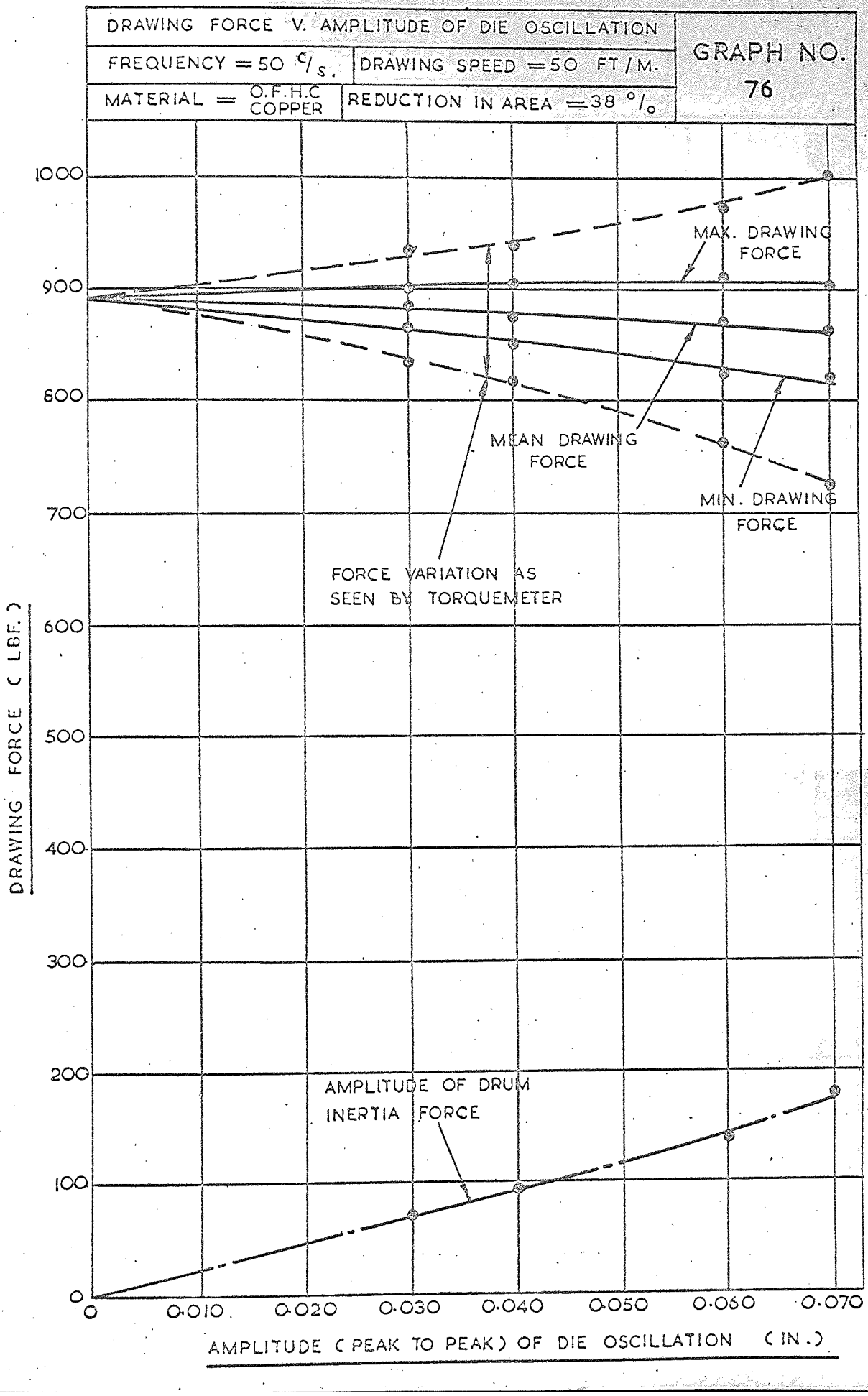
DRAWING FORCE V. AMPLITUDE OF DIE OSCILLATION
FREQUENCY = 50 C/S.
DRAWING SPEED = 50 FT/M.
MATERIAL = O.F.H.C COPPER
REDUCTION IN AREA = 38 %
GRAPH NO. 76
MAX. DRAWING FORCE
MEAN DRAWING FORCE
MIN. DRAWING FORCE
FORCE VARIATION AS SEEN BY TORQUEMETER
AMPLITUDE OF DRUM INERTIA FORCE
DRAWING FORCE (LBF.)
1000
900
800
700
600
500
400
300
200
100
0
0
0·010
0·020
0·030
0·040
0·050
0·060
0·070
AMPLITUDE (PEAK TO PEAK) OF DIE OSCILLATION (IN.)

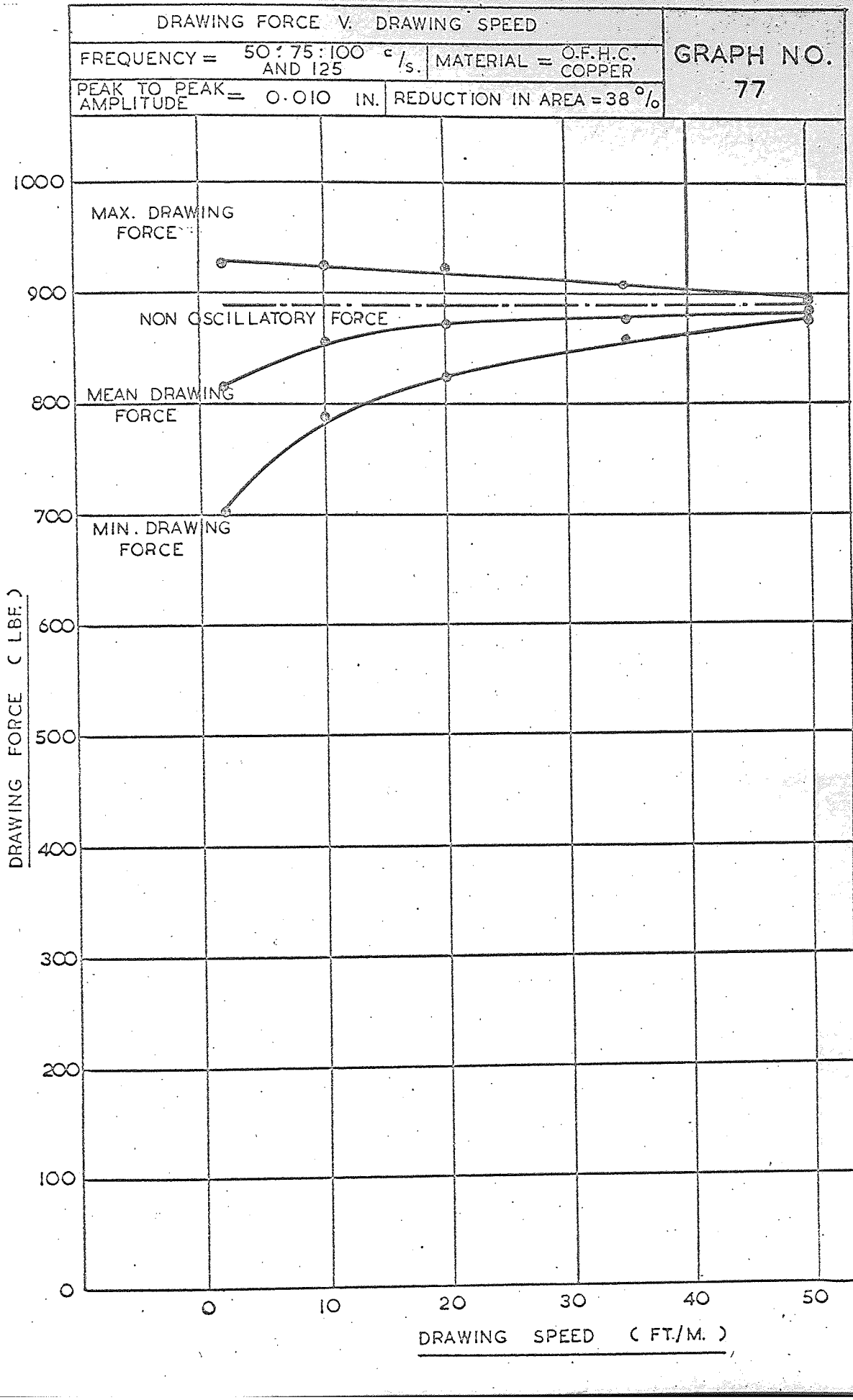
DRAWING FORCE V. DRAWING SPEED
FREQUENCY = 50 : 75 : 100 AND 125 c/s.
MATERIAL = O.F.H.C. COPPER
PEAK TO PEAK AMPLITUDE = 0·010 IN.
REDUCTION IN AREA = 38 %
GRAPH NO. 77
MAX. DRAWING FORCE
NON OSCILLATORY FORCE
MEAN DRAWING FORCE
MIN. DRAWING FORCE
DRAWING FORCE (LBF.)
1000
900
800
700
600
500
400
300
200
100
0
0
10
20
30
40
50
DRAWING SPEED (FT./M.)

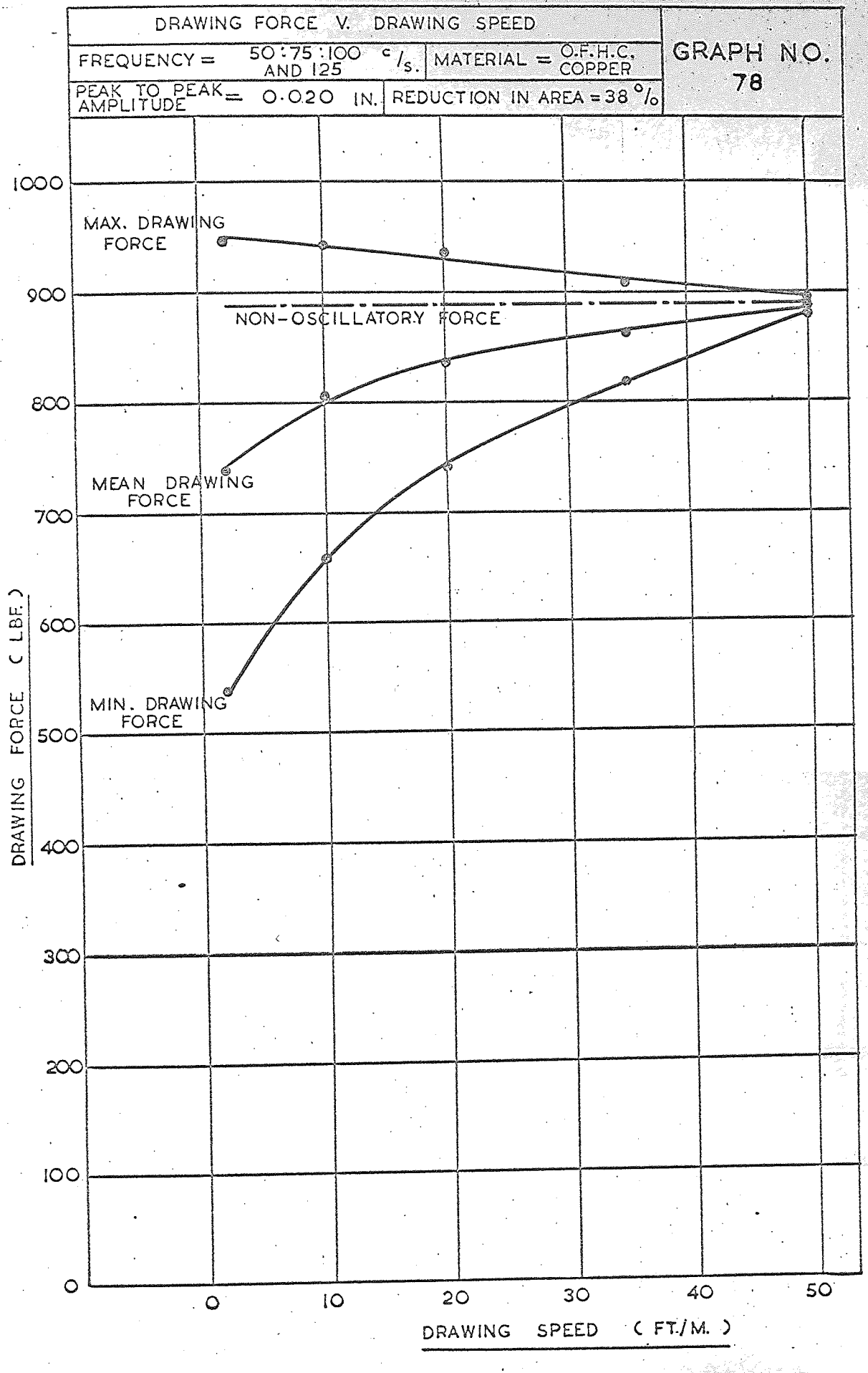
DRAWING FORCE V. DRAWING SPEED
FREQUENCY = 50 : 75 : 100 AND 125 c/s.
MATERIAL = O.F.H.C. COPPER
PEAK TO PEAK AMPLITUDE = 0.020 IN.
REDUCTION IN AREA = 38 %
GRAPH NO. 78
MAX. DRAWING FORCE
NON-OSCILLATORY FORCE
MEAN DRAWING FORCE
MIN. DRAWING FORCE
DRAWING FORCE (LBF.)
1000
900
800
700
600
500
400
300
200
100
0
0
10
20
30
40
50
DRAWING SPEED (FT./M.)

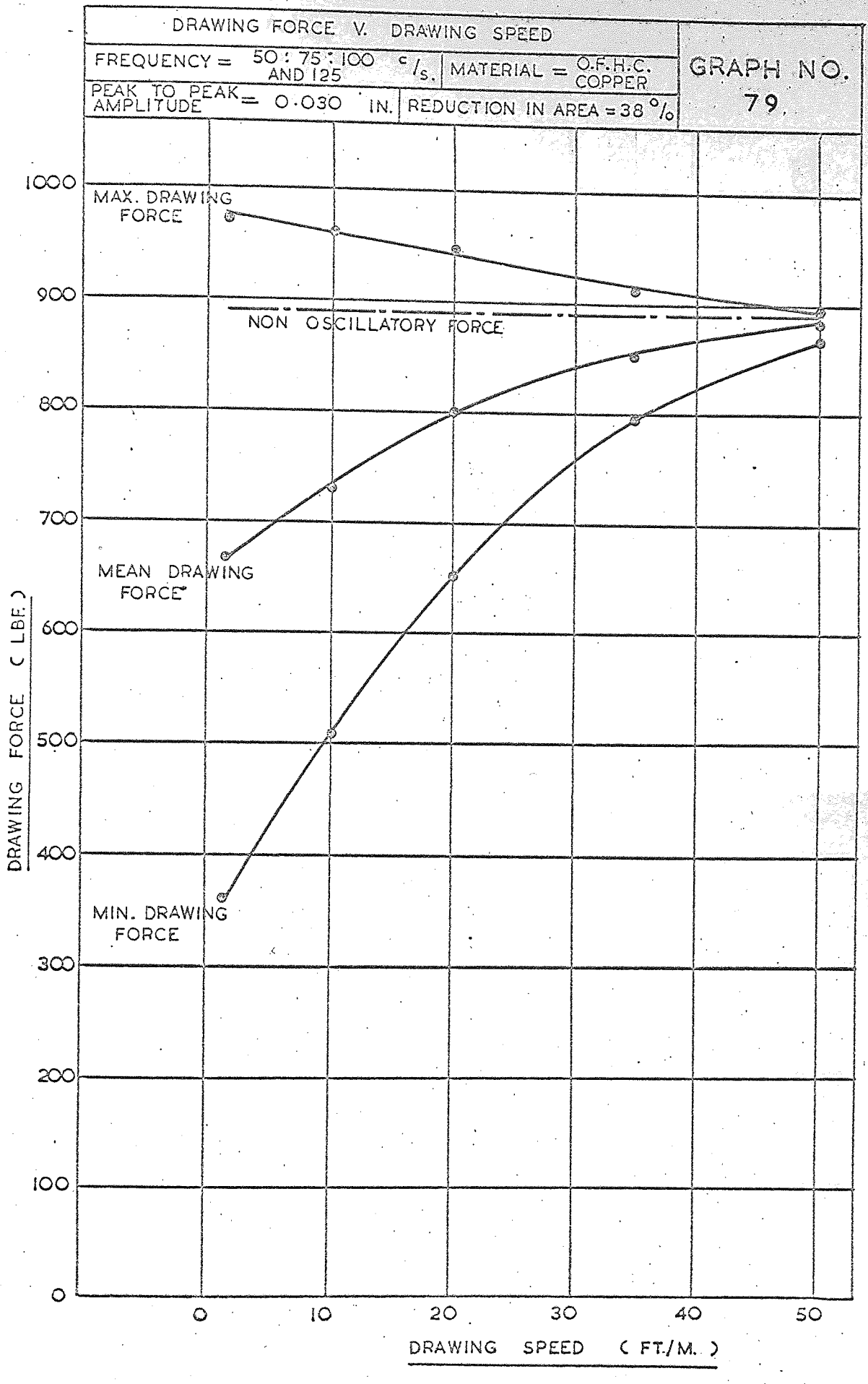
DRAWING FORCE V. DRAWING SPEED
FREQUENCY = 50 : 75 : 100 AND 125 c/s.
MATERIAL = O.F.H.C. COPPER
PEAK TO PEAK AMPLITUDE = 0.030 IN.
REDUCTION IN AREA = 38 %
GRAPH NO. 79.
MAX. DRAWING FORCE
NON OSCILLATORY FORCE
MEAN DRAWING FORCE
MIN. DRAWING FORCE
DRAWING FORCE (LBF.)
1000
900
800
700
600
500
400
300
200
100
0
0
10
20
30
40
50
DRAWING SPEED (FT./M.)

DRAWING FORCE V. DRAWING SPEED

FREQUENCY = 50 : 75 : 100 AND 125 $^{c}/_{s}$.

MATERIAL = O.F.H.C. COPPER

PEAK TO PEAK AMPLITUDE = 0·040 IN.

REDUCTION IN AREA = 38 %

GRAPH NO. 80

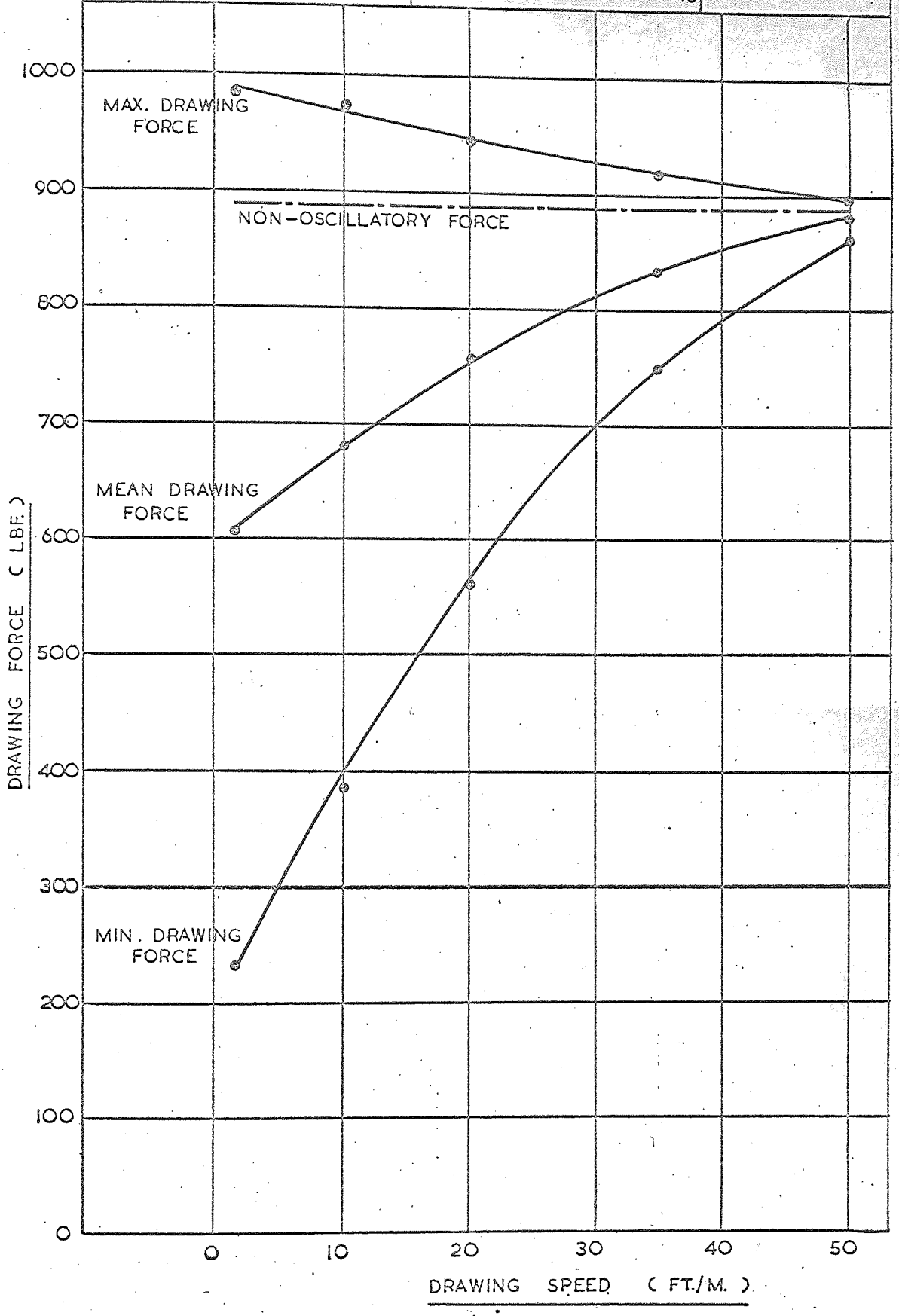

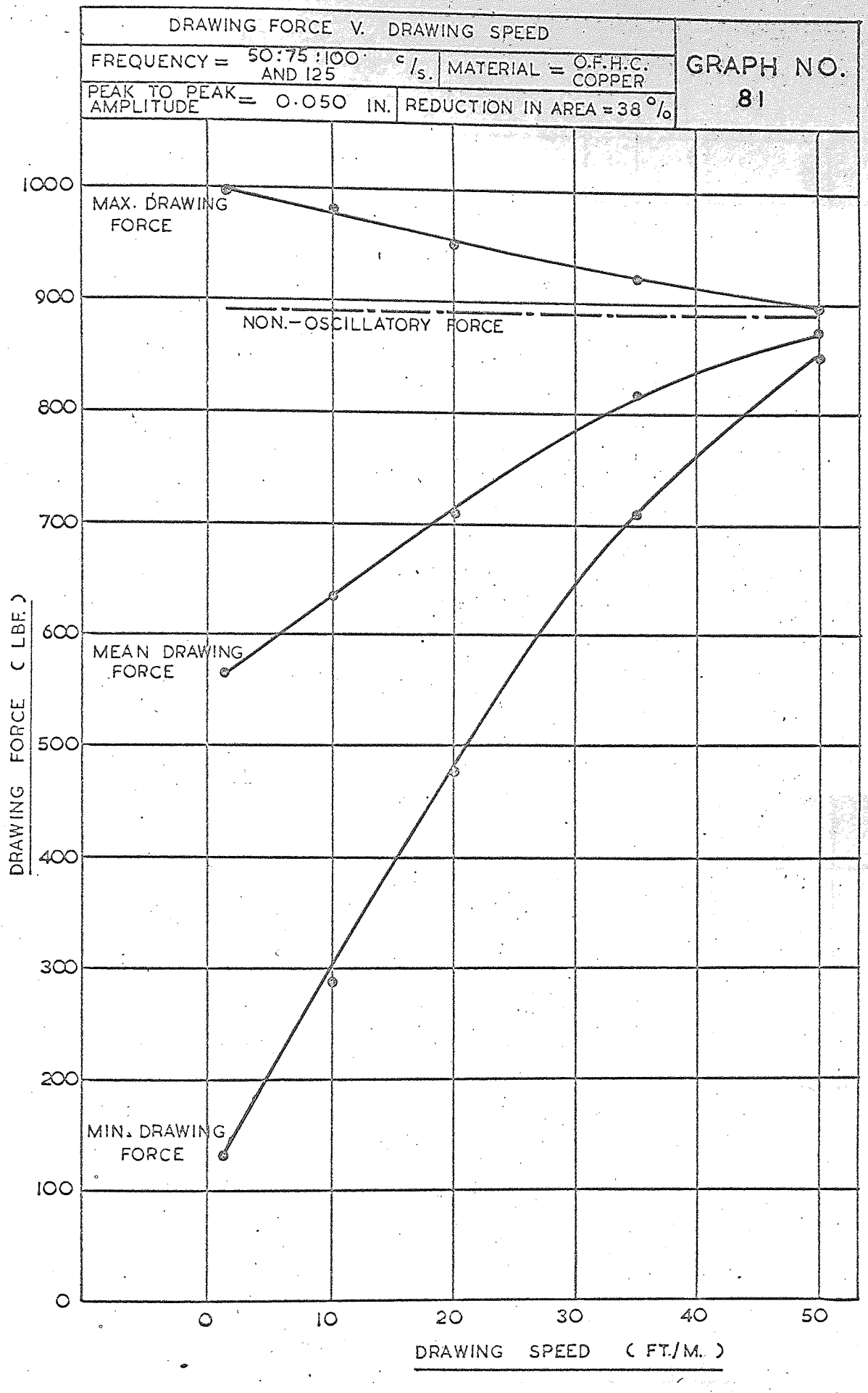
DRAWING FORCE V. DRAWING SPEED
FREQUENCY = 50:75:100 AND 125 c/s.
MATERIAL = O.F.H.C. COPPER
PEAK TO PEAK AMPLITUDE = 0.050 IN.
REDUCTION IN AREA = 38 %
GRAPH NO. 81
MAX. DRAWING FORCE
NON.-OSCILLATORY FORCE
MEAN DRAWING FORCE
MIN. DRAWING FORCE
DRAWING FORCE (LBF.)
1000
900
800
700
600
500
400
300
200
100
0
0
10
20
30
40
50
DRAWING SPEED (FT./M.)

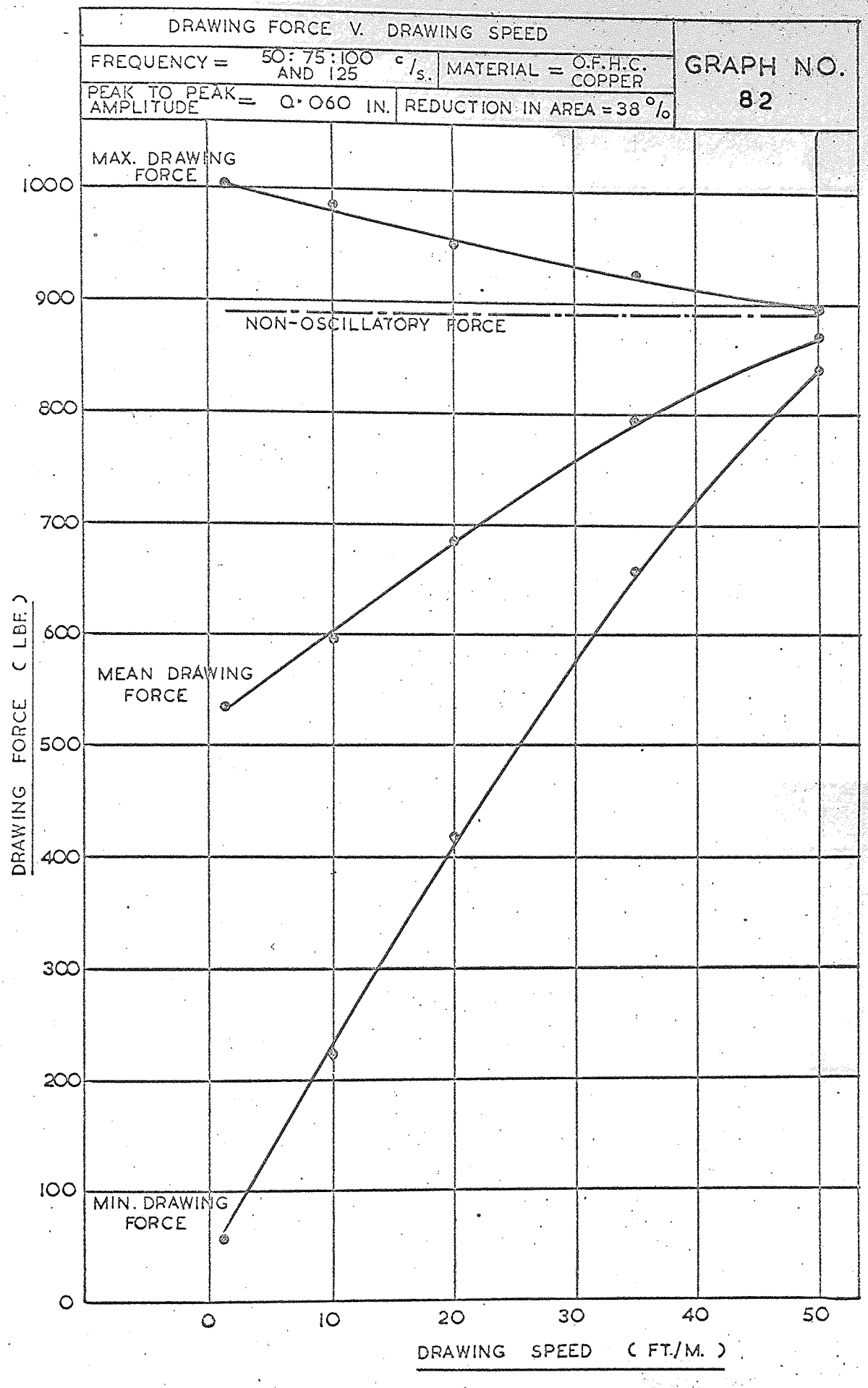
DRAWING FORCE V. DRAWING SPEED
FREQUENCY = 50: 75: 100 AND 125 c/s.
MATERIAL = O.F.H.C. COPPER
PEAK TO PEAK AMPLITUDE = 0·060 IN.
REDUCTION IN AREA = 38 %
GRAPH NO. 82
MAX. DRAWING FORCE
NON-OSCILLATORY FORCE
MEAN DRAWING FORCE
MIN. DRAWING FORCE
DRAWING FORCE (LBF.)
1000
900
800
700
600
500
400
300
200
100
0
0
10
20
30
40
50
DRAWING SPEED (FT./M.)

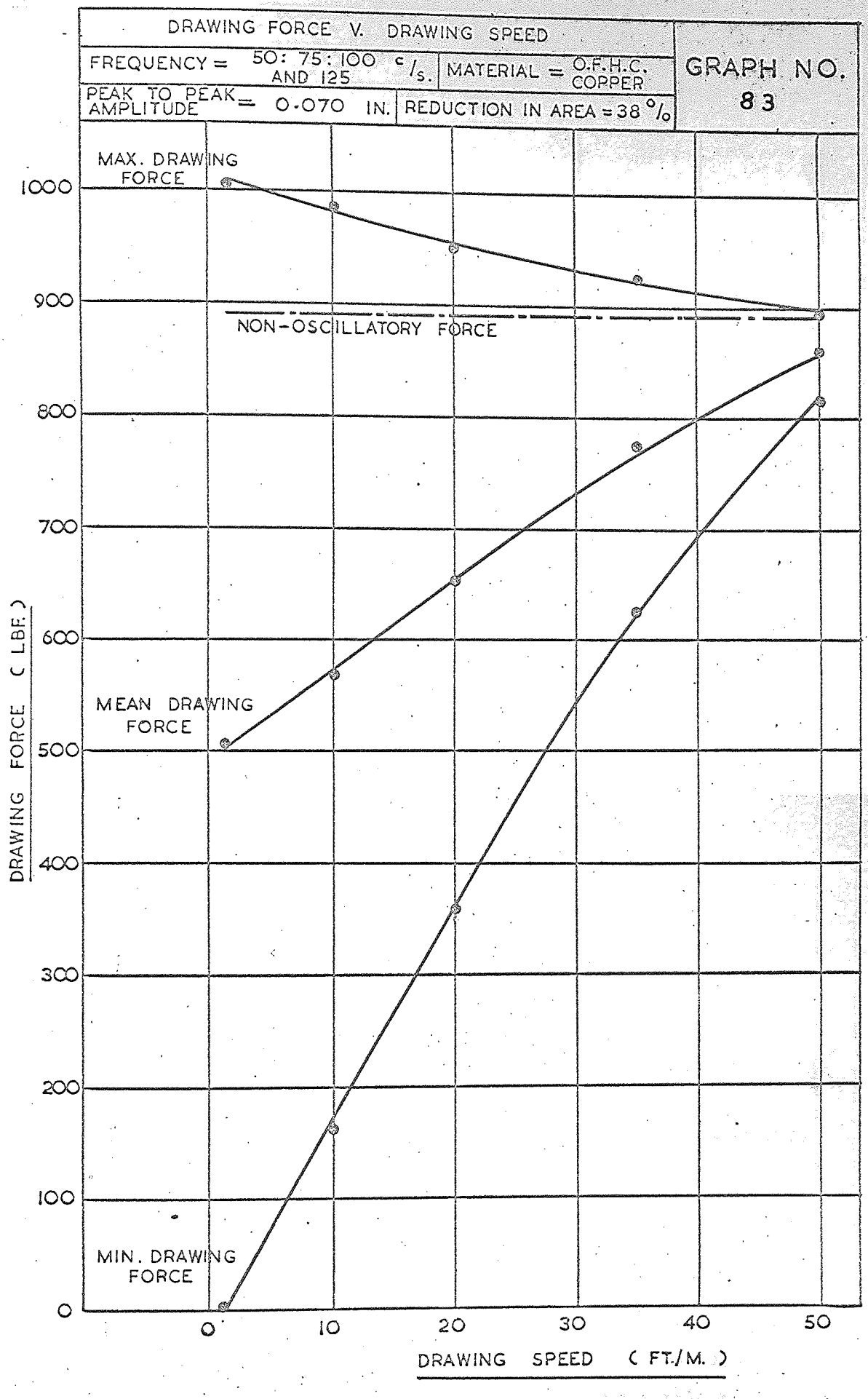
DRAWING FORCE V. DRAWING SPEED
FREQUENCY = 50: 75: 100 AND 125 c/s.
MATERIAL = O.F.H.C. COPPER
PEAK TO PEAK AMPLITUDE = 0·070 IN.
REDUCTION IN AREA = 38 %
GRAPH NO. 83
MAX. DRAWING FORCE
NON-OSCILLATORY FORCE
MEAN DRAWING FORCE
MIN. DRAWING FORCE
DRAWING FORCE (LBF.)
1000
900
800
700
600
500
400
300
200
100
0
0
10
20
30
40
50
DRAWING SPEED (FT./M.)

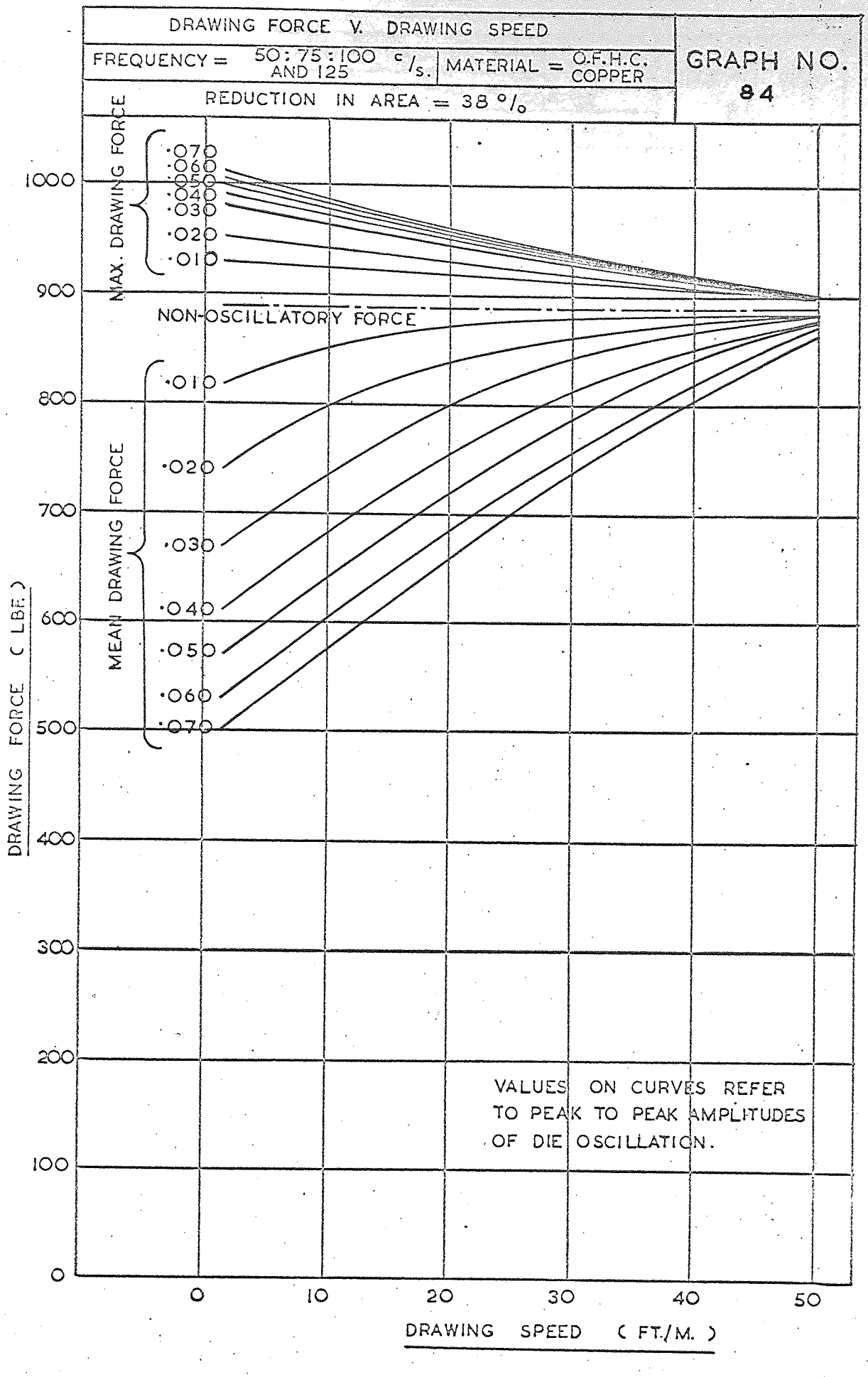
DRAWING FORCE V. DRAWING SPEED
FREQUENCY = 50 : 75 : 100 AND 125 c/s.
MATERIAL = O.F.H.C. COPPER
REDUCTION IN AREA = 38 %
GRAPH NO. 84
MAX. DRAWING FORCE
·070
·060
·050
·040
·030
·020
·010
NON-OSCILLATORY FORCE
MEAN DRAWING FORCE
·010
·020
·030
·040
·050
·060
·070
DRAWING FORCE (LBF.)
1000
900
800
700
600
500
400
300
200
100
0
0
10
20
30
40
50
DRAWING SPEED (FT./M.)
VALUES ON CURVES REFER TO PEAK TO PEAK AMPLITUDES OF DIE OSCILLATION.

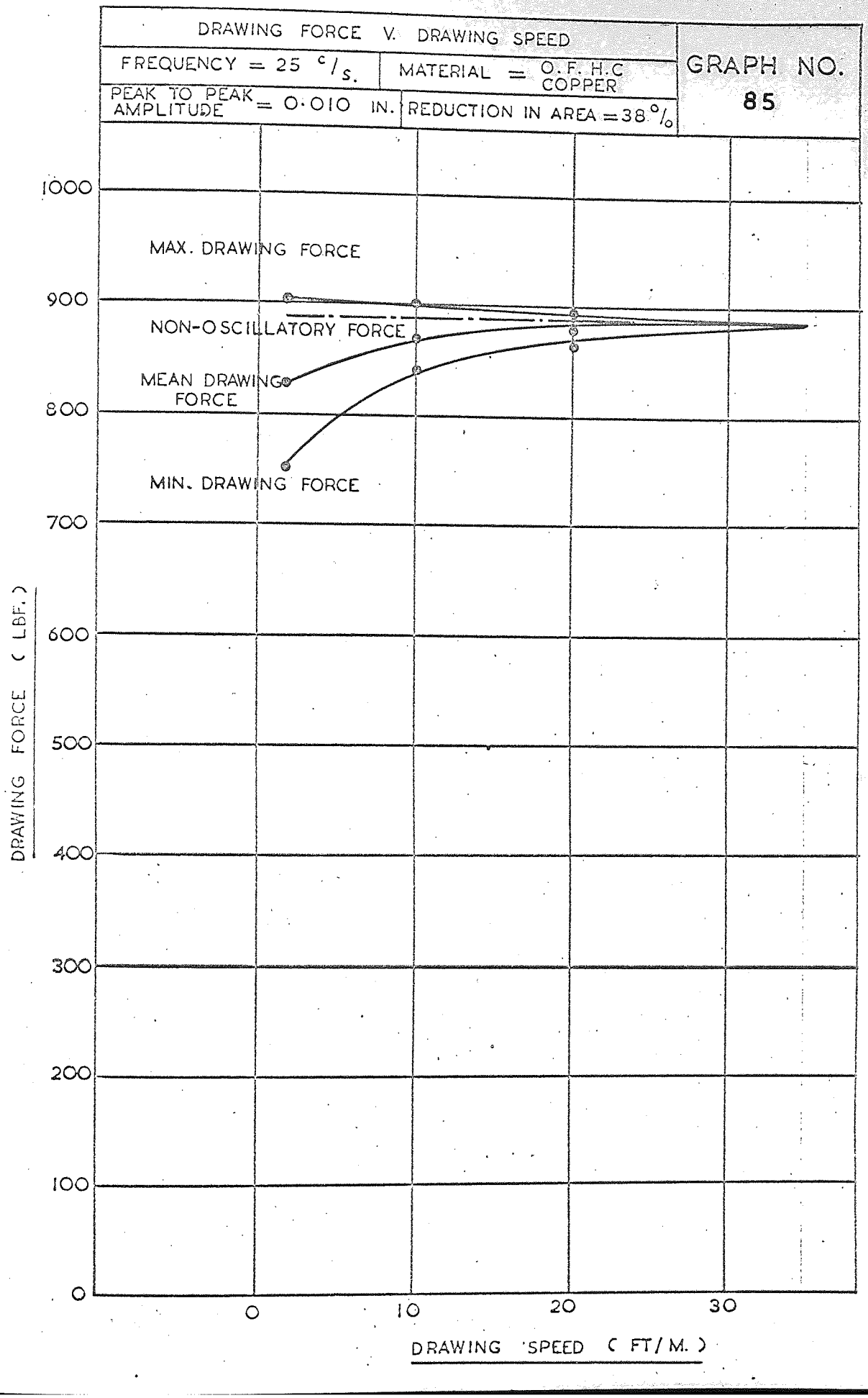
DRAWING FORCE V. DRAWING SPEED
FREQUENCY = 25 c/s.
MATERIAL = O.F. H.C COPPER
PEAK TO PEAK AMPLITUDE = 0·010 IN.
REDUCTION IN AREA = 38 %
GRAPH NO. 85
MAX. DRAWING FORCE
NON-OSCILLATORY FORCE
MEAN DRAWING FORCE
MIN. DRAWING FORCE
1000
900
800
700
600
500
400
300
200
100
0
DRAWING FORCE (LBF.)
0
10
20
30
DRAWING SPEED (FT/M.)

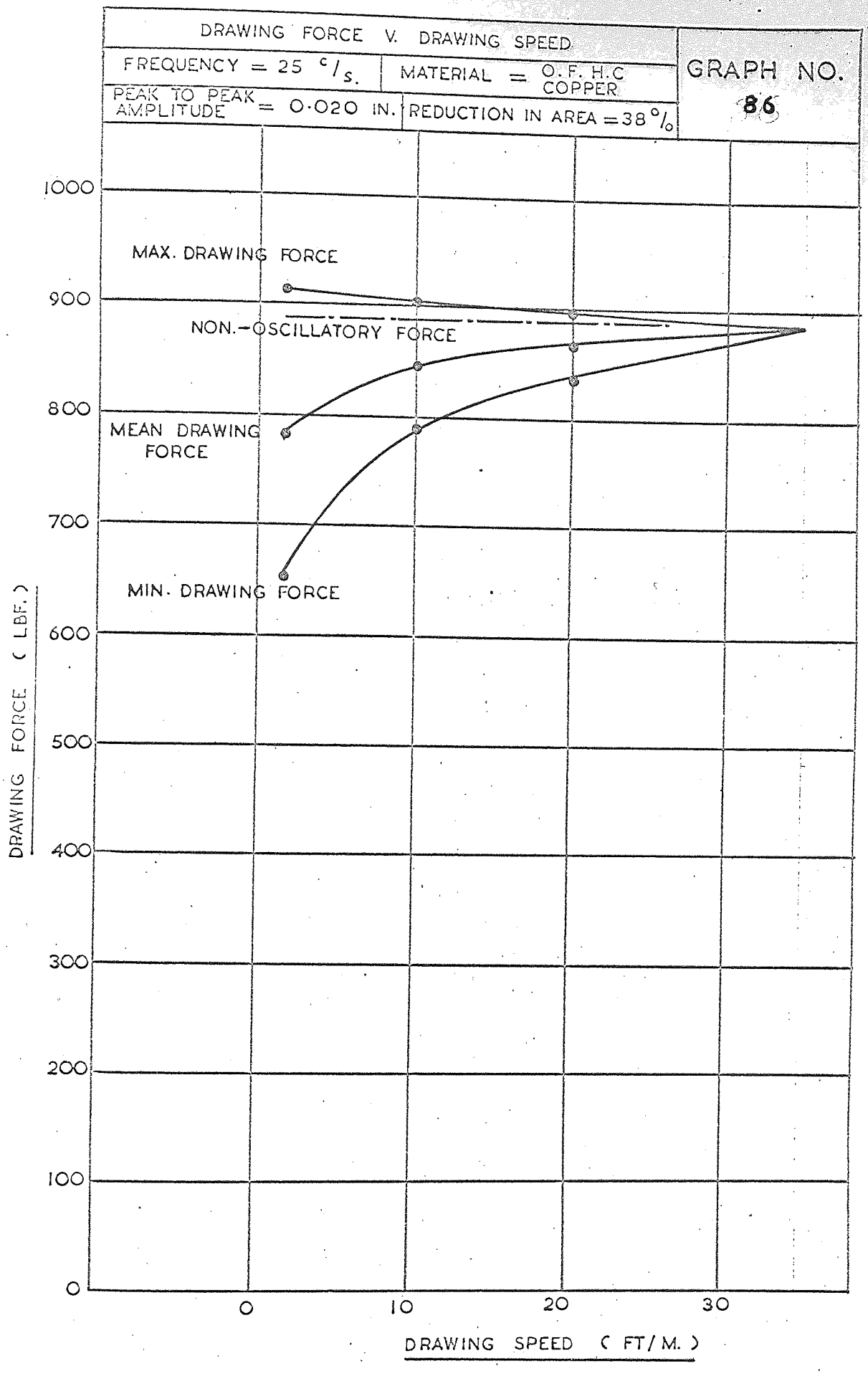
DRAWING FORCE V. DRAWING SPEED
FREQUENCY = 25 c/s.
MATERIAL = O.F.H.C COPPER
PEAK TO PEAK AMPLITUDE = 0·020 IN.
REDUCTION IN AREA = 38 %
GRAPH NO. 86
MAX. DRAWING FORCE
NON.-OSCILLATORY FORCE
MEAN DRAWING FORCE
MIN. DRAWING FORCE
DRAWING FORCE (LBF.)
1000
900
800
700
600
500
400
300
200
100
0
0
10
20
30
DRAWING SPEED (FT/M.)

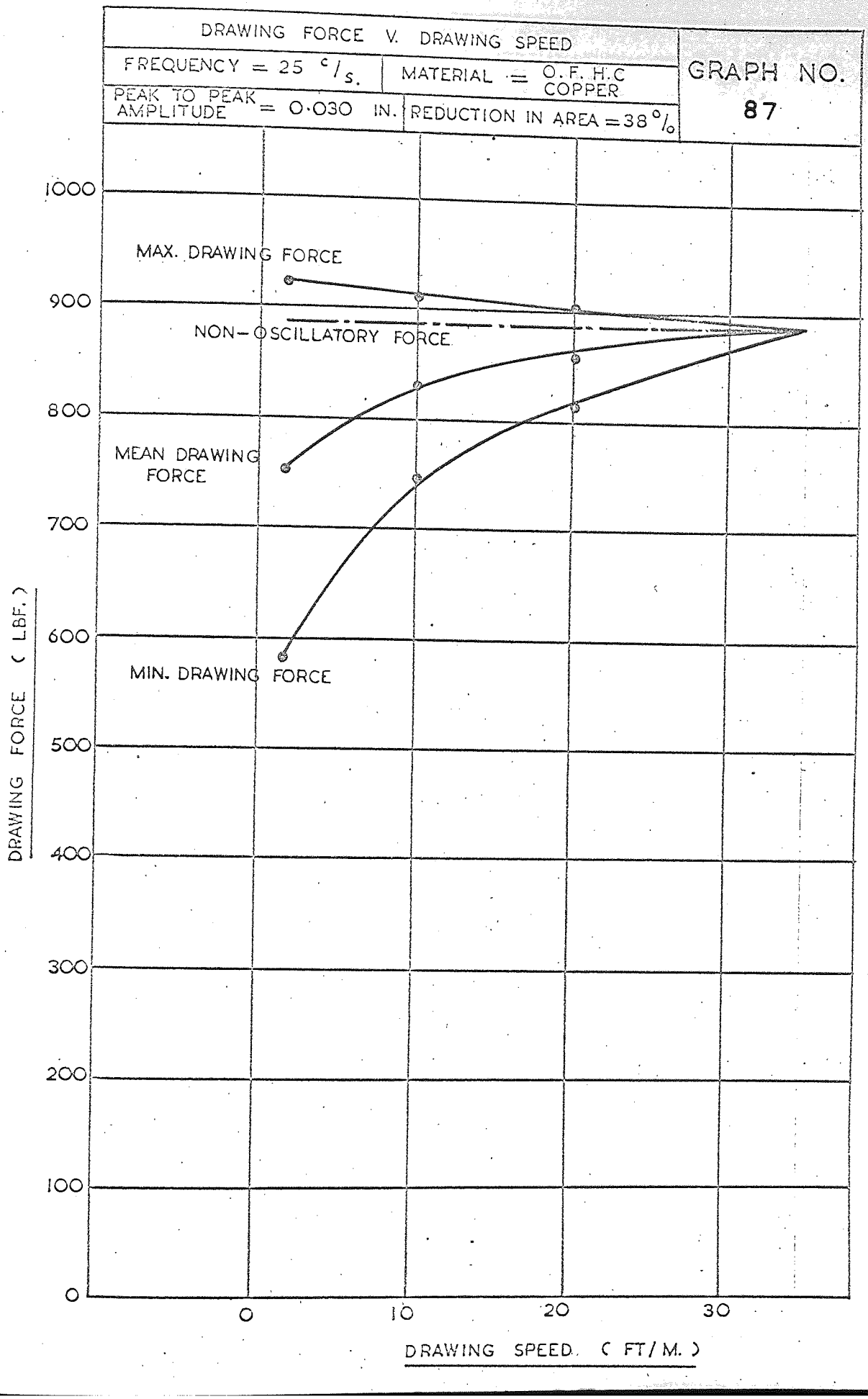
DRAWING FORCE V. DRAWING SPEED
FREQUENCY = 25 c/s.
MATERIAL = O.F. H.C COPPER
PEAK TO PEAK AMPLITUDE = 0·030 IN.
REDUCTION IN AREA = 38 %
GRAPH NO. 87
MAX. DRAWING FORCE
NON-OSCILLATORY FORCE
MEAN DRAWING FORCE
MIN. DRAWING FORCE
DRAWING FORCE (LBF.)
1000
900
800
700
600
500
400
300
200
100
0
0
10
20
30
DRAWING SPEED (FT/M.)

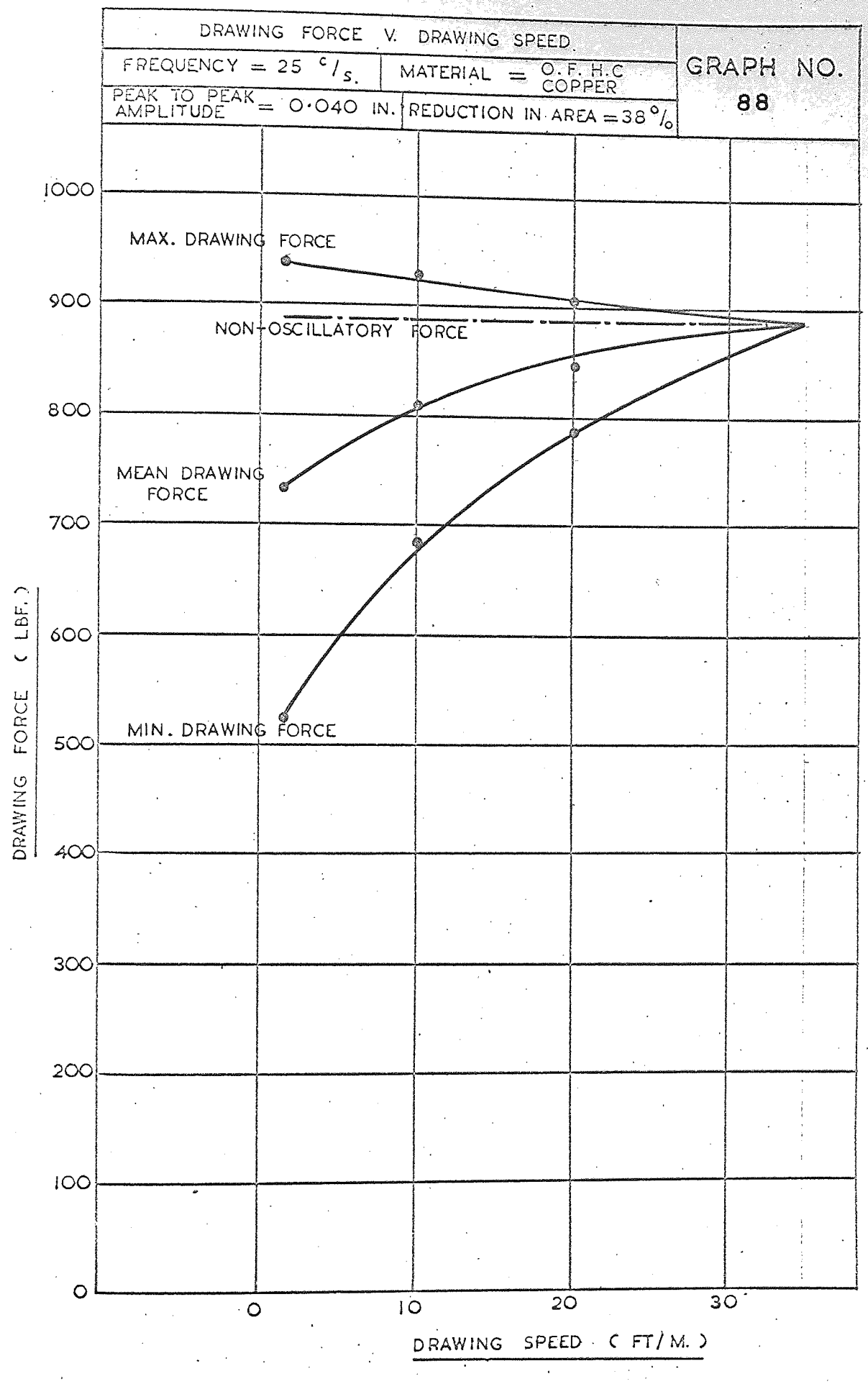
DRAWING FORCE V. DRAWING SPEED
FREQUENCY = 25 c/s.
MATERIAL = O.F.H.C COPPER
PEAK TO PEAK AMPLITUDE = 0·040 IN.
REDUCTION IN AREA = 38 %
GRAPH NO. 88
MAX. DRAWING FORCE
NON-OSCILLATORY FORCE
MEAN DRAWING FORCE
MIN. DRAWING FORCE
DRAWING FORCE (LBF.)
1000
900
800
700
600
500
400
300
200
100
0
0
10
20
30
DRAWING SPEED (FT/M.)

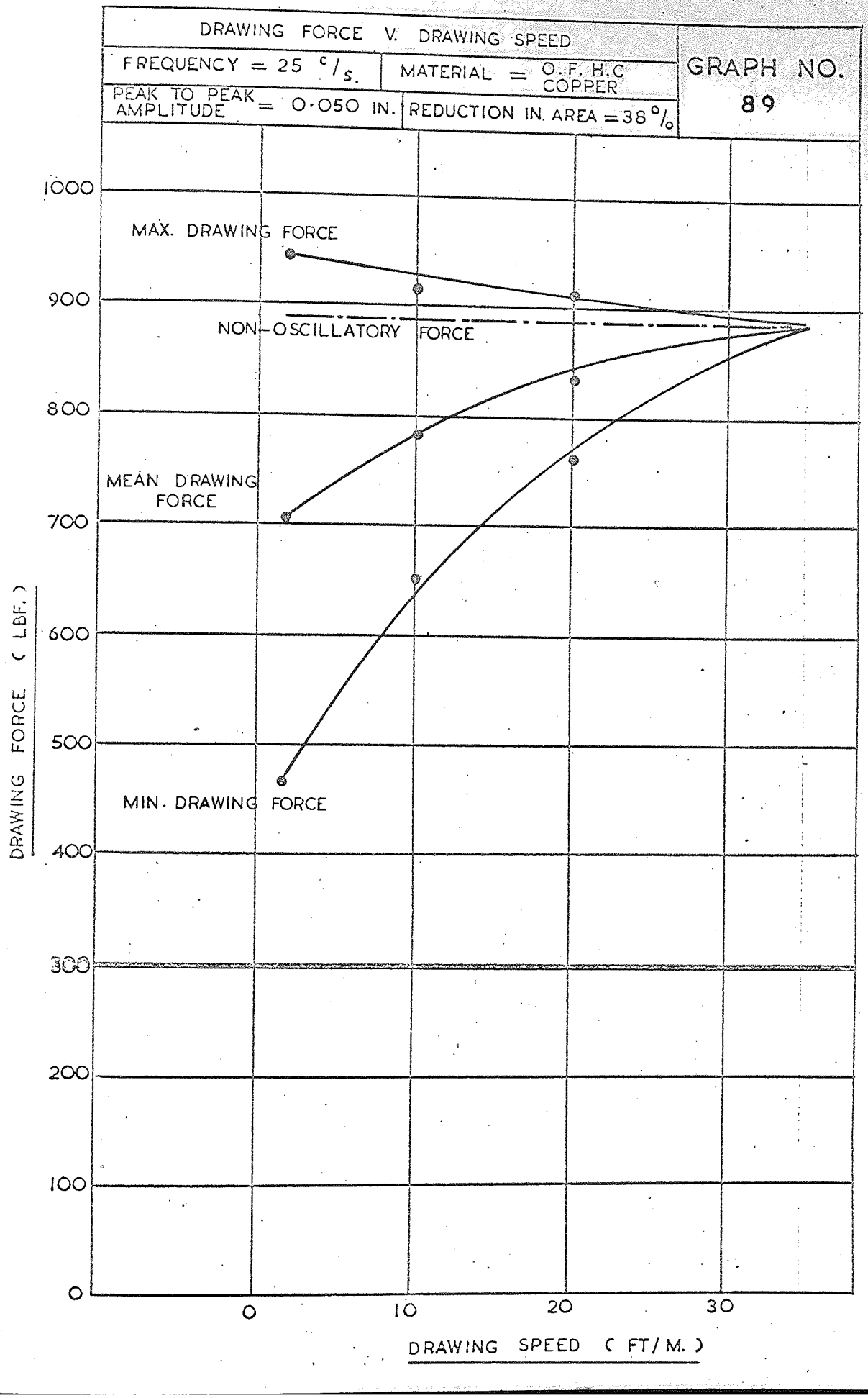
DRAWING FORCE V. DRAWING SPEED
FREQUENCY = 25 c/s.
MATERIAL = O.F.H.C COPPER
PEAK TO PEAK AMPLITUDE = 0·050 IN.
REDUCTION IN AREA = 38 %
GRAPH NO. 89
MAX. DRAWING FORCE
NON-OSCILLATORY FORCE
MEAN DRAWING FORCE
MIN. DRAWING FORCE
DRAWING FORCE (LBF.)
1000
900
800
700
600
500
400
300
200
100
0
0
10
20
30
DRAWING SPEED (FT/M.)

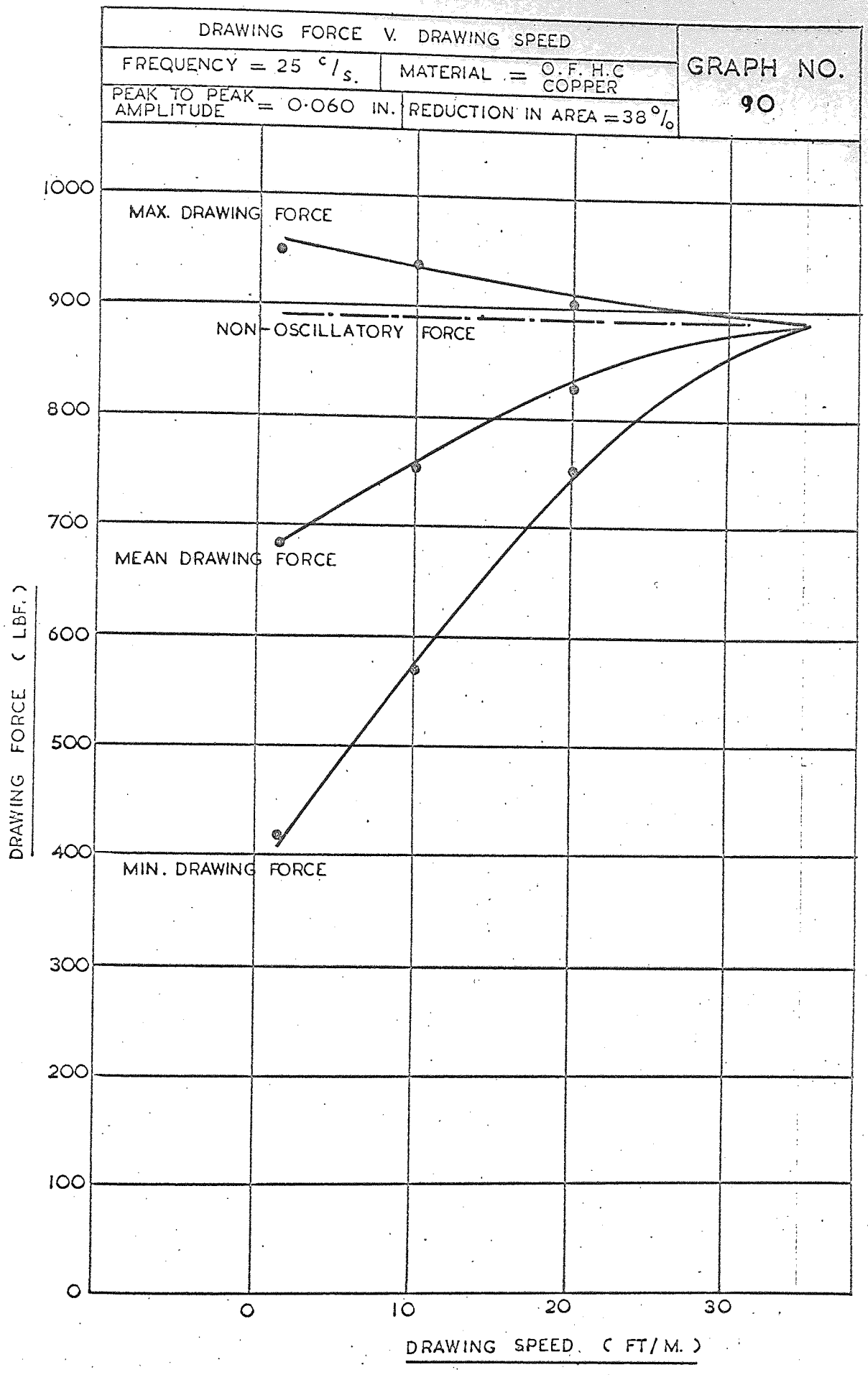
DRAWING FORCE V. DRAWING SPEED
FREQUENCY = 25 c/s.
MATERIAL = O.F.H.C COPPER
PEAK TO PEAK AMPLITUDE = 0·060 IN.
REDUCTION IN AREA = 38 %
GRAPH NO. 90
MAX. DRAWING FORCE
NON-OSCILLATORY FORCE
MEAN DRAWING FORCE
MIN. DRAWING FORCE
DRAWING FORCE (LBF.)
1000
900
800
700
600
500
400
300
200
100
0
0
10
20
30
DRAWING SPEED. (FT/M.)

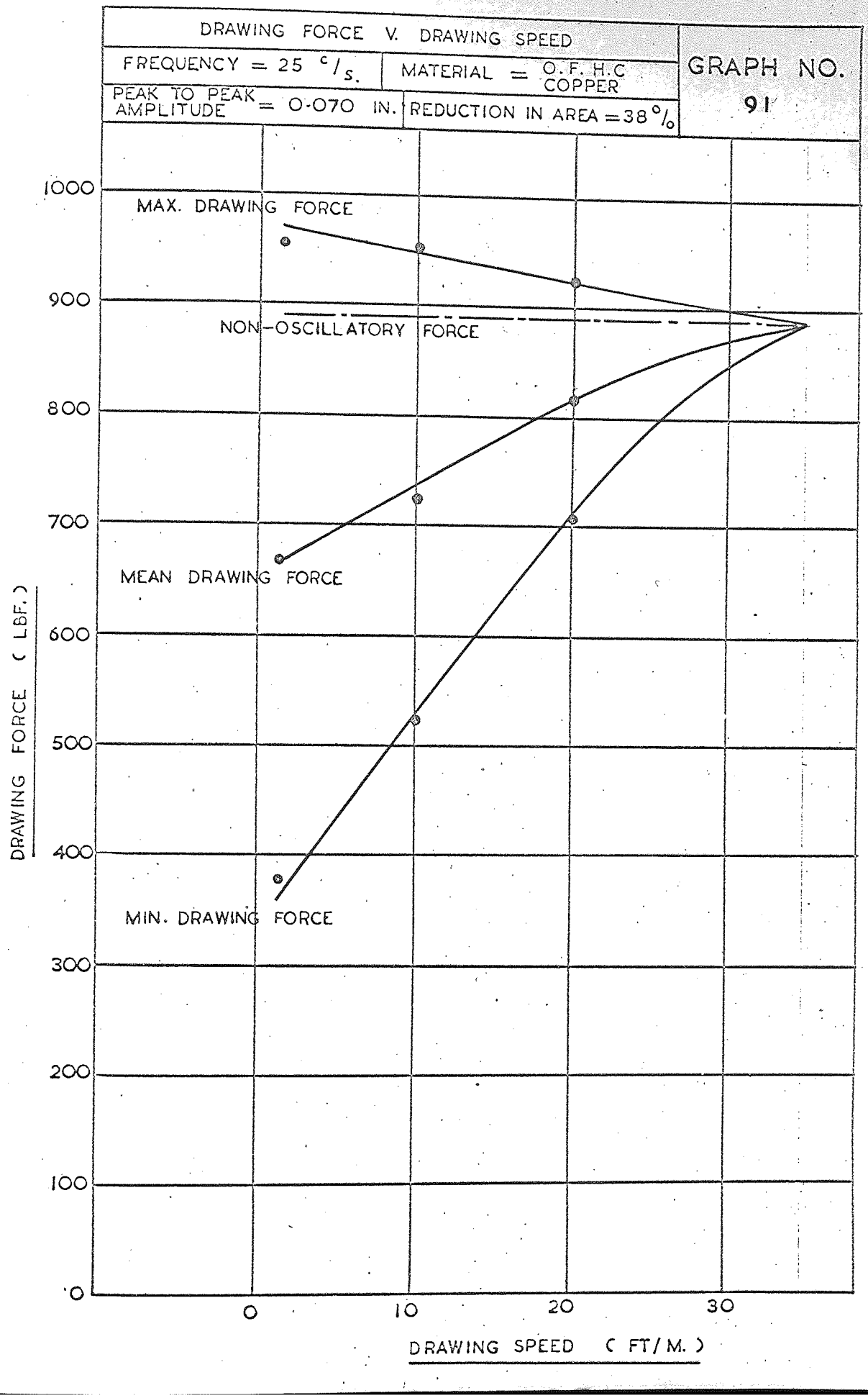
DRAWING FORCE V. DRAWING SPEED
FREQUENCY = 25 c/s.
MATERIAL = O.F. H.C COPPER
PEAK TO PEAK AMPLITUDE = 0·070 IN.
REDUCTION IN AREA = 38 %
GRAPH NO. 91
MAX. DRAWING FORCE
NON-OSCILLATORY FORCE
MEAN DRAWING FORCE
MIN. DRAWING FORCE
DRAWING FORCE (LBF.)
1000
900
800
700
600
500
400
300
200
100
0
0
10
20
30
DRAWING SPEED (FT/M.)

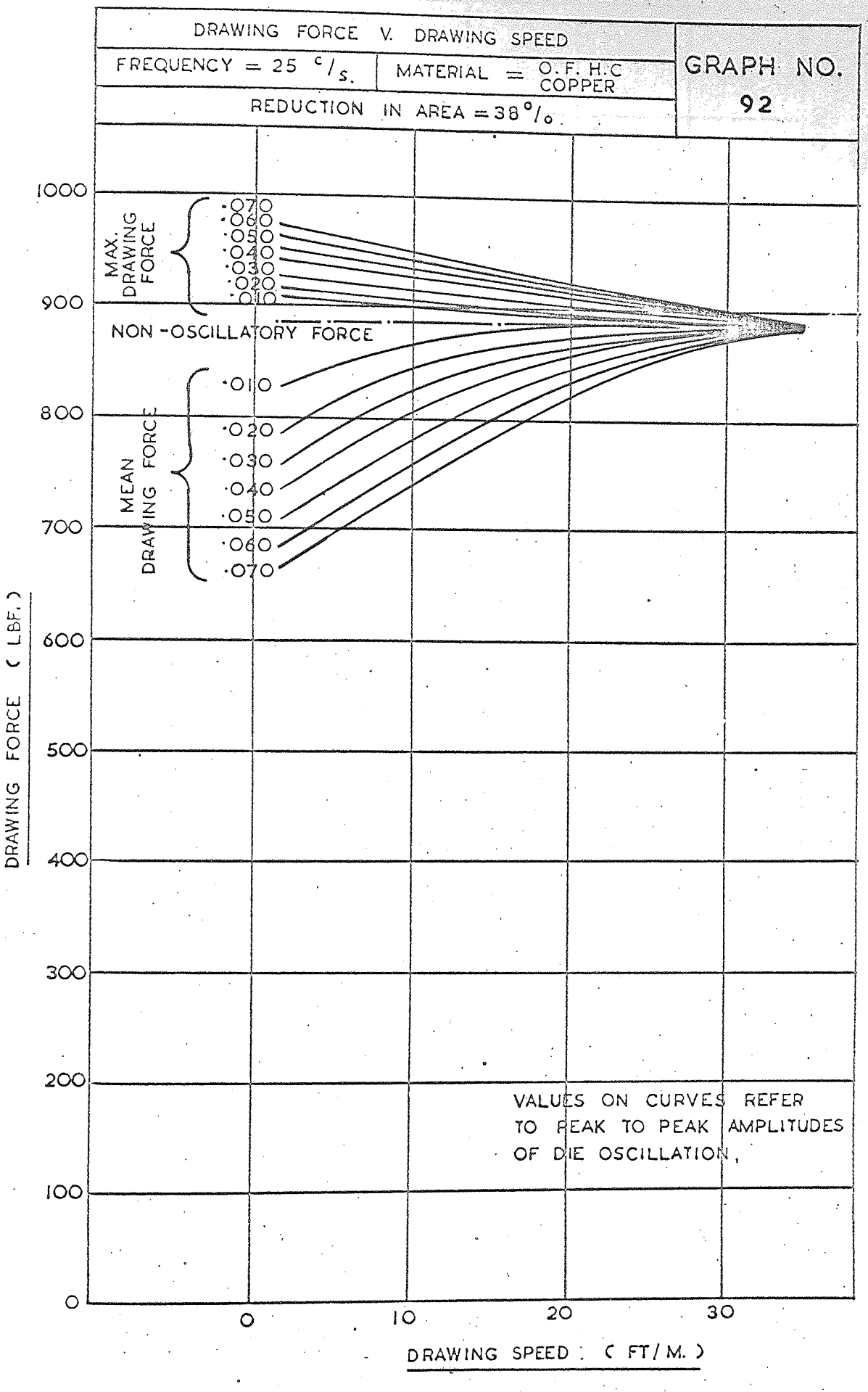
DRAWING FORCE V. DRAWING SPEED
FREQUENCY = 25 c/s.
MATERIAL = O.F. H.C COPPER
REDUCTION IN AREA = 38%.
GRAPH NO. 92
MAX. DRAWING FORCE
·070
·060
·050
·040
·030
·020
·010
NON-OSCILLATORY FORCE
MEAN DRAWING FORCE
·010
·020
·030
·040
·050
·060
·070
1000
900
800
700
600
500
400
300
200
100
0
DRAWING FORCE (LBF.)
0
10
20
30
DRAWING SPEED : (FT/M.)
VALUES ON CURVES REFER TO PEAK TO PEAK AMPLITUDES OF DIE OSCILLATION.

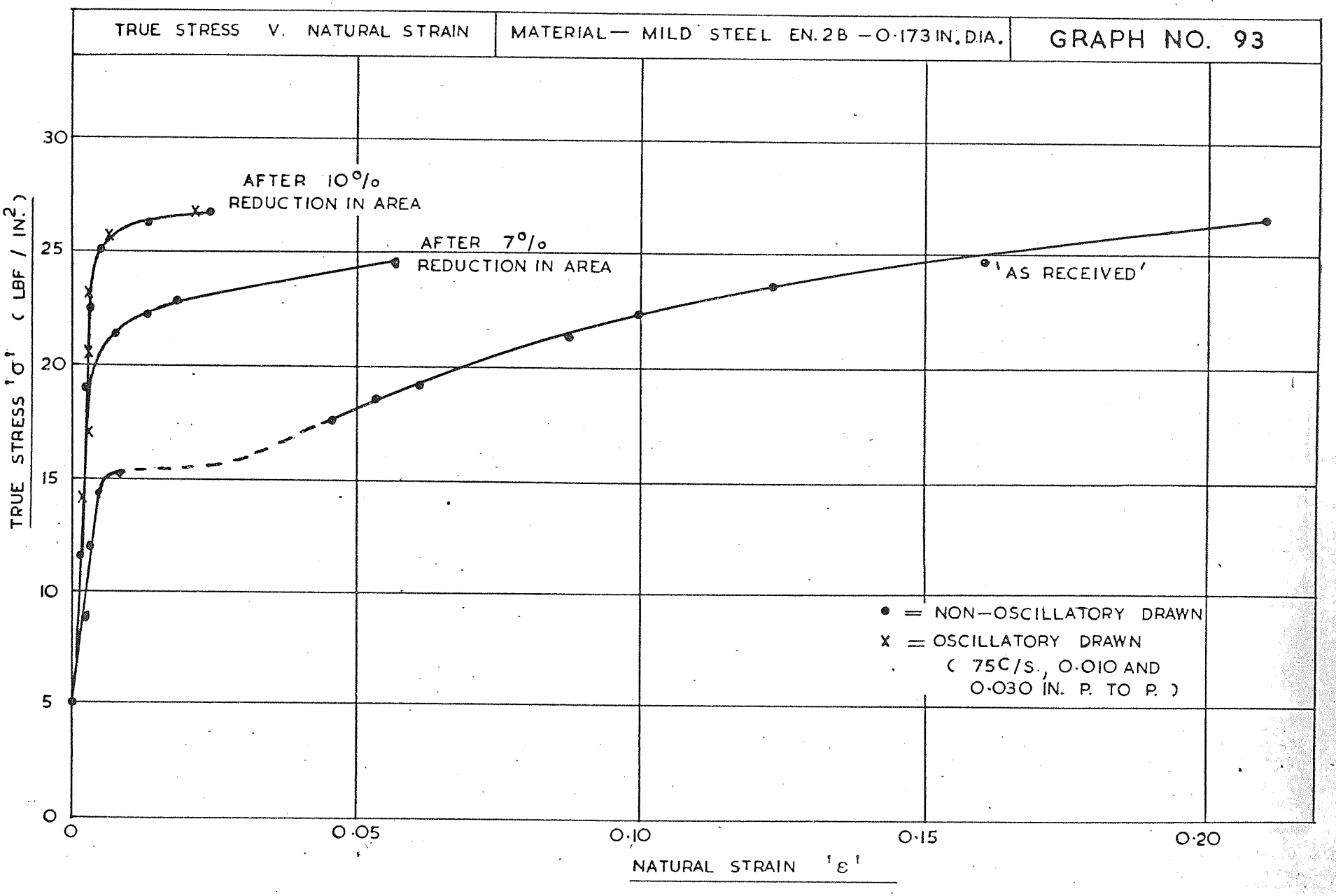
TRUE STRESS V. NATURAL STRAIN
MATERIAL— MILD STEEL EN. 2B —0·173 IN. DIA.
GRAPH NO. 93
AFTER 10% REDUCTION IN AREA
AFTER 7% REDUCTION IN AREA
'AS RECEIVED'
• = NON—OSCILLATORY DRAWN
X = OSCILLATORY DRAWN
(75C/S., 0·010 AND 0·030 IN. P. TO P.)
TRUE STRESS 'σ' (LBF / IN.2)
NATURAL STRAIN 'ε'
0
5
10
15
20
25
30
0·05
0·10
0·15
0·20

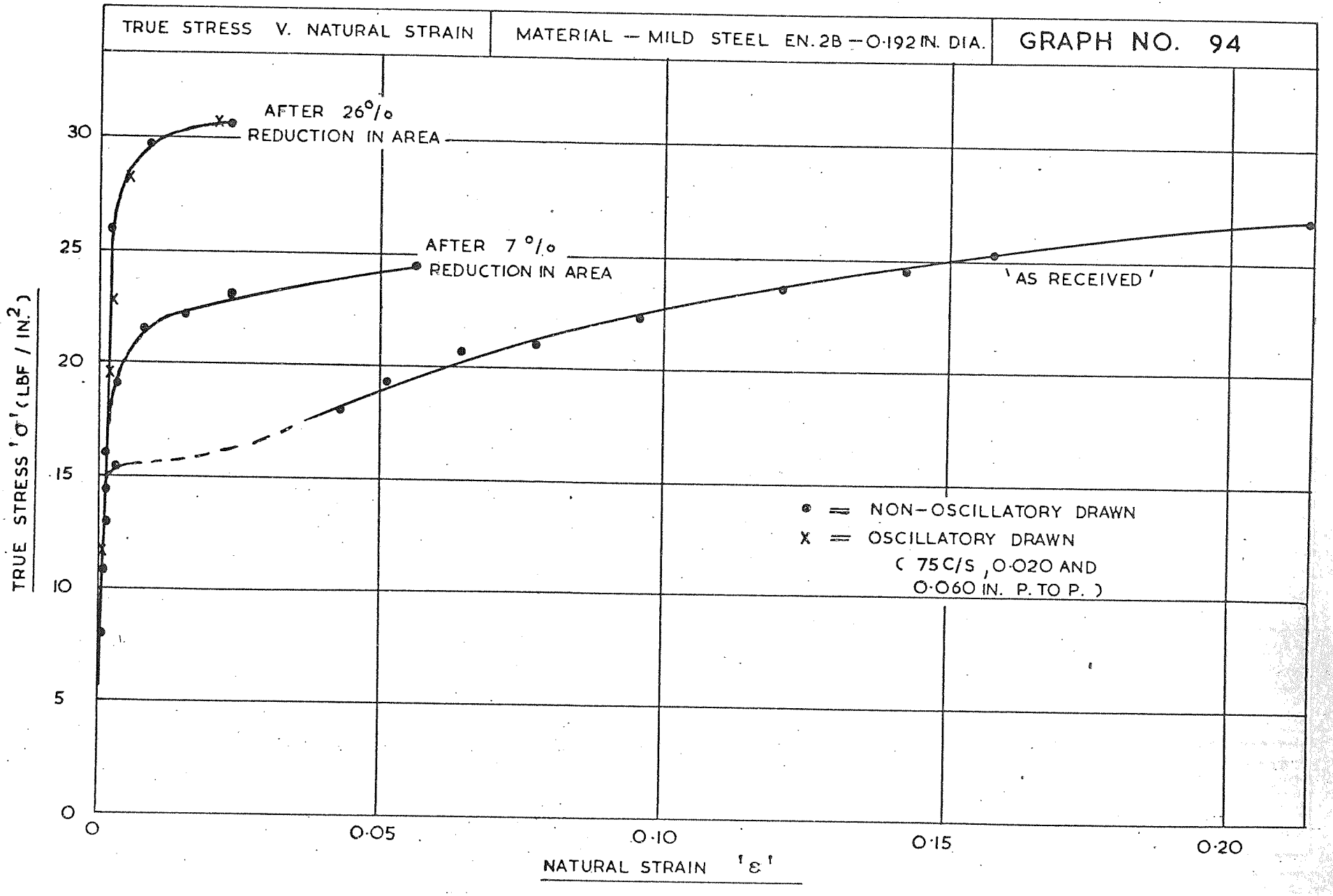
TRUE STRESS V. NATURAL STRAIN
MATERIAL — MILD STEEL EN. 2B — 0·192 IN. DIA.
GRAPH NO. 94
AFTER 26% REDUCTION IN AREA
AFTER 7 % REDUCTION IN AREA
'AS RECEIVED'
• = NON-OSCILLATORY DRAWN
X = OSCILLATORY DRAWN
(75 C/S , 0·020 AND 0·060 IN. P. TO P.)
TRUE STRESS 'σ' (LBF / IN.²)
NATURAL STRAIN 'ε'
0
5
10
15
20
25
30
0·05
0·10
0·15
0·20

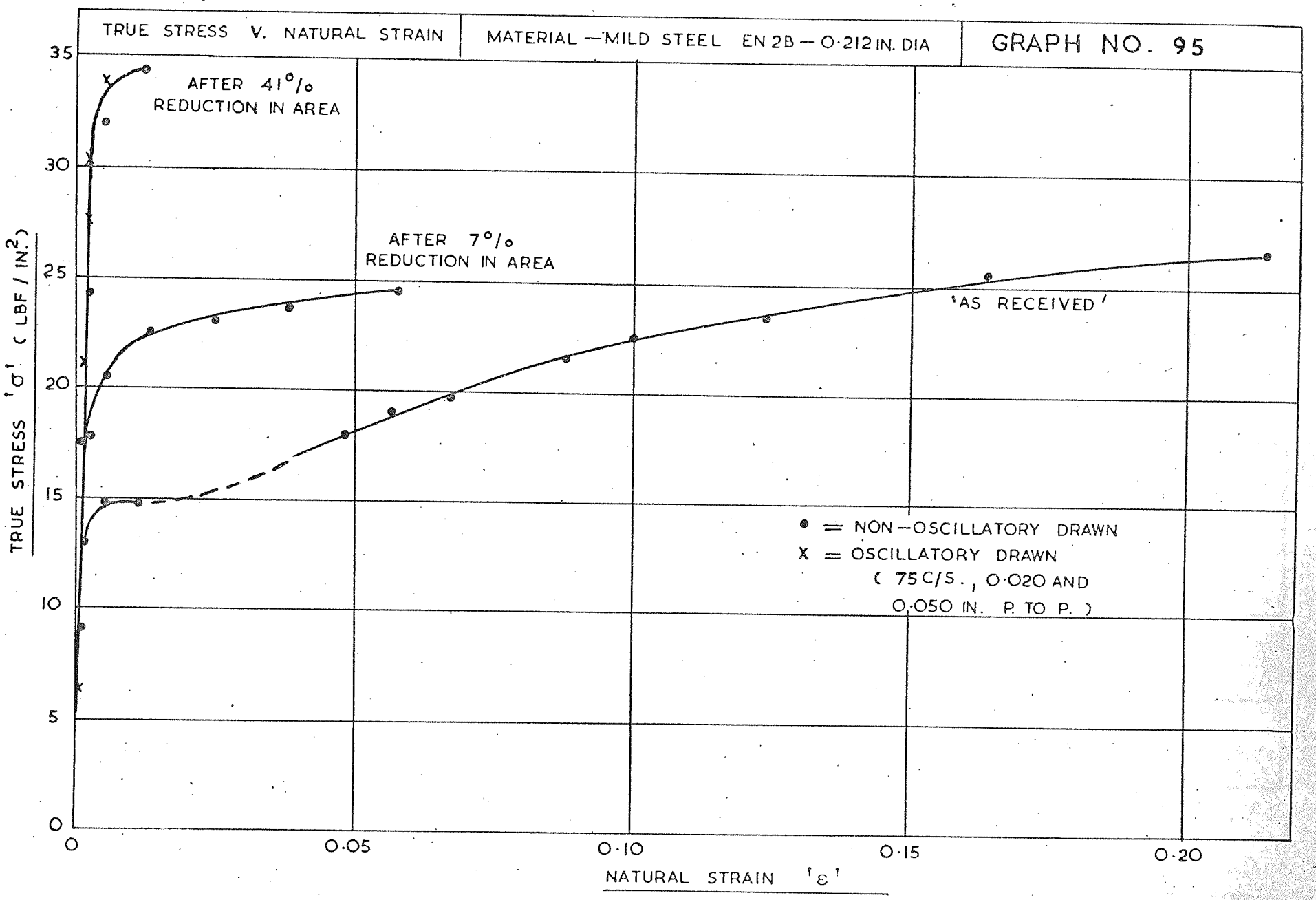
TRUE STRESS V. NATURAL STRAIN
MATERIAL — MILD STEEL EN 2B — 0·212 IN. DIA
GRAPH NO. 95
AFTER 41°/o REDUCTION IN AREA
AFTER 7°/o REDUCTION IN AREA
'AS RECEIVED'
• = NON-OSCILLATORY DRAWN
X = OSCILLATORY DRAWN (75 C/S., 0·020 AND 0·050 IN. P. TO P.)
TRUE STRESS 'σ' (LBF / IN.²)
NATURAL STRAIN 'ε'
0
5
10
15
20
25
30
35
0·05
0·10
0·15
0·20

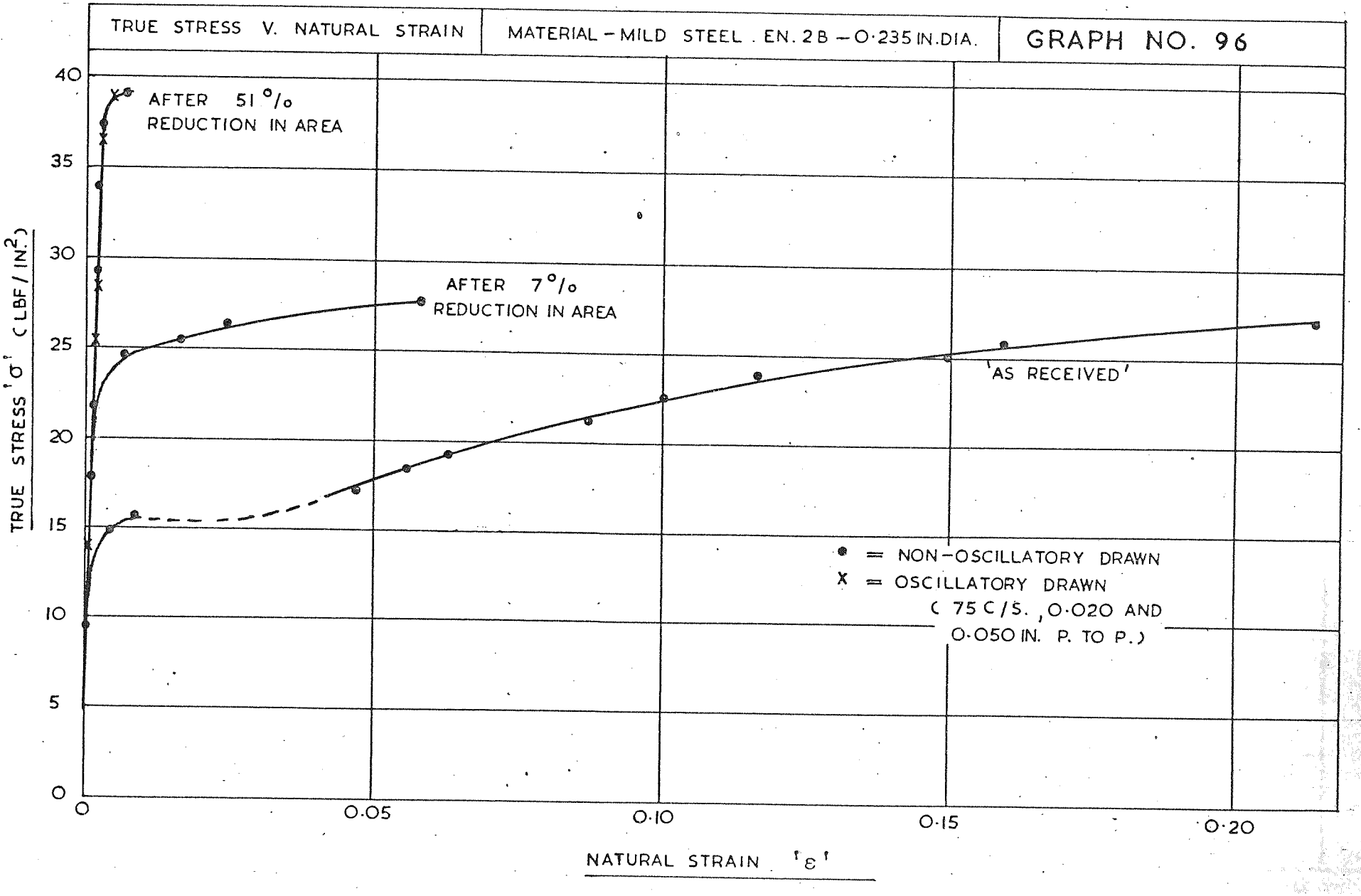
TRUE STRESS V. NATURAL STRAIN
MATERIAL – MILD STEEL . EN. 2B – 0·235 IN. DIA.
GRAPH NO. 96
AFTER 51 °/o REDUCTION IN AREA
AFTER 7 °/o REDUCTION IN AREA
'AS RECEIVED'
• = NON–OSCILLATORY DRAWN
X = OSCILLATORY DRAWN (75 C/S., 0·020 AND 0·050 IN. P. TO P.)
TRUE STRESS 'σ' (LBF/IN.²)
NATURAL STRAIN 'ε'
0
5
10
15
20
25
30
35
40
0·05
0·10
0·15
0·20

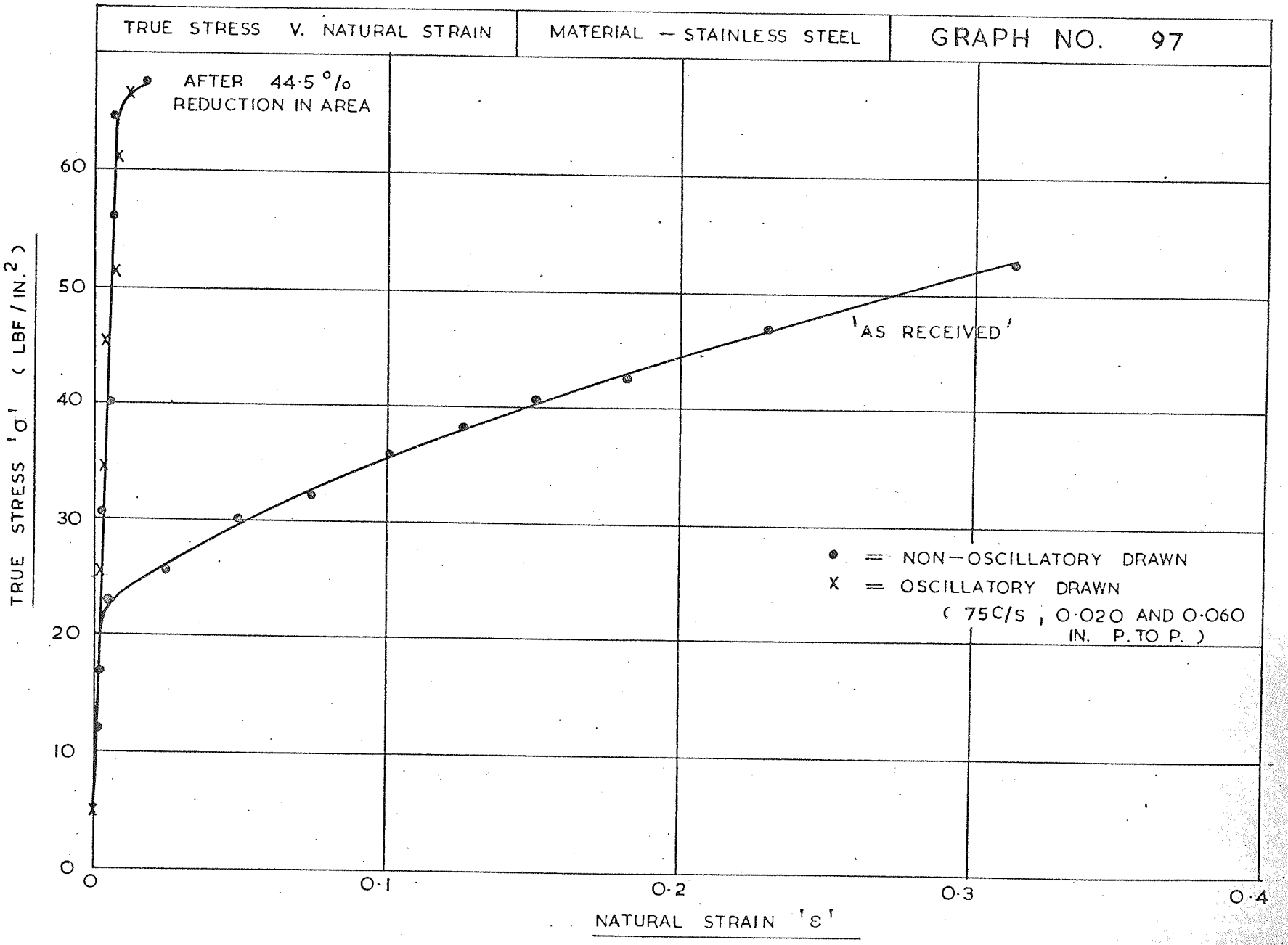
TRUE STRESS V. NATURAL STRAIN
MATERIAL — STAINLESS STEEL
GRAPH NO. 97
AFTER 44·5 °/o REDUCTION IN AREA
'AS RECEIVED'
• = NON—OSCILLATORY DRAWN
X = OSCILLATORY DRAWN
(75C/S , 0·020 AND 0·060 IN. P. TO P.)
TRUE STRESS 'σ' (LBF / IN.2)
NATURAL STRAIN 'ε'
0
10
20
30
40
50
60
0·1
0·2
0·3
0·4

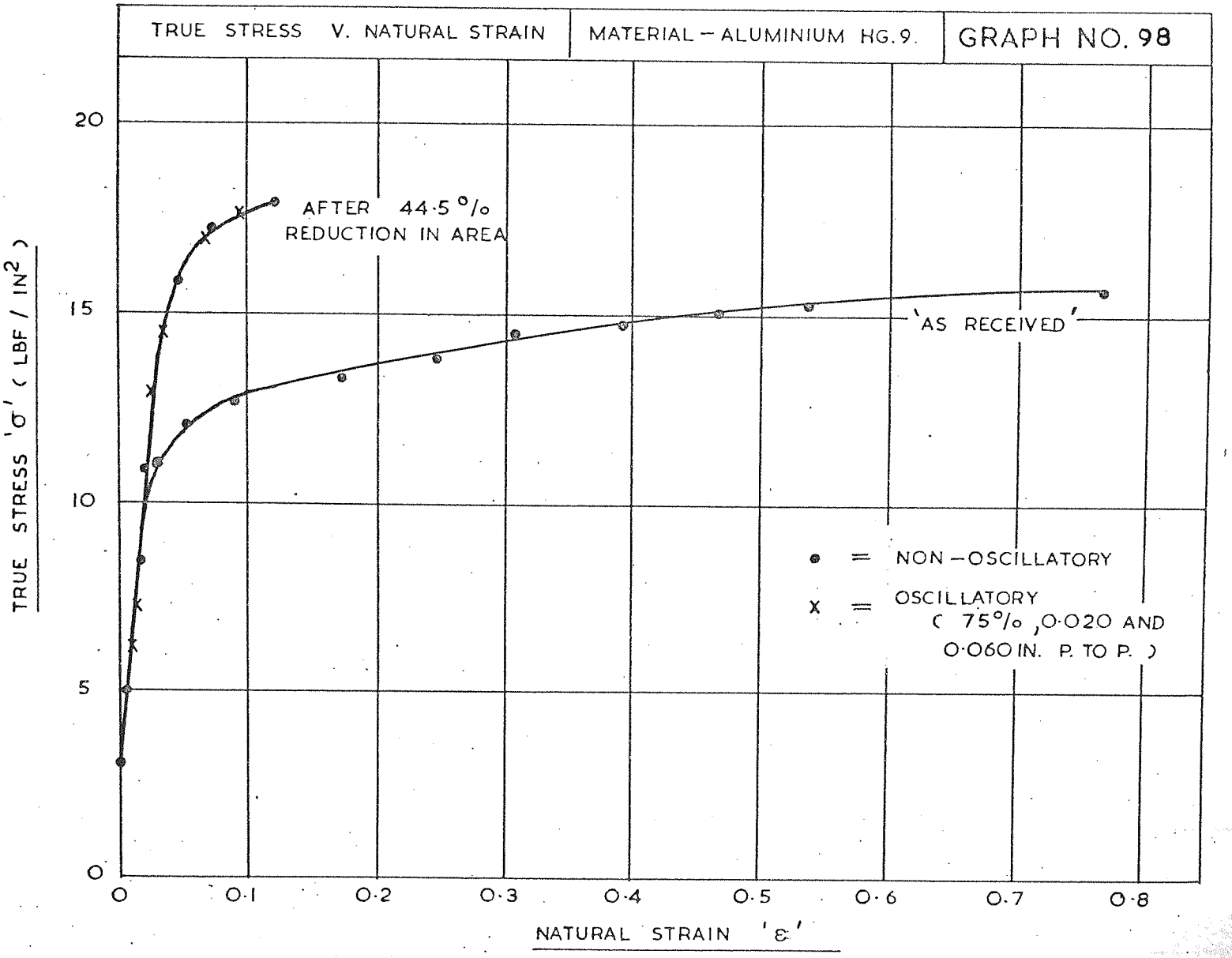
TRUE STRESS V. NATURAL STRAIN
MATERIAL – ALUMINIUM HG.9.
GRAPH NO. 98
AFTER 44·5 °/o REDUCTION IN AREA
'AS RECEIVED'
• = NON – OSCILLATORY
x = OSCILLATORY (75°/o , 0·020 AND 0·060 IN. P. TO P.)
TRUE STRESS 'σ' (LBF / IN2)
NATURAL STRAIN 'ε'
0
5
10
15
20
0·1
0·2
0·3
0·4
0·5
0·6
0·7
0·8

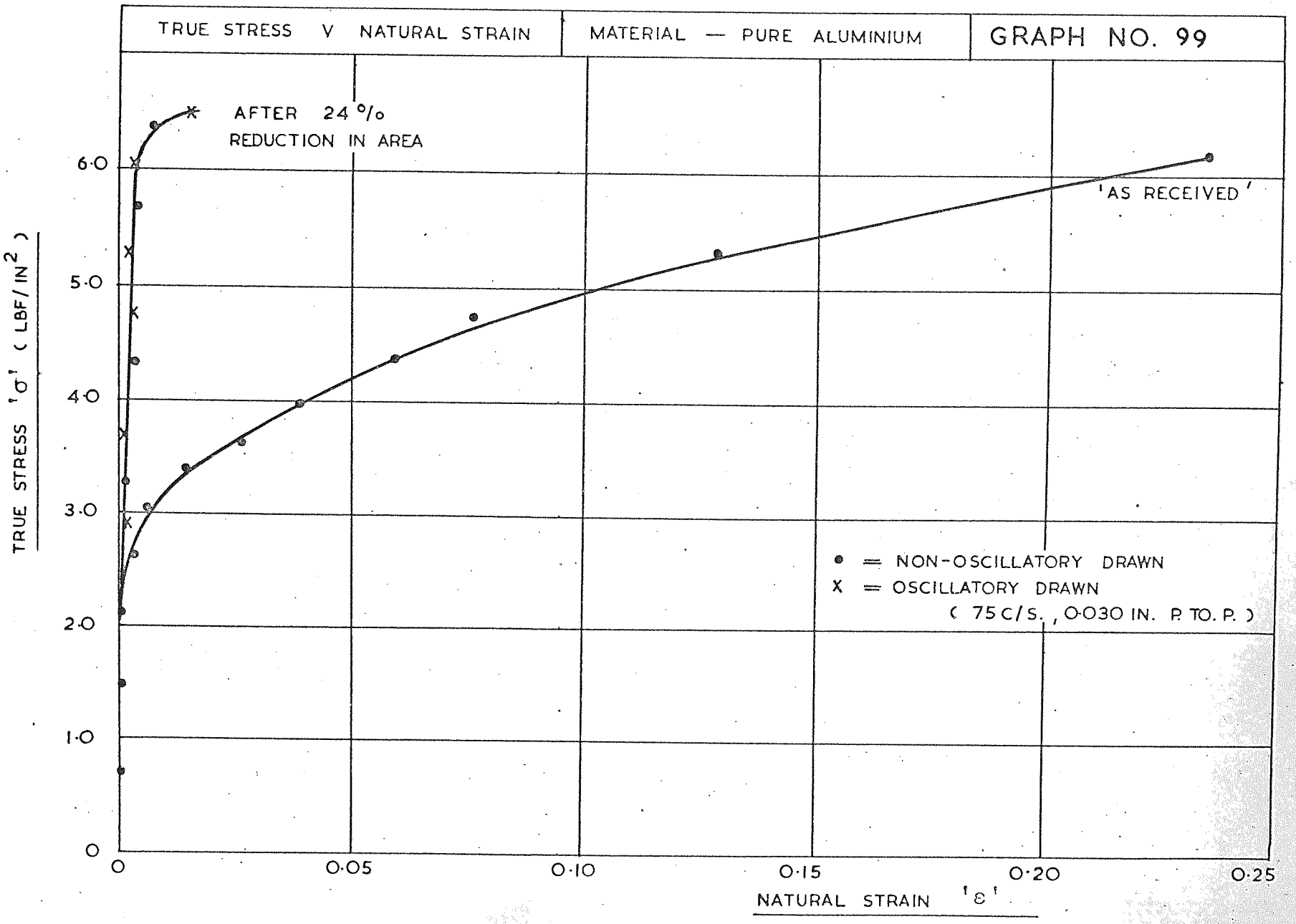
TRUE STRESS V NATURAL STRAIN
MATERIAL — PURE ALUMINIUM
GRAPH NO. 99
AFTER 24 % REDUCTION IN AREA
'AS RECEIVED'
• = NON-OSCILLATORY DRAWN
X = OSCILLATORY DRAWN
(75 C/S., 0·030 IN. P TO P.)
TRUE STRESS 'σ' (LBF/IN²)
NATURAL STRAIN 'ε'
0
1·0
2·0
3·0
4·0
5·0
6·0
0·05
0·10
0·15
0·20
0·25

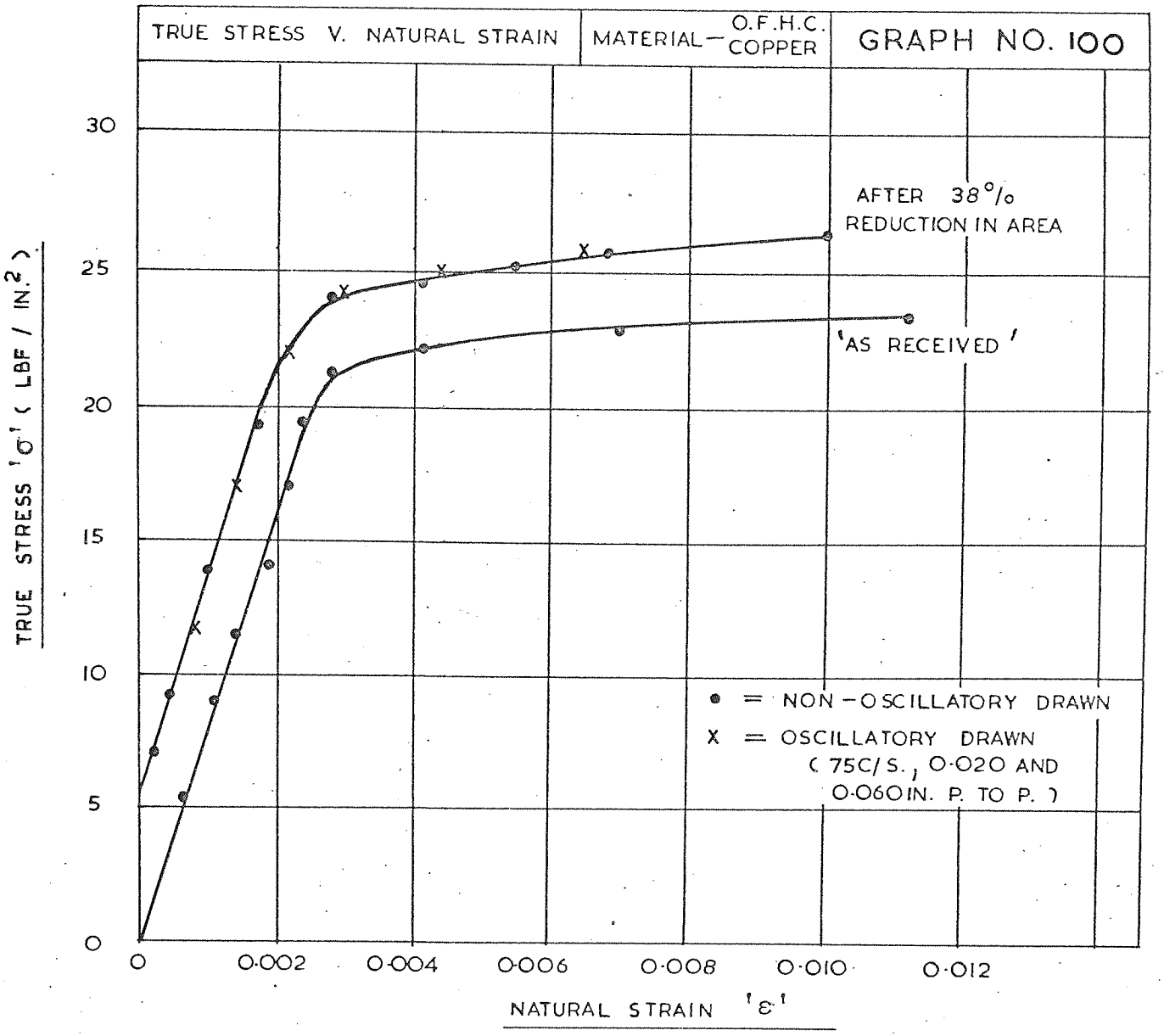
TRUE STRESS V. NATURAL STRAIN
MATERIAL — O.F.H.C. COPPER
GRAPH NO. 100
TRUE STRESS 'σ' (LBF / IN.²)
NATURAL STRAIN 'ε'
0
5
10
15
20
25
30
0
0·002
0·004
0·006
0·008
0·010
0·012
AFTER 38°/o REDUCTION IN AREA
'AS RECEIVED'
• = NON-OSCILLATORY DRAWN
X = OSCILLATORY DRAWN (75C/S., 0·020 AND 0·060 IN. P. TO P.)

11. Discussion of Results

11. Discussion of Results.

11.1. Slow Speed Tests (1.3 ft/m.)

11.1.1. Mild Steel.

It can be seen from Graph No's 2, 9, 16 and 23 that, for a given reduction in area, the mean drawing force falls as the amplitude of die oscillation is increased, and the magnitude of the fall is independent of the frequency of oscillation in the range 50 to 500 c/s. Graph No's. 3, 10, 17 and 24 show that for a frequency of 25 c/s., the mean drawing force is reduced also, but the magnitude of the reduction is less than that recorded at frequencies of 50 to 500 c/s.,ie. for a reduction in area of 51 per cent and a peak to peak amplitude of die oscillation of 0.050 in., the mean drawing force is reduced 30 per cent at frequencies in the range 50 to 500 c/s , while at 25 c/s.,the mean force is reduced 18 per cent. Furthermore, Graph No's. 2, 9, 16 and 23 show that, as the amplitude of oscillation is increased, the maximum drawing force rises and the magnitude of the rise is independent of the frequency in the range 50 to 500 c/s. Similarly, Graph No's 3, 10, 17 and 24 show the same phenomenon at a frequency of oscillation of 25 c/s., but again the magnitude of the rise is less than that observed at frequencies of 50 to 500 c/s.ie. for a reduction in area of 51 per cent and a peak to peak amplitude of die oscillation of 0.050 in., the maximum drawing force is increased by 9 per cent at

frequencies in the range 50 to 500 c/s., and increased by 2 per cent at a frequency of 25 c/s.

The effect of frequency of oscillation on the mean drawing force was expected, since at frequencies in the range 50 to 500 c/s., the die and drum oscillated nearly 180 degrees out of phase, while at a frequency of 25 c/s., they oscillated in phase. As a result of this, when the die and drum oscillate out of phase, the wire is subjected to an increased oscillatory strain, producing a greater variation of force in the drawn wire and consequently a greater reduction in mean force. The reasons why the peak drawing force is above the non-oscillatory drawing force are discussed later in section 11.5.

Graph No's.2, 9, 16 and 23, show that the rate of fall of the mean drawing force decreases as the amplitude of die oscillation increases. However, it is thought that, provided the wire oscillates in a longitudinal mode, the fall in mean force is directly proportional to the amplitude of die oscillation and any diversion from this linear relationship is attributable to secondary modes of oscillation being introduced into the system.During the investigation it was noted that, as the amplitude of die oscillation increased, some of the oscillatory energy was being transferred to the drawn wire in the form of transverse vibrations. As a result of this,the drum was subjected to smaller torsional oscillations than it would have been were

all the oscillatory energy being transferred to the wire as longitudinal oscillations, and consequently the wire was experiencing smaller longitudinal oscillatory strains. This phenomenon was less pronounced at high non-oscillatory drawing forces and is reflected in Graph No.23, where the relationship between the drawing force and the die amplitude is almost linear.

From Graph No's 30 and 31, it can be seen that the rate of fall of the mean drawing force decreases slightly, as the reduction in area decreases. The reason for this is that, at the smaller reduction in area, less oscillatory energy is transferred to the wire and hence the drum, and therefore the wire is subjected to smaller oscillatory strains.

During the slow speed drawing tests on mild steel wire, the control of the bull-block speed proved to be difficult and was found to be dependent on the magnitude of the drawing torque. For a constant setting on the oil gear speed control lever, the drum speed was found to increase considerably as the drawing torque was reduced. Consequently, when wire was being drawn under oscillatory conditions, the resulting reduction in the maximum value of drumtorque caused the drum to 'speed-up'. This increase in speed was found to be quite high, ie. for a 51 per cent reduction in area, and a frequency and peak to peak amplitude of die oscillation of 100 c/s. and 0.050 in.

respectively, the drawing speed was found to increase from 1.3 ft/m. up to 2.0 ft/m. However, this phenomenon only occurred at drawing speeds less than 4 ft/m., and therefore throughout the investigation this effect was neglected and the non-oscillatory drawing speed was recorded. Also during these early tests, attempts were made to draw mild steel wire at a 60 per cent reduction in area. However, this reduction was found to be impossible under both oscillatory and non-oscillatory conditions.

The magnitude of force variation in the drawn wire calculated from the theoretical analysis shows good correlation with experimental findings (see Graph No's 3, 8, 10, 15, 17, 22, 24 and 29). This suggests that the process of oscillatory drawing is merely a mechanical process of straining and unstraining sinusoidally the wire between the die and the drum. It is thought that, as the die moves in the direction of the drum, the strain in the drawn wire is released and hence the drawing force is reduced. When the die moves away from the drum, the strain is then 'taken-up' until a strain is reached where the wire draws through the die. The fact that the maximum force under oscillatory conditions is greater than the non-oscillatory force is dicussed in section 11.5.

From the results obtained for mild steel when drawing with superimposed, longitudinal, oscillatory stresses at frequencies in the range 25 to 500 c/s., it

was concluded that there is no reduction in yield stress in the material and no, or negligible, reduction in the coefficient of friction between the die and the wire.

During the experiments on mild steel, it was decided to try to increase the rate at which tests could be performed, and results analysed, by measuring the force variation in the wire directly. A strain gauge bridge on the wire had given satisfactory results, but had proven to be both an expensive and time consuming way of measuring the force. As a result of this, two different designs of loadmeter were manufactured, one to connect in parallel with the drawn wire, and the other to connect in series with the drum and the wire leaving the die. The meter designed for parallel operation was found to give spurious results because of its tendency to slip on the wire, while the meter designed for series operation functioned correctly, but, because of its weight, changed the vibration characteristic of the bull-block and wire. These difficulties were not overcome and hence the loadmeters were not used in the investigation. Details of the meters are included in Appendix No.11.10.

11.1.2. Stainless Steel.

It can be seen from Graph No's. 33 to 37 inclusive, that the results obtained when drawing stainless steel with superimposed oscillatory energy, are of the same form as those obtained when drawing mild steel.

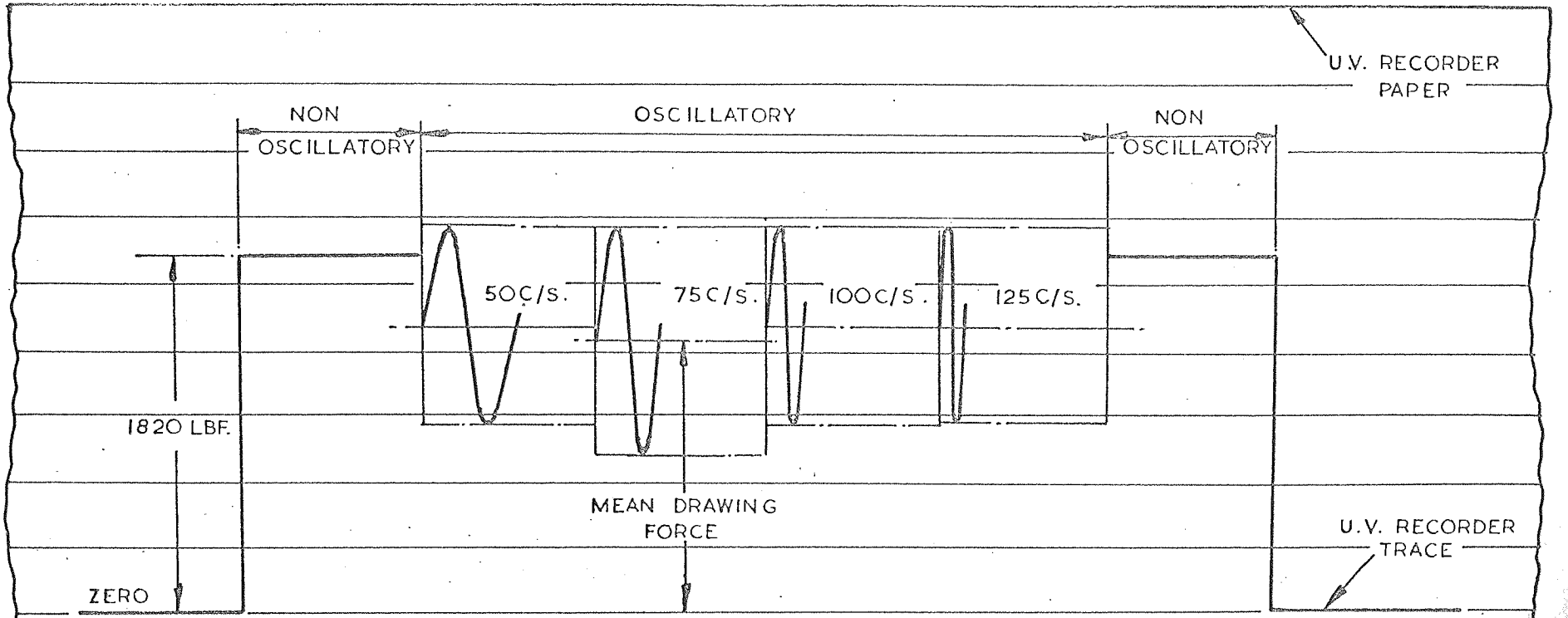

MATERIAL — STAINLESS STEEL

AMPLITUDE (PEAK TO PEAK) OF DIE OSCILLATION = 0·030 IN.

FIG. NO. 67. STRAIN GAUGE RECORD SHOWING THE EFFECT OF FREQUENCY

Comparing Graph No. 23 with Graph No.32, it can be seen that, at a constant amplitude of die oscillation, the magnitude of reduction in mean drawing force when drawing stainless steel is the same as that recorded when drawing mild steel with a 51 per cent reduction in area. This effect was expected since the theoretical analysis shows that the magnitude of the forces present during oscillatory drawing are dependent on Young's Modulus, the density and the cross-sectional area of the material being drawn. Therefore, because these parameters are constant for both stainless and mild steel, and since the maximum oscillatory drawing forces remain sensibly at the same value as the non-oscillatory force, the mean drawing forces will be the same

Graph No's. 35 and 38, show that, at a frequency of oscillation of 75 c/s., the mean drawing force is reduced by and amount greater than that recorded at frequencies of 50, 100 and 125 c/s., for a constant amplitude of die oscillation. This phenomenon was present throughout the complete series of experiments, but in the majority of cases the effect was negligible. However, the effect was magnified at the high non-oscillatory drawing forces required to draw stainless steel. This greater reduction in mean force is thought to be due to secondary modes of oscillation being introduced into the system at the higher drawing forces. Fig. No. 67, shows a record obtained from a strain gauge bridge bonded to the stainless steel

wire, illustrating the effect on the mean drawing force of varying the frequency of oscillation.

The calculated values of variation of force in the drawn wire, show again very good correlation with experimental findings (see Graph No. 38), and confirm further that this process of oscillatory drawing is mechanical. From these above observations it is concluded that, within the frequency range 25 to 500 c/s., the rate of work hardening of stainless steel is not reduced.

Note :- since the vibration analysis predicted that the die and drum oscillated in phase at 50 c/s., when in fact they oscillated nearly 180 degrees out of phase, the magnitude of the force variation in the wire was not computed at this frequency.

11.1.3. Hard and Pure Aluminium and OFHC. Copper.

Graph No's 39 to 59 inclusive, show that, hard and pure aluminium, and hard worked copper, behave similarly to mild and stainless steel when drawn with superimposed longitudinal oscillatory stresses.

It can be seen from Graph No. 60, in which the positions of the abscissi have been adjusted to enable all curves to start from the same non-oscillatory position, that the greatest reduction in mean drawing force is obtained for mild and stainless steel and minimum reduction is obtained for pure aluminium. The elastic vibrational analysis of the bull-block and wire confirm that this situation would obtain by its dependency on

Young's Modulus, density and cross-sectional area of the material being drawn. Graph No.60, shows also that the magnitude of the force variation induced in the drawn wire is greatest for stainless steel and a minimum for the pure aluminium. This again was expected, from the vibration analysis of the system. The reasons for the maximum drawing forces being, in the order shown in Graph No. 60. above the non-oscillatory drawing force are discussed in section 11.5.

From the above observations, it is concluded that during oscillatory drawing tests, at frequencies within the range 25 to 500 c/s. -

(a) Pure aluminium does not absorb oscillatory energy to ease the movement of dislocations.

(b) Hard aluminium is not softened by oscillatory energy being the equivalent of heat.

and (c) Hard drawn copper is not cyclically softened.

11.2. High Speed Tests on Hard Copper.

Graph No's 61 to 92 inclusive, show the effect of drawing speed on the process of oscillatory drawing. Experiments were performed to cover a range of drawing speeds up to a maximum of 50 ft/m. At speeds greater than this, the oscillatory mean drawing force is coincident with the non-oscillatory force and therefore no further advantage is to be gained at the amplitudes of oscillation available in this investigation.

It can be seen from Graph No's. 61 to 76 inclusive

that the fall in mean drawing force and the rise in maximum drawing force decrease as the drawing speed increases. This is because, as the drawing speed increases, less oscillatory energy is being transferred to unit volume of the wire leaving the die, and hence the wire is being subjected to smaller oscillatory strains. During these tests, it was observed that as the drawing speed increased, the amplitude of torsional oscillation of the drum decreased, until at a speed of 50 ft/m., the drum ceased to oscillate.

Experiments of 35 ft/m. and above, were carried out at a frequency of 50 c/s. only. This was necessary in order to minimise the length of wire being drawn. However, since all previous tests had indicated that the reduction in mean force was independent of frequency within the range 50 to 500 c/s., this was considered justifiable.

Graph No's. 77 to 92 inclusive, show that the effect of drawing speed on mean drawing force for constant amplitudes of die oscillation. The curves show that the amplitude of die oscillation must be increased, in order to maintain a constant reduction in the mean drawing force as the speed of draw is increased.

11.3. Mechanical Properties and Surface Finish of Wire.

Stress-strain curves obtained from tensile tests carried out on the drawn wire, with and without

superimposed oscillatory stresses, show that within the frequency range 25 to 500 c/s., oscillatory energy has no effect on the mechanical properties of the material, see Graph No's 93 to 100 inclusive. Furthermore, visual inspection of the drawn wire showed that oscillatory energy applied during drawing does not affect the surface finish of the drawn material.

11.4. Significance of Results.

The above results show that, for longitudinal oscillations of the die at frequencies within the range 25 to 500 c/s., the maximum drawing force is always greater than the non-oscillatory drawing force. Consequently, it will not be possible to obtain larger reduction in area per pass.

The maximum torque on the drum shaft is always below the non-oscillatory drawing torque and therefore, for all materials tested, the oscillatory action can be considered as being entirely mechanical in transferring power from the bull-block motor to the oscillator motor. This means that the capacity of a drawing machine can be increased substantially by the addition of a suitable oscillator . Furthermore, the oscillator takes a larger share of the load as the amplitude of die oscillation is increased and hence the greatest increase in capacity can be obtained at large amplitudes of die oscillation. By selecting

suitable values for the magnitude of drum inertia and the frequency and amplitude of die oscillation, the maximum torque on the drum can be arranged to be coincident with the mean drawing torque. This means that an even greater proportion of the work would be undertaken by the oscillator and hence the capacity of the drawing machine would be increased still further.

Since the mean force is always below the non-oscillatory drawing force, then, provided that die wear is dependent on die pressure and independent of fatigue effects due to oscillatory loading, the life of drawing dies will be increased.

11.5. Maximum Drawing Force.

In order to discuss the reasons why the maximum drawing force is always greater than the non-oscillatory drawing force, it is necessary to consider how the material being drawn can support an additional load without slipping through the die. The drawing force will be increased if -

(1) The value of the yield stress is increased.

(2) The die impacts on the wire, and

(3) The friction force is increased. This can occur either by an increase in the coefficient of friction, or by a change in the shape and/or the position of the deformation zone.

The yield stress of the materials could have been increased due to strain rate effects. However, since the maximum velocity of the die was only 84ft/m. and the non-oscillatory drawing force remained constant at drawing speeds up to 50 ft/m., this effect was considered to be negligible.

The maximum drawing force during oscillatory drawing is recorded when the die is at the end of its stroke and moving with zero velocity, and therefore at this instant the wire is not experiencing impact. Furthermore, since impact forces are dependent on the velocity of impact and the increase in maximum drawing force is independent of the velocity of die oscillation, the effect of impact is considered to be negligible.

Since the speed range investigated was small ie. 0 to 50 ft/m., it was thought unlikely that the lubrication mechanism changed during drawing and therefore it was concluded that the coefficient of friction remained unaltered. This conclusion is substantiated by the observation that the non-oscillatory drawing force is independent of the speed of draw.

From the preceding discussion, it is concluded that the maximum force is always above the non-oscillatory force because of an increase in friction forces, other than that which results from a change

Amplitude (peak to peak) of Die Oscillation = 0.030 in.			Frequency of Oscillation 25 to 125 c/s.	
Material	Reduction in Area (%)	Non Oscillatory Drawing Force (lbf.)	Magnitude of the Rise in Maximum Drawing Force Above the Non-Oscillatory Force (lbf.) (Measured)	(Calculated)
Mild Steel	51	1420	100	98
"	41	1148	84	79
"	26	810	63	56
"	10	405	30	28
Stainless Stl.	44.5	1820	125	125
Pure Aluminium	24	205	14	14
HC.9 Aluminium	44.5	675	35	46
OFHC. Copper	38	892	60	61
Note - Calculated fom the ratio of non-oscillatory drawing forces, - stainless steel as the reference.				

FIG. NO. 68

TABLE SHOWING THE MAGNITUDE OF THE RISE IN MAXIMUM DRAWING FORCE ABOVE THE NON-OSCILLATORY FORCE

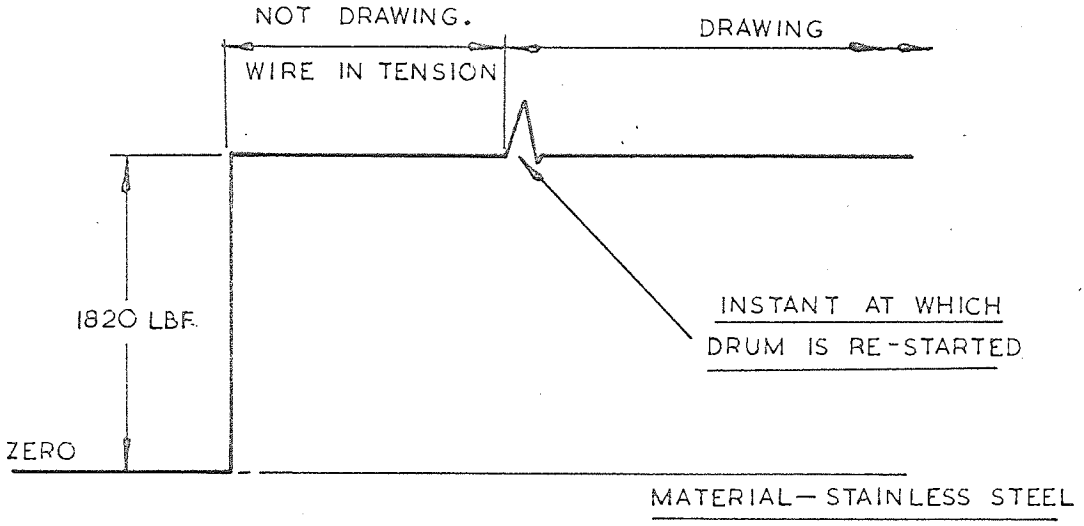

FIG.NO. 69 TORQUEMETER RECORD SHOWING THE EFFECT OF RE-STARTING THE DRUM DURING DRAWING

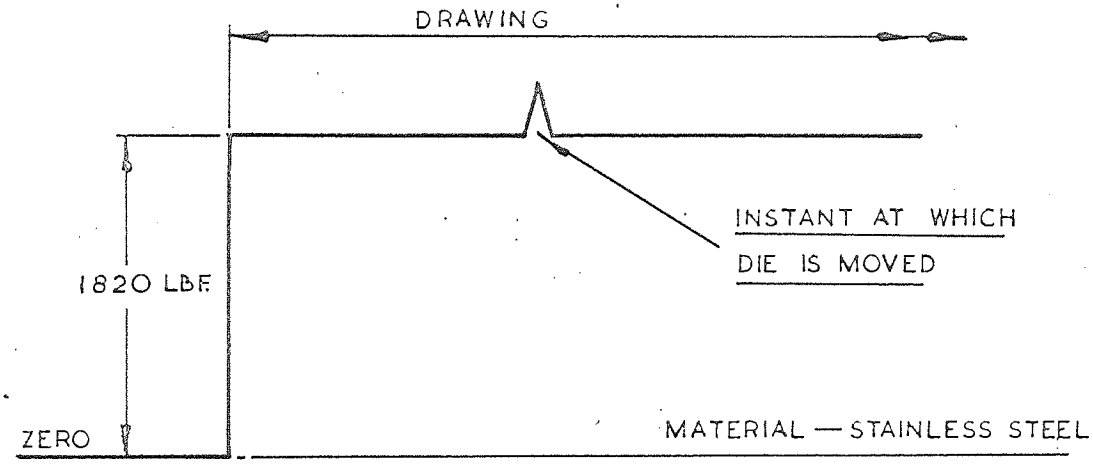

FIG.NO. 70 TORQUEMETER RECORD SHOWING THE EFFECT OF MOVING THE DIE DURING DRAWING

in the coefficient of friction. The table shown in Fig. No.68, substantiates this conclusion. It shows that the increase in maximum drawing force is directly proportional to the magnitude of the non-oscillatory drawing force and therefore, provided the coefficientof friction remains constant, on the friction forces.

To define this frictional effect, two simple non-oscillatory drawing experiments were carried out as follows -

(1) The bull-block was arranged to draw stainless steel wire at a slow drawing speed. After a length of wire had been drawn, the drum was stopped and the tension in thewire between the die and the drum allowed to remain. The drum was then re-started and a torquemeter record obtained, as shown in Fig. No. 69. The record shows that the drawing force increases momentarily before drawing commences, and since impact was neglected, this was attributed to a change in frictional conditions, ie. a change from sticking to slipping friction.

(2) The bull-block was arranged to draw stainless steel at a speed of 1.3 ft/m. and during the operation, the die was moved quickly in the opposite direction to that of drawing. During this operation, a torquemeter record was again obtained, and is shown in Fig. No. 70. This simple experiment

showed that the force was increased at the instant of moving the die although sticking friction was eliminated. This phenomenon was attributed to a change in friction forces occurring because of a change in the equilibrium drawing conditions.

From these simple experiments and the previous discussion, it is concluded that the drawing force is increased because of a combination of sticking friction and a change in die pressure due to a change in equilibrium conditions. It is thought that during the simple tests and during oscillatory drawing, the drawing equilibrium is upset momentarily because of an increase in the rate of working and consequently the position and shape of the deformation zone is altered momentarily. This results in an increase in die pressure and frictional forces and therefore an increase in the drawing force.

12. Conclusions

12. Conclusions :-

(1) For all metals tested the reduction in mean drawing force is dependent on the amplitude of die oscillation and independent of the frequency within the range 25 to 500 c/s.

(2) There is a negligible reduction in the coefficient of friction between the die and the wire when drawing with oscillations in the range 25 to 500 c/s.

(3) Within the frequency range 25 to 500 c/s.

(a) There is no reduction in yield stress of mild steel.

(b) There is no reduction in the rate of work hardening of stainless steel.

(c) Pure aluminium does not absorb oscillatory energy to ease the movement of dislocations.

(d) Hard aluminium is not softened by oscillatory energy as it is by the action of heat, ie. the diffusion process is not accelerated, and

(e) Hard drawn copper is not cyclically softened when drawn with superimposed oscillatory stresses.

(4) The maximum reduction in mean drawing force is obtained when drawing stainless steel and mild steel, while the minimum reduction is obtained when drawing pure aluminium.

(5) The magnitude of force variation in the drawn wire is smallest for pure aluminium and greatest for stainless steel.

(6) The maximum drawing force rises least above the non-oscillatory drawing force for pure aluminium and most for

stainless steel.

(7) As the drawing speed is increased and the amplitude of die oscillation maintained constant.

(a) The magnitude of force variation in the copper wire decreases and

(b) The mean and maximum drawing forces approach the non-oscillatory value of drawing force.

(8) Within the frequency range 25 to 500 c/s., oscillatory energy has no effect on the mechanical properties of the materials.

(9) Within the frequency range 25 to 500 c/s., oscillatory energy has no effect on the surface finish of the drawn wire.

(10) Drawing with superimposed oscillatory stresses at frequencies in the range 25 to 500 c/s., is a purely mechanical process of straining and unstraining the drawn wire.

(11) The energy required to draw metals with superimposed oscillatory stresses is shared between the bull-block motor and the oscillator motor. The magnitude of the energy supplied by the oscillator is dependent on the amplitude of die oscillation.

(12) The maximum drawing force is always greater than the non-oscillatory drawing force. The rise in force is attributed to a combination of sticking friction and an increase in die pressure due to a change in equilibrium conditions. The magnitude of the rise is dependent on the magnitude of the non-oscillatory friction forces and

therefore, provided the coefficient of friction is constant, on the magnitude of the non-oscillatory drawing force.

(13) The theoretical analysis shows that the reduction in mean drawing force is dependent on Young's Modulus, the density and the cross-sectional area of the material being drawn.

13. Suggestions for Future Work

13. Suggestions for Future Work.

It has been concluded when drawing with superimposed oscillatory energy at frequencies in the range 25 to 500 c/s., that the drawing operation is a mechanical process of straining and unstraining the drawn wire. However, the instant at which the wire moves relative to the die during a cycle of die oscillation cannot be deduced from the measurments made. It has not been possible to determine whether the die and wire move together until the non-oscillatory force is reached, or whether the wire passes through the die at values of force less than the non-oscillatory force, and since this effect has important implications, it is suggested that a series of experiments be carried out to ascertain whether this phenomenon occurs, and should it do so, to try to develop it to assist the drawing operation.

For all experimental conditions tested it was found that the maximum oscillatory drawing force was always greater than the non-oscillatory force. This phenomenon was concluded to be due to an increase in friction forces attributable to a combination of sticking friction, and a change in die pressure because of a change in the shape of the deformation zone. However, the proportion of each of these effects is not known. Therefore, it is suggested that tests be initiated to determine their magnitude and also, if the sticking friction effect proves to be the main contributor, to investigate the possibility of eliminating

sticking by rotating the die during the oscillatory drawing operation. It was thought during the investigation, that the reduction in mean drawing force was directly proportional to the amplitude of die oscillation and that any diversion from a linear relationship was attributable to secondary modes of oscillation. To check this, it is suggested that a series of tests be performed with an isolator die to prevent secondary modes of oscillation from occurring, ie. the die is not contributing to the overall reduction in area, but merely preventing transverse vibrations being induced in to the drawn wire.

Because of the limitations on amplitude imposed by the oscillator used in this investigation, it is possible only to obtain a reduction in mean drawing force for drawing speed up to 50 ft/m. To obtain a reduced force at higher values of speed, ie. at speeds closer to those used commercially when drawing wire, it is necessary to use an oscillator of greater power output. Furthermore, it is not possible, because of the very small amplitudes available at the higher frequencies, to show conclusively that the effect of oscillatory stresses at 500 c/s. is the same as that at 100 c/s. ie. the effect of drawing load reduction is not evident as the power density is not high enough. Therefore, it is suggested that this aspect be studied and also the speed range extended by carrying out an investigation using an oscillator which develops a large power output.

The theoretical analysis shows that the reduction

in mean drawing force is dependent on the stiffness of the drawn wire. If this parameter was increased, then the proportion of oscillatory energy transferred to the wire would be increased and therefore for a constant amplitude and frequency setting, the fall in mean drawing force would be greater and the drawing speed range at which a reduction in force is observed would be extended. It is suggested, therefore, that an investigation designed to study the effect of the length of drawn wire between the die and the drum would finally confirm the theory.

During the present investigation, it was observed that hard drawn copper did not soften when drawn with superimposed tensile oscillatory energy, and therefore it is concluded that, although large oscillatory stresses were applied, softening will occur only when the material is subjected to complete stress reversals. It is thought that, if hard copper, or indeed any metal which softens because of stress reversals is drawn through tandem dies which are oscillating 180 degrees out of phase, and provided the distance between the dies is small, stress reversals will take place resulting in a softening of the material being drawn, and therefore a reduction in tag load. Furthermore, drawing through tandem dies could take advantage of the mechanical straining and unstraining effect observed during this investigation. If the dies oscillate 180 degrees out of phase, then the tag load will be equal to the algebraic sum of the force variation induced in the wire by each die. Consequently,

under idealised conditions, it is argued that the total drawing force will be equal to the sum of the two mean forces. To investigate these possibilities, it is suggested that an extensive investigation be made into tandem drawing, studying such variables as, material drawn, die spacing, phase relationship between dies, the disposition of reductions in area and the speed of draw. This suggestion has important commercial implications.

Throughout this research, a very good lubricant, namely sodium stearate, was used which gave a very low coefficient of friction, ie. of the order of 0.025. Therefore, it is suggested that a series of tests be undertaken to study the effect of poor lubricants on the rise in the maximum oscillatory drawing force above the non-oscillatory force, and to see whether oscillatory energy could be used to improve poor frictional conditions and hence reduce the drawing force.

Also using the sodium stearate lubricant, the surface finish of the material drawn appeared to be unaffected by superimposing oscillatory stresses, however, only visual inspections were made of the wire. Since some investigators have claimed oscillations improve the surface, it is concluded that a series of experiments should be undertaken to study closely the effects of a variety of lubricants with and without oscillatory stresses on the variation of surface finish, diameter and tolerance of the drawn wire.

The investigation was restricted to wire drawing because of the reasons given on page 49, and it was thought that similar results would be obtained when drawing tube. This has yet to be proved. Also investigators applying low frequency vibrations during forging, have observed that residual stresses in the components are reduced significantly. Since the level of residual stresses is important in tube drawing and sinking it is suggested that a thorough investigation into tube drawing should be undertaken to study residual stresses and to satisfy the sceptics.

It was suggested in the introduction to this thesis that, if oscillatory energy had the desired effect of reducing the yield stress of the material being drawn and reducing the coefficient of friction between the die and the workpiece, the existing technological wire drawing theories could be used and modified to incorporate the effects of oscillatory energy by the selection of suitable values for the yield stress and the coefficient of friction. However, if the shape of the deformation zone changes appreciably during oscillatory drawing, it is suggested that a new theory should be developed for oscillatory drawing, perhaps by considering that oscillatory drawing is analogous to the flow of a fluid through a nozzle.

Finally, following conflicting claims in the literature, it is thought that fundamental research should be undertaken to answer the following questions :

What is the mechanism of yield under oscillatory conditions, and how is the energy absorbed? Is the reduction in yield stress dependent on frequency, and not independent as suggested by a number of investigators? Is there a greater readiness for dislocations to move and if there is, is this readiness associated with amplitude of vibration or frequency or both? Are hardness, tensile strength or indeed other mechanical properties of metals affected and if so what factors affect these properties? Is there a reduction in the coefficient of friction ? Do the tool and workpiece seperate during some oscillatory operations? Are some lubricants more effective than others in oscillatory metal working and if so why? If the tool and workpiece do not separate, is the coefficient of friction reduced? Is a lubricant needed at all?

14. Acknowledgments

14. Acknowledgments.

The author would like to express his sincere appreciation to Dr. D.H.Sansome for his invaluable help and direction throughout the three year research programme, and his thanks to Mr.J.Metcalfe, a Director of Tube Investments Limited, for supplying the bull-block and oscillatory equipment.

His thanks are due also to the following -

Professor A.C. Walshaw, for his permission to carry out the investigation in the Department of Mechanical Engineering at the University of Aston in Birmingham.

Mr.G.K. Steel, for his invaluable help with the design and manufacture of the d.c. amplifiers.

Mr.P.A. Clayton, Mr.I.M. Cole and Mr.W.H. Stableford for their many helpful discussions.

Mr.E.W. Denchfield, Mr.H.F. Pratt, Mr.G.M. Jones and members of the workshop of the Mechanical Engineering Department for their help in the manufacture of the apparatus.

Mr.E. Dummer of the Aluminium Wire and Cable Co. Ltd.,

Mr.G. Austin of G.K.N. Group of Companies and

Mr.R.C.W. Thomas of Imperial Metal Industries Ltd. for supplying the raw material,and lastly,

his wife for the many hours she has spent typing this thesis.

15. Bibliography

15. Bibliography

The Effect of Oscillatory Stresses on the Mechanical Properties of Metals.

(1). BLAHA,F., LANGENECKER,B.
'Dehnung von Zink-Kristallen unter Ultraschalleinwirkung'.
Die Naturwissenschaften 1955, Vol.42, p.556.

(2). AEROPROJECTS INCORPORATED.
'Fundamentals of Ultrasonic Welding, Phase II'
Research Project No.60-90, Navy Contract No.59-6070c
Dec. 1960.

(3). ROSENFIELD,A.R.
'The Application of Ultrasonic Energy in the Deformation of Metals'.
(Report on an Informal Symposium). Defence Metals Information Centre. Battelle Memorial Institute. Columbus, Ohio. Report No. 187, Aug.16th.1963.

(4). BLAHA,F., LANGENECKER,B.
'Untersuchungen zur Bearbeitungserholung'.
(Verformungsentfestigung), von Metallkristallen'.
Z.Metallk 1958, Vol.49,p.357.

(5). BLAHA,F., LANGENECKER,B.
'Plastizitatuntersuchungen von Metallkristallen in Altraschallfeld'.
Acta Met. 1959, Vol. 7, p.93.

(6). BLAHA,F., LANGENECKER,B., OELSCHLAGEL,D.
'Zum plastischen Verhalten von Metallen unter Schalleinwirkung'.
Zeitschraft fur Metallkunde 1960 Vol.51, p.636.

(7). BLAHA,F., LANGENECKER,B.
'Plastic Behaviour of Metal Crystals when exposed to Sound Waves'.
Bulletin of the National Institute of Sciences of India.
March 1959, No. 14.

(8). LANGENECKER,B., COLBERG,S., FRANSDEN,W.H.
'Plastic Deformation in Single Crystals of Zinc by Sound Waves'.
Bull.Am. Phys. Soc. 1962 Vol.8, p.362.

(9). LANGENECKER,B.
'Crystal Plasticity in Macrosonic Fields'.
Bull. Am. Phys. Soc. 1963 Vol.8, p.288.

(10). FITZGERALD,E.R.
'Mechanical Resonance Dispersion in Crystalline Polymers at Audio Frequencies'.
J. Chem. Phys. 1957, Vol.27, p1180.

(11). FITZGERALD,E.R.
'Mechanical Resonance Dispersion in Single Crystals'.
Phys. Rev. 1958, Vol. 102, p.1063.

(12). FITZGERALD,E.R.
'Yield Strength of Crystalline Solids from Dynamic Mechanical Measurements'.
J.E.Lay and L.E.Malvern, Eds., Developments in Mechanics, Vol.1, New York, Plenum Press 1961,p.10-38.

(13). NEVILL,G.E., BROTZEN,F.R.
'Effect of Vibrations on the Yield Strength of a Low-Carbon Steel'.
Technical Document No. AFOSR-TN-57-170.
Rice Institute, Houston, Texas, Air Force Contract AF49(638)-78, April 1957.

(14). SIEGEL,R.
'Der Einfluss von Ultachall auf das Kriechen von Kupferfedern'.
Annalen der Physik 1959, Vol.5, p.107.

(15). OELSCHLAGEL,D.
'The Deformation of Single Zinc Crystals under the Effect of Ultrasonics'.
Zeitschrift der Metallkunde 1962, Vol.53, No.6,p.361.

(16). SEVERDENKO,V.P., KLUBOVICH,V.V.
'The Effect of Ultrasonic Oscillations on the Process of Extension of Copper'.
'Primenenie Ul'trzuka v Machinostr'. Nauka i Teknika, Minsk, 1964, p.3-6.

(17). MELEKA,A.H., HARRIS,L.B.
'Cyclic-induced Ductility in Zinc'.
Nature 1962, Vol.193, No.4817, p.770-771.

(18). HAVERBECK,K.E., WEBER,R.R.
'Interim Engineering Progress Report'.
Air Force Contract AF33(657)-10821. Oct. 1963.

The Effect of Oscillatory Stresses on the Forming of Metals.

(19). BOBORYKIN,Iu.A.
'Use of the Vibration Process for the Working of Metals'
Kuznechno-Shtampovochnoe Proizvodstvo 1959,
No.6, p.21-22.

(20). FRIDMAN,H.D., LEVESQUE,P.
'Reduction of Static Friction by Sonic Vibrations'.
J.of App. Phys. 1959, Vol.30, p.1572-1575.

(21). BALAMUTH,L.
'Sonic Forging Press is a Possibility'.
Metal Working Production, March 17th., 1965.p.52-53.

(22). SHESTAKOV,S.N., KARNOV,M.Ya.
'Structure and Properties of Alloys (and Steel)
After Vibrational Working'.
Metallovedenie i Obrabotka Metallov, July 1958,
No.7, p.35-38. (Brutcher Trans. No.4281).

(23). SOGRISHIN,Yu.P.
'Vibrational Working of Metal'.
Metallovedenie i Permich. Obrabotka Metallov 1959.
No.1, p.55-57. (Brutcher Trans. No.4484).

(24). KARNOV,M.Ya., SHESTAKOV,S.N.
'Vibro-Forging of Aluminium Alloys'.
Metallovedenie i Termich. Obrabotka Metallov 1959.
No.1. p.57-59 (Brutcher Trans. No.4485).

(25). LYSAK,L.I., SOGRISHIN,Yu.P.
'Effect of Method of Plastic Deformation on
Internal Stresses in Metals'.
Sbornil nauch.rab.Inst. Metallofiz. Akad.Nauk Ukr.
(Kiev.) S.S.R. 1959, No,9. p.22-26.
(Translation No. BISI 2371).

(26). KARNOV,M.Ya., VORONIN,A.A.
'Deformation by Vibration'.
Kuznecho-Shtampovochnoe Proizvodstvo 1960,
Vol.2, No.3, p.3-8.
(Translation No.BISI 1987).

(27). KARNOV,M.Ya.
'Some problems of the Vibration Deformation of
Metals with Restriction of Spread'.
Kuznechno-Shtampovochnoe Proizvodstvo 1961,
Vol.3, No.3, p.16-18. (Translation No. BISI 2528).

(28). KARNOV,M.Ya.
'On the Determination of Work of Deformation
under Conditions of Vibrational Loading'.
Kuznechno-Shtampovochnoe Proizvodstvo 1961,
Vol.6, p.21-23. (Translation No. BISI 2903).

(29). FLEISCHHACKER,F.
'Forging Process Employing Superimposition of Vibratory Forces Concurrently with Normal Forging Forces'.
Ladish Co. ASD Technical Report 61-7-496, July 1961, U.S.A.F. Contract AF33 (600)-37462.

(30). SEVERDENKO,V.P., KLUBOVICH,V.V.
'Deformation of Metal in the Ultrasonic Field'.
Doklady akad. Nauk Belorusskoi S.S.R. 1961.
Vol.5, No.1, p.15-16.

(31). SEVERDENKO,V.P., KLUBOVICH,V.V.
'Distribution of the Deformation Height in a Ultrasonic Field'.
Izrestiya Vysshikh Uchebriich Zavedenii Chernaya Metallurgiya. Vol.1, 1965. p.61-64.

(32). BOCHAROV,Y., KOBAYASHI,S., THOMSEN,E.G.
'The effect of Vibration on Plastic Flow in Coining'.
A.S.M.E. Trans. (J. of Eng. for Indty). Nov.1962.
p.502-508.

(33). JONES,J.B., DePRISCO,C.F., MAROPIS,N., THOMAS,J.G.
'Ultrasonic Energy applied to Aluminium Extrusion Cladding of Tubes'.
Report No. DP-418. Aeroprojects Incorporated,West Chester, Pennsylvania. Contract No. AT (07-2)-1
Nov. 1959.

(34). TARPLEY,W.B., YOCOM,K.M., PHEASANT,R.
'Ultrasonic Extrusion; Reduction in Vehicle and Plasticizer Requirements for Non-Clay Ceramics'.
Report No.NYO-10006. Aeroprojects Incorporated, West Chester, Pennsylvania. Contract No.AT(30-1)-1836.
Nov. 1961.

(35). PEACOCK,J.
'Forming Goes Ultrasonic'.
American Machinist/Metalworking Manufacturing.
Vol. 105, No,24 Nov. 27th. 1961, p.83-85.

(36). LANGENECKER,B., FOUNTAIN,C.W., JONES,V.O.
'Ultrasonic Aid to Metal Forming'.
Metal Progress, April 1964, p97-101.

(37). TARPLEY,W.B., KARTLUKE,H.
'Ultrasonic Tube Drawing; Niobium, Zircaloy-2, and Copper'.
Report No. NYO-10008. Aeroprojects Incorporated, West Chester, Pennsylvania. Contract No. AT(30-1)-1836.

(38). SEVERDENKO,V.P., KLUBOVICH,V.V.
'Drawing of Copper Wire in an Ultrasonic Field'.
Trans. from Doklady S.S.S.R. 1963, Vol.7, No.2.
p.95-98.
Air Force Systems Command, Wright-Patterson Air Force Base, Ohio. (AD 417,408)

(39). ROBINSON,A.T., CONNELLY,J.C., STAYTON,L.M.
'The Application of Ultrasonics to Wire Drawing'.
U.S.Naval Test Ordnance Station, China Lake, California.

Report April - June 1963	N.T.P.3297,	TPR.328.
Report Oct. - Dec. 1963	N.T.P.3463,	TPR.352.
Report Jan. - Mar. 1964	N.T.P.3542,	TPR.304.
Report April - June 1964	N.T.P.3636,	TPR.375.
Report July - Sept.1964	N.T.P.3675,	TPR.382.
Report Oct. - Dec. 1964	N.T.P.3768,	TPR.390.
Report Jan. - Mar. 1965	N.T.P.3836,	TPR.399.
Report July - Sept 1965	N.T.P.3976,	TPR.420.

(40). RESEARCH & DEVELOPMENT DEPT.
THE STEEL CO. OF CANADA LTD.
'Ultrasonic Vibration of Wire Dies'.
File No.780. March 1965.

(41). NOSAL, V.V., RYMSHA,O.M.
'Reducing the Drawing Forces by Ultrasonic Oscillations of the Drawplate and Determination of the Technological Parameters of Tube Drawing'.
Stal in English, Feb.1966. p.135-137.

(42). ROBINSON, A.T.
Personal Communication to C.E.Winsper reference - 4513/ATR:fwb.
dated 8th.Aug. 1966.

Mechanics of Wire Drawing.

(43). WISTREICH J.G.
'The Fundamentals of Wire Drawing'.
Metallurgical Reviews,
Vol.3. No.10, 1958, p.97-142.

(44). WISTREICH.J.G.
'Investigation of the Mechanics of Wire Drawing'.
Proc. Inst. of Mech. Engrs.
Vol.169, 1955, p. 654.

(45). WHITTON.P.W.
'Calculation of Drawing Force and Die Pressure in Wire Drawing'.
J. Inst. Metals
Vol. 86, 1957/8,p.417-421.

Miscellaneous.

(46). HIGGINS, R.A.
'Engineering Metallurgy Part 1'.
English Universities Press 1957.

(47). JOHNSON,W., MELLOR, P.B.
'Plasticity for Mechanical Engineers'.
Van Nostrand Ltd. 1962.

(48). FORD,H., ALEXANDER, J.M.
'Advanced Mechanics of Materials'.
Longmans Press. 1963.

(49). ALEXANDER,J.M., BREWER.R.C.
'Manufacturing Properties of Materials.
Van Nostrand Ltd. 1963.

(50). OLDROYD, P.W.J., BURNS.D.J., BENHAM.P.P.
'Strain Hardening and Softening of Metals produced by Cycles of Plastic Deformation'.
Presented Applied Mechanics Convention. 1966.
Published Proc. Instn. Mech. Engrs. Vol.180, part 31.

(51). DEN HARTOG, J.P.
'Mechanical Vibrations'.
McGraw - Hill, 1956.

(52). SETO, W.W.
'Mechanical Vibrations'.
Schaum Publishing. 1964.

16. Appendices

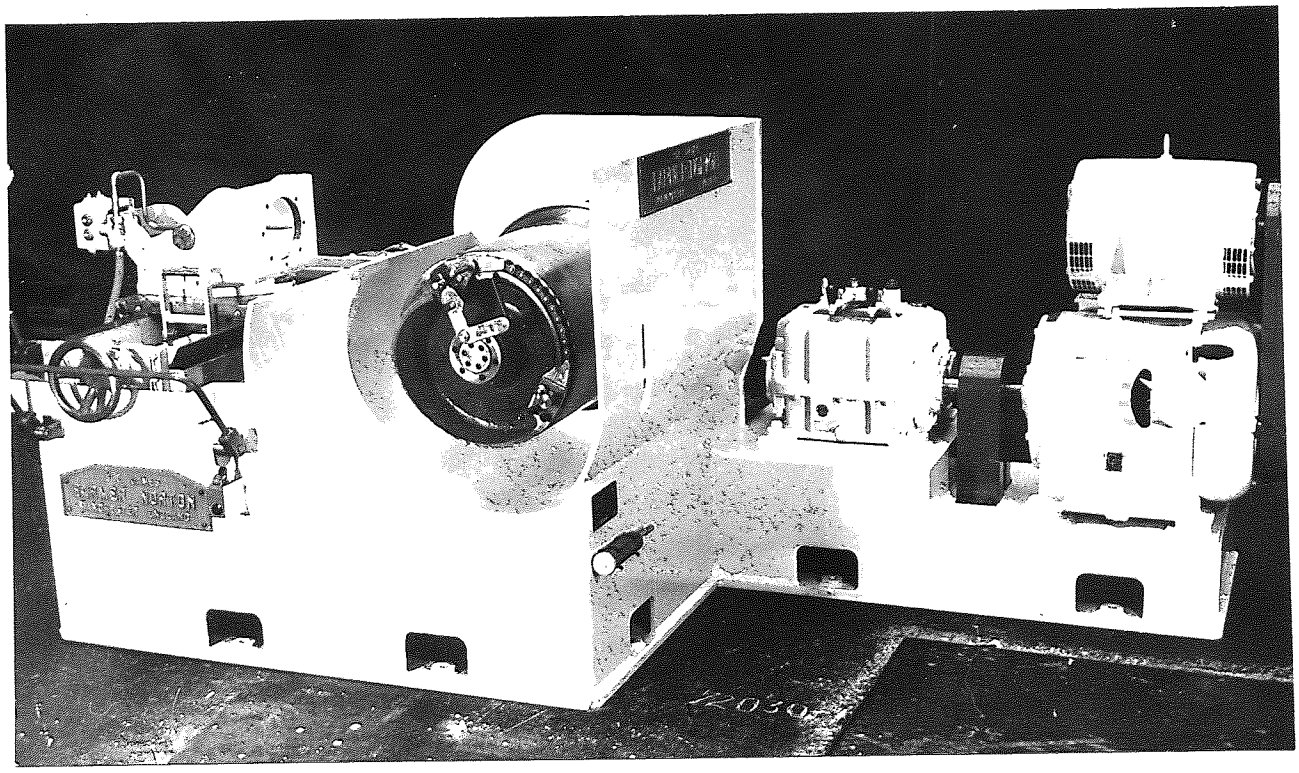

FIG. NO. 71 DETAILS OF BULL-BLOCK

16. Appendices

16.1. Description of Drawing Machine.

The drawing machine used was a horizontal bull-block. (see Fig. No.71). It consisted of a fabricated steel frame on which was mounted an 18 in. diameter drum having an 18 in. long working surface. The drum which was carried on a carbon steel shaft, was mounted horizontally and supported in heavy duty roller bearings and driven through a totally enclosed wormgear. The base of the frame formed a reservoir for the lubrication of the gears. The bull-block was provided with a traversing die-box for drawing tube, and the drum was designed with a back flange for drawing wire. The die-box was mounted on guides and was driven by a lead screw to give 0.75 in. traverse per revolution of the drum

The block was designed for drawing speeds of 120, 240, 360 and 480 ft/m. which were selected by means of a four speed gear box. The drum speed was infinitely variable from 1.3 ft/m. up to 480 ft/m. The drive was arranged so that a maximum die pull of 2,300 lbf. was available up to a maximum speed of 120 ft/m. At speeds above 120 ft/m. the die pull available was reduced gradually giving a value of 575 lbf. at 480 ft/m.

The drum shaft was driven through a variable speed oil gear and a four speed gear box by a 15 h.p. squirrel cage induction motor.

Gripping jaws were supplied for gripping wire up to 0.375 in. diameter.

16.2. Hydraulic Oscillator.

16.2.1. General Description.

The equipment was designed to operate over a frequency range of d.c. to 500 c/s. The actuator had a maximum thrust of 4,500 lbf. and a total stroke of 0.25 ins. The oscillator was controlled by a single channel servo-system and this allowed the actuator piston to be positioned conveniently. The position of the piston was measured by means of a rotary transducer which translated the linear motion of the piston to rotary motion.

The transducer was an a.c. pick-off energised by a 2.4×10^3 c/s. supply. Thefeed-back signal from the pick-off was demodulated before it was accepted by the d.c. amplifier. The output from the transducer was proportional to the displacement of the actuator and was fed to the servo amplifier in such a way as to tend to cancel the input signal.

The signal from the servo amplifier was fed to an electro-hydraulic servo valve which activated the first stage of the piston. The output from the amplifier was proportional to the difference between the signal voltage (from an oscillator), and the feed-back voltage.

Owing to capacitive effects the impedance of the electro-hydraulic servo valve increased as the frequency increased. Therefore, in order to counteract this effect, and maintain the frequency response characteristics of the

system, a constant current unit was built in the electronic control console.

16.2.2. The Actuator.

The actuator was a double acting jack with a rod extension at each end. Hydraulic fluid under pressure was delivered by the powerpack via the servo valves to the actuator. An adaptor block which carried the servo valves was fixed to the side of the actuator body. Oilways were drilled in the adaptor block and actuator to carry pressure and return line fluid, and to collect fluid which was allowed to leak in a controlled manner through the metal gland seals. These 'drained gland' seals allowed a controlled leakage from the pressure chamber inside the actuator which kept the oil cool when operating under high frequency, small amplitude conditions. A further advantage was realised by causing a pressure gradient along the length of the gland enabling the normal high pressure seal to be replaced by a low pressure seal, thus lengthening the working life.

A one inch diameter hole was provided through the piston rod to enable the wire to be passed through.

The total movement of the jack was 0.25in. and it had a cross-sectional area of 1.5 in^2. The hydraulic power unit was capable of delivering 6 gal/m. of hydraulic fluid at a pressure of 3000 lbf/in^2. to the actuator thus giving it a maximum dynamic thrust of 3000 lbf. at a maximum velocity of 18.5 in/s. The maximum static thrust

attainable was 4500 lbf.

16.2.3. Hydraulic Power Supply Unit.

The unit comprised a pressure-compensated variable-delivery pump driven by an electric motor. The pump was immersed inside the hydraulic reservoir and delivered the fluid under pressure through an accumulator, and a micro filter, to the actuator. The return flow passed through a cooler system back to the reservoir.

16.2.4. Electronic Control Unit.

Servo Unit - The servo unit controlled the actuator and power was supplied from an oscillator. The 'gain' control consisted of a decade attenuator with a 1/10 switch and a continuous rotary 'fine' control. A balance control was incorporated in the unit to enable the jack to be positioned at any point along its travel before vibration was superimposed. Also included in the design of the servo unit, was a constant current device to maintain a good response characteristic as high frequencies.

Carrier Generator Unit.- This unit supplied a 24 volt R.M.S. signal at 2.4×10^3 c/s. to the feed-back transducer, and the demodulator. The oscillator was a resistance capacitance type, designed to provide a very stable output.

Power Supply Unit- This unit provided a stabilised d.c. 12 - 0 - 12 voltage for operating the servo unit.

16.2.5. Specification.

Actuator

Bearing type	Drained Gland
Frequency Range	d.c. to 500 c/s.
Stroke	$\pm$ 0.125 in.
Effective Ram Area	1.5 in^2.
Maximum Thrust	4,500 lbf.
Thrust at Maximum Velocity.	3,000 lbf.
Maximum Velocity	18.5 in/s.
Mounting	Flange at end drilled with 7 holes 17/32 in.dia. on a 7 in. P.C.D.
Piston Rod	1 7/8 in. BSF.thread by 13/16 in. deep with a 1 in. dia. hole drilled through the piston centre along its axis.

Hydraulic Power Supply Unit.

Fluid Type	Shell Tellus 27
Fluid Capacity	15 gallons
Filter	5 micron
Pump Delivery	6 gal/m.
System Pressure	3,000 lbf./$in.^2$
Electronic Motor (Pump)	15 hp.
Electric Motor (Cooler)	0.5 hp.
Accumulator	Charged at 1500 lbf/in^2.

Electronic Control Unit.

Internal Oscillator Range.	0.01 to 1,000 c/s.
External Signal Input.	5 volt peak
Input Impedence	20 x 10^3 ohm.

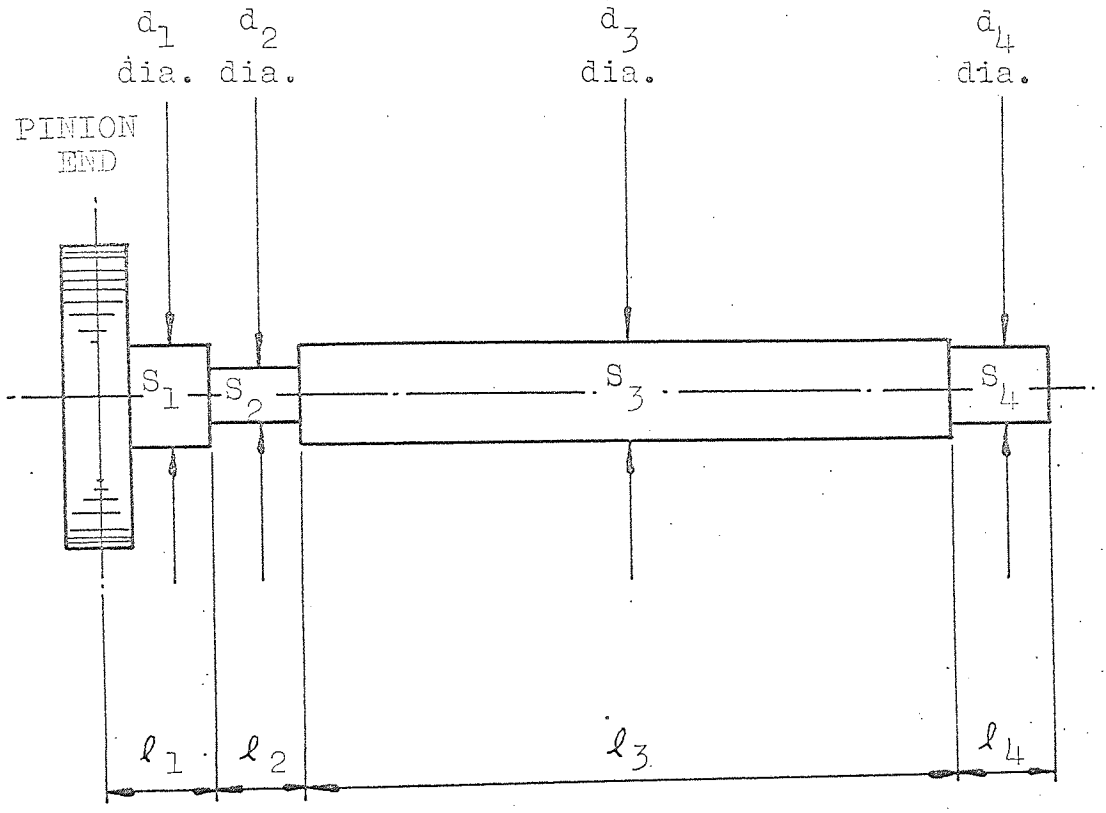

FIG.NO. 72 DIAGRAM TO ESTABLISH STIFFNESS OF DRUM SHAFT

16.3. Computation of Drawing Speed.

Ratio of worm shaft speed to pinion speed =14.66 to 1

let 't' = the time taken for the worm shaft to rotate a quarter of a revolution, then the time taken for the worm shaft to rotate a complete revolution = 1/14.66 times the time taken for the drum to rotate a complete revolution = 4 t seconds.

therefore, the speed of the drum 'V' $= \frac{60 \cdot 2\pi}{14.66 \cdot 4t}$ rad/m.

$$V = \frac{60 \cdot 2\pi \cdot 9}{12 \cdot 14.66 \cdot 4t} \text{ ft/m.}$$

$$\underline{\text{Drawing Speed} = \frac{4.82}{t} \text{ ft/m.}}$$

16.4. Stiffness Determination for the parts of the Bull-block.

16.4.1. Stiffness of Drum Shaft.

From Fig. No. 72,

$d_1 = d_3 = 4.0$ in. $\quad \ell_1 = 6.0$ in.

$d_2 = 2.5$ in. $\quad \ell_2 = 4.0$ in.

$d_4 = 3.0$ in. $\quad \ell_3 = 20.5$ in.

$\ell_4 = 3.5$ in.

Stiffness $S = \frac{GJ}{\ell}$ where $G = 12 \times 10^6$ lbf./in.^{2}, therefore

$$S_1 = \frac{12 \cdot 10^6}{6.0} \left[\frac{\pi \cdot 4.0^4}{32} \right]$$

$S_1 = 50.2 \times 10^6$ in. lbf/rad.

$$S_2 = \frac{12 \cdot 10^6}{4.0}\left[\frac{\pi \cdot 2.5^4}{32}\right]$$

$$S_2 = 11.52 \times 10^6 \text{ in.lbf/rad.}$$

$$S_3 = \frac{12 \cdot 10^6}{20.5}\left[\frac{\pi \cdot 4.0^4}{32}\right]$$

$$S_3 = 14.72 \times 10^6 \text{ in.lbf/rad.}$$

$$S_4 = \frac{12 \cdot 10^6}{3.5}\left[\frac{\pi \cdot 3.0^4}{32}\right]$$

$$S_4 = 27.30 \times 10^6 \text{ in.lbf/rad.}$$

If S = the equivalent stiffness of the drum shaft then

$$\frac{1}{S} = \frac{1}{S_1} + \frac{1}{S_2} + \frac{1}{S_3} + \frac{1}{S_4}$$

therefore

$$\frac{1}{S} = \left[\frac{1}{50.20} + \frac{1}{11.52} + \frac{1}{14.72} + \frac{1}{27.30}\right]\frac{1}{10^6}$$

$$S = 4.74 \times 10^6 \text{ in.lbf/rad.}$$

16.4.2. Stiffness of Bull-block Drive.

(for slow drawing speed, 1.3 ft/m.)

from Fig. No. 53.

$d_2 = 1.75$ in. $\quad \ell_2 = 25.0$ in. $\quad R_1 = 14.66$

$d_3 = 1.50$ in. $\quad \ell_3 = 27.0$ in. $\quad R_2 = 3.70$

$d_4 = 1.375$ in. $\quad \ell_4 = 13.0$ in. $\quad R_3 = 50.00$

$$S_1 = 4.74 \times 10^6 \text{ in.lbf/rad.}$$

$$S_2 = \frac{12 \cdot 10^6}{25.0}\left[\frac{\pi \cdot 1.75^4}{32}\right]$$

$$S_2 = 0.442 \times 10^6 \text{ in.lbf/rad.}$$

$$S_3 = \frac{12 \cdot 10^6}{27.0}\left[\frac{\pi \cdot 1.50^4}{32}\right]$$

$$S_3 = 0.221 \times 10^6 \text{ in.lbf/rad.}$$

$$S_4 = \frac{12 \cdot 10^6}{13.0}\left[\frac{\pi \cdot 1.375^4}{32}\right]$$

$$S_4 = 0.323 \times 10^6 \text{ in.lbf/rad.}$$

from equation (4), page 84,

$$\frac{1}{S_e} = \frac{1}{10^6}\left[\frac{1}{4.74} + \frac{1}{(14.66)^2 0.442} + \frac{1}{(14.66)^2(3.7)^2 0.221} + \frac{1}{(14.66)^2(3.7)^2(50.0)^2 0.323}\right]$$

$$\underline{S_e = 4.48 \times 10^6 \text{ in.lbf/rad.}}$$

16.4.3. Stiffness of Loadmeter and Drawn Wire.

$$\text{Stiffness} = K = \frac{EA}{\ell}$$

for the loadmeter assume $E = 29 \times 10^6$ lbf/in.^{2}, and therefore

$$K_1 = \frac{29 \cdot 10^6}{1.375}\left[\frac{\pi}{4}(1.2^2 - 1.0^2)\right]$$

$$\underline{K_1 = 7.29 \times 10^6 \text{ lbf/in.}}$$

for the drawn wire assume $E = 30 \times 10^6$ lbf/in.^{2}, and therefore

$$K_2 = \frac{30 \cdot 10^6}{18.0}\left[\frac{\pi}{4} \cdot 0.158^2\right]$$

$$\underline{K_2 = 0.032 \times 10^6 \text{ lbf/in.}}$$

16.5. Determination of Natural Frequencies of Bull-block when drawing Mild Steel wire, 0.158 in. diameter.

$K_1 = 7.29 \times 10^6$ lbf/in. $\quad m = 13.8$ lbf.

$K_2 = 0.032 \times 10^6$ lbf/in. $\quad s = 4.48 \times 10^6$ in.lbf/r.

$I_1 = 53.77$ lbf.in.s^2 $\quad r = 9.0$ in.

note :- 'm' was determined from the loadmeter signal for free oscillation of the die.

From the frequency equation (10), page 90,

$$\omega^2 = 12.9 \times 10^4 \text{ and } 203.5 \times 10^6 \text{ (rad/s.)}^2$$

$$\omega = 359 \text{ rad/s. and } 14{,}270 \text{ rad/s.}$$

$$\omega = 57 \text{ c/s. and } 2271 \text{ c/s.}$$

16.6 Determination of Damping Forces.

From Graph No.1 $C = 225$ ft.lbf.s/rad.

$$\text{now } \theta = \hat{\theta} \sin \omega t$$

$$\text{and the damping torque } T_F = C \frac{d\theta}{dt}$$

$$\text{and therefore } T_F = C\hat{\theta}\omega \cos \omega t$$

The maximum damping torque $= C\hat{\theta}\omega$ lbf.ft. ,and therefore the maximum damping force $= C\hat{\theta}\omega/0.75$ lbf. $= F_F$

at 125 c/s. $\quad F_F = \dfrac{225(125 \cdot 2\pi)(1.45 \cdot 10^{-4})}{0.75}$

$$F_F = 34 \text{ lbf.}$$

at 100 c/s. $\quad F_F = \dfrac{225(100 \cdot 2\pi)(2.53 \cdot 10^{-4})}{0.75}$

$$F_F = 47 \text{ lbf.}$$

at 75 c/s. $F_F = \frac{225\ (75\ .\ 2\pi)(4.97\ .\ 10^{-4})}{0.75}$

$F_F = 70$ lbf.

at 50 c/s. $F_F = \frac{225\ (50\ .\ 2\pi)(16.73\ .\ 10^{-4})}{0.75}$

$F_F = 156$ lbf.

at 25 c/s. $F_F = \frac{225\ (25\ .\ 2\pi)(6.54\ .\ 10^{-4})}{0.75}$

$F_F = 30$ lbf.

Note :- All values of F_F are peak to peak values and correspond to a peak to peak amplitude of die oscillation of 0.015 in.

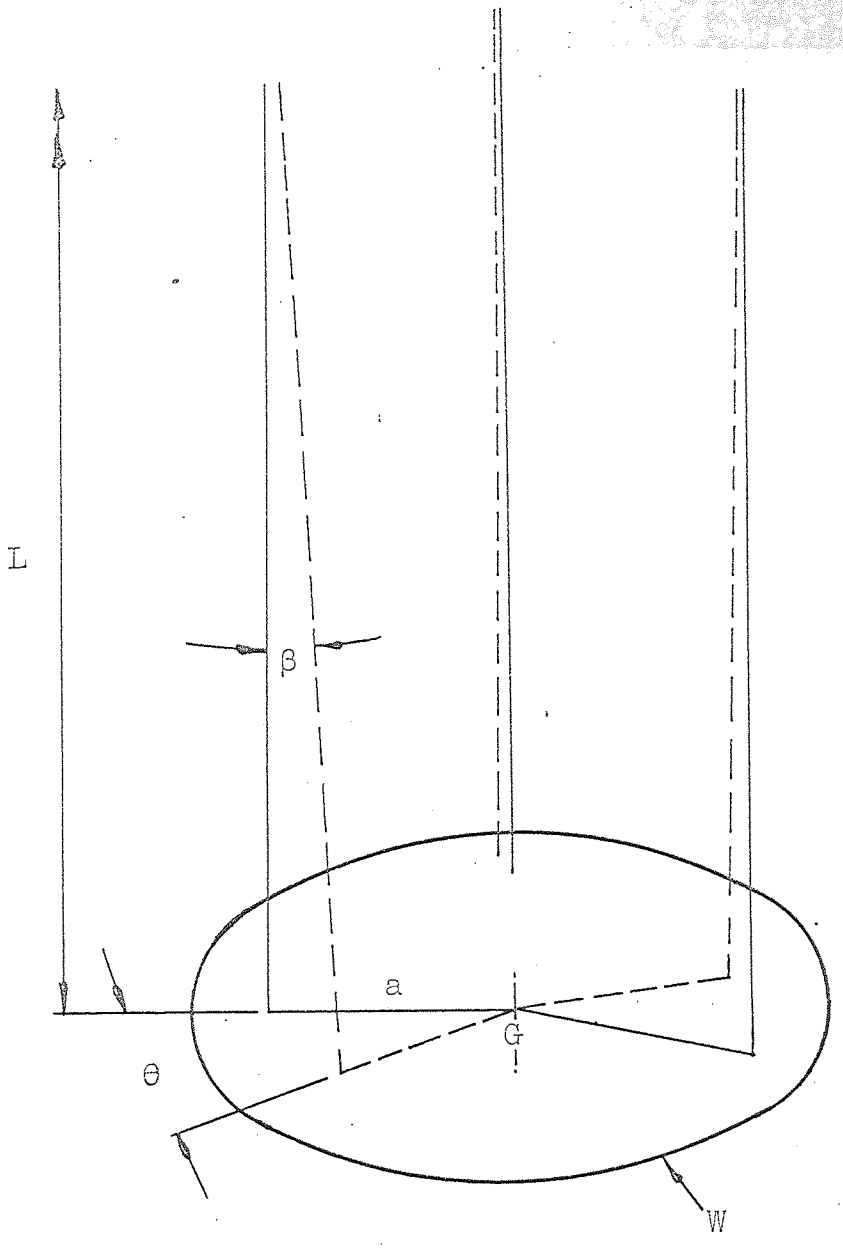

FIG. NO. 73 SYMBOLS USED IN TRIFILAR SUSPENSION CALCULATION

16.7. Determination of Drum Inertia by Trifilar Suspension.

16.7.1. Description of Tests.

A 24 in. diameter aluminium disc of known weight was supported from a bulk-head by three 65.5 in. long, alloy steel, multi-core cables approximately 1/16 in. diameter. The disc was given a small torsional displacement and allowed to oscillate freely. The time taken for the disc to complete fifty oscillations was then recorded. The bull-block drum was next weighed and then placed centrally on the disc and the new time for the disc and drum to complete fifty oscillations was recorded. From these observed periodic times, the moment of inertia of the drum was computed.

16.7.2. Theoretical Analysis.

From Fig. No. 73, let the tension in each wire be

$$F = \frac{W}{3}$$

and therefore the horizontal component P,

$$= F \tan \beta$$

$$= \frac{W}{3} \tan \beta$$

the moment of this component about the axis of the disc

$$= Pa \cos \frac{\theta}{2}$$

$$= \frac{W}{3} a \tan \beta \cos \frac{\theta}{2}$$

if θ and β are small then $\cos \frac{\theta}{2} \simeq 1$, and $\tan \beta \simeq \beta$

then the moment about the axis of the disc

$$= \frac{W}{3} a \beta$$

The total moment applied to the disc

$$= 3\left[\frac{Wa}{3}\,\beta\right] = Wa\beta \qquad \text{——————————(1)}$$

also the moment = the inertia torque, and therefore

$$= I\,\frac{d^2\theta}{dt^2} = \frac{W}{g}\,k^2\,\frac{d^2\theta}{dt^2} \qquad \text{——————————(2)}$$

equating equations (1) and (2),

$$\frac{W}{g}\,k^2\,\frac{d^2\theta}{dt^2} = Wa\beta$$

$$\frac{k^2}{g}\,\frac{d^2\theta}{dt^2} = a\beta \qquad \text{——————————(3)}$$

also $\ell\beta \triangleq a\theta$, and therefore $\beta = \frac{a\theta}{\ell}$

Substituting in equation (1),

$$\frac{k^2}{g}\,\frac{d^2\theta}{dt^2} = \frac{a^2\theta}{\ell}$$

$$\frac{d^2\theta}{dt^2} + \frac{ga^2}{k^2\ell}\,\theta = 0$$

which equals the equation of simple harmonic motion, where

$$\omega^2 = \frac{ga^2}{k^2\ell}$$

The periodic time t,

$$= \frac{2\pi}{\omega} = 2\pi\sqrt{\frac{k^2\ell}{ga^2}} \qquad \text{——————————(4)}$$

therefore, knowing the time 't' the value of k^2 and hence 'I' can be determined.

Also $I_{drum} = I_{(drum + disc)} - I_{disc}$ _____(5)

16.7.3. Computation of Drum Inertia.

weight of disc = 42.73 lbf.

weight of drum = 372.6 lbf.

effective length of cable = ℓ = 65.5 in.=5.46 ft.

radius of drum = a = 10.44 in. = 0.871 ft.

average time per 50 oscillations = 63.7 s.

and therefore periodic time =1.273s.(disc).

average time per 50 oscillations = 89.7 s.

and therefore periodic time = 1.792 s. (disc and drum)

Disc only

$$t = 2\pi\sqrt{\frac{k^2\ell}{ga^2}}$$

$$1.273 = 2\pi\sqrt{\frac{5.46 \cdot k^2}{32.2(0.871)^2}}$$

$$k^2 = 0.184 \text{ ft.}^2$$

therefore

$$I_{disc} = \frac{W}{g}k^2 = \frac{42.73 \cdot 0.184}{32.2}$$

$$\underline{I_{disc} = 0.24 \text{ lbf.ft.s.}^2}$$

Disc and Drum.

$$1.792 = 2\pi\sqrt{\frac{5.46 \cdot k^2}{32.2(0.871)^2}}$$

$$k^2 = 0.364 \text{ ft.}^2.$$

therefore

$$I_{(\text{disc + drum})} = 4.70 \text{ lbf.ft.s.}^2$$

substituting in equation (3),

$$I_{(\text{drum})} = (4.70 - 0.24) \text{ lbf.ft.s.}^2$$

$$I_{(\text{drum})} = 4.46 \text{ lbf.ft.s.}^2$$
$$= 53.52 \text{ lbf.in.s.}^2$$

Approximate moment of inertia of drum shaft

$$= 0.75 \text{ lbf.in.s.}^2$$

and therefore, the correction to be added to the moment of inertia of the drum = 0.25 lbf.in.s.^{2}

$$I_{(\text{drum})} = 53.77 \text{ lbf.in.s.}^2$$

16.8. Drawing Material Specification.

Mild Steel.

Mild Steel EN.2B, B.S.970, fully annealed and lubricated with a phosphate coating,

analysis -	Carbon	: 0.15 % max.
	Manganese	: 0.50 % max.
	Sulphur	: 0.050 % max.
	Phosphorus	: 0.050 % max.

Stainless Steel.

Niobium stabilised, SAE 305, copper coated to a depth of 3×10^{-4} to 5×10^{-4} in., supplied with a phosphate coating having received a 7 per cent reduction in area.

analysis -	Carbon	: 0.12 % max.
	Silicon	: 1.00 % max.
	Manganese	: 2.00 % max.
	Nickel	: 10.00 to 13.00 %
	Chromium	: 17.00 to 19.00 %
	Sulphur	: 0.030 % max.
	Phosphorus	: 0.045 % max.

Aluminium Alloy.

Aluminium HG.9, B.S.1475, Condition W.P., fully heated treated.

analysis -	Copper	: 0.10 % max.
	Magnesium	: 0.4 to 0.9 %
	Silicon	: 0.3 to 0.5 %
	Iron	: 0.5 % max.

Manganese : 0.03 % max.

Chromium : 0.10 % max.

Zinc : 0.10 % max.

Aluminium the remainder.

Pure Aluminium.

99.8 per cent Pure Aluminium G.1A, B.S.1475, condition 'O', fully annealed.

analysis - Copper : 0.02 % max.

Silicon : 0.15 % max.

Iron : 0.15 % max.

Manganese : 0.03 % max.

Zinc : 0.06 % max.

Copper + Silicon + Manganese + Zinc = 0.20 % max.

O.F.H.C. Copper.

Oxygen free high conductivity copper. B.S.2873, C.103, supplied cold worked having received a 40 per cent reduction in area.

analysis - Copper : 99.5 % max.

Lead : 0.005 % max.

Bismuth : 0.001 % max.

0.03 % impurities excluding oxygen and silver.

16.9. Specification of Recording Equipment.

Ultra Violet Galvanometer Recorder.

(S.E. Laboratories, type 2005)

The recorder is a 12 channel instrument, incorporating 15 paper speeds from 1.25 mm/s. to 2000 mm/s., in steps of 1.25, 5, 10 and 20 with a speed change over switch giving x1, x10 and x100. Accuracy of speed $\pm$ 2 per cent.

The recorder is supplied with a range of galvanometers enabling signals at frequencies up to 8×10^3 to be recorded.

Stabilised d.c. Supply.

(Thorn Electronics, type VP.21)

Output voltage	-	3 to 30 volt d.c. continuously variable.
Output current	-	Up to 1 ampere.
Output impedence	-	d.c. less than 0.01 ohm. a.c. less than 0.3 ohm at 10×10^{-3} c/s.
Ripple	-	less than 2 millivolt peak to peak.
Mains variation	-	Up to $\pm$ 10 per cent from nominal permissible.
Overload protection	-	Electronic cut-out incorporated.

Digital Counter.

(Research Electronics, model 5321)

This was used with the drawing speed measuring device.

Frequency measurement	- 5×10^3 c/s.
Speed of revolution measurement.	- 0 to 300×10^3 rpm.
Accuracy of time measured with a 10^3 c/s. reference signal.	- $\pm$ 0.001 s.

Oscillator.

(Dawe Instruments, type 445)

Frequency range	- 0.01 c/s. to 1000 c/s in five decades.
Calibration accuracy	- $\pm$ 3 per cent of scale reading. Scale was calibrated with an accuracy of $\pm$ 1 per cent on the 100 c/s. to 1000 c/s. range.
Distortion	- less than 0.5 per cent over the measured range 20 c/s. to 1000c/s.
Hum and noise level	- less than 0.2 per cent.
Output level	- 15 volt maximum continuously variable, in to a minimum load of 10×10^3 ohm .

Slip Ring Assembly.

Current rating	- 2.5 ampere R.M.S. maximum.
Circuit resistance (between slip ring and two brushes in parallel)	- 40 milliohm. max.
Starting torque	- 0.25 lbf.in. max.
Noise level	- less than 8 micro volt/ milliampere.

Vibration Meter.

(Bell and Howell Ltd.)

General :-	
Input impedance	- 10,000 ohm.
Linear deviation	- Less than $\pm$ 3 per cent of full scale deflection.
Attenuation accuracy	- Within $\pm$ 2 per cent of set value
Velocity Measurements :-	
Frequency response	- $\pm$ 3 per cent from 5 to 5×10^3 c/s.
Sensitivity (V x1.0 range)	- 278.0 to 834.0 millivolt.
(V x0.1 range)	- 27.8 to 83.4 millivolt.

Displacement Measurements :-

Frequency response - $\pm$ 4 per cent from 5 to 5×10^3 c/s.

Sensitivity (d x1.0 range)- 278.0 to 834.0 millvolt.
(d x0.1 range)- 27.8 to 83.4 millivolt.

Linear Seismic Transducer :-

Sensitivity - 135 $\pm$ 2 millivolt/in./s. at 100 c/s., into a 10×10^3 ohm load.

Frequency range - 15 to 2×10^3 c/s.

Natural frequency - 6 c/s.

Amplitude range - 0.25 in. peak to peak.

Torsiograph :-

Sensitivity - 9.4 millivolt/degree/s.

Frequency Response - 10 to 10^3 c/s.

Maximum Speed of Revolution- 6000 rpm.

Natural Frequency - 3 c/s.

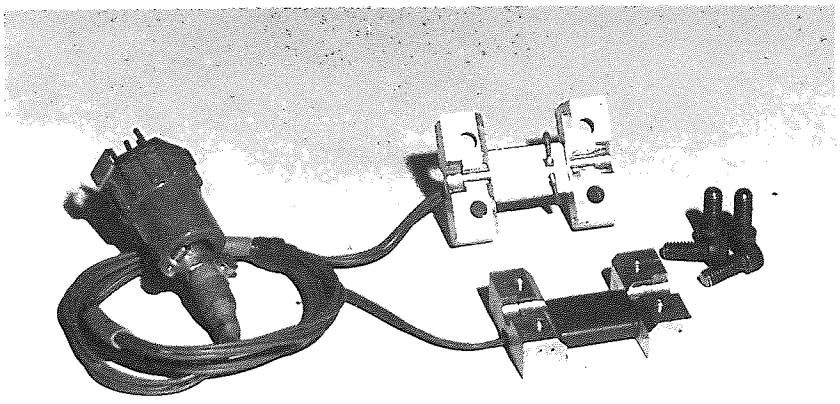

FIG. NO. 74. ALUMINIUM LOADMETER DETAILS

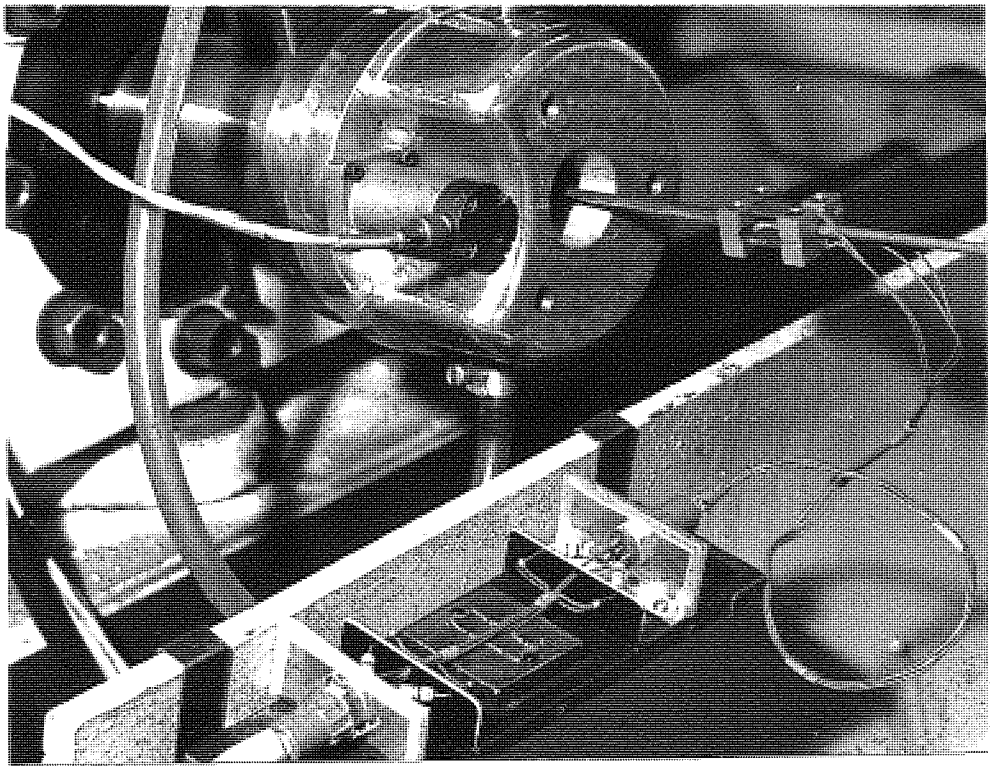

FIG. NO. 75 LOADMETER IN POSITION ON WIRE DURING A TEST

16.10 Design of Additional Loadmeters.

Because of the lengthy analysis required to determine the magnitude of force variation in the drawn wire, it was decided to try to measure this parameter directly. A strain gauge bridge bonded to the wire, provided a satisfactory method of measuring the force, but it took about a day to prepare and was expensive. It was possible to obtain five recordings only from each bridge before the wire carrying the gauges was wound on the drum and the bridge was destroyed. Furthermore, the time required for the preparation and bonding of the gauges meant that only a single set of readings could be obtained every twenty four hours. Therefore, to measure this force, two different types of loadmeter were designed. The details of these and the reasons for not using them in the main series of experiments are discussed in the following sections.

16.10.1. Aluminium Loadmeter.

The initial loadmeter was designed to clamp directly on the wire as shown in Fig. No.75. It was manufactured in two halves and was clamped to the wire by four small cap screws. The meter was made from an aluminium alloy, Duralumin, and was designed to give 0.1 per cent strain for a drawing force of 1800 lbf. Aluminium was selected because of its low density, ie. it was thought that, provided that the weight of the loadmeter was small, then

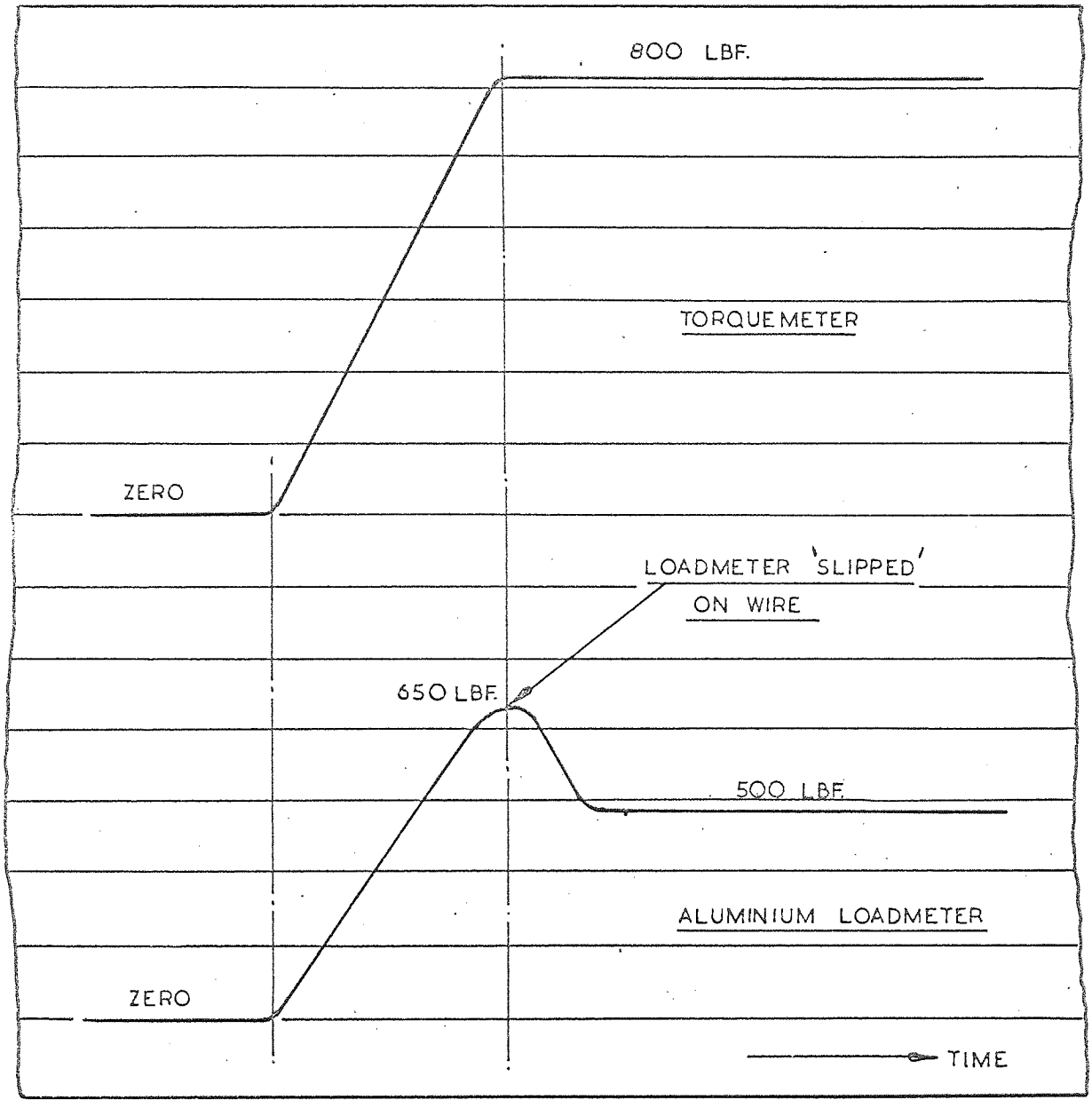

FIG. NO. 76 TYPICAL LOADMETER AND TORQUEMETER RECORD

its effect on the vibration characteristics of the bull-block and wire would be negligible.

Two 75 ohm. strain gauges were bonded to each half of the loadmeter and all four gauges were connected to form the active arm of a Wheatstone bridge. The three inactive arms were provided by twelve 75 ohm. gauges which were bonded to a block of Duralumin. The gauges on the block also provided the bridge with temperature compensation. All gauges were bonded by the same procedure as that adopted when manufacturing the torquemeter and main loadmeter.

The bridge current was supplied from a 24 volt stabilised d.c. supply and the bridge output signal was amplified and recorded on a channel of an ultra violet galvanometer recorder. The bridge was calibrated under non-oscillatory conditions before each test against the torquemeter and main loadmeter as described in section 6.3. Fig No. 74 shows details of the loadmeter.

16.10.2. Discussion of Results.

Commissioning tests with the loadmeter clamped to the wire showed that for small drawing forces (ie. less than 650 lbf.), the meter functioned correctly. However, for drawing forces above this level, the loadmeter was found to 'slip' on the wire (Fig. No. 76 shows a typical loadmeter record). The force at which slipping started was found to be dependent upon the loadmeter clamping pressure, and therefore a series of tests were performed with varying

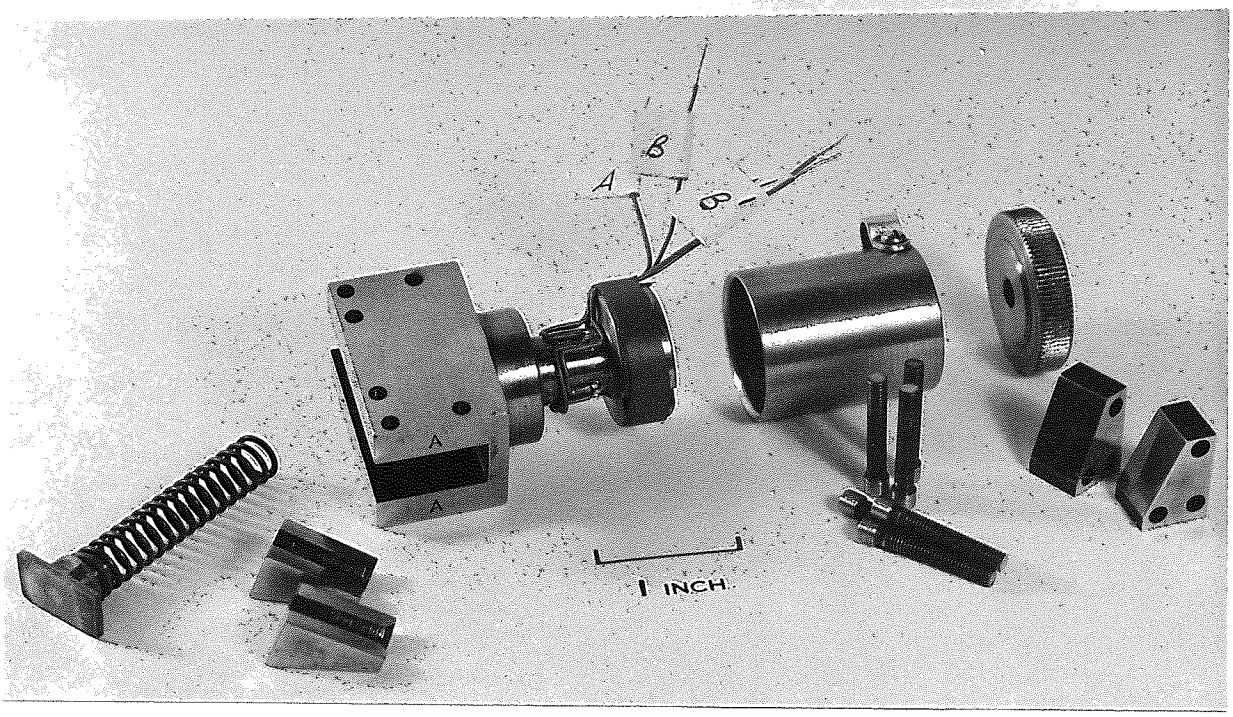

FIG. NO. 77. STEEL LOADMETER DETAILS

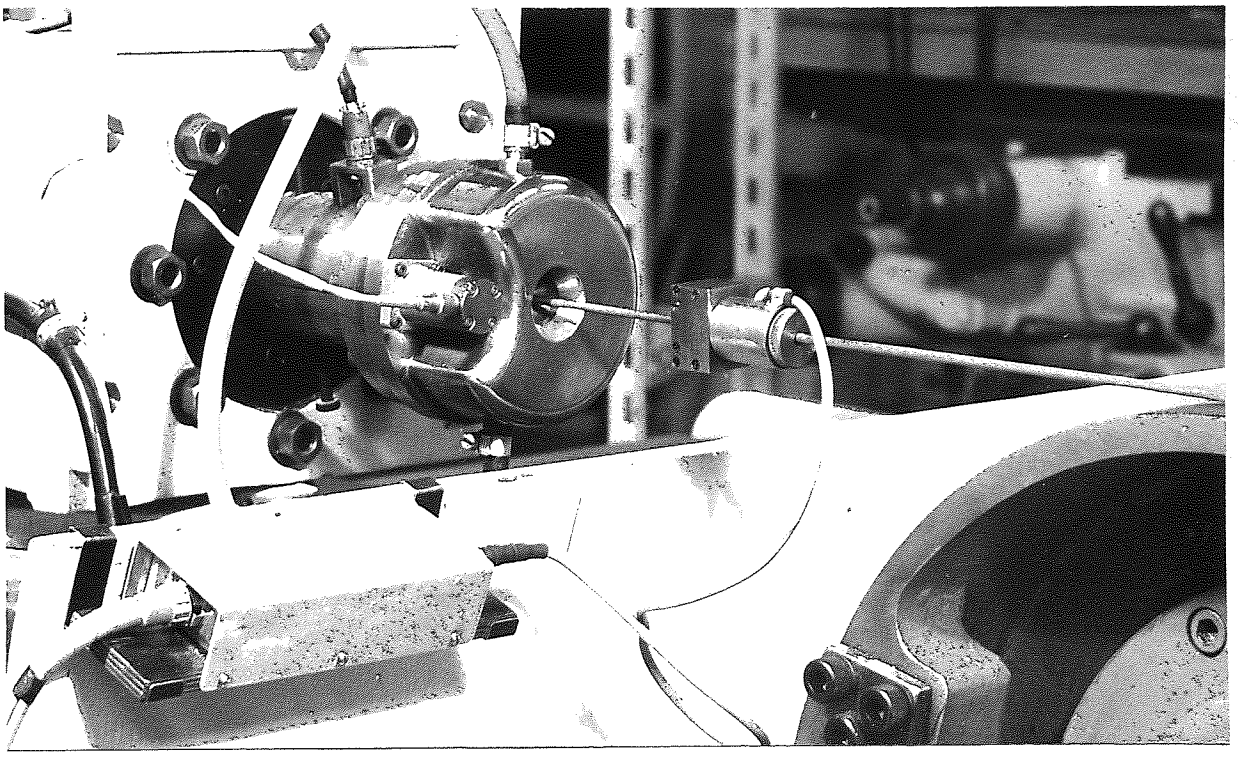

FIG. NO. 78 LOADMETER IN POSITION ON WIRE DURING A TEST

pressures up to a value where distortion of the loadmeter was observed. For all pressures tested, the loadmeter was found to 'slip' on the wire. This phenomenon could not be overcome and therefore the loadmeter design was discarded.

16.10.3. Steel Loadmeter.

After further deliberation, it was decided to manufacture a loadmeter which could be placed in series with the wire and gripping jaws.

The meter consisted essentially of a hollow cylinder which was ground to size, the outer and inner diameters being calculated to give a 0.1 per cent strain for a force of 1800 lbf. One end of the meter was screwed to provide fixing to the drum, while the other end was designed to house two spring loaded jaws for gripping the wire as it left the die (see Fig. No. 77). To provide connection between the meter and the bull-block drum, a length of wire of identical stiffness to that being drawn, was screwed in the loadmeter body, and then passed around the drum before being gripped by the bull-block jaws,(see Fig. No. 78). It was thought that the vibration characteristics of the bull-block and wire would remain unaltered, provided the weight of the loadmeter was kept as small as possible, and the stiffness maintained the same as that which prevailed when the wire was connected between the die and the drum directly.

Four 75 ohm. strain gauges were bonded to the

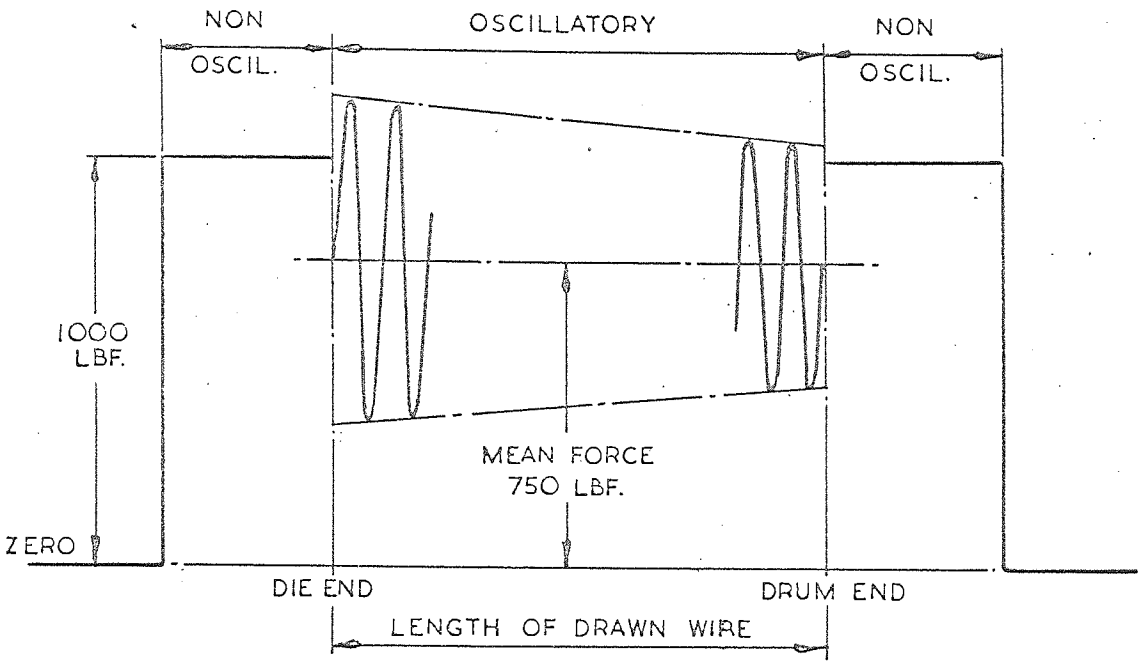

(1). FORCE IN WIRE — STEEL LOADMETER IN SERIES WITH WIRE AND DRUM

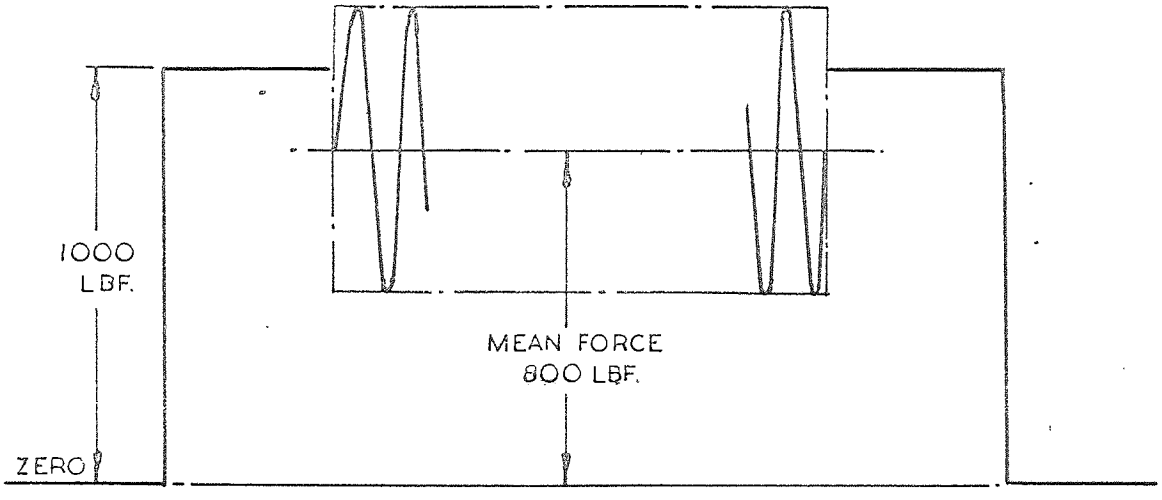

(2). FORCE IN WIRE — STEEL LOADMETER OMITTED

FIG. NO. 79 EFFECT OF STEEL LOADMETER ON THE VARIATION OF FORCE IN THE DRAWN WIRE

column of the loadmeter by the same procedure as that adopted throughout the research programme and were connected in series to form one arm of a Wheatstone bridge. The three other arms were made up by twelve 75 ohm. gauges which were mounted on a block of Vibrac steel.

The bridge current was supplied from a 24 volt d.c. supply and the output was amplified and recorded on a channel of an ultra-violet recorder. The bridge was calibrated before each test by the same procedure as that adopted for the aluminium loadmeter.

16.10.4. Discussion of Results.

The initial tests with the loadmeter in series with the drawn wire and drum showed that the meter was functioning correctly. However, the meter showed that, for a constant frequency and amplitude setting, the peak to peak value of force variation in the wire decreased as the length of drawn wire increased, whereas the strain gauges bonded to the wire had revealed a constant magnitude of force variation at all positions along the length of drawn wire. (see Fig. No. 79). Furthermore, the percentage reduction in mean drawing force was found to be greater than that recorded with the loadmeter omitted. From these observations, it was concluded that the addition of the loadmeter had changed the vibration characteristics of the bull-block and wire by introducing a further mode of vibration. Because of this phenomenon the design of the loadmeter was discarded.

16.11. List of Patents involving Oscillatory Energy for Metal Working.

(1). VANG,A.
'Material Forming and Drawing with the aid of Vibrations'
American Patent No. 2,393,131, Jan.15th., 1946.

(2). ROSENTHAL,A.H.
'Machine for Mechanically Working Materials'.
American Patent No. 2,452, 211. Oct. 26th., 1948.

(3). BALAMUTH,L.
'Method and Means for Removing Material from a Solid Body'.
American Patent No. 2, 580, 716. Jan 1st. 1952.

(4). SCHULTZ.
'Vibration Method and Device for Shaping Elongated Products eg. For Drawing Tube'.
German Patent 955, 943 (T.I. Translation,1411)

(5). ROGOV,V.K., ROGOV,K.R.
'Pulsating Equipment for Drawing Components'.
USSR. Patent No. 111, 247.
Committee of Inventions and Discoverics. Stal in English. Nov., 1959. p 851-852.

(6). KORSHUNOV,V.I., KORSHUNOV, N.V.
'Arrangment for Drawing Wire with the Use of Ultrasound'
Translation from Russian Patent No. 144, 140.
(Appl. No. 73838/22, July 14th., 1961, p.1-2.)
Air Force Systems Command, Wright-Patterson Air Force Base, Ohio. No. A.D. 433, 525.

(7). JONES,J.B.
'Vibrating Roll and Method'.
American Patent No. 3, 096, 672, July 9th. 1963.

(8). SANSOME,D.H., WINSPER,C.E.
'Apparatus for Carrying out Drawing Operations'.
Patent No. 29418/65. July 12th., 1965.

(9). BALAMUTH,L., ET.AL.
'Metal Forming'.
American Patent No. 3, 201, 967. Aug. 24th., 1965.

(10). JONES,J.B.
'Ultrasonic Extrusion Apparatus'.
American Patent No.3, 203, 215. Aug. 31st. 1965.

16.12. Loadmeter and Torquemeter Calibration Curves

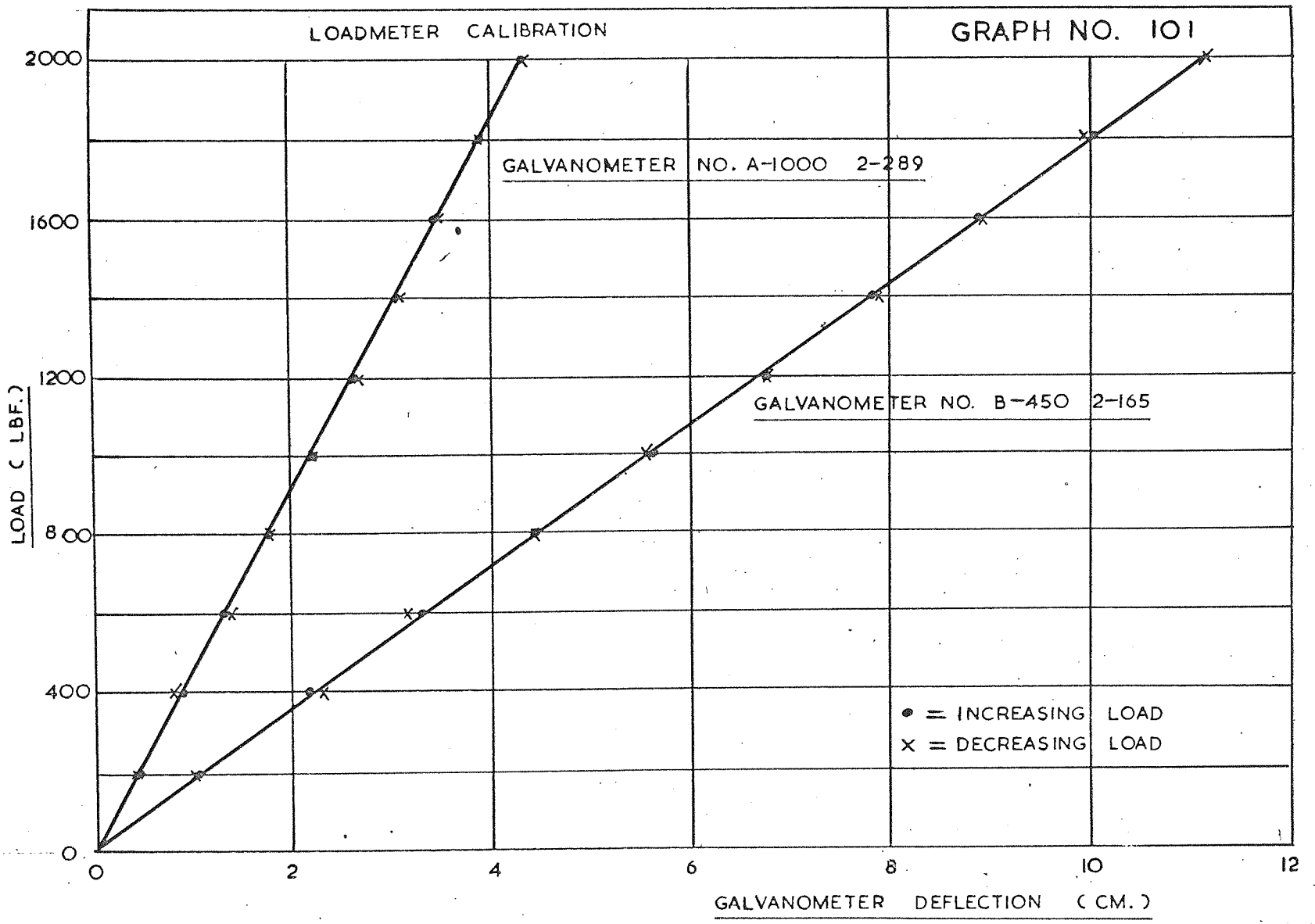
LOADMETER CALIBRATION
GRAPH NO. 101
GALVANOMETER NO. A-1000 2-289
GALVANOMETER NO. B-450 2-165
• = INCREASING LOAD
× = DECREASING LOAD
LOAD (LBF.)
2000
1600
1200
800
400
0
0
2
4
6
8
10
12
GALVANOMETER DEFLECTION (CM.)

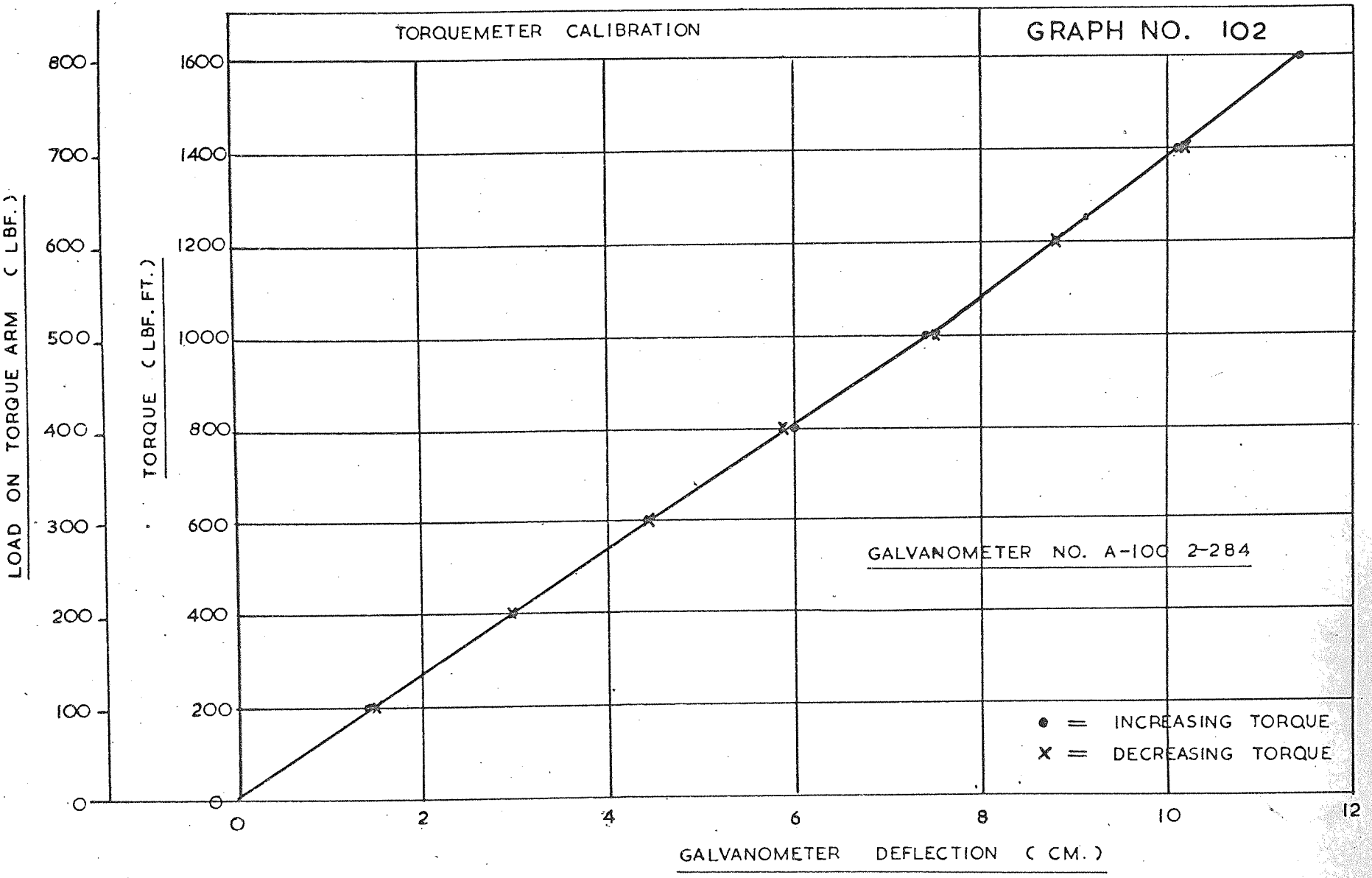
TORQUEMETER CALIBRATION
GRAPH NO. 102
LOAD ON TORQUE ARM (LBF.)
TORQUE (LBF. FT.)
800
700
600
500
400
300
200
100
0
1600
1400
1200
1000
800
600
400
200
0
0
2
4
6
8
10
12
GALVANOMETER DEFLECTION (CM.)
GALVANOMETER NO. A-100 2-284
● = INCREASING TORQUE
X = DECREASING TORQUE

16.13. Amplifier Frequency Response Curves

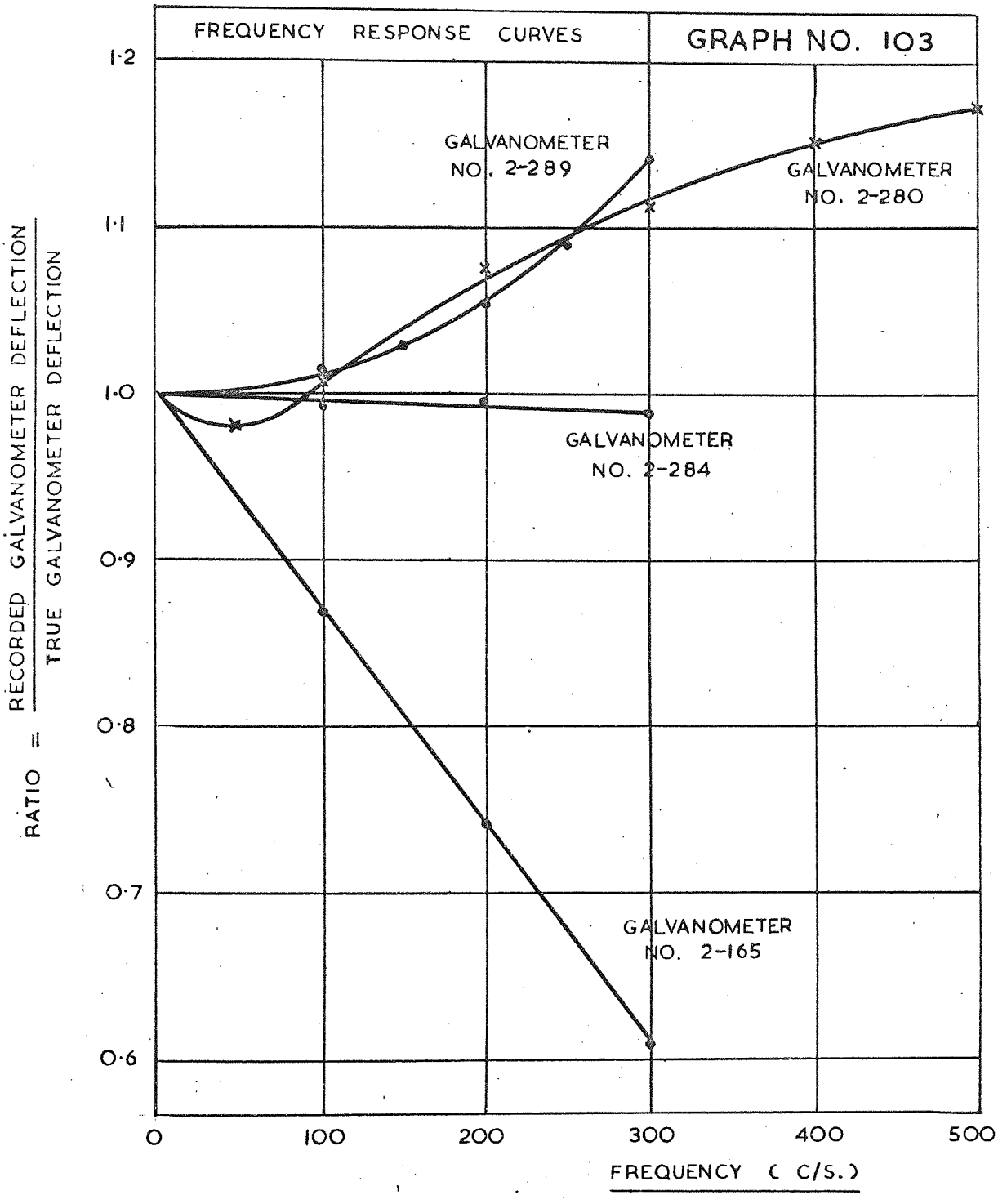
FREQUENCY RESPONSE CURVES
GRAPH NO. 103
RATIO = RECORDED GALVANOMETER DEFLECTION / TRUE GALVANOMETER DEFLECTION
1·2
1·1
1·0
0·9
0·8
0·7
0·6
0
100
200
300
400
500
FREQUENCY (C/S.)
GALVANOMETER NO. 2-289
GALVANOMETER NO. 2-280
GALVANOMETER NO. 2-284
GALVANOMETER NO. 2-165

16.14. Load-Extension Curves for Determination of Young's Modulus

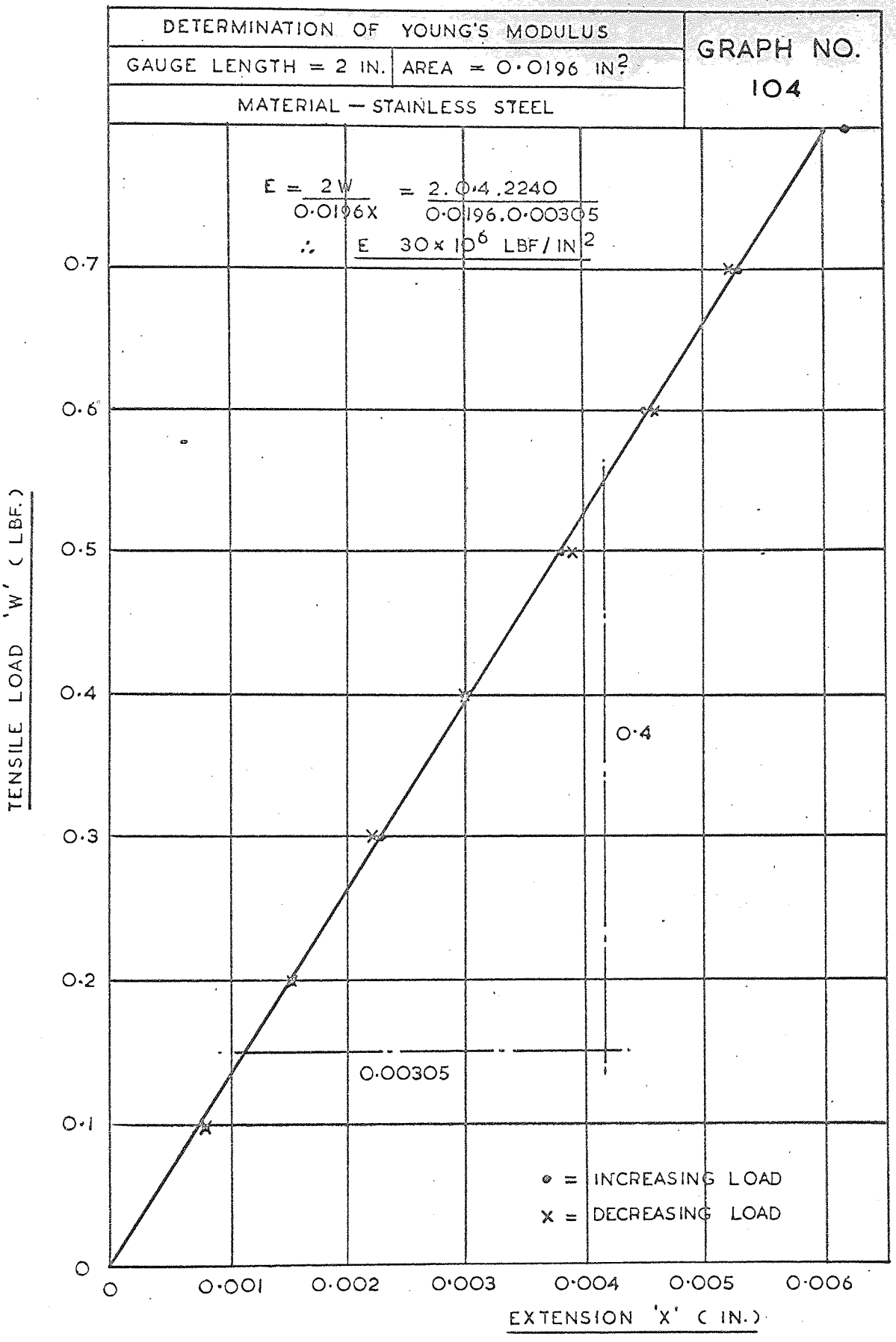
DETERMINATION OF YOUNG'S MODULUS
GAUGE LENGTH = 2 IN. | AREA = 0·0196 IN²
MATERIAL — STAINLESS STEEL
GRAPH NO. 104
E = 2W / 0·0196X = 2.0·4.2240 / 0·0196.0·00305
∴ E 30 × 10⁶ LBF/IN²
TENSILE LOAD 'W' (LBF.)
0·7
0·6
0·5
0·4
0·3
0·2
0·1
0
0·4
0·00305
⊙ = INCREASING LOAD
X = DECREASING LOAD
0
0·001
0·002
0·003
0·004
0·005
0·006
EXTENSION 'X' (IN.)

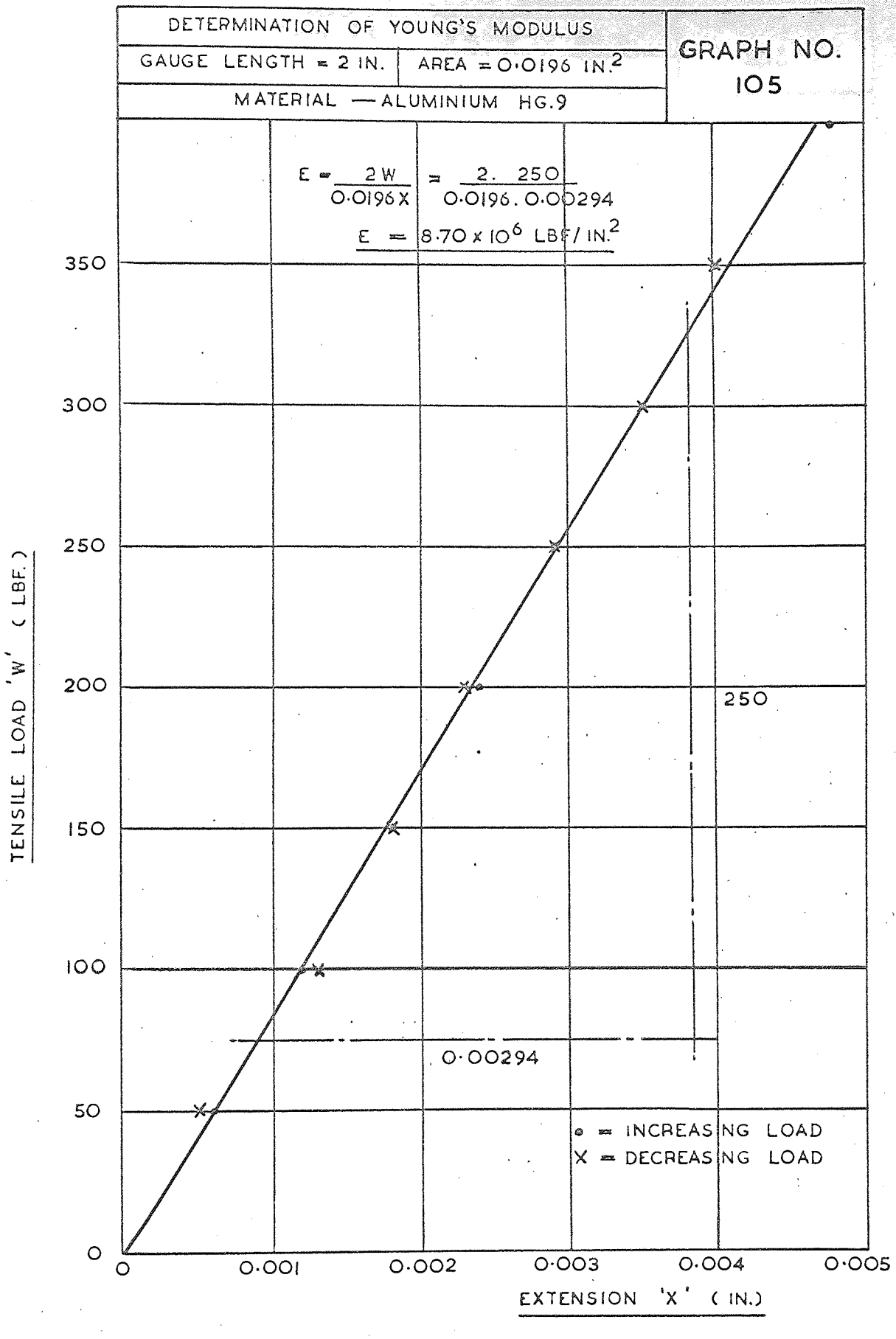
DETERMINATION OF YOUNG'S MODULUS
GAUGE LENGTH = 2 IN.
AREA = 0·0196 IN.²
MATERIAL — ALUMINIUM HG.9
GRAPH NO. 105
E = 2W / 0·0196X = 2. 250 / 0·0196. 0·00294
E = 8·70 x 10⁶ LBF/IN.²
TENSILE LOAD 'W' (LBF.)
350
300
250
200
150
100
50
0
250
0·00294
• = INCREASING LOAD
X = DECREASING LOAD
0
0·001
0·002
0·003
0·004
0·005
EXTENSION 'X' (IN.)

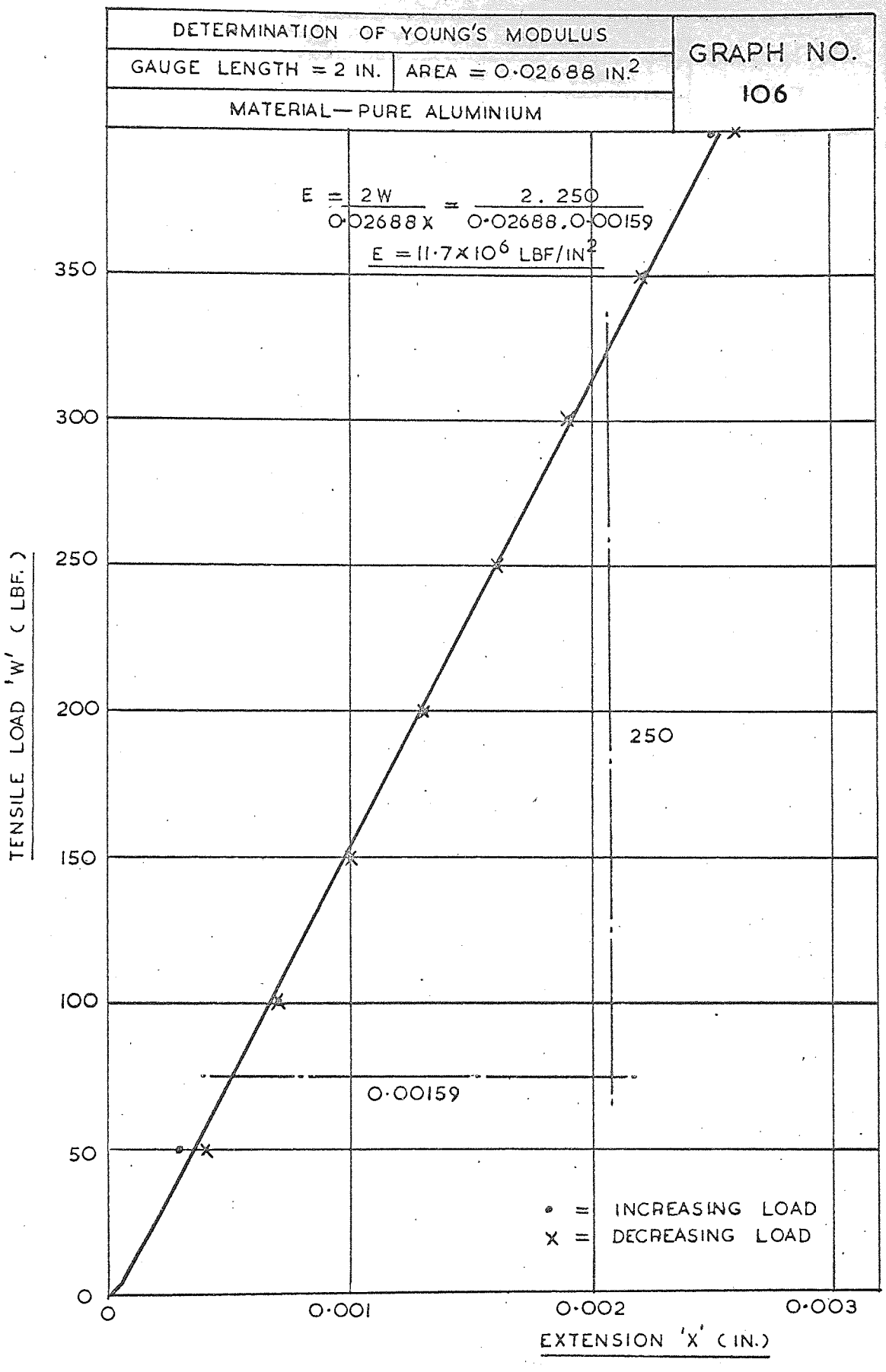
DETERMINATION OF YOUNG'S MODULUS
GAUGE LENGTH = 2 IN.
AREA = 0·02688 IN.²
MATERIAL — PURE ALUMINIUM
GRAPH NO. 106
E = 2W / 0·02688 X = 2.250 / 0·02688 . 0·00159
E = 11·7 × 10⁶ LBF/IN²
TENSILE LOAD 'W' (LBF.)
350
300
250
200
150
100
50
0
250
0·00159
• = INCREASING LOAD
X = DECREASING LOAD
0
0·001
0·002
0·003
EXTENSION 'X' (IN.)

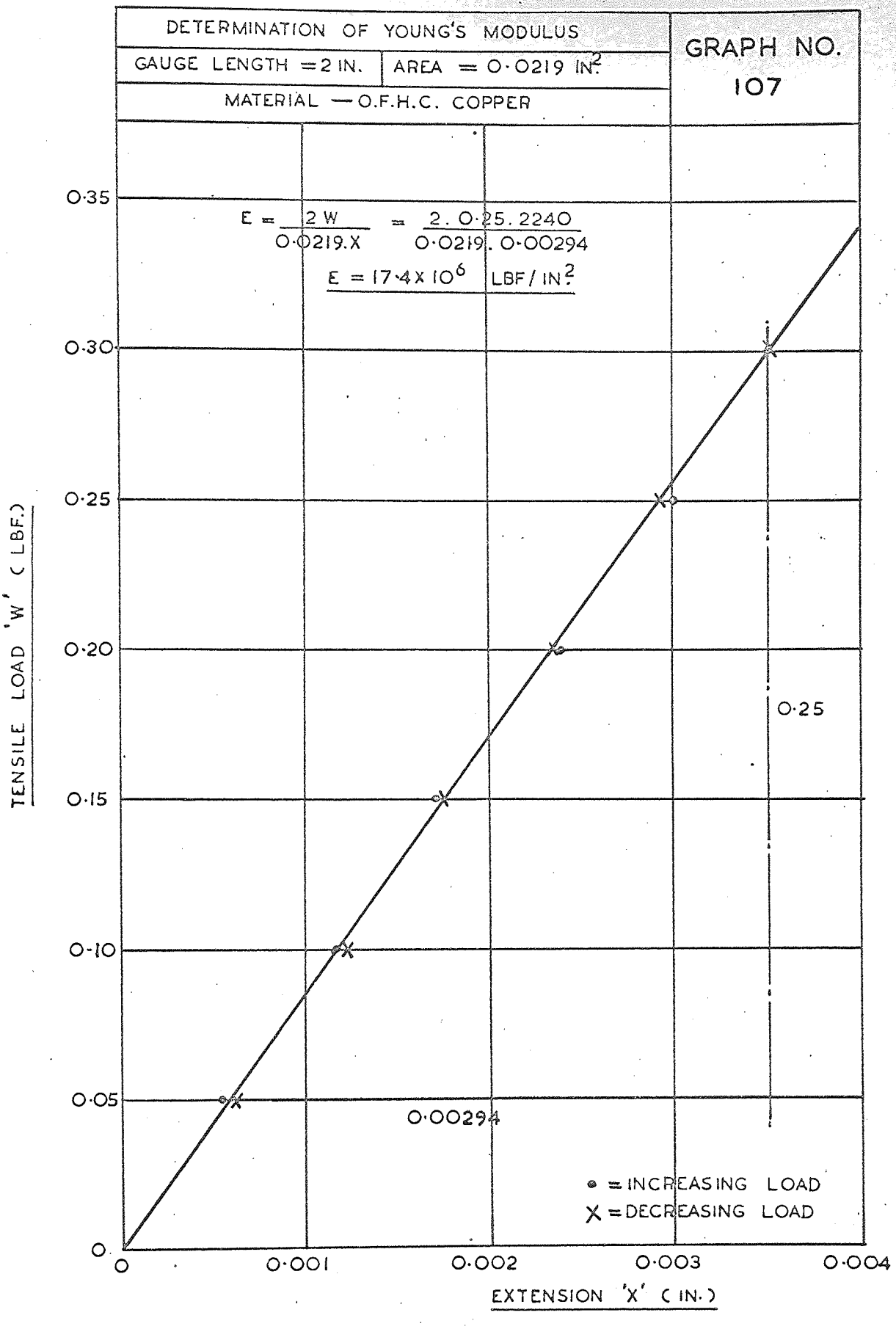
DETERMINATION OF YOUNG'S MODULUS
GAUGE LENGTH = 2 IN.
AREA = 0·0219 IN.²
MATERIAL — O.F.H.C. COPPER
GRAPH NO. 107
E = 2W / 0·0219.X = 2 . 0·25 . 2240 / 0·0219 . 0·00294
E = 17·4 X 10⁶ LBF / IN.²
TENSILE LOAD 'W' (LBF.)
0·35
0·30
0·25
0·20
0·15
0·10
0·05
0
0·25
0·00294
• = INCREASING LOAD
X = DECREASING LOAD
0
0·001
0·002
0·003
0·004
EXTENSION 'X' (IN.)

16.15. Tabulated Results

EXPERIMENTAL RESULTS												TABLE NO. 1.
Material - Mild Steel		Drawing Speed = 1.3 ft / m.							Reduction in Area = 51 %			
Amplitude of Die Oscil. (p to p) 'x' in.	Amplitude of Drum Oscil. 'θ' rads.	Drum Inertia Torque		Mean Drawing Force (Torquemeter)			Mean Drawing Force (Loadmeter)		Force Variation as seen by Torquemeter		
		lbf.ft	lbf.	cm.	lbf.ft	lbf.	cm.	lbf.	cm.	lbf.ft	lbf.
Frequency of Oscillation = 25 c/s.											
0	0	0	0	7.84	1055	1398	3.13	1414	0	0	0
0.010	1.74×10^{-4}	19.1	25	7.72	1042	1378	3.03	1370	1.09	145	192
0.020	3.14 "	34.5	46	7.41	1000	1321	2.97	1340	1.84	243	322
0.030	4.71 "	51.8	68	7.28	978	1298	2.85	1280	2.40	322	426
0.040	6.11 "	67.2	89	6.90	928	1228	2.74	1225	3.25	435	576
0.050	7.51 "	82.5	109	6.50	872	1153	2.63	1175	4.18	564	746
Strain Gauge Bridge on Wire (0.030 in. p to p)				1 cm. = 389 lbf.			∴ 0.74 cm.		= 294 lbf.		
Frequency of Oscillation = 50 c/s.											
0	0	0	0	7.93	1069	1415	3.13	1414	0	0	0
0.010	4.72×10^{-4}	207.5	274	7.32	982	1298	2.97	1335	1.92	258	342
0.020	10.12 "	445.0	588	6.84	918	1212	2.67	1210	3.46	462	612
0.030	14.82 "	653.0	864	6.34	848	1121	2.45	1108	4.85	650	860
0.040	18.32 "	806.0	1065	5.99	802	1060	2.41	1070	5.84	782	1030
0.050	20.60 "	906	1200	5.55	741	980	2.25	1005	6.25	835	1100
Strain Gauge Bridge on Wire (0.030 in. p to p)				1 cm. = 389 lbf.			∴ 1.97 cm.		= 787 lbf.		

EXPERIMENTAL RESULTS												TABLE NO. 2.
Material - Mild Steel			Drawing Speed = 1.3 ft / m.						Reduction in Area = 51 %			
Amplitude of Die Oscil. (p to p) 'x' in.	Amplitude of Drum Oscil. 'θ' rads.	Drum Inertia Torque		Mean Drawing Force (Torquemeter)			Mean Drawing Force (Loadmeter)		Force Variation as seen by Torquemeter		
		lbf.ft	lbf.	cm.	lbf.ft	lbf.	cm.	lbf.	cm.	lbf.ft	lbf.
Frequency of Oscillation = 75 c/s.											
0	0	0	0	7.84	1055	1398	3.13	1414	0	0	0
0.010	1.22×10^{-4}	120.8	160	7.50	1006	1331	2.94	1348	0.62	83	110
0.020	2.80 "	276.5	366	6.81	902	1232	2.72	1222	1.22	162	214
0.030	4.02 "	398.0	526	6.16	816	1110	2.49	1120	1.65	220	291
0.040	5.41 "	536.0	709	5.52	742	982	2.22	998	2.43	318	421
0.050	6.46 "	639.1	846	5.14	688	912	2.08	932	2.62	352	466
Strain Gauge Bridge on Wire				1 cm. = 389 lbf.			$\therefore$ 1.97 cm.		= 787 lbf.		
	(0.030 in. p to p)										
Frequency of Oscillation = 100 c/s.											
0	0	0	0	7.84	1055	1398	3.13	1414	0	0	0
0.010	0.68×10^{-4}	118.5	157	7.53	1010	1338	2.97	1338	0.43	59	78
0.020	1.33 "	233.0	309	6.89	922	1220	2.83	1238	0.65	88	116
0.030	1.67 "	294.2	389	6.33	846	1119	2.65	1136	0.90	122	161
0.040	2.53 "	446.0	592	5.86	785	1039	2.38	1030	1.00	135	179
0.050	3.06 "	539.0	713	5.35	716	947	2.18	943	1.14	152	201
Strain Gauge Bridge on Wire				1 cm. = 389 lbf.			$\therefore$ 2.12 cm.		= 816 lbf.		
	(0.030 in. p to p)										

EXPERIMENTAL RESULTS											TABLE NO. 3.
Material - Mild Steel		Drawing Speed = 1.3 ft / m.					Reduction in Area = 51 %				
Amplitude of Die Oscil. (p to p) 'x' in.	Amplitude of Drum Oscil. 'θ' rads.	Drum Inertia Torque		Mean Drawing Force (Torquemeter)			Mean Drawing Force (Loadmeter)		Force Variation as seen by Torquemeter		
		lbf.ft	lbf.	cm.	lbf.ft	lbf.	cm.	lbf.	cm.	lbf.ft	lbf.
Frequency of Oscillation = 125 c/s.											
0	0	0	0	7.84	1055	1398	3.13	1414	0	0	0
0.010	0.40×10^{-4}	110.5	146	7.50	1007	1332	2.94	1322	0.29	48	64
0.020	0.82 "	225.0	298	6.87	920	1238	2.77	1240	0.42	58	77
0.030	1.20 "	322.0	439	6.22	831	1100	2.46	1103	0.57	78	103
0.035	1.38 "	380.2	503	5.98	800	1058	2.36	1068	0.60	81	107
Strain Gauge Bridge on Wire				1 cm. = 389 lbf.				∴ 2.10 cm. = 800 lbf.			
	(0.030 in. p to p)										
	Frequency								Strain Gauge		Bridge
	of Oscil.								on wire 1cm. = 389 lbf.		
0.013	200			7.30	984	1302	2.92	1320	0.90cm. = 330		lbf.
0.007	300			7.72	1038	1373	3.02	1365	0.58cm. = 212		lbf.
0.005	400			7.75	1042	1381	3.06	1380	0.43cm. = 151		lbf.
0.003	500			7.80	1051	1392	3.10	1400	0.21cm. = 68		lbf.

EXPERIMENTAL RESULTS												TABLE NO. 4.
Material - Mild Steel			Drawing Speed = 1.3 ft / m.						Reduction in Area = 41 %			
Amplitude of Die Oscil. (p to p) 'x' in.	Amplitude of Drum Oscil. 'θ' rads.	Drum Inertia Torque		Mean Drawing Force (Torquemeter)			Mean Drawing Force (Loadmeter)		Force Variation as seen by Torquemeter		
		lbf.ft	lbf.	cm.	lbf.ft	lbf.	cm.	lbf.	cm.	lbf.ft	lbf.
Frequency of Oscillation = 25 c/s.											
0	0	0	0	6.44	863	1141	10.67	1140	0	0	0
0.010	1.92×10^{-4}	21.1	28	5.92	794	1052	10.05	1072	1.10	148	196
0.020	3.14 "	34.5	46	5.98	800	1060	10.20	1087	1.88	254	336
0.030	4.88 "	53.7	71	5.79	773	1026	9.56	1026	2.62	375	496
0.040	6.28 "	69.1	91	5.54	743	990	9.47	1012	3.45	462	611
0.050	7.51 "	82.5	109	5.36	718	952	9.08	970	4.35	580	767
0.060	7.87 "	86.5	115	4.92	660	872	8.14	870	4.70	632	835
Strain Gauge Bridge on Wire				1 cm.	= 411	lbf.		$\therefore$ 0.8	cm. = 335 lbf.		
Frequency of Oscillation = 50 c/s.											
0	0	0	0	6.47	868	1150	10.75	1145	0	0	0
0.010	5.41×10^{-4}	238	315	5.86	788	1042	10.02	1065	1.60	213	282
0.020	10.48 "	461	610	5.46	730	965	9.20	982	3.60	481	636
0.030	14.82 "	653	864	4.67	626	829	7.61	812	4.67	643	850
0.040	17.10 "	752	994	4.23	569	753	6.84	730	5.56	743	983
0.050	19.22 "	846	1120	4.01	537	710	6.54	700	5.80	775	1023
0.060	19.22 "	846	1120	3.75	500	665	6.34	675	5.40	725	960
Strain Gauge Bridge on Wire				1 cm.	= 411	lbf.		$\therefore$ 1.90	cm. =	800 lbf.	

EXPERIMENTAL RESULTS											TABLE NO. 5.
Material - Mild Steel		Drawing Speed = 1.3 ft / m.					Reduction in Area = 41 %				
Amplitude of Die Oscil. (p to p) 'x' in.	Amplitude of Drum Oscil. 'θ' rads.	Drum Inertia Torque		Mean Drawing Force (Torquemeter)			Mean Drawing Force (Loadmeter)		Force Variation as seen by Torquemeter		
		lbf.ft	lbf.	cm.	lbf.ft	lbf.	cm.	lbf.	cm.	lbf.ft	lbf.
Frequency of Oscillation = 75 c/s.											
0	0	0	0	6.45	866	1143	10.66	1135	0	0	0
0.010	2.01×10^{-4}	198.6	262	5.67	760	1005	9.42	1006	1.06	140	185
0.020	2.80 "	276.5	366	5.13	685	907	8.68	925	1.45	196	258
0.030	4.61 "	455.0	602	4.67	623	824	7.76	826	2.15	287	379
0.040	5.41 "	535.0	708	4.07	543	717	6.93	737	2.17	290	384
0.050	6.45 "	709.0	845	3.88	520	688	6.60	700	2.30	308	407
0.060	7.00 "	770.0	913	3.52	472	624	5.82	620	2.52	338	447
Strain Gauge Bridge on Wire				1 cm. = 411 lbf.				∴ 2.00 cm. = 824 lbf.			
Frequency of Oscillation = 100 c/s.											
0	0	0	0	6.57	880	1163	10.86	1158	0	0	0
0.010	0.84×10^{-4}	147.3	195	5.85	784	1038	9.70	1035	0.48	65	86
0.020	1.43 "	251.5	332	5.26	705	932	8.68	927	0.73	100	132
0.030	1.80 "	317.0	420	4.82	645	853	8.00	852	0.93	123	163
0.040	2.56 "	452.0	598	4.35	582	770	7.40	788	1.15	153	202
0.050	2.92 "	514.2	679	3.89	521	690	6.62	707	1.22	165	218
Strain Gauge Bridge on Wire				1 cm. = 411 lbf.				∴ 2.00 cm.		= 819	lbf.

EXPERIMENTAL RESULTS												TABLE NO. 6.
Material - Mild Steel				Drawing Speed = 1.3 ft / m.					Reduction in Area = 41 %			
Amplitude of Die Oscil. (p to p) 'x' in.	Amplitude of Drum Oscil. 'θ' rads.	Drum Inertia Torque		Mean Drawing Force (Torquemeter)			Mean Drawing Force (Loadmeter)		Force Variation as seen by Torquemeter		
		lbf.ft	lbf.	cm.	lbf.ft	lbf.	cm.	lbf.	cm.	lbf.ft	lbf.
Frequency of Oscillation = 125 c/s.											
0	0	0	0	6.45	866	1145	10.67	1138	0	0	0
0.010	0.47×10^{-4}	129.5	171	5.85	782	1032	9.90	1057	0.32	42	56
0.020	0.94 "	259.0	342	5.41	722	954	9.12	972	0.56	62	82
0.030	1.24 "	341.2	450	4.81	655	856	7.86	837	0.60	82	108
0.035	1.39 "	383.0	506	4.56	608	805	7.39	787	0.62	86	114
Strain Gauge Bridge on Wire (0.030 in. p to p)				1 cm. = 411 lbf.			∴ 2.0 cm. = 806 lbf.				
	Frequency of Oscil.								Strain Gauge Bridge on wire 1cm.= 411lbf.		
0.013	200			5.85	785	1038	9.69	1030	1.02cm. = 398 lbf.		
0.007	300			6.20	830	1098	10.32	1100	0.65cm. = 240 lbf.		
0.005	400			6.22	834	1102	10.32	1100	0.50cm. = 177 lbf.		
0.003	500			6.33	848	1122	10.68	1137	0.26cm. = 89 lbf.		

EXPERIMENTAL RESULTS									TABLE NO. 7.		
Material - Mild Steel		Drawing Speed = 1.3 ft / m.					Reduction in Area = 26 %				
Amplitude of Die Oscil. (p to p) 'x' in.	Amplitude of Drum Oscil. 'θ' rads.	Drum Inertia Torque		Mean Drawing Force (Torquemeter)			Mean Drawing Force (Loadmeter)		Force Variation as seen by Torquemeter		
		lbf.ft	lbf.	cm.	lbf.ft	lbf.	cm.	lbf.	cm.	lbf.ft	lbf.
Frequency of Oscillation = 25 c/s.											
0	0	0	0	4.55	608	806	7.6o	810	0	0	0
0.010	1.92×10^{-4}	21.1	28	4.37	585	774	7.27	775	1.13	150	199
0.020	3.14 "	34.5	46	4.06	550	728	7.01	747	1.72	229	303
0.030	4.88 "	54.7	71	3.92	530	702	6.46	690	2.64	354	469
0.040	5.93 "	65.3	86	3.76	503	666	6.24	665	3.35	448	570
0.050	7.34 "	80.7	107	3.50	469	620	5.76	615	3.58	480	700
Strain Gauge Bridge on Wire (0.025 in. p to p)				1 cm. = 355 lbf.				∴ 0.73 = 266 lbf.			
Frequency of Oscillation = 50 c/s.											
0	0	0	o	4.55	608	806	7.55	803	0	0	0
0.010	5.41×10^{-4}	238	315	3.86	502	684	6.67	710	2.25	302	399
0.020	9.60 "	422	559	3.59	480	635	5.85	625	3.57	478	633
0.030	11.51 "	506	670	3.31	442	584	5.26	560	3.92	523	692
0.040	12.72 "	560	741	2.90	388	513	4.74	507	3.68	495	655
0.050	13.42 "	591	781	2.70	362	478	4.30	461	3.41	455	692
Strain Gauge Bridge on Wire (0.025 in. p to p)				1 cm. = 355 lbf.				∴ 1.60 cm. = 584 lbf.			

EXPERIMENTAL RESULTS												TABLE NO. 8.
Material - Mild Steel		Drawing Speed = 1.3 ft / m.							Reduction in Area = 26 %			
Amplitude of Die Oscil. (p to p) 'x' in.	Amplitude of Drum Oscil. 'θ' rads.	Drum Inertia Torque		Mean Drawing Force (Torquemeter)			Mean Drawing Force (Loadmeter)		Force Variation as seen by Torquemeter		
		lbf.ft	lbf.	cm.	lbf.ft	lbf.	cm.	lbf.	cm.	lbf.ft	lbf.
Frequency of Oscillation = 75 c/s.											
0	0	0	0	4.55	610	807	7.60	810	0	0	0
0.010	1.57×10^{-4}	155.5	206	3.96	530	702	6.57	702	0.70	93	123
0.020	2.97 "	294.0	389	3.24	435	576	5.54	592	1.32	176	233
0.030	4.01 "	396.1	524	2.97	398	526	4.85	518	1.78	237	314
0.040	4.19 "	413.9	548	2.71	362	480	4.62	493	1.92	258	341
0.050	4.72 "	466.0	683	2.62	352	466	4.54	484	2.49	332	440
Strain Gauge Bridge on Wire (0.025 in. p to p)				1 cm. = 355 lbf.				∴ 1.70 cm.	= 605 lbf.		
Frequency of Oscillation = 100 c/s.											
0	0	0	0	4.56	611	808	7.48	795	0	0	0
0.010	0.70×10^{-4}	123.0	163	3.92	525	695	6.39	679	0.38	52	69
0.020	1.34 "	236.5	313	3.31	442	584	5.58	595	0.62	83	110
0.030	1.66 "	292.5	387	2.92	392	518	5.04	538	0.84	115	152
0.040	2.01 "	354.0	469	2.80	375	496	4.71	502	1.02	136	180
0.050	2.18 "	384.1	508	2.66	357	472	4.42	472	0.95	128	169
Strain Gauge Bridge on Wire (0.025 in. p to p)				1 cm.	=355 lbf.			∴ 1.70 cm.	= 600 lbf.		

EXPERIMENTAL RESULTS											TABLE NO. 9.
Material - Mild Steel		Drawing Speed = 1.3 ft / m.							Reduction in Area = 26 %		
Amplitude of Die Oscil. (p to p) 'x' in.	Amplitude of Drum Oscil. 'θ' rads.	Drum Inertia Torque		Mean Drawing Force (Torquemeter)			Mean Drawing Force (Loadmeter)		Force Variation as seen by Torquemeter		
		lbf.ft	lbf.	cm.	lbf.ft	lbf.	cm.	lbf.	cm.	lbf.ft	lbf.
Frequency of Oscillation = 125 c/s.											
0	0	0	0	4.55	608	806	7.60	810	0	0	0
0.010	0.38×10^{-4}	105.5	139	4.25	570	754	7.02	750	0.28	38	50
0.020	0.73 "	202.0	267	3.77	503	665	6.32	673	0.46	63	83
0.030	0.98 "	267.9	355	3.10	413	550	5.29	565	0.50	70	93
0.035	1.13 "	300.0	397	2.98	398	526	4.87	522	0.60	81	107
Strain Gauge Bridge on Wire (0.025 in. p to p)				1 cm. = 355 lbf.				1.7 cm. = 592 lbf.			
	Frequency of Oscil.								Strain Gauge Bridge on wire 1 cm. = 355 lbf.		
0.013	200			4.00	535	708	6.60	700	0.93cm.	= 311	lbf.
0.007	300			4.26	569	754	6.97	740	0.62cm.	= 198	lbf.
0.005	400			4.30	573	760	7.06	750	0.40cm.	= 123	lbf.
0.003	500			4.48	598	792	7.53	800	0.28cm.	= 83	lbf.

EXPERIMENTAL RESULTS												TABLE NO. 10.
Material - Mild Steel		Drawing Speed = 1.3 ft / m.							Reduction in Area = 10 %			
Amplitude of Die Oscil. (p to p) 'x' in.	Amplitude of Drum Oscil. 'θ' rads.	Drum Inertia Torque		Mean Drawing Force (Torquemeter)			Mean Drawing Force (Loadmeter)		Force Variation as seen by Torquemeter		
		lbf.ft	lbf.	cm.	lbf.ft	lbf.	cm.	lbf.	cm.	lbf.ft	lbf.
Frequency of Oscillation = 25 c/s.											
0	0	0	0	2.34	310	409	3.75	401	0	0	0
0.010	1.03×10^{-4}	11.3	15	2.24	298	394	3.62	387	0.56	74	98
0.020	1.75 "	19.2	25	2.08	274	363	3.34	358	1.06	140	185
0.030	2.79 "	30.6	41	1.82	240	318	2.97	318	1.57	207	274
Strain Gauge Bridge on Wire				1 cm.	= 157.5 lbf.		∴	0.57	cm. =	90 lbf.	
Frequency of Oscillation = 50 c/s.											
0	0	0	0	2.34	310	409	3.75	401	0	0	0
0.010	3.57×10^{-4}	157.2	208	1.67	222	293	2.83	303	0.90	121	160
0.020	5.41 "	238.0	315	1.30	175	232	2.10	225	1.48	198	262
0.030	6.64 "	292.1	386	1.01	135	179	1.71	182	1.50	202	267
Strain Gauge Bridge on Wire				1 cm.	= 157.5 lbf.		∴	1.90	cm. =	302 lbf.	
Frequency of Oscillation = 75 c/s.											
0	0	0	0	2.34	310	409	3.75	401	0	0	0
0.010	1.20×10^{-4}	120.0	160	1.68	224	296	2.87	306	0.49	68	90
0.020	2.10 "	188.0	249	1.29	171	226	2.10	229	0.65	88	116
0.030	2.53 "	249.8	331	1.19	157	208	1.78	191	0.90	121	160
Strain Gauge Bridge on Wire				1 cm.	= 157.5 lbf.		∴	2.00	cm. =	310 lbf.	

EXPERIMENTAL RESULTS												TABLE NO. 11.
Material - Mild Steel			Drawing Speed = 1.3 ft / m.						Reduction in Area = 10 %			
Amplitude of Die Oscil. (p to p) 'x' in.	Amplitude of Drum Oscil. 'θ' rads.	Drum Inertia Torque		Mean Drawing Force (Torquemeter)			Mean Drawing Force (Loadmeter)		Force Variation as seen by Torquemeter		
		lbf.ft	lbf.	cm.	lbf.ft	lbf.	cm.	lbf.	cm.	lbf.ft	lbf.
Frequency of Oscillation = 100 c/s.											
0	0	0	0	2.33	308	408	3.75	402	0	0	0
0.010	0.56×10^{-4}	98.4	130	1.72	227	300	2.72	290	0.33	42	56
0.020	0.96 "	169.5	224	1.21	159	210	2.02	217	0.38	53	70
0.030	1.22 "	217.0	285	1.00	135	179	1.62	173	0.41	58	77
Strain Gauge Bridge on Wire				1 cm. = 157.5 lbf.				∴	2.05 cm. = 312 lbf.		
Frequency of Oscillation = 125 c/s.											
0	0	0	0	2.34	310	410	3.75	402	0	0	0
0.010	0.33×10^{-4}	91.0	120	1.83	241	318	3.03	323	0.26	35	46
0.020	0.57 "	156.5	207	1.42	189	250	2.26	243	0.37	51	68
0.030	0.68 "	188.0	249	1.25	166	219	1.93	213	0.32	43	57
Strain Gauge Bridge on Wire				1 cm. = 157.5 lbf.				∴	2.00 cm. = 308 lbf		
	Frequency								Strain Gauge Bridge		
	of Oscil.								on wire 1cm. =		158lbf
0.013	200			1.62	214	284	2.71	290	1.82cm. = 272		lbf.
0.007	300			1.93	255	338	3.18	340	1.20cm. = 172		lbf.
0.005	400			2.08	274	364	3.55	370	0.90cm. = 123		lbf.
0.003	500			2.18	288	381	3.55	370	0.55cm. = 73		lbf.

EXPERIMENTAL RESULTS												TABLE NO. 12.
Material - Stainless Stl, Drawing Speed = 1.3 ft / m.									Reduction in Area = 44.5 %			
Amplitude of Die Oscil. (p to p) 'x' in.	Amplitude of Drum Oscil. 'θ' rads.	Drum Inertia Torque		Mean Drawing Force (Torquemeter)			Mean Drawing Force (Loadmeter)		Force Variation as seen by Torquemeter		
		lbf.ft	lbf.	cm.	lbf.ft	lbf.	cm.	lbf.	cm.	lbf.ft	lbf.
Frequency of Oscillation = 25 c/s.											
0	0	0	0	10.05	1382	1828	4.05	1832	0	0	0
0.010	1.74×10^{-4}	19.1	25	9.82	1350	1786	3.93	1778	1.02	140	185
0.020	3.14 "	34.6	46	9.68	1330	1760	3.83	1732	1.73	237	314
0.040	5.93 "	65.0	86	9.12	1252	1658	3.62	1635	3.20	443	586
0.060	8.72 "	96.0	127	8.62	1185	1568	3.49	1578	4.50	620	819
0.070	10.82 "	118.7	157	8.35	1155	1528	3.38	1532	5.45	751	993
Strain Gauge Bridge on Wire (0.030 in. p to p)				1 cm. = 463 lbf.			$\therefore$ 0.62 cm. = 290 lbf.				
Frequency of Oscillation = 50 c/s.											
0	0	0	0	10.00	1377	1820	4.02	1818	0	0	0
0.010	4.01×10^{-4}	176.2	234	9.53	1300	1718	3.82	1728	1.50	206	273
0.020	9.58 "	422.0	560	9.02	1248	1650	3.65	1642	3.46	476	561
0.040	18.52 "	818.0	1082	7.82	1088	1440	3.23	1460	6.08	837	1108
0.060	23.60 "	1038.0	1375	7.16	983	1300	2.83	1280	7.40	1020	1346
0.070	25.30 "	1113.3	1476	6.98	958	1268	2.79	1262	7.65	1052	1390
Strain Gauge Bridge on Wire (0.030 in. p to p)				1 cm. = 463 lbf.			$\therefore$ 1.58 cm. = 752 lbf.				

EXPERIMENTAL RESULTS												TABLE NO. 13.
Material - Stainless Stl.		Drawing Speed = 1.3 ft / m.							Reduction in Area = 44.5 %			
Amplitude of Die Oscil. (p to p)	Amplitude of Drum Oscil.	Drum Inertia Torque		Mean Drawing Force (Torquemeter)			Mean Drawing Force (Loadmeter)		Force Variation as seen by Torquemeter			
'x' in.	'0' rads.	lbf.ft	lbf.	cm.	lbf.ft	lbf.	cm.	lbf.	cm.	lbf.ft	lbf.	
Frequency of Oscillation = 75 c/s.												
0	0	0	0	10.04	1363	1826	4.02	1818	0	0	0	
0.010	1.66×10^{-4}	164.2	217	9.40	1290	1708	3.82	1728	0.62	85	113	
0.020	3.14 "	310.8	411	8.93	1230	1627	3.63	1638	1.42	195	258	
0.040	6.46 "	639.2	845	7.25	1002	1325	2.93	1325	2.40	332	438	
0.060	8.89 "	882.0	1168	6.12	893	1118	2.49	1123	4.32	597	790	
0.070	10.48 "	1038.2	1370	5.95	822	1088	2.34	1059	4.66	643	850	
Strain Gauge Bridge on Wire (0.050 in. p to p)				1 cm. = 463 lbf.			∴ 1.80 cm. = 855 lbf.					
Frequency of Oscillation = 100 c/s.												
0	0	0	0	10.00	1376	1820	4.02	1818	0	0	0	
0.010	0.70×10^{-4}	123.2	163	9.52	1293	1712	3.82	1728	0.38	52	69	
0.020	1.36 "	240.0	368	9.08	1247	1650	3.67	1660	0.57	79	104	
0.030	2.13 "	375.1	496	8.56	1166	1555	3.42	1542	0.88	121	160	
0.040	2.44 "	430.8	570	7.96	1095	1449	3.25	1470	1.00	138	182	
0.050	2.95 "	518.8	692	7.51	1033	1365	3.10	1402	1.20	165	218	
Strain Gauge Bridge on Wire (0.050 in. p to p)				1 cm. = 463 lbf.			∴ 1.62 cm. = 747 lbf.					

EXPERIMENTAL RESULTS — TABLE NO. 14.

Material - Stainless Stl. Drawing Speed = 1.3 ft / m. Reduction in Area = 44.5 %

Amplitude of Die Oscil. (p to p) 'x' in.	Amplitude of Drum Oscil. 'θ' rads.	Drum Inertia Torque		Mean Drawing Force (Torquemeter)			Mean Drawing Force (Loadmeter)		Force Variation as seen by Torquemeter		
		lbf.ft	lbf.	cm.	lbf.ft	lbf.	cm.	lbf.	cm.	lbf.ft	lbf.
Frequency of Oscillation = 125 c/s.											
0	0	0	0	10.00	1375	1820	3.96	1782	0	0	0
0.010	0.38×10^{-4}	105.7	140	9.38	1290	1708	3.78	1702	0.20	27	36
0.020	0.83 "	230.0	305	9.18	1253	1660	3.63	1640	0.43	60	79
0.030	1.24 "	340.2	450	8.62	1185	1568	3.40	1540	0.55	76	100
0.035	1.36 "	374.5	495	8.40	1155	1528	3.38	1528	0.62	86	113
Strain Gauge Bridge on Wire (0.030 in. p to p)				1 cm. = 463 lbf.			∴ 2.10 cm. = 773 lbf.				
	Frequency of Oscil.								Strain Gauge Bridge on wire 1cm. = 375lbf		
0.013	200			9.40	1290	1712	3.81	1712	0.90cm. = 337 lbf.		
0.007	300			9.82	1345	1783	3.95	1781	0.59cm. = 221 lbf.		
0.005	400			9.85	1355	1792	3.97	1792	0.45cm. = 146 lbf.		
0.003	500			9.96	1370	1812	4.00	1809	0.28cm. = 87 lbf.		

EXPERIMENTAL RESULTS												TABLE NO. 15.
Material - Aluminium HG9		Drawing Speed = 1.3 ft / m.							Reduction in Area = 44.5 %			
Amplitude of Die Oscil. (p to p) 'x' in.	Amplitude of Drum Oscil. 'θ' rads.	Drum Inertia Torque		Mean Drawing Force (Torquemeter).			Mean Drawing Force (Loadmeter)		Force Variation as seen by Torquemeter		
		lbf.ft	lbf.	cm.	lbf.ft	lbf.	cm.	lbf.	cm.	lbf.ft	lbf.
Frequency of Oscillation =				25 c/s.							
0	0	0	0	3.80	510	675	6.37	675	0	0	0
0.010	0.79×10^{-4}	9	11	3.67	492	652	6.12	662	0.78	103	137
0.020	1.31 "	14	19	3.52	472	625	5.83	620	1.25	168	222
0.040	3.49 "	38	51	3.18	426	564	5.29	562	2.03	294	390
0.060	4.88 "	54	71	2.95	395	524	5.03	534	2.96	392	520
0.070	5.58 "	61	81	2.74	368	487	4.74	503	3.36	445	590
Strain Gauge Bridge on Wire (0.030 in. p to p)				1 cm. = 166 lbf.			∴	1.15 cm. = 189 lbf.			
Frequency of Oscillation =				50 c/s.							
0	0	0	0	3.83	514	680	6.40	680	0	0	0
0.010	1.83×10^{-4}	81	107	3.53	472	626	5.94	632	0.77	103	137
0.020	3.58 "	157	209	3.25	436	577	5.65	598	1.21	162	214
0.040	6.54 "	288	382	3.03	409	542	5.02	532	2.12	284	376
0.060	8.03 "	353	470	2.45	329	435	4.28	454	2.35	315	417
0.070	8.78 "	384	510	2.32	311	412	4.07	432	2.32	329	435
Strain Gauge Bridge on Wire (0.030 in. p to p)				1 cm. = 166 lbf.			∴	1.70 cm. = 277 lbf.			

EXPERIMENTAL RESULTS												TABLE NO. 16.
Material -Aluminium HG9			Drawing Speed = 1.3 ft / m.						Reduction in Area = 44.5 %			
Amplitude of Die Oscil. (p to p) 'x' in.	Amplitude of Drum Oscil. 'θ' rads.	Drum Inertia Torque		Mean Drawing Force (Torquemeter)			Mean Drawing Force (Loadmeter)		Force Variation as seen by Torquemeter		
		lbf.ft	lbf.	cm.	lbf.ft	lbf.	cm.	lbf.	cm.	lbf.ft	lbf.
Frequency of Oscillation = 75 c/s.											
0	0	0	0	3.83	514	680	6.40	680	0	0	0
0.010	0.51×10^{-4}	50	66	3.58	479	635	5.96	634	0.27	36	48
0.020	1.12 "	111	147	3.22	432	572	5.52	587	0.50	66	87
0.040	2.05 "	199	263	2.75	373	493	4.93	524	0.88	118	157
0.060	2.70 "	268	354	2.50	335	444	4.30	456	1.15	154	204
0.070	3.22 "	319	422	2.30	308	408	3.92	416	1.20	161	213
Strain Gauge on Bridge on Wire (0.030 in. p to p)				1 cm. =		166 lbf.		∴ 1.77 cm.		= 294 lbf.	
Frequency of Oscillation = 100 c/s.											
0	0	0	0	3.80	509	675	6.32	672	0	0	0
0.010	0.26×10^{-4}	46	61	3.67	490	652	6.00	638	0.21	28	37
0.020	0.49 "	86	114	3.42	454	602	5.85	621	0.27	36	48
0.030	0.78 "	138	183	3.12	418	553	5.33	567	0.45	60	80
0.040	0.92 "	163	215	3.07	410	544	5.02	532	0.47	63	84
0.050	1.11 "	197	261	2.78	373	493	4.86	517	0.49	66	87
Strain Gauge Bridge on Wire (0.030 in. p to p)				1 cm. =		175 lbf.		∴ 1.80 cm.		= 302 lbf.	

EXPERIMENTAL RESULTS									TABLE NO. 17.		
Material -Aluminium HG9		Drawing Speed = 1.3 ft / m.							Reduction in Area = 44.5 %		
Amplitude of Die Oscil. (p to p) 'x' in.	Amplitude of Drum Oscil. '0' rads.	Drum Inertia Torque		Mean Drawing Force (Torquemeter)			Mean Drawing Force (Loadmeter)		Force Variation as seen by Torquemeter		
		lbf.ft	lbf.	cm.	lbf.ft	lbf.	cm.	lbf.	cm.	lbf.ft	lbf.
Frequency of Oscillation =				125 c/s.							
0	0	0	0	3.83	514	680	6.45	686	0	0	0
0.010	0.14×10^{-4}	39	51	3.62	484	642	5.96	634	0.15	20	26
0.020	0.31 "	86	114	3.36	450	596	5.42	576	0.20	27	36
0.030	0.47 "	129	171	3.13	420	556	5.19	552	0.20	27	36
0.035	0.48 "	132	175	3.00	402	532	4.92	522	0.20	27	36
Strain Gauge Bridge on Wire (0.030 in. p to p)				1 cm. = 166 lbf.			∴ 1.75		cm. = 276 lbf.		
	Frequency of Oscil.								Strain Gauge Bridge on wire 1 cm. = 166 lbf.		
0.013	200			3.50	468	621	6.10	648	0.90 cm. = 141		lbf.
0.007	300			3.73	501	663	6.28	666	0.58 cm. = 87		lbf.
0.005	400			3.70	496	656	6.30	670	0.45 cm. = 64		lbf.
0.003	500			3.80	510	674	6.37	676	0.28 cm. = 38		lbf.

EXPERIMENTAL RESULTS												TABLE NO. 18.
Material -Pure Aluminium		Drawing Speed = 1.3 ft / m.					Reduction in Area = 24 %					
Amplitude of Die Oscil. (p to p) 'x' in.	Amplitude of Drum Oscil. 'θ' rads.	Drum Inertia Torque		Mean Drawing Force (Torquemeter)			Mean Drawing Force (Loadmeter)		Force Variation as seen by Torquemeter		
		lbf.ft	lbf.	cm.	lbf.ft	lbf.	cm.	lbf.	cm.	lbf.ft	lbf.
Frequency of Oscillation = 25 c/s.											
0	0	0	0	1.18	155	205	1.80	198	0	0	0
0.010	1.04×10^{-4}	11.3	15	0.92	121	160	1.45	160	0.59	79	104
0.020	1.74 "	18.9	25	0.82	107	142	1.24	138	0.98	130	172
0.030	2.09 "	23.4	31	0.73	95	126	1.13	125	1.27	168	222
Strain Gauge Bridge on Wire				1 cm.	= 49	lbf.		∴ 2.40 cm.		= 118	lbf.
Frequency of Oscillation = 50 c/s.											
0	0	0	0	1.22	160	212	1.80	198	0	0	0
0.010	1.48×10^{-4}	65.7	87	0.99	130	172	1.42	156	0.48	63	84
0.020	2.52 "	111.0	147	0.68	89	118	1.07	118	0.62	82	109
0.030	3.14 "	138.2	183	0.58	76	101	0.90	99	0.73	97	128
Strain Gauge Bridge on Wire				1 cm.	= 49	lbf.		∴ 3.18 cm.		= 153	lbf.
Frequency of Oscillation = 75 c/s.											
0	0	0	0	1.20	157	208	1.82	200	0	0	0
0.010	0.63×10^{-4}	61.9	82	0.91	119	158	1.38	152	0.30	39	52
0.020	1.06 "	105.0	139	0.69	91	120	1.02	113	0.45	59	78
0.030	1.36 "	134.5	178	0.60	79	104	0.92	101	0.69	91	120
Stain Gauge Bridge on Wire				1 cm.	= 49	lbf.		∴ 3.25 cm.		= 154	lbf.

EXPERIMENTAL RESULTS — TABLE NO. 19.

Material - Pure Aluminium — Drawing Speed = 1.3 ft / m. — Reduction in Area = 24 %

Amplitude of Die Oscil. (p to p) 'x' in.	Amplitude of Drum Oscil. 'θ' rads.	Drum Inertia Torque lbf.ft	Drum Inertia Torque lbf.	Mean Drawing Force (Torquemeter) cm.	Mean Drawing Force (Torquemeter) lbf.ft	Mean Drawing Force (Torquemeter) lbf.	Mean Drawing Force (Loadmeter) cm.	Mean Drawing Force (Loadmeter) lbf.	Force Variation as seen by Torquemeter cm.	Force Variation as seen by Torquemeter lbf.ft	Force Variation as seen by Torquemeter lbf.
Frequency of Oscillation =				100 c/s.							
0	0	0	0	1.20	157	208	1.83	202	0	0	0
0.010	0.30×10^{-4}	52.2	69	0.97	127	168	1.45	160	0.18	23	31
0.020	0.51 "	89.2	118	0.73	96	127	1.07	118	0.22	29	38
0.030	0.58 "	101.2	134	0.65	85	112	0.88	97	0.23	30	40
Strain Gauge Bridge on Wire				1 cm. = 49 lbf.			∴ 3.23 cm. = 153 lbf.				
Frequency of Oscillation =				125 c/s.							
0	0	0	0	1.20	157	208	1.80	199	0	0	0
0.010	0.16×10^{-4}	43.2	57	0.94	123	163	1.38	155	0.14	18	24
0.020	0.27 "	74.8	99	0.77	98	130	1.08	122	0.13	17	23
0.030	0.34 "	94.2	125	0.64	84	111	0.90	100	0.13	17	23
Strain Gauge Bridge on Wire				1 cm. = 49 lbf.			∴ 3.20 cm. =		149 lbf.		
	Frequency								Strain Gauge Bridge		
	of Oscil.								on wire 1cm.=49 lbf.		
0.013	200			0.88	105	153	1.38	152	3.00cm. = 134		lbf.
0.007	300			0.98	128	170	1.51	167	1.90cm. = 82		lbf.
0.005	400			1.06	140	185	1.67	185	1.55cm. = 64		lbf.
0.003	500			1.10	144	191	1.68	186	0.73cm. = 30		lbf.

EXPERIMENTAL RESULTS — TABLE NO. 20.

Material - OFHC. Copper | Drawing Speed = 1.3 ft / m. | Reduction in Area = 38 %

Amplitude of Die Oscil. (p_x to p) in.	Amplitude of Drum Oscil. 'θ' rads.	Drum Inertia Torque		Mean Drawing Force (Torquemeter)			Mean Drawing Force (Loadmeter)		Force Variation as seen by Torquemeter		
		lbf.ft	lbf.	cm.	lbf.ft	lbf.	cm.	lbf.	cm.	lbf.ft	lbf.
Frequency of Oscillation = 25 c/s.											
0	0	0	0	4.92	662	875	8.30	882	0	0	0
0.010	1.57×10^{-4}	17.4	23	4.50	605	801	7.65	812	1.10	148	196
0.020	3.14 "	34.7	46	4.40	592	784	7.50	796	1.75	236	312
0.040	5.06 "	56.7	75	4.12	553	732	7.05	747	3.20	431	570
0.060	7.15 "	78.6	104	3.80	511	676	6.40	679	4.30	579	766
0.070	7.85 "	86.2	114	3.73	501	663	6.28	667	4.65	626	828
Strain Gauge Bridge on Wire (0.025 in. p to p)				1 cm.	= 307 lbf.			∴ 0.80 cm.	= 270 lbf.		
Frequency of Oscillation = 50 c/s.											
0	0	0	0	5.00	672	890	8.40	892	0	0	0
0.010	3.42×10^{-4}	154	204	4.52	606	803	7.64	812	1.25	168	222
0.020	6.97 "	307	407	4.15	558	739	7.11	754	2.37	319	422
0.040	11.50 "	508	673	3.48	467	618	6.00	636	3.52	473	626
0.060	13.61 "	602	796	2.90	390	516	4.98	530	3.65	491	650
0.070	13.93 "	618	819	2.92	392	520	4.76	506	3.55	476	632
Strain Gauge Bridge on Wire (0.025 in. p to p)				1 cm.	= 307 lbf.			∴ 1.70 cm.	= 508 lbf.		

EXPERIMENTAL RESULTS — TABLE NO. 21.

Material - OFHC. Copper | Drawing Speed = 1.3 ft / m. | Reduction in Area = 38 %

Amplitude of Die Oscil. (p to p) 'x' in.	Amplitude of Drum Oscil. 'θ' rads.	Drum Inertia Torque		Mean Drawing Force (Torquemeter)			Mean Drawing Force (Loadmeter)		Force Variation as seen by Torquemeter		
		lbf.ft	lbf.	cm.	lbf.ft	lbf.	cm.	lbf.	cm.	lbf.ft	lbf.
Frequency of Oscillation = 75 c/s.											
0	0	0	0	5.12	691	914	8.45	899	0	0	0
0.010	1.22×10^{-4}	121	160	4.58	617	817	7.60	800	0.60	81	107
0.020	2.46 "	244	322	4.07	547	724	6.90	733	0.87	117	155
0.040	4.09 "	406	536	3.30	446	590	5.63	597	1.50	202	268
0.060	5.31 "	528	698	2.90	391	517	4.92	521	2.32	311	412
0.070	5.74 "	570	754	2.82	379	502	4.60	489	2.69	363	480
Strain Gauge Bridge on Wire (0.025 in. p to p)				1 cm. = 307 lbf.				∴ 1.73 cm. = 519 lbf.			
Frequency of Oscillation = 100 c/s.											
0	0	0	0	5.02	677	895	8.47	901	0	0	0
0.010	0.59×10^{-4}	104	138	4.52	607	803	7.63	810	0.35	47	62
0.020	1.15 "	202	268	4.08	549	727	7.00	742	0.54	73	96
0.030	1.53 "	271	358	3.68	496	656	6.41	670	0.68	90	119
0.040	2.00 "	353	467	3.40	457	605	5.72	608	0.89	119	158
0.050	2.26 "	400	529	3.13	421	557	5.29	562	1.00	134	178
Strain Gauge Bridge on Wire (0.025 in. p to p)				1 cm. = 307 lbf.				∴ 1.73 cm. = 520 lbf.			

EXPERIMENTAL RESULTS — TABLE NO. 22.

Material - OFHC. Copper | Drawing Speed = 1.3 ft / m. | Reduction in Area = 38 %

Amplitude of Die Oscil. (p to p) 'x' in.	Amplitude of Drum Oscil. 'θ' rads.	Drum Inertia Torque		Mean Drawing Force (Torquemeter)			Mean Drawing Force (Loadmeter)		Force Variation as seen by Torquemeter		
		lbf.ft	lbf.	cm.	lbf.ft	lbf.	cm.	lbf.	cm.	lbf.ft	lbf.
Frequency of Oscillation = 125 c/s.											
0	0	0	0	5.00	672	890	8.35	886	0	0	0
0.010	0.31×10^{-4}	87	115	4.68	629	834	7.70	816	0.20	27	36
0.020	0.64 "	177	235	4.12	553	732	7.06	749	0.35	42	55
0.030	0.91 "	249	330	3.63	488	646	6.16	652	0.43	58	77
0.035	1.10 "	302	400	3.52	474	627	6.04	635	0.48	65	86
Strain Gauge Bridge on Wire (0.025 in. p to p)				1 cm. = 307 lbf.			∴ 1.70 cm. = 508 lbf.				
									Strain Gauge Bridge		
	Frequency								on wire 1cm. = 307lbf.		
	of Oscil.										
0.013	200			4.45	598	792	7.43	790	0.95cm. = 270 lbf.		
0.007	300			4.70	634	838	7.90	838	0.53cm. = 144 lbf.		
0.005	400			4.80	647	856	8.04	852	0.41cm. = 107 lbf.		
0.003	500			4.90	659	872	8.15	866	0.22cm. = 56 lbf.		

EXPERIMENTAL RESULTS — TABLE NO. 23.

Material - OFHC.Copper | Drawing Speed = 10 ft / m. | Reduction in Area = 38 %

Amplitude of Die Oscil. (p to p) 'x' in.	Amplitude of Drum Oscil. 'θ' rads.	Drum Inertia Torque		Mean Drawing Force (Torquemeter)			Mean Drawing Force (Loadmeter)		Force Variation as seen by Torquemeter		
		lbf.ft	lbf.	cm.	lbf.ft	lbf.	cm.	lbf.	cm.	lbf.ft	lbf.
Frequency of Oscillation =				25 c/s.							
0	0	0	0	5.00	672	890	8.30	882	0	0	0
0.010	0.70×10^{-4}	7	10	4.93	662	877	8.17	867	0.45	60	80
0.020	1.74×10^{-4}	20	26	4.80	644	854	8.03	852	0.90	121	160
0.040	3.48×10^{-4}	39	51	4.52	609	806	7.62	809	2.00	269	356
0.060	5.05×10^{-4}	56	74	4.25	571	756	7.14	757	3.10	417	552
0.070	5.75×10^{-4}	63	84	4.10	550	729	6.74	715	3.40	457	605
Frequency of Oscillation =				50 c/s.							
0	0	0	0	5.00	672	890	8.30	882	0	0	0
0.010	2.18×10^{-4}	96	127	4.88	656	868	8.10	858	0.85	114	151
0.020	5.58×10^{-4}	246	326	4.55	611	810	7.70	818	1.95	262	347
0.040	9.95×10^{-4}	438	580	3.90	523	693	6.55	695	3.22	433	573
0.060	11.50×10^{-4}	507	671	3.39	456	604	5.72	606	3.18	427	566
0.070	12.02×10^{-4}	529	702	3.24	435	576	5.50	583	3.22	433	573

EXPERIMENTAL RESULTS — TABLE NO. 24.

Material - OFHC. Copper | Drawing Speed = 10 ft / m. | Reduction in Area = 38 %

Amplitude of Die Oscil. (p to p) 'x' in.	Amplitude of Drum Oscil. 'θ' rads.	Drum Inertia Torque		Mean Drawing Force (Torquemeter)			Mean Drawing Force (Loadmeter)		Force Variation as seen by Torquemeter		
		lbf.ft	lbf.	cm.	lbf.ft	lbf.	cm.	lbf.	cm.	lbf.ft	lbf.
Frequency of Oscillation = 75 c/s.											
0	0	0	0	5.00	672	890	8.30	882	0	0	0
0.010	0.80×10^{-4}	79	105	4.85	652	862	8.10	858	0.25	34	45
0.020	1.48 "	147	195	4.52	607	803	7.46	792	0.60	81	107
0.040	3.22 "	320	423	3.80	512	677	6.55	695	1.20	161	213
0.060	4.36 "	432	571	3.39	444	598	5.70	605	2.02	272	360
0.070	4.71 "	466	617	3.10	417	552	5.30	562	2.36	317	420
Frequency of Oscillation = 100 c/s.											
0	0	0	0	5.00	672	890	8.30	882	0	0	0
0.010	0.35×10^{-4}	61	81	4.78	643	852	8.10	858	0.20	27	36
0.020	0.75 "	131	174	4.38	588	780	7.42	786	0.32	43	57
0.030	1.15 "	202	267	3.98	535	708	6.80	721	0.48	65	86
0.040	1.51 "	266	352	3.73	501	664	6.28	666	0.63	85	112
0.050	1.78 "	312	413	3.54	476	630	6.08	640	0.73	94	124

EXPERIMENTAL RESULTS — TABLE NO. 25.

Material - OFHC. Copper | Drawing Speed = 10 ft / m. | Reduction in Area = 38 %

Amplitude of Die Oscil. (p to p) 'x' in.	Amplitude of Drum Oscil. 'θ' rads.	Drum Inertia Torque		Mean Drawing Force (Torquemeter)			Mean Drawing Force (Loadmeter)		Force Variation as seen by Torquemeter		
		lbf.ft	lbf.	cm.	lbf.ft	lbf.	cm.	lbf.	cm.	lbf.ft	lbf.
Frequency of Oscillation = 125 c/s.											
0	0	0	0	5.00	672	890	8.30	882	0	0	0
0.010	0.24×10^{-4}	67	89	4.80	644	853	8.05	854	0.15	20	27
0.020	0.47 "	130	172	4.55	611	810	7.50	795	0.25	34	45
0.030	0.70 "	192	254	4.08	548	726	6.83	724	0.30	41	52
0.035	0.82 "	226	299	3.82	491	680	6.41	680	0.33	45	59

EXPERIMENTAL RESULTS — TABLE NO. 26.

Material - OFHC. Copper | Drawing Speed = 20 ft / m. | Reduction in Area = 38 %

Amplitude of Die Oscil. (p to p) 'x' in.	Amplitude of Drum Oscil. 'θ' rads.	Drum Inertia Torque		Mean Drawing Force (Torquemeter)			Mean Drawing Force (Loadmeter)		Force Variation as seen by Torquemeter		
		lbf.ft	lbf.	cm.	lbf.ft	lbf.	cm.	lbf.	cm.	lbf.ft	lbf.
Frequency of Oscillation =				25 c/s.							
0	0	0	0	5.00	672	890	8.30	882	0	0	0
0.010	0.52×10^{-4}	6	8	4.97	668	885	8.29	880	0.22	30	40
0.020	1.05 "	11	15	4.90	659	873	8.22	872	0.45	68	90
0.040	1.39 "	15	20	4.72	634	839	7.96	846	0.90	122	162
0.060	2.62 "	29	38	4.68	629	833	7.88	836	1.24	208	275
0.070	2.96 "	33	43	4.55	612	810	7.52	797	1.74	234	310
Frequency of Oscillation =				50 c/s.							
0	0	0	0	5.00	672	890	8.30	882	0	0	0
0.010	1.57×10^{-4}	69	92	4.82	646	856	8.08	868	0.55	74	98
0.020	3.14 "	139	184	4.73	635	842	7.95	844	1.08	145	192
0.040	7.14 "	316	419	4.30	577	764	7.18	762	2.62	352	466
0.060	9.58 "	424	562	3.95	532	703	6.70	711	3.40	458	606
0.070	10.45 "	462	612	3.70	497	658	6.20	658	3.40	458	606

EXPERIMENTAL RESULTS — TABLE NO. 27.

Material - OFHC. Copper | Drawing Speed = 20 ft / m. | Reduction in Area = 38 %

Amplitude of Die Oscil. (p to p) 'x' in.	Amplitude of Drum Oscil. 'θ' rads.	Drum Inertia Torque		Mean Drawing Force (Torquemeter)			Mean Drawing Force (Loadmeter)		Force Variation as seen by Torquemeter		
		lbf.ft	lbf.	cm.	lbf.ft	lbf.	cm.	lbf.	cm.	lbf.ft	lbf.
Frequency of Oscillation =				75 c/s.							
0	0	0	0	5.00	672	890	8.30	882	0	0	0
0.010	0.52×10^{-4}	52	69	4.98	669	886	8.26	878	0.13	17	23
0.020	1.01 "	99	132	4.78	642	852	8.10	859	0.36	48	64
0.040	2.18 "	215	285	4.28	576	763	7.20	765	1.00	134	178
0.060	2.96 "	293	388	3.82	514	682	6.50	690	1.70	228	302
0.070	3.18 "	345	457	3.55	476	632	6.08	646	1.70	228	302
Frequency of Oscillation =				100 c/s.							
0	0	0	0	5.00	672	890	8.30	883	0	0	0
0.010	0.24×10^{-4}	42	55	4.97	667	884	8.27	878	0.12	16	21
0.020	0.52 "	92	122	4.75	638	845	7.94	843	0.20	27	36
0.030	0.75 "	132	175	4.54	611	809	7.70	816	0.40	54	71
0.040	0.94 "	166	220	4.23	568	753	7.12	756	0.50	67	89
0.050	1.13 "	200	265	4.03	543	719	6.86	728	0.56	76	100

EXPERIMENTAL RESULTS — TABLE NO. 28.

Material - OFHC. Copper | Drawing Speed = 20 ft / m. | Reduction in Area = 38 %

Amplitude of Die Oscil. (p to p) 'x' in.	Amplitude of Drum Oscil. 'θ' rads.	Drum Inertia Torque		Mean Drawing Force (Torquemeter)			Mean Drawing Force (Loadmeter)		Force Variation as seen by Torquemeter		
		lbf.ft	lbf.	cm.	lbf.ft	lbf.	cm.	lbf.	cm.	lbf.ft	lbf.
Frequency of Oscillation =				125 c/s.							
0	0	0	0	5.00	672	890	8.30	882	0	0	0
0.010	0.17×10^{-4}	48	64	4.94	671	888	8.20	871	0.10	14	18
0.020	0.33 "	91	120	4.72	634	840	7.82	829	0.18	24	32
0.030	0.47 "	129	171	4.40	592	785	7.40	786	0.20	27	36
0.035	0.59 "	139	184	4.30	544	764	7.20	764	0.21	28	37

EXPERIMENTAL RESULTS — TABLE NO. 29.

Material - OFHC. Copper | Drawing Speed = ft / m. | Reduction in Area = 38 %

Amplitude of Die Oscil. (p to p) 'x' in.	Amplitude of Drum Oscil. '0' rads.	Drum Inertia Torque		Mean Drawing Force (Torquemeter)			Mean Drawing Force (Loadmeter)		Force Variation as seen by Torquemeter		
		lbf.ft	lbf.	cm.	lbf.ft	lbf.	cm.	lbf.	cm.	lbf.ft	lbf.
Frequency of Oscillation = 25 c/s.				Drawing Speed = 35 ft/m.							
0	0	0	0	5.00	672	890	8.30	882	0	0	0
0.030	0.26×10^{-4}	3	4	4.98	669	886	8.30	882	0.39	53	70
0.070	1.05 "	11	15	4.90	660	874	8.18	870	0.61	82	108
Frequency of Oscillation = 50 c/s.				Drawing Speed = 35 ft/m.							
0	0	0	0	5.00	672	890	8.30	882	0	0	0
0.010	0.73×10^{-4}	33	43	4.90	658	872	8.20	871	0.35	47	62
0.020	1.74 "	77	102	4.84	652	862	8.16	866	0.70	94	124
0.040	3.48 "	162	214	4.67	628	832	7.88	836	1.40	188	249
0.060	5.66 "	250	331	4.45	598	793	7.50	796	2.25	303	401
0.070	6.54 "	289	383	4.33	583	771	7.28	774	2.75	370	490
Frequency of Oscillation = 50 c/s.				Drawing Speed = 50 ft/m.							
0.030	0.12×10^{-4}	5	7	4.98	669	886	8.30	882	0.56	76	100
0.040	0.16 "	7	9	4.93	663	878	8.26	877	0.70	94	124
0.060	0.24 "	10	14	4.86	655	866	8.22	873	1.20	162	214
0.070	0.30 "	13	18	4.82	646	857	8.16	866	1.58	212	281

THEORETICAL CALCULATIONS — TABLE NO. 30

Material- Mild Steel — Reduction in Area= 51 %

Drawing Speed = 1.3 ft/m. — Length of Drawn Wire = 17.8in

Amplitude of Die Oscil ('x' in. (p to p))	Amplitude of Drum Osc. 'θ' rads.	Amplitude of Wire at Die 'x' in.	Amplitude of Wire at Drum. 'rθ' in.	$\frac{\omega L}{a}$ degr's	Cosec $\frac{\omega L}{a}$	Cot $\frac{\omega L}{a}$	Sin $\frac{\omega L}{a}$	Force Variation 'F' in Wire. lbf.
	x 10^{-4}		x 10^{-4}					
Frequency of Oscillation = 75 c/s.								
0.010	1.28	.0021	11.07	$2^{o}21'$	24.2	24.2	.041	215
0.020	2.80	.0048	25.20	"	"	"	"	488
0.030	4.02	.0068	36.18	"	"	"	"	702
0.040	5.41	.0092	48.69	"	"	"	"	944
0.050	6.46	.0110	58.14	"	"	"	"	1128
Frequency of Oscillation = 100 c/s.								
0.010	0.68	.0036	6.12	$3^{o}08'$	18.3	18.3	.055	266
0.020	1.33	.0065	11.97	"	"	"	"	518
0.030	1.67	.0082	15.03	"	"	"	"	702
0.040	2.53	.0125	22.77	"	"	"	"	987
0.050	3.06	.0151	27.54	"	"	"	"	1194
Frequency of Oscillation = 125 c/s								
0.010	0.40	.0037	3.60	$3^{o}54'$	14.7	14.7	.068	270
0.020	0.82	.0075	7.38	"	"	"	"	552
0.030	1.20	.0109	11.80	"	"	"	"	810
0.035	1.38	.0125	12.42	"	"	"	"	895
Frequency of Oscillation = 25 c/s.								
0.010	1.74	.0034	15.66	$0^{o}57'$	73.3	73.3	.016	122
0.020	3.14	.0061	28.26	"	"	"	"	211
0.030	4.71	.0092	42.39	"	"	"	"	330
0.040	6.11	.0119	54.99	"	"	"	"	429
0.050	7.51	.0147	67.59	"	"	"	"	525

THEORETICAL CALCULATIONS — TABLE NO. 31

Material- Mild Steel — Reduction in Area = 41 %

Drawing Speed = 1.3 ft/m. — Length of Drawn Wire = 17.8in

Amplitude of Die Oscil (p to p) 'x' in.	Amplitude of Drum Osc. 'θ' rads.	Amplitude of Wire at Die 'x'' in.	Amplitude of Wire at Drum. 'rθ' in.	$\frac{\omega L}{a}$ degr's	Cosec $\frac{\omega L}{a}$	Cot $\frac{\omega L}{a}$	Sin $\frac{\omega L}{a}$	Force Variation in Wire. 'F' lbf.
	$\times 10^{-4}$		$\times 10^{-4}$					
Frequency of Oscillation = 75 c/s.								
0.010	2.01	.0034	18.08	2°21'	24.2	24.2	0.04	350
0.020	2.80	.0048	25.20	"	"	"	"	488
0.030	4.60	.0078	41.40	"	"	"	"	803
0.040	5.41	.0092	48.69	"	"	"	"	950
0.050	6.45	.0110	59.05	"	"	"	"	1126
0.060	7.00	.0119	63.00	"	"	"	"	1222
Frequency of Oscillation = 100 c/s.								
0.010	0.84	.0041	7.56	3°08'	18.3	18.3	0.06	327
0.020	1.43	.0070	12.87	"	"	"	"	558
0.030	1.80	.0087	16.20	"	"	"	"	690
0.040	2.56	.0126	23.04	"	"	"	"	1000
0.050	2.97	.0144	26.73	"	"	"	"	1139
Frequency of Oscillation = 125 c/s.								
0.010	0.47	.0043	4.23	3°54'	14.7	14.7	0.07	317
0.020	0.94	.0085	8.46	"	"	"	"	635
0.030	1.24	.0113	11.16	"	"	"	"	834
0.035	1.39	.0127	12.51	"	"	"	"	939
Frequency of Oscillation = 25 c/s.								
0.010	1.92	.0038	17.28	0°57'	73.3	73.3	0.02	134
0.020	3.14	.0061	28.26	"	"	"	"	220
0.030	4.88	.0095	43.92	"	"	"	"	341
0.040	6.28	.0122	56.52	"	"	"	"	440
0.050	7.55	.0147	67.95	"	"	"	"	524
0.060	7.87	.0154	70.83	"	"	"	"	551

THEORETICAL CALCULATIONS							TABLE NO. 32	
Material- Mild Steel				Reduction in Area= 26 %				
Drawing Speed = 1.3 ft/m.				Length of Drawn Wire = 17.8in				
Amplitude of Die Oscil (p to p) 'x' in.	Amplitude of Drum Osc. 'θ' rads.	Amplitude of Wire at Die 'x'' in.	Amplitude of Wire at Drum. 'rθ' in.	$\frac{\omega L}{a}$ degr's	Cosec $\frac{\omega L}{a}$	Cot $\frac{\omega L}{a}$	Sin $\frac{\omega L}{a}$	Force Variation 'F' in Wire. 'F' lbf.
	$\times 10^{-4}$		$\times 10^{-4}$					
Frequency of Oscillation = 75 c/s.								
0.010	1.57	.0027	14.13	2°21'	24.2	24.2	0.04	270
0.020	2.97	.0051	26.73	"	"	"	"	518
0.030	4.01	.0068	36.09	"	"	"	"	700
0.040	4.19	.0071	37.71	"	"	"	"	731
0.050	4.72	.0080	42.48	"	"	"	"	824
Frequency of Oscillation = 100 c/s.								
0.010	0.70	.0034	6.30	3°08'	18.3	18.3	0.06	270
0.020	1.34	.0066	12.06	"	"	"	"	524
0.030	1.66	.0082	14.94	"	"	"	"	648
0.040	2.01	.0099	18.09	"	"	"	"	784
0.050	2.18	.0107	19.62	"	"	"	"	851
Frequency of Oscillation = 125 c/s.								
0.010	0.38	.0035	3.42	3°54'	14.7	14.7	0.07	259
0.020	0.73	.0067	6.57	"	"	"	"	494
0.030	0.98	.0089	8.82	"	"	"	"	658
0.035	1.13	.0103	10.17	"	"	"	"	762
Frequency of Oscillation 25 c/s.								
0.010	1.92	.0038	17.28	0°57'	73.3	73.3	0.02	134
0.020	3.14	.0061	28.26	"	"	"	"	220
0.030	4.83	.0095	43.47	"	"	"	"	341
0.040	5.93	.0116	53.37	"	"	"	"	415
0.050	7.34	.0143	66.06	"	"	"	"	514

THEORETICAL CALCULATIONS								TABLE NO. 33
Material- Mild Steel				Reduction in Area= 10 %				
Drawing Speed = 1.3 ft/m.				Length of Drawn Wire = 17.8in				
Amplitude of Die Oscil (p to p) 'x' in.	Amplitude of Drum Osc. 'θ' rads.	Amplitude of Wire at Die 'x'' in.	Amplitude of Wire at Drum. 'rθ' in.	$\frac{\omega L}{a}$ degr's	Cosec $\frac{\omega L}{a}$	Cot $\frac{\omega L}{a}$	Sin $\frac{\omega L}{a}$	Force Variation in Wire. 'F' lbf.
	x 10^{-4}		x 10^{-4}					
Frequency of Oscillation = 75 c/s.								
0.010	1.24	.0020	11.16	2°21'	24.2	24.2	0.04	209
0.020	2.10	.0036	18.90	"	"	"	"	365
0.030	2.53	.0043	22.77	"	"	"	"	455
Frequency of Oscillation 100 c/s.								
0.010	0.56	.0028	5.04	3°08'	18.3	18.3	0.06	218
0.020	0.96	.0047	8.64	"	"	"	"	376
0.030	1.22	.0060	10.98	"	"	"	"	476
Frequency of Oscillation = 125 c/s.								
0.010	0.33	.0030	2.97	3°54'	14.7	14.7	0.07	224
0.020	0.57	.0051	5.13	"	"	"	"	382
0.30	0.69	.0063	5.61	"	"	"	"	466
Frequency of Oscillation 25 c/s.								
0.010	1.05	.0020	9.45	0°57'	73.3	73.3	0.02	73
0.020	1.74	.0034	15.66	"	"	"	"	122
0.030	2.80	.0055	25.20	"	"	"	"	196

THEORETICAL CALCULATIONS — TABLE NO.34

Material-Stainless Steel — Reduction in Area = 44.5 %

Drawing Speed = 1.3 ft/m. — Length of Drawn Wire = 17.8in

Amplitude of Die Oscil (p to p) 'x' in.	Amplitude of Drum Osc. 'θ' rads.	Amplitude of Wire at Die 'x' in.	Amplitude of Wire at Drum. 'rθ' in.	$\frac{\omega L}{a}$ degr's	Cosec $\frac{\omega L}{a}$	Cot $\frac{\omega L}{a}$	Sin $\frac{\omega L}{a}$	Force Variation in Wire. 'F' lbf.
	x 10^{-4}		x 10^{-4}					
Frequency of Oscillation = 75 c/s.								
0.010	1.66	.0028	14.94	$2^{o}21'$	24.2	24.2	0.04	292
0.020	3.14	.0053	28.26	"	"	"	"	589
0.040	6.45	.0110	58.05	"	"	"	"	1125
0.060	8.90	.0150	80.10	"	"	"	"	1552
0.070	10.45	.0178	94.05	"	"	"	"	1823
Frequency of Oscillation = 100 c/s.								
0.010	0.70	.0034	6.30	$3^{o}08'$	18.3	18.3	0.06	272
0.020	1.36	.0067	12.24	"	"	"	"	531
0.030	2.13	.0105	19.17	"	"	"	"	829
0.040	2.45	.0120	22.05	"	"	"	"	954
0.050	2.97	.0146	26.73	"	"	"	"	1158
Frequency of Oscillation=125 c/s.								
0.010	0.38	.0035	3.42	$3^{o}54'$	14.7	14.7	0.07	258
0.020	0.84	.0076	7.56	"	"	"	"	564
0.030	1.24	.0112	11.16	"	"	"	"	832
0.035	1.36	.0124	12.24	"	"	"	"	916
Frequency of Oscillation = 25 c/s.								
0.010	1.74	.0034	15.66	$0^{o}57'$	73.3	73.3	0.02	122
0.020	3.14	.0061	28.26	"	"	"	"	221
0.040	5.94	.0116	53.46	"	"	"	"	416
0.060	8.72	.0170	73.48	"	"	"	"	609
0.070	10.81	.0211	91.29	"	"	"	"	756

THEORETICAL CALCULATIONS								TABLE NO.35
Material-Aluminium HG.9				Reduction in Area= 44.5 %				
Drawing Speed = 1.3 ft/m.				Length of Drawn Wire = 17.8in				
Amplitude of Die Oscil (p to p) 'x' in.	Amplitude Osc. of Drum 'θ' rads.	Amplitude of Wire at Die 'x' in.	Amplitude of Wire at Drum. 'rθ' in.	$\frac{\omega L}{a}$ degr's	Cosec $\frac{\omega L}{a}$	Cot $\frac{\omega L}{a}$	Sin $\frac{\omega L}{a}$	Force Variation in Wire. 'F' lbf.
	x 10^{-4}		x 10^{-4}					
Frequency of Oscillation = 75 c/s.								
0.010	0.25	.0040	2.25	$2^{\circ}32'$	22.75	22.73	0.05	87
0.020	1.12	.0085	10.08	"	"	"	"	187
0.040	2.01	.0155	18.09	"	"	"	"	340
0.060	2.71	.0210	24.39	"	"	"	"	460
0.070	3.23	.0253	29.07	"	"	"	"	558
Frequency of Oscillation=100 c/s.								
0.010	0.26	.0047	2.34	$3^{\circ}24'$	16.86	16.83	0.06	100
0.020	0.49	.0044	4.41	"	"	"	"	186
0.030	0.70	.0071	7.11	"	"	"	"	300
0.040	0.93	.0084	8.37	"	"	"	"	356
0.050	1.12	.0101	10.08	"	"	"	"	427
Frequency of Oscillation = 125 c/s.								
0.010	0.14	.0045	1.26	$4^{\circ}16'$	13.50	13.48	0.09	90
0.020	0.31	.0100	2.79	"	"	"	"	200
0.030	0.47	.0150	4.23	"	"	"	"	310
0.035	0.48	.0160	4.32	"	"	"	"	320
Frequency of Oscillation = 25 c/s.								
0.010	0.79	.0040	7.11	$0^{\circ}51'$	67.70	67.70	0.02	64
0.020	1.31	.0065	11.79	"	"	"	"	104
0.040	3.49	.0170	31.41	"	"	"	"	270
0.060	4.88	.0240	43.92	"	"	"	"	381
0.070	5.58	.0270	50.22	"	"	"	"	438

THEORETICAL CALCULATIONS								TABLE NO. 36
Material - Pure Aluminium				Reduction in Area = 24 %				
Drawing Speed = 1.3 ft/m.				Length of Drawn Wire = 17.8in				
Amplitude of Die Oscil (p to p) 'x' in.	Amplitude of Drum Osc. 'θ' rads.	Amplitude of Wire at Die 'x' in.	Amplitude of Wire at Drum. 'rθ' in.	$\frac{\omega L}{a}$ degr's	Cosec $\frac{\omega L}{a}$	Cot $\frac{\omega L}{a}$	Sin $\frac{\omega L}{a}$	Force Variation in Wire. 'F' lbf.
	$\times 10^{-4}$		$\times 10^{-4}$					
Frequency of Oscillation = 75 c/s.								
0.010	0.63	.0025	5.67	$2^{\circ}12'$	26.05	26.03	0.04	109
0.020	1.06	.0040	9.54	"	"	"	"	178
0.030	1.36	.0051	12.24	"	"	"	"	226
Frequency of Oscillation = 100 c/s.								
0.010	0.30	.0029	2.70	$2^{\circ}54'$	19.77	19.74	0.05	113
0.020	0.51	.0049	4.59	"	"	"	"	193
0.030	0.58	.0055	5.22	"	"	"	"	220
Frequency of Oscillation = 125 c/s.								
0.010	0.16	.0031	1.44	$3^{\circ}42'$	15.50	15.46	0.06	116
0.020	0.27	.0054	2.43	"	"	"	"	200
0.030	0.34	.0063	3.06	"	"	"	"	232
Frequency of Oscillation = 25 c/s.								
0.010	1.04	.0030	9.36	$0^{\circ}42'$	81.85	81.85	0.01	77
0.020	1.74	.0050	15.76	"	"	"	"	128
0.030	2.09	.0060	18.81	"	"	"	"	154

THEORETICAL CALCULATIONS							TABLE NO. 37	
Material- O.F.H.C Copper			Reduction in Area= 38 %					
Drawing Speed = 1.3 ft/m.			Length of Drawn Wire = 17.8in.					
Amplitude of Die Oscil (p to p) 'x' in.	Amplitude of Drum Osc. 'θ' rads.	Amplitude of Wire at Die 'x' in.	Amplitude of Wire at Drum. 'rθ' in.	$\frac{\omega L}{a}$ degr's	Cosec $\frac{\omega L}{a}$	Cot $\frac{\omega L}{a}$	Sin $\frac{\omega L}{a}$	Force Variation in Wire. 'F' lbf.
	x 10^{-4}		x 10^{-4}					
Frequency of Oscillation=75 c/s.								
0.010	1.22	.0038	10.98	3°17'	17.40	17.39	0.06	210
0.020	2.46	.0076	22.14	"	"	"	"	424
0.040	4.09	.0127	36.81	"	"	"	"	706
0.060	5.31	.0165	47.79	"	"	"	"	917
0.070	5.74	.0179	51.76	"	"	"	"	992
Frequency of Oscillation = 100 c/s.								
0.010	0.59	.0048	5.31	4°25'	12.99	12.95	0.09	229
0.020	1.15	.0094	10.35	"	"	"	"	447
0.030	1.53	.0125	13.77	"	"	"	"	594
0.040	2.00	.0164	18.09	"	"	"	"	768
0.050	2.26	.0185	2o.43	"	"	"	"	880
Frequency of Oscillation = 125 c/s.								
0.010	0.31	.0046	2.79	5°30'	10.43	10.39	0.09	210
0.020	0.64	.0095	5.76	"	"	"	"	432
0.030	0.91	.0133	8.19	"	"	"	"	605
0.035	1.10	.0161	9.90	"	"	"	"	736
Frequency of Oscillation = 25 c/s.								
0.010	1.57	.0042	14.13	1°06'	52.09	52.08	0.02	119
0.020	3.14	.0084	28.26	"	"	"	"	238
0.040	5.06	.0136	45.54	"	"	"	"	384
0.060	7.15	.0191	64.35	"	"	"	"	540
0.070	7.85	.0210	70.65	"	"	"	"	594

THEORETICAL CALCULATIONS — TABLE NO. 38

Material- O.F.H.C Copper — Reduction in Area = 38 %

Drawing Speed = 10. ft/m. — Length of Drawn Wire = 17.8in

Amplitude of Dic Oscil (p to p) 'x' in.	Amplitude of Drum Osc. of 'θ' rads.	Amplitude of Wire at Dic 'x' in.	Amplitude of Wire at Drum. 'rθ' in.	$\frac{\omega L}{a}$ degr's	Cosec $\frac{\omega L}{a}$	Cot $\frac{\omega L}{a}$	Sin $\frac{\omega L}{a}$	Force Variation in Wire. 'F' lbf.
	x 10^{-4}		x 10^{-4}					
Frequency of Oscillation = 75 c/s.								
0.010	0.80	.0025	7.20	3°17'	17.40	17.39	0.06	138
0.020	1.48	.0046	13.32	"	"	"	"	255
0.040	3.22	.0100	28.98	"	"	"	"	568
0.060	4.36	.0135	39.24	"	"	"	"	750
0.070	4.71	.0146	42.39	"	"	"	"	811
Frequency of Oscillation = 100 c/s.								
0.010	0.35	.0029	3.15	4°25'	12.99	12.95	0.09	135
0.020	0.75	.0061	6.75	"	"	"	"	290
0.030	1.15	.0094	10.35	"	"	"	"	446
0.040	1.51	.0124	13.59	"	"	"	"	587
0.050	1.78	.0145	16.02	"	"	"	"	690
Frequency of Oscillation = 125 c/s.								
0.010	0.24	.0036	2.16	5°30'	10.43	10.39	0.09	163
0.020	0.47	.0069	4.23	"	"	"	"	315
0.030	0.70	.0102	6.30	"	"	"	"	466
0.035	0.82	.0120	7.38	"	"	"	"	548
Frequency of Oscillation = 25 c/s.								
0.010	0.70	.0019	6.30	1°06'	52.09	52.08	0.02	52
0.020	1.74	.0048	15.66	"	"	"	"	133
0.040	3.48	.0094	31.32	"	"	"	"	265
0.060	5.05	.0136	45.45	"	"	"	"	384
0.070	5.75	.0154	51.57	"	"	"	"	436

THEORETICAL CALCULATIONS							TABLE NO. 39	
Material- O.F.H.C Copper				Reduction in Area= 38 %				
Drawing Speed = 20 ft/m.				Length of Drawn Wire = 17.8in				
Amplitude of Die Oscil (p to p) 'x' in.	Amplitude of Drum Osc. 'θ' rads.	Amplitude of Wire at Die 'x'' in.	Amplitude of Wire at Drum. 'rθ' in.	$\frac{\omega L}{a}$ degr's	Cosec $\frac{\omega L}{a}$	Cot $\frac{\omega L}{a}$	Sin $\frac{\omega L}{a}$	Force Variation in Wire. 'F' lbf.
	x 10^{-4}		x 10^{-4}					
Frequency of Oscillation = 75 c/s.								
0.010	0.52	.0016	4.68	3°17'	17.40	17.39	0.06	87
0.020	1.01	.0031	9.09	"	"	"	"	174
0.040	2.18	.0068	19.62	"	"	"	"	375
0.060	2.96	.0092	26.64	"	"	"	"	513
0.070	3.18	.0108	28.62	"	"	"	"	600
Frequency of Oscillation = 100 c/s.								
0.010	0.24	.0019	2.16	4°25'	12.99	12.95	0.09	92
0.020	0.52	.0043	4.68	"	"	"	"	203
0.030	0.75	.0061	6.75	"	"	"	"	291
0.040	0.94	.0077	8.46	"	"	"	"	365
0.050	1.13	.0092	10.17	"	"	"	"	439
Frequency of Oscillation = 125 c/s.								
0.010	0.17	.0026	1.53	5°30'	10.43	10.39	0.09	117
0.020	0.33	.0049	2.97	"	"	"	"	222
0.030	0.47	.0069	4.23	"	"	"	"	315
0.035	0.59	.0074	5.31	"	"	"	"	339
Frequency of Oscillation = 25 c/s.								
0.010	0.52	.0014	4.68	1°06'	52.09	52.08	0.02	40
0.020	1.05	.0028	9.45	"	"	"	"	79
0.040	1.39	.0037	12.51	"	"	"	"	106
0.060	2.62	.0070	23.58	"	"	"	"	199
0.070	2.96	.0078	26.64	"	"	"	"	221